48

ЖУРНАЛ
ЭКСПЕРИМЕНТАЛЬНОЙ И ТЕОРЕТИЧЕСКОЙ
ФИЗИКИ
Zhurnal Eksperimental'noi i Teoreticheskoi Fiziki

SOVIET PHYSICS
JETP

LIBRARY
THE BOEING COMPANY
WICHITA DIVISION

VOL. 13, No. 1 ~~July, 1961~~

A Translation
of the
Journal of Experimental and Theoretical Physics
of the
Academy of Sciences of the USSR

(Russian Original Vol. 40, No. 1 (January, 1961)

Published by the
AMERICAN INSTITUTE OF PHYSICS
INCORPORATED

SOVIET PHYSICS
JETP

A translation of the Journal of Experimental and Theoretical Physics of the USSR.

A publication of the

**AMERICAN INSTITUTE
OF PHYSICS**

Governing Board

RALPH A. SAWYER, *Chairman*
JAMES G. BAKER
R. H. BOLT
WALLACE R. BRODE
HARVEY BROOKS
DIRK BROUWER
J. H. ELLIOTT
HERBERT A. ERF
N. S. GINGRICH
S. A. GOUDSMIT
W. W. HAVENS, JR.
W. V. HOUSTON
WINSTON E. KOCK
R. BRUCE LINDSAY
DAVID L. MACADAM
H. VICTOR NEHER
LEONARD O. OLSEN
C. J. OVERBECK
RAY PEPINSKY
S. L. QUIMBY
FRANCIS W. SEARS
FREDERICK SEITZ
C. G. SUITS
MARY E. WARGA
WILLIAM R. WILLETS

Administration

ELMER HUTCHISSON
Director
WALLACE WATERFALL
Secretary and Treasurer
HENRY A. BARTON
Administrative Consultant
W. C. KELLY
Director of Education
EUGENE H. KONE
Director of Public Relations
HUGH C. WOLFE
Director of Publications
KATHRYN SETZE
Assistant Treasurer
JAMES E. MILLS
Supervisor, Editorial Department
SISTINA GRECO
Circulation Manager
EDWARD TOBER
Manager, Production and Distribution
THEODORE VORBURGER
Advertising Manager
EMILY WOLF
Manager, Special Services

American Institute of Physics Advisory Board on Russian Translations

ROBERT T. BEYER, *Chairman*
J. GEORGE ADASHKO, FREEMAN DYSON, DWIGHT GRAY,
MORTON HAMERMESH, DAVID HARKER, HAROLD F. WEAVER

Editor of SOVIET PHYSICS—JETP

J. GEORGE ADASHKO, 25 WEST 81ST ST., NEW YORK 24, NEW YORK

SOVIET PHYSICS—JETP is a monthly journal published by the American Institute of Physics and contains a complete translation of the JOURNAL OF EXPERIMENTAL AND THEORETICAL PHYSICS of the U.S.S.R. Academy of Sciences.

This translating and publishing project was undertaken by the institute in the conviction that dissemination of the results of researches everywhere in the world is invaluable to the advancement of science. The NATIONAL SCIENCE FOUNDATION of the United States has encouraged the project initially and is supporting it in large part by a grant.

The American Institute of Physics and its translators propose to translate faithfully all the material appearing in the original articles. The views expressed in the translations are therefore those of the original authors, and not those of the translators nor of the American Institute of Physics.

Volume 1 of SOVIET PHYSICS—JETP corresponds to Russian Volume 28 (1955). Two volumes are published annually, each of six issues. Each volume contains the translation of one volume of the JOURNAL OF EXPERIMENTAL AND THEORETICAL PHYSICS.

Beginning with Vol. 9 (36), the transliteration of the names of Russian authors follows British Standard 2979, which is being adopted by a large number of scientific journals in the United States. The Library of Congress transliteration is followed in the earlier volumes.

Subscription Prices

Per Year (12 issues), starting with Vol. 13, No. 1

General:	
United States and Canada	$75.00
Elsewhere	79.00
Libraries of non-profit degree-granting Institutions:	
United States and Canada	$50.00
Elsewhere	54.00
Single Copies	$ 8.00

Subscriptions should be addressed to the American Institute of Physics, 335 East 45th Street, New York 17, New York.

SOVIET PHYSICS, JETP is published monthly by the American Institute of Physics, Inc. Second Class postage paid at New York, N. Y. and Ann Arbor, Michigan.

Copyright by American Institute of Physics 1961

SOVIET PHYSICS

JETP

A translation of Zhurnal Éksperimental'noĭ i Teoreticheskoĭ Fiziki.

Vol. 13, No. 1, pp 1-261 (Russ. orig. Vol. 40, No. 1, pp 3-382, Jan., 1961) July, 1961

HYPERFINE INTERACTION IN THE DIPHENYLPICRYLHYDRAZYL MOLECULE

Yu. S. KARIMOV and I. F. SHCHEGOLEV

Institute for Physics Problems, Academy of Sciences, U.S.S.R.

Submitted to JETP editor July 22, 1960

J. Exptl. Theoret. Phys. (U.S.S.R.) **40**, 3-9 (January, 1961)

The structure of the proton resonance line due to the magnetic interaction between the unpaired electron and the protons in the diphenylpicrylhydrazyl (DPPH) free radical was measured in fields from 500 to 5000 oe, mainly at helium temperatures. When H/T is large enough, the resonance line splits into four components. One component is unshifted, one is shifted toward the low-frequency side, and the other two are shifted to the high frequency side. The twelve protons in DPPH can be assigned to the three shifted components in a manner that is consistent with the relative intensities of the lines. The existence of an unshifted line is unexpected and its origin remains unexplained.

INTRODUCTION

RECENTLY there has been a large amount of work, both experimental and theoretical, devoted to the study of the interaction between nuclei and unpaired electrons in free radicals (cf., for example, reference 1). Precise information on the unpaired electron probability distribution within the molecules has been obtained; in particular, a negative spin density has been found at certain nuclear positions. Most of these experimental studies have used electron paramagnetic resonance; there has been only a small amount of work devoted to studying the same phenomenon with nuclear resonance techniques. Yet it is just nuclear resonance that can apparently give more precise information about this interaction.

The free radical diphenylpicrylhydrazyl (DPPH), the structure of which is indicated schematically in Fig. 1, is typical of the materials studied in electron paramagnetic spectroscopy. A large amount of work has been devoted to the study of DPPH. It is known that every DPPH molecule has one unpaired electron; its paramagnetic susceptibility obeys Curie's law in the range from room temperature down to liquid helium temperature; a slight deviation from Curie's law begins only below 4° K.[2]

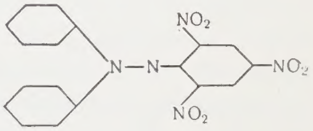

FIG. 1. Structure of the DPPH molecule.

In solid DPPH the electron resonance line is narrow; its width (1.5 — 2 oe) is much smaller than that which would be produced by a dipole interaction between electrons in different molecules. This phenomenon is explained[1] by the presence of a strong intermolecular exchange interaction which narrows the line. In dilute solutions the width of the DPPH electron resonance line increases and it splits into five hyperfine components, spaced about 10 oe apart.[3] In the work of Hutchinson et al.,[3] this hyperfine (h. f.) structure is attributed to the presence of an interaction between the nuclear spin $\mathbf{I}$ and the electron spin $\mathbf{S}$ of the form

$$\mathcal{H}_{\text{h.f.}} = \sum_i h a_i \mathbf{I}_i \mathbf{S},$$

with $a_1 \approx a_2$ for the two central nitrogen atoms, and $a_i \ll a_1, a_2$ for all the other coupling constants. On the other hand, Weissman[4] showed that if the exchange is strong the dipole-dipole interaction between the electron and nuclear spins averages to zero, and the only term contributing to the Hamiltonian is the Fermi contact interaction, proportional to the electron spin density[5] at the position of the particular nucleus.

Behrson,[6] using a simple molecular orbital method, made a rough calculation of the spin density in the DPPH molecule and obtained a result in agreement with experiment, namely $a_1 = a_2$. Besides this, his calculation led to the conclusion that there should be an observable interaction between the unpaired electron and the protons in ortho and para positions in the phenyl rings; this interaction will shift the resonance of these protons to lower frequency (in a given external field). At the same time, the protons in meta positions in the phenyl and picryl groups, according to this calculation, are not coupled to the unpaired electron and should give an unshifted proton line.

The first experimental indication that the DPPH molecule has at least two non-equivalent groups of protons was obtained by Berthet and Riemann,[7] who studied the proton resonance in DPPH at a field of ~6500 oe and a temperature of 77°K. Similar measurements were made somewhat more carefully later by Gutowsky et al.[8] The latter authors carried out a more exact calculation of the coupling constants using the localized-pair method, which gives the possibility of a negative spin density.[5] According to this calculation, the proton spectrum in DPPH should have four lines: the ortho and para protons in the phenyl groups should, as before, give two closely spaced lines shifted to the low-frequency side (in a given external field), while the meta protons in the phenyl and picryl groups should give lines shifted to the high-frequency side.

The present work is a study of the proton resonance in DPPH, mostly at liquid helium temperatures, where the high values of H/T needed to resolve the individual lines can be obtained. The proton resonance spectrum of DPPH was found to contain, besides the expected lines, an intense unshifted line; the origin of this unshifted line is not understood. This shows that our picture of the state of the unpaired electron in the molecule is apparently incomplete.

APPARATUS AND SAMPLES

The proton resonance was detected with a regenerative detector of the type used by Pound and Knight;[9] after narrow-band amplification and synchronous detection, the signal was recorded by an ÉPP-09 recording potentiometer. The coil was wound directly on a thin-walled glass ampoule 6 mm in diameter containing about 0.15 cm^3 of sample which was placed in a Dewar; the coil was connected to the electronic apparatus by a specially constructed coaxial cable.

The 935-oe magnetic field was obtained with a permanent magnet; the other fields were obtained with an electromagnet[10] fed by a motor generator with an electronic current stabilizer. The field was measured by a separate proton resonance system. The modulating field was supplied by supplementary windings on the magnet poles. The modulation frequency was 30 cps, amplitude ~1.5 oe. The time constant of the phase detector was 10 sec and a sweep through the whole frequency range took about 30 — 40 min.

Two polycrystalline DPPH preparates were used as samples: one prepared in A. E. Arbuzov's laboratory, the other obtained in France.* Both samples gave nearly the same results.

We note that the empty ampoule gave a weak proton line, probably due to protons in the insulation on the windings, in the glue applied to the windings, and in the walls of the ampoule; the intensity of this line did not exceed 1 — 2% of the intensity of the DPPH line.

RESULTS

Figure 2 shows typical traces of the absorption line in a 935-oe field at temperatures of 4.2°, 2.5°, and 1.55°K. Figure 3 shows integral curves for the 935-oe field and various temperatures; similar curves for 2000 oe are shown in Fig. 4. Each integral curve is the average of 4 or 5 traces taken on different days.

From Figs. 3 and 4 it is clear that the proton spectrum of DPPH has four components, one remaining at the position of the unshifted proton line, one shifted to lower frequency and two shifted to higher frequencies. The width of the central line is practically independent of H/T, while the satellite widths increase with increasing H/T.

Figure 5 shows the dependence of the shift on H/T for each of the satellites. The linear dependence of the shift on H/T shows that it is caused by the paramagnetism of the unpaired electron.

Table I gives the relative intensities of the satellite for various fields and temperatures. The relative intensity of a line is defined to be the ratio of its area to the total area of the whole integral curve. The accuracy of these measurements is determined

---

*We take this opportunity to thank V. M. Chibrykin, who furnished us with these samples.

FIG. 2. Trace of the derivative of the proton absorption lines in DPPH at 935 oe at temperatures 4.2°, 2.5°, and 1.55° K.

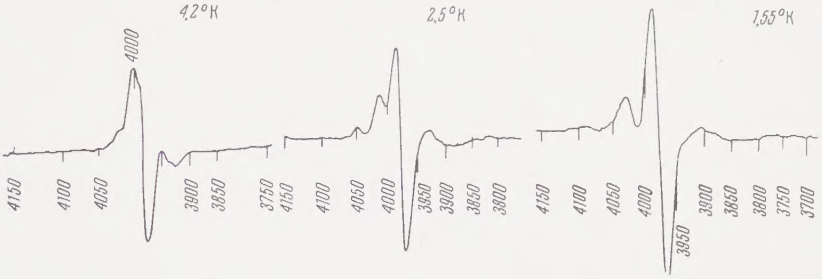

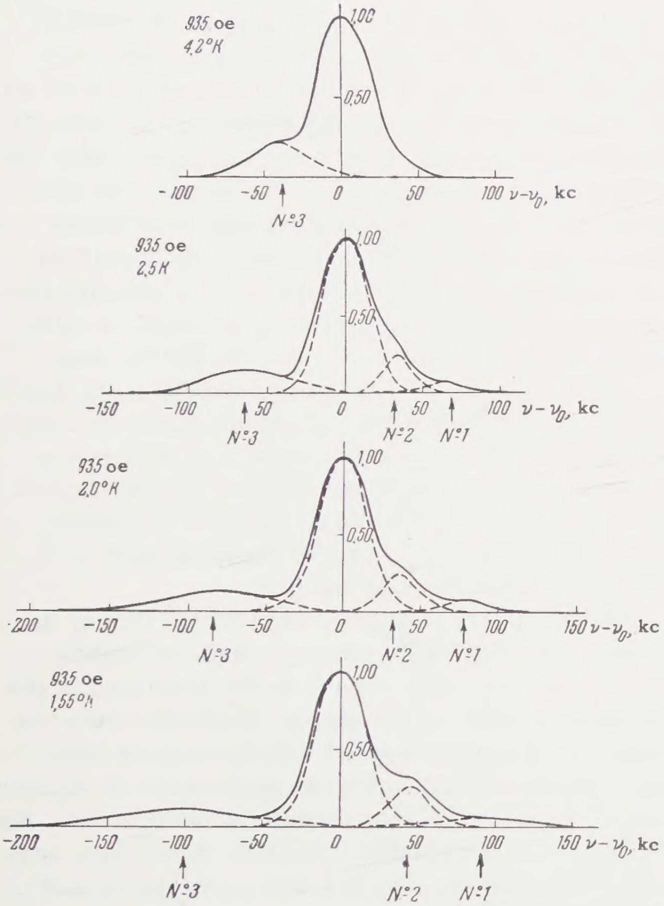

FIG. 3. Proton line in DPPH at 935 oe.

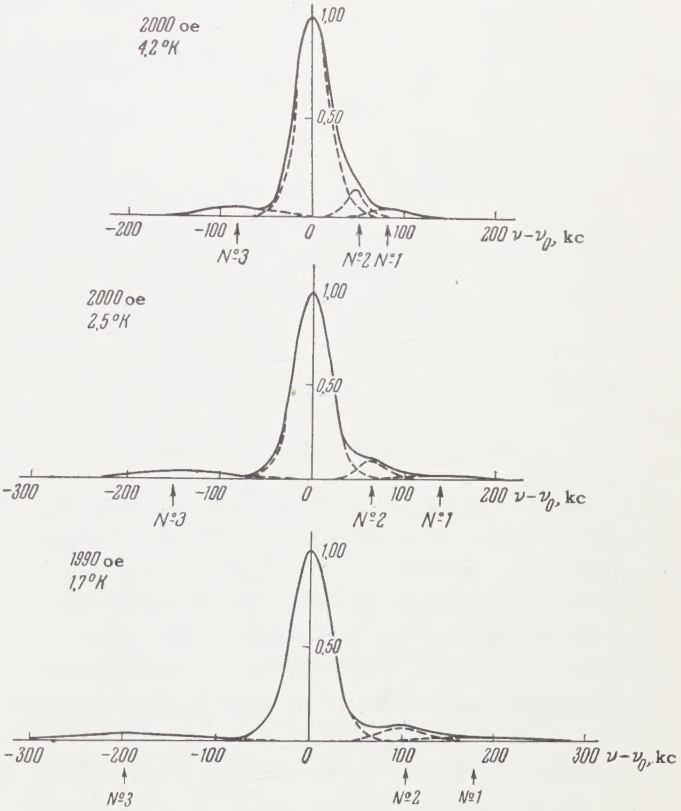

FIG. 4. Proton line in DPPH at 2000 oe.

from the scatter in the different integral curves obtained in different runs. Besides this scatter, there is also an arbitrariness in splitting the full curve up into its components; as a result, the probable error in the intensities is 15 — 20%.

It is clear that in a fixed magnetic field, the satellite relative intensities are independent of temperature in the helium temperature range, but they decrease noticeably in going from 935 oe to 2000 oe. In a further increase in field to 5000 oe the satellites continue to become weaker, but not so rapidly; in this field it is difficult to measure the shifts and intensities with any accuracy.

In a field of about 5000 oe, measurements were also made at 77° K. Here the resonance line is asymmetric, like that observed in references 7 and 8. Because the shifts are so small, it is hopeless to try to split the line into its components. One can only conclude that the satellite intensities apparently increase on going from helium temperatures to nitrogen temperature.

DISCUSSION OF THE RESULTS

From Table I it is clear that the intensities of the lines are in the ratios 1 : 2 : 3 : 11 at 935 oe and 1 : 2 : 3 : 25 at 2000 oe. Thus, while the satellite intensities maintain a constant ratio, the relative intensity of the central line increases with increasing field. Moreover, the central line is so intense that if the weakest line (No. 1) is assumed to be produced by one proton, then all 12 protons in the DPPH molecule are not sufficient to produce the observed intensity of the central line.

If we neglect for the moment the existence of

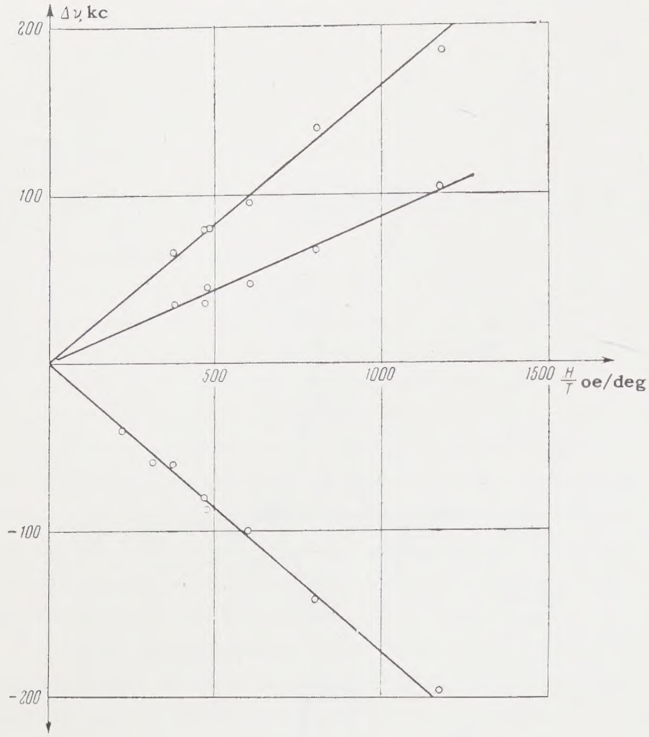

FIG. 5. Satellite shift, Δν versus H/T.

the unshifted proton line, it is easy to assign the 12 DPPH protons to the three satellites. Namely, in qualitative agreement with calculations,[8] the two protons in the picryl group can be assigned to line No. 1, the four meta protons in the phenyl groups to No. 2, and the six ortho and para protons in the phenyl groups to No. 3. In Table II are listed the values of the coupling constants a_i calculated from the slopes of the curves in Fig. 5 by the formula

$$\Delta\nu_i = a_i(\gamma_e/2\pi)(g\beta H/4kT),$$

where $\Delta\nu_i$ is the line shift, γ_e is the electron gyromagnetic ratio, and β is the Bohr magneton. In the same table, the corresponding calculated[6,8] coupling constants are listed for comparison. It is clear that the calculations using the localized pair method are in qualitative agreement with experiment.

Let us now return to the central line. What is

TABLE II Coupling constants a_i

Proton position	Experiment	Theory* (ref. 6)	Theory (ref. 8)
meta (picryl)	1.74	0.0	2.2
meta (phenyl)	0.92	0.0	1.58
ortho (phenyl)	—1.84	—0.90	—3.00
para (phenyl)	—1.84	—0.90	—2.79

*Calculated according to[11] $a_i = -22.5\rho_{c_i}$, with ρ_{c_i} taken from reference 6.

its origin? Obviously, some part of its intensity may be due to the presence of nonmagnetic compounds. However, to ascribe it entirely to such an admixture is difficult on the following grounds: a) the admixture would have to be too large, since the central line constitutes 60 — 80% of the total intensity; b) two compounds synthesized in different places give identical results within the accuracy of the measurements; c) it is difficult to imagine how the magnetic field could change the relative intensities of the admixture line and the DPPH lines.

On the other hand, magnetic susceptibility data[2] show that DPPH has normal paramagnetic properties down to the lowest temperatures, and every molecule has one unpaired electron. Therefore it is apparently not possible to ascribe the central line to the pairing of some of the molecules with consequent diamagnetic behavior.

One might try to explain the central line by assuming that the DPPH molecule has two states, one having zero spin density at the positions of the hydrogen nuclei. If the energy difference between these two states increased with increasing magnetic field, then the observed dependence of relative intensity on field strength could be understood. But in this case, the relative intensity should also vary with temperature. Table I, however, shows that this does not happen.

In conclusion, we express our profound gratitude to academician P. L. Kapitza for his constant interest in this work and to A. S. Borovik-Romanov for discussions.

TABLE I Satellite relative intensities

H, oe	460	935					2000		
T, °K	1.7	4.2	3	2.5	2	1,55	4.2	2.5	1.7
I_1	—	—	—	0,06	0,05	0.06	0,03	0.03	0.03
I_2	—	—	—	0.11	0,12	0.12	0.07	0.06	0.06
I_3	0.22	0.20	0.17	0.19	0.18	0.18	0.09	0.08	0.08
$I_1+I_2+I_3$				0,36	0.35	0.36	0.19	0.17	0.17

Remark: I_1, I_2, I_3 are the intensities of lines No. 1, 2, and 3.

---

[1] D. J. E. Ingram, Free Radicals as Studied by Electron Spin Resonance, Butterworth, London 1958.

[2] Gerristen, Okkes, Gijman, and van den Handel, Physica **20**, 13 (1954).

[3] Hutchison, Pastor, and Kowalsky, J. Chem. Phys. **20**, 534 (1952).

[4] S. I. Weissman, J. Chem. Phys. **22**, 1378 (1954).

[5] H. M. McConnell, J. Chem. Phys. **28**, 1188 (1958).

[6] R. Bersohn, Arch. Sci. **11**, Fasc. sp. 177 (1958).

[7] G. Berthet and R. Riemann, Compt. rend. **246**, 1830 (1958).

[8] Gutowsky, Kusumoto, Brown, and Anderson, J. Chem. Phys. **30**, 860 (1959).

[9] R. Pound and W. Knight, Rev. Sci. Instr. **21**, 219 (1950).

[10] S. P. Kapitza, Приборы и техника эксперимента (Instr. and Exptl. Techn.) **2**, 97 (1958).

[11] H. M. McConnell, J. Chem. Phys. **28**, 107 (1958).

Translated by M. Bolsterli
1

SOVIET PHYSICS JETP VOLUME 13, NUMBER 1 JULY, 1961

β-γ POLARIZATION CORRELATION IN THE β DECAY OF Sc^{46}

V. M. LOBASHOV, V. A. NAZARENKO, and L. I. RUSINOV

Leningrad Physico-Technical Institute, Academy of Sciences, U.S.S.R.

Submitted to JETP editor June 22, 1960

J. Exptl. Theoret. Phys. (U.S.S.R.) 40, 10-12 (January, 1961)

The correlation between the β-ray transverse polarization and γ-ray circular polarization was measured. The degree of correlation is theoretically proportional to an interference term of the type Im (VT, SA). The experimental result indicates with statistical accuracy ~ 30% that the term is absent. This is not inconsistent with the present theory of β decay.

THE time-reversal invariance of β decay has been tested in several experiments. Direct experiments such as the determination of β - ν correlation in polarized-neutron decay and of β - γ correlation in oriented-nucleus decay indicate with accuracy of 15 — 30% that the β-interaction Hamiltonian does not include an imaginary part. The magnitude of the correlation in these experiments depends on the imaginary part of V, A interference terms. Since S- and T-interaction terms have so far not been excluded, it was of interest to perform a direct experiment in order to estimate the Im (VT, SA) term.

The verification of time-reversal invariance is known to require the measurement of pseudoscalar quantities with respect to time. Our experiment was devised to measure the pseudoscalar $\mathrm{P}_\gamma \mathbf{k}_\gamma \times [\mathbf{p}_\mathrm{e} \times \boldsymbol{\zeta}_\mathrm{e}]$, where P_γ is the circular polarization of the γ ray, $\mathbf{k}_\gamma$ is its momentum, and $\mathbf{p}_\mathrm{e}$ and $\boldsymbol{\zeta}_\mathrm{e}$ are the momentum and polarization of the β electron. The correlation between the transverse polarization of the electron and the circular polarization of the γ ray was measured. The experimental geometry is shown in Fig. 1.

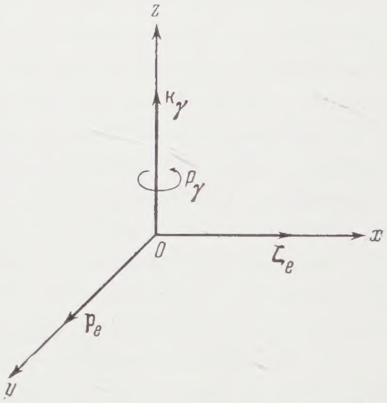

FIG. 1. Experimental geometry

The correlation coefficient in the case of allowed transitions is, according to Dolginov,[1]

$$\begin{aligned}K = -\frac{B_{1\sigma}}{|\xi|}\Big\{2\,\frac{v}{c}\,\mathrm{Im}\,(C_V C_T'^{*} + C_V' C_T^{*} - C_S C_A'^{*} - C_S' C_A^{*})\,M_F M_{GT}^{*} \\ - \frac{2\alpha Z}{E}\,\mathrm{Re}\,(C_S' C_T^{*} + C_S C_T'^{*} - C_V C_A'^{*} - C_V' C_A^{*})\,M_F M_{GT}^{*} \\ - \lambda_{j_1 j_0}\Big[\frac{v}{c}\,\mathrm{Im}\,(C_A C_T'^{*} + C_A' C_T^{*})\,|M_{GT}|^2 \\ - \frac{\alpha Z}{E}\,\mathrm{Re}\,(C_T C_T'^{*} - C_A C_A'^{*})\,|M_{GT}|^2\Big]\Big\},\end{aligned} \qquad (1)$$

where

$$|\xi| = (|C_A|^2 + |C_A'|^2 + |C_T|^2 + |C_T'|^2)\,|M_{GT}|^2$$

$$+ (|C_S|^2 + |C_S'|^2 + |C_V|^2 + |C_V'|^2)\,|M_F|^2,$$

$$B_{1\sigma} = \frac{j_1(j_1+1) - j_2(j_2+1) + I(I+1)}{2I(I+1)\sqrt{j_1(j_1+1)}},$$

$$\lambda_{j_1 j_0} = \frac{j_1(j_1+1) - j_0(j_0+1) + 2}{2\sqrt{j_1(j_1+1)}},$$

j_0 is the spin of the level from which β decay proceeds, and j_1 and j_2 are the spins of product-nucleus levels. The magnitude of the correlation obviously depends on the degree of interference between Gamow-Teller and Fermi matrix elements. We therefore used as our source the Sc^{46} nucleus, for which experiments on β-γ circular polarization correlation have indicated large interference of the matrix elements.

The correlation can obviously be determined in two ways: 1) by detecting γ rays with specified circular polarization in order to measure electron polarization; 2) by detecting β rays with specified polarization, to measure the circular polarization of γ rays. The second method is favored because the measurement of γ-ray circular polarization does not require any change of experimental geometry. Errors associated with instrumental asymmetry are thus excluded.

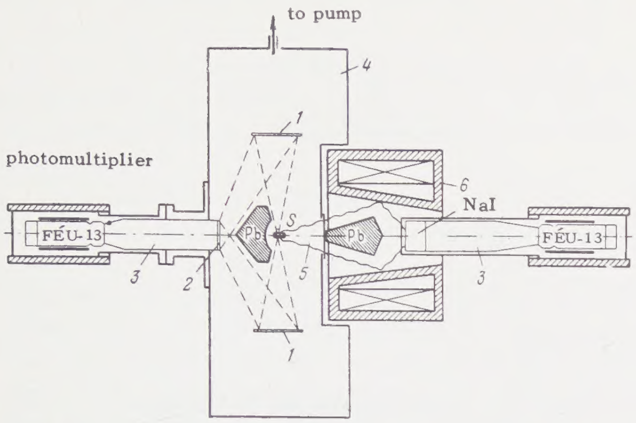

FIG. 2. Diagram of apparatus: S – source, 1 – electron scatterer, 2 – plastic scintillator, 3 – light pipes, 4 – vacuum chamber, 5 – γ-ray exit window, 6 – magnet of γ polarimeter,

The experimental arrangement is shown diagramatically in Fig. 2. Collimated electrons from the source S strike a 0.5-mg/cm^2 bismuth film, and after scattering at ~ 135° are registered by a scintillator combined with a light pipe and photomultiplier. Because of azimuthal asymmetry associated with Mott scattering, the beam of scattered electrons will be polarized in the $\mathbf{p}_1 \times \mathbf{p}_2$ direction, where $\mathbf{p}_1$ and $\mathbf{p}_2$ are the electron momentum before and after scattering, respectively.

Circular geometry was used to increase the counting rate. The circular polarization of γ rays was measured through forward Compton scattering on magnetized iron.[2] The photomultiplier outputs of the β and γ detectors were connected to a fast-slow coincidence scheme with $2\tau = 1.8 \times 10^{-8}$ sec. In order to avoid errors associated with changing sensitivity of the coincidence scheme, the magnetization of the γ-polarimeter magnet was reversed automatically every 3.5 minutes.

The measurements were used to calculate

$$\Delta = 2(I_1 - I_2)/(I_1 + I_2), \qquad I_{1,2} = R_{\text{coinc}} / R_\beta R_\gamma;$$

the subscripts 1 and 2 here pertain to the magnetic field directed away from and toward the source, respectively.

The correlation coefficient K was obtained from the formula

$$K = \Delta / P_\gamma P_\beta,$$

where P_γ and P_β are the efficiencies of the γ and β polarimeters.

We obtained Δ = + 0.15 ± 0.11%, from which the correlation coefficient K = 0.08 ± 0.06 was calculated. The sign corresponds to the notation in Dolginov's paper, and is the opposite of our previous convention in reference 3.

The efficiency P_β of the β polarimeter was determined from the known scattering geometry, extrapolating the azimuthal asymmetry coefficients from Sherman's tables[4] to Z = 83 (bismuth). We followed Wegener[5] in taking account of multiple scattering. The polarization efficiency P_γ of the γ polarimeter was also calculated from the scattering geometry.

The absence of instrumental asymmetry was checked by repeating the experiment with a thick ($\sim 5\ \text{mg/cm}^2$) scatterer. As a result of multiple electron scattering spin-associated azimuthal asymmetry here disappears, and the investigated effect should also disappear. The result Δ = − 0.03 ± 0.09% indicates the absence of instrumental asymmetry.

We used the value $|M_{GT}|/|M_F| = 2.2$ given in reference 2 for the interference of Gamow-Teller and Fermi matrix elements. From Eq. (1) we then obtain

$$K = +0.04 \quad \text{assuming} \quad \operatorname{Im}(VT,\ AS) = 0,$$

$$K = \begin{cases} +0.23 \\ -0.15 \end{cases} \quad \text{assuming maximum} \quad \operatorname{Im}(VT,\ AS).$$

Our result therefore agrees, with statistical accuracy ~ 30%, with the hypothesis that the Im(VT, AS) term is not present. This term can fail to appear not only because the interaction constants have no imaginary parts, but also because VT, AS interference terms are forbidden in the existing β-decay theory. Our results can therefore be regarded as an additional confirmation of the present theory of β decay.

As an independent check of our experimental procedure we performed experiments on the β-γ circular polarization correlation in the β decay of Sc^{46} and Co^{60}, obtaining results in agreement with those of other investigators.

We are indebted to A. Z. Dolginov for discussions and for his continued interest, and to O. M. Saltykovskiĭ, V. V. Andryukevich, and A. V. Kurakin for assistance with the apparatus and measurements

---

[1] A. Z. Dolginov, JETP **35**, 178 (1958), Soviet Phys. JETP **8**, 123 (1959).

[2] F. Boehm and A. H. Wapstra, Phys. Rev. **109**, 456 (1958).

[3] Lobashov, Nazarenko, and Rusinov, JETP **37**, 1810 (1959), Soviet Phys. JETP **10**, 1277 (1960).

[4] N. Sherman, Phys. Rev. **103**, 1601 (1956).

[5] H. Wegener, Z. Phys. **151**, 252 (1958).

Translated by I. Emin
2

SOVIET PHYSICS JETP VOLUME 13, NUMBER 1 JULY, 1961

FORMATION OF SLOW NEGATIVE IONS IN SINGLE COLLISIONS BETWEEN FAST NEGATIVE HYDROGEN AND OXYGEN IONS AND GAS MOLECULES

Ya. M. FOGEL', A. G. KOVAL', and Yu. Z. LEVCHENKO

Physico-Technical Institute, Academy of Science, Ukrainian S.S.R.

Submitted to JETP Editor June 27, 1960

J. Exptl. Theoret. Phys. (U.S.S.R.) **40**, 13-22 (January, 1961)

The total cross sections for the formation of negative ions have been measured for single collisions between H^- and O^- ions and O_2, CCl_4 and SF_6 molecules in the energy range from 10 to 50 kev. The slow negative and positive ions formed when H^- and O^- ions pass through these gases have been analyzed by a mass-spectrometer technique. An analysis has also been made of the negative ions formed in collisions between O^- ions and H_2O and CO_2 molecules. The experimental data for ion collisions are compared with the corresponding data for electron collisions.

INTRODUCTION

SLOW negative ions can be formed as a result of two processes when fast negative ions move through a rarefied gas:

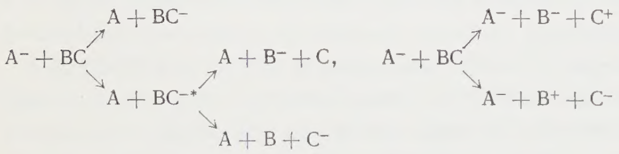

$$A^- + BC \begin{cases} \nearrow A + BC^- \\ \searrow A + BC^{-*} \begin{cases} \nearrow A + B^- + C, \\ \searrow A + B + C^- \end{cases} \end{cases} \qquad A^- + BC \begin{cases} \nearrow A^- + B^- + C^+ \\ \searrow A^- + B^+ + C^- \end{cases} \qquad (1)$$

(BC^{-*} is the excited ion).

Although the analogous reactions that occur when electrons move through a gas have been studied, very little work has been done on the formation of slow negative ions due to the passage of fast negative ions through a rarefied gas. We are acquainted only with reference 1, in which cross sections have been measured for the formation of slow negative ions in collisions between O_2 molecules and Na^-, K^-, O^-, Cl^-, OH^-, and O_2^- with energies of 720 ev. No mass analysis was made of the slow negative ions in this work.

In order to obtain further data on the formation of slow negative ions in the interaction of fast negative ions with gas molecules, we have measured the cross sections for the formation of negative ions in collisions of H^- and O^- ions with energies from 10 to 15 kev and the molecules O_2, CCl_4, and SF_6. In addition to measuring the total cross sections for the formation of negative ions we have carried out a mass-spectrometer analysis of the negative and positive ions formed in the gas.

APPARATUS AND METHOD OF MEASUREMENT

The experimental apparatus used to investigate the formation of slow negative ions has been described by the authors in detail in earlier papers[2,3] in which the ionization of gases by negative ions was investigated.

The total cross section for the formation of slow negative ions σ_i^- is measured by the familiar potential technique. In order to distinguish slow negative ions from electrons produced by stripping a fast negative ion and by ionization of the gas molecules, we used a magnetic field parallel to the axis of the primary beam. The same field suppressed the secondary electron emission from the electrodes of the measurement capacitor.

Before measuring σ_i^-, we obtained for each ion-molecule pair the characteristic curves $i_H^-/I_0^- = f(H)$ and $i_H^-/I_0^- = f(V)$, where i_H^- is the negative current to the measurement electrode with the magnetic field on, and I_0^- is the primary beam current. Using these characteristic curves we determined the magnetic field strength necessary for complete separation of the slow negative ions from the electrons, and the potential difference V between the electrodes of the measurement capacitor required to obtain saturation current. To find the conditions which must be satisfied to obtain single collisions, we studied the dependence of i_H^-/I_0^- for the investigated gas on the pressure in the collision chamber. For all gases studied (except SF_6) and for all beam energies, the curve $i_H^-/I_0^- = f(p)$ is linear up to 1.5×10^{-4} mm Hg, indicating that we are dealing with single collisions. In the single-collisions region the cross section

σ_i^- was computed from the formula

$$\sigma_i^- = i_H^- / I_0^- nL, \tag{2}$$

where n is the number of gas molecules per cubic centimeter and L is the length of the measurement electrode.

In SF_6, the $i_H^-/I_0^- = f(p)$ curve is found to be parabolic, starting at low gas pressures. In this case σ_i^- was determined from the pressure dependence of the quantity $(i_H^-/I_0^-)/p$ by a method which has been described earlier.[4] The error in the measurement of σ_i^-, as estimated from the spread in the measured results, is ±10%. The error in the energy measurement is ±3%.

The slow negative and positive ions were analyzed in a magnetic mass spectrometer with a beam turning angle of 60° and a mean trajectory radius of 16.4 cm. The relative intensity of a mass spectrometer line was computed from the formula

$$\alpha_n = h_n \Big/ \sum_i h_i, \tag{3}$$

where h_n is the height of the line corresponding to the n-th ion while $\sum\limits_i h_i$ is the sum of the heights for all the spectral lines.

The cross section for the formation of a given negative ion σ_n^- was computed from the intensity of the mass-spectrometer line and from the total cross section for the formation of slow negative ions, by means of the formula

$$\sigma_n^- = \alpha_n \sigma_i^-. \tag{4}$$

Fedorenko and Afrosimov[5] have shown that α_n gives the true composition of the slow ions in the zone of interaction between the primary beam and the gas only when it is independent of the mass spectrometer exit slit width, the extraction potential V_e, the acceleration voltage V_a, and the focusing voltage V_f (cf. Fig. 1. in reference 1). For each ion-molecule pair and for each primary-ion energy we determined the dependence of α_n on the parameters given above. The operating values of V_e, V_a, V_f and the slit width were then chosen to correspond to points on the plateaus of the appropriate curves.

In order to find the gas pressure in the collision chamber necessary to ensure single collisions, we obtained the curve $I_n^-/I_0^- = f(p)$, where I_n^- is the current at the peak of a given mass-spectrometer line. Most of the measurements of α_n were carried out at a gas pressure of $1-1.5 \times 10^{-4}$ mm Hg. The error in the measurement of σ_n^- is made up of the errors in σ_i and α_n and is ±10% for high intensity peaks and ±35% for low intensity peaks.

RESULTS OF THE MEASUREMENTS

The total cross sections for the formation of slow negative ions in oxygen are shown in Fig. 1 as a function of the velocities of the H^-, D^- and O^- ions. The cross section for $H^- - O_2$ is $(1-3) \times 10^{-17}$ cm^2; for $O^- - O_2$ these cross sections are an order of magnitude larger. Il'in, Afrosimov, and Fedorenko[6] have estimated the cross sections for the dissociation of O_2 molecules into positive and negative ions by collisions with protons with energies of 10 to 30 kev. These cross sections are of the order of 10^{-19} cm^2. Since it is not very likely that the cross sections for the dissociation of the O_2 molecules by impact with H^- ions are much larger than the corresponding cross sections for the H^+ ion, it is reasonable to assume that σ_i^- for $H^- - O_2$ and $O^- - O_2$ represents the cross section for charge exchange of H^- and O^- ions in oxygen. The following conclusions follow from an analysis of the curves in Fig. 1.

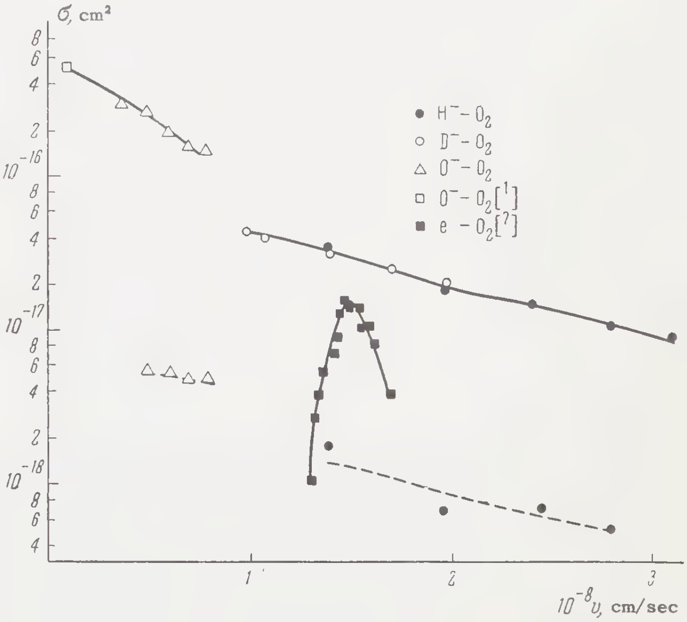

FIG. 1. The cross sections for the formation of slow negative ions σ_i^- in oxygen as a function of velocity (solid curve); the dashed curve is the function $\sigma_0^-(v)$.

1. The cross section σ_i^- is independent of ion mass, since the experimental points for H^- and D^- ions lie on the same curve.

2. The reduction in σ_i^- with increasing ion velocity is fairly well described by the formula $\sigma_i^- = \sigma_0 e^{-kv}$. The constant k in this formula is different for hydrogen and oxygen ions. It should be noted that the experimental point for $O^- - O_2$ at 720 ev[1] also lies on the curve $\sigma_i \sim e^{-kv}$.

The mass spectrum for the slow negative ions from $H^- - O_2$ and $O^- - O_2$ contains the O_2^- ion and, in very small quantities, the O^- ion. This result indicates that when H^- or O^- ions pass through O_2 the most important reaction is $A^- + O_2 \rightarrow A + O_2^-$; the reactions $A^- + O_2 \rightarrow O_2^{-*} \rightarrow O$ and $A^- + O_2 \rightarrow A^- + O^- + O^+$ are characterized by low probabilities.

The formation of negative ions in collisions between electrons and molecules exhibits entirely different characteristics. In this case the dependence of the negative ion formation cross section on the electron velocity is characterized by a resonance effect. In Fig. 1 we show this dependence in O_2, using the data reported by Buchel'nikova.[7] When the electron "sticks" to the O_2 molecule, the reaction $O_2 + e \rightarrow O_2^{-*} \rightarrow O^- + O$ occurs, that is to say, the O^- ion is formed only as a result of the dissociation of the excited O_2^- ion.[8] As has been noted above, charge exchange of H^- and O^- with O_2 molecules results primarily in the formation of O_2^- ions. This difference in charge exchange of negative ions and attachment of electrons to molecules is completely reasonable. Since the radiation process $O_2 + e \rightarrow O_2^- + h\nu$ is characterized by a small probability, the attachment of the electron to the O_2 molecule leads to the formation of the excited O_2^- ion. Because of the low gas pressure this ion cannot be stabilized by transfer of excitation energy to another particle so that it must dissociate. In the case of charge exchange, say for $O^- - O_2$, the resonance defect ΔE is equal to the difference in the electron affinity for O_2 and O, more precisely, to $0.15 - 1.48 = -1.33$ ev, so that ΔE is negative;* therefore, energy is absorbed rather than released. A stable O_2^- ion can be formed in charge exchange because of this effect.

In charge exchange of negative ions, as in electron capture by singly-charged positive ions and neutral atoms, the maximum cross section as a function of velocity is determined by the well-known Massey adiabatic criterion;[11,12] assuming that the quantity a which appears in the adiabatic criterion is the same for this process as for one-electron charge exchange in singly-charged positive ions, i.e. 8 A, we find the peak for $O^- + O_2 \rightarrow O + O_2^-$ at an energy of 5.5 kev. However, it is not very likely that the maximum value of $\sigma_i^-(v)$ for this process lies at 5.5 kev; the value of σ_i^- in the energy range 10 — 50 kev, obtained in the present work, and the value at 0.7 kev, obtained by Dukel'skiĭ and Zandberg,[1] correspond to a smooth curve which increases monotonically between 0.7 and 50 kev. It is more probable that the maximum value of $\sigma_i^-(v)$ for $O^- - O_2$ lies at an energy lower than 0.7 kev. If this is the case, then the condition for applying the Massey adiabatic criterion to charge exchange of negative ions means that the value of a for $O^- + O_2 \rightarrow O + O_2^-$ is considerably smaller than 8 A. The resonance defect for $H^- + O_2 \rightarrow H + O_2^-$ is -0.58 ev, which is still smaller than for $O^- + O_2 \rightarrow O + O_2^-$; therefore the maximum cross section for the first process is also expected to be at a low energy.

In Fig. 2 we show the $\sigma_i^-(v)$ curves for $H^- - CCl_4$ and $O^- - CCl_4$. The cross section σ_i^- for $H^- - CCl_4$ remains essentially constant over the velocity range studied; for $O^- - CCl_4$ this cross section diminishes as the velocity increases, in accordance with the empirical relationship established for $H^- - O_2$ and $O^- - O_2$.

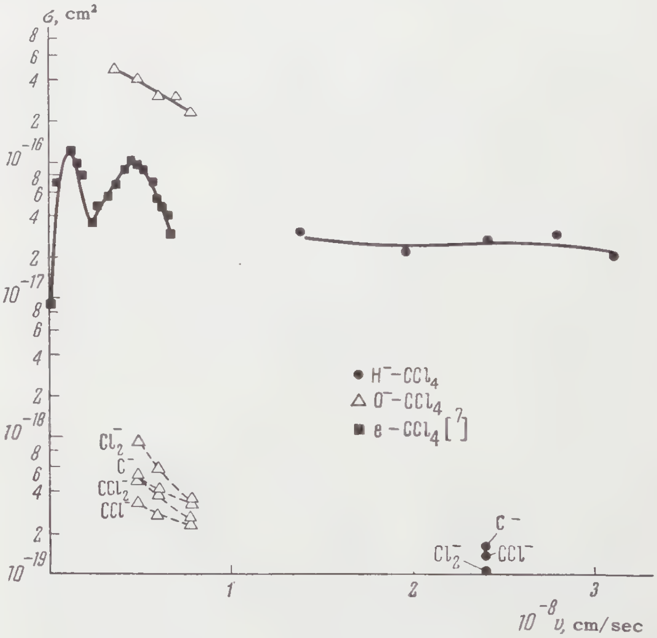

FIG. 2. The cross sections for the formation of slow negative ions in CCl_4 gas as a function of velocity (solid curve). The dashed curves show the corresponding curves for the individual ions. For the ions C^-, CCl^- and Cl_2^-, the cross sections for bombardment by H^- have been measured only at 30 kev.

The relative intensities of the mass-spectrometer lines, for negative and positive ions produced when H^- and O^- ions with energies of 30 kev bombard CCl_4, are shown in the table. For purposes of comparison we also show in this table the corresponding data for electrons with energies of 75 ev.[13] The data in the table indicate that in the negative-ion spectra characteristic of collisions of negative ions and electrons with the CCl_4 molecule, the greatest relative intensity is to be assigned to the Cl^- ion so that $\sigma_i^- \approx \sigma_{Cl}^-$. This result

---

*The electron-affinity values are taken from references 9 and 10.

CCl_4				SF_6			CCl_2F_2			
Secondary ion	Particle in the primary beam			Secondary ion	Particle in the primary beam		Secondary ion	Particle in the primary beam		
	O^-	H^-	e		O^-	e		O^-	H^-	e
Cl^{++}	2	0.34	—	F^+	16.2	1.93	C^{++}	0.17	—	—
Cl^+	38.3	28	14.1	S^+	21	3.4	F^{++}	0,02	—	—
CCl_2^{++}	—	—	0.4	SF^+	13.4	5.24	C^+	6.9	4.05	4.9
CCl_2^+	9.2	12.5	12	SF_2^+	7.1	3.47	F^+	7.5	4.18	0.65
CCl^+	18.8	15	14.2	SF_3^+	8.5	16.8	CCl^{++}	0.6	0.7	—
CCl_3^{++}	—	—	0.8	SF_4^+	2.5	5.43	CF^+	14.3	17.2	10.8
Cl_2^+	1.0	1.26	0.18	SF_5^+	31.2	60.2	Cl^+	20	18.35	10
CCl_3^+	23.5	38	51.3	SF_2^{++}	—	0.82	$CCl_2F_2^{++}$	—	—	0.48
CCl_4^+	0,05	0.09	0.01	SF_3^{++}	—	0.22	$CCl^+ + CF_2^+$	39.3	40,5	—
C^+	7.1	3.8	7.4	SF_4^{++}	—	2.46	CCl^+	—	—	3.5
C^-	0.13	0.28	0.01	SF_6^-	63	96.1	CF_2^+	—	—	8.1
Cl^-	99.4	99.3	99,9	SF_5^-	3.5	3.9	CCl_2F^{++}	—	—	0.4
CCl^-	0,09	0.18	0,005	F^-	33.5	0.04	$CClF^+$	8.4	12.3	2.3
Cl_2^-	0.2	0.24	0.1				CCl_2F^+	—	—	4.3
CCl_2^-	0.12	—	—				$CClF_2^+$	2.5	2.8	54
							F_2^+	—	—	0.24
							Cl_2^+	—	—	0.16
							$CCl_2F_2^+$	0.1	—	0.16
							C^-	4	4.1	0.22
							F^-	73.5	74.6	30.4
							Cl^-	22.6	21.3	69.4

Note: For O^- the velocity is 6×10^7 cm/sec; for H^- $v = 2.4 \times 10^8$ cm/sec; for the electrons $v = 5.18 \times 10^8$ cm/sec.

has been verified by other authors.[14,15] On the other hand, the CCl_4^- ion has not been observed in any of this work. Thus, charge exchange (negative ions) and electron attachment in CCl_4 lead to dissociation of the CCl_4^- ion which is formed. Inasmuch as a stable negative molecular ion can be formed in charge exchange (cf. above), the absence of such ions in the present case can be explained by the fact that the electron affinity of the CCl_4 molecule is negative. Judging from the relative intensity of the mass lines in the negative-ion spectrum, at least for $O^- - CCl_4$, we can say that this ion decays chiefly via the reaction $CCl_4^{-*} \rightarrow Cl^- + CCl_3$. In the case of H^- ions and electrons with higher velocities than the O^- ion, a contribution to the formation of the Cl^- ion arises from the well-known dissociation process $CCl_4 \rightarrow Cl^- + CCl_3^+$. To some extent this interpretation is verified by the presence of a large number of CCl_3^+ ions in the positive-ion spectrum. It should be kept in mind, however, that these ions can be formed as a result of ionization and subsequent dissociation of the excited CCl_4 ion. It is interesting to note that the number of CCl_4^+ ions is very small. It is found that in CCl_4 both attachment and detachment of an electron lead to the formation of unstable molecular ions. The absence of the CCl_3^- ion in the negative ion spectrum* indicates the small probability of the decay of the CCl_4^- ion via the reaction $CCl_4^{-*} \rightarrow CCl_3^- + Cl$ as compared with the decay reaction $CCl_4^{-*} \rightarrow Cl^- + CCl_3$. The situation which has been pointed out is understandable because in the decay of the CCl_4^- ion the excess electron will be attached to the shell with the higher electron affinity, that is to say, to the Cl atom rather than the CCl_3 radical. On the other hand, the absence of the CCl_3^- ion indicates the small probability for the dissociation process $CCl_4 \rightarrow CCl_3^- + Cl^+$ whereas in electron impact the process $CCl_4 \rightarrow Cl^- + CCl_3^+$ has a rather high probability.[14]

Thus, in their general features, the spectra of the negative and positive ions are the same for H^- and O^- and for electrons. However, there is a big difference in the cross section for the formation of negative ions as a function of velocity of the primary particles, as is apparent from Fig. 2; in this figure, we show the $\sigma_1^-(v)$ curves obtained in the present work and the $\sigma(v)$ curve for the electron attachment process in CCl_4 taken from the work of Buchel'nikova.[7]

The cross sections for the formation of negative ions in SF_6 bombarded by H^- and O^- ions are weak functions of ion velocity in the velocity region which has been studied (Fig. 3). σ_1^- for SF_6 is considerably smaller than for O_2 and CCl_4, as is apparent from Fig. 4, in which we compare the $\sigma_1^-(v)$ curves for these three gases. Just as in O_2 and CCl_4, the $\sigma_1^-(v)$ curve for electron attachment in SF_6 is very different from the curve for charge exchange between O^- ions and the SF_6 molecule (cf. Fig. 3).[7]

In the table we give the results of a mass-spec-

---

*The CCl_3^- ion has been observed in work reported by Dibeler and Mohler, but the relative content was very small (approximately 0.1%).[16]

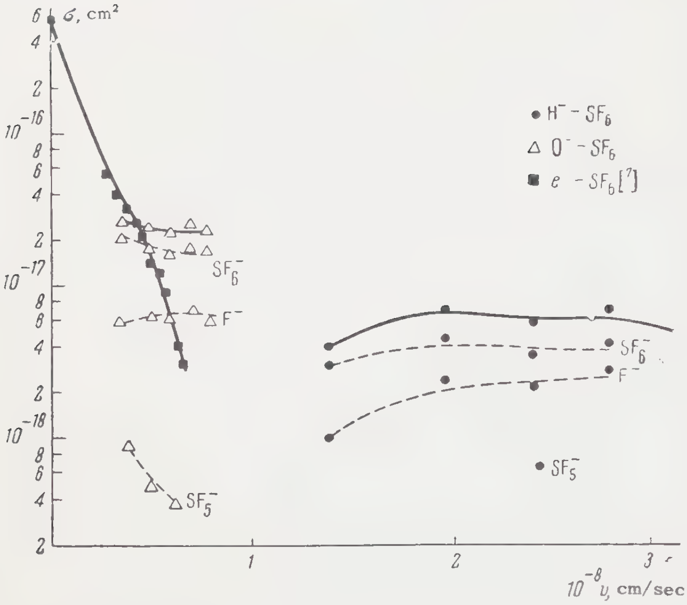

FIG. 3. The cross sections for the formation of slow negative ions in the gas SF_6 as a function of velocity (solid curve). The dashes indicate the corresponding curves for the individual ions. For the ion SF_5^- the cross section for bombardment by H^- has been measured at only 30 kev.

trometer analysis of the negative and positive ions formed by passing 30-kev O^- ions through SF_6. For purposes of comparison, in this same table we give data on the composition of the positive ions formed in SF_6 by electrons with energies of 50 ev.[16] The data on negative ions given in the table refer to electron energies close to zero, since it is at this energy that there is a maximum cross section for the formation of the ions SF_6^-, SF_5^-, and F^-.[17] It is apparent that there is a considerable difference in the relative intensities for the SF_6^- and F^- ions when they are formed by O^- ions and by electrons. In electron collisions, excited SF_6^{-*} ions are formed in the overwhelming majority of cases; these excited ions have lifetimes which exceed the time-of-flight in the mass spectrometer. In charge exchange of O^- ions with SF_6 molecules, however, a large portion of the SF_6^- ions which are formed decay with the formation of F^- ions ($SF_6^{-*} \rightarrow SF_5 + F^-$) while a considerably smaller part of these ions decay via the process $SF_6^{-*} \rightarrow SF_5^- + F$. In this case, just as in decay of CCl_4^- ion, the more probable decay process is the one in which the electron becomes attached to the shell with the higher electron affinity. Attention is merited by the fact that the positive ion spectrum does not contain the SF_6^+ ion whereas SF_6^- exhibits the highest intensity in the negative ion spectrum. This means that the detachment of the electron from the SF_6 molecule always results in dissociation of the SF_6^+ ion formed. Attachment of the electron to the SF_6 molecule is much more likely, especially the attachment of a free low-energy electron, which results in the formation of an excited SF_6^{-*} ion with an appreciable lifetime.

The investigation of the spectrum of the negative ions formed in collisions of H^- and O^- with the freon molecule CCl_2F_2 shows, that in addition to the ions F^-, Cl^- and C^-, this spectrum contains a large number of H^- ions (approximately 50%). Inasmuch as the water vapor is carefully removed from the freon in the collision chamber, we may assume that the H^- ion appears as a consequence of impurities (in the freon) containing molecules in which one or more halogen atoms are replaced by hydrogen atoms. It is well known that it is difficult to remove these impurities from freon. For this reason, a systematic investigation of $\sigma_i^-(v)$ was not carried out for CCl_2F_2. However, we have estimated $\sigma_i^-(v)$ for $H^- - CCl_2F_2$ for H^- energies of 30 kev. This estimate yields a value of 2.5×10^{-18} cm², which is 25 times smaller than

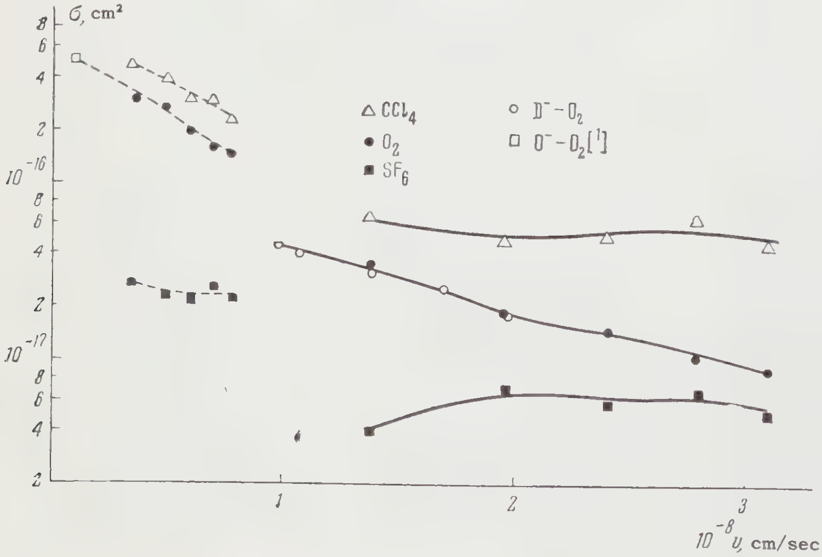

FIG. 4. The solid curves show the function $\sigma_i^-(v)$ for H^- while the dashed curves apply for O^-.

for $H^- - CCl_4$ at the same ion energy. From this result we may conclude that replacement of Cl atoms by F atoms in CCl_4 causes a marked reduction in σ_i^-.

The relative numbers of different negative and positive ions which appear in collisions of H^- and O^- ions with CCl_2F_2 molecules is given in the table together with the data on electron impact.[13] It is apparent from these data that in charge exchange with H^- and O^- and in electron attachment, the CCl_2F_2 molecule does not form the ion $CCl_2F_2^-$; on the other hand, in ionization by these particles only a very small number of $CCl_2F_2^+$ ions are formed. In this respect, CCl_2F_2 is similar to CCl_4 (cf. above). We may note that electron impact results in the formation of more Cl^- ions than F^-. On the other hand, in ion impact, more F^- is formed than Cl^-.

In addition to the investigation of O_2, CCl_4, SF_6 and CCl_2F_2, attempts were made to measure σ_i^- in bombardment of CO, CO_2, H_2O, NO and NH_3 by H^- and O^-. In all these molecules σ_i^- was found to be much smaller than in O_2, CCl_4, and SF_6. Furthermore, the characteristic curves for $i_H^-/I_0^- = f(V)$ obtained in the bombardment of these gases by O^- show that i_H^-/I_0^- increases continuously with increasing potential difference V; this effect is apparently caused by scattered ions from the primary beam, which strike the measurement electrode, or by the high initial velocities of the negative ions formed. In any case, because the $i_H^-/I_0^- = f(V)$ characteristic does not have a plateau, it is impossible to obtain reliable values for σ_i^- in CO, CO_2, H_2O, CH_4, NO and NH_3. When H^- ions pass through these gases, the $i_H^-/I_0^- = f(V)$ characteristic does exhibit a plateau, but the value of i_H^-/I_0^- at the plateau cannot be measured reliably because of the low sensitivity of the device used to measure the current i_H^-. In any case σ_i^- in these gases is smaller than $2-3 \times 10^{-18}$ cm^2.

For the same reason (small current at the mass-spectrometer collector) negative ion spectra could be analyzed only for the molecules H_2O and CO_2. In $O^- - H_2O$ the spectrum exhibits H^- ions (58%) and O^- ions (42%). Judging from the relative intensity of the H^- and O^- peaks, the decay processes $H_2O^- \rightarrow H^- + OH$ and $H_2O^- \rightarrow O^- + H_2$ have approximately the same probability. Similar results have been obtained in investigations of the negative ion spectra for collisions of electrons with the H_2O molecule.[18,19] In the negative ion spectrum for $O^- - CO_2$ we observe O^- (85%) and O_2^- ions (15%). Thus, the probability for the decay process $CO_2^- \rightarrow CO + O^-$ is appreciably greater than for the process $CO_2^- \rightarrow C + O_2^-$. In the negative ion spectrum characteristic of electon attachment to the CO_2 molecule, only the O^- ions are observed.[20] The maximum electron attachment cross section is 5×10^{-19} cm^2.

The experimental data reported in the present paper indicate that there is an important difference in the cross sections σ_i^- and the shapes of the $\sigma_i^-(v)$ curves for the attachment of free electrons in molecules and for charge exchange of negative ions with the same molecules. This difference arises because in the first case the negative ion is formed as a consequence of attachment of a free electron to the molecule. In this case the transition from molecule into a negative ion proceeds in accordance with the Franck-Condon principle and the $\sigma_i^-(v)$ curve must exhibit a resonance.[21] In the second case the negative ion is formed by electron transitions between discrete states of the fast negative ion and the gas molecule, so that the general features of the $\sigma_i^-(v)$ curve are similar to these curves in other charge exchange processes.

The data presented on the formation of negative ions in atomic collisions, point to the desirability of further investigations at low velocities, where the maxima of the $\sigma_i^-(v)$ curves are located. The locations of these maxima (v_{max}) and the behavior of the $\sigma_i^-(v)$ curves for $v < v_{max}$ will allow us to examine the applicability of the adiabatic hypothesis to charge exchange of negative ions.

We wish to thank A. F. Khodyachikh, who helped in these measurements.

In conclusion the authors also wish to take this opportunity to express their gratitude to Professor A. K. Val'ter for his continued interest in this work.

---

[1] V. M. Dukel'skiĭ and E. Ya. Zandberg, Doklady Akad Nauk SSSR **82**, 33 (1952).

[2] Fogel', Koval', and Levchenko, JETP **38**, 1053 (1960), Soviet Phys. JETP **11**, 760 (1960).

[3] Fogel', Koval', Levchenko and Khodyachikh, JETP **39**, 548 (1960), Soviet Phys. JETP **12**, 384 (1961).

[4] Fogel', Ankudinov, and Slabospitskiĭ, JETP **32**, 453 (1957), Soviet Phys. JETP **5**, 382 (1957).

[5] N. V. Fedorenko and V. V. Afrosimov, J. Tech. Phys. (U.S.S.R.) **26**, 1941 (1956), Soviet Phys.-Tech. Phys. **1**, 1872 (1957).

[6] Il'in, Afrosimov, and Fedorenko, JETP **36**, 41 (1959), Soviet Phys. JETP **9**, 29 (1959).

[7] N. S. Buchel'nikova, JETP **35**, 1119 (1958), Soviet Phys. JETP **5**, 783 (1959).

[8] Craggs, Thorburn, and Tozer, Proc. Roy. Soc. **A240**, 473 (1955).

[9] L. M. Branscomb and S. J. Smith, Phys. Rev. **98**, 1127 (1955).

[10] Burch, Smith and Branscomb, Phys. Rev. **112**, 171 (1958).

[11] J. B. H. Stedeford and J. B. Hasted, Proc. Roy. Soc. **A227**, 466 (1955).

[12] Ya. M. Fogel', Usp. Fiz. Nauk, **71**, 243 (1960), Soviet Phys.-Uspekhi **3**, 390 (1960).

[13] R. F. Baker and J. T. Tate, Phys. Rev. **53**, 683 (1938).

[14] Craggs, McDowell, and Warren, Trans. Faraday Soc., **48**, 1093 (1952).

[15] Reese, Dibeler, and Mohler, J. Res. NBS, **57**, 367 (1956).

[16] V. H. Dibeler and F. L. Mohler, J. Res. NBS, **40**, 25 (1948).

[17] W. M. Hickam and R. E. Fox, J. Chem. Phys. **25**, 642 (1956).

[18] Mann, Hustrulid, and Tate, Phys. Rev. **58**, 340 (1940).

[19] L. Kerwin and M. Cottin, Can. J. Phys. **36**, 184 (1958).

[20] J. D. Craggs and B. A. Tozer, Proc. Roy. Soc. **A254**, 229 (1960).

[21] H. S. W. Massey, Negative Ions, Cambridge Univ. Press, (1950) p. 47.

Translated by H. Lashinsky
3

RADIATIONS FROM Eu^{145}, Eu^{146} *AND* Eu^{147}

N. M. ANTON'EVA, A. A. BASHILOV,* B. S. DZHELEPOV, K. G. KAUN, A. F. A. MEYER, and V. B. SMIRNOV

Submitted to JETP editor July 1, 1960

J. Exptl. Theoret. Phys. (U.S.S.R.) 40, 23-27 (January, 1961)

The europium and gadolinium fractions separated from Ta irradiated by 680-Mev protons were investigated by means of a magnetic spectrometer and a luminescent γ spectrometer. New γ transitions have been detected. The relative intensities of hard γ rays from Eu^{146} have been determined. More precise values have been determined for the energies as well as intensities of the conversion lines due to previously observed γ transitions in the decay of Eu^{145} ($T_{1/2} = 5.6 \pm 0.3$ days), Eu^{146} ($T_{1/2} = 4.6 \pm 0.3$ days), and Eu^{147} ($T_{1/2} = 25$ days). The conversion electron spectrum of the europium fraction was measured between ~20 and ~2600 kev, and the hard γ ray spectrum was investigated up to 3500 kev. The level schemes of Eu^{145}, Eu^{146} and Eu^{147} are discussed.

WE investigated the radiations from the europium and gadolinium fractions, separated from tantalum bombarded with 680-Mev protons, using a Ketron-type[1] magnetic spectrometer ($\Delta H\rho / H\rho \sim 0.5\%$) and a scintillation γ spectrometer (resolving power 7.5% at the 662-kev γ line of Cs^{137}). The new lines were identified by the time variation of their intensity in both the europium and in the gadolinium fractions.

RADIATION FROM THE Eu^{145} NUCLEUS

In addition to observing in the conversion-electron spectrum of the europium fraction the conversion lines belonging to Eu^{146} ($T_{1/2} = 4.6$ days), Eu^{147} ($T_{1/2} = 25$ days) and Eu^{149} ($T_{1/2} \sim 100$ days), which we reported earlier,[2] we observed also the conversion lines due to an europium isotope with a half-life 5.6 ± 0.3 days.[3,4] The energy of the corresponding nuclear transitions and the relative intensities of the conversion lines are listed in Table I.

The lines belonging to the europium with the 5.6-day half life could be distinguished reliably from the Eu^{146} lines ($T_{1/2} = 4.6$ days). In the gadolinium fraction, the Eu^{146} lines grew stronger; whereas the lines indicated in the table were absent. The gadolinium fraction, containing Gd^{146} ($T_{1/2} \sim 45$ days), was separated twelve hours after the end of irradiation of the target, and did not contain Gd^{145} ($T_{1/2} = 24$ min). In addition, we observed that Sm^{145} accumulated in the europium fraction.[4] For these reasons, we ascribed the γ lines listed in Table I to the decay of Eu^{145}. This interpretation agrees with the data of Rasmussen et al.,[5] who assigned a half-life $T_{1/2} = 5$ days to Eu^{145}. In a recently published paper,[6] only one γ transition of 180 kev energy was observed for Eu^{145}. Grover[7] ascribes the ~0.53-, 0.645-, and 0.890-Mev γ transitions to the decay of Eu^{145}, and leaves doubtful the weak 1.30- and 1.65-Mev γ transitions.

Table I. Energy of Transitions and Relative Intensities I of the Conversion Lines of Eu^{145}

E_γ, kev	Observed conversion lines	$100 \cdot I_K / I_K$ (894 kev)	I_K / I_L
110,3±0.5	*K, L, M*	750±50	6±1
191±1	*K*	20±5	—
543±2	*K*	15±3	—
656±3	*K, L*	13±2	—
766±4	*K*	6±1	—
894±4	*K, L, M*	100	5,9±0,5
1663±5	*K, L*	4,5±0,5	5.8±0,5
1830±8	*K*	0.4±0,1	—
2001±6	*K, L*	2,1±0,3	—

We have also made preliminary measurements of the coefficient of internal conversion of the 894-kev γ transition by the method described in reference 8. The coefficient of internal conversion α_K is determined by measuring with a magnetic spectrometer the number of conversion electrons and (by the photoelectrons) the number of γ quanta emitted from one and the same source. The value obtained for α_K is

$$\alpha_K = (2.2 \pm 0.4) \cdot 10^{-3}.$$

This value of α_K, as well as the ratio of the intensities of the K and L lines, make it possible to classify the 894-kev transition as E2.

---

*Deceased.

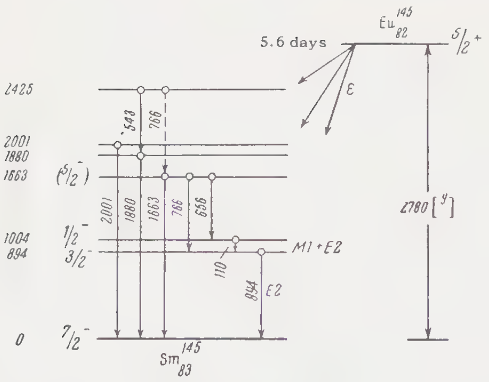

FIG. 1. Proposed scheme of the transitions in Sm^{145}.

Figure 1 shows the proposed scheme of the transitions in Sm^{145}. It is based essentially on energy data. The scheme includes all the transitions which we have observed, except for the transition with energy $E_\gamma = 191$ kev. The 766-kev transition is energetically feasible also between the 1663 and 2425 kev levels (shown dotted in the figure).

The nucleus Sm^{145} has only one neutron on top of the filled shell, and apparently fits the Mayer scheme. According to this model, the spin and parity of the ground state should be $7/2^-$ or $9/2^-$. We assume that the spin and parity of the ground state of Sm^{145} is $7/2^-$. The first excited level has an energy 894 kev. The direct transition from this level is of the E2 type (from the measurement of the coefficient of internal conversion). On can therefore assign spin and parity $3/2^-$ to the first excited level. It is apparently necessary to ascribe to the second excited 1004-kev level a spin and parity $1/2^-$. This follows from the multipolarity of the transition with $E_\gamma = 110$ kev, found to be M1 + E2 by the I_K/I_L ratio (Table I), and also from the absence of a direct 1004-kev transition to the ground state.

RADIATION OF THE Eu^{146} NUCLEUS

We have observed several new γ lines of Eu^{146}, both by conversion electrons and by γ rays. The lines attributed to Eu^{146}, observed in the gadolinium fraction, first built with a period of approximately 5 days, and then decayed with the half-life of the parent Gd^{146} ($T_{1/2} = 45$ days). In the europium fractions, the lines constantly decayed with a half life 4.6 ± 0.3 days.

Table II lists the energies of the nuclear transitions, the relative intensities of the conversion lines, and the ratios I_K/I_L for the most intense lines, as well as the relative intensities of the γ rays.

We also measured the relative intensities of the 635- and 748-kev γ rays (by the photoelectrons)

$$I\,(635\,\text{kev})/I(748\,\text{kev}) = 0.7 \pm 0.1.$$

Gold foil ($\sigma \sim 7$ mg/cm^2) and uranium ($\sigma \sim 7$ mg/cm^2) foils were used as emitters.

Table II. Transition Energies and Relative Intensities of Conversion Electrons and γ Rays from Eu^{146}

E_γ, kev	Observed conversion lines	100 I_K/I_K (748 kev)	I_K/I_L	I_γ/I_γ (748 kev)
188±1	*K*	50±20	—	—
399±1	*K*, *L*	6±1	—	—
413±1	*K*, *L*	4±1	—	—
432±1 *	*K*, *L*	19±1	5,0±0,5	—
635±3	*K*, *L*	75±5	5,5±0,5	75
667±3	*K*, *L*	14±2	—	24
705±4	*K*	10±1	—	
748±2	*K*, *L*, *M*	100	5.8±04	100
(900±5)?	*K*	(<5)	—	(9)
1061±5	*K*	1,0±0.2	—	7
1154±5	*K*	0,7±0,2	—	7
1180±5	*K*	0,5±0.1	—	
1298±5	*K*, *L*	1,1±0,2	7±1	3
1384±5	*K*	0,5±0,2	—	2
1412±7	*K*	0.3±0.1	—	2
1451±7	*K*	~0,3	—	2
1539±7	*K*, *L*	0,6±0.2	6±1	6
1765±8	*K*	<0,3	—	3
2100	—	—	—	2
2180 ?	—	—	—	1
2300	—	—	—	1
2400	—	—	—	1
2540	—	—	—	~0.7
2670	—	—	—	~0.2
2860	—	—	—	≲0.2
3100	—	—	—	<0.2

*The 423-kev transition was first observed by Zh. Zhelev.[10]

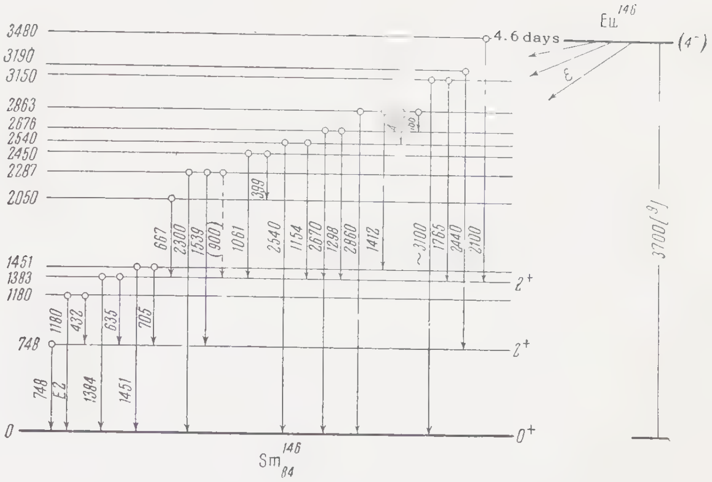

FIG. 2. Proposed scheme of the transitions in Sm^{146}.

Our results do not agree with the data of French workers,[6] who ascribed to Eu^{146} γ rays with energies 125 and 570 kev, but are in agreement with the work Funk et al.[11]

Figure 2 shows the proposed scheme of transitions in Sm^{146}. This scheme includes all the nuclear transitions which we have observed, except the transition with $E_\gamma = 2180$ kev. The decay scheme is based essentially on energy considerations. For most transitions the energy balance holds within 1 — 3 kev. In the construction of the scheme we used the cascade γ transitions, determined by Alexandrov et al.[12] and by Berlovich et al.,[13] namely: 745 — 635 — 667, 745 — 635 — 900, 745 — 635 — 1060, 748 — 635 — 1300, 745 — 635 — 1800, 745 — 1550, 745 — 635 — 2100, and 745 — 2400 kev; the 635-kev γ transition does not agree in time with the 1550- and 2400-kev transitions.

Sm^{146}_{84} is an even-even nucleus and is apparently spherically symmetrical (there are only two neutrons on top of the filled shell). The characteristic of the ground state is 0^+ and the energy of the first excited state of the nucleus is 748 kev. The latter is derived from the following considerations: first, from the intensities of the γ transitions (this is the most intense transition), second from the presence of a coincidence cascade, and third from the systematics of the first excited levels of the even-even nuclei in the region of atomic numbers close to 82.

The characteristic of the first excited state is 2^+. This follows both from the systematics of the even-even nuclei, and from the experimentally determined multipolarity of the 748-kev transition (the ratio $I_K/I_L = 5.8 \pm 0.4$ and the coefficient $\alpha_K = (4.1 \pm 0.6) \times 10^{-3}$ unequivocally point to an E2 transition).

The second excited level of Sm^{146}, with energy 1180 kev, is introduced only on the basis of energy considerations. This level is "de-excited" by two transitions: $E_\gamma = 432$ and $E_\gamma = 1180$ kev.

The 1383-kev level must apparently be assigned spin and parity 2^+. This follows from the presence of a direct transition to the ground state, the multipolarity of which is determined by our data to be E2 or E2 + M1, and also from experiments on correlation,[11] by which the 1384-kev level cannot be assigned a spin 4^+.

RADIATION OF THE Eu^{147} NUCLEUS

We have investigated the radiation of Eu^{147} previously.[2] In the present investigation we observed two additional new γ transitions, with energies 957 and 1080 kev. These transitions were observed both in the europium and in the gadolinium fractions. In the latter fraction, the observed lines first built up with a period ~ 1.5 days, and then decayed with a period of 25 days. Table III lists the transition energies and the relative intensities of the new conversion lines referred to the 187.6-kev line.

Energies of new γ transitions and relative intensities I of the conversion electrons of Eu^{147}

E_γ, kev	Observed conversion lines	$100 \cdot I_K/I_K$ (197,5 kev)	I_K/I_L
197.5±0,5	K, L, M	100	4,0±0,5
957±4	K	0,4±0,1	—
1080±4	K, L	0.6±0.2	3.2±0.6

The scheme of the $Eu^{147} \rightarrow Sm^{147}$ decay was studies by us earlier. We are now able to supplement this scheme with new transitions, with energies 957 and 1080 kev (see Fig. 3).

The spin of the ground state of Sm^{147} was determined experimentally as $7/2$ while the Mayer model predicts for the ground state of Sm^{147} spin

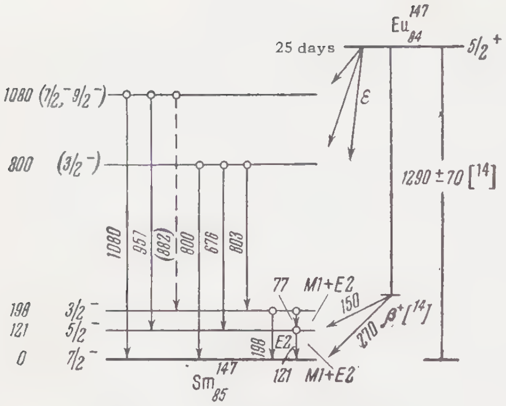

FIG. 3. Decay scheme of Eu^{147}.

and parity values of $7/2^-$ or $9/2^-$.

The spin and parity of the first excited 121-kev level is $5/2^-$, since the $E_\gamma = 121$ kev transition is of the M1 + E2 type. The spin and parity of the second excited level is $3/2^-$; this agrees with the multipolarity of the 77- and 198-kev transitions. The 800- and 1080-kev levels can apparently be assigned, with certain reservations, spins and parities of $3/2^-$ and $7/2^-$ or $9/2^-$, respectively.

An analogous placement of the levels is observed in the case of Nd^{147} (reference 15), which differs from Sm^{147} by two protons and two neutrons. The 900-kev transition observed in reference 14 was not observed by us distinctly, and are therefore shown dotted on our scheme.

We have also observed weak conversion lines corresponding to γ transitions with energies 1139, 1167, 1527, and 2050 kev. These lines, present in the gadolinium and europium fractions, have not been identified in view of their low intensity.

The authors are deeply grateful to L. K. Peker for interest in the work and for a discussion of the decay schemes.

---

[1] B. S. Dzhelepov and A. A. Bashilov, Izv. Akad. Nauk SSSR, Ser. Fiz. **14**, 263 (1950).

[2] Anton'eva, Bashilov, Dzhelepov, and Preobrazhenskii, JETP **36**, 28 (1959), Soviet Phys. JETP **9**, 20 (1959); Izv. Akad. Nauk SSSR, Ser. Fiz. **22**, 906 (1958) and **23**, 204 (1959), Columbia Tech. Transl. pages 889 and 196.

[3] Anton'eva, Bashilov, and Dzhelepov, Тезисы докладов X ежегодного совещания по ядерной спектроскопии (Topics of Papers of the Tenth Annual Conference on Nuclear Spectroscopy), Acad. Sci. Press, 1960, p. 76.

[4] Bashilov, Larionov, Nikitin, and Smirnov, Izv. Akad. Nauk SSSR, Ser. Fiz. **24**, 788 (1960), Columbia Tech. Transl. in press.

[5] Hoff, Rasmussen and Thompson, Phys. Rev. **83**, 1068 (1951).

[6] Olkowsky, Le Papc, Gratot, and Cohen, J. phys. rad. **20**, 549 (1959).

[7] J. R. Grover, Phys. Rev. **116**, 411 (1959).

[8] Anadmchuk, Bshilov, and Preobrazhenskii, Izv. Akad. Nauk SSSR, Ser. Fiz. **22**, 919 (1958), Columbia Tech. Transl. p. 911.

[9] A. Cameron, A Revised Semi-Empirical Atomic Mass Formula AECL No. 433 (1957).

[10] Dzhelepov, Zhelev, and Kudryavtseva, Материалы 3-го совещания по ядерной спектроскопии нейтронодефицитных изотопов редких земель Materials of the Third Conference on Nuclear Spectroscopy of Neutron-Deficient Isotopes of Rare Earths, Dubna, Joint Inst. Nuc. Res., in press.

[11] Funk, Schwedtfeger, and Mihelich, BAPS **5**, 254 (1960).

[12] Aleksandrov, Kroga, and Nikitin, op. cit. ref. 10.

[13] Berlovich, Klement'ev, Krasnov, and Nikitin, op. cit. ref. 10.

[14] C. F. Schwedtfeger and J. W. Mihelich, BAPS **4**, 426 (1959).

[15] Brosi, Ketelle, Thomas, and Kerr, Phys. Rev. **113**, 239 (1959).

Translated by J. G. Adashko
4

SOVIET PHYSICS JETP VOLUME 13, NUMBER 1 JULY, 1961

DIFFERENT LATTICE CONSTANTS OF SOLID NEON ISOTOPES

V. S. KOGAN, B. G. LAZAREV, and R. F. BULATOVA*

Physico-Technical Institute, Academy of Sciences, Ukrainian S. S. R.

Submitted to JETP editor July 6, 1960

J. Exptl. Theoret. Phys. (U.S.S.R.) **40**, 29-31 (January, 1961)

X-ray diffraction investigations of Ne^{20} and Ne^{22} were performed at 4.2° K. Both isotopes have face-centered cubic lattices, with the constants $a = 4.471 \pm 0.004$ A and 4.455 ± 0.004 A, respectively. The relative difference in the molar volumes, $\Delta V/V = 1.1 \pm 0.5\%$, agrees satisfactorily with calculations taking into account the difference in zero-point vibration energy. The difference in the molar volumes of the neon isotopes is much greater than that for lithium isotopes, which, according to the literature, is negligible despite the larger relative mass difference of the latter. This is apparently associated with a difference in the nature of the binding forces in neon and lithium lattices.

WE have found only report[1] of an attempt to detect differences in the lattice constants of isotopes of elements heavier than helium. For the difference between the lattice constants of Li^6 and Li^7 Covington and Montgomery obtained 0.0015 kxu, which was close to the limit of their experimental accuracy. They considered the principal result of their work to be the direct confirmation of zero-point vibrations of lattice atoms, varying in energy for different isotope masses. This effect should evidently be more pronounced in inert gases, where different isotopes of the same element are not characterized by identical forces which result from free electrons, and which are the principal determinant of structure in metallic crystals. The different lattice constants of inert-gas isotopes or, equivalently, their different molar volumes in the solid phase, have been considered in several theoretical papers.[2-4] $\Delta V/V = 0.6\%$ has been obtained for neon at absolute zero.

We used x rays to study the structure of Ne^{20} (99% pure) and Ne^{22} (98% pure). Air impurities were removed by passing the neon through a coil cooled by liquid hydrogen, while helium contamination was eliminated by pumping from a vessel in which solid neon had been produced by liquid-helium cooling. Neon isotope samples were obtained in the form of polycrystalline layers deposited from the gaseous phase on a copper capillary tube that was cooled internally by liquid helium. The x-ray diffraction apparatus was described in reference 5. The figure shows typical x-ray diffraction patterns, including both neon lines and lines of the copper backing serving as standards.

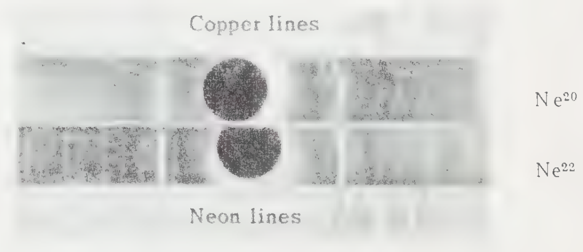

We used CuKα and FeKα radiation from a Pines fine-focus x-ray tube, and a casette 40 mm in diameter. In the photometric study the separations of interference maxima were determined within ± 0.03 — 0.05 mm. The effective diameter of the cassette was determined within ± 0.05 mm by means of the standard lines. Corrections for sample thickness were introduced by the Kurdyumov procedure, taking account of characteristics associated with the use of a fine-focus tube.[6] Results obtained from the x-ray patterns are given in the table; the lattice constants are accurate to within ±0.004 kxu.

The table shows that both neon isotopes have face-centered cubic lattices with constants differing by 0.016 kxu, which is one order of magnitude greater than in the case of lithium isotopes, despite a smaller relative mass difference. $\Delta V/V = 1.1 \pm 0.5\%$ for the relative difference in molar volumes was calculated from the lattice constants of the neon isotopes. The theoretical value $\Delta V/V = 0.6\%$ is within the range of experimental accuracy, but is considerably smaller than the mean value of $\Delta V/V$ obtained from the x-ray data.

The value $a = 4.471$ kxu obtained for the lattice constant of the lighter neon isotope, which constitutes ~91% of natural neon, improves the values

---

*Assisted by the graduate student A. S. Bulatov.

Computations for Ne^{20} and Ne^{22} based on x-ray (CuKα) diffraction patterns

[illegible]	Intensity for Ne^{22}		θ (Ne^{20})	θ (Ne^{22})	a (Ne^{20}), kxu	a (Ne^{22}), kxu
	computed	exper.				
(111)	100	[illegible]				
(200)	48	8				
(220)	27	21	29°06′	29°13.5′	4.470	4.459
(311)	25	20.5	34°48′	34°57′	4.472	4.456
(222)	6.4					
(400)	4.2					
(331)	7.0					
(420)	6.4	10.5	50°26.4′	50°38.3′	4.470	4.456
(422)	4.9	8	57°29′	57°53′	4.471	4.451
(333)(511)	6.0	10.5		63°55.5′		4.452
				Mean:	4.471	4.455

for the lattice constant of the natural mixture that are given in the literature: a = 4.52 kxu from x-ray diffraction[7] and 4.429 kxu from neutron diffraction.[8]

The neon line intensities in the x-ray patterns differ considerably from the calculated values. For CuKα and FeKα rays the (200) line intensities, compared with the (111) intensities, are much lower than the calculated values. With FeKα the (222) intensity was enhanced. This redistribution of the intensities is evidently associated with the fact that the neon layer deposited from the gaseous phase on the copper capillary tube has its [111] axis along capillary radii. It is interesting that the intensity ratio of identical x-ray interferences from the heavier and lighter isotopes $[I_{hkl}(Ne^{22})/I_{hkl}(Ne^{20})]$ is greater, and increases more rapidly with the scattering angle, than could have been expected from the calculation of a thermal factor. The last lines that are distinctly visible in the x-ray patterns for the heavier isotope merge with the background in the case of the lighter isotope.

---

[1] E. J. Covington and D. J. Montgomery, J. Chem. Phys. **27**, 1030 (1957).

[2] J. H. Henkel, J. Chem. Phys. **23**, 681 (1955).

[3] I. J. Zucker, J. Chem. Phys. **25**, 915 (1956).

[4] T. F. Johns, Phil. Mag. **3**, 27 (1958).

[5] Kogan, Lazarev, and Bulatova, JETP **37**, 678 (1959), Soviet Phys. JETP **10**, 485 (1960).

[6] B. Ya. Pines, Острофокусные рентгеновские трубки (Fine-Focus X-ray Tubes), Gostekhizdat, 1955.

[7] Keesom, De Smedt, and Mooy, Comm. Phys. Univ. Leiden **18**, 203e (1930).

[8] D. G. Henshaw, Phys. Rev. **111**, 1470 (1958).

Translated by I. Emin
5

SOVIET PHYSICS JETP VOLUME 13, NUMBER 1 JULY, 1961

THE OVERHAUSER EFFECT AND THE ELECTRON PARAMAGNETIC RESONANCE "SECONDARY SIGNAL"

A. V. KESSENIKH

Moscow State University

Submitted to JETP editor July 8, 1960

J. Exptl. Theoret. Phys. (U.S.S.R.) 40, 32-33 (January, 1961)

The relative increase in the polarization of the protons in a free radical as the electron paramagnetic resonance is saturated has been measured by observing the increase in the nuclear magnetic resonance signal. It is shown that at large saturating power an electron paramagnetic resonance "secondary signal" is observed simultaneously with the nuclear magnetic resonance signal, corresponding to the emission or absorption of an additional quantum by the electron spin system.

WE have observed dynamic nuclear polarization (d.n.p.) in solid diphenylpicrylhydrazyl at room temperature in fields of approximately 3300 oe. The apparatus described in reference 1 has enabled us to measure the d.n.p. of the protons by means of the relative amplitude of the nuclear magnetic resonance (n.m.r.) signal on an oscillograph screen.

The coil with the sample containing 30 mm^3 of diphenylpicrylhydrazyl placed into a teflon container was situated within a rectangular three centimeter resonant cavity excited in the H_{102} mode. The sample was cooled by a stream of air. The amplitude of the high frequency magnetic field H_1 was determined from the power dissipated in the resonator. The position of the coil in the resonant cavity and its dimensions are such that there should be no significant variations in the magnitude of the high frequency magnetic field over the volume of the sample where H_1 is perpendicular to the axis of the coil, and this is confirmed by the observation of the electron paramagnetic resonance (e.p.r.) signal with the coil present in the cavity.

The dependence on H_1 of the increase in the n.m.r. signal is shown in Fig. 1. The accuracy of determining H_1 and the relative increase in the signal amounts to approximately 10%. As an example, we show in Fig. 2 an oscillogram of the n.m.r. signal in the absence of the high frequency field. In order to obtain reliable results at higher values of the high frequency power and field in the resonator we shall need more intensive cooling, since starting with $H_1 > 2$ oe appreciable heating begins to be observed, while for $H_1 > 3$ oe partial melting of the sample is observed, as can be inferred from the n.m.r. line.

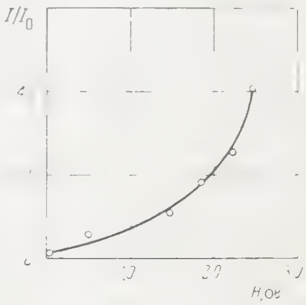

FIG. 1. Dependence of the relative increase in the nuclear magnetic resonance signal due to protons in diphenylpicrylhydrazyl on the amplitude of the high frequency magnetic field saturating the electron paramagnetic resonance.

We have also observed at $H_1 > 1.5$ oe the "double quantum emission" effect (9300 and 14 Mc/sec) in e.p.r. described by Winter.[2] This effect occurs when the electron spin system, situated in a constant magnetic field H_0, is simultaneously acted upon by electromagnetic radiation of frequency ω_1 and another radiation of frequency ω_2. The condition for the appearance of a "secondary signal" at the frequency ω_2 is $\omega_1 \pm \omega_2 = \gamma_e H_0$. Fig. 3 shows an oscillogram of the signal which

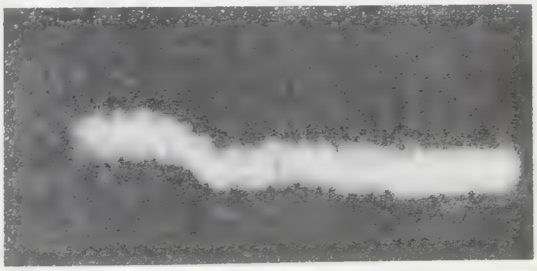

FIG. 2. Oscillogram of the nuclear magnetic resonance signal due to protons in solid diphenylpicrylhydrazyl. Amplification K = 30.

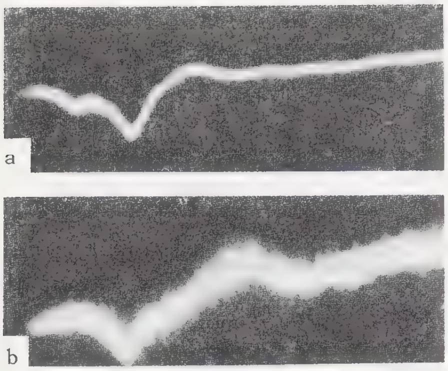

FIG. 3. a – Signal representing the superposition of the nuclear magnetic resonance signal (middle peak) and of the electron paramagnetic resonance "secondary signal" (outer peaks). Amplification K = 1 (the signal is applied to the oscillograph plates), $H_1 = 2.5$ oe; b – Electron paramagnetic resonance "secondary signal," $H_1 = 2.2$ oe, amplification K = 3.

represents the superposition of an n.m.r. signal with a maximum in the field H_0 and of an e.p.r. "secondary signal" at the same frequency ν_n which consists of the absorption and emission signals displaced respectively by $\pm \omega_n/\gamma_e = 5$ oe from the field H_0. The detuning of the autodyne n.m.r. detector by several tens of kilocycles does not change the shape and the position of the e.p.r. "secondary signal", but sharply affects the amplitude (and, of course, the position) of the n.m.r. signal.

In our opinion, the signals described in reference 3 represent a superposition of an n.m.r. signal and an e.p.r. "secondary signal", with the n.m.r. signal displaced from the maximum value corresponding to the Overhauser effect.

I wish to express my gratitude to Professor E. I. Kondorskiĭ and E. S. Goryunov for active participation in this work.

---

[1] A. V. Kessenikh, Приборы и техника эксперимента (Instruments and Exptl. Techn.) in press.

[2] I. M. Winter, J. phys. radium **19**, 843 (1958).

[3] You Hing-Tchao and J. Herve, Compt. rend. **250**, 700 (1960).

Translated by G. Volkoff
6

SOVIET PHYSICS JETP VOLUME 13, NUMBER 1 JULY, 1961

DISSOCIATION OF MOLECULAR HYDROGEN IONS IN COLLISIONS WITH GAS MOLECULES

L. I. PIVOVAR, V. M. TUBAEV, and M. T. NOVIKOV

Submitted to JETP editor July 18, 1960

J. Exptl. Theoret. Phys. (U.S.S.R.) 40, 34-39 (January, 1961)

The cross sections for the dissociation of molecular hydrogen ions (H_2^+) in single collisions with H_2 and N_2 molecules and with He, Ar, and Kr atoms are measured at energies from 200 to 1200 kev.

1. INTRODUCTION

RECENT measurements of the cross sections for the dissociation of molecular hydrogen ions have been connected mainly with the problem of injecting hydrogen ions into thermonuclear devices and accelerators. Measurements have been performed by Damodaran,[1] Fedorenko et al.,[2] and Barnett[3] at energies up to 200 kev in hydrogen, nitrogen, helium, and argon. Barnett[3] has also investigated H_2^+ dissociation at 500 — 2200 kev in the same gases. Sweetman[4] very recently reported cross sections for H_2^+ dissociation in hydrogen at 100 — 800 kev. The cross sections for proton production given in the first three of the aforementioned papers do not agree; it is indicated in reference 2 that different geometries can account for the discrepancies.

There have been no measurements of the cross section for H_2^+ dissociation within the 200 — 500 kev range in any gas besides hydrogen. Because of the scientific and practical importance of such cross sections, we have investigated molecular hydrogen ion dissociation in different target gases from 200 to 1200 kev.

2. APPARATUS AND EXPERIMENTAL TECHNIQUE

We produced molecular hydrogen ions by means of an electrostatic accelerator, using an ion source with a cold cathode. We have described the accelerator in reference 5.

Figure 1 is a diagram of our apparatus. The hydrogen ion beam from the electrostatic accelerator passed through a collimating aperture 1 of diameter 4 mm into a magnetic mass monochromator (analyzer) 2, in which the ion beam was deflected 17°. The H_2^+ beam passed from the monochromator through a 2-mm diaphragm 4 and channel of diameter 6.5 mm and length 100 mm into the collision chamber 3, from which the ions emerged through a channel of the same dimensions. The collision chamber, of effective length 310 mm, was fastened to two supports 5 which were regulated by means of vacuum-sealed screw rods for accurate positioning of the chamber with respect to the ion beam. After traversing the collision chamber the beam entered an electrostatic analyzer 6, which consisted of a copper tube 200 mm in diameter and 1000 mm long containing the plates of a flat condenser.

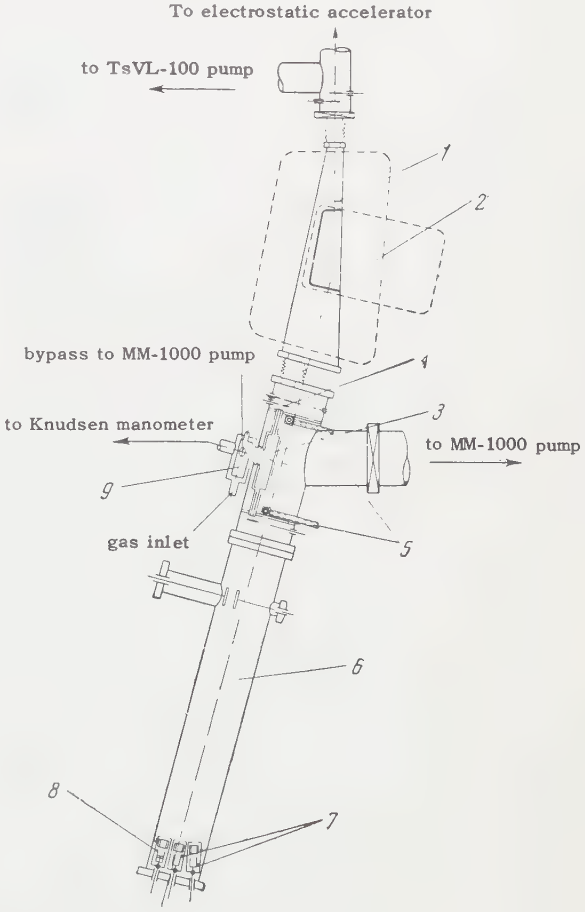

FIG. 1. Diagram of apparatus.

The electric field of the condenser separated the beam into a neutral component and H^+ and H_2^+ components. The currents of positive components were measured by vacuum-tube electrometers connected to Faraday cups 7. The intensity of the neutral beam formed from H_2^+ was measured by a thermocouple detector 8 similar to that described by Damodaran.[1] The thermocouple emf was measured by an M-21/4 mirror galvanometer. All currents were measured simultaneously in order to reduce the error resulting from fluctuations of the primary beam intensity. For the purpose of reducing the background and contaminations, the collision chamber was sealed by means of lead gaskets, and a liquid-nitrogen trap 9 was introduced to freeze condensing fractions. An auxiliary vacuum duct and valve accelerated the exhaustion of residual gas and gas liberated from the chamber walls as they were heated to 100 – 120° C.

The residual gas pressure in the collision chamber did not exceed $(4-5)\times 10^{-6}$ mm Hg. Gas was exhausted at the entrance and outlet of the collision chamber by an MM-1000 pump and liquid-nitrogen trap. The pressure in the space surrounding the collision chamber and in the analyzer did not exceed 3×10^{-6} mm. The accelerating tube and chamber of the mass monochromator were exhausted by a TsVL-100 pump and liquid-nitrogen trap. During the experiment the pressure at the accelerating-tube exit and in the mass monochromator varied from 7×10^{-6} to 1.2×10^{-5} mm. Gas pressure in the collision chamber was measured by a Knudsen manometer calibrated against a McLeod manometer.

Total cross sections for proton production (σ_{H^+}) and for the production of fast hydrogen atoms (σ_{H^0}) were measured mass-spectrometrically. The following formulas were used in the calculations:

$$\sigma_{H^+} = \left\{\frac{d}{d(nL)}\left[2N_{H^+}/(N_{H^+}+N_{H^0})+2N_{H_2^+}\right]\right\}_{nL\to 0}, \qquad (1)$$

$$\sigma_{H^0} = \left\{\frac{d}{d(nL)}\left[2N_{H^0}/(N_{H^+}+N_{H^0})+2N_{H_2^+}\right]\right\}_{nL\to 0}. \qquad (2)$$

Here N_{H^+}, N_{H^0}, and $N_{H_2^+}$ are the numbers of protons, hydrogen atoms, and molecular hydrogen ions, respectively, traversing the collision chamber after subtraction of the particles produced in the residual gas and at the edges of apertures; n is the concentration of target gas molecules, and L is the effective length of the collision chamber with adjacent segments of the beam path taken into account.

For the purpose of checking on the occurrence of single collisions we recorded the ratios of secondary to primary particles as functions of the gas pressure in the collision chamber. With these ratios extrapolated to zero pressure, σ_{H^+} and σ_{H^0} were determined from (1) and (2).

Since the cross sections were measured using thin targets, σ_{H^+} could be determined neglecting the effect of the $H_2^+ \to H_2^0$ process even at low energies. The result obtained for σ_{H^0} can be too high because H_2^0 molecules resulting from charge exchange of H_2^+ reach the detector along with H^0 atoms. However, the cross section for electron capture by molecular hydrogen ions is very small at 200 kev and falls off very rapidly with increasing primary ion energy. Sweetman's data[4] for energies above 250 – 300 kev show that the systematic error resulting from this process is small. For these reasons, and assuming also that the cross sections for processes leading to the production of negative hydrogen ions are negligibly small at the given energies, we find that the total dissociation cross section is determined practically by the following three processes:

$$\text{I. } H_2^+ \to H^+ + H^0,$$
$$\text{II. } H_2^+ \to H^+ + H^+,$$
$$\text{III. } H_2^+ \to H^0 + H^0.$$

The total dissociation cross section σ_d is therefore given by

$$\sigma_d = (\sigma_{H^+} + \sigma_{H^0})/2. \qquad (3)$$

The foregoing considerations regarding the smallness of the cross section for $H_2^+ \to H_2^0$ can also be applied to process III at energies beginning with 400 – 500 kev. In the range 500 – 1200 kev we can therefore assume without large error that the total dissociation cross section is the sum of the cross sections for processes I and II; the corresponding partial cross sections σ_I and σ_{II} can be evaluated accordingly. The partial cross section σ_I is then given directly by σ_{H^0}, while σ_{II} is determined from

$$\sigma_{II} = (\sigma_{H^+} - \sigma_{H^0})/2. \qquad (4)$$

Diaphragm openings of different diameters at the collision-chamber exit were used to check for unequal scattering of primary and secondary particles. With openings of diameters greater than 4 mm the ratio of secondary to primary particles remained constant within the limits of error. Since the exit channel of the collision chamber had a 6.5-mm diameter, only a small systematic error resulting from unequal scattering is thus indicated. We estimated random errors of ± 12% for σ_{H^+} and ± 15% for σ_{H^0}. The energy of molecular hydrogen ions was determined from the accelerating voltage of the electrostatic generator, measured by a rotary voltmeter that had been calibrated by means of γ-ray resonances. The error of primary ion energies does not exceed ± 2%.

3. RESULTS AND DISCUSSION

The target gases were hydrogen passed through a palladium filter, 99.97% pure nitrogen, and helium, argon, and krypton with at most 0.1% impurities.

The curves in Figs. 2, 3, and 4 represent the cross sections σ_{H^+} for proton production, and σ_d for hydrogen dissociation as functions of H_2^+ energy. Values of σ_{H^+} and σ_d given by other investigators are also shown. Figs. 2 — 4 show that over the entire investigated energy range σ_{H^+} and σ_d decrease steadily with increasing energy; σ_d decreases more rapidly than σ_{H^+}. The cross sections are enhanced with increased atomic number of the target gas, in agreement with the observations of other investigators. Besides the higher absolute values of σ_{H^+} and σ_d, in heavy gases the cross sections fall off less rapidly with increasing H_2^+ energy.

It is interesting to compare our results with those obtained by other workers. For hydrogen our data agrees satisfactorily with those of Sweetman,[4] are close to those of Barnett at relatively low energies,[3] and join only poorly at 200 kev with those of Damodaran[1] and Fedorenko et al.[2]

Our values for σ_{H^+} and σ_d in the cases of nitrogen and argon differ by 15 — 60% from the cross sections measured by Damodaran and by Barnett. Also, our curves for σ_d in the range 500 — 1200 kev fall off more rapidly with increasing energy than those of Barnett.

Considerably greater discrepancies between our data and those of other investigators were observed in the case of helium, for which our values of σ_{H^+} and σ_d were about 1.5 — 2 times smaller than the results given in references 1 — 3. The cause for the disagreement could lie in different degrees of purity of the helium in the collision chamber, since small admixtures of heavier gases can obviously result in highly exaggerated measurements of H_2^+ dissociation cross sections in helium.

FIG. 3. Cross sections for H_2^+ dissociation and proton production in nitrogen. Solid curves – present work; △–σ_d, ▲–σ_{H^+} – reference 1; dot-dash curve – reference 2; dashed curve – reference 3.

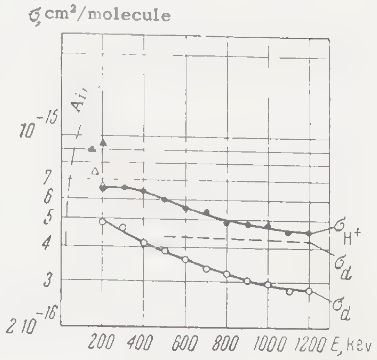

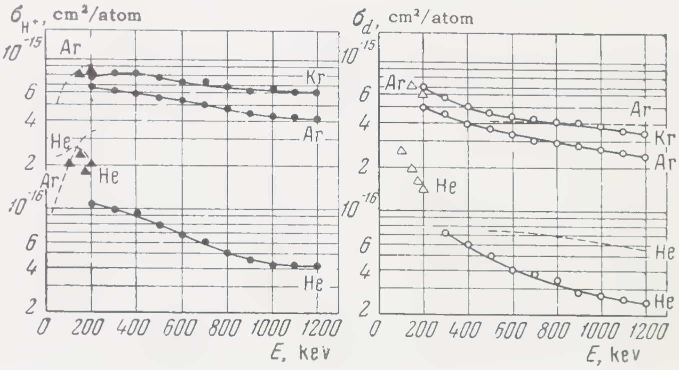

FIG. 4. Cross sections for H_2^+ dissociation and proton production in helium, argon, and krypton. Solid curves – present work; △, ▲ – reference 1; dot-dash curves – reference 2; dashed curves – reference 3.

The partial cross sections for processes I and II in the range 500 — 1200 kev were evaluated (see the table) from our data on the basis of the foregoing considerations regarding the smallness of the $H_2^+ \rightarrow 2H^0$ cross section at high energies. In all of the investigated gases σ_{II} decreases slowly and monotonically as the H_2^+ energy is increased. σ_I decreases considerably more rapidly in the same energy range.

Our calculated partial cross sections σ_I and σ_{II} can be compared with Sweetman's direct

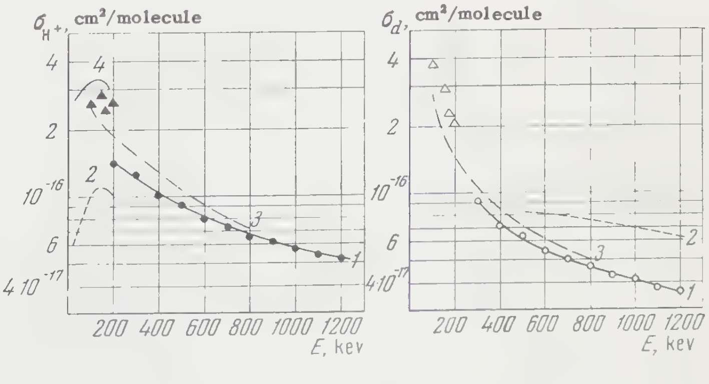

FIG. 2. Cross sections for H_2^+ dissociation and proton production in hydrogen: 1 – present work, 2 – reference 3, 3 – reference 4, 4 – reference 2, △, ▲ – reference 1.

Energy, kev	H_2		N_2		He		Ar		Kr	
	σ_I^*	σ_{II}	σ_I	σ_{II}	σ_I	σ_{II}	σ_I	σ_{II}	σ_I	σ_{II}
500	3.7	2.8	17	21	2,3	2.6	18	19,5	23	25
600	3,0	2.5	16	20	1.8	2.3	17	18	20	24
700	2.6	2.4	14	20	1.6	2,2	14	18	18	25
800	2,5	2.2	13	18	1.4	2.0	12	18	17	25
900	2.2	2.1	12	18	1.2	1.7	11	17	16	25
1000	2.2	1.9	11	17	1,1	1.6	10.5	16	15	25
1100	2	1.8	9	17	1.0	1,6	10	15	13	24
1200	1,9	1.7	9	16	0.9	1,55	9.5	15	12	24

*Cross sections are given in units of 10^{-17} cm²/molecule

measurements[4] only in the case of hydrogen. Our values are consistently lower than Sweetman's results by 15 — 20%, which is approximately the same discrepancy that occurred for the total cross sections σ_{H^+} and σ_d.

Salpeter[6] has performed the only theoretical calculation of the dissociation cross sections of fast molecular hydrogen ions in collisions with gas molecules, employing the Born approximation for high H_2^+ energies. Our cross sections for H_2^+ dissociation in hydrogen at 300 — 400 kev agree satisfactorily with Salpeter's calculations. We used energies that are too low to permit a comparison between the theoretical and experimental cross sections for H_2^+ dissociation in N_2 and Ar.

In conclusion we wish to thank Academician A. K. Val'ter of the Academy of Sciences, Ukrainian S.S.R., for his interest in this work, and Ya. M. Fogel' for a discussion of the results.

[1] K. K. Damodaran, Proc. Roy. Soc. (London) **A239**, 382 (1957).

[2] Fedorenko, Afrosimov, Il'in, and Kaminker, JETP **36**, 385 (1959), Soviet Phys. JETP **9**, 267 (1959).

[3] C. F. Barnett, Proc. of the Second International United Nations Conference on the Peaceful Uses of Atomic Energy, Geneva, 1958 (United Nations, Geneva, 1959), Vol. 15, Paper No. P/1789.

[4] D. R. Sweetman, Phys. Rev. Letters **3**, 425 (1959).

[5] Pivovar, Tubaev, and Novikov, J. Tech. Phys. (U.S.S.R.) **30**, 74 (1960), Soviet Phys.-Tech. Phys. **5**, 67 (1960).

[6] E. E. Salpeter, Proc. Phys. Soc. (London) **A63**, 1295 (1950).

Translated by I. Emin
7

SOVIET PHYSICS JETP VOLUME 13, NUMBER 1 JULY, 1961

LOSS OF PLASMA FROM A MAGNETIC-MIRROR SYSTEM. II

M. S. IOFFE, R. I. SOBOLEV, V. G. TEL'KOVSKIĬ, and E. E. YUSHMANOV

Submitted to JETP editor July 20, 1960

J. Exptl. Theoret. Phys. (U.S.S.R.) 40, 40-48 (January, 1961)

The anomalously rapid loss of plasma from a magnetic-mirror system described earlier[1] has been investigated. Measurements of the ionic component of the current to the walls of the system show that the loss is due to the motion of plasma across the magnetic field lines and that most of the charged particles are lost at the side walls of the system.

INTRODUCTION

IN experiments described by us in an earlier communication[1] we have studied the containment of a hydrogen plasma with a density of the order of 10^9 cm^{-3} consisting of fast ions ($E_i = 1 - 2$ kev) and slow electrons ($E_e \sim 10$ ev). The containment time of the plasma in the system was determined by measuring the time rate of decay of the fast-ion density after the plasma-production process was terminated. In addition to charge exchange, which should be the principal mechanism by which fast ions are lost under the present experimental conditions, it has been found that there is another mechanism which causes loss of ions from the system.

To determine the direction in which ions escape by virtue of this other mechanism (i.e., along the magnetic field, through the mirrors, across the field, to the side walls), we have carried out direct measurements of the number of fast ions which leave the plasma at the ends (mirrors) and at the side walls of the system.

MEASUREMENT OF THE NUMBER OF FAST IONS ESCAPING AT THE ENDS (ALONG THE MAGNETIC FIELD)

The number of ions escaping along the magnetic field of the system is measured by means of a metal electrode in the form of a sector of a disc, which is fastened to one of the diaphragms. The area of the sector is $1/6$ of the total end surface (cf. Fig. 1); a bias of -20 v is applied to the electrode and is sufficient to suppress plasma electrons. The signal from the sector is integrated in an RC circuit which has a time constant of 5 millisec. Thus, the total ion charge carried to the sector is measured. A correction is made for secondary electron emission; the secondary electron coefficient is approximately unity (cf. reference 2). To measure the charge after the accelerating-voltage pulse we use a blanking system in which the amplifier is switched on at the end of the pulse.

It is apparent that this method of measuring charge does not allow us to separate the fast ions from the slow ions. The slow ions are formed in this system by charge exchange of fast ions on the neutral gas. The decay of the plasma is characterized by two simultaneous processes: charge exchange, in a time* $\tau_{ce} = 1/n_0 v_i \sigma_{ce}$, and the other escape mechanism, characterized by a time τ_s; thus, the number of ions which experience charge exchange during the plasma decay time is

$$\int_0^\infty \frac{N_0}{\tau_{ce}} \exp\left[-\left(\frac{1}{\tau_{ce}}+\frac{1}{\tau_s}\right)t\right]dt = N_0\frac{\tau_s}{\tau_s+\tau_{ce}},$$

where N_0 is the initial number of fast ions in the system. Then the number of ions which escape the system because of the supplementary loss mechanism is $N_0\,\tau_{ce}/(\tau_s + \tau_{ce})$. It is apparent that if plasma decay is due primarily to the supplementary loss mechanism, then the fraction of the ions which experience charge exchange (forming slow ions) will be small. According to reference 1, if $H_0 = 5000$ oe, $p = 1 \times 10^{-6}$ mm Hg and $U_0 = 30$ kv, $\tau_s = 200\,\mu$sec and $\tau_{ce} = 700\,\mu$sec so that the total number of slow ions which is formed is 20% of N_0. On the basis of these results, it is reasonable to expect that the ion current which reaches the measurement electrode consists primarily of fast ions. In the results of the measurements given below it is assumed that all of the measured current is due to fast ions. (The experimental basis for the validity of this assumption will be given at the end of this section.)

The charge carried by the fast ions which escape at the ends is measured with $H_0 = 5000$ oe, $p = 1 \times 10^{-6}$ mm Hg, $U_0 = 30$ kv and $\alpha \equiv H_{max}/H_0$

---

*The notation is the same as in reference 1.

Table I. Number of fast ions escaping at the ends for various values of the mirror ratio

α	1.33	1.55	2.0	2.35
10^7 Q_s, Coul.	3,3	8.7	12.8	10.8
10^7 Q, Coul.	46	125	200	200
q_{end}, percent	7.0	7.0	6.4	5.4

= 1.33, 1.55, 2.0, and 2.35. The quantity which is obtained is compared with the charge due to the total number of fast ions which escape the system because of the supplementary loss mechanism. The quantity N_0 is determined from the mean density of fast ions at the central cross section under the assumption that the fast-ion concentration is uniform over the entire volume of the system.

The magnitude of the charge-exchange current, which must be known to find the density, is measured together with the fast-ion charge. The values of the measured charges, converted for the entire surface of both ends Q_e are given in Table I. The table also gives the charge of the fast ions which escape the system because of the supplementary loss mechanism, Q, as well as the ratio of these charges q_e for each value of the mirror ratio $\alpha = H_{max}/H_0$. It is apparent from the table that only a small portion of the fast ions which escape the system leave via the ends.

Since there is a measurement electrode at only one mirror, it is necessary to check that the results which have been obtained are not caused by some small asymmetry in the mirrors. If the mirror ratio is somewhat larger in the mirror in which the electrode is located (as compared with the opposite mirror), the particle loss can be stronger at the end with the smaller value of α. For this reason control experiments were performed with asymmetric mirrors; the mirror-ratio at the mirror containing the electrode was several percent smaller than the mirror ratio at the opposite end. Under these conditions the charge measured by the sector was approximately doubled. This result would seem to indicate that the results which have been obtained are not due to a mirror asymmetry.

It has been noted earlier, that during the plasma decay time slow ions amounting to 20% of the total number of fast ions in the system are formed. According to the results given in Table I, not more than 10% of the ions which escape from the system by virtue of the additional loss mechanism escape through the ends (the fraction of this charge compared with the total number of fast ions in the system is still smaller). A comparison of these data shows that the charge measured at the ends is undoubtedly not due to the fast ions, which have velocities which are predominantly in the transverse direction, but rather to the slow ions, which are not well contained by the mirrors. To investigate this problem we have compared the ion currents at the ends as measured with the sector electrode and with a special electrode system in which only the fast ions are detected. This system consists of eight metal plates 0.8 mm thick which form a curved comb. The height of the plates is 20 mm and the distance between them is 18 mm. In Fig. 1 we show schematically the shape and arrangement of the plates in the comb and the location of the comb with respect to the sector electrode.

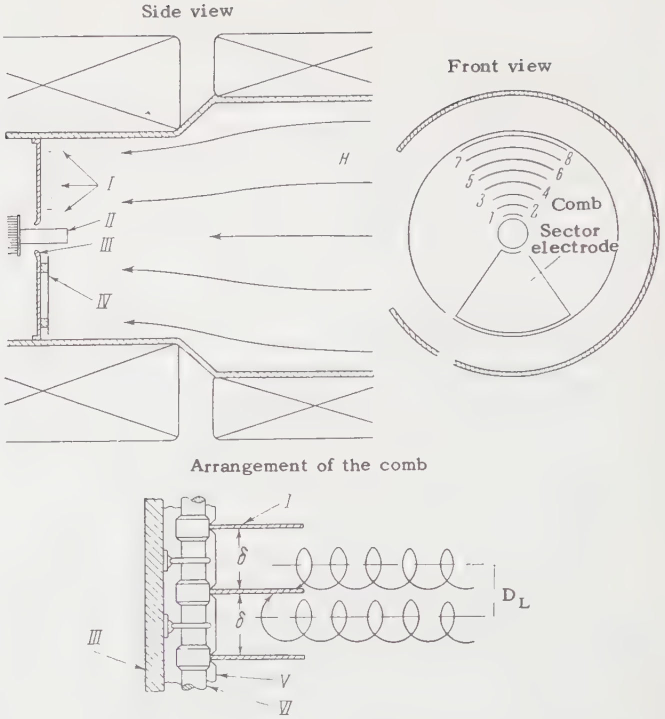

FIG. 1. Electrodes for measuring the ion current at the ends of the system. I) Measurement electrodes (comb), II) cap, III) diaphragm, IV) sector electrode, V) shield, VI) insulator.

The current measured by a given electrode in the comb is due essentially to the flow of fast ions from a portion of a cylindrical layer with a mean radius equal to the radius of the electrode. The thickness of this layer is equal to the Larmor diameter of the fast ions. The slow ions can be neglected because their Larmor orbits are small compared with those of the fast ions. This situation holds even more strongly for the electrons in the plasma. The secondary electron emission from the plates in the comb is small because the plates are parallel to the magnetic field.

Table II. Number of slow ions in the ion flux which escapes at the ends

α	1.33	1.55
$10^8\ Q_s$, Coul.	5,5	19.0
$10^8\ Q_c$, Coul.	2.4	7.6
Q_{slow}/Q_{fast}, percent	~5	~15

In measuring the charge collected by the comb, we must take account of the fact that the comb measures only a fraction of the total flux of fast ions at the region of the diaphragm occupied by the comb electrodes if the Larmor diameter of the ions D_L in the mirrors is smaller than the separation between the plates of the comb δ. To take account of the "transparency" of the comb we multiply the charge Q_c by the quantity δ/D_L.

The charge measured by the sector Q_s is equal to the sum of the charges carried by the fast ions Q_{fast}, the slow ions Q_{slow}, and the secondary electrons produced by the fast ions. By comparing the charges measured by the sector and by the comb under the same conditions we can determine the ratio of the number of slow ions to fast ions at the ends

$$Q_{slow}/Q_{fast} = (Q_s/Q_c)(D_L/\delta) - (1+k)$$

(k is the secondary emission coefficient).

The results of the measurements are shown in Table II (for $k = 1$). In calculating D_L we assume an ion energy of 1.5 kv.[1]

From the expression given for Q_{slow}/Q_{fast} it is apparent that the final result is sensitive to the magnitude of the secondary emission coefficient. However, even if we take $k = 0$, which is not very probable, the particle flux at the ends contains at least 50% slow ions. These relative measurements show that the charge measured by the sector is due primarily to fast ions. We may note that because the slow ions have been neglected the true charge carried to the ends by the fast ions is actually smaller than the measured charge.

Thus, the end-current measurements show that fast ions do escape through the mirrors, but that this loss is only an insignificant part of the total supplementary loss.

MEASUREMENT OF THE NUMBER OF FAST IONS LOST AT THE SIDE WALLS

In order to measure the number of fast ions lost at the side walls we use a system which consists of six insulated electrodes arranged along the length of the system at one side of the central cross section, as shown in Fig. 2. The electrodes are $2 \times 8\ \text{cm}^2$ in size and are at a distance of 10 mm from the walls of the chamber. In order to keep the electrodes from protruding beyond the walls of the chamber, they are inserted in windows in a wide guard plate (150 mm) which is bent to follow the shape of the chamber and which is 10 mm from the walls. A bias of − 20 v is applied to the electrodes; this bias is sufficient to prevent plasma electrons from reaching the electrodes.

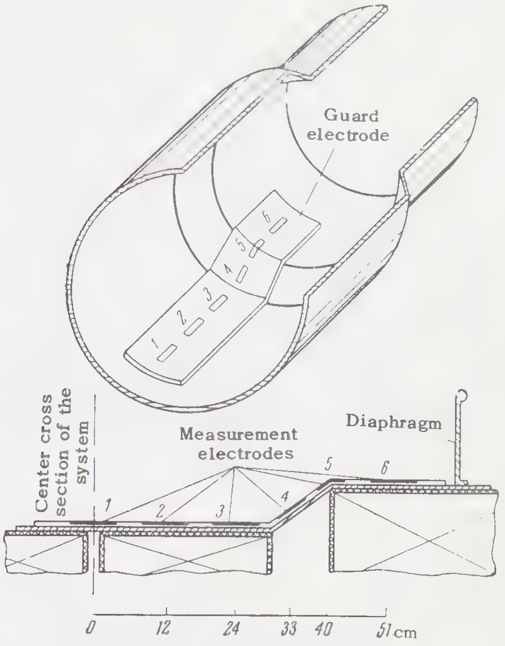

FIG. 2. Electrodes for measuring the ion current at the side walls of the system.

The particle flux at the side walls consists of fast ions and fast neutral particles (the slow ions can be neglected for reasons which have been indicated earlier). Secondary electrons can be emitted at any or all of the electrodes, depending on the orientation of a given electrode with respect to the magnetic field. Thus, in determining the number of fast ions which escape from the system at the side walls, we must subtract off the part due to secondary electrons from the total charge measured by the electrodes.

To estimate the number of secondary electrons roughly we assume that secondary emission due to fast ions and fast neutral particles occurs only at electrodes 4 and 5 (Fig. 2) since these are at large angles with respect to the lines of force of the magnetic field (for $\alpha \leq 1.55$); we assume that the charge at electrodes 1, 2 and 3 is due to fast ions only, while the charge at electrodes 4 and 5 is due to fast ions and secondary electrons. (In all cases no charge is measured at electrode 6.)

Table III. Number of fast ions escaping at the side walls for different values of the mirror ratio

α	1.33	1.55	2.0	2.35
10^6 Q^+_{fast}, Coul.	0.83	1.8	4.4	5,8
10^6 Q, Coul.	1.9	5,3	16.3	23.2
q_{side}, percent	43	34	27	25

Thus, by measuring the charges $q_{1,2,3}$ at electrodes 1, 2, and 3, and $q_{4,5}$ at electrodes 4 and 5, and finding the total number of fast neutral particles formed during the plasma decay time Q^0_{ce} (from the amount of charge exchange), we determine the number of fast ions q^+_{fast} at the electrodes:

$$q^+_{\text{fast}} = q_{1,2,3} + (q_{4,5} - Q^0_{\text{L}} \cdot 1{,}6 \cdot 10^{-3} k)/(1 + k), \quad (1)$$

where k is the secondary emission coefficient and the factor 1.6×10^{-3} is introduced to take account of the fast neutral particles which strike electrodes 4 and 5. (It is assumed that the fast neutral particle flux at the side walls is distributed uniformly over the length of the system.)

The charge at the side-wall electrodes is measured in the same way as the charge at the end electrodes. The quantity q^+_{fast} is found from Eq. (1) under the assumption, as before, that the secondary emission coefficient is unity. The number of fast ions striking the side wall of the system Q^+_{fast} is obtained by multiplying q^+_{fast} by the ratio of lateral surface of the system to the total area of the measurement electrodes.

In Table III we show the values of Q^+_{fast} obtained for the same values of magnetic field, accelerating voltage, pressure, and mirror ratio as for the measurements of ion loss at the ends. We also show the charge due to fast ions Q which escape from the system by virtue of the supplementary loss mechanism, as well as the ratio of these quantities q_{side}. It is apparent from the table that up to 40% (depending on α) of the fast ions which escape from the system (because of the supplementary loss mechanism) do so at the side walls.

A comparison of the charges measured separately at each of the five electrodes shows that the ion losses at the side walls are not uniform over the length and that the loss distribution depends on the mirror ratio. As expected, the majority of ions escape at those portions of the loss surface which intersect the lines of force which are close to the axis of the system. For mirror ratios of 1.33 and 1.55 these regions are the points at which the chamber is constricted, where electrodes 4 and 5 are located. At higher mirror ratios ($\alpha = 2.0$ and 2.35) the lines of force touch the walls at the central cross section of the system and accordingly the largest part of the loss occurs in the region in which electrodes 1 and 2 are located.

The values of q_{end} and q_{side} obtained by comparison of the fast-ion charge measured at the ends and at the side walls, and the fast ions lost to the system because of the supplementary loss mechanism, are not very accurate. The principal error is the uncertainty in the number of fast ions in the system at the end of the acceleration-voltage pulse. This quantity is determined from the mean density of the fast ions at the central cross section (the cross section at which the neutral particle detector is located) and it is tacitly assumed that the density is the same over the entire length of the system. The total number of ions in the system is actually smaller than the number obtained in this way because of the lower density of charged particles in the high-field regions (mirrors). The fact that the exact value of the secondary emission coefficient is not known introduces an additional error. Because of these errors, the measurements carried out at the ends and at the side walls under identical conditions give values of q_{end} and q_{side} whose sum is less than 100%.*

It should be kept in mind, however, that the uncertainties in q_{end} and q_{side} due to these errors are the same for both quantities. Hence, we can compare the ratios $q_{\text{end}}/(q_{\text{end}} + q_{\text{side}})$ and $q_{\text{side}}/(q_{\text{end}} + q_{\text{side}})$, which characterize the relative ion losses at the ends and at the side walls. A comparison of this kind, made on the basis of the data in Tables I and III, shows that for $H_0 = 5000$ oe, $p = 1 \times 10^{-6}$ mm Hg and $U_0 = 30$ kv, not less than 80% of the ions lost at the walls of the system escape across the magnetic field and are lost at the side walls; correspondingly, no more than 20% of the ions escape along the magnetic field to the ends. This ratio between the ion losses transverse to the field and along the field is found at all mirror ratios.

Similar measurements of the ion losses at the ends and at the side walls have been carried out for $H_0 = 8000$ oe, $U_0 = 30$ kv, $p = 1 \times 10^{-6}$ mm Hg, and $\alpha = 1.33$ and 1.55. The analysis of the results of these measurements is more complicated; when $H_0 = 8000$ oe the measured charge may contain a

---

*The sum $q_{\text{end}} + q_{\text{side}}$ decreases with increasing mirror ratio α (cf. Tables I and III), because in finding the total number of ions in the system we do not take account of the contraction of the region occupied by the plasma when the mirror ratio is increased.

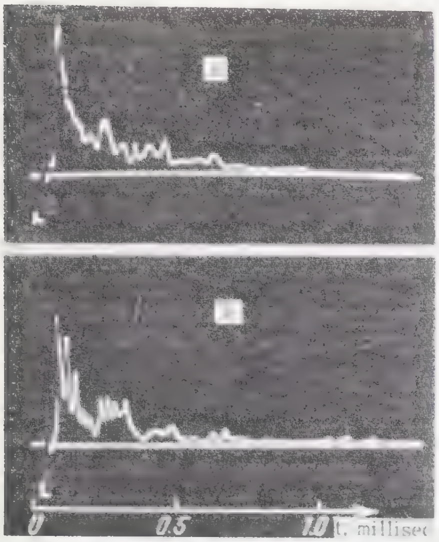

FIG. 3. Oscillograms of the current. a) at the comb electrode in the mirror and b) at the side walls.

considerable slow-ion component because charge-exchange becomes the predominant source of loss. Nonetheless, at this field we also find qualitatively that most of the fast ions move across the magnetic field in escaping from the system.

TIME VARIATION OF THE ION CURRENT AT THE WALLS

Oscillograms of the ion current at the wall electrodes show that this current is highly modulated by irregular fluctuations; the phase and amplitude of the fluctuations are both irregular. Typical oscillograms of the current at individual electrodes in the mirrors and in the side walls are shown in Fig. 3. These oscillograms would seem to indicate that the mechanism responsible for the escape of ions from the system is nonstationary. In this connection it is important to note that the depth of modulation depends on the area of the electrode at which the ion current is measured.

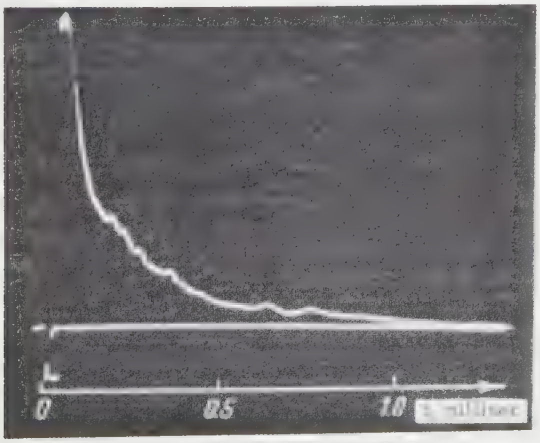

FIG. 4. Oscillogram of the current at the sector electrode.

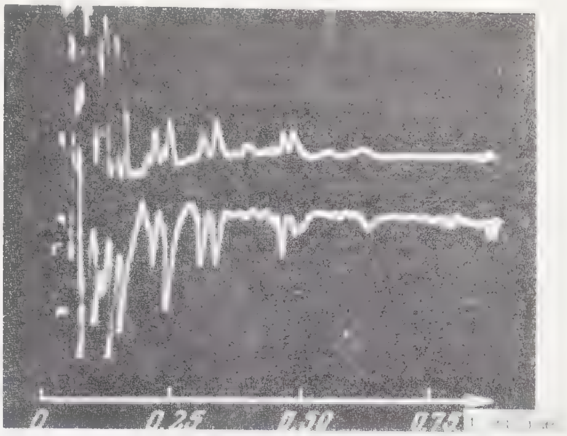

FIG. 5. Oscillograms of the current at electrodes 1 and 5, located at the side walls of the chamber.

In Fig. 4 we show an oscillogram of the current to the isolated sector located at the same diaphragm as the comb electrodes. It is apparent that the current modulation at the sector is much weaker than that at an individual comb electrode. This means that the plasma perturbations responsible for the observed fluctuations do not arise over the entire volume of the plasma simultaneously, but are localized in separate regions; moreover, the transverse dimensions of these regions (perpendicular to the magnetic field) are appreciably smaller than the transverse dimensions of the system.

The longitudinal dimensions of these regions can be investigated by making simultaneous oscillograms of the current at different electrodes located along one of the lines of force. In Fig. 5 we show an oscillogram of the current at electrodes 1 and 5 located at the side walls of the chamber; electrode 1 is located at the central cross section of the system while electrode 5 is at a distance of 400 mm; this distance represents $^2/_3$ of the distance from the central cross section to the region of maximum mirror field (cf. Fig. 2). At the cross section at which electrode 5 is located the mirror ratio is 1.33; the maximum mirror ratio is 1.55.

It is apparent from the oscillogram that the current fluctuations at these electrodes are synchronous; we may also note a distinct correlation in the amplitudes of the individual maxima. On the basis of these results we can conclude that the plasma perturbations extend along the magnetic field over the entire length of the system.

CONCLUSION

The anomalously rapid loss of plasma from a mirror system, which has been observed earlier[1] in measurements of the fast ion lifetime, has been verified in the present work through a study of ion losses at the walls of the system. Direct measurements of the ion current at the walls have shown that the greatest part of these losses (at least 80%) is due to the escape of ions at the side walls of the system (perpendicular to the magnetic field); no more than 20% of all the ions lost from the system escape through the mirrors (along the magnetic field). The process in which the charged particles escape from the system is a nonstationary one. Fluctuations in the current at electrodes located at the ends of the system and at the side walls show that the charged particles are ‘‘expelled’’ from separate regions which are not connected; these regions are small in the direction perpendicular to the magnetic field as compared with the transverse dimensions of the system, and extend over the entire length of the system in the direction of the field.

The way in which the charged particles escape would seem to indicate that in the experiments described here the plasma containment time is limited by a flute type instability, inherent to the convex magnetic-field configuration.

---

[1] Ioffe, Sobolev, Tel'kovskiĭ, and Yushmanov, JETP **39**, 1602 (1960), Soviet Phys. JETP **12**, 1117 (1961).

[2] V. G. Tel'kovskiĭ, Dissertation, Moscow State University, 1959.

Translated by H. Lashinsky
8

SOVIET PHYSICS JETP VOLUME 13, NUMBER 1 JULY, 1961

MEASUREMENT OF THE SPIN-LATTICE RELAXATION TIME IN COMPOUNDS WITH STRONG COVALENT BONDING

P. P. PASHININ and A. M. PROKHOROV

P. N. Lebedev Physics Institute, Academy of Sciences, U.S.S.R.

Submitted to JETP editor July 22, 1960

J. Exptl. Theoret. Phys. **40**, 49-51 (January, 1961)

The spin-lattice relaxation time T_1 for Fe^{3+} and Cr^{3+} ions in $K_3(Fe, Cr)(CN)_6$ was measured by the methods of pulsed and continuous saturation. For Fe^{3+} concentrations of 0.1 and 0.21% the relaxation time T_1 was found to be independent of concentration in the temperature range from 2.1 to 40°K and equal to $0.64\,T^{-5}$ sec. The experiment shows in a qualitative way that there is a strong cross relaxation between the lines from the two non-equivalent ions. The measurements of T_1 for Cr^{3+} also indicate the existence of cross relaxation.

INTRODUCTION

THE study of spin-lattice relaxation has received a new impetus in connection with the development of quantum paramagnetic amplifiers. Several series of experiments[1-4] on spin-lattice relaxation point to an anomaly which cannot be explained by the existing theory. Some effects observed in the work of Giordmaine et al.[3] were explained by the existence of cross relaxation.[5] We wished to study spin-lattice relaxation in the simplest system having two levels without hyperfine structure.

For this purpose we chose Fe^{3+} ions in the compound $K_3Fe(CN)_6$ with strong dilution by Co^{3+} ions. Because of the considerable convalent bonding the Fe^{3+} ion has an effective spin $S = 1/2$.

We studied crystals with different relative concentrations of Fe and Co, namely 1 : 1000 and 2.1 : 1000. Baker et al.[6] have studied the spectrum of $K_3Fe(CN)_6$ at $T = 20$°K. They showed that there are two magnetically non-equivalent Fe^{3+} ions and gave the values of the g factors. In our experiments we aimed to have the lines from the two non-equivalent ions coinciding.

We used both the continuous saturation and the pulse methods to investigate spin-lattice relaxation.

Figure 1 shows the block diagram of the spectroscope used. The klystron K_1 operated under pulsed conditions, giving 25 μsec pulses with a rise time of < 1 μsec at a repetition rate of 100 to 0.1 cps. The power of 1.5 w in the pulse was quite sufficient to achieve appreciable saturation during the period of the pulse. The rest of the apparatus consists of a superheterodyne spectroscope working on the low power level of the signal klystron K_2 at a frequency of 9400 Mc/sec. For measurements by the continuous saturation method, klystron K_1 operates under CW conditions and the power at which saturation is reached is fed to the power measurer LPM through the waveguide directive feed. A relaxation curve for Fe^{3+} is shown in Fig. 2.

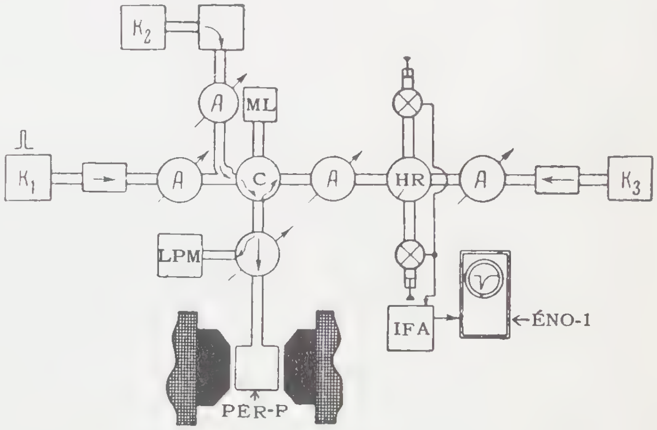

FIG. 1. Block diagram of spectroscope for measuring the spin-lattice relaxation time by the pulse method. K_1, K_2, K_3 – klystrons. A – attenuator. LPM – lower power meter. ML – matched load. C – circulator. HR – hybrid ring. R – resonator. IFA – intermediate frequency amplifier. ÉNO-1 – oscillograph.

EXPERIMENTAL RESULTS

The spin-lattice relaxation time T_1 at 4.2°K, measured for both Fe^{3+} concentrations by the pulse method, was found to be $(4.9 \pm 0.4) \times 10^{-4}$ sec. The corresponding spin-spin relaxation times T_2 are 1.4×10^{-8} and 0.66×10^{-8} sec. The continuous saturation method, the accuracy of which is lower, gave good agreement with these data. At 2.1°K, T_1 for both concentrations is $(1.6 \pm 0.2) \times 10^{-2}$ sec. Examination of the relaxation curve showed it

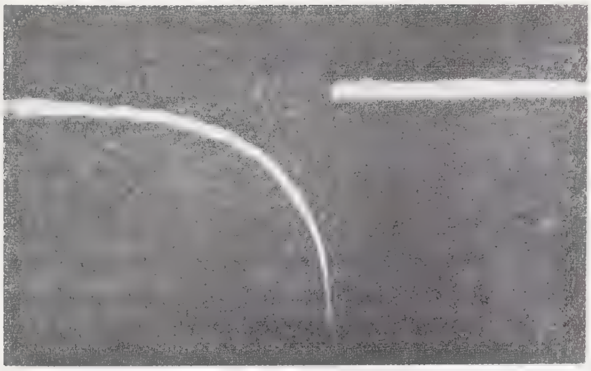

FIG. 2. Oscillogram of relaxation curve of the Fe^{3+} ion.

to be exponential with a single characteristic time, as expected for a two-level system.

It follows that at helium temperatures the spin-lattice relaxation time is independent of concentration for the Fe^{3+} ion concentrations studied, and is inversely proportional to the fifth power of the temperature. Such a strong temperature dependence of T_1 indicates that second-order processes are dominant at liquid helium temperatures. We measured the line width for the 0.21% specimen between 4.2 and 40°K to check the temperature dependence of T_1 at higher temperatures. Between 2.1 and 19°K the line width does not change, showing the small contribution of spin-lattice interaction to the line width. The width rapidly increases above 20°K, owing to the decrease in T_1 and the corresponding contribution of spin-lattice interaction to the overall line width. The relaxation time T_1 calculated from the line width also follows a T^{-5} law up to 40°, where the line is very strongly broadened and becomes difficult to observe.

Thus from 2.1 to 40°K, T_1 is independent of concentration and is given by

$$T_1 = 0.64\, T^{-5} \quad \text{sec}.$$

A preliminary study by the pulse method of the influence of cross relaxation between the two lines from non-equivalent ions did not yield results. This is probably due to the short cross-relaxation time. We therefore carried out another experiment to determine qualitatively whether there is cross relaxation in the present case. For this, a specimen with a Fe^{3+} ion concentration of 0.46% and 24 oe line width was placed in the resonator in which two types of wave were excited, differing in frequency by 300 Mc/sec (reference 2). The specimen was oriented in such a way that the distance between the lines from the two non-equivalent ions was also 300 Mc/sec, so that both lines were observed simultaneously on two spectroscopes on modulating the frequency. One of the lines was saturated and the behavior of the other studied. At the orientation mentioned, when the distance between the lines was approximately four line widths, the lines are saturated together.

It requires a much larger power to achieve an analogous saturation of the line using a klystron at the same frequency difference. This indicates the existence of cross relaxation.

We also carried out a preliminary study of the relaxation processes in $K_2Cr(CN)_6$ with a 0.24% Cr^{3+} concentration. The constant magnetic field was directed along the z axis in the crystallographic ac plane and the $2 \leftrightarrow 3$ transition was studied by the pulse method. It appeared that the relaxation curve at 4.2 and 2.1°K can be represented quite accurately by the sum of two exponentials with very different relaxation times. One exponential time is independent of temperature and is 4.5×10^{-4} sec, while the other is inversely proportional to temperature and is 1.9×10^{-3} sec at 4.2°K. We are certainly concerned here with cross relaxation, the existence of which was indicated in earlier work.[2,4,7,8] Such a rapid cross relaxation is evidently connected, on the one hand with the fairly large concentrations and on the other with the fact that for the given orientation the frequency of the $3 \leftrightarrow 4$ transition is almost exactly half the frequency of the $2 \leftrightarrow 3$ transition. The pulse method, using short saturating pulses, can certainly give much more information about rapid cross relaxation processes than a method using long pulses.

In conclusion, the authors express their thanks to R. P. Bashuk and A. S. Bebchuk for providing the crystals used in this work.

---

[1] A. A. Manenkov and A. M. Prokhorov, JETP **38**, 729 (1960), Soviet Phys. JETP **11**, 527 (1960).

[2] G. M. Zverev and A. M. Prokhorov, JETP **39**, 545 (1960), Soviet Phys. JETP **12**, 382 (1961).

[3] Giordmaine, Alsop, Nash, and Townes, Phys. Rev. **109**, 302 (1958).

[4] van der Marel, van den Broek, and Gorter, Physica **23**, 361 (1957).

[5] Bloembergen, Shapiro, Pershan, and Artman, Phys. Rev. **114**, 445 (1959).

[6] Baker, Bleaney, and Bowers, Proc. Phys. Soc. **B69**, 1205 (1956).

[7] S. Shapiro and N. Bloembergen, Phys. Rev. **116**, 1453 (1959).

[8] B. Bölger and B. J. Robinson, Physica **26**, 133 (1960).

Translated by R. Berman
9

SOVIET PHYSICS JETP VOLUME 13, NUMBER 1 JULY, 1961

MAGNETIC PROPERTIES OF THIN SUPERCONDUCTING TIN AND INDIUM FILMS

B. K. SEVAST'YANOV

Submitted to JETP editor July 23, 1960

J. Exptl. Theoret. Phys. (U.S.S.R.) 40, 52-63 (January, 1961)

The conditions under which there is no normal phase in a finite size superconducting film placed at a small angle to a uniform magnetic field are determined. The torques acting on such a film are measured. The dependence of the transverse component of the magnetic moment M on temperature and thickness is determined for tin and indium films 4×10^{-3} to 2×10^{-6} cm thick. The critical field values derived from these measurements are analyzed.

INTRODUCTION

ALTHOUGH the magnetic properties of thin superconducting layers are of considerable interest in the theory of superconductivity (see, for example, references 1 — 3), they have not been investigated experimentally to any extent. There is only one paper[4] reporting the measurements of the magnetic moments of a stack of superconducting films, the thinnest of which were 3.7×10^{-5} cm thick. We know of no study of the magnetic moments of thinner films.

One of the main difficulties in setting up such experiments lies in the following. The magnetic moment investigated in the theory is that of an infinite layer in a parallel field. In the experiment, however, the measurements must be carried out on films of finite dimensions, which are only approximately parallel. A case close to that considered theoretically can be realized by measuring the longitudinal component $M_{\parallel}$ of the magnetic moment in a field parallel to the surface of the film. It is practically impossible, however, to align the film perfectly parallel to the field, and therefore the magnetic moment $M_{\perp}$ normal to the surface of the layer will be different from zero and consequently, there will always exist the probability that the presence of $M_{\perp}$ affects the measurement results. Nor is it possible to calculate $M_{\perp}$, since its dependence on the temperature and on the thickness of the layer has been determined neither theoretically nor experimentally. A determination of this dependence is of interest in itself, since it will permit a considerable simplification in the experimental determination of the magnetic moments of superconducting films, for the difficult measurement of $M_{\parallel}$ is replaced by a measurement of $M_{\perp}$.

To determine $M_{\perp}$ we measured the torque acting on a layer placed at a small angle, $\varphi \approx 10^{-3} - 10^{-4}$ rad with the direction of the uniform magnetic field. The torque K is given by

$$K = \tfrac{1}{2}(\chi_{\parallel} - \chi_{\perp})\, vH^2 \sin 2\varphi, \qquad (1)$$

where $\chi_{\parallel}$ and $\chi_{\perp}$ are the magnetic susceptibilities of the film in a parallel and a perpendicular field, respectively; the susceptibility is defined as $\chi = M/H$, H is the external field, and v is the volume of the layer. For a "bulky" ($d \gg \delta$) superconducting layer of thickness d (δ is the depth of penetration of the magnetic field in the superconductor) the inequality $\chi_{\perp} \gg \chi_{\parallel}$ holds true. In this case the torque is determined only by the transverse component of the magnetic moment $M_{\perp} = \chi_{\perp} vH \sin \varphi$. Consequently, apart from the sign, we have

$$M_{\perp} = 2K / H \cos\varphi \qquad (2)$$

We can expect the dependence of $M_{\perp}$ on the temperature and on the thickness to be substantially different for bulky layers and thin ($d \lesssim \delta$) films. If a bulky layer is in the form of a round disc of diameter D, the vanishing of the field in the layer causes the expression for $M_{\perp}$ to be independent of d, namely[5]

$$M_{\perp} = (1/12\pi)\, HD^3 \sin\varphi. \qquad (3)$$

On the other hand, the field in a sufficiently thin film should be different from zero (see, for example, reference 6). Its intensity is determined by the ratio δ/d, and $M_{\perp}$ can be expected to depend on the thickness and on the film temperature. Although the truth of the inequality $\chi_{\perp} \gg \chi_{\parallel}$ is not as evident for thin films as it is for bulky superconductors, this inequality apparently remains valid in a certain thickness range. We therefore determined the value of $M_{\perp}$ for films, as for bulky layers, from formula (2).

In the investigation of the magnetic properties of superconducting films, there is always the danger that the film contains domains of the normal phase. If it is assumed that the film can be approximated

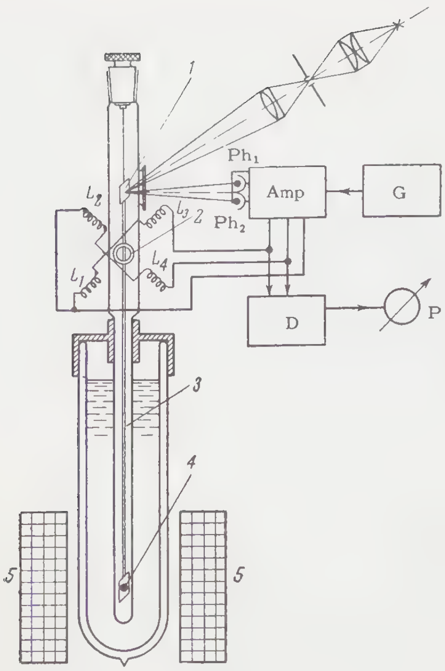

FIG. 1. Diagram of the apparatus: 1 – mirror, 2 – aluminum ring, 3 – glass rod, 4 – sample, 5 – magnet, Amp – amplifier, G – generator, D – detector, P – type KL-48 potentiometer with type M25/3 galvanometer.

by a flat ellipsoid of revolution, one of the axes of which is small, we can, in analogy with a bulky superconductor, write the condition for the absence of a normal phase in the following form:[6]

$$H_{\perp}/(1-N) \leqslant H_{\mathrm{cr}}, \tag{4}$$

where H_{cr} is the critical field and $H_{\perp}$ is the magnetic field component perpendicular to the surface of the film, equal to H sin φ. Taking into account the value of the demagnetizing factor N for a layer in the form of a round disc,[5] we obtain the following condition for the absence of normal phase in the layer

$$\varphi_0 \leqslant \tfrac{1}{2}\pi (d/D)(H_{\mathrm{cr}}/H). \tag{5}$$

If the angle between the film and the field is less than φ_0, it can be assumed that the film is wholly in the superconducting state.

EXPERIMENTAL PROCEDURE AND SAMPLES

The torque K was measured with a magnetic torsion balance[1] with feedback, described in detail elsewhere.[8] A block diagram of the apparatus is shown in Fig. 1. A glass rod 3 (diameter ~ 1 mm) carries the sample 4 and a light aluminum ring 2. The latter is located in an alternating magnetic field (10 kc/sec) produced by two pairs of coils $L_1 - L_4$, fed in phase with alternating current. The coils are so arranged that the field vector of one pair is perpendicular to that of the other. The plane of the ring is parallel to the direction of the resultant field. When the amplitude of the field of one of the coil pairs is changed, the vector of the resultant field rotates and causes the ring to turn. The amplitude of the field in each pair of coils is determined by the illumination of photocells Ph_1 and Ph_2, and depends on the position of mirror 1. If no torque acts on the suspension system, the illumination from the diaphragm of the light-source is equally distributed between the photocells; the amplitudes of the magnetic fields are equal and no torque acts on the ring. Once a force couple is applied to the sample, the photocell illumination changes, and the resultant torque on the ring is used to cancel out the torque of the sample. If the system parameters are suitably chosen, the angle between the field and the film remains practically constant during the measurements. The accuracy of the position of the film in the field is 5×10^{-5} rad. What is measured is the feedback current, which depends in such a system linearly on the torsion force acting on the suspension. Such a magnetic balance can measure torques ranging from 5×10^{-5} to 4 dyne-cm.*

The homogeneous magnetic field was produced by air-core coils. The earth's magnetic field was canceled out accurate to approximately 1%. The temperature was determined from the vapor tension of helium.

The samples were films of tin and indium (the purity of the original metal was 99.995 and 99.992%, respectively) obtained by evaporation in vacuo (~ 10^{-7} mm Hg). A special evaporator was used. The films were condensed on a substrate cooled with liquid nitrogen. The substrates were flat optically polished quartz plates measuring 15 × 10 × 1.5 mm. The substrate was covered with a shield to produce a film in the form of a circular disc. The disc diameters were chosen, in accordance with the film thickness, to satisfy condition (5) and ranged from 0.5 to 0.05 cm.

The magnetic moments of films ~ 10^{-5} cm thick were measured with discs of diameter D = 0.2 – 0.3 cm. Smaller values of D were used for thinner films. Since the torque K decreases with decreasing disc diameter, several discs were condensed on the substrate whenever d was less than 0.2 cm, to obtain measurable torques. The thinnest films measured ($d \approx 3 \times 10^{-6}$ cm, D = 0.05 cm) were condensed through a screen with round holes spaced more than 2D apart.

---

*This procedure is a further development of the method used by Alekseevskiĭ[7] to measure the critical fields of superconducting films.

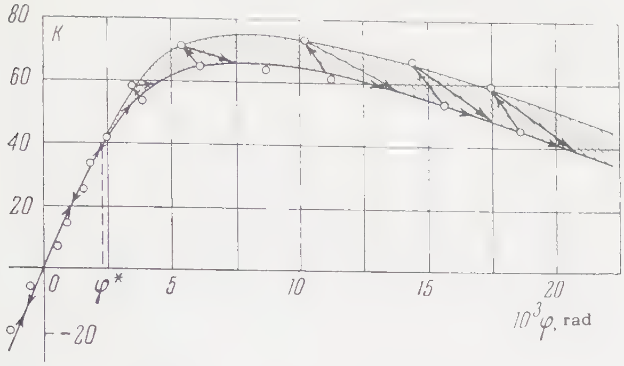

FIG. 2. Dependence of the torque K on the angle φ for a tin film: d = 1 × 10^{-5} cm, D = 0.06 cm, T = 3.65° K, H_0 = 30 oe. The values of K are given in units proportional to the galvanometer deflection.

The films were evaporated at a rate $\sim 10^{-5}$ cm^3/min. The layers had a mirror surface down to thicknesses of $\sim 1\mu$, and disclosed no surface defects when viewed under a microscope with magnification × 1500. It should be noted that in individual cases the evaporation rate was $10^{-2} - 10^{-3}$ cm^3/min, in order to study the effect of film structure on the magnetic properties. The surfaces of such films were granular. The condensed film was heated to room temperature and transferred to the measuring instrument. Its stay in air did not exceed 10 or 15 minutes. The bulky layers used were foils 5 — 40 μ thick, produced by rolling.

MEASUREMENT RESULTS

Before starting the measurements of the magnetic moment, the films were oriented in the field. For this purpose the nature of the dependence $K(\varphi)$ was determined (Fig. 2). Its linearity in the range of small angles made it possible to establish a film position parallel to the field with great accuracy, and to maintain an angle $\sim 10^{-3} - 10^{-4}$ rad during the measurements. It is seen from the figure that no hysteresis is observed in the linear portion of the $K(\varphi)$ curve. This proves that there are no domains of the normal phase in the film when $\varphi < \varphi^*$ (Fig. 2). The value of φ^* for all the investigated films was of the same order of magnitude as the values of φ_0 given by formula (5).

The value of $M_\perp$ for bulky superconducting layers[*] increases linearly with increasing field, up to values close to H_{cr} (see Fig. 3[*]). The value of $M_\perp$ is determined by the cube of the disc diameter, in accordance with formula (3).[†] The loss of superconductivity of bulky layers occurs abruptly, so that the curve representing this loss occupies a field interval amounting to a fraction of an oersted. As the field is decreased from $H > H_{cr}$, the magnetic-moment curve is duplicated, that is, the field is crowded out from the layer (Meissner effect).[‡]

It was noted earlier that in sufficiently thin films one can expect $M_\perp$ to depend on the film temperature and on the thickness. However, as can be seen from Figs. 4 — 6, no dependence of $M_\perp$ on these parameters is observed, although the thickness of the films in Figs. 4 and 5 is comparable with δ, and in the case corresponding to Fig. 6 it is less than δ. The value of $M_\perp$ for thin films in weak fields is found to be the same as that for bulky layers (Fig. 3), and is determined by formula (3).

The dependence of $M_\perp$ on the temperature has been observed only in films only several times 10^{-6} cm thick. Here, apparently, the size of the disc diameter D becomes important. Thus, at D = 0.05 cm, a temperature dependence is observed in the initial slope of the magnetization curves only for films with $d \leq 3 \times 10^{-6}$ cm. For smaller values of D, a temperature dependence of $M_\perp$ is observed also in thicker films. The initial slope of the magnetic moment curves increases with decreasing temperature, in the case of films with $d \approx 3 \times 10^{-6}$ and D = 0.05 cm, in the temperature interval $\Delta T = T_{cr} - T \approx 1°$ K, after which $M_\perp$ reaches the same value as for a bulky layer. Figure 7 shows the experimental points obtained in some experiments for a tin film.

The appearance of domains of normal phase in films can be readily noted by controlling the occurrence of hysteresis in the magnetic field. A typical hysteresis picture is shown in Fig. 8. The hysteresis always takes place when the $M_\perp(H)$ curve deviates from linear. As can be seen from Figs. 4 — 7, such a deviation takes place in fields

---

[*] The measurements of the magnetization curves at a given temperature were made only after the sample was heated (by light from a special illuminator) to a temperature above critical and was made superconducting in the absence of the field.

[*] Since the magnetization curves of tin and indium films of equal thickness are similar, $M_\perp(H)$ is plotted for indium films in Fig. 5 only. In all other cases the curves pertaining to indium films have been omitted to save space.

[†] To facilitate comparison of the magnetic moments of films with different values of D and measured at different angles φ, the quantity $M_\perp^* = M_\perp/D^3 \sin\varphi$ is shown in Fig. 3, and in Figs. 4–10 later on, in a certain arbitrary scale, which is, however, the same for all plots.

[‡] The supercooling that takes place on the layers is not considered in the present work.

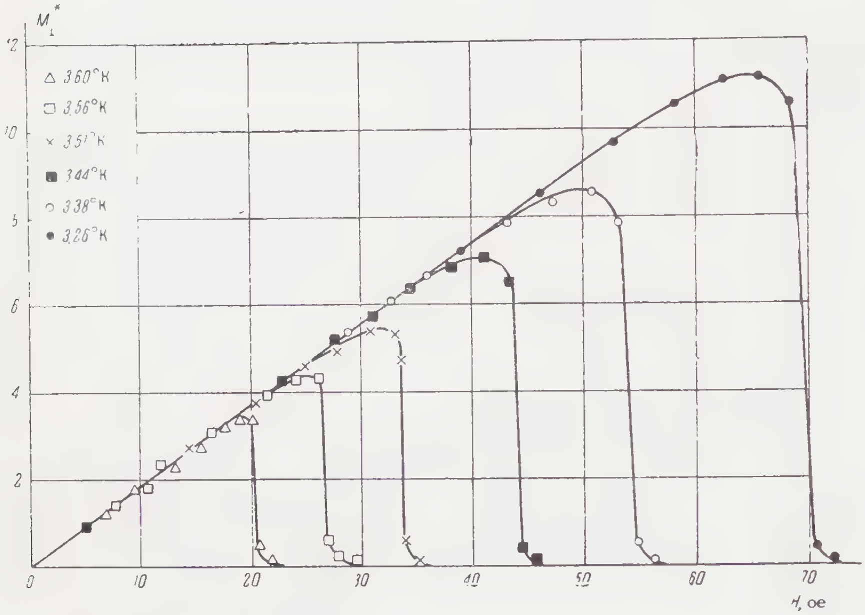

FIG. 3. Magnetization curves of tin foil: d = 4 × 10^{-3} cm, D = 0.5 cm, $\varphi = 1 \times 10^{-3}$ rad, T_{cr} = 3.73° K. Here and elsewhere $M_\perp^* = M_\perp / D^3 \sin\varphi$.

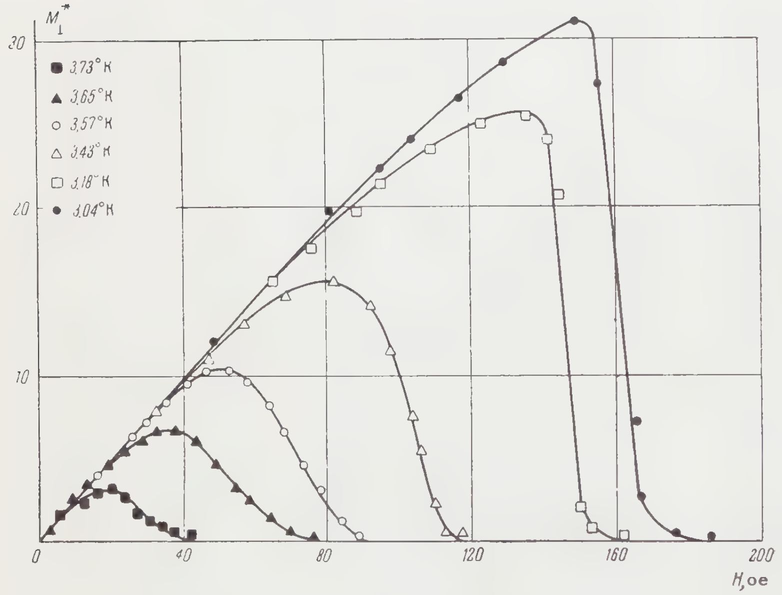

FIG. 4. Magnetization curves of tin film: d = 3 × 10^{-5} cm, D = 0.1 cm, T_{cr} = 3.81° K, $\varphi = 1 \times 10^{-3}$ rad.

considerably below H_{cr}, even when the ratio D/d does not exceed 10^3 and the film makes an angle less than 10^{-3} rad with the field. It is found here that the external field in which the normal phase is produced in the film is of the same order of magnitude as given by (5).

If the geometrical dimensions of the film and the angle φ are such that double connectivity takes place even in weak fields, the magnetic-moment curves are as shown in Fig. 9. Their initial slope has in this case a temperature dependence. However, unlike the films of Figs. 4 — 7, hysteresis takes place even on the linear portions of the curves. This shows that the temperature dependence of the initial slope of the magnetic-moment curve is due in this case only to the temperature variation of the geometric parameters of the superconducting loop produced in the film, and is not connected with the depth of penetration δ. Thus, the presence of domains of normal phase in the film is always accompanied by hysteresis. The absence of hysteresis on the initial portion of the curves of the magnetic moment $M_\perp$ was therefore watched with particular care in all the measurements.

The magnetic properties of films depend appreciably on the structure of their surface. Thus, the absence of temperature dependence in the initial slope of the $M_\perp(H)$ curves for layers with $d > 3 \times 10^{-6}$ cm occurs only for films with mirror surface, in which no defects are seen under a microscope with magnification ~ 1500. On the other

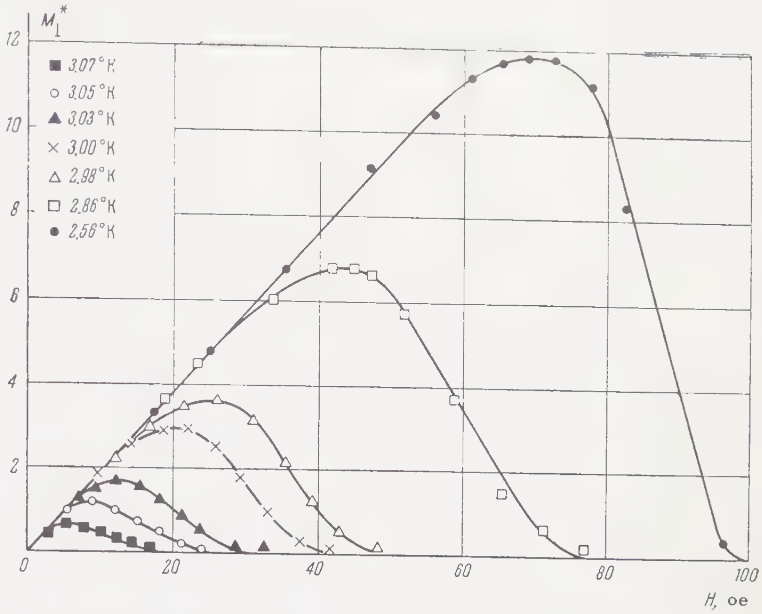

FIG. 5. Magnetization curves of indium films: $d = 3 \times 10^{-5}$ cm, $D = 0.1$ cm, $T_{cr} \approx 3.10°$ K, $\varphi = 1 \times 10^{-3}$ rad.

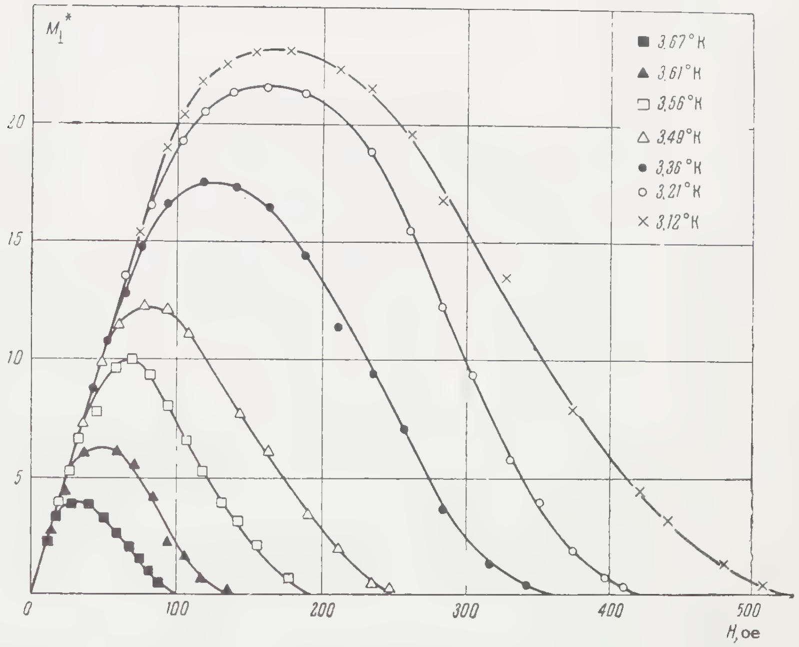

FIG. 6. Magnetization curves of tin films: $d = 1.2 \times 10^{-5}$ cm, $D = 0.06$ cm, $T_{cr} = 3.77°$ K, $\varphi = 4 \times 10^{-4}$ rad.

hand, films with granular surfaces display a temperature dependence of the initial slope of the magnetization curves (Fig. 10) even when $d > 10^{-5}$ cm. In this case there is no hysteresis in the linear portions of the curves. The increase in the moment $M_\perp$ with decreasing temperature takes place in an interval $\Delta T \approx 0.1°$K. The value of $M_\perp$ at the lowest temperature is somewhat lower than would follow from (3).

The form of the magnetic-moment curves (Figs. 3 — 7) depends on the ratio d/d_{cr}, where d_{cr} is the "critical thickness," defined in the Ginzburg-Landau theory as $d_{cr} = \sqrt{5}\,\delta$ (Fig. 11). In the case when $d > d_{cr}$ and the superconducting transition is a first-order phase transition, the loss of superconductivity occurs abruptly. The magnetic-moment curve has in this case a sharp discontinuity at fields close to H_{cr}. On the other hand, when $d < d_{cr}$, there are no sharp breaks in the curve to evidence any supercooling. One can therefore conclude that in films with $d < d_{cr}$ the superconducting transition is apparently a phase transition of second order. It is interesting to note in this connection that the temperature dependence of the slope of the superconductivity-loss curves is observed only in films with thickness $d \approx d_{cr}$ (Figs. 4, 5).

The curves obtained for the magnetic moment enable us to determine the critical fields H_{cr} of the films.[7] The value of H_{cr} was determined by extrapolating the most steeply drooping portion of the superconductivity-loss curve to the field axis. This excludes the possibility of obtaining exaggerated

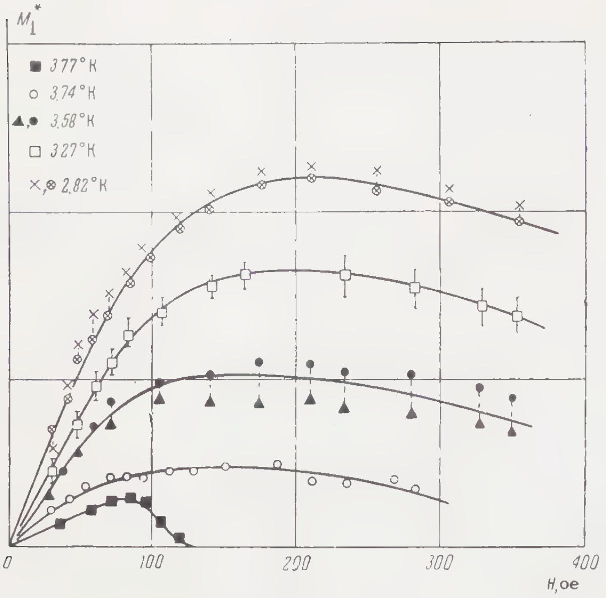

FIG. 7. Magnetization curves of a tin film with temperature dependent susceptibility; d = 2 × 10⁻⁶ cm, D = 0.05 cm, φ = 2.5 × 10⁻⁴ rad, T_{cr} = 3.78° K.

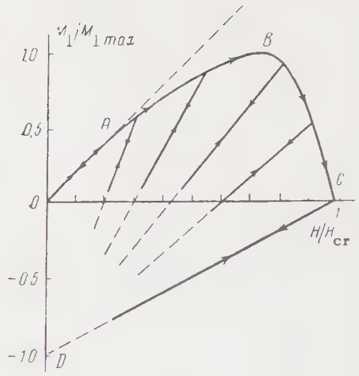

FIG. 8. Typical picture of hysteresis phenomena in thin superconducting films.

values of H_{cr} as a result of stresses in the film. The value of dH_{crb}/dT, determined in this manner for a bulky layer of tin ($d = 4 \times 10^{-3}$ cm) amounts to 151 oe/deg, which is in good agreement with the data given in the literature. The temperature dependence of H_{cr} is well described by the Ginzburg-Landau formulas:[9]

$$H_{cr}/H_{crb} = 2\sqrt{6}\,(\delta/d)\ \text{ for }\ d \ll \delta, \tag{7}$$

$$H_{cr}/H_{crb} = 1 + \delta/d\ \text{ for }\ d \gg \delta, \tag{8}$$

where $\delta = \frac{1}{2}\,\delta_0\sqrt{T_{cr}/\Delta T}$. As can be seen from Fig. 11, the experimental points fit the theoretical curves quite well. The value of δ_0 for tin films, determined from their critical fields by means of formulas (7) and (8), is found to be $(8.5 \pm 0.5) \times 10^{-6}$ cm. For indium films, $\delta_0 = (10 \pm 0.5) \times 10^{-6}$ cm.

As is well known,[10] at temperatures near T_{cr} tin is a "London" type metal, and the following relation should therefore be satisfied for tin films[11,12]

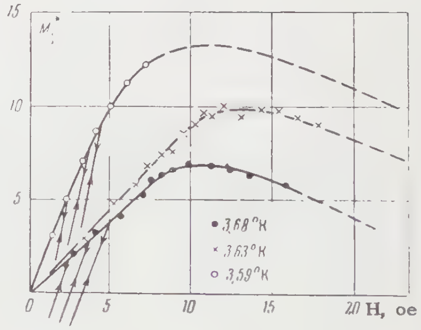

FIG. 9. Magnetization curves of films that do not satisfy condition (5); d = 1.3 × 10⁻⁵ cm, D = 0.7 cm, φ = 1.5 × 10⁻² rad.

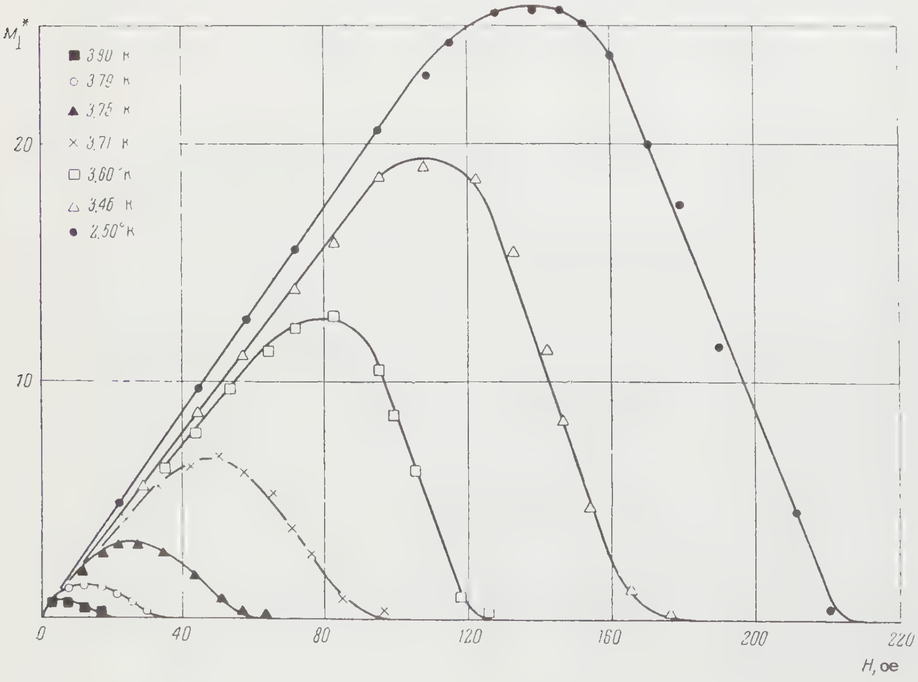

FIG. 10. Magnetization curves of a tin film with granular surface. The initial slope of the curves has a temperature dependence. d = 2.5 × 10⁻⁵ cm, D = 0.1 cm, φ = 1 × 10⁻³ rad, T_{cr} = 3.86° K.

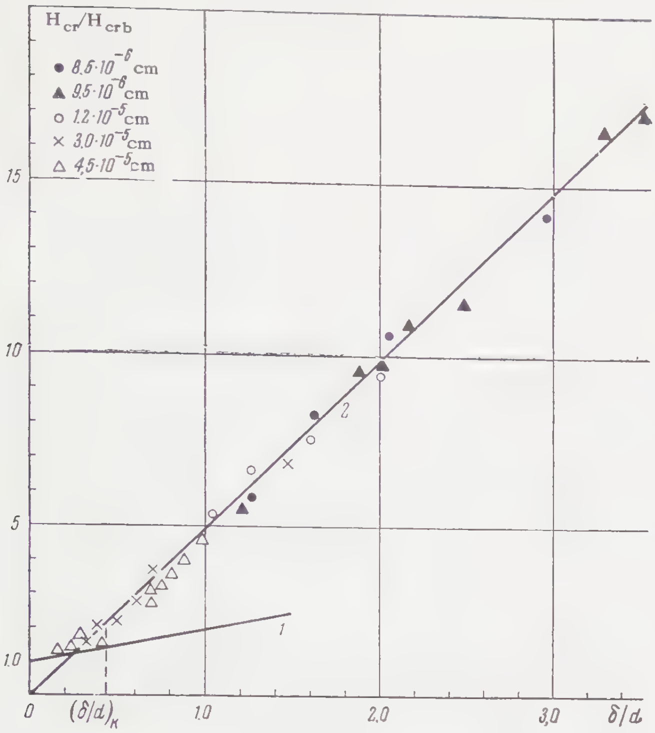

FIG. 11. Dependence of H_{cr}/H_{crb} on the ratio δ/d for tin films: curves 1 and 2 are based on formulas (8) and (7), respectively.

$$H_{cr} = \sqrt{6}\ (\delta_0/d)\sqrt{T_{cr}}\,|dH_{crb}/dT\,|\sqrt{\Delta T}. \qquad (9)$$

The dependence of H_{cr} on $1/d$ and on $\sqrt{\Delta T}$ was found to be linear (Fig. 12) for tin films. The indium films also display a linear dependence of H_{cr} on these parameters. The value of δ_0 determined for tin and indium films from (9) coincides with the values determined from formulas (7) and (8).

DISCUSSION OF THE RESULTS

Proceeding to analyze the results, we note that in our measurements φ amounted to $10^{-2} - 10^{-4}$ rad. Such an angle can readily arise in measurements of the magnetic moment $M_\perp$ in a parallel field. For example, one can assume that in the experiments by Lock[4] and Schawlow[13] the film was parallel to the field not closer than to within 10^{-3} rad, since neither the orientation of the films in the field nor the quality of the substrate surface were specially controlled. Consequently the data on the domains of normal phase in the films and on the character of the superconductivity-loss curves, obtained in the present investigation, can be said to pertain to films measured practically in a parallel field.

The results obtained show that normal-phase domains occur in films in fields considerably lower than H_{cr}, even when the linear dimensions of the film amount to a fraction of a millimeter, and $\varphi \approx 10^{-4}$ rad. Therefore, in investigations of $\delta(T)$ and in particular of $\delta(H)$ near H it is essential to ensure the absence of no normal-phase domains in the film. We note that in Lock's experiments the films were probably doubly-connected in fields close to H_{cr}, for the magnetization curves displayed hysteresis as the field was decreased from $H > H_{cr}$. However, the instants when the normal-phase domains were produced in the films was not checked in Lock's experiments.

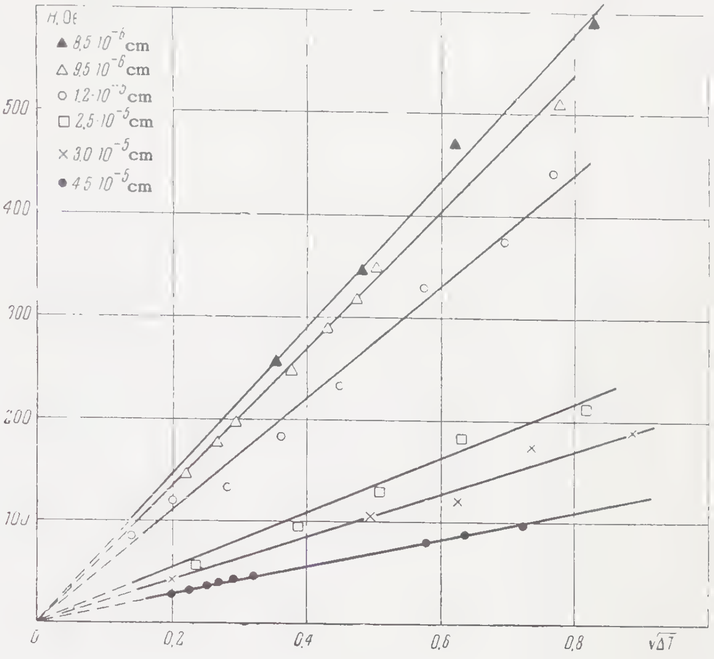

FIG. 12

In spite of the fact that the film thickness becomes comparable with the depth of penetration δ even when $d = (5-6)\times10^{-5}$ cm, a temperature dependence of $M_\perp$ is observed in weak fields only for the thinnest films, of thickness on the order of 10^{-6} cm (Fig. 7). Unfortunately, it is still impossible to make a detailed evaluation of these results, since there is no theoretical expression for $M_\perp$.*

In the discussion of the results, notice must be taken of the fact that the region of the superconductivity-loss curve (BC in Fig. 8) increased as the thickness d was decreased and T approached T_{cr}, (Figs. 3 — 7), although it might have been expected (see, for example, references 6 and 14) that, in view of the decrease in the absolute value of the magnetic susceptibility of a thin film, the distortion which the susceptibility produces in the configuration of the magnetic field would become smaller, and the region of superconductivity loss should also decrease.

---

*G. F. Zharkov was kind enough to advise us that he derived formulas for the dependence of $M_\perp$ on the temperature and on the thickness of the layer.

Notice should be taken of the convenience of determining the value of H_{cr} of films with the aid of a magnetic torsion balance with feedback, since it dispenses with the need of using current leads for the film. By keeping the position of the sample fixed during the experiments the difficulties[6] which have arisen in the work of Alekseevskii[7] are eliminated, and it becomes possible to perform the measurements starting with values $\Delta T = 0.02°K$.

The depth of penetration δ_0, determined from the critical fields, was found to be greater in films than in bulk superconductors. Although the films did disclose previously[12,15] an increased value of δ_0, nevertheless, in the determination of H_{cr} from the electric resistance, this might have been due to the shunting action of the stressed portions of film, which have higher values of H_{cr}. On the other hand, if H_{cr} is determined by magnetic measurements, the influence of the stressed portions is eliminated. Nevertheless, the value of δ_0 obtained for tin and indium films in the present investigation exceeds considerably the values of δ_0 of bulk single-crystal samples. This result is apparently explained by the fact[10] that the parameter ξ of the Bardeen-Schrieffer-Cooper theory is smaller for films than for bulk single-crystal superconductors.

In conclusion, the author is deeply grateful to Professor N. E. Alekseevskiĭ for many valuable hints and for a discussion of the results, to G. F. Zharkov for discussing many theoretical problems, and to Yu. V. Sharvin for useful remarks when the article was prepared for press. The author is grateful to Professor A. I. Shal'nikov for his interest. Great help in the performance of the experiments was rendered by V. A. Sokolin and E. G. Kharakhash'yan, for which the author expresses his thanks.

---

[1] V. L. Ginzburg, Doklady Akad. Nauk SSSR **83**, 385 (1952).

[2] V. L. Ginzburg and L. D. Landau, JETP **20**, 1064 (1950).

[3] J. R. Schrieffer, Phys. Rev. **106**, 47 (1957).

[4] J. M. Luck, Proc. Roy. Soc. **208**, 391 (1951).

[5] L. D. Landau and E. M. Lifshitz, Электродинамика сплошных сред (Electrodynamics of Continuous Media), Fizmatgiz, 1959.

[6] D. Shoenberg, Superconductivity, Cambridge, 1952.

[7] N. E. Alekseevskiĭ, J. Phys. U.S.S.R. **4**, 401 (1941).

[8] B. K. Sevast'yanov, Приборы и техника эксперимента (Instruments and Exptl. Techniques) No. 5, 137 (1960).

[9] V. L. Ginzburg, Usp. Fiz. Nauk **42**, 169 (1950).

[10] V. L. Ginzburg, Doklady Akad. Nauk SSSR **118**, 464 (1958), Soviet Phys.-Doklady **3**, 102 (1958).

[11] V. L. Ginzburg, JETP **36**, 1930 (1959), Soviet Phys. JETP **9**, 1372 (1959).

[12] N. I. Ginzburg and A. I. Shal'nikov, JETP **37**, 399 (1959), Soviet Phys. JETP **10**, 285 (1960).

[13] A. L. Schawlow, Phys. Rev. **109**, 1856 (1958).

[14] D. Shoenberg, Proc. Roy. Soc. **175**, 49 (1940).

[15] N. V. Zavaritskii, Doklady Akad. Nauk SSSR **75**, 665 (1951).

Translated by J. G. Adashko
10

SOVIET PHYSICS JETP VOLUME 13, NUMBER 1 JULY, 1961

A STUDY OF LOW-LYING EXCITED STATES IN Mn^{56} *AND* Ho^{166} *BY MEASURING CASCADE QUANTUM COINCIDENCES*

A. S. MELIORANSKIĬ, I. V. ÉSTULIN, and L. F. KALINKIN

Institute of Nuclear Physics, Moscow State University

Submitted to JETP editor July 17, 1960

J. Exptl. Theoret. Phys. (U.S.S.R.) 40, 64-71 (January, 1961)

The technique for measurement of the intensity of cascade γ quanta was employed to investigate the low-lying levels of the odd-odd nuclei Mn^{56} and Ho^{166}. The multipolarity of the 25- and 85-kev radiative transitions in Mn^{56} was determined. The level scheme of the strongly deformed Ho^{166} nucleus, which exhibits a rotational band, is discussed.

INTRODUCTION

SOME low-lying excited states of the odd-odd nuclei Mn^{56} and Ho^{166} have been studied in this research; these states arise in the radiative capture of thermal neutrons. The technique of measurement of the coincidences of cascade γ quanta by means of a luminescence spectrometer was employed.[1,2] The general measuring arrangements were described previously.[1] The further development of the coincidence technique used in the present research is given below.

2. NOTE ON THE TECHNIQUE OF MEASUREMENT OF CASCADE γ -QUANTUM COINCIDENCES

The technique of the measurement of multiple coincidences of γ quanta is usually applied to the detection of cascade transitions, with the aim of making clear the decay scheme. In a number of cases, this technique makes it possible to determine certain characteristics of the radiative transitions entering into the cascades.

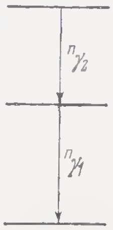

FIG. 1.

We assume that there is a cascade of γ quanta with intensity of radiations $n_{\gamma 2}$ and $n_{\gamma 1}$, (Fig. 1). In the general case, $n_{\gamma 1} \neq n_{\gamma 2}$ because of the additional transitions to the lower excited level, or because of the internal conversion of the γ quanta entering into the cascades. In the measurement of the coincidences by a luminescence spectrometer, one of the γ rays is isolated in the control channel and the spectrum of pulses coinciding with the pulses in the control channel is measured in the other (main) channel. The ratio of the number of pluses in the main channel N_{coin}, determined from the area of the light spikes, to the number of pulses from the separated γ line in the control channel N_{cont} will be equal to

$$N_{coin}/N_{cont} = (q/n_{cont})\, \varepsilon\omega, \tag{1}$$

where q is the intensity of the cascade, n_{cont} is the intensity of the γ quanta which control the coincidences, ϵ and ω are the efficiency and the solid angle of the main channel. The quantity q, having the same dimension as n_{cont}, is determined by the intensity of the γ quanta of the upper transition $n_{\gamma 2}$ and by the total coefficient of internal conversion α of the lower transition on the electrons of the atom:

$$q = n_{\gamma_2}/(1+\alpha)_{\gamma_1}. \tag{2}$$

The value of q/n_{cont} entering into (1) will be different in the equations for the upper (3a) or lower (3b) γ quanta:

$$q/n_{cont} = 1/(1+\alpha)_{\gamma_1} \tag{3a}$$

$$q/n_{cont} = n_{\gamma_2}/n_{\gamma_1}(1+\alpha)_{\gamma_1} \tag{3b}$$

In a number of experiments in coincidence spectra, a spike appears from the characteristic x-radiation of the atom, which is connected with the internal conversion of the radiated γ quanta by the electrons of the K shell of the atom. For this spike we obtain

$$q/n_{cont} = [\alpha_K/(1+\alpha)]_{\gamma_1} W_K, \tag{4a}$$

$$q/n_{cont} = (n_\gamma \alpha_K)_{\gamma_2} W_K/[n_\gamma (1+\alpha)]_{\gamma_1}, \tag{4b}$$

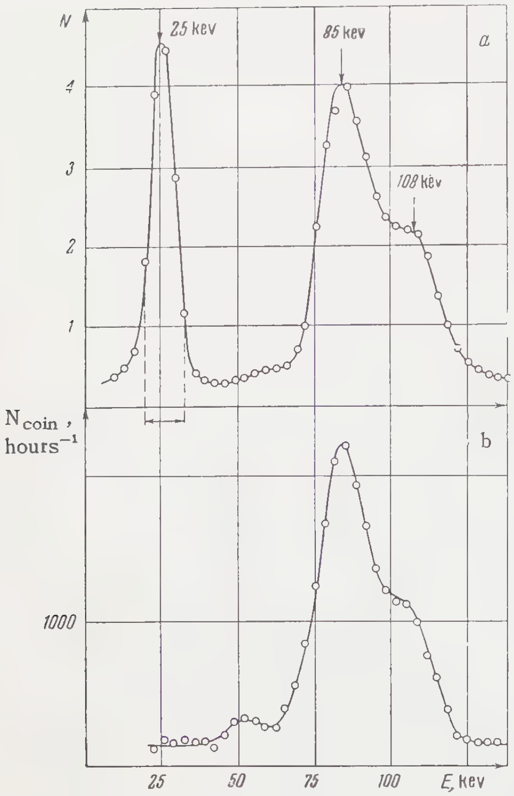

FIG. 2. Spectra from γ ray pulses of the reaction $Mn^{55}(n, \gamma)Mn^{56}$; a – in one channel; b – in coincidence with the line of 25 kev.

respectively, in place of (3a) and (3b). Here W_K is the yield of the K fluorescence.

Experimentally, the ratio N_{coin}/N_{cont} is determined; then q/n_{cont} is found from (1) and the result is compared with the theoretical values for the cases a) and b) in the case of different multipolarity radiative transitions. By the suitable analysis, it is possible in certain cases to find the succession of the radiative transitions, to find the intensity of the γ transitions, and to determine the coefficients of internal conversion and the multipolarity of the radiative transitions under consideration. Examples of the use of these techniques are contained in the succeeding sections of this paper, in which we report the results of experiments with Mn^{56} and Ho^{166}.

For an exact determination of the ratio q/n_{cont}, it is necessary to make use of the correct values of N_{cont}, ε, and ω. The number of pulses N_{cont} includes only a part of the pulses incident on the "slit" of the amplitude analyzer of the control channel and produced by the controlling γ lines. To determine N_{cont}, the pulse spectrum is divided into components by filtering the radiation.[1] The procedure used to determine the efficiency of the spectrometer according to the light spike ε was described by us earlier.[3] To find the solid angle ω, experiments were made with a compound of Te^{123m} (E_γ = 159 kev), which was identical in form with the target, with the compound located at the place of the target with a distance of 30 cm between the source and the collimator of the γ rays; in the second case, the solid angle was computed. For the determination of the multipolarity of the γ transition, use was made of the theoretical values[4–6] of the coefficients of internal conversion of γ quanta on atomic electrons.

The measurement of the coincidence spectrum was combined with measurements of the spectrum in one of the channels with the aim of determining the absolute intensities expressed in γ quanta per captured neutron.[3]

2. EXPERIMENTS WITH Mn^{56}

The spectrum of the γ rays with energies up to several hundred kev, emitted in the radiative capture of thermal neutrons in Mn^{55}, was measured by a number of authors.[7–10] However, the maximum in the spectrum which appears in the region of energies 80 — 110 kev was attributed in these works to one γ line with energy of either 85 kev[10] or 105 kev,[7,9] while the γ line with energy of 105 kev was assumed to be connected with the transition from the second excited level to the ground state of Mn^{56}. The γ quanta with energy 25 kev, which correspond to a transition from the first excited level, were recorded only in the work of D'Angelo.[10]

Measurements were carried out in the research reported here on the energy and absolute intensities of soft γ quanta of the reaction $Mn^{55}(n, \gamma)Mn^{56}$, and the coincidences between them. The very soft region of the spectrum is shown in Fig. 2. The measurements were made with the aid of a single-crystal luminescence spectrometer. Light spikes from γ quanta with energies of 25 ± 2 kev are seen in this spectrum, and the complicated character of the maximum in

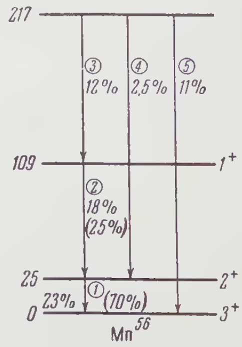

FIG. 3. Scheme of the low-lying levels of Mn^{56}. The intensities of transitions (radiative and total) are indicated in percent per captured neutron.

Table I. Gamma lines of the reaction $Mn^{55}(n, \gamma)Mn^{56}$

No. of line	Energy of gamma line, kev	Intensity of the gamma line, per cent per captured neutron	Concurrent lines, kev	
1	25±2	23±3	85, 108,	>6200
2	85±2	18±2	25, 108,	
3	108±3	12±2	25, 85,	
4	190±4	2.5±0.5	**	
5	217±4	11±2		
6	280±5	8±3*	85, 108	

*The intensity of the γ line with energy 280 kev was determined from $\gamma\gamma$ coincidences.

**The spectrum of the γ quanta that coincide with the γ lines of 25 kev was measured in the energy region up to 140 kev.

the region 85 — 110 kev is apparent. As measurements of the absorption of gamma rays in different filters have shown, this maximum consists of light spikes from γ quanta with energies of 85 ± 2 and 108 ± 3 kev. In addition to those previously known, a low-intensity γ line with energy 190 ± 4 kev was also found. Data on the energies and intensities of γ lines are given in Table I.

Gamma quantum spectra coinciding with the gamma lines of 25 and 85 kev and with the sum of the lines of 85 and 108 kev were measured. In the measurement of coincidences with γ quanta with energies of 85 kev, the γ line of 108 kev was filtered by lead, in which the first of the γ quanta mentioned were weakly absorbed. In addition to coincidences between soft γ lines, the spectrum of soft γ quanta coinciding with hard γ rays whose energies were close to the binding energy of the neutron was measured. This experiment confirmed that the γ lines discovered corresponded to transitions between the lower excited states.

Data on $\gamma\gamma$ coincidences for Mn^{56} are also given in Table I. The spectrum of γ quanta coinciding with the γ lines of 25 kev was studied in the region of energies below 140 kev. In the analysis of the results, it was noted that the ratio of the areas of the light spikes from γ quanta with energies of 108 and 85 kev, which appear in coincidences with γ lines of 25 kev (Fig. 2b), is equal, within the limits of error of the experiment, to the ratio of the areas of the spikes from these same γ lines in the spectrum measured on a single-crystal spectrometer with the same crystal (respectively, 0.60 ± 0.01 and 0.63 ± 0.04). This means that the γ line with energy 108 kev is practically completely caused by a transition from the third excited level to the second (Fig. 3). The equality of the areas of the S light spikes from γ quanta of 85 and 108 kev in the coincidence spectrum with the sum of these γ lines ($S_{85}/S_{108} = 1.02 \pm 0.05$) also bears witness to this fact. The upper limit of the intensity of the γ quanta, which is associated with the possible transition from the second excited level (109 kev) to the ground state, does not exceed 1.3 per cent for one captured neutron.

The method of analysis of the results of $\gamma\gamma$ coincidences, described in the previous section, was used for the determination of the total conversion coefficients of γ transitions with energies of 25 and 85 kev. The experimental values obtained from Eqs. (3), and the theoretical total conversion coefficients for the K, L and M shells are given in Table II.[4–6] The experimental data for the radiative transition with 85 kev energy can be made to agree with theoretical values under the assumption either of a transition of the M2 type, or of a mixture of the multipoles M1 + E2. We can eliminate the first possibility because of the too long lifetime of the excited state in this case, a result which contradicts experiment.[10] Thus the transition with energy of 85 kev is a mixture of the multipoles M1 + E2 (admixture of radiation of the type E2 is 45 per cent) and consequently does not change the parity of the states. To the level with

Table II. Multipolarity of transitions for Mn^{56}

Transition energy, kev		25			85			
Conversion coefficient $1+\alpha$	Theory	$E1$ 3,36	$M1$ 2.37	$E2$ 79.7	$E1$ 1,05	$M1$ 1,05	$E2$ 1,83	$M2$ 1.55
	Experiment	3,0±0.2			1,4±0.2			
Multipolarity of transition		$99M1+1E2$			$55M1+45E2$			
Reduced probability	$B(M1)\cdot 10^5$, $e^2\cdot b$,	0.83			0,3			
	$B(E2)$, $e^2\cdot b^2$	1.4			4			

energy 109 kev there is a direct transition of the type E1 from the initial state of Mn^{56} with characteristics 2^- or 3^- (the first is more probable), which is realized in the capture of a thermal neutron.[11] Thus the states of 109 and 25 kev have positive parity.

The presence in the spectrum of an intense γ line with energy 25 kev gives evidence that the corresponding transition can only be dipole, since in the case of higher multipolarities it would have been practically completely converted. The measured value of the total internal conversion coefficient (Table II) is close to the theoretical value for the transition of type E1. However, the parities of the ground and first excited states are identical, and there cannot be such a transition between them. The experimental value of $(1 + \alpha)$ for 25 kev exceeds the theoretical value for the transition M1, which compels us to regard this transition as a mixture of the multipoles M1 + E2. The strong difference in the conversion coefficients for transitions of such multipolarities makes it possible to determine a small admixture of radiation of the type E2, amounting to (0.8 ± 0.3 per cent).

The results of the study of $\gamma\gamma$ coincidences confirm the scheme of γ transitions between the lower levels of Mn^{56} given in reference 8. The values of the multipolarities of γ transitions with energies of 25 and 85 kev do not contradict the results of D'Angelo,[10] who measured the lifetimes of the first three excited levels of Mn^{56}, nor of the research of reference 12 on the study of the radiation of Cr^{56}. In using the results of reference 10 in conjunction with our data on the conversion coefficients and mixtures of multipolarities (Table II), the experimental values of the reduced probabilities of transitions M1 and E2 with energies of 25 and 85 kev were computed (see Table II). The reduced probability of the transition M1 with energy 25 kev was computed with an accuracy of ± 25 per cent, and the others with ± 50 per cent. Transitions of the type M1 were retarded by a factor of 10 — 40 relative to single-particle transitions, while those of type E2 were accelerated by two or three orders of magnitude.

3. EXPERIMENTS WITH Ho^{166}

Soft γ quanta produced in the reaction $Ho^{165}(n, \gamma)Ho^{166}$ with energies of 120 and 140 kev were discovered by Sklyarevskiĭ et al.[13] and by Draper.[14] In the present work, the connection between these γ quanta and the levels of Ho^{166}, which are populated in the β decay of Dy^{166}, was studied.[15,16] One could expect the appearance of a band of rotational levels, since the odd-odd nucleus Ho^{166} is located in a region of strongly deformed nuclei.

In the investigation of the radiative capture of thermal neutrons, a target of Ho_2O_3 was used with a weight of 70 mg and in the shape of a disc 20 mm in diameter. Possible impurities of other rare-earth elements required additional checks of the purity of the target material. As a criterion, we had the γ radiation, and also the energy and peak form of the K-shell x-radiation which arises in the exposure of the specimen to the neutrons. The Dy impurity amounted to (2 ± 0.5) per cent. A small peak with energy 180 kev, which appears in the spectrum of a single channel, was connected with the Dy impurity, which was observed by its induced activity with a period of 1.25 min. About one quarter of the neutrons captured in the target were in the Dy fraction, a fact which complicated the identification of the low-intensity γ lines.

In Table III we give the energy and intensity of the γ quanta involved in the reaction $Ho^{165}(n, \gamma)Ho^{166}$. In previously published researches, the γ lines 1 and 2 were not shown. The intensity of the γ lines 3 and 4 found in the present work differs somewhat from the result of Sklyarevskiĭ et al.[13] and, in particular, of Draper,[14] whose data on the γ line with energy 121 kev are inaccurate. The peak with energy 47 ± 2 kev is demonstrated by the K-shell x-radiation of the Ho atom. The intensity of this radiation, which is shown in the table, has been adjusted for the x-radiation of Dy (a correction of the order of 7 per cent is obtained by recalculation of the data of references 13 and 14).

Table III. Lines of the reaction $Ho^{165}(n, \gamma)Ho^{166}$

No. of line	Energy of γ line, kev	Intensity, in percent per captured neutron	Coincident γ lines kev	Multipolarity of the γ transition
X	47±2	58±12	X, 121, >1750	
1	56—66	19±5*	121	M1
2	82±2	2.5	X, >1750	M1
3	121±3	16±2	X, >1750	E2
4	140±3	22±3	—	E1+M2

*Strong conversion, the total intensity of the transition is shown.

Four different series of measurements of coincidences were carried out with x-radiation by γ lines of 121 and 140 kev, and also with hard γ quanta with energy of 1.75 Mev, which are generated in the target under the action of the neutrons. In these experiments, no coincidences were found with γ quanta of energy 140 kev, which indicates the long lifetime of the level with which the transition under consideration is realized, in accord with the work of Alexander and Bredel.[17] The gamma transition with energy 140 kev can lead either to the ground state of Ho^{166} or to the first excited state with energy 54.2 kev,[16] since it was not possible to find coincidences with these γ quanta, because of their appreciable conversion on the atomic electrons. Alexander and Bredel[17] determined the coefficient of internal conversion of the γ quanta with energy of 140 kev on the K shell of the atom, the value of which ($\alpha_K \approx 0.4$) indicates two possible variants of multipolarity: E2 or E1, with 5 per cent addition of M2. Such a strongly retarded E2 transition ($\tau = 2.14 \times 10^{-4}$ sec[17]) is scarcely probable, but E1 transitions with a retardation factor as large as $10^6 - 10^9$ are known. The intensity of the transition also supports a multipolarity of the E1 type. Therefore, it is more probable to regard the γ transition with energy of 140 kev as a mixture transition, which contradicts the assumption that it leads to the ground state. Apparently, there exists a level in the Ho^{166} nucleus with excitation energy 194 kev with the characteristic 3^+ (see Fig. 4). In this case, the absence of γ transitions to the second excited level and to the ground state is satisfactorily explained.

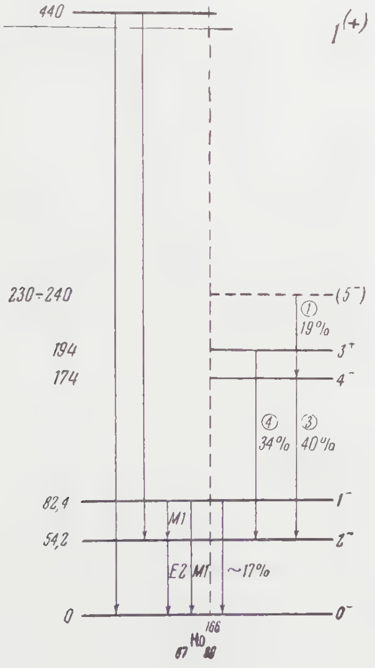

FIG. 4. Level scheme of Ho^{166}. On the left are the levels which appear in the decay of Dy^{166}.[16] On the right are those of the reaction Ho(n, γ). The total intensity of transitions is shown in per cent per captured neutron.

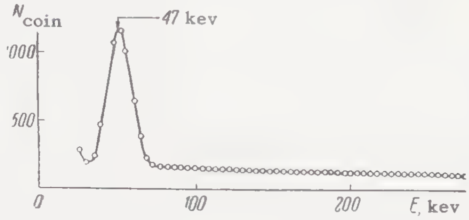

FIG. 5. Spectrum of pulses, which coincides with the gamma lines of 121 kev in the reaction Ho(n, γ).

In the measurement of coincidences with γ quanta of energy 121 kev there is a peak of energy 47 ± 2 kev, within the limits of error of experiment, which corresponds to K radiation of Ho, and no other γ lines are observed. The results of one of many similar experiments are shown in Fig. 5. In picking out the coincidences with the x radiation, coincidences are also observed with γ quanta of energy 121 kev. Thus the γ quanta with energy of 121 kev are found in a cascade with strongly converted γ lines (we denote them by y), whose conversion coefficient on the electrons of the K shell of the atom is $\alpha_K \geq 10$. A similar estimate eliminates the possibility of transitions E1 and E2, but permits a multipolarity of the type M1 with energy of 56 — 65 kev, or of type M2 with energy 56 — 120 kev. If the energy of the transition under consideration, $E_y = 47 \pm 2$ kev, is identical with the energy of the K radiation, then this multipolarity can only be E1.

The intensity of the cascade from the lines y and 121 kev is determined from Eq. (1):

$$(q/n_{121})_{\text{exp}} = 0{,}34 \pm 0{,}06. \tag{5}$$

This value was compared with the theoretical, obtained from (4), for various assumptions on the multipolarity of the radiative transitions under consideration. If the γ transition with energy 121 kev is considered as the upper transition [case (4a)], then the estimate of the multipolarity of the transition y, which corresponds to the value (5), contradicts the estimate of the multipolarity according to α_K. Therefore, case (4a) is rejected. Similar analysis for γ quanta with energy of 47 kev leads to the same conclusion. The given analysis did not consider the possibility of the transition 0 — 0. However, introduction of an excited level with spin 0 makes it necessary to forbid also a series of transitions between the lower excited levels of Ho^{166}, which are realized in the reaction (n, γ), and in the decay of Dy^{166}. More justifiable is the conclusion that the lower transition has the energy 121 kev [case (4b)]. Making use of the experimental value of (5) from an expression similar to (4b), we determine the total intensity of the transition y: $n_y = 19$ per cent for a single captured neutron with a multipolarity of the γ quanta with energy 121 kev of the type M1 or E2. The multipolarity of the γ quanta with energy 121 kev is found from the intensity of the x radiation (Table III) with account of the internal conversion of these γ transitions on the K shell of the atom, where the choice of the multipolarity E2 is preferable.

The intense cascade of lines y and 121 kev can lead to the ground state or to the lowest excited level. We assume that the cascade leads to the second excited level (Fig. 4). In this case, the absence of coincidences between the lines 121 and 82 kev (Fig. 5) should have sufficed to account for the low intensity of the direct transition (of the order of 5 per cent) in comparison with the intensity of the cascade transition from the level with energy 82.4 kev. But the low intensity of the direct transition contradicts the results of the study[15,16] of the radiation of Dy^{166}. In the transition of the cascade to the ground state, it is advantageous to introduce new levels of Ho^{166} with the quantum characteristics 1^- or 2^- which could also be populated in the β decay of Dy^{166}. We would expect transitions here from the 121-kev level not only to the ground state, but also to the first two levels. The scheme of γ transitions shown in Fig. 4 is free of the foregoing contradictions. In this scheme, the transition with energy 121 kev is accomplished from the level with energy 174 kev. For the level with energy 230 — 240 kev, the characteristic 5^- is chosen, which guarantees the transition to the level 174 kev with the suppression of the other transitions.

In the suggested scheme of levels of Ho^{166} (Fig. 4) there is seen a rotational band 0 (state 0^-), 54.2 kev (2^-) and 174 kev (4^-) for $K = 0$. The moment of inertia of this rotational band is characterized by the value $A = \hbar^2/2J = 9.20 \pm 0.07$ kev (for $B = 0.05 \pm 0.011$ kev) and is identical with the calculations of Peker[18] for odd-odd nuclei for the case $K = 0$ and $I_0 = 0$. The level of energy 82.4 kev, through which pass about 17 per cent of all transitions, can serve as the beginning of a new rotational band with odd spins. In the measurement of coincidences with x-radiation and hard γ quanta ($E_\gamma > 1.75$ Mev) γ quanta are observed with energy of 82.4 kev, and x-radiation not connected with the cascade of the lines y and 121 kev is observed. Evidently there is a soft γ radiation which leads to the level with energy 82.4 kev; however, we did not observe the corresponding γ quanta. The nucleus Ho^{166} has a long-lived isomeric level with spin and parity 7^- (references 19 and 20), which has an excitation energy ~ 900 kev. This state can have $K = 7$ and the transition from it to the observed level will be connected with the strong K forbideness.

---

[1] Melioranskiĭ, Estulin, Kalinkin, and Kudinov, JETP **38**, 758 (1960), Soviet Phys. JETP **11**, 548 (1960).

[2] A. S. Melioranskiĭ, Приборы и техника эксперимента (Instrum. and Exptl. Techn.) in press.

[3] Estulin, Kalinkin, and Melioranskiĭ, JETP **32**, 979 (1957), Soviet Phys. JETP **5**, 801 (1957).

[4] L. A. Sliv and N. M. Band, Таблицы коэффициентов внутренней конверсии гамма излучения (Tables of Internal Conversion Coefficients of Gamma Radiation) (Acad. Sci. Press, Moscow-Leningrad, 1958).

[5] M. E. Rose, Tables of Internal Conversion Coefficients, Beta and Gamma Spectroscopy, under the editorship of K. Siegbahn, Appendix IV, North Holland, 1955.

[6] M. E. Rose, Internal Conversion Coefficients (Amsterdam, 1958).

[7] M. Reier and M. H. Shames, Phys. Rev. 100, 1302 (1955).

[8] Kennett, Bollinger, and Carpenter, Phys. Rev. Lett. 1, 76 (1958).

[9] Urbanec, Kopecky, and Kajfosz, Czechoslovak J. Phys. **9**, 544 (1959).

[10] N. D'Angelo, Phys. Rev. **117**, 510 (1960).

[11] Groshev, Demidov, Lutsenko, and Pelekhov, Атлас спектров γ-лучей радиационного захвата тепловых нейтронов (Atlas of Gamma Ray Spectra of Radiative Capture of Thermal Neutrons) Atomizdat, 1958.

[12] Dropesky, Schardt, and Shull, Nucl. Phys. **16**, 357 (1960).

[13] Sklyarevskiĭ, Stepanov, and Obinyakov, Атомная энергия (Atomic Energy) **4**, 22 (1959).

[14] J. E. Draper, Phys. Rev. **114**, 268 (1959).

[15] R. G. Helmer and S. B. Surson, Bull. Amer. Phys. Soc. **4**, 427 (1959).

[16] Geiger, Graham, and Ewan, Bull. Amer. Phys. Soc. **5**, 255 (1960).

[17] K. Alexander and V. Bredel, Nucl. Phys. **16**, 153 (1960).

[18] L. K. Peker, Izv. Akad. Nauk SSSR, Ser. Fiz. **24**, 365 (1960), Columbia Tech. Transl. p. 350.

[19] P. Baskma and H. DeWoard, Nucl. Phys. **12**, 533 (1959).

[20] Pastima, Miederna, and Smulders, Physica **25**, 671 (1959).

Translated by R. T. Beyer
11

SOVIET PHYSICS JETP VOLUME 13, NUMBER 1 JULY, 1961

CIRCULAR POLARIZATION OF THE γ RAYS ACCOMPANYING THE β DECAY OF Nd^{147}

A. A. PETUSHKOV and I. V. ÉSTULIN

Nuclear Physics Institute, Moscow State University, Institute for General and Inorganic Chemistry, Academy of Sciences, U.S.S.R.

Submitted to JETP editor July 27, 1960

J. Exptl. Theoret. Phys. (U.S.S.R.) 40, 72-75 (January, 1961)

The asymmetry coefficient for $\beta\gamma$ correlation was determined by measuring the degree of circular polarization of 530-kev γ rays accompanying the β decay of Nd^{147} and found to be $A = -0.093 \pm 0.15$. This value is consistent with a spin of $7/2$ for the state of Pm^{147} in question and for a mixed E2 + M1 transition, with an amplitude ratio E2/M1 equal to $+1.75 \pm 0.15$.

INTRODUCTION

ONE of the consequences of parity nonconservation in β decay is that the γ rays emitted by excited nuclei after β decay are circularly polarized. The first measurements of γ-ray circular polarization were done to check the nonconservation of parity.[1,2] At the present time, the fundamental principles involved in the nonconservation of parity in β decay have been established.[3] Measurements of the degree of circular polarization of γ rays can be used to establish quantum numbers for nuclear levels, the multipolarity of radiative transitions, and nuclear matrix elements for β transitions. The theory is sufficiently detailed[4,5] that experimental results can be interpreted from this point of view. There have been only a few papers published[6,7] on measurements of circular polarization for spectroscopic purposes.

In this paper we report on measurements of $\beta\gamma$ correlation and circular polarization of the 530-kev γ rays accompanying the β decay of Nd^{147}. Nd^{147} has been also studied by Bishop et al.[8] using a low temperature technique, but the results obtained did not allow firm conclusions to be drawn.

MEASUREMENT PROCEDURE

In general, the measurements were made using conventional techniques. The γ-ray circular polarization was detected by using the cross section of forward Compton scattering from polarized electrons. The scattering cylinder was made of a magnetic material with induction $B = 2.2 \times 10^4$ gauss in a field $H = 15$ oersted. The mean scattering angle for the γ rays was $\sim 55°$. To minimize the magnetic field at the photomultiplier (FÉU-13) we used a 15 cm light pipe. The electrons were detected by an anthracene crystal 2 mm thick; a threshold could be set to discriminate against electrons having small values of v/c. The γ rays reflected from the scatterer were detected by a NaI(Tl) crystal having dimensions 40×40 mm^2. The γ-ray pulses were passed through a single channel analyzer with variable window. This selected the pulses due to γ rays of the desired energy. $\beta\gamma$ coincidences were selected with a resolving time of $\tau = 3 \times 10^{-8}$ sec, the total (i.e., sum of true and accidental coincidences) and accidental coincidence rates being recorded simultaneously.[9] We measured the quantity

$$\varepsilon = 2[N_{\beta\gamma}(\uparrow) - N_{\beta\gamma}(\downarrow)] / [N_{\beta\gamma}(\uparrow) + N_{\beta\gamma}(\downarrow)],$$

where $N_{\beta\gamma}(\downarrow)$ is the $\beta\gamma$ coincidence rate when the magnetic field in the scatterer was directed away from the source, and $N_{\beta\gamma}(\uparrow)$ was the coincidence rate with the magnetic field directed to the source. The direction of the magnetic field was changed every 10 minutes. The effect on the mean counting rate in the various channels was not greater than 0.05%. From the value of ϵ we calculated the asymmetry coefficient A for $\beta\gamma$ correlation with circularly polarized γ rays. To test the apparatus, measurements were made on Co^{60} and Na^{22}. The results are shown in the table. The experimental values of A agree both with theory and also with the results of other authors. From the measurements on Co^{60} and Na^{22} we concluded that there were no instrumental asymmetries.

MEASUREMENTS ON Nd^{147}

In the measurements on Nd^{147}, coincidences were recorded between 530-kev γ rays and elec-

	ε, %	*A*	
		experiment	theory
Co^{60}	$+1.44 \pm 0.27$	$-0,34 \pm 0,06$	-0.33
Na^{22}	$-1,45 \pm 0.32$	$+0.30 \pm 0.07$	$+0.33$
Nd^{147}	$+0,21 \pm 0.34$	-0.093 ± 0.15	$-0,21$

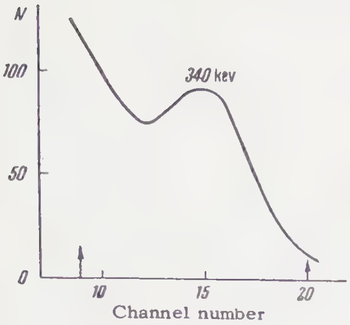

FIG. 1. Spectrum of scattered γ rays from Nd^{147} (the arrows show the window of the discriminator).

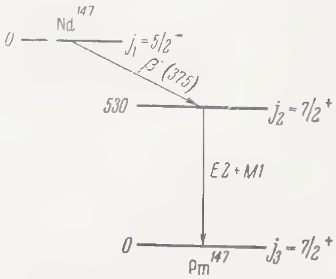

FIG. 2. Decay scheme for the transition $Nd^{147} \to Pm^{147}$.

trons of the β spectrum having an upper limit of 375 kev. The threshold in the β channel was set at 140 kev, which corresponds to a mean value $\bar{v}/c = 0.71$. Figure 1 shows the spectrum of pulses from the NaI(Tl) crystal. These pulses are due to scattered γ rays. The diffuse photopeak corresponds to an energy of 340 kev and is due to γ rays with initial energy 530 kev. The arrows on Fig. 1 indicate the part of the spectrum selected by the single-channel analyzer. About one coincidence was counted per second, true and accidental coincidences being approximately equally probable. The result of the measurement is given in the table, together with its mean square error. One possible source of systematic error is that the part of the γ-ray spectrum measured may have contained γ quanta due to other transitions. The correction for this is not greater than one fifth the mean square error.

The β transition in Nd^{147} is a first-forbidden one. For Nd^{147}, $Z = 60$. According to Gaponov, the β transition should be of the Coulomb type, i.e., the β spectrum should have the allowed shape and the angular distribution of the γ rays about the direction in which the electron is emitted should be isotropic. As a test, we made some measurements of $\beta\gamma$ correlation without looking at the circular polarization of the γ rays. The angular distribution obtained was isotropic to 0.5%, which confirms that the β decay is of the Coulomb type. Hence the formulae in reference 5 may be used to interpret our results.

DISCUSSION

According to Gaponov,[5] the asymmetry coefficient A for Coulomb type β transitions depends on the angular momenta of the initial nucleus (j_1) and of the final nucleus both in its excited state (j_2) and in its ground state (j_3). The value of A depends also on the multipolarity of the radiative transition. For $j_1 = j_2$ the matrix elements for the β decay must also be known.

Using a paramagnetic resonance technique, Kadzic et al. have measured the spin of the ground state of Nd^{147} to be $j_1 = {}^5\!/_2$.[10] From optical spectroscopy, Klinkenburg and Tomkins have found the spin of the ground state of Pm^{147} to be $j_3 = {}^7\!/_2$.[11]

Bishop et al.[8] have established that the 530-kev radiative transition in Pm^{147} has a mixed multipolarity E2 + M1 (see Fig. 2). However, in analyzing their data, they used spins $j_1 = {}^9\!/_2$ and $j_3 = {}^5\!/_2$, in contradiction with the results of references 10 and 11. We reviewed the analysis given by Bishop et al.,[8] and found that if the spin j_2 were assumed to be ${}^5\!/_2$, it would be very difficult to fit the experimental data, no matter what ratio δ were assumed for the amplitudes of the electric quadrupole and magnetic dipole radiations (E2/M1). On the other hand, the assumption $j_2 = {}^7\!/_2$ gave good agreement with the data for two values of $\delta : \delta_1 = +1.75 \pm 0.15$ and $\delta_2 = -1.02 \pm 0.13$. The spin assignment $j_2 = {}^9\!/_2$ is not excluded by this data, but does imply a unique β transition and an anisotropy in the $\beta\gamma$ correlation (summed over circular polarizations) and so is ruled out by our results.

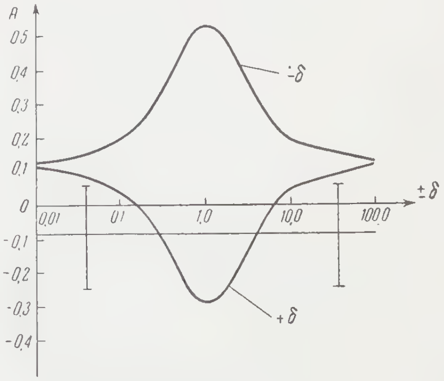

FIG. 3. The asymmetry coefficient A in $\beta\gamma$ correlation with circularly-polarized γ rays as a function of δ, the amplitude ratio E2/M1.

Figure 3 shows the asymmetry coefficient A as a function of the amplitude ratio δ for $j_2 = {}^7\!/_2$.[5] Our experimental result for A agrees with $j_2 = {}^7\!/_2$ if δ is taken with a plus sign. We conclude that the excited state in Pm^{147} at 530 kev must have spin $j_2 = {}^7\!/_2$, and the amplitude ratio E2/M1 for the radiative transition to the ground state must be $\delta = +1.75 \pm 0.15$.

In conclusion, the authors wish to thank I. S. Shapiro for stimulating their interest in this problem, Yu. V. Gaponov for help in interpreting the results and finally Kh. Yungklaussen, I. I. Miroshnichenko and B. G. Kiselev, students in the physics faculties at the Moscow State University and Voronezh State University, for their assistance.

---

[1] H. Schopper, Phil. Mag. **2**, 710 (1957).

[2] F. Boehm and A. H. Wapstra, Phys. Rev. **107**, 1462 (1957).

[3] A. I. Alikhanov, Слабые взаимодействия. Новейшие исследования β-распада. (Weak Interactions. The Present Status of β Decay), Fizmatgiz, 1960.

[4] Yu. V. Gaponov and V. S. Popov, JETP **33**, 256 (1957), Soviet Phys. JETP **6**, 197 (1958).

[5] Yu. V. Gaponov, JETP **36**, 193 (1959), Soviet Phys. JETP **9**, 191 (1959).

[6] R. M. Steffen, Bull. Am. Phys. Soc. **3**, 205 (1958).

[7] G. Hartwig and H. Schopper, Phys. Rev. Lett. **4**, 293 (1960).

[8] Bishop, Grace, Johnson, Lemmer, and Jorba, Phil. Mag. **2**, 534 (1957).

[9] A. S. Melioranskiĭ and A. A. Petushkov, Приборы и техника эксперимента (Instrum. and Exptl. Techn.) (in press).

[10] Kadzie, Abraham, and Jeffries, Phys. Rev. **108**, 854 (1957).

[11] P. F. A. Klinkenburg and F. S. Tomkins, Physica **26**, 103 (1960).

Translated by R. Krotkov
12

SOVIET PHYSICS JETP VOLUME 13, NUMBER 1 JULY, 1961

TEMPERATURE DEPENDENCE OF THE HALL EFFECT IN $MnAu_2$

V. N. NOVOGRUDSKIĬ and I. G. FAKIDOV

Institute of Metal Physics, Academy of Sciences, U.S.S.R.

Submitted to JETP editor July 30, 1960

J. Exptl. Theoret. Phys. (U.S.S.R.) **40**, 76-78 (January, 1961)

It is shown that the ordinary Hall effect in $MnAu_2$ is supplemented by an additional effect in the antiferromagnetic temperature range. It is suggested that this additional effect is caused by the presence of a high magnetic susceptibility.

MANY substances are known to exhibit more than one form of spin ordering. The magnetic properties of these substances have been investigated thoroughly, but their electrical properties have been studied fully only in the case of ferromagnets. It therefore appeared interesting to investigate the galvomagnetic properties of antiferromagnets in order to determine those parts of the observed effects that are directly associated with antiferromagnetism.

We have investigated the Hall effect in the intermetallic compound $MnAu_2$, which is antiferromagnetic but becomes ferromagnetic in magnetic fields above a certain threshold ($H > H_{th}$).[1,2] Our specimen exhibited the Néel temperature $T_N = 92°$ C and $H_{th} = 8000$ oersteds. In earlier work[3] we showed that the Hall emf for $MnAu_2$ in the region $0 < H < H_{th}$ depends linearly on the magnetic field strength H. In the present work we investigated the temperature dependence of the Hall emf in the same specimen, using magnetic fields in which $MnAu_2$ remains antiferromagnetic. An abrasive disk was used to saw the specimen from an ingot, thus excluding large residual deformations. The emf and magnetic susceptibility were measured as in reference 3.

The figure shows the temperature dependence of the Hall emf for an internal magnetic field $H = 5000$ oe. Curve 1 exhibits a peak located near the Néel temperature T_N, which was determined from the temperature dependence of the magnetic susceptibility. In this respect $MnAu_2$ can be contrasted with manganese telluride, where the Hall emf falls off rapidly around the Néel temperature.[4]

Let us consider the portion of the curve that lies in the paramagnetic region. It has been shown by Kikoin and others[5-7] that in strongly paramagnetic substances and in ferromagnetics above the Curie point the Hall emf can be represented by

$$E_x = [R_0 H + R_1 \chi H] I/d = R_0 [1 + 4\pi\alpha\chi] HI/d, \qquad (1)$$

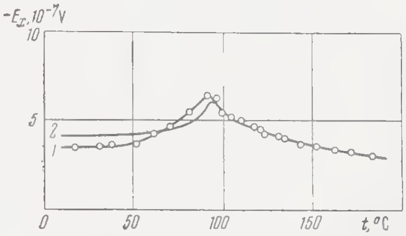

Temperature dependence of the Hall emf for $MnAu_2$ with an internal magnetic field $H = 5000$ oe. 1 – experimental curve; 2 – curve calculated from Eq. (1).

where H is the magnetic field, I is the current flowing through the specimen, d is the thickness of the specimen, R_0 is the magnetic susceptibility, R is the Hall constant for the ordinary effect, and R_1 is the Hall constant for the part of the effect that is associated with magnetization. Since it was shown in the same investigation that R_1 is independent of temperature, we have assumed that (1) is also valid in antiferromagnetics above the Néel temperature. The figure shows that the experimental curve 1 can be closely approximated by (1) when the following numerical constants are used:

$$R_0 = -2.19 \times 10^{-12} \text{ v-cm/amp-oe}$$
$$R_1 = -2.42 \times 10^{-10} \text{ v-cm/amp-gauss}$$
$$\alpha = 8.8. \qquad (2)$$

These values were determined by the method of least squares from the experimental results in the paramagnetic temperature region. It should be noted that $\alpha = 8.8$ is small compared with the value for ferromagnetics; e.g. for very pure nickel near the Curie point we have $\alpha \sim 10^2$.

It therefore follows from the high magnetic susceptibility of $MnAu_2$ ($\chi \approx 5 \times 10^{-3}$ cm^{-3}) that a considerable fraction of the Hall effect depends on magnetization. Since it can hardly be supposed that at temperatures below T_N the parameter α is immediately reduced to the order of unity, a

Hall effect resulting from a paramagnetic process must evidently exist in the antiferromagnetic region.

Curve 2, which represents Eq. (1) with the values of R_0 and R_1 given in Eq. (2), is seen to agree well with the experimental curve 1 above the Néel temperature, but to differ considerably below that temperature. The temperature dependence of the Hall emf can therefore not be represented by (1) in the antiferromagnetic region if R_0 and R_1 are assumed to be temperature-independent. Since $MnAu_2$ has the electrical properties of a metal, its conduction-electron concentration is temperature-independent, and this must also apply to R_0. We can therefore assume that either R_1 or α is temperature-dependent below the Néel temperature.

It should be noted that when α is of the order of a few tens the magnetization-induced part of the Hall effect can be appreciable only in substances where the susceptibility exceeds 10^{-4} cm^{-3}. In antiferromagnets with low susceptibility, such as MnTe, the additional magnetization-induced Hall emf can therefore be imperceptible.

However, the anomalous Hall effect in manganese telluride around the Néel temperature is evidence that antiferromagnetism results in an additional Hall emf, which is apparently produced by a different mechanism than in $MnAu_2$.

---

[1] A. J. Meyer and P. Taglang, J. Phys. Radium **17**, 457 (1956).

[2] A. Herpin and P. Meriel, Compt. rend. **250**, 1450 (1960).

[3] I. G. Fakidov and V. N. Novogrudskiĭ, Физика металлов и металловедение (Physics of Metals and Metallography) **10**, 158 (1960).

[4] Uchida, Kondoh, and Fukuoka, J. Phys. Soc. Japan **11**, 27 (1956).

[5] I. K. Kikoin, J. Phys. (U.S.S.R.) **9**, 1 (1936).

[6] Kevane, Legvold, and Spedding, Phys. Rev. **91**, 1372 (1953).

[7] Kikoin, Buryak, and Muromkin, Doklady Akad. Nauk SSSR **125**, 1011 (1959), Soviet Phys.-Doklady **4**, 386 (1959).

Translated by I. Emin
13

SOVIET PHYSICS JETP VOLUME 13, NUMBER 1 JULY, 1961

ON THE LEVEL SCHEME OF Eu^{153}

L. I. RUSINOV*, R. L. APTEKAR', V. S. GVOZDEV, S. L. SAKHAROV, and Yu. L. KHAZOV

Leningrad Physico-Technical Institute

Submitted to JETP editor August 3, 1960

J. Exptl. Theoret. Phys. (U.S.S.R.) 40, 79-84 (January, 1961)

The decay scheme of Sm^{153} ($T_{1/2}$ = 47 hours) obtained in the (n, γ) reaction was investigated. The γ transition types were determined for transitions with energies of 69.7 kev (96.4 percent M1 + 3.6 percent E2); 84.4 kev (60 percent M1 + 40 percent E2); 103.2 kev (98.5 percent M1 + 1.5 percent E2) and 98 kev (M1). The 98-kev transition has been observed for the first time. The experimental results are compared with theory. Some new details of the level scheme of Eu^{153} are presented.

INTRODUCTION

THE nucleus Eu^{153} is formed both in β decay of Sm^{153} with a half-life $T_{1/2} = 47$ hours and also from Gd^{153} in the capture of orbital electrons with a half-life $T_{1/2} = 230$ days. The scheme of the excited levels of Eu^{153} was investigated in great detail in a large number of researches, and the spins and parities of the excited levels were established up to energies of 200 kev. However, there are a number of peculiarities which require further determination.

1. The excited level with energy of 97.5 kev is observed only in the formation of Eu^{153} from Gd^{153}.

2. The intensity of transitions with energies 89.5 and 172.9 kev is small in comparison with the intensity of transition with energy of 69.7 kev.

3. The transition with energy 83.4 kev between the rotational levels with $K = 5/2$ has a larger admixture of the E2 type than the transition with energy 69.7 kev between the rotational levels with $K = 3/2$. In connection with the foregoing, an investigation of the level scheme of the Eu^{153} nucleus, formed in β decay of Sm^{153} was again undertaken in the present research.

EXPERIMENTAL RESULTS

The spectrum of internal conversion electrons was measured on a β spectrometer with focusing of the electrons at an angle of $\pi\sqrt{2}$ with a resolving power $\Delta H\rho/H\rho = 0.25$ per cent and with an aperture of 0.25 percent of 4π. As a source, we used samarium oxide enriched by the isotope Sm^{152} to 98.5 percent, which was coated on aluminum foil of 4μ thickness in the form of a layer of thickness 0.03 — 0.05 mg/cm^2. The prepared source was exposed for 4 — 5 days in the flux of thermal neutrons of the reactor. The K, L, M and N lines of the γ transitions were observed in the spectrum of internal conversion electrons, with energies of 69.7, 83.4 and 103.2 kev, as well as the L and M lines of the γ transition with energy of 89.5 kev and the K line of the γ transition with energy of 172.9 kev. The transition with energy 89.5 kev was observed for the first time in the decay of Sm^{153}.

The types of transitions with energies of 69.7, 83.4 and 103.2 kev were determined from a comparison of the experimental and theoretical[1] relations of the coefficients of internal conversion on the L sub-shells (Table I). The results obtained for γ transitions of 83.4 and 103.2 kev are identical with the data of Graham et al.[2] For the transition with energy of 69.7 kev, there is an important difference: in reference 2, the admixture of the transition of type E2 is shown to be equal to 1.5 percent.

It should be noted that the values of the ratio α_L/α_M obtained by us differ sharply from the theoretical.[3]

In addition to the conversion lines mentioned, an electron line was discovered in the spectrum with an energy of 49.5 kev (Fig. 1). It was interpreted by us as a K line of the γ transition with energy of 98 kev in Eu^{153}. The ratio of the intensities of the K internal conversion electrons of the γ transition of 98 kev and the L electrons of the γ transition of 69.7 kev was shown to be equal to 0.06 per cent.

For clarifying the location of the γ transition of 98 kev in the level scheme of Eu^{153}, investigations were carried out on the $\gamma\gamma$ coincidences

---

*Deceased.

Table I

<table>
<tr><th rowspan="3">E_γ, kev</th><th colspan="5">$\alpha_{L_I} : \alpha_{L_{II}} : \alpha_{L_{III}}$</th><th rowspan="3">Type of transition</th><th colspan="3">α_L / α_M</th><th rowspan="3">Intensity of the transition</th></tr>
<tr><th colspan="4">Theoretical values</th><th rowspan="2">Experimental values</th><th colspan="2">Theoretical values</th><th rowspan="2">Experimental values</th></tr>
<tr><th colspan="2">M1</th><th colspan="2">E2</th><th>M1</th><th>E2</th></tr>
<tr><td>69.7</td><td colspan="2">65.8:5.57:1</td><td colspan="2">0.09:0.89:1</td><td>9.47:1.53:1</td><td>96.4±0,5% M1 +3.6∓0.5% E2</td><td>0,44</td><td>0,47</td><td>0.20±0,01</td><td>100</td></tr>
<tr><td>83.4</td><td colspan="2">66.8:5.57:1</td><td colspan="2">0.15:0,93:1</td><td>0,74:1.02:1</td><td>60±2% M1+40∓2% E2</td><td>0.44</td><td>0.47</td><td>0.18</td><td>3</td></tr>
<tr><td>103.2</td><td colspan="2">68.1:5,55:1</td><td colspan="2">0.26:0.995:1</td><td>24:2.75:1</td><td>98.5±0.1% M1 +1,5∓0.1% E2</td><td>0.44</td><td>0.47</td><td>0.181±0.005</td><td>220,5</td></tr>
<tr><td>89.5</td><td colspan="2"></td><td colspan="2"></td><td></td><td>>85% M1+<15% E2*</td><td></td><td></td><td></td><td>1,49</td></tr>
<tr><td>172.9</td><td colspan="2"></td><td colspan="2"></td><td></td><td>60% M1+40% E2*</td><td></td><td></td><td></td><td>0,24</td></tr>
<tr><td></td><th colspan="5">α_K</th><td></td><td></td><td></td><td></td><td></td></tr>
<tr><td></td><th colspan="4">Theoretical values</th><th rowspan="2">Experimental values</th><td></td><td></td><td></td><td></td><td></td></tr>
<tr><td></td><th>E1</th><th>E2</th><th>M1</th><th>M2</th><td></td><td></td><td></td><td></td><td></td></tr>
<tr><td>98</td><td>0,24</td><td>1.18</td><td>1,62</td><td>14</td><td>1,5±0.5</td><td>M1 (+E2)</td><td></td><td></td><td></td><td>1.3</td></tr>
</table>

*Taken from reference 2.

(Fig. 2). The measurements were made on a coincidence circuit with a resolving time of $\tau = 2 \times 10^{-8}$ sec. In one of the channels of the coincidence circuit, there was a differential amplitude analyzer which made it possible to select any portion of the gamma spectrum. The coincidence spectrum was recorded by a 100 channel amplitude analyzer.

In tuning of the amplitude analyzer to the line of 103.2 kev in the spectrum for a single channel (the portion a in the upper curve of Fig. 2), a γ line with energy 98 ± 5 kev was observed in the coincidence spectrum (lower curves). The spectrum of $\gamma\gamma$ coincidences is shown in the figure; here random coincidences have been deducted.

In order to eliminate the effect of coincidences of γ rays with energies of 103.2 and 69.7 kev, the analogous spectrum of coincidences with the portion b (upper curve) was also studied. The relation of the intensities of the γ lines with energies of 98 and 69.7 kev remained the same in both series of measurements (coincidence with the portion a and coincidence with the portion b) and was equal to 0.03 ± 0.01.

For the γ transition with energy of 69.7 kev, the internal conversion coefficient on the L shell was calculated for the value of the mixture 96.4 percent M1 + 3.6 per cent E2. From the relation of the intensities of the conversion electrons for the γ transition of 98 kev on the L shell and for

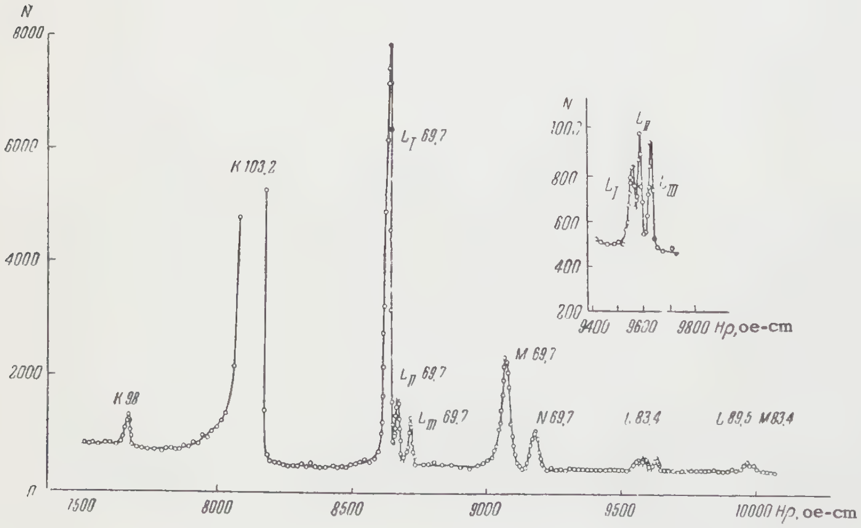

FIG. 1. A portion of the spectrum of internal conversion electrons of Eu^{153}.

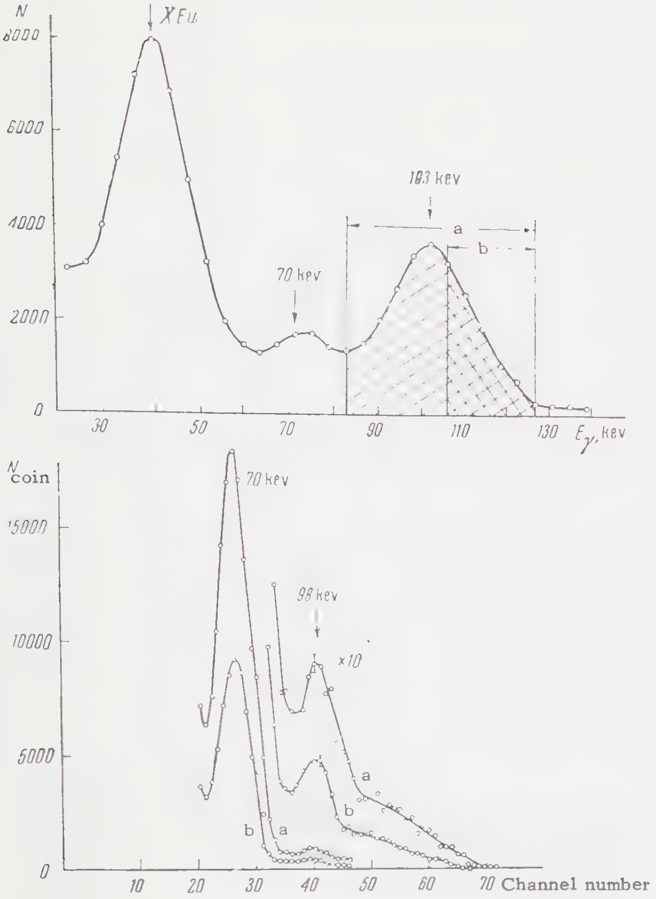

FIG. 2. Spectrum for a single channel (upper curve) and the spectrum of $\gamma\gamma$ coincidences. The curves a and b have been partially expanded in scale by a factor of 10, XEu is the characteristic x-radiation of europium.

the γ transition of 69.7 kev on the L shell, and also from the relation of the intensities of γ rays for the same transitions, we can compute the coefficient of internal conversion on the K shell for the transition of 98 kev. It turned out to be equal to 1.5 ± 0.5, which corresponds to an M1 transition or to a mixture of M1 and E2.

DISCUSSION OF RESULTS

The value of the internal conversion coefficient for the γ transition of 98 kev, and the presence of coincidences of γ quanta of this transition with γ quanta of 103.2 kev indicate that the observed transition does not take place from the level of 97.5 kev.

There are two rotational structures in the level scheme of Eu^{153}. One of these is connected with the ground state of the nucleus. The first excited level of this structure (E = 83.4 kev and I = $^7\!/_2$) is formed both in the decay of Sm^{153}, and also in the decay of Gd^{153}. The second excited level (E = 190 kev and I = $^9\!/_2$) is not discovered in the decay of Sm^{153} and Gd^{153} because of the large value of the spin, and is observed only in the experiments on Coulomb excitation.

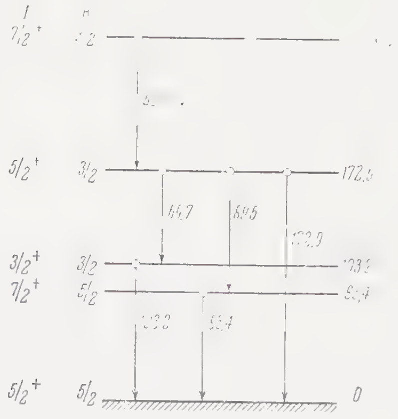

FIG. 3. Level scheme of Eu^{153}.

The second rotational structure has its ground state level with excitation energy 103.2 kev (I = $^3\!/_2$). The transition from the first excited level of this structure (E = 172.9 kev) to its ground state takes place with energy of 69.7 kev. The excitation energy of the next level is computed by a well-known formula (see reference 10) and is equal to 271 kev (relative to the ground state of Eu^{153}). The transition from the second excited level to the first should take place with energy of 97.6 kev. This value is identical with the value of the energy of the observed transition.

Thus one can draw the conclusion that the γ transition with energy of 98 kev is a transition of type M1 with a possible admixture of E2. This transition refers to the second rotational structure and takes place between the levels with excitation energies of 271 and 172.9 kev (Fig. 3).

In the decay of Gd^{153}, the level of 271 kev in Eu^{153} is not generated because of the small total energy of decay.[4]

In strongly deformed nuclei, the relations of the probabilities of transitions from any state to the rotational state belonging to one rotational band are computed according to the well-known rule of Alaga.[5] It was noted by Gnedich et al.[6] that there are certain cases of violation of this rule. The deviation consists in the fact that the transitions to the excited states of the rotational band are more intense (in comparison with the transition to the ground state of the same band) than follows from Alaga's rule. In this case a higher probability of transition is observed to the second excited state than to the first excited state.

It is of interest in the case of Eu^{153} to compare the probabilities obtained for the transitions B(λ) with energies of 89.5 and 172.9 kev (transitions to

Table II

Type of transition	$B(\lambda)_{89.5}/B(\lambda)_{172.9}$		Favoring of 89.5-kev transition
	By Alaga's rule	Experiment	
$M1$	2.5 : 1	24.8 : 1	9.9
$E2$	0.037 : 1	17.9 : 1	483

the first excited state and to the ground state of the rotational band). Both transitions are mixed and it is necessary to make the comparison independently for each type of transition, M1 or E2. The relation of the intensities of γ rays for these transitions was computed from the intensities of the internal conversion electrons. The value of the mixture M1 and E2 is taken from the work of Grant et al.[2] The comparison of the theoretical and experimental relations for the probabilities obtained for different transitions B(λ) is written down in Table II. As is seen from the table, the transition of 89.5 kev is facilitated in a considerable degree in comparison with the theoretical predictions.

The reason for the departure from Alaga's rule is not known at the present time. In the case of Eu^{153}, it is impossible to explain this deviation by a mixture of the wave functions of the states (both states have spin and parity of $^5/_2{}^-$), because such a mixture can bring about only the opposite effect — the facilitating of the transition of 172.9 kev in comparison with the γ transition of 89.5 kev.

As is seen from Table I, the intensities of transitions with energies of 89.5 and 172.9 kev are very small in comparison with the transition intensity for the energy of 69.7 kev. The reasons for this circumstance consist of the following. The initial state of the internal excitation with energies of 89.5 and 172.9 kev is a state characterized by the asymptotic quantum numbers N, n_z, λ, Σ, equal to [4, 1, 1, —], the final state is characterized by the numbers [4, 1, 3, —].[7] The transition of the type M1 between these states, in accord with the rules of the review of reference 8, is seen to be forbidden according to the asymptotic quantum number λ, while the transition of the type E2 remains allowed. This prohibition leads to a certain "retardation" of transitions with energies of 89.5 and 172.9 kev. This circumstance also clearly explains the fact of the larger admixture of E2 in transitions with energy of 89.5 and 172.9 kev in comparison with transitions of 69.7, for which there are no prohibitions.

A striking fact is the higher value of the admixture of E2 for the transition of 83.4 kev than for the transition of 69.7 kev, in spite of their rotational character. One can attempt to explain this fact in the following fashion.

The probability of the electromagnetic transition of multipolarity λ is connected with the reduced transition probability B(λ) by a well-known relation (see reference 10). For strongly deformed nuclei and for transitions within the limits of a single rotational band, B(λ) is expressed in terms of the statistical moment of the ground state of the K band, μ, Q_0, the general magnetic ratios g_K and g_R, and the Clebsch-Gordan coefficients.[9] From these relations, and with a knowledge of the partial lifetime,[10] the value of the mixture of E2 and M1 for the corresponding transition, and the value of the magnetic moment for the ground state of the rotational band, one can determine the values of Q_0, g_K, and g_R for this state.

The lifetime of the 172.9-kev level of the Eu^{153} nucleus is known. The partial lifetime for the 69.7-kev transition can be determined from the relations of the intensities of the 69.7-, 89.5-, and 172.9-kev transitions. As the value of the magnetic moment of the Eu^{153} nucleus in a state with excitation energy 103.2 kev, we can take a quantity equal to the magnetic moment μ of the Tb^{159} nucleus in the ground state ($\mu = 1.52$). Under these conditions, the values of Q_0, g_K, and g_R for Eu^{153} in the 103.2-kev state were found to be equal respectively to 5.1×10^{-24} cm^2, 1.4 and 0.44.

The quadrupole moment of the Eu^{153} nucleus in the ground state is known from experiments on Coulomb excitations[11] and is equal to 7.7×10^{-24} cm^2. Thus the experimental data testifies to the fact that the different deformation corresponds to different internal states.

The value of the mixture of M1 and E2 for any transition is determined by the ratio of probabilities B(M1)/B(E2) for this transition. From the known values of Q_0, g_K and g_R for the Eu^{153} nucleus in the ground and excited states, we can determine the ratio $[B(M1)/B(E2)]_{83.4}$: $[B(M1)/B(E2)]_{69.7}$, which is shown to be equal to 0.03. In the same way, it is explained why the transition with 83.4 kev energy has a much larger admixture of E2 than the transition with energy of 69.7 kev.

In conclusion, the authors express their deep gratitude to D. A. Varshalovich for discussion of the results.

---

[1] L. A. Sliv and I. M. Band, Таблицы коэффициентов внутренней конверсии гамма-излучения (Conversion Coefficients of Gamma Radiation) Acad. Sci. Press, 1958, p. 2.

[2] Graham, Ewan, and Geiger, Bull. Am. Phys. Soc. Ser II, **5**, No. 1 (1960).

[3] M. E. Rose, Internal Conversion Coefficients, Amsterdam, 1958.

[4] Anton'eva, Bashilov, Dzelepov, and Preobrazhenskiĭ, Izv. Akad. Nauk SSSR, Ser. Fiz. **22**, 135 (1958), Columbia Tech. Transl. p. 134.

[5] Alaga, Alder, Bohr, and Mottelson, Kgl. Danske Vidensk. Selsk. Mat.-fys. Medd. **29**, No. 9 (1955).

[6] Gnedich, Kryukova, and Murav'eva, JETP **38**, 726 (1960), Soviet Phys. JETP **11**, 524 (1960).

[7] S. G. Nilsson, Kgl. Danske Vidensk. Selsk. Mat.-fys. Medd. **29**, No. 16 (1955).

[8] L. I. Rusinov and D. A. Varshalovich, Атомная энергия (Atomic Energy) **5**, 432 (1958).

[9] Collection, Строение атомного ядра (Structure of the Atomic Nucleus) IIL, 1959, pp. 552 and 556.

[10] R. Graham and J. Walker, Phys. Rev. **94**, 794 (1954).

[11] N. F. Ramsey, Nuclear Moments, New York, 1953.

Translated by R. T. Beyer
14

SOVIET PHYSICS JETP VOLUME 13, NUMBER 1 JULY, 1961

AN INVESTIGATION OF THE $Sn^{112}(\gamma, n)$ AND $Sn^{124}(\gamma, n)$ REACTIONS

KUO CH'I-TI, B. S. RATNER, and B. V. SERGEEV

P. N. Lebedev Physics Institute, Academy of Sciences, U.S.S.R.

Submitted to JETP editor August 3, 1960

J. Exptl. Theoret. Phys. (U.S.S.R.) 40, 85-87 (January, 1961)

The yield curves for the (γ, n) reaction in Sn^{112} and Sn^{124} were measured by means of the induced radioactivity. The peaks of the cross section curves for the reactions $Sn^{112}(\gamma, n)Sn^{111}$ and $Sn^{124}(\gamma, n)Sn^{123}$ are located at 16.0 ± 0.5 and 15.5 ± 0.5 Mev, respectively. The corresponding integral cross sections are 1.82 ± 0.10 and 1.56 ± 0.08 Mev-barn.

1. The (γ, n) reaction in different isotopes of the same element has hitherto been investigated almost exclusively for light nuclei, where the total cross section for γ-ray absorption includes additional important contributions from (γ, p), (γ, np) and $(\gamma, 2n)$ reactions. For medium-weight and heavy nuclei, where the (γ, n) reaction furnishes ~ 90% of the entire giant-resonance cross section, we have only the data obtained by Katz and Cameron[1] for antimony. A surprisingly large difference was found between the integral cross sections for the (γ, n) reaction in Sb^{121} and Sb^{123}.

It was of interest to obtain data on the integral cross section and the resonance energy and width of the (γ, n) reaction in isotopes of a single element with greatly different numbers of neutrons. For this purpose the two extreme isotopes Sn^{112} and Sn^{124} were selected.

2. Both reactions were investigated through the activity induced by synchrotron-generated γ rays ($E_{\gamma max} = 30$ Mev). In the case of the $Sn^{112}(\gamma, n)Sn^{111}$ reaction ($T_{1/2} = 35$ min) a 29.3% enriched sample of Sn^{112} was used,* while for $Sn^{124}(\gamma, n)Sn^{123}$ ($T_{1/2} = 40$ min) chemically pure natural tin was used. The (γ, n) yield was measured relative to $Cu^{63}(\gamma, n)Cu^{62}$ at energies above the threshold of the latter reaction, and relative to readings from an integrating ionization chamber in the case of lower energies. Residual β activity was registered by means of two BFL-25 end-window counters in an anticoincidence scheme, with ~ 0.55 registration efficiency. The scalar output was fed to a time discriminator. The scale of the energy stabilization system of the synchrotron was calibrated by means of the thresholds of $Cu^{63}(\gamma, n)$ (10.75 Mev) and $C^{12}(\gamma, n)$ (18.72 Mev), as well as the bend at $E_{\gamma max} = 17.15$ Mev in the $O^{16}(\gamma, n)$ curve. The relative yield curve for $Sn^{112}(\gamma, n)$ includes a correction for 0.9% content of Sn^{124}. The yield from $Sn^{124}(\gamma, n)Sn^{123}$ takes into account ~ 7% of activity from Sn^{112}. For $E_{\gamma max} > 20$ Mev an ~ 8-min activity also appears, which at $E_{\gamma max} = 24.0$ Mev amounts to ~ 10% (assuming the same number of nuclei) of the 40-min activity of Sn^{123}. The self-absorption of Sn^{123} and Cu^{62} β rays for the given experimental geometry was obtained by irradiating samples of different thickness.

3. The yields Y of the reactions $Sn^{112}(\gamma, n)$ and $Sn^{124}(\gamma, n)$ are shown in Fig. 1. The $Sn^{112}(\gamma, n)$ threshold is 10.2 ± 0.2 Mev, which differs considerably from the binding energy 11.1 Mev given in reference 2 for a neutron in Sn^{112}.

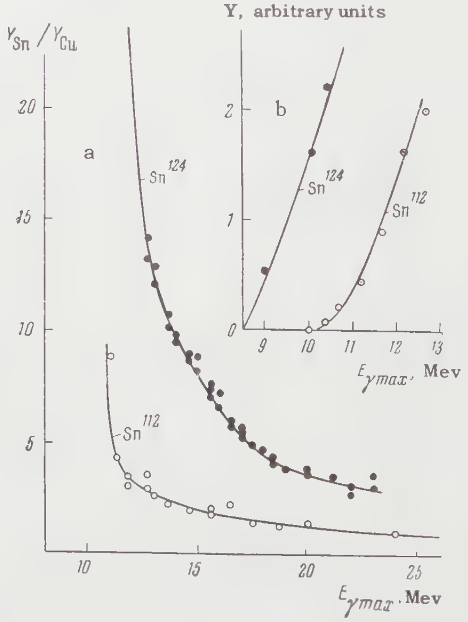

FIG. 1. a – Yields of the reactions $Sn^{112}(\gamma, n)$ and $Sn^{124}(\gamma, n)$ relative to the yield of $Cu^{63}(\gamma, n)$ as a function of $E_{\gamma max}$; b – yields of $Sn^{112}(\gamma, n)$ and $Sn^{124}(\gamma, n)$ as a function of $E_{\gamma max}$ near threshold.

---

*The authors,are very grateful to workers in the laboratory of V. S. Zolotarev, who prepared this sample.

The reaction threshold 8.5 ± 0.3 Mev obtained for $Sn^{124}(\gamma, n)$ agrees with mass data.[2] The (γ, n) cross sections were plotted from the relative yield curves and the $Cu^{63}(\gamma, n)$ cross section by the method described in reference 3. Corrections were introduced that take account of the Sn^{111} decay scheme[4] and the contribution from $Sn^{124}(\gamma, n)Sn^{123*}$. Irradiation at $E_{\gamma max} = 19.0$ Mev for the purpose of measuring the 126-day activity of Sn^{123*} showed a 0.24 ± 0.09 yield ratio for final-nucleus formation in the isomeric $(I = 9/2)$ and ground $(I = 3/2)$ states, respectively. This indicates a high probability for transitions with small spin change.

Figure 2 shows the energy dependence of the $Sn^{112}(\gamma, n)$ and $Sn^{124}(\gamma, n)$ cross sections, for which we have the following results:

	$Sn^{112}(\gamma, n)Sn^{111}$	$Sn^{124}(\gamma, n)Sn^{123}$
Peak energy, Mev	16.0±0.5	15.5±0.5
Cross section peak, mb	340±40	300±30
Half-width, Mev	5.0±0.5	5.0±0.5
Integral cross section, Mev-barn	1.82±0.10	1.56±0.08

The $Sn^{124}(\gamma, n)$ cross section peak agrees with values obtained for a natural tin isotope mixture. A comparison of data for the two isotopes must take into account the considerable difference between the $Sn^{112}(\gamma, n)$ and $Sn^{124}(\gamma, n)$ thresholds, 21.0 and 14.0 Mev, respectively. This evidently accounts for the very close peak energies and integral cross sections for γ-ray absorption by Sn^{112} and Sn^{124}, as would be expected from the sum rule.

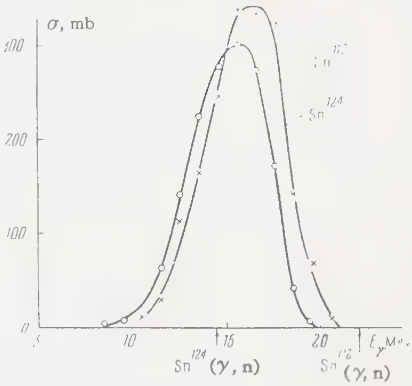

FIG. 2. Cross sections for the reactions $Sn^{112}(\gamma, n)$ and $Sn^{124}(\gamma, n)$. Thresholds are indicated by arrows.

---

[1] L. Katz and A. G. W. Cameron, Can. J. Phys. **29**, 518 (1951).

[2] V. A. Kravtsov, Usp. Fiz. Nauk **54**, 3 (1954).

[3] Kuo Ch'i-Ti and B. S. Ratner, JETP **39**, 1578 (1960), Soviet Phys. JETP **12**, 1098 (1961).

[4] C. L. McGinnis, Phys. Rev. **81**, 734 (1951).

[5] Fuller, Petree, and Weiss, Phys. Rev. **112**, 554 (1958).

Translated by I. Emin
15

SOVIET PHYSICS JETP VOLUME 13, NUMBER 1 JULY, 1961

OBSERVATION OF RESONANCE ABSORPTION OF GAMMA RAYS IN Zn^{67}

S. I. AKSENOV, V. P. ALFIMENKOV, V. I. LUSHCHIKOV, Yu. M. OSTANEVICH, F. L. SHAPIRO, and YEN WU-KUANG

P. N. Lebedev Physics Institute, Academy of Sciences, U.S.S.R. and Joint Institute for Nuclear Research

Submitted to JETP editor August 3, 1960

J. Exptl. Theoret. Phys. (U.S.S.R.) **40**, 88-90 (January, 1961)

Experiments on the observation of recoilless resonance absorption of the 92-kev γ rays of Zn^{67} are described. A positive result was obtained for metallic zinc at liquid-helium temperature. However the effect is very small.

THE radioactive isotope Ga^{67} (half-life $T = 78$ hr) emits γ quanta with energy $E = 92$ kev, which appear in the transition of the Zn^{67} nucleus from its first excited state ($T = 9.3 \times 10^{-6}$ sec, relative width $\Gamma/E = 5.3 \times 10^{-16}$) to the ground state.[1] Resonance scattering of these quanta by Zn^{67}, using the Mössbauer effect,[2] is of considerable interest, for example, for the study of the gravitational red shift under laboratory conditions,[3,4] since the relative width of the Zn^{67} gamma line is three orders of magnitude smaller than that of the line in Fe^{57}, which has been used in various experiments.[5,6] In the present paper we describe the results of the first experiments undertaken to detect resonance scattering in Zn^{67}.

EXPERIMENTAL ARRANGEMENT

The resonance scattering effect was measured by the increase in intensity of the filtered radiation when the resonance condition was destroyed. A source of Ga^{67} was produced on one side of a sample containing Zn^{67} by a preliminary irradiation of this side with 6.7-Mev protons. The source thickness did not exceed 0.1 mm, while the rest of the sample (4 — 6 mm thick) served as a filter (cf. the figure). The resonance was destroyed by applying to the sample an inhomogeneous magnetic field with a maximum magnetic field strength of 1500 oe. As a result of the nuclear Zeeman effect, the magnetic field produced a shift of the emission line relative to the absorption line which was by a factor of ten greater than the natural line width. The detectors were FÉU-11B photomultipliers with NaI crystals 15 mm thick.

For the "poor geometry" shown here, Compton and resonance scattering of quanta in the detector reduces the observed effect by a factor of 2 — 3 compared to the effect in an ideal geometry. However we felt that this defect was compensated by two advantages: a) to a large extent, the possibility of relative motions of source and filter is eliminated; b) we reduce the danger of shifts of the emission and absorption lines resulting from nonidentical composition and treatment of source and filter.

The change in the amplification of the multiplier when the field was turned on did not exceed 10^{-5}. To eliminate errors resulting from drifts in the detection equipment, measurements with and without field were alternated every 20 — 40 sec. The time intervals were given by a quartz-stabilized frequency generator. After each switching on of the field, a demagnetization was carried out, so that the residual field did not exceed 1 oe.

The principal measurements were done at 4.2° and 300° K with a polycrystalline sample of zinc, enriched to 33% in Zn^{67}. As a control, we also measured the intensity of 92-kev radiation passing

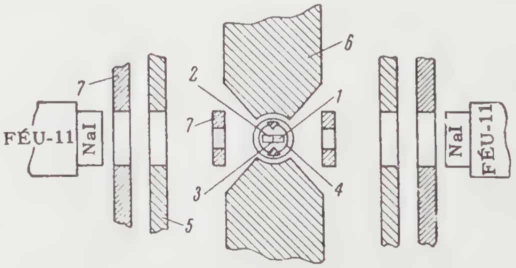

Schematic of the experimental apparatus: 1 – sample of enriched Zn, 2 – sample of normal Zn, 3 – face of enriched sample, irradiated at cyclotron, 4 – shield at 80°K, with Armco iron pole pieces, 5 – magnetic shield (iron), 6 – pole of electromagnet, 7 – lead collimators. Samples 1 and 2 were soldered to the bottom of a container of liquid helium. The photomultipliers were surrounded by a permalloy screen 5 mm thick.

Relative change in intensity of filtered radiation when the magnetic field is applied (10^2 δ, %)

Series of measurements	4°K				300° K			
	Enriched Zn		Normal Zn		Enriched Zn		Normal Zn	
	E_γ=92 kev	180 kev	92 kev	180 kev	92 kev	180 kev	92 kev	180 kev
I	4.48±2.69		—1.36±2.85					
II	2,74±1,65		—0.75±1,83		0,84±1,40		—1,17±1,61	
III	2.22±1,04	—0.67±1.32	+1,35±1.12	0.09±1.18	0.63±0,84	—0.88±0.97	0,70±0.89	0,36±0,98
average	2.58±0.84	—0.67±1.32	0.55±0.91	0.09±1.18	0.68±0.73	—0.88±0.97	0.26±0.79	0,36±0.98

through a sample of normal zinc (4.1% Zn^{67}). In some of the experiments we also recorded the intensity of filtered 180- and 270-kev radiation, which should not undergo resonance absorption.

In addition to metallic zinc, we also investigated an ordered alloy of brass and normal zinc (β′ brass, 50% Cu, 50% Zn) and an alloy of Cu + 1.5% Zn, with an enrichment to 71% in Zn^{67}. Within the limits of statistical accuracy of the measurements, which were 2.2×10^{-2} and 7.5×10^{-2}%, respectively, the brass and the Cu-Zn alloy showed no resonance absorption effect.

The results of the measurements with metallic zinc are shown in the table.

DISCUSSION OF RESULTS

As we see from the table, the intensity of the 92-kev radiation, filtered through enriched zinc at a temperature of 4.2° K, increases when the magnetic field is applied by an amount $\delta = (2.58 \pm 0.84) \times 10^{-2}$%. The sign of the change corresponds to the presence of a Mössbauer effect in zinc, and its magnitude is three times greater than the mean square statistical error of the measurements. At the same time, there was not a single control measurement in which δ exceeded the mean square error.

In computing the Mössbauer effect in zinc, we should not use the Debye approximation, since the Debye temperature of zinc depends very strongly on temperature.[7] Kazarnovskiĭ,[8] starting from experimental data on the specific heat of zinc, found that the effective Debye temperature of zinc for the Mössbauer effect is 213° K. Using this figure, taking account of the quadrupole splitting of the levels of Zn^{67} in the hexagonal zinc lattice, and introducing a factor of ½ — ⅓ for the "dilution" of the effect because of the "poor geometry" of the experiment, we get an expected value for the effect of $\delta = (6 - 9) \times 10^{-2}$%. This is somewhat greater than the observed value, which may be explained by a broadening or shift of the Mössbauer line, or by an incorrect location of some of the atoms of Ga^{67} in the zinc lattice.

Recently Pound and Rebka[9] reported an unsuccessful attempt to detect resonance absorption in normal zinc. Obviously this result is in agreement with our data since even in enriched zinc the effect is four times less than the error in the experiments of Pound and Rebka, which was 0.1%. Craig et al.[11] have observed the resonance absorption in zinc oxide.

The low value of the resonance absorption effect in zinc makes difficult any further investigation or use by the filter method. At present we are preparing experiments for recording scattered Zn^{67} radiation, where for better separation from the nonresonant background we propose to use detectors with better energy resolution (xenon proportional counters) and to modulate the beam of γ quanta incident on the scatterer by means of a rotating chopper. Such a modulation is technically feasible because of the relatively long mean life of the isomeric level of Zn^{67}.

In addition one should consider the possibility of increasing the yield of the Mössbauer line by introducing the Zn^{67} into a material with high atomic weight. Using the classical theory of the Mössbauer effect,[10] one can see that for the case of a small amount of impurity the relative area of the Mössbauer line is determined not by the mass of the radiating atom but rather by the mass of the solvent atom and the Debye temperature of the solvent.

In conclusion the authors thank I. Ya. Barit, A. G. Zel'dovich, Ya. B. Zel'dovich, and M. I. Podgoretskiĭ for valuable discussions, A. B. Fradkov for liquefying the helium, and E. Ya. Pikel'ner, V. A. Otroshchenko and A. I. Sekirin for help with the measurements.

The samples were irradiated at the cyclotron of the Nuclear Physics Institute of Moscow State University. The authors take this opportunity to express their profound gratitude to S. S. Vasil'ev, G. V. Koshelyaev, A. F. Tulinov and the operating crew of the cyclotron.

---

[1] B. S. Dzhelepov and L. K. Peker, Схемы распада радиоактивных ядер (Decay Schemes of Radioactive Nuclei), 1958.

[2] R. L. Mossbauer, Z. Physik **151**, 124 (1958); Z. Naturforsch. **14a**, 211 (1959).

[3] Barit, Podgoretskiĭ, and Shapiro, JETP **38**, 301 (1960), Soviet Phys. JETP **11**, 218 (1960).

[4] R. V. Pound and G. A. Rebka, Jr., Phys. Rev. Letters **3**, 439 (1959).

[5] R. V. Pound and G. A. Rebka, Jr., Phys. Rev. Letters **4**, 337 (1960).

[6] Cranshaw, Schiffer, and Whitehead, Phys. Rev. Letters **4**, 163 (1960).

[7] M. Blackman, Handbuch der Physik, vol. VII/1, p. 325, 1955.

[8] M. V. Kazarnovskiĭ, JETP **38**, 1652 (1960), Soviet Phys. JETP **11**, 1191 (1960).

[9] R. V. Pound and G. A. Rebka, Jr., Phys. Rev. Letters **4**, 397 (1960).

[10] F. L. Shapiro, Usp. Fiz. Nauk **72**, 685 (1960), Soviet Phys. Uspekhi **3**, 881 (1961).

[11] Craig, Nagle, and Cochran, Phys. Rev. Letters **4**, 561 (1960). Nagle, Craig, and Keller, Nature **186**, 707 (1960).

Translated by M. Hamermesh
16

SOVIET PHYSICS JETP VOLUME 13, NUMBER 1 JULY, 1961

DECAY SCHEME OF Te^{131m}

A. BǍDESCU, O. M. KALINKINA, K. P. MITROFANOV, A. A. SOROKIN, N. V. FORAFONTOV, and V. S. SHPINEL'

Institute of Nuclear Physics, Moscow State University

Submitted to JETP editor August 7, 1960

J. Exptl. Theoret. Phys. (U.S.S.R.) **40**, 91-100 (January, 1961)

The γ and β radiation accompanying the decay of the Te^{131m} isomer ($T_{1/2} = 30$ hr) was measured with a scintillation γ coincidence spectrometer, a two-lens β spectrometer and a $\beta\gamma$-coincidence spectrometer. A decay scheme for the decay of the Te^{131m} nucleus is proposed. Levels at 0.15, 0.60, 0.78, 0.92, 1.62, 1.82, 1.92, 2.00, and 2.24 Mev have been established for the daughter nucleus I^{131}. The spins and parities of a number of levels have been determined from the data on the multipolarities and relative intensities of the γ and β transitions.

INTRODUCTION

THE present work is a continuation of the investigations of the decay scheme of the Te^{131} nucleus ($T_{1/2} = 30$ hr), the preliminary results of which have been published previously.[1] One can also find in reference 1 a brief survey of other work devoted to the decay of this isotope. In reference 1, we made an accurate determination of the γ spectrum and established the excited levels of the I^{131} nucleus with energies of 147, 595, 780, and 2200 kev. It was shown there that the I^{131} level scheme presented by Hebb[2] is inaccurate. However, the results were not sufficiently complete to determine the positions of the levels lying between the 780- and 2200-kev levels. In the present work, the measurements were made under better conditions than previously. First, for the preparation of the source we used 99.9% Te^{130}-enriched tellurium. (The methods of eliminating the daughter isotope I^{131} from the source and of obtaining the samples have been described previously.[1]) Second, for the measurements of the $\gamma\gamma$ coincidences, we used NaI(Tl) crystals of large size and recorded the spectra with the aid of a 100-channel pulse-height analyzer of type AI-100. Moreover, the partial β spectra were separated by the method of $\beta\gamma$ coincidences. All this made it possible to obtain more complete information on the Te^{131m} decay scheme.

γ SPECTRUM

After removal of the I^{131} isotope from the sample, we measured the γ-ray spectrum of Te^{131m} on a scintillation spectrometer. For the measurement of the hard γ rays ($E_\gamma > 400$ kev) we used a 40 × 40 mm NaI(Tl) crystal with a resolving power of 10% on the 660-kev Cs^{137} line. The soft region of the spectrum was measured with a crystal of diameter 30 mm and height 14 mm, having a better resolving power (8.5%). Figure 1 shows the γ-ray spectrum in the low-energy region below 400 kev. The γ-ray spectrum in the high-energy region (to 2500 kev) has been given previously.[1]

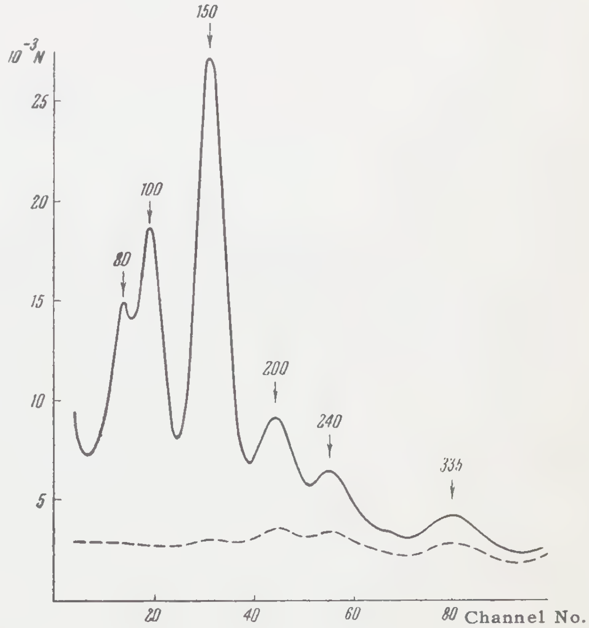

FIG. 1. γ spectrum of Te^{131m} in the energy region up to 400 kev. The spectrum measured with a 2 mm Pb + 0.5 mm Cd filter is indicated by the dotted line. This makes it possible to take into account the contribution from the Compton distributions of the harder γ transitions. In this figure and in subsequent figures, the energies in kev are shown above the peaks.

Table I
Energy and Intensities of Te^{131m} γ Lines

E_γ, kev			I_γ, % (scintillation spectrometer)
Scintillation spectrometer	Photoelectron spectrum	Conversion-electron spectrum	
80±5	—	81±0,5	5±1
100±5	101±1	101,5±0,5	8±2
150±5	149±2	149±1	25±5
—	183±2	182±0.2	—
200±5	201±3	—	~8
240±5	240±5	241±5	~4
—	—	277±5	—
335±5	333±5	330±5	18±6
450±10	~454	~454	12±3
590±10	~588	—	~4
780±10	780±5	780±5	100
850±15	840±10	840±10	50±10
920±20	925±10	—	14±5
1080±20	—	—	6±2
1140±20	1140±15	—	27±5
1220±20	1220±15	—	20±5
1350±30	—	—	~2
1540±30	—	—	~1,5
1650±30	—	—	3±1
1920±30	—	—	2,5±0,5
2000±30	—	—	4,6±0,5
2240±30	—	—	0,94±0,2

In the present experiment we determined more accurately the energy of some hard lines and made a more careful resolution of the spectrum. The energies (E_γ) and intensities (I_γ) of the γ rays obtained from these measurements are shown in Table I. Columns 2 and 3 of this table give the γ-transition energies obtained from the photoelectron and internal-conversion electron spectra, respectively, measured on a two-lens β spectrometer. The spectrum of the photoelectrons were measured with lead radiators of 8-mm diameter and thicknesses of 11 mg/cm^2 and 4 mg/cm^2. The half-width of the lines was 4%. The intensities of the γ transitions in the energy region > 700 kev obtained from the photoelectron spectrum are in agreement with the data of the scintillation γ spectrum. In the softer region the determination of the intensities from the photoelectron lines was not carried out, owing to the large Compton background from hard γ rays.

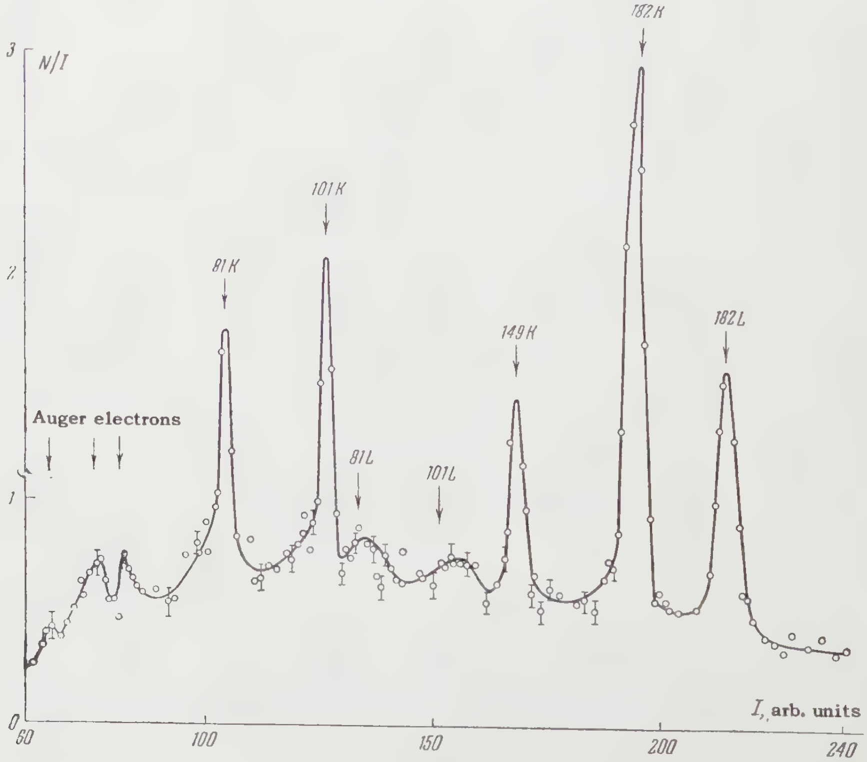

FIG. 2. Conversion-electron (I – Current in spectrometer coils).

Table II
Internal-Conversion Coefficients for γ Transitions

E_γ, kev	α_K	α_K/α_L	Theoretical value of α_K			Proposed multipolarity
			$E2$	$M1$	$E1$	
81±0.5	2.06±0.45	⩾5	2.3	1.2	0.3	$M1+E2$
101.5±0.5	1.23±0.28	⩾5	1.12	0.603	0.166	$M1+E2$
149±1	0.26±0,05	—	0.3	0.195	0.05	$M1+(E2)$

CONVERSION-ELECTRON SPECTRUM

The conversion-electron spectrum in the 10 — 200 kev region measured on a two-lens β spectrometer is shown in Fig. 2. A source ~ 0.1 mg/cm^2 thick was used in the measurements of this spectrum. The thickness of the counter window was ~ 0.1 mg/cm^2 and its transmission threshold was 8 kev. The resolving power of the spectrometer in these measurements was 2%. The intensity ratio of the 81-, 101.5-, and 149-kev conversion lines can be determined from the spectrum. Using the ratio of intensities corresponding to the γ lines in the γ spectrum and the value of the conversion coefficient $\alpha_K = 0.26 \pm 0.05$ for the 149-kev transition obtained by Sorokin,[3] we can obtain the value of α_K for the 81- and 101.5-kev transitions. Moreover, we can estimate for these transitions the value of the ratio α_K/α_L. These data are shown in Table II, which also gives the theoretical values of α_K for various multipolarities. Comparison of our data for α_K with the theoretical values indicates that the 81- and 101.5-kev transitions can be of the M1 or E2 type, or a mixture of both, but the large value of the ratio α_K/α_L (≥ 5) indicates that in all probability they are preferentially of the M1 type with a possible admixture of E2.

Also visible in the spectrum shown in Fig. 2 are the intense K and L peaks from the 182-kev γ transition occurring in Te^{131} (isomeric transition of the M4 type). Apart from the peaks shown in Fig. 2, peaks from γ-rays of energies 24, 277, 330, 780, and 840 kev were also visible in the spectrum. In reference 1, the coefficient α_K for the 780-kev transition was determined from a comparison of the intensities of the conversion and photoelectron lines from the 780-kev γ transition in I^{131} with the intensities of the corresponding lines from the 364-kev γ transition in Xe^{131} (I^{131} was not separated from the sample), whose conversion coefficient α_K is known. It turned out to be $(0.8 \pm 0.2) \times 10^{-3}$ and corresponded to a transition of the E1 type.

In the present work we repeated these measurements by a somewhat different method. We prepared sources of Te^{131} and Cs^{137} and, under identical geometrical conditions, we measured the relative intensities of the conversion lines on a β spectrometer and of the γ lines with a scintillation spectrometer. The coefficient α_K for the 662-kev transition in Ba^{137} is known well[4] and the conversion coefficient for the 780-kev transition can be determined from the expression

$$\alpha_{K780} = \alpha_{K662}\,(I_{\gamma 662}/I_{\gamma 780})\,(I_{e780}/I_{e662}).$$

These measurements gave the value $\alpha_{K780} = (1 \pm 0.3) \times 10^{-3}$, in agreement with the value obtained by us previously and with the multipolarity ascribed to this transition. The conversion coefficient for the 840-kev transition was not specifically determined, but, by using the available experimental data, we could estimate it to be ~ 2×10^{-3}, which is also in agreement with the previously[1] reported value $(1.6 \pm 0.6) \times 10^{-3}$ and corresponds to the multipole orders M1, E2, or a mixture of both.

BETA SPECTRUM

The β spectrum was measured on a two-lens β spectrometer with a source thickness of 1 mg/cm^2, resolving power of ~ 4%, and a transmission of ~ 5%. A Fermi plot was made of the spectrum and the partial β spectra were separated (Fig. 3). In subtracting the hardest spectrum ($E_{max} = 2460$ kev), which was a unique spectrum ($\Delta J = 2$, yes)^2, we introduced a correction factor of the form

$$a_1(W) = (W^2 - 1) + (W_0 - W)^2.$$

The spectrum was not resolved in the soft-energy region (< 300 kev). The shape of the spectrum in this region indicates the existence of a component with $E_{max} \approx 200$ kev. This was confirmed by measurements based on the $\beta\gamma$-coincidence method. All the data on the Te^{131} β spectra are shown in Table III. In this table, the energies of the soft components are taken from the measurements of the partial β spectra by the $\beta\gamma$-coincidence method. Apart from the β spectra shown in Table III, we observed a spectrum with E_{max} = 690 ± 40 kev and intensity ~ 6.5% of the full

Table III

β spectra of Te^{131}

$E_{\beta max}$, kev	Relative intensity, %			log ft
	Full β spectrum	β-spectra of isomer with $T_{1/2}=25$ min	β spectra of isomer with $T_{1/2}=30$ hr	
2457±10	3.76±0.4	—	3.76±0.4	9.45
2150±20	7.85±0.8	42.3±4	—	6.81
1680±50	3±0.3	16.2±2	—	6.30
1365±25	7.67±0.8	41.4±4	—	5.54
570±30	30.9±3	—	30.9±3	6.15
420±30	43.4±4	—	43.4±4	5.56
215±15	3.6	—	3.6	5.69

spectra. It can be assumed that it is associated with the decay of Te^{127}, a small admixture of which could have been contained in our sample. An intensive β spectrum with $E_{max} = 695$ kev is emitted in the decay of Te^{127}.[4] The β spectrum with $E_{max} = 980$ reported by Hebb[2] was not disclosed by our measurements. The intensities of the partial spectra which we obtained were also somewhat different from that given by Hebb.[2]

$\beta\gamma$ AND γe^- COINCIDENCES

Measurements of $\beta\gamma$ and γe^- coincidences were carried out on an arrangement consisting of a two-lens β spectrometer and a scintillation γ spectrometer connected in a coincidence circuit. This arrangement has already been described in detail.[5,6] In our work, we used a commercial coincidence circuit of type BDS-1, a preamplifier of an improved type, and a new high-voltage stabilizer, which kept the supply voltage of the photomultipliers in the β and γ channels constant to within 0.06%. In the γ channel, we used a NaI (Tl) crystal 40 mm in diameter and 40 mm thick. The relative half-width of the Cs^{137} γ lines was 11%. In the β channel, we used an anthracene crystal 15 mm in diameter and 2 mm thick. The radioactive source had the shape of a circle 8 — 12 mm in diameter and 2 — 3 mg/cm^2 thick. The resolving power of the β spectrometer was then ~ 4% with a transmission of the order of 2%. All the measurements were carried out with a resolving time of $2\tau = 7 \times 10^{-8}$ sec. Under these conditions, the relative counting efficiency attained 80%. To separate the partial β spectra, the differential window of the β-channel analyzer was set on the photopeak of the γ line under study and the number of $\beta\gamma$ coincidences was measured as a function of the energy of the electrons focused by the β spectrometer. From the corresponding Fermi plot, we obtained the values of the maximum energies of the β spectra. In some cases an integral threshold was used in the β channel.

All the obtained results are shown in Table IV. In this table, column 1 lists the energies of the γ lines with which the coincidences were measured. Also shown are the mean values of the maximum energies of the partial spectra which were calculated from the values of the maximum energy obtained in the coincidences with various γ quanta.

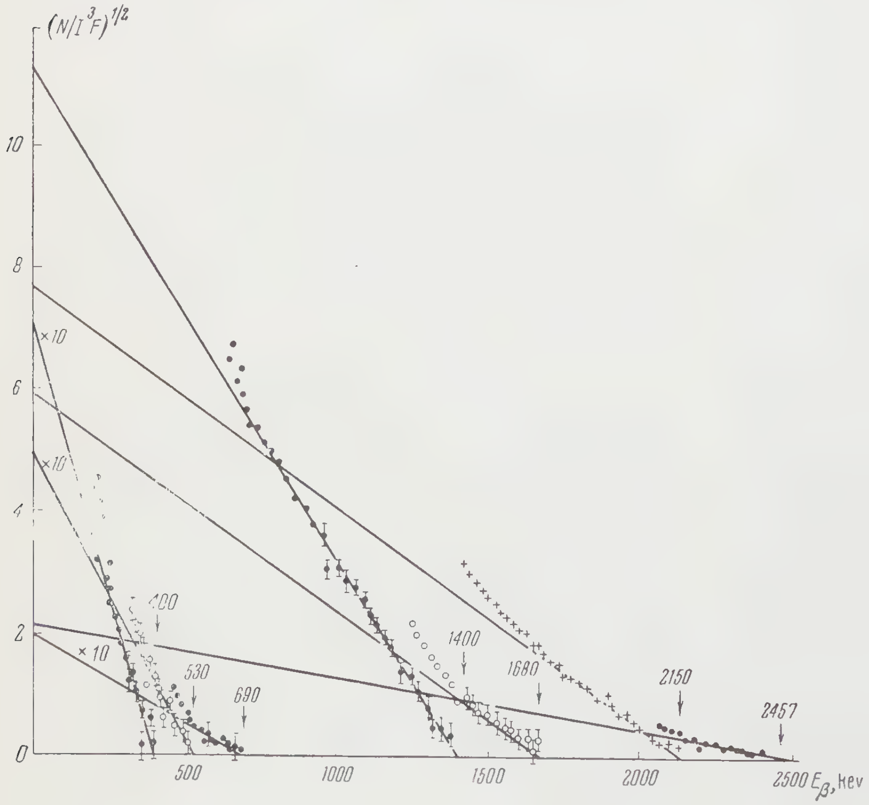

FIG. 3. Fermi plot for β spectrum of Te^{131m}.

Table IV
$\beta\gamma$ Coincidences of Te^{131}

E_γ, kev	$E_{\beta\ max}$, kev			
780	1350±30	590±30	460±40	225±40
850 920	1380±40	590±30	420±40	200±40
1140	—	535±50	380±40	—
1650	—	580±50	420±100	220±50
⩾1300	—	680±100	425±25	—
⩾1900	—	545±30	345±70	—
Mean value of $E_{\beta_{max}}$, kev	1365±25	570±30	420±30	215±15

Shown in Fig. 4a is a Fermi plot for the β spectra in coincidence with 780-kev γ lines; Fig. 4b shows a Fermi plot for β spectra in coincidence with γ quanta whose energy exceeds 1900 kev.

γ RAYS FOLLOWING THE HARD β SPECTRA (E ≥ 600 KEV)

We presented previously[1] the results of $\beta\gamma$ coincidence measurements on a scintillation spectrometer. It was then reported that γ rays with energies of 850, 780, 590, 450, 330, and 150 kev were observed in coincidences with γ rays of energy ≥ 600 kev. In these measurements, however, the contribution from coincidences was not taken into account. In the present experiment, similar measurements were made, in which this contribution was taken into account. The results are shown in Fig. 5. As seen from the figure, only γ transitions with energies of 150, 450, 590 kev and possibly ~ 900 kev take part in the coincidences. It is evident that all the remaining γ transitions proceed from levels that are populated as a result of soft β spectra.

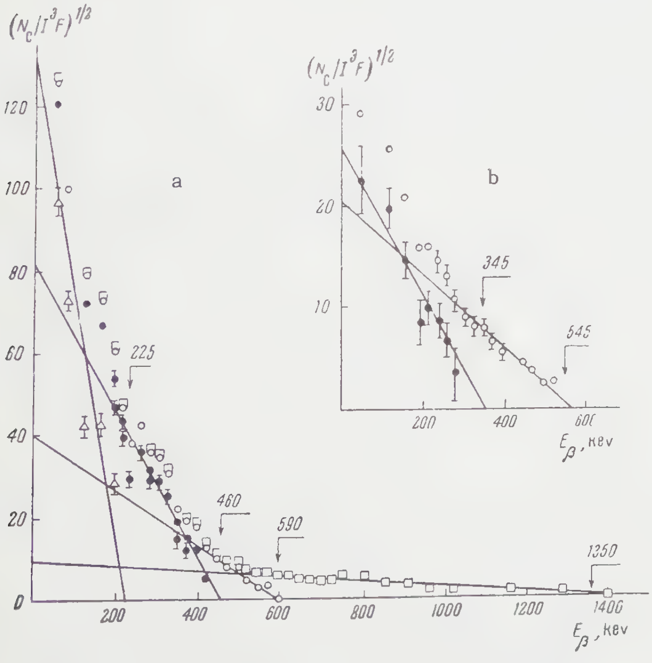

FIG. 4. a – Fermi plot of the spectrum of β particles in coincidence with 780-kev γ rays; b – Fermi plot for coincidences with γ rays ≥ 1900 kev. Here and elsewhere N_c is the coincidence counting rate.

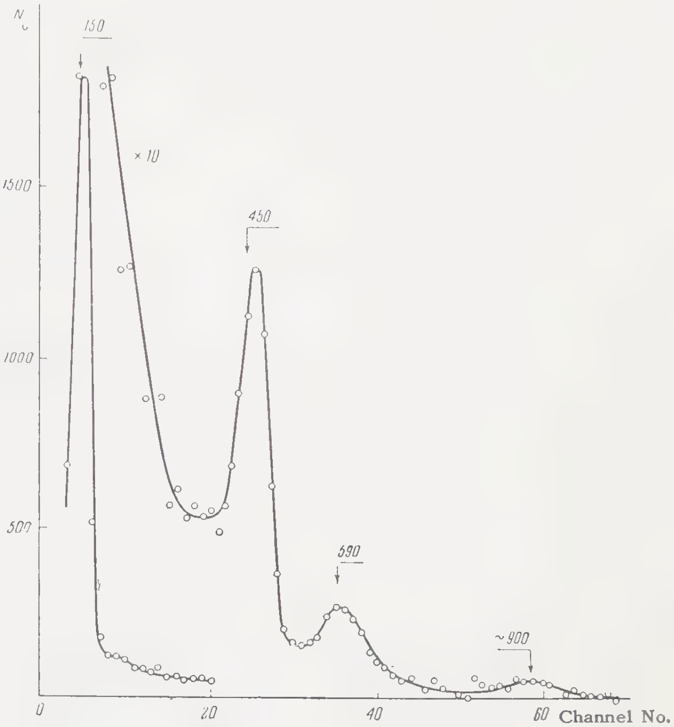

FIG. 5. γ-ray spectrum in coincidence with β electrons of energy ≥600 kev.

$\gamma\gamma$ COINCIDENCES AND CONSTRUCTION OF THE DECAY SCHEME

Shown in Figs. 6 and 7 are the γ spectra obtained in coincidences with the hardest γ rays of Te^{131}. Peaks from γ rays of 81 and ~ 240 kev (Fig. 6) stand out in the spectrum of coincidences with all γ rays of energy ≥ 1800 kev (i.e., 1920, 2000, and 2240 kev). The absence of a peak from 150-kev γ rays (transition from the first excited level) indicates that all these transitions proceed to the ground state of I^{131}. Then it is natural to interpret the 81- and 240-kev γ rays as transitions between the levels 1.92 and 2.0 Mev (80 kev) and 2.0 and 2.24 Mev (240 kev). During the measurements of the spectrum shown in Fig. 7, the window of the control analyzer was set on the peak from the 1650-kev γ rays. In comparison with the spectrum of Fig. 6, there are the additional peaks here from 100- and 330-kev γ rays. In the energy region of 180-260 kev, a plateau is observed. Evidently, apart from the 240-kev peak, there is also a 200-kev γ ray peak. The peak at 150 kev, as shown by an estimate, can largely be explained

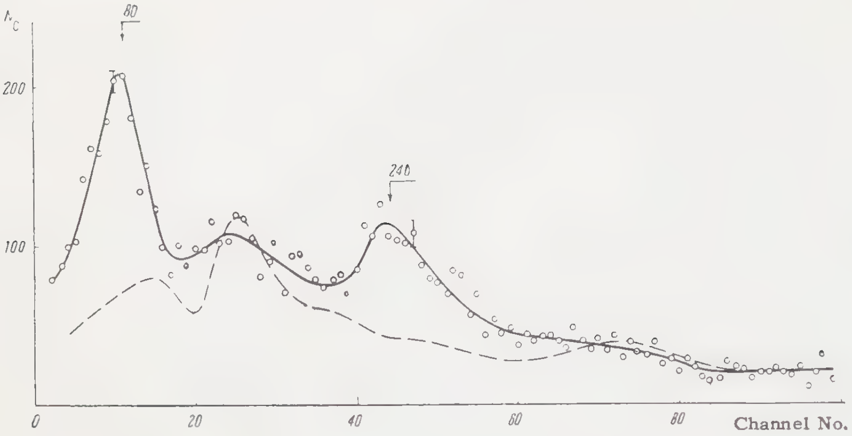

FIG. 6. γ spectrum in coincidence with γ rays of energy $\geq$1800 kev. The dotted line indicates the contribution from random coincidences.

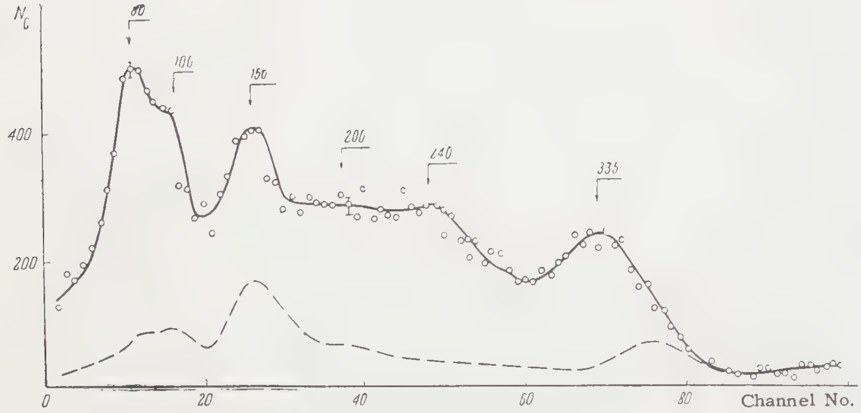

FIG. 7. γ spectrum in coincidence with 1650-kev γ rays. The dotted line indicates the contribution from random coincidences.

by the random-coincidence background. Hence, it is clear that the 1650-kev transition also proceeds to the ground state. Transitions with energies of 100, 200, and 330 kev evidently occur between levels lying in the interval of 1.92 — 1.65 Mev. The energy of the 1650-kev transition was determined to an accuracy of ± 1 kev. A more accurate value of the energy of the level from which this transition takes place can be obtained from the fact that the 780- and 840-kev γ rays are emitted in cascade. This was demonstrated earlier[1,2] and is confirmed in the present experiment. We thus obtain an energy of 1.620 ± 0.015 Mev for this level.

Furthermore, $\gamma\gamma$ cascades of 780-1140, 780-1220, and 1140-80 kev were also observed. This indicates that the 1140-kev and 1220-kev transitions proceed from the 1.920 ± 0.20 Mev and 2.000 ± 0.20 Mev levels, respectively. It should be noted that, since the energy of the 81-kev transition is known to an accuracy of ± 0.5 kev, the difference in the energies of these two levels is determined to the same accuracy. The levels lying in the 1.92 — 1.62 Mev interval were not reliably established by us, since direct transitions from them to the ground state were not observed, and the spectrum of soft γ quanta between them had a quite complex character and could not be reliably inter-

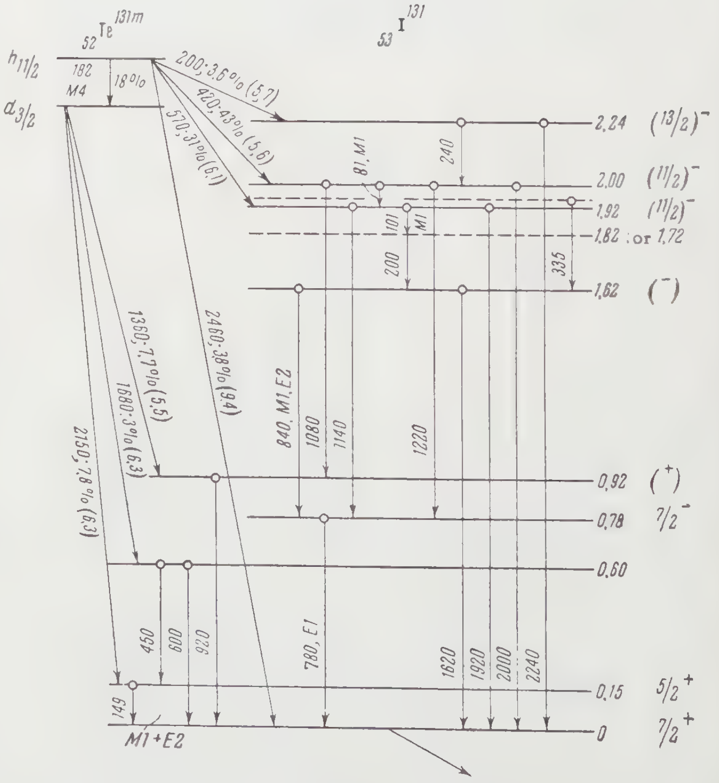

FIG. 8. Decay scheme of Te^{131}. The energies of the levels are given in Mev and the energies of the transitions in kev.

preted. Moreover, the energies of the partial β transitions were not determined with sufficient accuracy. We also established the presence of coincidences between 920- and 1080-kev γ rays. The energy of this cascade is 2000 kev, and we therefore assumed that it proceeds from the 2.0 Mev level to the ground state. Since in the resolution of the singles γ spectrum it was found that the intensity of the 920-kev transition is greater than the intensity of the 1080-kev transition (see Table I), then this cascade evidently goes through the 0.920-Mev level and not through the 1.08-Mev level. Moreover, in the spectrum of coincidences with β electrons of energy > 600 kev (Fig. 5) there is an indication of the presence of a peak with energy ~ 900 kev which can be associated with a 920-kev γ transition following the 1360-kev β transition. The position of the levels at 0.15, 0.6, and 0.78 Mev was established by us earlier.[1]

Figure 8 shows the general scheme of the decay of Te^{131} nuclei which agrees with the results of the measurements described above.

DISCUSSION OF THE DECAY SCHEME. SPINS AND PARITIES OF THE LEVELS

The most intensive β transitions of the Te^{131} nucleus are the β transitions of energies 420 and 570 kev proceeding to levels that are close to 2 Mev. From energy considerations they should proceed from the isomeric state Te^{131m} with the characteristic $^{11}/_{2}^{-}$. The values of the quantity log ft for β transitions of 420, 570, and 200 kev (see Table III) indicate that these transitions are evidently allowed. Therefore the 2.24-, 2.0-, and 1.92-Mev levels (and also, possibly, other high-lying levels) have high spin values, from $^{9}/_{2}$ to $^{13}/_{2}$, and negative parity. Furthermore, 780-kev level has a negative parity, since the transition from this level to the ground state is of the E1 type. This level is populated almost entirely as a result of the intense γ transitions of 840, 1140, and 1220 kev. The β transitions to this level were not observed either from the isomeric or ground state of Te^{121}. This result can be explained only if the 780-kev level has a spin and parity of $^{7}/_{2}^{-}$. The characteristics of the I^{131} levels proposed on the basis of the available experimental data (log ft for β transitions, intensities and multipole orders of γ transitions) are also shown in Fig. 8. The ground and first excited states of I^{131} are the $g_{7/2}$ and $d_{5/2}$ states predicted by the single-particle model given in reference 1. The 600-kev level can also be a single-particle $d_{3/2}$. The remaining levels apparently cannot be explained within the framework of the single-particle model.

In conclusion, the authors express their gratitude to M. Radoevich for aid in carrying out the experiments and in the analysis of the experimental data, to S. A. Sergeev for considerable help in setting up the apparatus, and to V. O. Kordyukevich for performing part of the radiometric work.

---

[1] Bǎdescu, Mitrofanov, Sorokin, and Shpinel', Izv. Akad. Nauk SSSR, Ser. Fiz. **23**, 1434 (1959), Columbia Tech. Transl. p. 1424.

[2] E. Hebb, Phys. Rev. **97**, 987 (1955).

[3] A. A. Sorokin, Izv. Akad. Nauk SSSR, Ser. Fiz. **23**, 1445 (1959), Columbia Tech. Transl. p. 1434.

[4] B. S. Dzhelepov and L. K. Peker, Схемы распада радиоактивных ядер (Decay Schemes of Radioactive Nuclei), Press of the Acad. Sci. U.S.S.R., 1958.

[5] Delyagin, Sorokin, Forafontov, and Shpinel', Izv. Akad. Nauk SSSR, Ser. Fiz. **20**, 913 (1956), Columbia Tech. Transl. p. 828.

[6] Parfenova, Forafontov, and Shpinel', Izv. Akad. Nauk SSSR, Ser. Fiz. **21**, 1601 (1957), Columbia Tech. Transl. p. 1590.

[7] L. A. Sliv and I. M. Band, Таблицы коэффициентов внутренней конверсии на K-оболочке (Table of Internal-Conversion Coefficients for the K-Shell), Press of the Acad. Sci. U.S.S.R. 1956.

Translated by E. Marquit
17

SOVIET PHYSICS JETP VOLUME 13, NUMBER 1 JULY, 1961

SHORT-LIVED ISOMERS OF Ga, Ge, AND As PRODUCED BY 19.2-Mev PROTONS

A. M. MOROZOV

Institute of Chemical Physics, Academy of Sciences, U.S.S.R.

Submitted to JETP editor August 9, 1960

J. Exptl. Theoret. Phys. (U.S.S.R.) 40, 101-104 (January, 1961)

Improved data are presented relating to the short-lived isomers previously observed when gallium, germanium, and arsenic were irradiated with fast protons.[1,2] A more detailed investigation revealed two short-lived activities in germanium, one of which is produced in the reaction $Ge^{76}(p, 2n)As^{75m}$ and the other apparently in $Ge^{72}(p, pn)Ge^{71m}$. The isomeric activities which followed the bombardment of gallium and arsenic were shown to result from $Ga^{71}(p, n)Ge^{71m}$ and $As^{75}(p, p')As^{75m}$, respectively. The energy dependence of the cross sections for $Ga^{71}(p, n)Ge^{71m}$ and $Ge^{76}(p, 2n)As^{75m}$ were measured from the reaction threshold to 19.2 Mev.

THE present experiments were stimulated by the fact that in earlier irradiation of gallium with fast protons an error in the reaction-threshold measurement led to incorrect identification of the reaction which produced a short-lived isomer.[2] The technique used in the present measurements was described in detail in reference 3. As in the earlier work, a proton beam impinging on an internal target was used in the measurement of excitation curves. Protons were counted by means of a current integrator connected to the target.

Arsenic. The present investigation showed that the gamma emission which we had detected in proton-irradiated metallic arsenic[2] has the energy $E_\gamma = 0.29 \pm 0.01$ Mev and half-life $T_{1/2} = 15.6 \pm 0.4$ millisec, in good agreement with our earlier results.[2] The excitation curve of the isomeric activity was measured using a thick arsenic target. Figure 1 shows that the isomeric level is excited by protons with $E_p \leq 2$ Mev. This result, as well as the good agreement with the corresponding data for As^{75m} from arsenic irradiated with 22-Mev gamma rays[4] ($E_\gamma = 284 \pm 5$ kev and $T_{1/2} = 17 \pm 1$ millisec), confirms our earlier identification of the reaction as $As^{75}(p, p')As^{75m}$.[2]

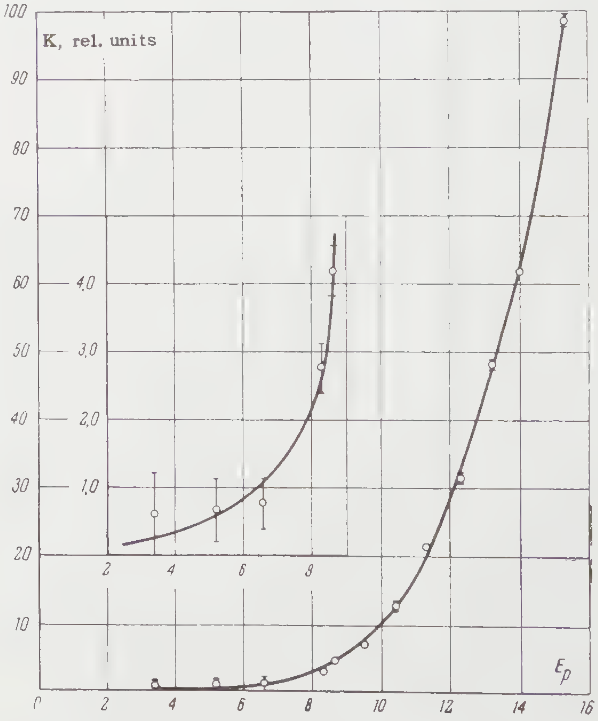

FIG. 1. Yield of short-lived isomer As^{75m} (from a thick arsenic target) as a function of proton energy. Statistical errors are indicated. The background from a neutral (carbon) target was taken into account. The pulse-height analyzer had a 10-volt channel width; the photomultiplier gate of length $\tau = 55$ millisec was delayed 3.7 millisec following the start of the proton pulse. The isomer yield at the reaction threshold is also shown on a larger scale.

Gallium. In the investigation of short-lived gamma rays from metallic gallium bombarded with fast protons we improved our earlier data for the isomer,[2] obtaining $E_\gamma = 0.18 \pm 0.01$ Mev and $T_{1/2} = 19.4 \pm 0.4$ millisec (instead of $E_\gamma = 0.19 \pm 0.01$ Mev and $T_{1/2} = 19.0 \pm 1.0$ millisec). Experiments with enriched gallium isotopes confirmed the fact that this isomer is produced through a reaction in Ga^{71}. Figure 2 represents the measurement of the cross section for the production of this isomer as a function of proton energy. The shape of the curve and the measured reaction threshold (below 2 Mev) indicate the reaction $Ga^{71}(p, n)Ge^{71m}$. Numerous measure-

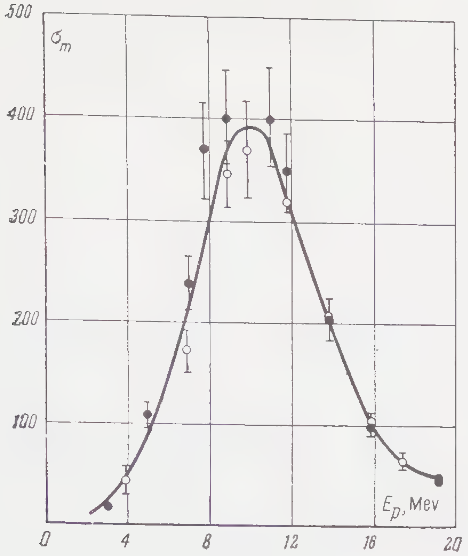

FIG. 2. Cross section (in millibarns) for Ge^{71m} production as a function of proton energy. The target was gallium oxide with 24.7 mg/cm² surface density. The black and open circles represent measurements on different days. The rms errors were calculated from the formula for the reaction threshold given in reference 3.

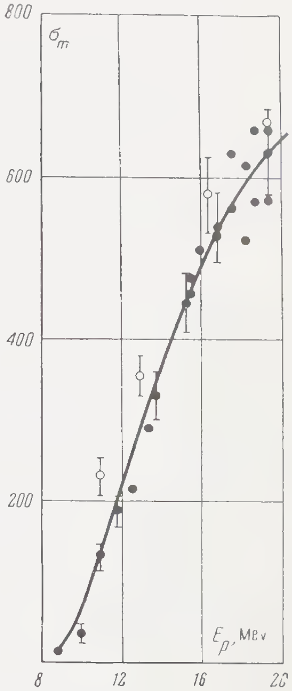

FIG. 3. Cross section (in millibarns) for As^{75m} production as a function of proton energy, from a 28.1-mg/cm² germanium oxide target.

ments yielded $\sigma_m = 50 \pm 6$ mb for the production of the isomer by 19.2-Mev protons.

The decay scheme of Ge^{71} is known. Transition energies of ~23 and ~175 kev in the decay of As^{71} have been reported in references 5 and 6. It was established that the two lines are in cascade and belong to Ge^{71}. Both groups of investigators have proposed a decay scheme for Ge^{71} on the basis of shell theory, β-decay theory, and data from other authors. The more likely scheme, in our opinion, is given in reference 6:

$$g_{9/2} \xrightarrow[M2]{23,3\ \text{keV}} f_{5/2} \xrightarrow[E2]{174,5\ \text{keV}} p_{1/2}.$$

The lifetime of the $f_{5/2}$ level is $\sim 0.07 \times 10^{-6}$ sec.[5] No measurements were obtained for the lifetime of the $g_{9/2} \rightarrow f_{5/2}$ transition, although $\sim 10^{-3}$ sec was the expected value.[6] In the different decay scheme given in reference 5, spin and parity $7/2^+$ are assigned to the 198-kev level, in conjunction with a $7/2^+ \rightarrow 5/2^-$ electric dipole transition. We have estimated $\lesssim 10^{-11}$ sec for the lifetime of a ~23-kev E1 radiative transition.

A comparison of the short-lived emitted energy which we observed in Ge^{71} decay with the data in references 5 and 6 indicates clearly that $T_{1/2} = 19.4$ millisec pertains to a ~198-kev level. Our value $E\gamma = 0.18$ Mev agrees with the value ~175 kev given in references 5 and 6. Low-energy emission (~23 kev) was not registered by our apparatus. We note that the theoretical[6] internal conversion coefficient for an M2 transition at ~23 kev is ~500.

A 0.17-Mev emission with half-life 16 ± 1 millisec was also observed when germanium was bombarded with 14-Mev neutrons.[7] The cross section (~0.3 barn) for isomer production in this case indicated the highest likelihood of a (n, 2n) reaction, and that this reaction cannot occur in Ge^{73} and Ge^{76}. Assuming that the radiation which we had previously observed[1] in proton-bombarded gallium and the radiation from neutron-bombarded germanium belong to the same isomer, and assuming also that the level scheme of Ge^{71} includes a 0.17-Mev state, it was suggested in reference 7 that Ge^{71m} had most probably been detected.

Germanium. When metallic germanium was irradiated we observed not one,[2] but two γ lines with $E\gamma_1 = 0.17 \pm 0.01$ Mev and $E\gamma_2 = 0.30 \pm 0.01$ Mev, and with half-lives 19.2 millisec and 16.3 ± 0.3 millisec, respectively. It has been shown in our earlier work that the 0.30-Mev line with 16-millisec half-life belongs to As^{75m} from $Ge^{76}(p, 2n)As^{75m}$.[2] This identification is confirmed by the shape of the curve (Fig. 3) representing our measurements of the production cross section for this isomer as a function of proton energy. The computed threshold for $Ge^{76}(p, 2n)As^{75}$ is ~9.2 Mev.

Several measurements yielded $\sigma_m = 6.35 \pm 60$ mb for the production of As^{75m} by 19.2-Mev protons.

The good agreement between the results $E\gamma_1 = 0.17$ Mev and $T_{1/2} = 19.2$ millisec from proton-

Target	Gamma-ray energy, Mev	Half-life, millisec	Cross section, mb	Yield from thick target, rel. un.	Reaction
Ga	0.18±0.01	19.4±0.4	50±6	2	Ga^{71} (p, n) Ge^{71m}
Ge	0.17±0.01	19.2	—	—	Ge^{72} (p, pn) Ge^{71m}
	0.30±0.01	16.3±0.3	635±60	2	Ge^{76} $(p, 2n)$ As^{75m}
As	0.29±0.01	15.6±0.4	—	0,2	As^{75} (p, p') As^{75m}

irradiated germanium, and the emission that we observed in gallium ($E\gamma = 0.18$ Mev, $T_{1/2} = 19.4$ millisec) and which we identified as belonging to Ge^{71m}, suggests that in proton-irradiated germanium in addition to As^{75m} an isomer of Ge^{71} is formed [$Ge^{72}(p, pn)Ge^{71m}$ with the computed reaction threshold ~ 11.2 Mev].

We also measured the yields of isomeric activities in thick targets of gallium ($E\gamma = 0.18$ Mev), germanium ($E\gamma = 0.30$ Mev), and arsenic ($E\gamma = 0.29$ Mev), irradiated with 19.2-Mev protons. These yields were, as previously, compared with that of the short-lived isomeric activity ($E\gamma = 0.37$ Mev) from a thick tantalum target.[3]

The results of the present investigation are given in the table.

In conclusion the author wishes to thank P. A. Yampol'skiĭ for a discussion of the results, A. P. Klyucharev for substantial assistance, and V. V. Remaev for aid in measuring cross sections.

---

[1] Leĭpunskiĭ, Morozov, Makarov, and Yampol'skiĭ, JETP **32**, 393 (1957), Soviet Phys. JETP **5**, 305 (1957).

[2] A. M. Morozov and P. A. Yampol'skiĭ, JETP **36**, 950 (1959), Soviet Phys. JETP **9**, 671 (1959).

[3] Morozov, Remaev, and Yampol'skiĭ, JETP **39**, 973 (1960), Soviet Phys. JETP **12**, 674 (1961).

[4] R. B. Duffield and S. H. Vegors, Phys. Rev. **112**, 1958 (1958).

[5] W. E. Graves and A. C. G. Mitchell, Phys. Rev. **97**, 1033 (1955).

[6] Thulin, Moreau, and Atterling, Arkiv Fysik **8**, 219 (1954).

[7] Glagolev, Kovrizhnykh, Makarov, and Yampol'skiĭ, Report, Inst. Chem. Phys. Acad. Sci. U.S.S.R., 1958; JETP **36**, 1046 (1959), Soviet Phys. JETP **9**, 742 (1959).

Translated by I. Emin
18

SOVIET PHYSICS JETP VOLUME 13, NUMBER 1 JULY, 1961

MODIFICATIONS OF BERYLLIUM AND IRON IN FILMS CONDENSED ONTO COLD SUBSTRATES

B. G. LAZAREV, E. E. SEMENENKO, and A. I. SUDOVTSOV

Physico-Technical Institute, Academy of Sciences, Ukrainian S.S.R.

Submitted to JETP editor August 10, 1960

J. Exptl. Theoret. Phys. (U.S.S.R.) 40, 105-108 (January, 1961)

A study has been made of the variation with temperature of the electrical resistance of films of beryllium, iron, and copper, condensed onto substrates cooled with liquid helium, hydrogen, or nitrogen. In the beryllium films the existence of two low-temperature modifications, obtained under differing conditions of condensation, was discovered. One of these modifications becomes superconducting at ~ 8° K and exists over the temperature region up to ~ 40° K; the other becomes superconducting at ~ 6° K and is stable up to at least 130° K. In the iron films a polymorphic transition is found at a temperature of ~ 40° K. No polymorphic transitions are observed in copper films.

IT is well known at the present time that certain metals, at least bismuth and beryllium, are not superconductors in the bulk state (down to 10^{-2}° K), while in films produced by low-temperature condensation they do show superconductivity, at relatively high temperatures (bismuth films, at ~ 6° K[1,2]; beryllium films, at ~ 8° K[3,4]).

In the present communication the results are presented of a further study of the superconducting properties and the temperature dependence for beryllium films, in connection with the question of the occurrence in them of new modifications.

In view of the data appearing in the literature concerning the possibility of low-temperature polymorphism in iron,[5] the electrical conductivity of films of this metal was also studied. Films of copper — a metal which has no low temperature modifications — were also investigated by the same method.

Production of the films and measurements of their electrical conductivity were carried out in the apparatus represented schematically in Fig. 1. The glass capsule 9 was evacuated to a pressure of 10^{-7} mm Hg, and pumping was continued with heating at this pressure for several hours; following this, the capsule was sealed off and placed in the helium cryostat. During evaporation of the metal to be studied the capsule was immersed in liquid helium. Below 4.2° K the temperature was controlled by helium vapor pumping, while for production of temperatures above 4.2° a jacket 1 in the form of a Dewar vessel was lowered over the capsule, whereupon the desired temperature was established within it with the aid of the heater 4.

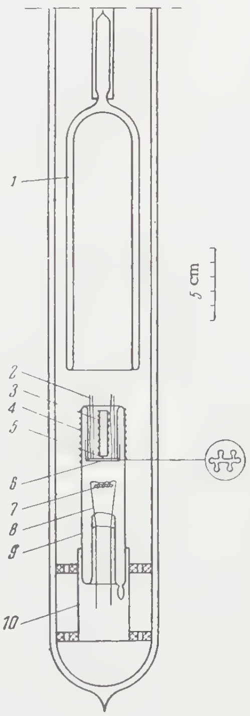

FIG. 1. Apparatus for production of films and measurement of their electrical conductivity: 1 – jacket in the form of a Dewar vessel; 2 – platinum leads from film; 3 – resistance thermometer; 4 – heater; 5 – polished glass surface onto which the film is condensed; 6 – mask defining the form chosen for the film; 7 – charge of metal to be evaporated; 8 – platinum leads for the evaporator; 9 – glass capsule; 10 – sleeve for centering capsule in cryostat.

Warming of the films was usually conducted at a rate of 2 deg/min. From 4.2 to 300° K the temperature was measured with the platinum or indium resistance thermometer 3, while from 4.2 to

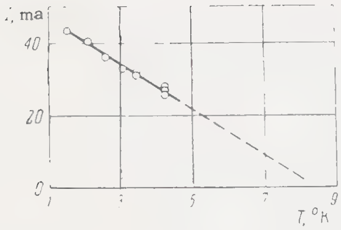

FIG. 2. Curve showing dependence of critical current upon temperature for one of the films.

1.23°K, it was determined from the vapor pressure of the helium bath. The electrical resistance of the thermometer and of the films was measured on a PPTN-1 potentiometer.

For destruction of superconductivity in beryllium films by current, the capsule could be filled with liquid helium subsequent to the deposition of the film.

In a previous paper[4] it was reported that beryllium films produced by low temperature condensation have a polymorphic transition at ~ 30°K. The films were obtained by rapid evaporation (evaporation time ~ 10 sec, temperature of the beryllium charge ~ 1500°C) onto a substrate cooled by liquid helium, and had a sharply-defined superconducting transition in the vicinity of 8 — 9°K. The same transition temperature is obtained by extrapolation of the curve showing the temperature dependence of the critical current (Fig. 2). The superconducting modification is preserved under heating to ~ 30°K. The region over which it exists is characterized by a horizontal segment in the curve showing the temperature variation of the electrical conductivity of the film, in the range from 8.5 to 30°K. Films heated to this temperature show, upon re-cooling, the same properties as freshly-condensed ones — the same complete superconducting transition is present in the same temperature region.

Heating of the films to 60°K leads to the disappearance of the superconducting modification, and this limiting heating temperature falls somewhat with increasing annealing time.

Films produced by condensation onto a substrate cooled with liquid hydrogen, following the same evaporation process, behave in a similar fashion.

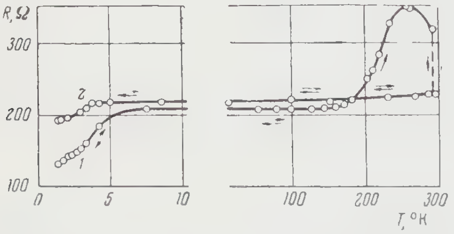

FIG. 3. Variation of electrical resistance with temperature for a beryllium film produced by slow condensation at low temperature: curve 1 – for the film after deposition; curve 2 – for a film maintained at room temperature 360 hours.

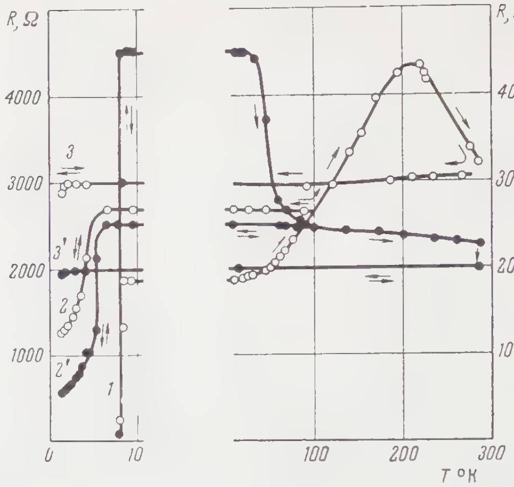

FIG. 4. Variation of electrical resistance with temperature for two beryllium films produced by slow condensation onto a surface cooled by liquid helium: 1 – initial curves; 2 and 2′ – after heating to 80° K; 3 and 3′ – following annealing at 290° K for 1 hr. Left-hand resistance scale refers to curves 1, 2, 3; right-hand, to curves 1, 2′, 3′.

It has recently become known that the mechanisms of evaporation of beryllium from the solid and liquid states are different.[7] While the beryllium evaporates primarily from the solid phase in the form of diatomic molecules, evaporation from the liquid phase proceeds chiefly in the atomic state. It was expected that condensation of vapor existing in such different states would influence the state of the films produced. A difference in the properties of films formed by slow evaporation (from the solid state) and films produced by rapid evaporation (from molten charges) is in fact observed.

Evaporation from solid beryllium (evaporation time ~ 1000 sec, charge temperature ~ 900°C) produces films that possess, in all probability, still another superconducting modification. The superconducting transition for these films (curve 1, Fig. 3) is smeared out over the region from 6°K on down. This second superconducting modi-

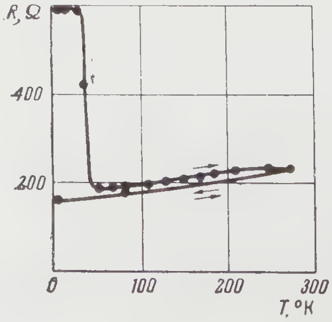

FIG. 5. Variation of electrical resistance with temperature for an iron film produced by condensation onto a surface cooled by liquid helium.

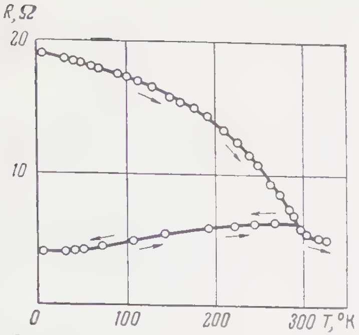

FIG. 6. Variation of electrical resistance with temperature for a copper film produced by low temperature condensation.

fication is stable to more elevated temperatures. Heating of the films to 130° K leads to no change in the second superconducting modification — the same fall in resistance below 6° K persists upon re-cooling. Moreover, the second superconducting modification can be obtained by slow evaporation onto a substrate cooled with liquid nitrogen. The temperature dependence of the electrical conductivity for films produced in this fashion is also shown in Fig. 3. After annealing at room temperature for 360 hrs. the film, on re-cooling still has a pronounced drop in electrical resistance below 5° K (curve 2).

Evaporation from the solid phase of beryllium onto a substrate cooled by liquid helium (Fig. 4) evidently leads to a mixture of the two superconducting beryllium modifications. The first superconducting modification has a sharp superconducting transition at ~ 8.4° K (curves 1 and 1′). This modification exists up to 30° K, while heating to 60° leads to its complete disappearance. Before annealing, the first modification, which becomes superconducting at the higher temperature (~ 8.4° K), apparently shunts the second modification, with the lower superconducting transition temperature (~ 6° K). The second modification is revealed following warming of the film to 60° K and subsequent cooling (curves 2 and 2′, Fig. 4). It is preserved when the film is maintained for as long as may be desired at a temperature of 130° K. Further, the second modification survives briefly (1 — 2 hrs) heating to room temperature (curves 3 and 3′). To be sure, this modification is considerably more stable when condensed slowly onto a wall cooled by liquid nitrogen (Fig. 3).

Analysis of curves showing the temperature dependence of the electrical conductivity is, evidently, a sensitive method for detection of polymorphism in metals. This circumstance can clearly be regarded at present as definitely established.

In a series of experiments, low temperature polymorphism has been found by the present method in bismuth,[1,2] beryllium,[3,4] gallium,[2] lithium, sodium, and potassium.[8] In bismuth, beryllium, and gallium, the existence of the new phases is further confirmed by their superconductivity. It is of interest that for bismuth there probably occurs in the film one of the modifications which exists at high pressures. This is evidently also the case for gallium; the same situation should be looked for in beryllium as well.

It seemed of interest also to investigate iron, for which, according to the data available,[5] the existence of a low temperature modification is possible. A curve showing the variation of electrical resistance with temperature for one of the iron films studied is presented in Fig. 5. This film was condensed onto a substrate cooled by liquid helium (evaporation time ~2 hr).

In the vicinity of 40° K there occurs a sharply-defined, irreversible drop in the electrical resistance. It appears that in iron there is indeed a low temperature modification produced which is stable up to 40° K. We should remark that superconductivity was not detected in any of the eleven films studied.

For comparison, we present the R(T) curve (Fig. 6) obtained for a copper film condensed at 4.2° K. No low temperature modifications have been found for this metal[9]. The curves are monotonic; they have none of the characteristic features typical of such curves for metals which possess new modifications in freshly-condensed films. Thus, low temperature modifications in freshly-condensed films have been observed for a whole series of metals: two in gallium, two in beryllium, one in bismuth, one in iron, and two each in sodium, lithium, and potassium.

---

[1] N. V. Zavaritskiĭ, Dokl. Akad. Nauk SSSR **86**, 687 (1952).

[2] W. Buckel and R. Hilsch, Z. Physik. **138**, 109, 136 (1954); F. Baumann, Nachr. Akad. Wiss. Göttingen, Math-physik Kl. IIa **15**, 285 (1956).

[3] Lazarev, Sudovtsov, and Smirnov, JETP **33**, 1059 (1957), Soviet Phys. JETP **6**, 816 (1958).

[4] Lazarev, Sudovtsov, and Semenenko, JETP **37**, 1461 (1959), Soviet Phys. JETP **37**, 1035 (1960).

[5] Mikhaĭlov, Nikulin, Reĭnov, and Smirnov, J. Tech. Phys. (U.S.S.R.) **29**, 931 (1959), Soviet Phys.-Tech. Phys. **4**, 844 (1960).

[6] A. I. Shal'nikov, Nature **142**, 74 (1938); JETP **10**, 630 (1940). N. E. Alekseevskiĭ, Dokl. Akad. Nauk SSSR **24**, 27 (1939); JETP **10**, 1392 (1940).

[7] Amonenko, Ryabchikov, Tikhinskiĭ, and Finkel', Dokl. Akad. Nauk SSSR **128**, 977 (1959).

[8] Lazarev, Semenenko, and Sudovtsov, JETP **39**, 1165 (1960), Soviet Phys. JETP **12**, 811 (1961).

[9] E. Feldtkeller, Z. Physik **157**, 65 (1959).

Translated by S. D. Elliott
19

SOVIET PHYSICS JETP VOLUME 13, NUMBER 1 JULY, 1961

POLARIZATION OF SOME RADIOACTIVE ISOTOPES IN ALLOYS

A. V. KOGAN, V. D. KUL'KOV, L. P. NIKITIN, N. M. REĬNOV, I. A. SOKOLOV, and M. F. STEL'MAKH

Leningrad Physico-Technical Institute, Academy of Sciences, U.S.S.R.

Submitted to JETP editor August 10, 1960

J. Exptl. Theoret. Phys. (U.S.S.R.) 40, 109-113 (January, 1961)

Polarization of the nuclei of the radiactive isotopes Au^{199}, Ir^{192}, Ir^{191m}, Re^{186}, and V^{48} alloyed with iron was studied at ultra-low temperatures. The magnetic field acting on the nuclei of the isotope mixture was $H_{eff} \geq 2 \times 10^6$ oe for Au^{199}, $H_{eff} \geq 2 \times 10^5$ oe for Re^{186}, and $H_{eff} \sim 10^6$ oe for Ir^{192}. No polarization was found in the Ir^{191m} isomer produced as a result of β decay of Os^{191m} introduced in the iron or in V^{48} in an alloy containing iron and 2% titanium. The comparatively small value of H_{eff} for Re^{186} may be due to the large disorientation of the nuclei during the β transition. The increase in the value of H_{eff} with the atomic number of the weakly magnetic mixture is in qualitative agreement with the theory proposed by Marshall.

THE method proposed by Samoĭlov, Sklyarevskiĭ, and Stepanov[1] for orienting nuclei of weakly magnetic elements alloyed with ferromagnetics opens new possibilities for carrying out investigations with oriented nuclei.

The nature of the large magnetic fields acting on the nuclei of weakly magnetic elements is still not entirely clear.

The only theoretical work deveoted to the question of the production of internal fields in metallic ferromagnetics, that of Marshall,[2] is only qualitative in character. As shown by that author, in general, both the conduction electrons and the atomic shell play a role in the production of this field; its value also depends on the type of lattice of the alloy. Recently, Khutsishvili[3] showed that at sufficiently low temperatures one may expect an essential orientation of nuclei and ions in the lattice of a dielectric antiferromagnetic.

Thus far, there are not very many experimental data on the orientation of nuclei in ferromagnetics[4-7] and, apart from the work of Samoĭlov, Sklyarevskiĭ, and Stepanov,[1,8,9] they deal with the question of the size of the internal field in ions of cobalt in cobalt single crystals and its various alloys.

In the present article, we present the results obtained from the orientation of Au^{199}, Ir^{192}, Ir^{191m}, Re^{186}, and V^{48} alloyed with iron. The first results for Sc^{46} and Co^{60} and the experimental method are described in a previous report.[10]

The study of the anisotropy of γ radiation of oriented nuclei allows one to obtain data on the value of μH_{eff}, where μ is the magnetic moment of the nucleus and H_{eff} is the effective magnetic field producing the orientation of the nucleus in the alloy.

However, for all the isotopes investigated in the present work, apart from V^{48}, the effect of the β transition on the anisotropy following γ radiation cannot be calculated in a single-valued way.

The temperature dependence of the anisotropy of the γ radiation was calculated without taking into account the preceding β transition.

The quantity $\beta = \mu H_{eff}/IkT$, where μ and I are the magnetic moment and spin of the nucleus, k is Boltzmann's constant, and T is the absolute temperature, serves as the temperature parameter. From the experimental dependence $\sqrt{\epsilon} = f(1/T)$ at a given source temperature, we determined the quantity $\epsilon = [J(\pi/2) - J(0)]/(\pi/2)$, and then, from the calculated curve, the value of β. In order to find H_{eff}, we inserted in the expression for β the value of the gyromagnetic ratio for the initial β active nucleus. Such a calculation does not take into account the fact that the nuclei are partially disoriented after the β decay, and the degree of orientation of the initial nuclei can be greater than the calculated value. Of course, the estimate of the value of H_{eff} obtained in this way is only the lower limit of the quantity we are seeking.

Au^{199}

Au^{199} is the daughter nucleus of the Pt^{199} obtained by neutron irradiation of Pt^{198}. Alloy samples with a 0.7% platinum content (by weight) were irradiated by neutrons and annealed in vacuo for two days after irradiation, in which time the Pt^{199} isotope is almost entirely transformed into Au^{199}. The polarization of the Au^{199} nuclei was measured from the anisotropy of the 158-kev γ radiation. The part of the decay scheme of interest to us is shown in Fig. 1. A plot of $\sqrt{\epsilon}$ vs the reciprocal of the temperature of the cooling salt is shown on the same figure.

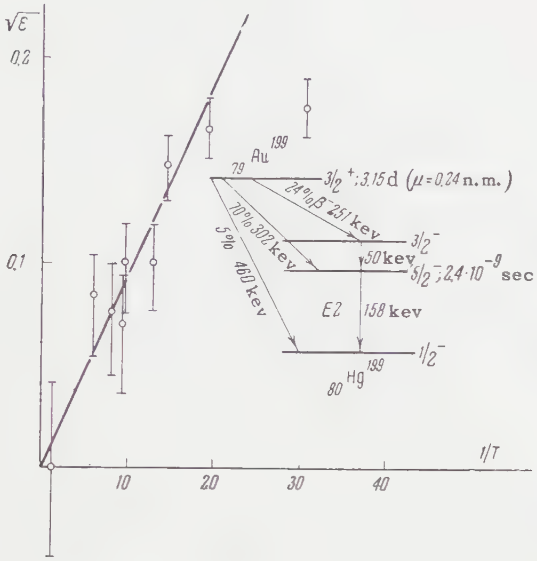

FIG. 1

Since the magnetic moment of the Au^{199} nucleus is known [μ = 0.24 nuclear magnetons (n.m.)], the analysis of the experimental data leads to a value $H_{eff} \geq 2 \times 10^6$ oe. The value $H_{eff} \geq 10^6$ oe obtained for the Au^{198} isotope by Samoĭlov et al.[1] is in agreement with our value of H_{eff}. The presence of a level of Hg^{199} with a lifetime of $\sim 10^{-9}$ sec in the decay scheme of Au^{199} does not lead to any essential disorientation of the nuclei.

Ir^{192}

The iron-iridium alloy samples contained less than 0.2% iridium by weight. The anisotropy of the γ radiation was measured after the decay of the Ir^{194} isotope.

Figure 2 shows the basic decay scheme of Ir^{192} and a plot of $\sqrt{\epsilon}$ vs 1/T. The value of ϵ attained 40%. We note that the 537-kev β transition is unique and its effect on the anisotropy of the subsequent γ radiation can be evaluated. However, the cascade γ transitions with energies 308 and 296 kev are mixtures, and small errors in determining the mixture coefficients lead to considerable errors in the calculation of the γ-radiation anisotropy. Therefore in order to determine the internal field, we used the 468-kev γ transition following the 673-kev β transition. As in the case of the Au^{199} nucleus, we determined only the lower limit of the quantity μH_{eff}:

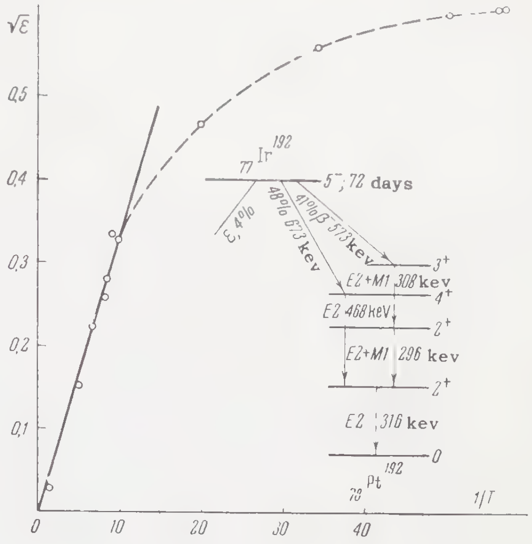

FIG. 2

$$\mu H_{eff} \geqslant 1.5 \cdot 10^{-17} \text{ erg}.$$

The value of μ for Ir^{192} was not determined experimentally, and there were not sufficiently complete data for calculating the magnetic moment from the formulas of the nuclear shell theory. It is evident that $H_{eff} \sim 10^6$ oe for Ir^{192}, since there is no basis to expect values of μ greater than a few nuclear magnetons.

Ir^{191m}

The Ir^{191m} isomer with an excitation energy of 171 kev and half-life period of 6.9 sec is obtained from the β decay of Os^{191}.

The decay scheme $Os^{191} \rightarrow Ir^{191}$ is shown in Fig. 3. The sample of the alloy of iron with 0.5% osmium was prepared in the same way as the previous samples. After the decay of Os^{193}, we investigated the anisotropy of the 129-kev γ radiation. One can expect considerable anisotropy for this γ radiation, since the internal field in iridium is sufficiently large and the value of μ for Ir^{191m}

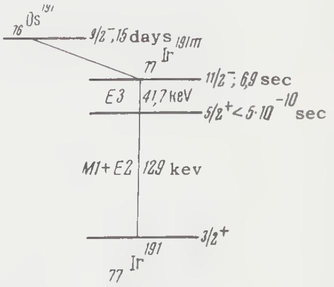

FIG. 3

estimated from Schmidt's curve is ~5 n.m. In the experiment, however, it turned out that $|\epsilon| < 0.3\%$. It can be assumed that the absence of an anisotropy in the given case is connected with a mixture of transitions of the M1 and E2 type. However, our experiments on the measurement of the plane polarization of the 129-kev radiation indicates the absence of the effect within the limits of 3%. It is clear that the Ir^{191m} nucleus in an alloy with iron is practically unoriented.

Re^{186}

Samples of the alloy with Re^{186} were prepared by the usual method. The Re content in the alloy did not exceed 0.2%. The decay scheme of Re^{186} and the plot of $\sqrt{\epsilon}$ vs T^{-1} is shown in Fig. 4. We obtained the value $\mu H_{eff} \geq 2 \times 10^{-18}$ erg. The magnetic moment of Re^{186} can be calculated from the formulas of the nuclear shell model: $\mu \sim 2$ mn.

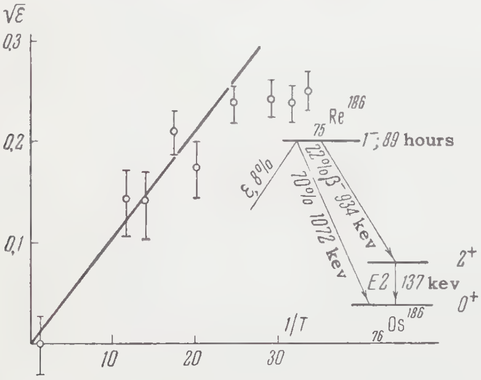

FIG. 4

Thus, $H_{eff} \geq 2 \times 10^5$ oe for Re^{186}.

V^{48}

The orientation of the V^{48} nucleus is of interest in investigating the question of the conservation of combined parity in β decay. The V^{48} was introduced into the iron together with metallic titanium, from which it was obtained by means of the (d, n) reaction. The titanium content in the alloy did not exceed 2% and the V^{48} content was minute. We investigated the anisotropy for 1320- and 990-kev γ transitions. The effect did not exceed 0.7%. If we estimate the magnetic moment of V^{48} from the formulas of the nuclear shell model, we obtain $H_{eff} \leq 50{,}000$ oe, while in the field of the V^{+++} ion $H_{eff} \sim 250{,}000$ oe. It is not excluded that the presence of titanium in the alloy has some effect on the effective magnetic field. We note, however, that the solubility of titanium and vanadium in iron is quite high. In the experiments with Au^{199}, the presence of an ~0.7% admixture of platinum did not lead to any essential effect on the orientation of the Au^{199} nucleus. It is more likely that the internal field in the metal is essentially different from the field in vanadium sulfate. It is possible that there is also a partial compensation of the effective field component associated with the atomic shell and conduction electrons. This possibility follows from the work of Marshall.[2]

The authors express their profound gratitude to S. Ya. Nikitin for supplying the V^{48} radioactive isotope, to A. Z. Dolginov for discussion of the results, and to D. A. Varshalovich for aid in the calculation of the magnetic moments of the radioactive nuclei.

---

[1] Samoĭlov, Sklyarevskiĭ, and Stepanov, JETP **36**, 644 (1959), Soviet Phys. JETP **9**, 448 (1959).

[2] W. Marshall, Phys. Rev. **110**, 1280 (1958).

[3] G. R. Khutsishvili, JETP **38**, 1647 (1960), Soviet Phys. **11**, 1187 (1960).

[4] Grace, Johnson, Jurti, Scurlock and Taylor, Communications, Conference de Physique des Basses Temperatures, Paris, 1955, p. 263.

[5] T. M. Daniels and M. A. R. Le-Blank, Can. J. Phys. **37**, 1321 (1959).

[6] N. Kurti, J. Appl. Phys. Suppl. **4**, 215 (1959).

[7] C. V. Heer and R. A. Erickson, Phys. Rev. **108**, 896 (1957).

[8] Samoĭlov, Sklyarevskiĭ, and Stepanov, JETP **36**, 1944 (1959), Soviet Phys. JETP **9**, 1383 (1959).

[9] Samoĭlov, Sklyarevskiĭ, and Stepanov, JETP **38**, 359 (1959), Soviet Phys. JETP **11**, 261 (1960).

[10] Kogan, Kul'kov, Nikitin, Reĭnov, Sokolov, and Stel'makh, JETP, in press.

Translated by E. Marquit
20

SOVIET PHYSICS JETP VOLUME 13, NUMBER 1 JULY, 1961

CONSERVATION LAWS IN THE GENERAL THEORY OF RELATIVITY

M. E. GERTSENSHTEĬN

Submitted to JETP editor October 8, 1959; resubmitted March 9, 1960

J. Exptl. Theoret. Phys. (U.S.S.R.) 40, 114-122 (January, 1961)

To determine the integral of a vector function in Riemannian geometry, and a vector field corresponding to a displacement of the origin of coordinates, a geometric operation of "harmonic" translation of the vector is introduced, which is defined in a unique manner by means of the first-order generally-covariant linear differential equations (13). The covariant vector components do not change during harmonic translation in a harmonic coordinate system, and this enables one to integrate the vectors by components. Therefore the energy-momentum vector, energy-momentum pseudotensor, energy density, and Hamiltonian of the system should be computed in a harmonic system. For the canonical energy-momentum tensor a unique expression is obtained which goes over to the Landau-Lifshitz pseudotensor after symmetrization.

1. STATEMENT OF THE PROBLEM

TWO points are unclear from a mathematical point of view about conservation laws in the general theory of relativity:

1. The definition of an integral over a vector function. In the energy-momentum vector of a system[1]

$$P_i = \int t_i^k dS_k \tag{1}$$

the expression under the integral is a vector. However, the operation of addition of two vectors at different points in space is not defined.[2] It is true that the generalized Stokes theorem[3] is treated in differential geometry; however, the integrand in the generalized Stokes theorem is a scalar (skewsymmetric differential form).

2. The conservation laws are a consequence of invariance under a continuous group of coordinate transformations — displacements or rotations.[4] If $\delta\omega^j$ are the parameters of an element of this group in the neighborhood of unity, then the corresponding coordinate transformation has the form[4,1]

$$\delta x^i = \xi^i(x) = x_j^i(x)\,\delta\omega^j, \tag{2}$$

however, it is not defined which functions $\xi^i(x)$ correspond to displacements.

Integrals of type (1) arise in the general theory of relativity in investigations of the conservation laws. If t_i^k is the energy-momentum pseudotensor, and the summation (integration) is carried out component-wise, while the coordinates are Euclidean at infinity, then the integral does not depend on the coordinate system. Similarly, if the quantities ξ^i tend to become constant as $x^\alpha \to \infty$, the integrals of the different energy-momentum tensors generated by (2) agree with each other. However, it is an unsatisfactory situation when mathematical operations are used which are not defined, and which acquire meaning only through the physical nature of the integrand. In our opinion the definitions of the integral and of the displacement are purely geometrical ones, and should be given independently of the physical content of the problem.

There are two points of view about this possibility: a) a covariant definition of the integral and the displacement is possible in the general theory of relativity, b) a generally covariant definition of the integral does not exist in a Riemannian space. In the present work we develop the first point of view for an isolated mass distribution, when the metric becomes Euclidean at infinity.

2. FREE-VECTOR FIELDS

In arbitrary curvilinear coordinates only vectors defined at the same point can be added. Therefore before performing the integration, all vectors must be transferred to one point, which we shall call the observation point x_0. It is then natural to define the integral by

$$P_i(x_0) = \int dP_i(x,\ x_0) = \int t_i^k(x,\ x_0)\, dS_k. \tag{3}$$

The integration in (3) is to be carried out over the points with coordinates x.

Consequently we must define an operation of transfer of a vector, which we shall call "harmonic" translation,* and which has the following properties: 1) The "harmonic" translation is unique and consequently must not depend on the path; 2) it is defined by a generally covariant linear differential equation of first order; 3) In Euclidean space the "harmonic" translation is identical with the usual parallel transport.

An arbitrary vector $P_i(x_0)$ which is given at some point can be transferred to any other point with the help of the harmonic translation. It thus defines a vector field $P_i(x)$:

$$P_i(x) = \hat{C}P_i(x_0), \tag{4}$$

where $\hat{C}$ denotes the operator of harmonic translation. Thus condition 1) implies the existence of the vector field (4), which we may call a field of free-vectors.

We now turn to Eq. (2). By the $\xi^i(x)$ in (2) we now mean a vector field that satisfies the following conditions: (a) $\xi^i(x, x_0)$ is a unique function of two points, the field point x, and the point x_0 from which the translation originated; (b) in Euclidean space the vectors $\xi^i(x)$ are parallel to each other. Clearly these conditions are satisfied by the field

$$\xi^i(x) = \hat{C}\xi^i(x_0). \tag{5}$$

Thus both problems posed in Sec. 1 have been reduced to a single geometric problem, that of finding the harmonic translation.

The harmonic translation must be defined uniquely, at least in topologically Euclidean spaces. It should be stressed that the harmonic translation differs from the parallel transport (Π transport), which is defined by somewhat different conditions: a) Π transport conserves the scalar product

$$\Pi(P_sQ^s) = (\Pi P_s)(\Pi Q^s); \tag{6}$$

b) In Euclidean space the Π transport is the usual parallel transport.

3. DEFINITION OF HARMONIC TRANSLATION

Consider first Euclidean space and introduce a Cartesian coordinate system. In this case the free vector clearly has constant components:

$$\partial P^s(x)/\partial x^k = 0; \quad s, k = 0, 1, 2, 3. \tag{7}$$

Equation (7) is of first order; therefore it is natural to demand that in the general case the harmonic translation also be defined by differential equations of first order. These equations must be linear: if ξ_1^i and ξ_2^i are two vector fields corresponding to a displacement of the origin, then the sum of these fields must correspond to a displacement of the origin by the vector $\xi_1^i(x_0) + \xi_2^i(x_0)$. The requirement of linearity also follows from the linearity of the operation of integration.

In curvilinear coordinates in pseudo-Euclidean space, Eq. (7) takes the form

$$\nabla_k P^s(x) = 0, \tag{8}$$

where ∇_k denotes the covariant derivative. $P^s(x)$ is obtained by integrating Eq. (8); to do this, boundary conditions must be imposed, namely boundedness at infinity.

Let us study Eq. (8) in Riemannian geometry. Since the indices k and s are independent, Eq. (8) constitutes 16 conditions. If (8) is fulfilled, the curvature tensor vanishes because of the noncommutation of the covariant derivatives,

$$(\nabla_k\nabla_s - \nabla_s\nabla_k)P_i(x) = R^m_{iks}P_m = 0. \tag{9}$$

In the general theory of relativity condition (8) must therefore be replaced by weaker ones, which can be fulfilled even when $R^m_{iks} \neq 0$.

From the second-rank tensor $\nabla_k P_i$ one can construct the invariant

$$\zeta = \nabla_k P^k \equiv \operatorname{div} P \tag{10}$$

and introduce the symmetric and skewsymmetric parts

$$\xi_{ik} = \nabla_k P_i + \nabla_i P_k, \quad \eta_{ik} = \nabla_k P_i - \nabla_i P_k. \tag{11}$$

Thus the following generally covariant conditions can be imposed on the vector field $P_i(x)$:

$$\xi_{ik} = 0 \quad (10\ \text{conditions}). \tag{12}$$

These conditions have been investigated by Fock.[5] They can be fulfilled only in spaces of constant curvature, $\nabla_s R = 0$, and therefore must be rejected.

$$\zeta = 0, \quad \eta_{ik} = 0 \quad (7\ \text{conditions}). \tag{13}$$

These conditions can be fulfilled for arbitrary R^m_{iks}. The solution of Eq. (13) is

$$P_k = \nabla_k\varphi = \partial\varphi/\partial x^k; \quad \Box\varphi = 0. \tag{14}$$

At the point x_0 we must have

$$\left.\frac{\partial\varphi}{\partial x^k}\right|_{x=x_0} = P_k(x_0), \tag{15}$$

in order that

$$P_k(x) = \hat{C}P_k(x_0). \tag{16}$$

To calculate the integral (1) one must translate the integrand harmonically from the field point to the point x_0. Hence Eq. (14) must be integrated for every field point x. This is a rather cumbersome operation.

---

*This nomenclature was suggested by V. A. Fock.

In Euclidean space a vector with vanishing curl and divergence, and bounded at infinity, is constant. Therefore the requirement (2) for "harmonic" translation is also fulfilled. In Euclidean space the harmonic translation is identical with parallel transport. The definition of harmonic translation introduced above is feasible only if one confines attention to first-order linear differential conditions.

4. A PREFERRED COORDINATE SYSTEM

Up to this point all equations were generally covariant. In Euclidean space a "preferred" coordinate system exists, namely, a Galilean system, in which the components of a vector remain unchanged during parallel transport. In this coordinate system addition and integration of vectors at different points can be performed component-wise. In the present section such a preferred system will be defined for spaces of arbitrary curvature.

Let us find the conditions that define the class of coordinate systems in which the components of a covariant field of "free" vectors [in the sense of Eq. (13)] are constant:

$$P_i(x) = \hat{C}P_i(x_0) = P_i(x_0). \tag{17}$$

Consider again Eq. (14). We have

$$\operatorname{div} P = \Box\varphi = \frac{1}{\sqrt{-g}}\frac{\partial}{\partial x^i}(\sqrt{-g}\,g^{ik}P_k) = 0,\quad \frac{\partial P_k}{\partial x^i} = 0, \tag{18}$$

hence

$$\partial(\sqrt{-g}\,g^{ik})/\partial x^i = 0, \qquad g^{im}\Gamma^k_{im} = 0. \tag{19}$$

Condition (19) defines the class of "harmonic" coordinate systems.[5] Subject to corresponding boundary conditions, these systems are defined uniquely up to Lorentz transformations.

We note that the components of a contravariant vector do not remain constant after the translation:

$$P^i(x) = \hat{C}P^i(x_0) = g^{is}(x)\,g_{si}(x_0)\,P^i(x_0). \tag{20}$$

One can show that in general no coordinate systems exist in which the contravariant components remain constant under harmonic translation.

In this section we have found the "preferred" coordinate system for a covariant vector. We write the word "preferred" in quotes since we mean by this only that addition of vectors at different points can be performed by components in this coordinate system. Thus in arbitrary coordinate systems the translation is generally covariantly defined by Eq. (13). In a harmonic coordinate system these differential conditions can be integrated and lead to formulas (17) and (20).

The situation with respect to "preferred" coordinate systems in the general theory of relativity is entirely analogous to the situation in electrodynamics. The equations of electrodynamics can be written down and solved in an arbitrary coordinate system. The calculation of integrals over vectors or tensors is carried out in the "preferred" Galilean coordinate systems, where vectors can be added by components.

The class of harmonic coordinate systems has been thoroughly investigated.[5] In particular, the uniqueness proof for harmonic translation reduces to the uniqueness proof for harmonic coordinates. This question was investigated in detail by Fock (see reference 5, Sec. 93), and we shall not treat it here. The question of the existence and uniqueness of the solution of Eqs. (14) and (15) and the precise mathematical formulation of boundary conditions in finite-sized regions or in a space of non-Euclidean topology will not be considered in the present paper.

5. CONSERVED QUANTITIES

So far our reasoning was purely geometric in character and the formulas we developed were considered independent of the physical nature of the vectors. Consider now an integral of type (1)

$$P_i(x_0) = \int_\sigma t_i^k dS_k = P_i(x_0,\ \sigma), \tag{21}$$

where the integration extends over a hypersurface σ. The integrand is a function of two points: the point x_0, where all vectors are collected and where their component-wise summation is carried out, and the variables of integration, x. As was pointed out in Sec. 4, to be able to integrate by components, we must use a harmonic coordinate system.

The vector $P_i(x_0, \sigma)$ is said to be conserved if, for fixed x_0, it does not depend on the hypersurface σ. It is usual to require that P_i be independent of the hypersurface of integration; the stipulation concerning a fixed x_0 is necessary in general relativity, where measuring rods and clocks may change from point to point, i.e., where the units of space and time measurement, and, consequently, any units in which P_i is measured, may change. We note that the point x_0 may also lie outside the hypersurface σ.

It follows immediately from the definition of conserved quantities that the tensor t_i^k satisfies the condition

$$\partial t_i^k(x,\ x_0)/\partial x^k = 0. \tag{22}$$

Formula (22) is a consequence of integration by components and therefore is correct for non-translated quantities only in harmonic coordinates.

6. INFINITESIMAL COORDINATE TRANSFORMATIONS

Conservation laws are a consequence of the invariance of the action under infinitesimal coordinate transformations. Let the action be expressed by the integral

$$S = \int \mathscr{L}\, d^4x, \quad \mathscr{L} = \mathscr{L}_0 \sqrt{-g}, \tag{23}$$

where the Lagrangian density $\mathscr{L}_0$ is a function of the field variables and their first derivatives:

$$\mathscr{L}_0 = \mathscr{L}_0 (u_k^A;\, u_{,k}^A), \quad u_{,k}^A = \partial u^A/\partial x^k \tag{24}$$

and does not contain the coordinates x explicitly (the index A denotes the totality of the tensor indices of the field). Consider the infinitesimal coordinate transformation

$$\xi^i (x) = x_j^i (x, x_0)\, \xi^j (x_0), \tag{25}$$

corresponding to a displacement of the origin x_0 by the infinitesimal vector $\xi^j (x_0)$, which characterizes the direction of the displacement.

The change of the field functions at some point in space will be[1,4]

$$\delta^* u^A = (\psi_j^A - x_j^k\, \partial u^A/\partial x^k)\, \xi^j (x_0). \tag{26}$$

Here $\delta^* u^A$ is the variation of the field function at the original point in space, which has new coordinates after the transformation, ψ_j^A is the matrix that relates total variation of the field variables (due to polarization properties as well as due to the displacement to the new point) with the displacement of the origin.[1,2,4] The canonical energy-momentum tensor is then defined by the relation by the relation

$$\Theta_j^k (x, x_0)\, \xi^j (x_0) = -\, \delta^* u^A\, \partial \mathscr{L}/\partial u_{,k}^A - \mathscr{L} x_j^k \xi^j (x_0) \tag{27}$$

and satisfies Eq. (22):

$$\partial \Theta_j^k/\partial x^k = 0. \tag{28}$$

The integral over the hypersurface

$$P_j (x_0, \sigma) = \int \Theta_j^k\, dS_k \tag{29}$$

is conserved. The integration in (29) is carried out component-wise. The quantities Θ_j^k in Eqs. (28) and (29) are referred to the observation point x_0, where x_0 may be located anywhere, not only at infinity.

The physical significance of the relationships obtained in this way depends on the coordinate transformation being considered. If one adopts the point of view expressed above, that the coordinate transformation corresponding to displacement or rotation must be uniquely defined, then the tensor Θ_j^k will also be unique.

7. THE GRAVITATIONAL FIELD

The general formula (27) is correct for an arbitrary field. Let us apply it to the gravitational field. The simplified action for the gravitational field is

$$\mathscr{L}_0 = g^{ik} (\Gamma_{im}^s \Gamma_{ks}^m - \Gamma_{ik}^s \Gamma_{sm}^m). \tag{30}$$

According to Sec. 4, the operation of harmonic translation can be written in a finite, non-differential form only in a system of harmonic coordinates. Therefore $\mathscr{L}_0$ should also be calculated in harmonic coordinates. The second term in (30) the vanishes, and

$$\mathscr{L}_0 = g^{ik} \Gamma_{im}^s \Gamma_{ks}^m. \tag{31}$$

Since harmonic coordinates form an affine group, $\mathscr{L}_0$ is a true scalar in harmonic coordinates. The components of the metric tensor g^{ik} are the field variables. The quantity $\Theta_0^0 (x)$ is the energy density of the system, or the Hamiltonian density. We note that Dirac[6] has pointed out the necessity of fixing the coordinates for a Hamiltonian formulation.

For infinitesimal coordinate transformations[2] we have

$$\delta^* g^{ik} = -(\nabla^i \xi^k_{\cdot} + \nabla^k \xi^i) = -\xi^{ik}, \tag{32}$$

where ξ^i is defined by Eq. (2). In the literature the case $\xi^i = \text{const}$ is usually discussed, and the coordinate system is not restricted. This leads to Einstein's canonical pseudotensor

$$t_i^k = g_{,i}^{ml}\, \partial \mathscr{L}/\partial g_{,k}^{ml} - \mathscr{L} \delta_i^k. \tag{33}$$

However, the vector field $\xi^i = \text{const}$ cannot be defined generally covariantly by means of first-order differential conditions.

We demand that the vector field $\xi^i (x)$ be derived from the vector of the displacement of the origin $\xi^i (x_0)$ by harmonic translation. In harmonic coordinates

$$x_j^i (x, x_0) = g^{is} (x)\, g_{sj} (x_0). \tag{34}$$

The change in field variables must be calculated from Eq. (32):

$$\delta^* g^{ik} = -2 \Gamma^{ik,\, l} (x)\, g_{lj} (x_0)\, \xi^j (x_0), \tag{35}$$

so that the energy-momentum tensor equals

$$t_j^k = 2\frac{\partial \mathscr{L}}{\partial g^{lm}_{,k}}\Gamma^{ml,\,s}(x)\,g_{sj}(x_0) - \mathscr{L}g^{ks}(x)\,g_{sj}(x_0)$$

$$= t^{ks}(x)\,g_{sj}(x_0). \tag{36}$$

The infinitesimal coordinate transformation (34) can be written in the form

$$\xi^i(x) = g^{is}(x)\,\xi_s, \quad \xi_s = \text{const.} \tag{37}$$

As Bergmann[7] showed, the transformation (37) leads to a tensor t^{ks} which, after addition of a strictly conserved quantity, becomes the tensor of Landau and Lifshitz. Thus the geometrical definition of the displacement leads to the tensor of Landau and Lifshitz, and not to that of Einstein.

As follows from the derivation, the quantities t_i^k and, consequently, the Hamiltonian[6] must be calculated in harmonic coordinates. Therefore the question raised again recently by Møller about the localization of the energy-momentum of the gravitational field makes sense, although, in our opinion, Møller's solution is wrong. Consider two mechanical oscillators much less than a wavelength apart, so that oscillation of one excites the other via gravitational interaction. The energy transfer calculated in the nonrelativistic approximation, using the canonical symmetric tensor, agrees with the result obtained from the equations of motion; the same calculation using Møller's tensor gives a zero result. For the Schwarzschild solution, Møller's energy density vanishes in any coordinate system, whereas the canonical energy density in harmonic coordinates is positive definite.

The principal objection against the Landau-Lifshitz energy-momentum tensor was, of course, the incorrect weight.[8,9] However, it is clear from Eqs. (33) and (36) that the canonical tensors have the same weights. Goldberg's conserved expressions of arbitrary weight are not connected with infinitesimal coordinate transformations and must be rejected.

8. THE GRAVITATIONAL FIELD AS A PERTURBATION

Let us analyze the case when the gravitational field can be considered a small perturbation, and compare the results of calculations in different coordinate systems. It is well known that the scattering angle of light in a centrally-symmetric field is given by

$$\theta = 4\varkappa M/c^2R, \qquad \theta \ll 1, \tag{38}$$

where R is the distance of closest approach, which in general relativity depends sensitively on the coordinate system employed.[10] From (38) we obtain for the effective scattering cross section, for $\theta \ll 1$:

$$d\sigma = \frac{R(\theta)}{\sin\theta}\left|\frac{dR}{d\theta}\right| do = 16\left(\frac{\varkappa M}{c^2}\right)^2\frac{do}{\theta^4}. \tag{39}$$

There is a difference in principle between Eqs. (38) and (39). The latter depends only on the scattering angle θ, which is measured away from the gravitating masses, at infinity, where the metric is Galilean, whereas (38) contains the distance of closest approach, a quantity measured near the mass.

Let us find the effective scattering cross section using the methods of quantum-mechanical perturbation theory. The Lagrangian density for the electromagnetic field equals

$$\mathscr{L} = \frac{1}{8\pi}F_{ik}^2 = \frac{1}{8\pi}g^{is}g^{km}F_{ik}F_{sm}. \tag{40}$$

For a weak field we have, in the notation of reference 2,

$$\mathscr{L} = \mathscr{L}_0 + \Delta\mathscr{L} = \frac{1}{8\pi}F_{ik}F^{ik} + \frac{1}{4\pi}h^k_m F^{im}F_{ik}. \tag{41}$$

The second summand in (41) can be considered as the interaction Lagrangian of the electromagnetic and gravitational fields. In (41) the indices are raised and lowered with the zero-order metric tensor $\overset{(0)}{g}_{ik}$.

The small additions to the Lagrangian and Hamiltonian have opposite signs:[2]

$$\Delta\mathscr{H} = -\Delta\mathscr{L} = -\frac{1}{4\pi}h^k_m F^{im}F_{ik}. \tag{42}$$

For a weak gravitational field in harmonic coordinates we have

$$h^\beta_\alpha = -2c^{-2}\delta^\beta_\alpha\varphi, \quad h^0_0 = 2c^{-2}\varphi, \quad h^0_\alpha = 0, \tag{43}$$

where φ is the gravitational potential. Thus we find, for a light wave

$$\Delta\mathscr{H} = \frac{1}{4\pi c^2}\varphi(\mathbf{E}^2 + \mathbf{H}^2) = \frac{2}{c^2}\frac{\varphi}{8\pi}(\mathbf{E}^2 + \mathbf{H}^2). \tag{44}$$

The quantity $(\mathbf{E}^2 + \mathbf{H}^2)/8\pi c^2$ can be treated like an inertial and gravitational mass density of the photon. The factor 2 corresponds to the well-known fact that the angle of deflection of light in the general theory of relativity is twice as large as in the special theory.

We shall consider the interaction Hamiltonian (44) as a perturbation, where for F_{ik} we must substitute the wave functions in zeroth order, namely plane waves. If we let the normalization volume be Ω, we find the normalized wave functions:

$$\mathbf{E} = \sqrt{4\pi\hbar\omega/\Omega}\,\mathbf{e}_{\mathbf{k}} e^{i\mathbf{kr}},$$

$$\langle \Delta \mathscr{H}_{12} \rangle = \frac{2}{c^2}\frac{\hbar\omega}{\Omega}\int \exp\{i(\mathbf{k}_1 - \mathbf{k}_2)\mathbf{r}\}\,dv = \frac{8\pi}{\Omega}\frac{\varkappa M}{c^2}\frac{\hbar\omega}{k^2\theta^2}, \quad (45)$$

and we can easily see that the scattering cross section agrees with the classical result:

$$d\sigma = \frac{2\pi}{\hbar c}\langle \Delta \mathscr{H}_{12} \rangle^2 \frac{\Omega^2}{(2\pi)^3} k^2 \frac{dk}{\hbar\, d\omega}\, do = 16\left(\frac{\varkappa M}{c^2}\right)^2 \frac{do}{\theta^4}. \quad (46)$$

The whole calculation could have been performed by perturbing the wave equation. The quantum notation was used only for brevity and because it is more familiar.

We show that $\langle \Delta \mathscr{H}_{12} \rangle$ depends on the coordinate system chosen. When applying perturbation theory one must use plane waves as wave functions in the zero-order approximation. In flat space and Galilean coordinates $h_{ik} \equiv 0$ and $\langle \mathscr{H}_{12} \rangle = 0$. After an infinitesimal coordinate transformation we have

$$\delta \langle \Delta \mathscr{H}_{12} \rangle = -\frac{1}{4\pi} \overset{(0)}{F}{}^{mi} \overset{(0)}{F}{}^{k}_{m\ldots} \int e^{i(\mathbf{k}_1 - \mathbf{k}_2)\mathbf{r}} (\nabla_i \xi_k + \nabla_k \xi_i)\, dV \neq 0, \quad (47)$$

and, therefore, an arbitrary coordinate system does not satisfy the correspondence principle, and we must use the harmonic system for the calculations as we have concluded above.

The author wishes to thank V. L. Bonch-Bruevich, Prof. A. Z. Petrov, A. A. Fedorov, and L. G. Soloveĭ for valuable discussions.

[1] W. Pauli, The Theory of Relativity, Pergamon Press, New York 1958, Secs. 21, 23, 25.

[2] L. D. Landau and E. M. Lifshitz, Теория поля (The Classical Theory of Fields) Gostekhizdat 1948, 2nd ed. Sec. 98, p. 266 [Addison Wesley, 1951].

[3] P. K. Rashevskiĭ, Геометрическая теория уравнений с частными производными (Geometrical Theory of Partial Differential Equations) OGIZ 1947, Chap. 2.

[4] N. N. Bogolyubov and D. B. Shirkov, Введение в теорию квантованных полей (Introduction to the Theory of Quantized Fields), Gostekhizdat 1957, Sec. 2 [Interscience, 1959].

[5] V. A. Fock, Теория пространства, времени и тяготения (Theory of Space, Time, and Gravitation), Gostekhizdat 1955, Secs. 49, 93.

[6] P. A. M. Dirac, Phys. Rev. **114**, 924 (1959).

[7] P. Bergman, Phys. Rev. **112**, 287 (1958).

[8] C. Møller, article in Max Planck Festschrift, Berlin, 1958.

[9] J. N. Goldberg, Phys. Rev. **111**, 315 (1958).

[10] E. P. Wigner, Revs. Modern Phys. **29**, 255 (1957).

Translated by D. Brill
21

SOVIET PHYSICS JETP VOLUME 13, NUMBER 1 JULY, 1961

THE INTERACTION OF FAST ELECTRON BEAMS WITH LONGITUDINAL PLASMA WAVES

Yu. A. ROMANOV and G. F. FILIPPOV

Submitted to JETP editor May 6, 1960

J. Exptl. Theoret. Phys. (U.S.S.R.) 40, 123-132 (January, 1961)

Equations are derived that yield the time variation of the plasma wave spectral density and of the fast electron distribution function for arbitrary velocity distributions. The dispersion relation for the stationary problem is solved, and the spatial extent of the exponential stage of the slowing down of the monochromatic beam is estimated.

1. There are many articles which deal with the generation of plasma oscillations by fast electron beams. It has been established that intense plasma oscillations can react on the beam and produce anomalous electron scattering, in which one observes a spatial localization of zones of intense plasma oscillation and zones of anomalous scattering.

In a recent paper Gabovich and Pasechnik[1] show that l, the distance traveled by an electron beam in a plasma before scattering, increases with a decrease in the beam current density, and that for a given l there exists a critical current density beyond which there occurs a considerable increase in fast-electron scattering. If the beam flux is more than critical, the average energy loss for an interaction with the plasma over a distance l amounts to 10 — 20%.

In the interpretation of their measurements, Gabovich and Pasechnik[1] refer to Vlasov[2] and Bohm and Gross,[3] who, in order to explain the anomalous scattering in the experiments of Merill and Webb,[4] assumed that an electron beam penetrating a plasma is velocity modulated by a fluctuating voltage ΔU. The beam modulation causes the formation of electron bunches and the appearance of intense plasma oscillations. Vlasov associates the voltage fluctuation with thermal surface oscillations of the plasma, the amplitude of which is on the order of the temperature T (in energy units). However, it can be shown that the amplitude of the surface oscillations is in fact many times less, $\approx T\sqrt{n_0\lambda_D^3}$ (where λ_D is the Debye length and n_0 is the electron density). Bohm and Gross attribute the appearance of the initial modulating voltage to the overall instability of the beam in the plasma and compare this voltage with the initial velocity spread in the beam. It is to be noted that the random fluctuations which are intensified by the action of the electron beam appear as longitudinal plasma waves. Their group velocity is directed along the beam, and for a semi-infinite plasma with no reflecting surfaces these waves cannot induce sufficient modulation at the penetration into the beam.* Besides, what is absent from the mechanism described by Vlasov and Bohm and Gross is the clear relationship between the scattering length l and the electron beam density n, a relationship observed by Gabovich and Pasechnik even when the frequency of the plasma oscillations was determined entirely by n_0 ($n_0 \gg n$).

To explain the anomalous phenomena in the interaction between a beam and plasma, one need not assume that there is a modulation voltage on the order of several volts at the plasma boundary; it is enough to assume that an electron beam in the plasma is unstable.[6,7] Because of this instability, the small disturbances (which always occur whenever the beam penetrates) grow exponentially with the distance from the boundary, and at a depth of about 1 cm their measured[1,4] amplitude becomes sufficient to effect anomalous beam scattering. We hasten to add that the above mechanism has no bearing on the interpretation of Looney and Brown's experiments,[8] in which the resonance properties of the system were sharply pronounced.

A theory of plasma wave excitation for two interpenetrating plasmas of the same density was developed in the hydrodynamic approximation by Kahn.[9] To explore the problem thoroughly, a kinetic equation must be used. This has been done by Klimontovich,[10] who has derived a kinetic equation describing the excitation and absorption processes for plasma waves. Similar equations, though of wider applicability, are derived in the present paper (Secs. 2 and 3). These are applicable even when the plasma oscillations are not in thermal equilibrium and the electron distribution function is non-Maxwellian.

---

*Gabor et al.[5] found a variable field at the plasma boundary with a large amplitude ($\approx$T) and with a frequency 4-5 times smaller than the Langmuir frequency. The nature of this field is not clear to us.

Klimontovich developes a non-linear theory to explain why fast electron beams with a rather large velocity dispersion slow down in a plasma. However, the requirement that the fast electron beam be only slightly excited by the plasma waves induced by the beam renders Klimontovich's extension of the solution to steady waves incorrect. In Sec. 4 we derive equations that can be used to analyze the non-exponential growth in time of the plasma wave intensity, induced by beams with an arbitrary velocity distribution. It is shown that during the deceleration a strong scattering occurs in the beam, accompanied by the appearance of electrons with energies greater and smaller than the average initial energy. These equations, when applied to electron beams with a large velocity dispersion, reduce to the kinetic equations derived in Secs. 2 and 3. The accuracy of the equations is tested for a specific case in Sec. 5. The electric field in the equations that we have derived is characterized by the spectral density of plasma waves. Therefore, the phenomena of the velocity modulation of the entering beam and its subsequent bunching cannot be described by the proposed system of equations. In Sec. 7 we obtain the dispersion relation for the growth of the plasma wave intensity in the stationary linearized approximation and compare the theoretical and experimental values for the spatial extent of the linear stage of the deceleration.

In the following analysis it is assumed that the density of the fast electrons is much less than that of the plasma and that there are no external magnetic and electric fields.

2. Let us use the Focker-Planck equation to derive a kinetic equation for the beam electrons, in which we include the interaction with plasma waves, thus

$$\partial N/\partial t + u_i \partial N/\partial x_i + \partial I_i/\partial u_i = 0. \tag{1}$$

Here I is the electron current in velocity space, which is found by computing the average decelerating force F_i and diffusion coefficient D_{ik}:

$$I_i = F_i N/m - \partial D_{ik} N/\partial u_k,$$

$$F_i = m\overline{\Delta u_i/\Delta t}, \qquad D_{ik} = \overline{\Delta u_i \Delta u_k/2\Delta t}.$$

The bar designates an average over the various possible variations in velocity Δu during time Δt.

N(u, r, t) is the electron distribution function and is obtained by averaging the exact distribution function over a volume whose linear dimension exceeds the plasma-oscillation wavelength that is characteristic for the problem. To describe the plasma oscillations we employ the plasma-wave spectral energy density ϵ(q, r, t), where q is the wave vector. The total plasma wave energy per unit volume, W, is given by:

$$W = \int \varepsilon\, d^3q.$$

The decelerating force F due to the collective interaction is composed of a force F_0, which is due to spontaneous plasma wave radiation ($\epsilon = 0$), and a force F_ϵ, which is proportional to the wave intensity. The force F_0 has been computed in different ways by various authors (see, for example, references 11 — 13) and is given by

$$F_0 = -(e^2\omega_0^2/u^2)\ln(q_{max}/q_{min}). \tag{3}$$

The minimum wave number (or q_{min}) corresponds to waves radiated in the direction of motion of the particles ($\cos\theta = 1$) and is determined by the condition

$$\omega(q_{min})/q_{min}u = 1. \tag{4}$$

Since plasma waves with $q > 1/\lambda_D$ are strongly damped, one can set q_{max} equal to $1/\lambda_D$.

To compute F_ϵ we need to find the average acceleration imparted to a particle by the electric field of the plasma wave, viz.,

$$\mathbf{F}_\varepsilon = m\frac{\overline{\Delta \mathbf{u}}}{\Delta t} = \frac{e}{\Delta t}\int_0^{\Delta t} \overline{\mathbf{E}(\mathbf{r}(t), t)\,dt},$$

$$\mathbf{r}(t) = \mathbf{r}_0 + \mathbf{u}_0 t + \frac{e}{m}\int_0^t \mathbf{E}(\mathbf{r}(t'), t')(t - t')\,dt'. \tag{5}$$

The time interval Δt must satisfy the condition

$$1/\gamma \gg \Delta t \gg 1/\Delta q u, \tag{6}$$

where γ is the logarithmic time derivative of the plasma wave amplitude, and Δq characterizes the width of the plasma wave spectrum.

Expanding (5) in a power series of the electric field vector E, we obtain for $\mathbf{F}_\epsilon$ an expression which is proportional to ϵ, viz.,

$$\mathbf{F}_\varepsilon = \frac{4\pi^2 e^2\omega_0^2}{m}\int \frac{\mathbf{q}}{\omega^2}\varepsilon\delta'(\mathbf{qu} - \omega)\,d^3q. \tag{7}$$

To compute the diffusion coefficient D_{ik} we express the velocity increment in Eq. (2) in terms of the electric fields,

$$\overline{\Delta u_i \Delta u_k} = \frac{e^2}{m^2}\int_0^{\Delta t} dt \int_0^{\Delta t} \overline{dt' E_i(\mathbf{r}(t), t)\, E_k(\mathbf{r}(t'), t')}.$$

Effecting the above simple computation, we finally obtain

$$D_{ik} = \frac{4\pi e^2\omega_0^2}{m^2} \int \frac{q_i q_k}{q^2} \frac{\varepsilon}{\omega^2} \delta(\mathbf{qu} - \omega) \, d^3q. \tag{8}$$

Consequently the electron flux in velocity space is given by

$$I_i = -\frac{e^2\omega_0^2}{m} \left[\frac{u_i N}{u^3} \ln \frac{q_{max}}{q_{min}} + \frac{4\pi^2}{m} \frac{\partial N}{\partial u_k} \int \frac{q_i q_k}{q^2\omega^2} \varepsilon \delta(\mathbf{qu} - \omega) \, d^3q \right]. \tag{9}$$

In deriving Eq. (9) we have neglected terms proportional to ϵ^2 in the series expansion of (5). This is permissible if the inequality

$$\int \varepsilon d^3q \ll (\Delta q/q)^4 n_0 m u^2 \tag{10}$$

is satisfied. Condition (10) applies even when the plasma wave spectrum differs appreciably from a thermal spectrum. In the particular case when the wave spectrum differs only slightly from equilibrium, Eq. (9) reduces to Klimontovich's.[10]

3. Let us set up an equation to define the plasma wave spectrum, i.e., an equation for the function $\epsilon(\mathbf{q}, \mathbf{r}, t)$. The variation of ϵ in time will be determined by the transfer of plasma wave quanta (plasmons) with the group velocity $\partial\omega/\partial\mathbf{q}$, by the spontaneous radiation of plasmons (a term independent of ϵ), and by their absorption or induced emission which is proportional to $\epsilon(\mathbf{q}, \mathbf{r}, t)$:

$$\frac{\partial\varepsilon}{\partial t} + \frac{\partial\omega}{\partial q_i} \frac{\partial\varepsilon}{\partial x_i} = A + B\varepsilon.$$

Here B is twice the growth rate of the plasma wave amplitude.

The quantity B is to be found from a dispersion relation that depends on the electron distribution function $N(\mathbf{u})$. If the function $N(\mathbf{u})$ can be expanded in a series in the complex plane near the point $\mathbf{q}\cdot\mathbf{u} = \omega$ and if moreover the value of the function at the pole $\mathbf{q}\cdot\mathbf{u} - \omega - i\gamma$ can be found from just the first term of the expansion, then the following expression is obtained for B,

$$B = 2\gamma = \frac{4\pi\omega_0^2 e^2}{m\omega q^2} \int q_i \frac{\partial N}{\partial u_i} \delta(\mathbf{qu} - \omega) \, d^3u. \tag{11}$$

In the particular case of a Maxwell distribution, the Landau[14] damping formula is obtained. A corresponding expression for γ was previously derived by Bohm and Gross.[6]

The next pure imaginary term in the expansion of $N(\mathbf{u})$ can be neglected if the inequality

$$| u^6 n_0^{-2} N'(u) N'''(u) | \ll 1 \tag{12}$$

is satisfied. For a beam of fast electrons of density n, moving at velocity u through a plasma with an electron density n_0 and possessing a velocity dispersion Δu, this inequality assumes the following form

$$(u/\Delta u)^3 (n/n_0) \ll 1. \tag{13}$$

On the other hand, condition (6), when applied to a beam of fast electrons, has the following form

$$\Delta q/q \gg (n/n_0)(u/\Delta u)^2, \tag{14}$$

where, as in Eq. (10), Δq and q characterize the plasma wave spectrum. If the plasma waves are generated by the fast electrons themselves, then $\Delta q/q \approx \Delta u/u$, and conditions (10), (13), and (14) become equivalent.

The intensity of the spontaneous radiation is found by analyzing the motion of a charged particle in the plasma.[12]

Thus, for the kinetic equation for $\epsilon(\mathbf{q}, \mathbf{r}, t)$, we obtain

$$\frac{\partial\varepsilon}{\partial t} + \frac{\partial\omega}{\partial q_i} \frac{\partial\varepsilon}{\partial x_i} = \frac{e^2\omega_0^2}{2\pi q^2} \int N \delta(\mathbf{qu} - \omega) \, d^3u + \frac{4\pi^2 e^2\omega_0^2}{m\omega q^2} \varepsilon \int q_i \frac{\partial N}{\partial u_i} \delta(\mathbf{qu} - \omega) \, d^3u. \tag{15}$$

Equations (1), (9), and (15) can be derived from a quantum representation of the plasma waves if the probabilities of emission and absorption by the electron of a quantum with frequency ω and wave vector $\mathbf{q}$ are assumed to be, respectively,[15]

$$W^+ = \frac{\omega_0^2}{2\pi\omega q^2}(N_\omega + 1), \qquad W^- = \frac{\omega_0^2}{2\pi\omega q^2} N_\omega,$$

where N_ω is the density in phase space of quanta with frequency ω.

It should be noted further that the description of plasmon transfer by a group velocity concept is justified provided that

$$\frac{\partial\varepsilon}{\partial t} \gg \frac{\partial\omega}{\partial q_i} \frac{\partial\varepsilon}{\partial x_i}. \tag{16}$$

If this inequality is not satisfied then the region of applicability of Eq. (15) is determined by a more stringent requirement on the velocity dispersion of the electron beam, viz.,

$$\Delta u/u \gg (n/n_0)^{1/3} (mu^2/T)^{1/4}. \tag{17}$$

Condition (17) defines simultaneously the boundaries of the quantum representation of plasma waves.

4. Equations (1), (9), and (15) are applicable when the electron distribution is a sufficiently smooth function of the velocity. Now let us derive equations for the time variation of the plasma wave spectral density and for the distribution function of fast electrons with an arbitrary velocity spread. We begin with the dispersion relation[14]

$$1 = \frac{4\pi e^2 i}{mq^2} \int_C q_i \frac{\partial N}{\partial u_i} \frac{d^3u}{i(\mathbf{qu} - \omega) + \gamma}. \tag{18}$$

We are interested in the case in which the electron distribution function can be represented as the sum of a Maxwellian distribution, $N_0(u)$, and a fast-electron distribution, $N(\mathbf{u}, \mathbf{r}, t)$, in which the average velocity is assumed to be considerably larger than the thermal velocity of the plasma. Since the distribution function for the fast electrons is different from zero only within a certain limited region of velocity space, this region is best separated in the dispersion relations where the integration is over $\mathbf{u}$. Neglecting terms proportional to $(n/n_0)^{2/3}$ and $(a/\omega)^4$ where $a^2 = q^2T/2m$, we find from (18) that

$$1 - \frac{\omega_0^2}{\omega^2} - \frac{6a^2\omega_0^2}{\omega^4} = -\frac{\omega_0^2}{q^2 n_0}\int d^3u \frac{\omega - \mathbf{qu}}{\gamma^2 + (\omega - \mathbf{qu})^2} q_i \frac{\partial N}{\partial u_i}, \tag{19}$$

$$\gamma\left(1 + \frac{12a^2}{\omega^2}\right) = \frac{\omega^2}{2q^2 n_0}\int d^3u \frac{|\gamma|}{\gamma^2 + (\omega - \mathbf{qu})^2} q_i \frac{\partial N}{\partial u_i}. \tag{20}$$

The integration in (19) and (20) is to be performed over the region $\omega - \mathbf{q}\cdot\mathbf{u} \ll \omega_0$. These equations are applicable if ω and ω_0 differ only slightly, which is not the case when $q \ll \omega/u$, although such small values of q are essentially absent from the plasma-wave spectrum when the waves are generated by fast electrons.

In the case of a monochromatic electron beam $((n/n_0)(u/\Delta u)^3 \gg 1,\ n \ll n_0)$ with velocity u_0, Akhiezer and Faĭnberg[7] have found that

$$\gamma = \gamma_a - (\omega - \mathbf{qu}_0)^2/12\gamma_a,$$
$$\gamma_a = \sqrt{3}\cdot 2^{-4/3}(n/n_0)^{1/3}\omega_0^{2/3}(\tilde{\omega} - q\partial\tilde{\omega}/\partial q)^{1/3}. \tag{21}$$

Here $\tilde{\omega}$ represents the oscillation frequency for a Maxwellian distribution $(n = 0)$:

$$\tilde{\omega}(q) = \omega_0 + \tfrac{3}{2}Tq^2/m\omega_0. \tag{22}$$

When the electron beam is not monochromatic $((n/n_0)(u/\Delta u)^3 \ll 1)$, then γ is determined by Eq. (11).

The derivation of Eqs. (24) and (25) which follow is based on the assumption that the electron distribution function changes more slowly than the plasma wave amplitude, i.e., that the system is "quasi-stationary." If $(n/n_0)(u/\Delta u)^3 \gg 1$, then one can show that the "quasi-stationary" approximation holds when

$$\int \varepsilon d^3q \ll (n/n_0)^{2/3}(\Delta u/u)^2 n_0 m u^2. \tag{23}$$

Despite the fact that the "quasi-stationary" conditions are essentially fulfilled only for electron beams that are sufficiently spread out in velocity, this approximation is useful in describing the entire slowing down process. In this case the equation for the plasma wave intensity is given by

$$\frac{\partial\varepsilon}{\partial t} + \frac{\partial\omega}{\partial q_i}\frac{\partial\varepsilon}{\partial x_i} = 2\gamma\varepsilon. \tag{24}$$

As before, the description of the plasma wave transfer by means of the group velocity concept[†] is applicable if

$$\frac{\partial\omega}{\partial q}\frac{\partial\varepsilon}{\partial x} \ll \frac{\partial\varepsilon}{\partial t}.$$

This inequality is not satisfied, for example, in the case of the stationary problem whose solution is examined below. Equation (24) does not take into account the radiation of plasma waves by individual, randomly moving electrons, but this radiation is important only for finding the initial values of ϵ in the exponential stage of growth of the oscillation and during the approach to equilibrium.

The corresponding equation for the electron distribution function for a given spectral density $\epsilon(\mathbf{q}, \mathbf{r}, t)$ will be of the form

$$\partial N/\partial t + u_i\partial N/\partial x_i + \partial I_i/\partial u_i = 0, \tag{25}$$

where

$$I = \int d^3q \frac{A_{ik}}{\gamma^2 + (\omega - \mathbf{qu})^2}\frac{\partial N}{\partial u_k}. \tag{26}$$

A_{ik} is determined uniquely by stipulating that Eqs. (18), (24), (25), and (26) satisfy the conservation of energy and also that in the limit, when $(n/n_0)(u/\Delta u)^3 \ll 1$, Eq. (26) reduces to the corresponding term in Eq. (9). In this case we have

$$A_{ik} = -\frac{8\pi e^2}{m^2}\frac{q_i q_k \varepsilon(\mathbf{q})|\gamma|}{q^2[1 + \omega_0^2/\omega^2 + 18a^2\omega_0^2/\omega^4]}. \tag{27}$$

Unlike the linearized kinetic equations, Eqs. (24), (25), and (26) take into account the reaction of the plasma wave field on the fast electrons. On the other hand, the effects due to the nonlinearity and non-sinusoidality of the wave are not included in our equations. These effects can be described by terms proportional to ϵ^2 and are seemingly essential when the plasma waves die out.

5. Equation (25) describes the diffusion of the fast electrons in velocity space during their interaction with the plasma waves. In case the beam is almost monochromatic one can obtain, assuming $(\omega - \mathbf{q}\cdot\mathbf{u})^2 \ll \gamma^2$, the following expression for I_i,

$$I_i = -\frac{4\pi e^2}{m^2\gamma}\frac{\partial N}{\partial u_k}\int \varepsilon \frac{q_i q_k}{q^2} d^3q. \tag{28}$$

Let us assume that, in the main, waves are generated with a wave vector directed along the z axis, in a direction parallel to the velocity of the fast electrons, i.e., that $q_z \approx q$ and $q_r \ll q_z$. This occurs, for example, in the case of a fast electron beam with a small cross section. Neglecting, moreover, the density variation in a homogeneous electron beam due to scattering, we can write the equation for diffusion in the u_z direction as

$$\frac{\partial N}{\partial t} = \frac{4\pi e^2}{m^2\gamma}\int \varepsilon d^3q\, \frac{\partial^2 N}{\partial u_z^2}\,. \tag{29}$$

By means of (29) it is possible to determine the induced velocity dispersion, viz.,

$$\overline{\Delta u_z^2} = (4\pi e^2/m^2\gamma^2)\, W. \tag{30}$$

Equation (30) is derived from Eq. (25), whose applicability to a monochromatic beam has not been, strictly speaking, proved. Therefore, in order to determine the accuracy of Eq. (25), a numerical calculation was made of the variation in the velocity of single electrons in a beam initially uniform in space and monochromatic in velocity.*

In dimensionless variables the equation for the motion of an electron in the field of an exponentially increasing plasma wave is

$$d^2x/dt^2 = \alpha e^{\gamma t}\cos(x - t), \qquad \alpha = 10^{-4}, \qquad \gamma = 0{,}1.$$

The initial electron coordinate $x_0\ (0 \le x_0 \le \pi)$ and initial velocity, $u_0\ (|u_0 - 1| < 10^{-3})$ were selected randomly. The value of $\alpha^{-2}(u - 1)^2e^{-2\gamma t}$ at various times, which is shown below, was obtained by averaging over 135 different trajectories:

t =	0	10	20	30	40	50
$\alpha^{-2}(u-1)^2e^{-2\gamma t}$ =	32	22.4	36.5	44	46.3	43.5

These results are in good agreement with Eq. (30), which gives

$$\alpha^{-2}(u - 1)^2e^{-2\gamma t} \approx 1/2\gamma^2 = 50.$$

6. Let us now consider an idealized problem dealing with the growth of the instability in a uniform monochromatic beam of electrons moving in an infinite plasma of constant density. Let us imagine that the interaction between the fast electrons and plasma is switched on instantly at $t = 0$. For $t < 0$, only a thermal background of oscillations exists in the plasma these being due to the random movement of Maxwell electrons ($\epsilon = T/(2\pi)^3$. Once the interaction is turned on, the plasma wave intensity which increases exponentially is given by

$$\varepsilon(\mathbf{q}, t) = (2\pi)^{-3}\left[\tfrac{1}{9}\, 2^{2/3}(n/n_0)^{1/3}mu_0^2 + \tfrac{4}{9}\, T\right] e^{2\gamma t}. \tag{31}$$

The pre-exponential factor is obtained by solving the kinetic equation with the inclusion of the random motion of the electrons.

Integrating (31) over $\mathbf{q}$ we obtain the total intensity of the excited plasma waves. This result is applicable so long as it is possible to neglect the variation in γ due to the fact that the monochromaticity of the fast electron beam is disturbed. During this exponential growth stage a narrow region of wave vectors stand out for which q_z is close to ω/u_0, so that when ϵ is integrated over q_z with γ given by Eq. (21), the dependence of γ_a on q_z becomes insignificant. The integration over q_r is to be restricted at some upper limit, $q_{r\,max}$, which in the case of a beam is determined by its diameter. Hence we find that

$$W = \int \varepsilon d^3q \sim \frac{1}{(2\pi)^3}\left[\frac{2^{2/3}}{9}\left(\frac{n}{n_0}\right)^{1/3} mu_0^2 \right.$$
$$\left. + \frac{4}{9}\, T\right]\sqrt{\frac{6\gamma_a\pi^3}{t}}\,\frac{1}{u_0}\, q_{r\,max}^2 e^{2\gamma_a t}. \tag{32}$$

From geometric considerations we have that $q_{r\,max} \approx q_z d/u_0 t$, where d is the diameter of the beam. If the diameter of the beam is significantly larger than the path length to the scattering zone, then the integral over q_r converges when Landau damping and the dependence of γ_a on q are taken into account.

The average velocity loss by the beam, Δu, which follows from the conservation of total energy, is found from the relation

$$W = nmu_0\Delta u.$$

On the other hand, according to (30) the rms spread in velocities is proportional to the square root of W. Furthermore, bearing in mind that $\gamma \approx \omega_0(n/n_0)^{1/3}$, we have

$$\sqrt{\overline{(\Delta u)^2}} \sim (n_0/n)^{1/3}(W/mn_0)^{1/2}.$$

The mean velocity loss is comparable with the rms spread for $W \approx nmu_0^2(n/n_0)^{1/3}$, at which time γ already differs considerably from its original value and Eq. (32) becomes inapplicable. Assuming in (32) that $W = nmu_0^2(n/n_0)^{1/3}$, we can find the time τ, during which the oscillation energy increases exponentially,

$$\tau = L/2\gamma_a, \tag{33}$$

where L is the logarithm determined from Eq. (32).

7. In the case of the stationary linearized problem the solution for the growth of the longitudinal oscillations due to a beam of fast electrons in a semi-infinite plasma with specified boundary plasma oscillations can be determined from the dispersion relations derived by A. A. Luchina.[16] As applied to a monochromatic electron beam entering a plasma, the dispersion relation is given by

$$\frac{1}{\omega_0^2} - \frac{1}{\omega^2} - \frac{n}{n_0}\,\frac{1}{(\omega - ku)^2} + \frac{3Tk^2}{m\omega^4}\,, \tag{34}$$

where $k = q + i\mu$ is the complex wave vector whose imaginary part μ characterizes the spatial growth in the plasma wave intensity.

If the plasma temperature is zero, $T = 0$, which corresponds to the hydrodynamic description of two mutually penetrating beams, then $\mu_{\max} = \infty$, i.e. there is no stationary solution. The value of $\mu_{\max}$ is finite if the temperature of the plasma is different from zero. Provided that $T \ll mu^2$, the solution of Eq. (34) becomes

---

*L. P. Strotseva and M. P. Bronnikova performed the computation for this problem.

$$\mu_{max} = \frac{\omega_0}{u}\left(\frac{nmu^2}{6n_0T}\right)^{1/3}\frac{\sqrt{\mathrm{ch}^2 t - 1/4}}{\mathrm{ch}^2\, t}, \quad \mathrm{sh}\, 2t = \left(\frac{4nmu^2}{3n_0T}\right)^{1/6} \qquad (35)^*$$

The spatial extent of the exponential growth of the plasma wave intensity, which corresponds to l, the distance to the first scattering zone in the electron beam, is found, as in (33), from the equation

$$l = L/2\mu. \qquad (36)$$

Equations (35) and (36), which determine the dependence of the length l, on the plasma density and the beam density, are qualitatively confirmed by the experimental results. Unfortunately it is impossible to make a thorough quantitative comparison because we do not know accurately enough some of the quantities which occur in Eqs. (35) and (36). In the first place, Eq. (32) only sets the upper limit to the value for the logarithm ($L \approx 20$); in fact the true value of L could turn out to be somewhat smaller if the excitations on the plasma boundary were strengthened by reflection of plasma waves in the experimental apparatus. In the second place, our estimates disregard the finite energy spread in the electron beam, which would diminish the value of μ. These data are not given in the paper by Gabovich and Pasechnik.[1] Finally, the published results[1,4] do not contain the actual plasma temperature.

If, nevertheless, we neglect the initial velocity spread in the beam and assume $T = 2$ ev, then on the basis of the experimental data given by Merill and Webb,[4] the logarithm, L, for the two different measurements made by these authors proves to be 15 and 19 respectively, which can be considered as a completely satisfactory confirmation of Eq. (36). The value of L in the experiments of Gabovich and Pasechnik falls within the range of from 12 to 70 for the different beam and plasma parameters employed. This disagrees with what would be theoretically expected for this quantity ($15 < L < 30$). Evidently additional measurements are needed to definitely clarify the problem of the divergence between the theoretical and empirical values for the length, l, which differ in some cases by as much as a factor of two or three.

The concepts developed above also provide for an understanding of such experimentally observed phenomena accompanying anomalous scattering as the change in the monochromaticity of the beam, which causes the appearance of electrons with an energy greater than the initial, and the small value of the average energy lost by the beam in the first scattering zone. The appearance of a second scattering zone, which was especially sharply defined in the experiments performed by Merill and Webb,[4] should, apparently, be attributed to the modulation of the beam velocity and a subsequent bunching of the beam after passage through the first scattering zone.

In conclusion, the authors wish to express their gratitude to V. S. Imshennik, Yu. I. Morozov, É. Z. Tarumov, and V. A. Teplyakov for their valuable consultation on several matters.

---

*sh = sinh, ch = cosh.

[1] M. D. Gabovich and L. L. Pasechnik, JETP **36**, 1025 (1959), Soviet Phys. JETP **4**, 727 (1959).

[2] A. A. Vlasov, Теория многих частиц (Many Body Theory), Gostekhizdat (1950).

[3] D. Bohm and E. P. Gross, Phys. Rev. **79**, 992 (1950).

[4] H. J. Merill and H. W. Webb, Phys. Rev. **55**, 1191 (1939).

[5] Gabor, Ash, and Dracott, Nature **176**, 916 (1955).

[6] D. Bohm and E. P. Gross, Phys. Rev. **75**, 1864 (1949).

[7] A. I. Akhiezer and Ya. B. Faĭnberg, JETP **21**, 1262 (1951).

[8] D. H. Looney and S. C. Brown, Phys. Rev. **93**, 965 (1954).

[9] F. D. Kahn, J. Fluid Mech. **2**, 601 (1957).

[10] Yu. L. Klimontovich, JETP **36**, 1405 (1959), Soviet Phys. JETP **9**, 999 (1959).

[11] A. A. Vlasov, Уч. зап. МГУ (Sci. Notes, Moscow State University) **75**, 2 (1945).

[12] A. I. Akhiezer and S. G. Sitenko, JETP **23**, 161 (1952).

[13] Gasiorowitz, Neuman, and Riddel, Jr, Phys. Rev. **101**, 922 (1956).

[14] L. D. Landau, JETP **16**, 574 (1946).

[15] B. I. Davydov, Физика плазмы и проблема управляемых термоядерных реакций (Plasma Physics and the Problems of Controlled Thermonuclear Reactions) Vol. 1, Acad. Sci. Press, 1958, p. 77.

[16] A. A. Luchina, JETP **28**, 17 (1955), Soviet Phys. JETP **1**, 12 (1955).

Translated by A. Skumanich
22

SOVIET PHYSICS JETP VOLUME 13, NUMBER 1 JULY, 1961

ON THE THEORY OF DOUBLE ELECTRON AND NUCLEAR RESONANCE IN SYSTEMS WITH HYPERFINE INTERACTION

T. G. IZYUMOVA and G. V. SKROTSKIĬ

Ural Polytechnic Institute

Submitted to JETP editor May 18, 1960

J. Exptl. Theoret. Phys. (U.S.S.R.) 40, 133-142 (January, 1961)

The complex susceptibility of electron spins interacting with a nuclear system is calculated on the basis of the statistical perturbation theory. The dependence of the conditions for the saturation of the electron system on the resonance conditions of the nuclear system is obtained.

1. INTRODUCTION

THE method of double magnetic resonance is applied to systems containing two different kinds of magnetic moments. The sample to be investigated is placed in a constant magnetic field $H_0 = H_Z$ and in two periodic fields of frequencies close to the Larmor precession frequencies for both kinds of magnetic moments. The existence of an interaction between the magnetic moments of the two systems (for example, hyperfine interaction) leads to the result that resonance in one of the systems has an effect on the nature of the resonance in the other system. In systems exhibiting both nuclear and electronic paramagnetism the existence of hyperfine interaction results in a number of effects which may be divided into two groups.

To the first group belong the effects associated with the influence of the electron paramagnetic resonance on the nuclear resonance. As the electron system approaches saturation an increase in the polarization of the nuclear magnetic moments (the Overhauser effect) may be achieved. The Overhauser effect[1] can be observed in substances with a "rapidly fluctuating lattice": in this case the method of double resonance is ordinarily used in order to intensify the nuclear magnetic resonance signal.

To the second group belong the effects associated with the influence of the nuclear resonance on the electron resonance. The first to observe this phenomenon experimentally and to give it a qualitative explanation was Feher.[2] The saturation of the nuclear system does not result in any appreciable polarization of the electron spins. However, it alters the conditions for the saturation of the electron system and, consequently, leads to a change in the absorption of energy from the radio frequency field by the electron system.

In order to explain this phenomenon Feher[2] considers a simple system consisting of electrons ($s = 1/2$) and nuclei ($I = 1/2$). In strong constant magnetic fields the energy level spectrum of such a system is of the form shown in the diagram. Transitions induced by a microwave field of frequency ω_S obey the selection rules $\Delta m_S = 1$ and $\Delta m_I = 0$. The amplitude of the signal due to these transitions is proportional to the difference in the populations of the levels E_1 and E_2'. If we partially saturate the electron system, then the signal due to the absorption of microwave power will be decreased. If at the same time we induce nuclear transitions of frequency ω_I, then the possibility arises of equalizing the populations of levels E_1 and E_2', as a result the difference in the populations of the levels E_2 and E_2' will increase, and this will in turn lead to an increase in the electron resonance signal. By inducing the nuclear transitions $E_1' \to E_1$, we can observe a sharp decrease in the electron resonance signal.

With such a formulation of the problem the method of double resonance turns out to be a sensitive means for studying the phenomenon of nuclear resonance. It enables us to determine, in particular, the value of the nuclear factor g_I. The method may be successfully applied in the case when the value of the hyperfine interaction $A(\mathbf{s}\cdot\mathbf{I})$ is small compared to the width of the electron resonance line, and therefore the hyperfine structure can not be resolved by the usual method of observing the absorption signal due to the electron system.[3] However, this turns out to be possible if the observations are made by the double resonance method, because of the small width of the nuclear resonance line.

The method enables us to resolve the hyperfine structure of a line due to an unpaired electron present in a complicated chemical compound arising from the interaction of this electron with the surrounding nuclei. Among such compounds we can include organic free radicals, irradiated crystals, and structures with displaced atoms or ruptured bonds. In this case we can obtain information with regard to the distribution of the electron density in molecules, crystals, F centers, etc.[4] Thus, the method of double resonance is of great practical interest.

In this paper we present a quantum-mechanical analysis of the phenomenon of the effect of nuclear magnetic resonance on the electron paramagnetic resonance in systems with hyperfine interaction. Such an analysis can not be carried through within the framework of the linear theory of magnetic resonance, since the very formulation of the problem assumes the possibility of applying strong radio frequency and microwave fields sufficient for the saturation both of electron and of nuclear resonance.

In this paper we have used the method of the statistical perturbation theory developed by Tomita[5] for the case of circularly-polarized radiation of arbitrary amplitude.

2. FORMULATION OF THE PROBLEM

We consider a system consisting of uncompensated electron spins $\mathbf{s}^k$, surrounded by several nuclei with different angular momenta $\mathbf{I}^l$. We assume the existence of a scalar interaction between the electrons and the nuclei, and also of an interaction of the electrons with the lattice. We place the sample in the magnetic field

$$\mathbf{H} = \mathbf{H}_0 + \mathbf{h}_s(t) + \mathbf{h}_l(t), \tag{1}$$

where $\mathbf{h}_S$ and $\mathbf{h}_I$ are respectively the intensities of the microwave and of the radio-frequency fields. These fields are circularly polarized in the plane perpendicular to H_0.

We write the Hamiltonian for the system of electrons and nuclei in the following form

$$\hat{\mathscr{H}} = -g_s\mu_s \sum_k \hat{\mathbf{s}}^k\mathbf{H} - \sum_l g_l^l \mu_l^l \hat{\mathbf{I}}^l\mathbf{H} + \sum_{l,k} A_l \hat{\mathbf{s}}^k \hat{\mathbf{I}}^l + \hat{\mathbf{s}}\hat{\mathbf{F}} + \hat{\mathscr{H}}_F, \tag{2}$$

where μ_S and μ_I are the electron and the nuclear magnetons, while A_l is the hyperfine interaction constant. The term $\hat{\mathbf{s}} \cdot \hat{\mathbf{F}}$ where $\mathbf{s} = \Sigma \mathbf{s}^k$ takes into account the interaction of the electrons with the lattice, while $\mathscr{H}_F$ is the operator for the energy of the "lattice".

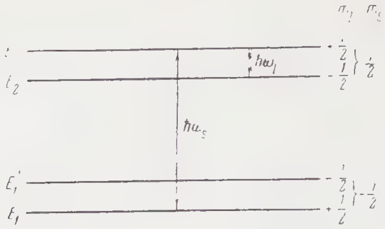

For subsequent discussion it will be convenient to go over to the circular variables

$$\hat{s}_{\pm 1} = \frac{1}{\sqrt{2}}(\hat{s}_x \pm i\hat{s}_y), \quad \hat{s}_0 = \hat{s}_z,$$

$$\hat{I}_{\pm 1} = \frac{1}{\sqrt{2}}(\hat{I}_x \pm i\hat{I}_y), \quad \hat{I}_0 = \hat{I}_z, \tag{3}$$

in terms of which the microwave and the radio frequency fields assume the form

$$h_{+1}^s = h^s e^{-i\omega_s t}, \qquad h_0^s = h_{-1}^s = 0;$$
$$h_{+1}^l = h_0^l = 0, \qquad h_{-1}^l = h_0^l e^{i\omega_l t}, \tag{4}$$

while the Hamiltonian (2) may be written in the following form:

$$\hat{\mathscr{H}} = -g_s\mu_s \sum_k \hat{s}_0^k H_0 - g_s\mu_s \sum_{k,\mu\neq 0} \hat{s}_\mu^k h_{-\mu}^s - g_s\mu_s \sum_{k,\mu\neq 0} \hat{s}_\mu^k h_{-\mu}^l$$
$$- \sum_l g_l^l \mu_l^l \hat{I}_0^l H_0 - \sum_{l,\mu\neq 0} g_l^l \mu_l^l \hat{I}_\mu^l h_{-\mu}^s - \sum_{k,\mu\neq 0} g_l^l \mu_l^l \hat{I}_\mu^l h_{-\mu}^l$$
$$+ \sum_\mu \hat{s}_\mu \hat{F}_{-\mu} + \sum_{lk} A_l \hat{s}_\mu^k \hat{I}_{-\mu}^l + \hat{\mathscr{H}}_F. \tag{5}$$

In future we shall assume that the energy of the hyperfine interaction is small compared to the Zeeman energy of the electrons. In this case the electron and the nuclear spins precess about the strong constant field H_0 independently of each other. The hyperfine interaction introduces only a perturbation of this motion. This latter circumstance enables us to pose the problem of finding the complex susceptibility of the electron spin system by itself. The hyperfine interaction will lead to the "inhomogeneous broadening"[6] of the electron paramagnetic resonance line.

"Inhomogeneous broadening" occurs when in the spin system under consideration interactions are possible not only with spins of the same kind ("homogeneous broadening"), but also with other kinds of spins not belonging to this system. Interactions giving rise to "inhomogeneous broadening" do not leave the spin system in equilibrium. They may vary slowly with time. In the case under consideration the second last term in (5) depends on the time, since the nuclear system is also in a state of magnetic resonance.

3. EQUATIONS OF MOTION FOR THE MAGNETIZATION VECTOR OF THE ELECTRON SYSTEM

The density matrix for the whole system in the case under consideration may be written in the form

$$\hat{\rho} \sim e^{-\beta\hat{\mathscr{H}}}, \qquad \hat{\mathscr{H}} = \hat{\mathscr{H}}_0 + \hat{\mathscr{H}}_1, \qquad \beta = 1/kT, \tag{6}$$

$$\hat{\mathscr{H}}_1 = \sum_{lk} A_l \hat{s}^k_\mu \hat{I}^l_{-\mu} + \sum_\mu \hat{s}_\mu \hat{F}_{-\mu}. \tag{7}$$

In accordance with (5) $\mathscr{H}_0$ consists of three parts corresponding to the energy of the electrons and of the nuclei in the external field, and also to the lattice energy $\hat{\mathscr{H}}_F$.

On utilizing the operator identity

$$\exp(-\beta(\hat{\mathscr{H}}_0 + \hat{\mathscr{H}}_1)) = \exp(-\beta\hat{\mathscr{H}}_0)\Big\{1 - \int_0^\beta d\lambda \exp(\lambda\hat{\mathscr{H}}_0) \times \hat{\mathscr{H}}_1 \exp(-\lambda\hat{\mathscr{H}}_0) + \int_0^\beta d\lambda_1 \int_0^{\lambda_1} d\lambda_2 \exp(\lambda_1\hat{\mathscr{H}}_0)\hat{\mathscr{H}}_1 \exp[-(\lambda_1 - \lambda_2)\hat{\mathscr{H}}_0]\hat{\mathscr{H}}_1 \exp(-\lambda_2\hat{\mathscr{H}}_0) + \ldots\Big\} \tag{8}$$

and on taking into account that the energy of the hyperfine interaction $\hbar\omega_{\text{int}}$ is small compared to the Zeeman energy, while at the same time $\delta = \hbar\omega_{\text{int}}/kT \ll 1$, we shall write the density matrix (6) in the form of a product of three independent factors

$$\hat{\rho} = \hat{\sigma}\hat{\sigma}'\hat{\rho}'. \tag{9}$$

Here $\hat{\sigma}$ is the density matrix for the electron spin system, $\hat{\sigma}'$ is the density matrix for the nuclear spin system and $\hat{\rho}'$ is the density matrix for the lattice.

The magnetization for the electron system is, evidently, determined in the following manner:

$$\langle\hat{M}_s\rangle = \mathrm{Sp}(\hat{\sigma}\mu_s\hat{s}) = \mu_s\,\mathrm{Sp}(\hat{\sigma}_+\hat{s}) - \mu_s\,\mathrm{Sp}(\hat{\sigma}_-\hat{s}). \tag{10a}$$

Here $\hat{\sigma}_+$ describes the ensemble of electrons whose spins are opposite to the field, while $\hat{\sigma}_-$ describes those whose spins are parallel to the field.

Similarly, for the nuclear system we have

$$\langle\hat{M}_I\rangle = \mathrm{Sp}(\hat{\sigma}'\mu_I\hat{I}) = \mu_I\,\mathrm{Sp}(\hat{\sigma}'_-\hat{I}) - \mu_I\,\mathrm{Sp}(\hat{\sigma}'_+\hat{I}). \tag{10b}$$

On taking (10a) and (10b) into account we can rewrite (9) in the form

$$\hat{\rho} = (\hat{\sigma}_+ - \hat{\sigma}_-)(\hat{\sigma}'_+ - \hat{\sigma}'_-)\hat{\rho}' = (\hat{\sigma}_+\hat{\sigma}'_+ + \hat{\sigma}_-\hat{\sigma}'_- - \hat{\sigma}_+\hat{\sigma}'_- - \hat{\sigma}_-\hat{\sigma}'_+)\hat{\rho}'. \tag{10c}$$

It is necessary to carry out such a decomposition because in the problem under consideration when energy is absorbed from the microwave field transitions occur not from both hyperfine sublevels of the ground state, but only from the one which, for example, corresponds to the value of the nuclear magnetic quantum number $m_I = +\frac{1}{2}$. The transition may occur to the upper level $m_S = \frac{1}{2}$ which also corresponds to $m_I = \frac{1}{2}$.

The variation of $\hat{\rho}$ with time is determined by the equation of motion

$$-i\hbar\,\partial\hat{\rho}/\partial t = [\hat{\rho}\hat{\mathscr{H}}]. \tag{11}$$

If we do not restrict ourselves to the case of small amplitudes of the microwave field h_S, then we cannot assume that the system of electron spins is in a state of thermodynamic equilibrium, since it is acted upon by a large secular time-dependent perturbation. In a system of coordinates rotating about the direction of the constant magnetic field with frequency ω_S, the system of electron spins will be acted upon by an effective magnetic field which is independent of the time. Now only those terms will depend on the time which describe a weak interaction of the electrons with the nuclei and with the lattice. In this system of coordinates there exists an equilibrium distribution of electron spins determined by the Boltzmann factor. The effective field H_{eff} is inclined to the z axis at an angle ϑ:

$$\sin\vartheta = h^s[(H_0 + \omega_s/\gamma_s)^2 + h^{s2}]^{-1/2}, \qquad \cos\vartheta = (H_0 + \omega_s/\gamma_s)[(H_0 + \omega_s/\gamma_s)^2 + h^{s2}]^{-1/2}, \tag{12}$$

$$H_{eff} = [(H_0 + \omega_s/\gamma_s)^2 + h^{s2}]^{1/2}. \tag{13}$$

The transition to the coordinate system rotating about the effective field is accomplished by means of the canonical transformation

$$\hat{s}^T_\mu = \exp(i\omega_s\hat{s}_0 t)\Big(\sum_\nu a_{\mu\nu}(\vartheta)\hat{s}_\nu\Big)\exp(-i\omega_s\hat{s}_0 t). \tag{14}$$

The matrix $a_{\mu\nu}(\vartheta)$ has the form

$$a_{\mu\nu}(\vartheta) = \begin{vmatrix} \frac{1}{2}(\cos\vartheta + 1) & 2^{-1/2}\sin\vartheta & \frac{1}{2}(\cos\vartheta - 1) \\ -2^{-1/2}\sin\vartheta & \cos\vartheta & -2^{-1/2}\sin\vartheta \\ \frac{1}{2}(\cos\vartheta - 1) & 2^{-1/2}\sin\vartheta & \frac{1}{2}(\cos\vartheta + 1) \end{vmatrix}. \tag{15}$$

Here μ and ν take on in turn the values 1, 0, − 1.

Upon application of the transformation (14), Eq. (11) is written in the following form:

$$-i\hbar\,d\hat{\rho}^T/dt = [\hat{\rho}^T\hat{\mathscr{H}}^T]. \tag{16}$$

Here

$$\hat{\mathscr{H}}^T = \hat{\mathscr{H}}^T_0 + \hat{\mathscr{H}}^T_1(t), \tag{17}$$

$$\hat{\mathscr{H}}^T_0 = -\sum_k \gamma^s\hbar\hat{s}^k_0\left(H_0 + \frac{\omega_s}{\gamma_s}\right) - \sum_{k,\mu\neq 0}\gamma^s\hbar\hat{s}^k_\mu h^s_{-\mu} + \hat{\mathscr{H}}_F - \sum_l g^l_I\mu^l_I\hat{I}^l_0 H_0 \tag{18}$$

$$\hat{\mathscr{H}}^T_1(t) = \sum_{l,k,\mu} A_l\hat{s}^k_\mu I^l_{-\mu}e^{i\mu\omega_s t} + \sum_{k,\mu}\hat{s}^k_\mu F_{-\mu}e^{i\mu\omega_s t}, \quad \hbar\gamma^s = g_s\mu_s \tag{19}$$

On assuming that the time interval t defined by the inequality $\epsilon = \mathscr{H}^T_1 t/\hbar \ll 1$ is greater than the relaxation time for the electron spin system we can utilize time-dependent perturbation theory. In order to do this it is convenient to go over to the interaction representation, and to expand the density matrix in powers of the parameter ϵ retaining second order terms:

$$\rho^{T*}(t) = \hat{\rho}^{T*}(0) - \frac{i}{\hbar}\int\limits_0^t [\hat{\rho}^{*T}(0)\,\hat{\mathscr{H}}_1^{*T}(t_1)]\,dt_1 - \frac{1}{\hbar^2}\int\limits_0^t\int\limits_0^{t_1} dt_1 dt_2\,[[\hat{\rho}^{*T}(0)\,\hat{\mathscr{H}}_1^{*T}(t_1)]\,\hat{\mathscr{H}}_1^{T*}(t_2)]. \tag{20}$$

We note that ϵ^2 always remains greater than δ, and, therefore, the neglect of terms linear in δ in (8) is quite legitimate.

It is necessary to average expression (20) over the canonical ensemble of the nuclei and the "lattice." After averaging and differentiation with respect to time we shall obtain the approximate equation for the density matrix of the electron system in the interaction representation:

$$\frac{\partial\hat{\sigma}^{T*}(t)}{\partial t} = -\frac{i}{\hbar}\frac{\partial}{\partial t}\int\limits_0^t \langle[\hat{\rho}^{*T}(0)\,\hat{\mathscr{H}}_1^{*T}(t_1)]\rangle_{\sigma',\,\rho'}dt_1 - \frac{1}{\hbar^2}\frac{\partial}{\partial t}\int\limits_0^t\int\limits_0^{t_1} dt_1 dt_2\,\langle[[\hat{\rho}^{*T}(0)\,\hat{\mathscr{H}}_1^{*T}(t_1)]\,\hat{\mathscr{H}}_1^{*T}(t_2)]\rangle_{\sigma',\rho'}. \tag{21}$$

In averaging over the ensemble of the nuclei we must distinguish two cases, depending on what type of nuclear transitions are induced. In the transitions $E_1' \rightarrow E_1$ it is necessary to take into account only the nuclei coupled to the electrons parallel to the field, and the averaging is taken only over the part of the density martix $\sigma_+(\sigma_+' - \sigma_-')$ from (10c). If the transitions $E_2 \rightarrow E_2'$ are being induced, then it is necessary to average over the other part of (10c) $\sigma_-(\sigma_+' - \sigma_-')$, since in this case we consider only the nuclei coupled to the electrons whose spins are directed oppositely to the field. In these two cases the averages of the terms including the hyperfine interaction will differ only in their sign.

It is necessary to substitute expression (19) into equation (21), and in doing so it is necessary to keep in mind that in the problem under consideration we neglect the satellite absorption lines of the electron system (their frequencies lie far from the main line). Therefore, in the term linear in $\mathscr{H}_1$ it is necessary to set $\mu = 0$, and in the quadratic term to set $\mu = -\mu'$. Then after a straightforward calculation we obtain:

$$\begin{aligned}\frac{\partial\hat{\sigma}^{*T}(t)}{\partial t} = &-\frac{i}{\hbar}e^{-i\nu\Omega_1 t}\sum_{k\nu} a_{0\nu}(\vartheta)\left\{\langle\hat{F}_0^*(t_1)\rangle \mp \sum_i A_i\langle\hat{I}_{i0}^*(t_1)\rangle\right\}\\ &\times[\hat{\sigma}^{*T}(0)\,\hat{s}_{k\nu}] - \frac{1}{\hbar^2}\sum_{k\mu\nu\nu'} a_{\mu\nu}(\vartheta)\,a_{-\mu\nu}(\vartheta)\exp(-i\nu\Omega_1 t\\ &- i\nu'\Omega_1 t)\int\limits_0^t d\tau\exp(i\mu\omega_1\tau + i\nu'\Omega_1\tau)\left\{\Big(\langle\hat{F}_{-\mu}^*(\tau)\,\hat{F}_\mu^*(0)\rangle\right.\\ &\mp\sum_l A_l^2\langle\hat{I}_{-\mu}^*(\tau)\hat{I}_\mu^*(0)\rangle\Big)[\hat{s}_\nu\hat{s}_{\nu'}\hat{\sigma}^{*T} - \hat{s}_{\nu'}\hat{\sigma}^{*T}\hat{s}_\nu]\\ &+\Big(\langle\hat{F}_\mu^*(0)\,\hat{F}_{-\mu}^*(\tau)\rangle \mp \sum_l A_l^2\langle\hat{I}_\mu^*(0)\,\hat{I}_{-\mu}^*(\tau)\rangle\Big)[\hat{\sigma}^{*T}\hat{s}_{\nu'}\hat{s}_\nu\\ &\left.- \hat{s}_\nu\hat{\sigma}^{*T}\hat{s}_{\nu'}]\right\}.\end{aligned} \tag{22}$$

The left hand side of (22) can be written in the form

$$\begin{aligned}\frac{\partial}{\partial t}\hat{\sigma}^{*T} &= \frac{\partial}{\partial t}\left\{\exp\left(-i\frac{\hat{\mathscr{H}}_0^T}{\hbar}t\right)\hat{\sigma}^T\exp\left(i\frac{\hat{\mathscr{H}}_0^T}{\hbar}t\right)\right\}\\ &= \exp\left(-i\frac{\hat{\mathscr{H}}_0^T}{\hbar}t\right)\left\{\frac{\partial\hat{\sigma}^T}{\partial t} + i\left[\hat{\sigma}^T, \frac{\hat{\mathscr{H}}_0^T}{\hbar}\right]\right\}\exp\left(i\frac{\hat{\mathscr{H}}_0^T}{\hbar}t\right).\end{aligned} \tag{23}$$

On multiplying both parts of (22) on the left by $\exp(i\mathscr{H}_0 t/\hbar)$ and on the right by $\exp(-i\mathscr{H}_0 t/\hbar)$, and on noting that in the energy representation ($\hat{\mathscr{H}}_0^T$ diagonal) we have

$$\exp\left\{i\frac{\hat{\mathscr{H}}_0^T}{\hbar}t\right\}\hat{s}_\nu\exp\left\{-i\frac{\hat{\mathscr{H}}_0^T}{\hbar}t\right\} = \hat{s}_\nu e^{i\nu\Omega_1 t},$$

we go over in (22) from the interaction representation again to the rotating coordinate system:

$$\begin{aligned}\frac{\partial\hat{\sigma}^T}{\partial t} = &-i\left[\hat{\sigma}^T, \frac{\hat{\mathscr{H}}_0^T}{\hbar}\right] - \frac{i}{\hbar}\sum_{k\mu\nu} a_{\mu\nu}(\vartheta)\left\{\sum_l\langle\hat{F}_0^*(0)\rangle_{\rho'}\right.\\ &\left.\mp A_l\langle\hat{I}_0^{l*}(0)\rangle_{\sigma'}\right\}[\hat{\sigma}^T, \hat{s}_\nu^k]\\ &-\frac{i}{\hbar^2}\sum_{k\mu\nu\nu'} a_{\mu\nu}(\vartheta)\,a_{-\mu\nu'}(\vartheta)\int\limits_0^t d\tau\exp(i\mu\omega_1\tau + i\nu'\Omega_1\tau)\\ &\times\left\{\Big[\langle\hat{F}_{-\mu}^*(\tau)\,\hat{F}_\mu^*(0)\rangle_{\rho'} \mp \sum_l A_l^2\langle\hat{I}_{-\mu}^{l*}(\tau)\,\hat{I}_\mu^{l*}(0)\rangle_{\sigma'}\Big][\hat{s}_\nu\hat{s}_{\nu'}\hat{\sigma}^T\right.\\ &-\hat{s}_{\nu'}\hat{\sigma}^T\hat{s}_\nu] + \Big[\langle\hat{F}_\mu^*(0)\,\hat{F}_{-\mu}^*(\tau)\rangle_{\rho'}\\ &\left.\mp\sum_l A_l^2\langle\hat{I}_\mu^{l*}(0)\,\hat{I}_{-\mu}^{l*}(\tau)\rangle_{\sigma'}\Big][\hat{\sigma}^T\hat{s}_{\nu'}\hat{s}_\nu - \hat{s}_\nu\hat{\sigma}^T s_{\nu'}]\right\}.\end{aligned} \tag{24}$$

Here $<\ >_{\sigma'}$ and $<\ >_{\rho'}$ denote averages over σ' and ρ', while

$$\begin{aligned}\hat{I}^{*T}(t) &= \exp\left\{i\frac{\hat{\mathscr{H}}_0^T}{\hbar}t\right\}\hat{I}\exp\left\{-i\frac{\hat{\mathscr{H}}_0^T}{\hbar}t\right\},\\ \hat{F}^{*T}(t) &= \exp\left\{i\frac{\hat{\mathscr{H}}_F}{\hbar}t\right\}\hat{F}\exp\left\{-i\frac{\hat{\mathscr{H}}_F}{\hbar}t\right\}\end{aligned} \tag{25}$$

are the operators for the nuclear spin and for the "lattice" in the interaction representation.

In order to obtain the equations of motion for the magnetization of the spin system we multiply (24) on the left by $\boldsymbol{\mu}_S \cdot \mathbf{s}$ and sum over the states of the electron system. As a result of this we obtain

$$\begin{aligned}\frac{d}{dt}\langle\hat{\mathbf{M}}^T\rangle = &\frac{i}{\hbar}\langle[\hat{\mathbf{M}}^T, \hat{\mathscr{H}}_0^T]\rangle - \frac{i}{\hbar}\sum_\nu a_{0\nu}(\vartheta)(\Phi_0 \mp \Psi_0)\langle[\hat{\mathbf{M}}^T, \hat{s}_\nu]\rangle\\ &-\sum_{\mu\nu\nu'} a_{\mu\nu}(\vartheta)\,a_{-\mu\nu'}(\vartheta)\{(\Phi_{\mu\nu'} \mp \Psi_{-\mu\nu'})\langle[\hat{\mathbf{M}}^T, \hat{s}_\nu]s_{\nu'}\rangle\\ &-(\Phi_{\mu\nu'} \mp \Psi_{\mu\nu'})\langle\hat{s}_{\nu'}[\hat{\mathbf{M}}^T, \hat{s}_\nu]\rangle\}.\end{aligned} \tag{26}$$

Here we have introduced the notation

$$\begin{aligned}&\frac{1}{\hbar^2}\int\limits_0^t d\tau\exp(i\mu\omega_s\tau + i\nu'\Omega_s\tau)\left\langle\hat{F}_{\mp\mu}^*\begin{pmatrix}\tau\\0\end{pmatrix}\hat{F}_{\pm\mu}^*\begin{pmatrix}0\\\tau\end{pmatrix}\right\rangle\\ &\qquad\equiv\Phi_{\mp\mu\nu'}(t),\\ &\frac{1}{\hbar}\langle\hat{F}_0^*(0)\rangle\equiv\Phi_0;\end{aligned} \tag{27}$$

$$\sum_l a_l^2 \int_0^t d\tau \exp(i\mu\omega_s\tau + i\nu'\Omega_s\tau)\left\langle \hat I^{l*}_{\mp\mu}\binom{\tau}{0}\hat I^{l*}_{\pm\mu}\binom{0}{\tau}\right\rangle_{\sigma'}$$

$$\equiv \Psi_{\mp\mu\nu'}(t), \qquad \sum a_l\left\langle \hat I^{l*}_0(0)\right\rangle \equiv \Psi_0. \tag{28}$$

where $a_l = A_l/\hbar$. The functions $\Phi_{\mu\nu}$ determine the nature of the relaxation processes due to the interaction of the electron spins with the lattice, and, in general, with one another. The expressions for these functions agree with those introduced in Tomita's paper.[5]

The functions $\Psi_{\mu\nu}$ are characteristic for the problem under consideration. They are due to the hyperfine interaction and lead to "inhomogeneous" broadening of the electron line. As will be seen from the following discussion, they depend in an essential manner on the resonance conditions for the system of nuclear spins.

In order to obtain the final form of the functions $\Psi_{\mu\nu}$ it is necessary to evaluate the average values appearing in (28). As we have already mentioned, $I^{l*}_{-\mu}(\tau)$ — the operator for the nuclear spin in the interaction representation — is the solution of the equation

$$i\hbar\, d\hat I^{l*}/dt = [\hat I^{l*}\mathscr{H}^*_{\text{int}}]. \tag{29}$$

$\mathscr{H}^*_{\text{int}}$ contains all the interactions within the nuclear system which we do not introduce explicitly. In order to utilize in subsequent calculations the representation in which $\mathscr{H}_{0\,\text{nucl}}$ (the Zeeman energy of the nuclei) is diagonal, it is necessary, just as in the case of the electron system, to go over to the system of coordinates in which we can speak of an equilibrium ensemble. This is the system of coordinates rotating about the effective field

$$H^l_{eff} = [\{(H_0 \pm a_l s_0) - \omega_I/\gamma^l_I\}^2 + h^{l2}]^{1/2} \tag{30}$$

with frequency ω_I. The field H^l_{eff} is inclined to the z axis at an angle θ_l determined by the expressions

$$\cos\theta_l = [(H_0 \pm a_l s_0) - \omega_I/\gamma^l_I]/H^l_{eff}, \quad \sin\theta_l = h^l/H^l_{eff}. \tag{31}$$

In this case the old operators will be expressed in terms of the new ones in the following manner:

$$\hat I^{l*}_\mu(\tau) = \sum_\lambda a_{\mu\lambda}(\theta_l)\, e^{i\mu\omega_I\tau}\hat I^{l*}_\lambda(\tau). \tag{32}$$

The matrix $a_{\mu\lambda}(\theta_l)$ is of the same form as (15). On taking (32) into account we obtain

$$\left\langle \hat I^{l*}_{-\mu}(\tau)\hat I^{l*}_\mu(0)\right\rangle = \sum_{\lambda\lambda'} a_{-\mu\lambda}(\theta_l)\, a_{\mu\lambda'}(\theta_l)\, e^{i\mu\omega_I\tau}\left\langle \hat I^{l*}_\lambda(\tau)\hat I^{l}_{\lambda'}(0)\right\rangle$$

$$= \sum_{\lambda\lambda'} a_{-\mu\lambda}(\theta_l)\, a_{\mu\lambda}(\theta_l)\exp(i\lambda\Omega_I\tau + i\mu\omega_I\tau)\left\langle \hat I^l_\lambda \hat I^l_{\lambda'}\right\rangle.$$

However,

$$\left\langle \hat I^l_\lambda \hat I^l_{\lambda'}\right\rangle = \exp(-\hbar\Omega_I/kT)\left\langle \hat I^l_{\lambda'}\hat I^l_\lambda\right\rangle, \tag{33}$$

and, therefore, we have

$$\Psi_{-\mu\nu'} = \Psi_{\mu\nu'}. \tag{34}$$

Thus, we have

$$\Psi_{\mu\nu}(t) = \sum_l\sum_{\lambda\lambda'} a_l^2\int_0^t d\tau\exp(-i\nu\Omega_s\tau + i\mu\omega_s\tau$$

$$+ i\mu\omega_I\tau)\, a_{-\mu\lambda}(\theta_l)\, a_{\mu\lambda'}(\theta_l)\left\langle \hat I^{l*}_\lambda(\tau)\hat I^{l*}_{\lambda'}(0)\right\rangle. \tag{35}$$

It may be seen from (35) that for $\mu \neq 0$ these functions vanish, since they contain a factor oscillating rapidly with frequency ω_S. On taking into account the fact that

$$\left\langle \hat I_x \hat I_z\right\rangle = \left\langle \hat I_y \hat I_z\right\rangle = \left\langle \hat I_x \hat I_y\right\rangle = 0,$$

we obtain for $\Psi_{0\nu}$ the expression

$$\Psi_{0\nu} = \sum_l a_l^2\int_0^t d\tau e^{-i\nu\Omega_s\tau}\left\{\cos^2\theta_l\left\langle \hat I^*_0(\tau)\hat I^*_0(0)\right\rangle\right.$$

$$\left. + \sin^2\theta_l\left\langle \hat I^{l*}_x(\tau)\hat I^{l*}_x(0)\right\rangle\right\}. \tag{36}$$

The quantity $\langle\hat I^{l*}_x(\tau)\hat I^{l*}_x(0)\rangle$ is the usual relaxation function for the nuclear system introduced in the linear theory of Kubo and Tomita.[7] On substituting in place of $\hat I^{l*}_x(\tau)$ the solution of (29) up to quantities of the second order in $\mathscr{H}^*_{\text{int}}\tau/\hbar$, we obtain:

$$\left\langle \hat I^{l*}_x(\tau)\hat I^{l*}_x(0)\right\rangle = \frac{1}{2}\left\langle \hat I^l_x \hat I^l_x\right\rangle\{\exp(-i\Omega_I - \Phi_l)\tau$$

$$+ \exp(i\Omega_I - \Phi_l)\tau\}. \tag{37}$$

The parameter Φ_l has the meaning of an inverse relaxation time determined by the interactions within the nuclear system. For t greater than the time of occurrence of the relaxation processes in the electron system the value of the integral (27) will not be altered if t is allowed to go to infinity, while

$$\Psi_{0,\pm1} = \sum_l \frac{a_l^2}{3}\frac{\Phi_l I^l(I^l+1)}{\Omega_s^2}\sin^2\theta_l$$

$$\pm i\sum_l \frac{a_l^2}{3}\frac{I^l(I^l+1)}{\Omega_s} = \Psi' + i\Psi''. \tag{38}$$

Formula (38) has been obtained in the approximation $(\Omega_I/\Omega_S)^2 \ll 1$, which holds practically always.

On utilizing (34), and on taking into account the fact[5] that

$$\Phi_{\mu\nu'} = \exp(-\hbar\Omega_F/KT)\,\Phi_{-\mu\nu'}, \tag{39}$$

we obtain in the approximation linear with respect to $\hbar\Omega_F/kT$ the desired equation of motion for the magnetization of the electron system:

$$\frac{d}{dt}\left\langle \hat{\mathbf{M}}^{T}\right\rangle = \frac{i}{\hbar}\left\langle [\hat{\mathbf{M}}^{T},\ \mathscr{H}_0^{T}]\right\rangle - i\sum_{\nu} a_{0\nu}(\vartheta)(\Phi_0$$

$$\mp \Psi_0)\left\langle [\hat{\mathbf{M}}^{T},\ \hat{s}_{\nu}]\right\rangle - \sum_{\mu\nu\nu'} a_{\mu\nu}(\vartheta)\, a_{-\mu\nu'}(\vartheta)\Big\{(\Phi_{-\mu\nu'}$$

$$\mp \Psi_{-\mu\nu'})\left\langle \Big[[\hat{\mathbf{M}}^{T}\,\hat{s}_{\nu}]\,\hat{s}_{\nu'}\Big]\right\}$$

$$+ \sum_{\mu\nu\nu'} a_{\mu\nu}(\vartheta)\, a_{-\mu\nu'}(\vartheta)\frac{\hbar\Omega_P}{kT}\,\Phi_{-\mu\nu'}\left\langle \hat{s}_{\nu'}[\hat{\mathbf{M}}^{T},\ \hat{s}_{\nu}]\right\rangle. \qquad (40)$$

If the hyperfine interaction is absent then equations (40) agree with the equations obtained by Tomita.[5] As was shown in that paper, in the case of a rapidly fluctuating lattice they reduce to equations of the Bloch type.

4. COMPLEX SUSCEPTIBILITY OF THE ELECTRON SYSTEM

As the nuclear system approaches resonance, a change in the absorption of energy from the microwave field by the electrons occurs which is described by the system of equations (40). In experiments this change is observed under the condition of resonance of the electron system $\omega_S = |\gamma_S|\,H_0$. In this case after simple but awkward operations of commutation and summation Eqs. (40) assume the form

$$\frac{d}{dt}\begin{bmatrix} M_x^T \\ M_y^T \\ M_z^T \end{bmatrix} + \begin{bmatrix} \Phi_x \mp \Psi' & 0 & 0 \\ 0 & \Phi_y \mp \Psi' & -\gamma_s h^s \\ 0 & \gamma_s h^s & \Phi_z \end{bmatrix}\begin{bmatrix} M_x^T \\ M_y^T \\ M_z^T \end{bmatrix}$$

$$= \chi_0 \begin{bmatrix} \Phi_x h^s \\ 0 \\ \Phi_z H_0 \end{bmatrix}, \qquad (41)$$

where $\chi_0 = \mu_S^2\, s(s+1)/3kT$ is the static electron susceptibility. In the derivation of (41) we have neglected second-order perturbation-theory terms which lead to shifts of the resonance frequency.

In the case under consideration[5] $\Phi_x = \Phi_y$. On introducing the notation

$$\Phi_x = \Phi_y = 1/T_2, \qquad \Phi_z = 1/T_1, \qquad \Psi' = 1/T', \qquad (42)$$

we obtain

$$\frac{dM_x^T}{dt} + \left(\frac{1}{T_2} \mp \frac{1}{T'}\right) M_x^T = \chi_0\,\frac{h^s}{T_2},$$

$$\frac{dM_y^T}{dt} + \left(\frac{1}{T_2} \mp \frac{1}{T'}\right) M_y^T - \gamma_s\, h^s M_z^T = 0, \qquad (43)$$

$$\frac{dM_z^T}{dt} + \gamma_s\, h^s\, M_y^T + \frac{M_z^T}{T_1} = \chi_0\,\frac{H_0}{T_1}.$$

Equations (43) differ from the Bloch equations in the rotating coordinate system under the conditions of resonance by terms containing T′. The expressions for T_1 and T_2 determine the usual longitudinal and transverse-relaxation times, and have been evaluated by Tomita.[5] The time T′ is due to the presence of the hyperfine interaction.

In the stationary state ($\dot{M}_X^T = \dot{M}_Y^T = \dot{M}_Z^T = 0$) we have

$$M_x^T = \chi_s' h^s, \quad M_y^T = \chi_s'' h^s, \quad M_z^T = \chi_0 H_0 Z_s^{\mp}, \qquad (44)$$

where

$$\chi_s' = \chi_0/(1 \mp T_2/T') \qquad (45)$$

is the real, and

$$\chi_s'' = \chi_0 T_2 \gamma_s H_0/(1 + (\gamma_s h^s)^2 T_1 T_2 \mp T_2/T') \qquad (46)$$

is the imaginary part of the complex susceptibility of the electron system, and

$$Z_s^{\mp} = \left\{1 + T_1 T_2 (\gamma_s h^s)^2/(1 \mp T_2/T')\right\}^{-1} \qquad (47)$$

is the saturation factor. The minus sign corresponds to the transitions between the sublevels of the hyperfine structure corresponding to $m_S = 1/2$, while the plus sign corresponds to the transitions with $m_S = -1/2$ (cf. diagram). In accordance with (30), (31), (38) we have

$$\frac{1}{T'} = \frac{1}{3}\sum_{l} a_l^2\,\frac{I^l(I^l+1)}{T_2^l}\,\frac{(\gamma_l^l h^l)^2}{(\gamma_s h^s)^2}\,\frac{1}{[(\gamma_s H_0 \pm a_l s_0) - \omega_l]^2 + \gamma_l'^2 h'^2}, \qquad (48)$$

where $1/T_2^l = \Phi^l$ is the transverse relaxation time for the nuclear system.

The expression for $1/T'$ has a resonance character, and attains a maximum when the frequency of the radio frequency field

$$\omega_I = |\gamma_I|\,H_0 \pm a_l s_0 \qquad (49)$$

corresponds to the interaction energy of the uncompensated electron with one of the neighboring nuclei (I^l). The number of maxima and the distances between them are determined by the specific configuration of the system.

Thus, as the frequency ω_I is varied the saturation parameters $Z_S^{\mp}$ will vary in a resonance fashion, diminishing (plus), or increasing (minus) the signal. By observing the absorption of energy from the microwave field, it is possible to find a number of maxima corresponding to the resonance values (49) of the frequency ω_I.

The variation of χ'' depends on a_l^2 and on the value of the ratio of the relaxation time of the electron system T_2 to the relaxation time of the nuclear system T_2^l. The longer is the time T_2, the more slowly will be upset the changes produced in the electron system by the hyperfine interactions.

Therefore, double resonance experiments of such a kind are carried out at low temperatures.[4]

The theory developed for $I = \frac{1}{2}$ exhibits the main features of the phenomenon observed experimentally and can be generalized to the case $I > \frac{1}{2}$.

---

[1] A. W. Overhauser, Phys. Rev. **92**, 411 (1953).

[2] G. Feher, Phys. Rev. **103**, 834 (1956).

[3] Kip, Kittel, Levi, and Portis, Phys. Rev. **91**, 1066 (1953).

[4] G. Feher, Phys. Rev. **105**, 1122 (1957).

[5] K. Tomita, Progr. Theoret. Phys. (Kyoto) **19**, 541 (1958).

[6] A. M. Portis, Phys. Rev. **91**, 1071 (1953).

[7] R. Kubo and K. Tomita, J. Phys. Soc. Japan **9**, 888 (1954).

Translated by G. Volkoff
23

SOVIET PHYSICS JETP VOLUME 13, NUMBER 1 JULY, 1961

THRESHOLD PHENOMENA IN SUPERCONDUCTORS

V. L. POKROVSKIĬ

Institute of Radiophysics and Electronics, Siberian Section, Academy of Sciences, U.S.S.R.

Submitted to JETP editor May 27, 1960

J. Exptl. Theoret. Phys. (U.S.S.R.) 40, 143-151 (January, 1961)

Decay thresholds of elementary excitations are established for superconductors at absolute zero. It is shown that ultrasonic waves in a superconductor are not absorbed up to threshold frequency $\omega_t = 2\Delta$; at the threshold point the absorption jumps abruptly to a finite value $\sim 10^{-2}\,\omega_t$. Processes of sound emission and electron-hole pair production are considered. The relative role of these processes is clarified for various electron energies.

PHENOMENA of decay of elementary excitations in a superconductor have a number of peculiarities that distinguish them from similar phenomena in a normal metal. The presence of decay thresholds is especially characteristic for superconductors.

In the normal metal, phonons of suitably low frequencies can decompose into an electron-hole pair; an electron (hole) on the Fermi surface can produce a phonon, since the Fermi velocity v_F is much larger than the sound velocity c. Finally, the electron (hole) on the Fermi surface can eject a pair from the Fermi sphere

All these phenomena become possible in a superconductor only at certain threshold values of the energies of the elementary excitations. This is connected with the existence of a gap Δ in the energy spectrum of the electrons. Obviously, the decay of a phonon into an electron-hole pair is possible only for phonons with energies $\omega > 2\Delta$; the creation of an electron pair is possible for electrons with energies $\epsilon > 3\Delta$. Finally, the electron on the Fermi surface cannot excite a phonon, since the velocity of the electrons on the Fermi surface is equal to zero in a superconductor. Therefore, there exists an electron energy threshold for this phenomenon also. This threshold is very close to the origin of the spectrum (at a distance of the order $c^2\Delta/v_F^2$).

From the experimental viewpoint, the phonon decay threshold $\omega_t = 2\Delta$ is clearly of most interest, i.e., the threshold frequency of ultrasonic absorption ($\omega_t \sim 10^{10} - 10^{11}\ \mathrm{sec}^{-1}$), below which absorption vanishes at the temperature of absolute zero.

The purpose of the present research is the study of the decay phenomena mentioned, close to threshold.* The successive determination of the spectrum of the elementary excitations in the superconductor should be based on the solutions of the Dyson equations, to which we now proceed. We shall give a representation of these equations in a somewhat different form from that of Éliashberg,[1] which is, however, equivalent to it. Our representation appears to us to be more convenient.

1. THE DYSON EQUATIONS

As a starting point, we shall make use of Froelich's Hamiltonian in the form in which it was written in the research of Migdal,[2] and also the Green's function D for the phonon, introduced in the same paper [see Eqs. (1), (3) in reference 2]. The electrons in the superconductor are characterized by two functions:

$$G_{\alpha\beta}(\mathbf{p}, t - t') = i\langle T a_{\alpha\mathbf{p}}(t)\, a^{+}_{\beta\mathbf{p}}(t')\rangle, \tag{1}$$

$$F_{\alpha\beta}(\mathbf{p}, t - t') = \langle N + 2 \,|\, T a_{\alpha\mathbf{p}}(t)\, a_{\beta,-\mathbf{p}}(t') \,|\, N\rangle\, e^{2\mu t}. \tag{2}$$

(Here < > denotes averaging over the ground state of the system, |N> is the ground state of a system composed of N particles.) The function $F_{\alpha\beta}(\mathbf{p}, t - t')$ describes the formation of a condensed pair of two electrons or the decay of the pair into two holes.

We shall seek the functions G and F in the momentum representation. The set of Dyson equations for the functions G, F, D has the form

---

*In a recently published work,[1] Éliashberg considered the interaction of electrons and phonons in a superconductor. Threshold phenomena were not noted, since he identified the Green's function of the phonon with that obtained by Migdal[2] for the normal conductor, and relied on an inexact theorem on the adiabatic properties of the Green's functions for electrons.

$$G(P) = G_0(P) + G_0(P)\Sigma_1(P)G(P) - G_0(P)\Sigma_2(P)F(P), \tag{3}$$

$$F(P) = G_0(-P + 2\mu)\Sigma_1(-P + 2\mu)F(P) + G_0(-P + 2\mu)\Sigma_2(P)G(P), \tag{4}$$

$$D(Q) = D_2(Q) + D_0(Q)\Pi(Q)D(Q), \tag{5}$$

$$\Sigma_1(P) = \frac{1}{i(2\pi)^4}\int D(Q)[G(P-Q)\Gamma_1(P, Q) + F(P-Q)\Gamma_2(P, Q)]\,d^4Q \tag{6}$$

$$\Sigma_2(P) = \frac{1}{i(2\pi)^4}\int D(Q)[F(P-Q)\Gamma_1(P, Q) - G(P-Q)\Gamma_2(P, Q)]\,d^4Q, \tag{7}$$

$$\Pi(Q) = -\frac{1}{i(2\pi)^4}\int\{[G(P)G(P-Q) - F(P)F(P-Q)]\Gamma_1(P, Q) + G(P)[F(P-Q) + F(P+Q)]\Gamma_2(P,Q)\}\,d^4p. \tag{8}$$

The letters P and Q denote 4-vectors with components $P = (\mathbf{p}, \eta)$, $Q = (\mathbf{q}, \omega)$; $p = |\mathbf{p}|$, $q = |\mathbf{q}|$; μ denotes a 4-vector whose only non-zero component coincides with the chemical potential of the system, $\mu\,[\mu = (0, 0, 0, \mu)]$.

The system (3) – (8) is similar to that introduced by Belyaev[3] for a gas of interacting Bose particles below the condensation point. The functions $G_0(P)$, $D_0(Q)$ are given by the formulas

$$G_0(P) = \frac{1}{\xi_p - \eta - i\delta\theta(\xi_p)}, \quad \xi_p = \frac{p^2}{2} - \mu, \quad \eta = \varepsilon - \mu, \tag{9}$$

$$D_0(Q) = \frac{\lambda_0\pi^2}{p_0}\,\omega_q\left(\frac{1}{\omega_q - \omega - i\delta} + \frac{1}{\omega_q + \omega - i\delta}\right), \quad \omega_q = cq. \tag{10}$$

Equations cannot be written down for the vertex parts $\Gamma_1(P, Q)$, $\Gamma_2(P, Q)$. The procedure for their construction is completely analogous to the usual, but some pairs of vertices are joined not by the usual lines which represent the function G, but by lines with oppositely directed ends, which represent the function F. At each vertex, one electron line must enter, and the other must leave.

The quantities G, F, Σ_i, Γ_i are matrices over the spin indices. By virtue of the isotropy of space, $G_{\alpha\beta}$ has the form

$$G_{\alpha\beta}(p, \eta) = \delta_{\alpha\beta}G(p, \eta). \tag{11}$$

By the law of conservation of the projection of the spin, the diagonal elements of the matrix $\hat{F}$ are equal to zero. Also, from the isotropy of space, the other two elements are either equal or are opposite in sign. To decide on one of these possibilities, we note that it follows from (2) that

$$F_{\alpha\beta}(p, \eta) = -F_{\beta\alpha}(p, -\eta).$$

This equality yields $F_{\alpha\beta}(p, 0) = F_{\beta\alpha}(p, 0)$ for $\eta = 0$, whence we derive the result (from continuity) that the matrix $\hat{F}$ has the form:

$$\hat{F}(p, \eta) = \hat{\sigma}_2 F(p, \eta), \tag{12}$$

where $\hat{\sigma}_2$ is the Pauli matrix.

Equations (3) – (7) show that Σ_1 and Γ_1 have the same matrix structure as G, while Σ_2 and Γ_2 are similar to F.

2. THE WEAK-COUPLING APPROXIMATION

The theory of Bogolyubov[4] corresponds to the assumption $\lambda_0 \ll 1$. Setting $\Gamma_1 = 1$ and $\Gamma_2 = 0$ in the lowest approximation, and replacing D and G by D_0 and G_0 in Eqs. (6) and (7), we get the equations of weak coupling:

$$G(P) = \overline{G}_0(P) - \overline{G}_0(P)\Sigma_2(P)F(P), \quad F(P) = \overline{G}_0(-P + 2\mu)\Sigma_2(P)G(P); \tag{13}$$

$$\overline{G}_0(P) = G_0(P)(1 + G_0(P)\Sigma_1(P))^{-1}. \tag{14}$$

It is not difficult to see that $\overline{G_0}(P)$ differs from $G_0(P)$ by the small renormalization of the velocity v_F on the Fermi surface and of the chemical potential μ. We shall assume these quantities to be renormalized and shall omit the bar in $\overline{G_0}$ in what follows.

The solution of the system (13) has the form

$$G(P) = \frac{\xi_p + \eta}{\varepsilon_p^2 - \eta^2 - i\delta} = \frac{u_p^2}{\varepsilon_p - \eta - i\delta} - \frac{v_p^2}{\varepsilon_p + \eta - i\delta}, \tag{15}$$

$$F(P) = \frac{\Sigma_2(P)}{(\varepsilon_p - \eta - i\delta)(\varepsilon_p + \eta - i\delta)}, \tag{16}$$

$$\varepsilon_p^2 = \xi_p^2 + \Sigma_2^2(P), \quad u_p^2 = \tfrac{1}{2}(1 + \xi_p/\varepsilon_p), \quad v_p^2 = \tfrac{1}{2}(1 - \xi_p/\varepsilon_p). \tag{17}$$

Equations (15) and (16) represent a generalization of the formulas of Gor'kov[5] to the case of electron-phonon interaction.

For $\Sigma_2(P)$ we have the equation

$$\Sigma_2(P) = \frac{2\lambda_0\pi^2}{i(2\pi)^4 p_0}\int\frac{\Sigma_2(P-Q)}{\varepsilon_{p-q}^2 - (\eta - \omega)^2 - i\delta}\,\frac{\omega_q^2}{\omega_q^2 - \omega^2 - i\delta}\,d^4Q. \tag{18}$$

In the integral of (18), as we shall establish below, the values of $|\mathbf{p} - \mathbf{q}|$ close to p_0 will play a role; more precisely, $|\mathbf{p} - \mathbf{q}| - p_0 \sim \Delta/p_0$, where $\Delta = \Sigma_2(p_0, \mu)$. We can therefore assume $\Sigma_2(p, \epsilon)$ to be independent of the spatial momentum p, and replace $\Sigma_2(p, \epsilon)$ by $C(\eta) = \Sigma_2(p_0, \mu + \eta)$.

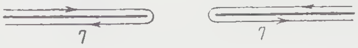

FIG. 1

We transform to the variables $\epsilon_{p-q} = \epsilon'$, $\omega_q = \omega'$, and extend the integral over ϵ' to infinity. We get

$$C(\eta) = \frac{\lambda_0 \pi^2}{2i(2\pi)^3 \omega_0^2} \int_0^{\omega_0} \omega'^2 d\omega' \int_{-\infty}^{\infty} d\omega C(\eta-\omega) \Big(\frac{1}{\omega' - \omega - i\delta}$$

$$+ \frac{1}{\omega' + \omega - i\delta} \Big) \int_L \varepsilon' d\varepsilon' / \sqrt{\varepsilon'^2 - C^2(\eta-\omega)}\, (\varepsilon' - \eta$$

$$+ \omega - i\delta)(\varepsilon' + \eta - \omega - i\delta), \tag{19}$$

where the integration over ϵ' runs along the contour L enclosing two cuts from $\pm C(\eta - i\omega)$ to $\pm\infty$, as is shown in Fig. 1. The integral along the contour L can be replaced by the difference in the residues at the corresponding poles $\epsilon' = \pm(\eta - \omega) - i\delta$ if $(\eta - \omega)^2 > \Delta^2$, or by zero if $(\eta - \omega)^2 < \Delta^2$. We thus obtain

$$C(\eta) = \frac{\lambda_0}{8\omega_0^2} \int_0^{\omega_0} \omega'^2 d\omega' \int_\Delta^\infty \frac{C(\varepsilon')}{\sqrt{\varepsilon'^2 - C^2(\varepsilon')}} \Big(\frac{1}{\omega + \varepsilon' + \eta}$$

$$+ \frac{1}{\omega - \varepsilon' + \eta} \Big). \tag{20}$$

Here we have omitted $i\delta$ in the denominator, since it is not difficult to show that the imaginary part of Σ_2 is small in comparison with the real.

At small $\eta \lesssim \Delta$, Eq. (20) is identical with Bogolyubov's equation for $C(\eta)$ and qualitatively gives the same results for $\eta \gg \Delta$. The reasons for some divergence of Eq. (20) from Bogolyubov's equation were given by Éliashberg[1] and we shall not consider them here.

We now proceed to the calculation of successive approximations in the weak coupling theory. We shall be interested in decay processes of elementary excitations near the threshold. As Pitaevskiĭ[6] has pointed out, the damping, both in the case of weak and in the case of strong coupling, is determined by diagrams which correspond to the decay process under examination, wherein the distance to threshold appears as a really small parameter. The results of weak and strong coupling theories can be distinguished only when the spectrum close to threshold in the weak coupling theory splits up (in the analogous case in strong coupling theory, the threshold is the end point of the spectrum). Further results show that there is no splitting of the spectrum in a superconductor. Therefore, our results, which we obtained in the weak coupling case, also remain valid for strong coupling, if we assume $\lambda_0 \sim 1$ and replace the velocity v_F, the chemical potential μ and the value of the gap Δ by the renormalized values.

Moreover, these results will correctly describe the damping of quasi-particles far from the threshold if the electronic energy ξ is less than or of the order of the Debye energy ω_0. This is related to the fact that the damping of phonons in the strong coupling case is determined by the process of decay into a pair, while the damping of the electrons in the given energy region is determined either by radiation of phonons or by pair creation.[2]

3. ULTRASONIC DAMPING

Kinematically, the decay of a phonon with wave vector q into an electron-hole pair is possible with satisfaction of the equality

$$\omega_q = \varepsilon_p + \varepsilon_{p-q}. \tag{21}$$

Eq. (21) can be satisfied only starting with $\omega_q = 2\Delta$, which also determines the decay threshold.

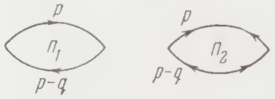

FIG. 2

For calculation of the damping associated with phonon-pair decay, we must take into account the contribution to the polarization operator of the phonon $\Pi(q, \omega)$ from the diagrams of Fig. 2.

$$\Pi(q, \omega) = \Pi_1 + \Pi_2, \tag{22}$$

$$\Pi_1(q, \omega) = \frac{i}{(2\pi)^4} \int d^4p \Big[\frac{u_p^2}{\varepsilon_p - \eta - i\delta} - \frac{v_p^2}{\varepsilon_p + \eta - i\delta} \Big]$$

$$\times \Big[\frac{u_{\mathbf{p-q}}^2}{\varepsilon_{\mathbf{p-q}} - \eta + \omega - i\delta} - \frac{v_{\mathbf{p-q}}^2}{\varepsilon_{\mathbf{p-q}} + \eta - \omega - i\delta} \Big], \tag{23}$$

$$\Pi_2(q, \omega) = \frac{\Delta^2}{i(2\pi)^4} \int d^4p \, [(\varepsilon_p - \eta - i\delta)(\varepsilon_p + \eta - i\delta)$$

$$\times (\varepsilon_{\mathbf{p-q}} - \eta + \omega - i\delta)(\varepsilon_{\mathbf{p-q}} + \eta - \omega - i\delta)]^{-1}. \tag{24}$$

Integrating over η and carrying out the substitution $\xi_p = \xi$, $\xi_{p-q} = \xi_1$, we get

$$\Pi_1(q, \omega) = \frac{1}{(2\pi)^2 q} \int_{-\infty}^{\infty} d\xi \int_{\xi - p_0 q}^{\xi + p_0 q} d\xi_1 \Big(\frac{u_\xi^2 v_{\xi_1}^2}{\varepsilon_\xi + \varepsilon_{\xi_1} - \omega - i\delta}$$

$$+ \frac{v_\xi^2 u_{\xi_1}^2}{\varepsilon_\xi + \varepsilon_{\xi_1} + \omega - i\delta} \Big), \tag{25}$$

$$\Pi_2(q, \omega) = \frac{\Delta^2}{4(2\pi)^2 q} \int_{-\infty}^{\infty} d\xi \int_{\xi - p_0 q}^{\xi + p_0 q} d\xi_1 \frac{1}{\varepsilon_\xi \varepsilon_{\xi_1}} \Big(\frac{1}{\varepsilon_\xi + \varepsilon_{\xi_1} - \omega - i\delta}$$

$$+ \frac{1}{\varepsilon_\xi + \varepsilon_{\xi_1} + \omega - i\delta} \Big). \tag{26}$$

In Eqs. (25) and (26), the integration over ξ_1 can be extended to $\pm\infty$ since $p_0 q \gg \omega_q$ in all cases, and just ξ, $\xi_1 \sim \omega_q$, appear in the essential region of integration in the calculation of $\operatorname{Im} \Pi(q, \omega)$. Taking this into account, we transform to the variables $\epsilon = \epsilon_\xi$, $\epsilon_1 = \epsilon_{\xi_1}$ and obtain*

$$\operatorname{Im} \Pi_1(q, \omega) = \frac{\pi}{(2\pi)^2 q} \int_\Delta^\infty d\varepsilon \int_\Delta^\infty d\varepsilon_1 \frac{\varepsilon \varepsilon_1 \delta(\varepsilon + \varepsilon_1 - |\omega|)}{\sqrt{(\varepsilon^2 - \Delta^2)(\varepsilon_1^2 - \Delta^2)}} \tag{27}$$

---

*We neglect the weak dependence of $C(\eta)$ on η.

$$\operatorname{Im}\Pi_2(q,\ \omega)=\frac{\pi}{(2\pi)^2 q}\int\limits_{\Delta}^{\infty}d\varepsilon\int\limits_{\Delta}^{\infty}d\varepsilon_1\,\frac{\Delta^2\delta(\varepsilon+\varepsilon_1-|\omega|)}{\sqrt{(\varepsilon^2-\Delta^2)(\varepsilon_1^2-\Delta^2)}}\,. \qquad (28)$$

Then

$$\operatorname{Im}\Pi(q,\ \omega)=\frac{\pi}{(2\pi)^2 q}\int\limits_{\Delta}^{\infty}d\varepsilon\int\limits_{\Delta}^{\infty}d\varepsilon_1\,\frac{(\varepsilon\varepsilon_1+\Delta^2)}{\sqrt{(\varepsilon^2-\Delta^2)(\varepsilon_1^2-\Delta^2)}}$$

$$\times\,\delta(\varepsilon+\varepsilon_1-|\omega|). \qquad (29)$$

It is easy to establish from (29) that $\operatorname{Im}\Pi=0$ for $\omega<2\Delta$. We shall consider the behavior of $\operatorname{Im}\Pi(q,\omega)$ in two limiting cases. First, let $\omega=2\Delta(1+\alpha/2)$ (for $\alpha\ll1$). We have

$$\operatorname{Im}\Pi=\frac{\pi}{(2\pi)^2 q}\int\limits_{\Delta}^{\Delta(1+\alpha)}\frac{d\varepsilon\,(\varepsilon\varepsilon_1+\Delta^2)}{\sqrt{(\varepsilon^2-\Delta^2)(\varepsilon_1^2-\Delta^2)}}, \qquad (30)$$

where $\epsilon_1=|\omega|-\epsilon$. Making the substitution $\epsilon=\Delta(1+\eta)$ in (30), we obtain

$$\operatorname{Im}\Pi=\frac{\pi\Delta}{(2\pi)^2 q}\int\limits_{0}^{\alpha}\frac{d\eta}{\sqrt{\eta(\alpha-\eta)}}=\frac{\Delta}{4q}. \qquad (31)$$

The ultrasonic damping is determined by the equation

$$D_0^{-1}-\Pi=0 \qquad (32)$$

and has near threshold the form

$$\operatorname{Im}\omega_q=-\frac{\lambda_0\pi^2}{4}\frac{\Delta}{p_0 q}\omega_q=-\frac{\lambda_0\pi^2}{4}\frac{\Delta}{\sqrt{M}}. \qquad (33)$$

Equation (33) shows that the damping at threshold increases abruptly from zero to a finite quantity. For $\omega_q=2\Delta$, the ratio $(\operatorname{Im}\omega_q)/\omega_q$ has a value $\sim1/\sqrt{M}\sim10^{-2}$.

In the discussion above, there was a certain lack of rigor. One can show that $\operatorname{Re}\Pi$ near the threshold $\omega=2\Delta$ has a logarithmic singularity of the form

$$(\Delta/4q)\ln[(2\Delta-\omega)/\omega_0],$$

and, strictly speaking, there is no discontinuity in the damping at threshold. However, the region in which the logarithmic term in $\operatorname{Re}\Pi$ [in the solution of Eq. (32)] is appreciable is very small:

$$|\omega-\omega_0|\sim\omega_0\exp(-A/\lambda_0\sqrt{M}),$$

where A is a quantity of the order of unity. Clearly, the physical smearing of the jump in the damping in such a region is completely imperceptible.

In the other limiting case $\omega\gg2\Delta$, we can set $\Delta=0$ in (30), from which we easily obtain

$$\operatorname{Im}\Pi(q,\ \omega)=|\omega|/4\pi q. \qquad (34)$$

This result is identical with the result of Migdal [see Eq. (12) of reference 2].

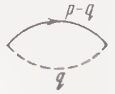

FIG. 3

4. PHONON EMISSION BY AN ELECTRON

The conservation laws in this process yield

$$\varepsilon_p=\varepsilon_{\mathbf{p}-\mathbf{q}}+\omega_q. \qquad (35)$$

In a superconductor, the velocity of the electron is zero on the Fermi surface. Therefore emission of a phonon is possible only if we start with the value of the momentum $p_1=p_0+(\Delta/p_0)(c/v_F)$ for which the velocity of the electron becomes equal to the velocity of sound. In this case, Eq. (35) can for the first time be satisfied.

We find the damping of the electron excitations corresponding to this process by calculating the contribution to the "self energy" of the electron $\Sigma_1(p,\eta)$ (Fig. 3):

$$\Sigma_1(p,\ \eta)=\frac{1}{i(2\pi)^4}\int G_0(P-Q)\,D_0(Q)\,d^4Q. \qquad (36)$$

Calculation of the integral (36) leads to the result:

$$\operatorname{Im}\Sigma_1(p,\ \eta)=\frac{\lambda_0\pi}{4pp_0}\int\limits_{0}^{q_m}q\omega_q dq\int\limits_{\xi_{|\mathbf{p}-\mathbf{q}|}}^{\xi_{\mathbf{p}+\mathbf{q}}}\delta(\varepsilon_{\xi_1}+\omega_q-|\eta|)\,d\xi_1. \qquad (37)$$

If we substitute $\eta=\epsilon_p$ in (37), it is then evident that the argument of the δ function can vanish only if $d\epsilon/dp\geq d\omega/dq=c$. The value of $\eta=\eta_0\approx\Delta(1+c^2/2v_F^2)$ is the threshold of the process. It is not difficult to transform (3) to the form

$$\operatorname{Im}\Sigma_1(p,\ \eta)=\frac{\lambda_0\pi}{4pp_0}\sigma(\eta-\eta_0)\int\limits_{\eta_0}^{\eta}\frac{\varepsilon(\eta-\varepsilon)^2}{(\varepsilon^2-\Delta^2)^{1/2}}\,d\varepsilon$$

$$=\frac{\lambda_0\pi}{4pp_0}\sigma(\eta-\eta_0)\int\limits_{0}^{q_\eta}\frac{q\omega_q\varepsilon_q dq}{(\varepsilon_q^2-\Delta^2)^{1/2}}. \qquad (38)$$

We consider the behavior of $\operatorname{Im}\Sigma_1(p,\eta)$ in three cases.

1) $\eta=\eta_0(1+\alpha)$, $\alpha\ll c^2/v_F^2\sim1/M$. Calculation of the integral (38) gives

$$\operatorname{Im}\Sigma_1(p_0,\ \eta)=\frac{\lambda_0\pi}{12\sqrt{2}}\left(\frac{\Delta}{\omega_0}\right)^2\Delta\alpha^3. \qquad (39)$$

2) $\eta=\eta_0(1+\alpha)$, $1/M\ll\alpha\ll1$,

$$\operatorname{Im}\Sigma_1(p_0,\ \eta)=\frac{\lambda_0\pi}{10\sqrt{2}}\left(\frac{\Delta}{\omega_0}\right)^2\Delta\alpha^{5/2}. \qquad (40)$$

The latter result is identical, with accuracy up to a numerical factor of the order of unity, with the result of Éliashberg [see reference 1, Eq. (30)].

3) For $\eta\gg\Delta$, Eq. (38) goes over into the corresponding equation for the normal metal.

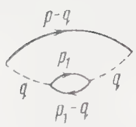

FIG. 4

5. CREATION OF AN ELECTRON-HOLE PAIR BY AN ELECTRON

The threshold of this process is obviously $\eta = 3\Delta$. By the conservation law applicable to the given case,

$$\varepsilon_p = \varepsilon_{\mathbf{p-q}} + \varepsilon_{p_1} + \varepsilon_{p_1-\mathbf{q}}. \tag{41}$$

The contribution to $\Sigma_1(\mathrm{p}, \eta)$ corresponding to this process is given by the diagram of Fig. 4:

$$\Sigma_1(p, \eta) = \frac{\lambda_0^2}{4ip_0^2}\int d^4Q\left(\frac{\omega_q^2}{\omega_q^2 - \omega^2 - i\delta}\right)^2 \Pi(q, \omega)$$

$$\times\left(\frac{u_{\mathbf{p-q}}^2}{\varepsilon_{\mathbf{p-q}} - \eta + \omega - i\delta} - \frac{v_{\mathbf{p-q}}^2}{\varepsilon_{\mathbf{p-q}} + \eta - \omega - i\delta}\right), \tag{42}$$

where $\Pi(\mathrm{q}, \omega)$ is determined by Eqs. (22), (23), and (24). It is clear from (41) that in pair creation all four energies should be of the same order of magnitude. Therefore, the values $\omega \sim \eta$ are important in the integral in (42). If $\eta \ll \omega_0$, then $\omega \ll \omega_\mathrm{q}$. By virtue of (42), for $\eta \ll \omega_0$, we can transform to

$$\Sigma_1(p, \eta) = \frac{\lambda_0^2}{4ip_0^2}\int d^4Q\Pi(q, \omega)\left(\frac{u_{\mathbf{p-q}}^2}{\varepsilon_{\mathbf{p-q}} - \eta - \omega - i\delta}\right.$$

$$\left.- \frac{v_{\mathbf{p-q}}^2}{\varepsilon_{\mathbf{p-q}} + \eta - \omega - i\delta}\right). \tag{43}$$

We change to the variables $\epsilon = \epsilon_{\mathrm{p-q}}$ and extend the integration over ϵ to the interval (Δ, ∞). The integration over ϵ is completed without difficulty, and yields

$$\int_\Delta^\infty\left(\frac{1}{\varepsilon - \tilde{\eta} - i\delta} - \frac{1}{\varepsilon + \tilde{\eta} - i\delta}\right)\frac{\varepsilon d\varepsilon}{(\varepsilon^2 - \Delta^2)^{1/2}}$$

$$= i\pi\int_\Delta^\infty [\delta(\varepsilon - \tilde{\eta}) - \delta(\varepsilon + \tilde{\eta})]\frac{\varepsilon\, d\varepsilon}{(\varepsilon^2 - \Delta^2)^{1/2}}, \tag{44}$$

where $\tilde{\eta} = \eta - \omega$. We have carried out the integration over ϵ to the end here, in order to give a smoother form to the result. Substituting (44) in (43), we get

$$\operatorname{Im}\Sigma_1(p, \eta) = \frac{\pi\lambda_0^2}{2pp_0^2}\int_{-\infty}^{\infty} d\omega \int_0^{q_m} qdq \operatorname{Im}\Pi(q, \omega)$$

$$\times\int_\Delta^\infty [\delta(\eta - \omega - \varepsilon) - \delta(\eta + \omega + \varepsilon)]\frac{\varepsilon d\varepsilon}{(\varepsilon^2 - \Delta^2)^{1/2}}. \tag{45}$$

Here we have made use of the parity of $\Pi(\mathrm{q}, \omega)$ relative to ω.

Now let $\eta > 0$. Making use of Eq. (29) for Im Π, we get from (45)

$$\operatorname{Im}\Sigma_1(p, \eta) = \frac{\lambda_0^2}{2}\frac{q_m}{4\pi pp_0^2}\int_\Delta^\infty d\varepsilon_1\int_\Delta^\infty d\varepsilon_2$$

$$\times\int_\Delta^\infty d\varepsilon_3\frac{(\varepsilon_1\varepsilon_2 + \Delta^2)\,\varepsilon_3}{[(\varepsilon_1^2 - \Delta^2)(\varepsilon_2^2 - \Delta^2)(\varepsilon_3^2 - \Delta^2)]^{1/2}}\delta(\eta - \varepsilon_1 - \varepsilon_2 - \varepsilon_3). \tag{46}$$

Near threshold, we have $\eta = 3\Delta\ (1 + \alpha/3)$, $\epsilon_\mathrm{i} = \Delta\ (1 + \eta_\mathrm{i})$, $(\alpha, \eta_\mathrm{i} \ll 1)$, and Eq. (46) gives

$$\operatorname{Im}\Sigma_1(p_0, \eta) = \frac{\lambda_0}{16\pi\sqrt{2}}\frac{q_m\Delta^2}{p_0^3}\int_0^\alpha d\eta_1$$

$$\times\int_0^{\alpha-\eta_1}\frac{(\eta_1 + \eta_2)\,d\eta_2}{[\eta_1\eta_2(\alpha - \eta_1 - \eta_2)]^{1/2}} = \frac{\lambda_0^2}{12\sqrt{2}}\frac{q_m}{p_0}\frac{\Delta}{p_0^2}\Delta\alpha^{3/2}. \tag{47}$$

For $\alpha \sim 1$, $\operatorname{Im}\Sigma_1 \sim \lambda_0^2\Delta^2/\mathrm{p}_0^2$. Comparing (47) with (40), we get the ratio of the frequency of emission of the phonons ν_1 to the frequency of pair creation ν_2: $\nu_1/\nu_2 = (\Delta/\omega_0)(\mathrm{p}^2/\omega_0)$ (we assume $\lambda_0 \sim 1$ here). Under real conditions, $\Delta/\omega_0 \sim \omega_0/\mathrm{p}_0^2 \sim 10^{-2}$. Therefore, the contribution to the damping made by the pair creation process increases rapidly beyond threshold to a value exceeding the damping due to phonon emission.

If $\eta \gg \Delta$, we must set $\Delta = 0$ in the integral (46), whence

$$\operatorname{Im}\Sigma_1(p_0, \eta) \sim (\lambda_0^2/M)\,\omega_0\,(\eta/\omega_0)^2. \tag{48}$$

This value becomes (for $\lambda_0 \sim 1$) of the same order as the damping due to phonon emission ($\operatorname{Im}\Sigma_1 \sim (\lambda_0/\sqrt{\mathrm{M}})\,\omega_0\,(\eta/\omega_0)^3$) for $\eta/\omega_0 \sim \mathrm{M}^{-1/2}$. Equation (48) is identical with Eq. (31) of Migdal's research, with accuracy up to a numerical factor.[2]

Thus, for energies η lying in the range $(\Delta, 3\Delta)$, the electrons radiate sound. In the interval $(3\Delta, \omega_0^2/\mathrm{p}_0^2)$ the decay of the electron is principally in the form of pair creation. Finally, in the range $(\omega_0^2/\mathrm{p}_0^2, \omega_0)$, phonon emission plays the principal role.

The author is grateful to A. P. Kazantsev for a number of valuable comments.

---

[1] G. M. Eliashberg, JETP **38**, 966 (1960), Soviet Phys. JETP **11**, 696 (1960).

[2] A. B. Migdal, JETP **34**, 1438 (1958), Soviet Phys. JETP **7**, 996 (1958).

[3] S. T. Belyaev, JETP **34**, 417 (1958), Soviet Phys. JETP **7**, 289 (1958).

[4] N. N. Bogolyubov, JETP **34**, 58 (1958), Soviet Phys. JETP **7**, 41 (1958).

[5] L. P. Gor'kov, JETP **34**, 735 (1958), Soviet Phys. JETP **7**, 505 (1958).

[6] L. P. Pitaevskiĭ, JETP **36**, 1168 (1959), Soviet Phys. JETP **9**, 830 (1959).

[7] V. L. Pokrovskiĭ and A. M. Dykhne, JETP **39**, 720 (1960), Soviet Phys. JETP **12**, 503 (1961).

Translated by R. T. Beyer
24

SOVIET PHYSICS JETP VOLUME 13, NUMBER 1 JULY, 1961

CALCULATION OF THE ENERGY CHANGE IN A SYSTEM OF ELECTRONS IN A LATTICE WHEN DEFECTS ARE FORMED

V. I. OSHEROV

L. Ya. Karpov Physico-Chemical Institute

Submitted to JETP editor June 24, 1960

J. Exptl. Theoret. Phys. (U.S.S.R.) 40, 152-155 (January, 1961)

A system of non-interacting electrons in a lattice is considered. In the single-band approximation the changes of energy and thermal capacity of this system when defects are formed are calculated.

In the theory of local perturbations in crystals the most important problems are, on the one hand, finding the discrete levels and the scattering problem,[1,2] and, on the other hand, the calculation of the changes in the various thermodynamic quantities. The latter problem was first posed and solved in the general case by I. Lifshitz[3] (see also references 4 and 5).

We consider the change of the electronic energy of a crystal when defects are formed. This problem is of particular interest in connection with the possibility of thus finding the contribution to the electronic thermal capacity of the crystal made by lattice defects. We use the one-electron approximation, and neglect electron interactions. We write the Schrödinger equation for the wave function of an electron in an ideal lattice as

$$H_0\psi_{\mathbf{k}} = \varepsilon_{\mathbf{k}}\psi_{\mathbf{k}}; \tag{1}$$

H_0 includes the kinetic energy and the periodic potential averaged over the lattice, $\psi_{\mathbf{k}}$ is a Bloch function. We limit the spectrum of $\epsilon_{\mathbf{k}}$ to one band.

For a lattice with a defect we have

$$(H_0 + V)\,\varphi_{\mathbf{k}} = \varepsilon'_{\mathbf{k}}\varphi_{\mathbf{k}}. \tag{2}$$

Here V is the perturbing potential localized about the same point $\mathbf{r}_0$; $\epsilon'_{\mathbf{k}}$ and $\varphi_{\mathbf{k}}$ are the perturbed eigenvalues and eigenfunctions.

Our problem consists in calculating the energy change of the electron system ΔE, which, using the invariance of the trace of operators, we will write in the form

$$\Delta E = \mathrm{Sp}\,\{\Omega\,(H_0 + V) - \Omega\,(H_0)\}, \tag{3}$$

$$\Omega\,(\varepsilon) = -kT\ln\left(1 + e^{(\mu-\varepsilon)/kT}\right), \tag{4}$$

where μ is the chemical potential, T is the temperature, k is Boltzmann's constant. If P_ϵ and $P_{\epsilon'}$ (the projection operators into the states $\psi_{\mathbf{k}}$ and $\varphi_{\mathbf{k}}$) are introduced, then

$$\Delta E = \int \mathrm{Sp}\,(P_\varepsilon - P'_\varepsilon)\,\Omega'\,(\varepsilon)\,d\varepsilon. \tag{5}$$

The trace of the difference of projection operators has been calculated in the case of a degenerate regular perturbation by I. Lifshitz.[3] We use for the perturbation operator the first order approximation. With this aim we expand $\psi_{\mathbf{k}}$, normalized to a δ-function, in terms of the Wannier functions $a_{\mathbf{n}}(\mathbf{r})$, localized at the lattice sites:

$$\psi_{\mathbf{k}}\,(\mathbf{r}) = (2\pi)^{-3/2}\sum_{\mathbf{n}} e^{i\mathbf{k}\mathbf{n}}a_{\mathbf{n}}\,(\mathbf{r}). \tag{6}$$

The diagonal matrix elements of V in $\psi_{\mathbf{k}}$ space, which are of interest to us in this approximation, will have the form

$$\langle\psi_{\mathbf{k}}\,|\,V\,|\,\psi_{\mathbf{k}}\rangle = (2\pi)^{-3}\sum_{\mathbf{n},\mathbf{n}'}\langle a_{\mathbf{n}}\,|\,V\,|\,a_{\mathbf{n}'}\rangle\, e^{i\mathbf{k}\,(\mathbf{n}-\mathbf{n}')}. \tag{7}$$

Limiting ourselves to the largest of all the elements $<a_{\mathbf{n}}\,|\,V\,|\,a_{\mathbf{n}'}>$

$$\alpha = (2\pi)^{-3}\alpha_0 = (2\pi)^{-3}\,\langle a_{\mathbf{n}_0}\,|\,V\,|\,a_{\mathbf{n}_0}\rangle \tag{8}$$

($\mathbf{n}_0$ is the site closest to $\mathbf{r}_0$), we obtain

$$\langle\psi_{\mathbf{k}}\,|\,V\,|\,\psi_{\mathbf{k}}\rangle = \alpha. \tag{9}$$

It is now possible to use the results of reference 3 for the case of a one-dimensional first-order perturbation. We have

$$\mathrm{Sp}\,(P_\varepsilon - P'_\varepsilon) = \frac{1}{\pi}\arg\left(1 + \int\frac{c\,(\varepsilon')}{\varepsilon' - \varepsilon - i0}\,d\varepsilon'\right),$$

$$c\,(\varepsilon) = \int\limits_{\varepsilon_{\mathbf{k}} = \varepsilon}\frac{d\omega}{|\,\nabla\varepsilon_{\mathbf{k}}\,|}. \tag{10}$$

The last integral is taken over a surface of constant energy, $d\omega$ is the element of its area.

The Stieltjes integral (5) gives

$$\Delta E = 2\,[\Omega\,(\varepsilon_0) - \Omega\,(\varepsilon_g)] + \frac{2}{\pi}\int\tan^{-1}\Big[\pi\alpha c\,(\varepsilon)\Big/\Big(1 + \alpha\mathrm{P}\int\frac{c\,(\varepsilon')}{\varepsilon' - \varepsilon}\,d\varepsilon'\Big)\Big]\,\Omega'\,(\varepsilon)\,d\varepsilon. \tag{11}$$

Here the spin degeneracy has already been taken into account, and the level of the localized state ϵ_0

is determined from the equation

$$1+\alpha\int d\varepsilon c(\varepsilon)/(\varepsilon-\varepsilon_0)=0; \tag{12}$$

ϵ_g is the upper or lower edge of the band, depending upon the sign of α.

The possibility of approximating by a one-dimensional perturbation has no rigorous foundation, but we shall establish a criterion for its approximate feasibility. To do this we note that for sufficiently small values of α (in the three-dimensional case) Eq. (12) has no solutions at all, there is no localization due to the perturbation, and, consequently, the approximation is demonstrably inapplicable.

In order to obtain a more accurate estimate we write

$$\int\limits_{\varepsilon_{\mathbf{k}}=\varepsilon} d\omega/\,|\nabla\varepsilon_{\mathbf{k}}| = \int\delta(\varepsilon_{\mathbf{k}}-\varepsilon)\,d\mathbf{k}. \tag{13}$$

It then becomes possible to introduce a new function

$$I_\varepsilon(\mathbf{n}-\mathbf{n}')=(2\pi)^{-3}\,\mathrm{P}\int d\mathbf{k}e^{i\mathbf{k}(\mathbf{n}-\mathbf{n}')}/(\varepsilon_{\mathbf{k}}-\varepsilon-i0), \tag{14}$$

which is the Green's function in the discrete space of lattice sites. We have

$$\operatorname{Re}I_\varepsilon(0)=(2\pi)^{-3}\mathrm{P}\int d\varepsilon' c(\varepsilon')/(\varepsilon'-\varepsilon),$$

$$\operatorname{Im}I_\varepsilon(0)=(2\pi)^{-2}c(\varepsilon). \tag{15}$$

If we now consider that (in the three-dimensional case) $\operatorname{Re}I_\epsilon(0)$ is continuous through the boundary of the spectrum and attains a maximum (minimum) at it, then it is possible to write down the inequality

$$1/\alpha<\mathrm{P}\int d\varepsilon' c(\varepsilon')/(\varepsilon'-\varepsilon_g). \tag{16}$$

We write $\epsilon=\epsilon^0+\beta f(\mathbf{k})$, where $\mathbf{k}$ is the quasi-momentum, and β determines the energy width of the band, then

$$1/\alpha_0<\mathrm{const}/\beta. \tag{17}$$

The constant appearing here has a value of the order of unity. Thus, our approximation is most justified when

$$\alpha_0\gg\beta. \tag{18}$$

We now turn to a study of the contribution of a small number of defects η to the electronic heat capacity at low temperatures. As is easily verified, the localized electrons give an exponentially small contribution and can, therefore, be ignored. For the energy change we find in the usual way[6]

$$\Delta E=\Delta E_0+\frac{\pi}{3}\eta(kT)^2\Phi'(\varepsilon_F),\ \Phi(\varepsilon)=\tan^{-1}\frac{\alpha_0\operatorname{Im}I_\varepsilon(0)}{1+\alpha_0\operatorname{Re}I_\varepsilon(0)}. \tag{19}$$

Here ϵ_F is the Fermi energy, ΔE_0 is the energy change at $T = 0$:

$$\Delta E_0=2(\varepsilon_0-\varepsilon_g)+\frac{2}{\pi}\int^{\varepsilon_F}\tan^{-1}\frac{\alpha_0\operatorname{Im}I_\varepsilon(0)}{1+\alpha_0\operatorname{Re}I_\varepsilon(0)}\,d\varepsilon. \tag{20}$$

It must be pointed out that, in fact, in the nature of the problem, the integrals in (15) are taken over the unperturbed spectrum, but the integral in (20) over the perturbed. This becomes of particular importance near to the edges of the unperturbed spectrum, where it is not permissible to expand in terms of β/α_0 (see reference 7). In addition the relationships obtained are only valid when the band is not too full, because otherwise it is impossible to use the procedure of extending the integrals over ϵ from the distribution function to infinity. We do not consider here the complicated processes when there is a gap between two bands.

Thus we have, for the contribution to the heat capacity,

$$\Delta c=\tfrac{2}{3}(\pi k)^2\alpha_0\eta T$$

$$\times\frac{[\operatorname{Im}I_\varepsilon(0)]'+\alpha_0\{[\operatorname{Im}I_\varepsilon(0)]'\operatorname{Re}I_\varepsilon(0)-[\operatorname{Re}I_\varepsilon(0)]'\operatorname{Im}I_\varepsilon(0)\}}{[\alpha_0\operatorname{Im}I_\varepsilon(0)]^2+[1+\alpha_0\operatorname{Re}I_\varepsilon(0)]^2} \tag{21}$$

We note that $\operatorname{Im}I_\epsilon(0)$ and $\operatorname{Re}I_\epsilon(0)$ possess characteristic singularities in their first derivatives at the boundary of the unperturbed spectrum.

When the inequality (18) is satisfied, the quantity Δc ceases to depend on the perturbation, and we obtain

$$\Delta c=\tfrac{2}{3}(\pi k)^2\eta T\Phi_0(\varepsilon_F),$$

$$\Phi_0(\varepsilon)=\{[\operatorname{Im}I_\varepsilon(0)]'\operatorname{Re}I_\varepsilon(0)-[\operatorname{Re}I_\varepsilon(0)]'\operatorname{Im}I_\varepsilon(0)\}/|I_\varepsilon(0)|^2 \tag{22}$$

In the other limiting case ($\beta\gg\alpha_0$), provided the first order approximation remains applicable (for example, with modified α_0^*), we find

$$\Delta c=\tfrac{2}{3}(\pi k)^2\alpha_0^*\eta\,[\operatorname{Im}I_{\varepsilon_F}(0)]'\,T. \tag{23}$$

These two possibilities are realized, apparently, in dielectrics and metals.

The author takes the opportunity to express his gratitude to Prof. I. M. Lifshitz for a number of valuable discussions.

---

[1] I. M. Lifshitz, JETP **17**, 1017 (1947).
[2] I. M. Lifshitz, JETP **17**, 1076 (1947).
[3] I. M. Lifshitz, Usp. Mat. Nauk **7**, 171 (1952).
[4] M. G. Kreĭn, Matem. Sbornik **33**, 597 (1953).
[5] I. M. Lifshitz, Nuovo cimento **3**, Suppl. 4, 716 (1956).
[6] L. D. Landau and E. M. Lifshitz, Статистическая физика (Statistical Physics), Gostekhizdat (1951).
[7] I. M. Lifshitz and G. I. Stepanova, JETP **30**, 938 (1956), Soviet Phys. JETP **3**, 656 (1956).

Translated by K. F. Hulme
25

SOVIET PHYSICS JETP VOLUME 13, NUMBER 1 JULY, 1961

ON THE AZIMUTHAL ANGULAR DISTRIBUTION OF SHOWER PARTICLES

V. M. CHUDAKOV

Physico-Technical Institute, Academy of Sciences, Uzbek S.S.R.

Submitted to JETP editor June 27, 1960

J. Exptl. Theoret. Phys. (U.S.S.R.) **40**, 156-162 (January, 1961)

It is shown that the χ^2 criterion can be employed to investigate the azimuthal angular distribution of a small number of shower particles. The azimuthal angular distribution of secondary particles in jets produced in photographic emulsions by cosmic-ray particles is analyzed by the proposed method. It is concluded that peripheral collisions of high-energy nucleons play an important role.

A possible consequence of the two-center model of multiple particle production in collisions of fast nucleons is the azimuthal anisotropy of secondary particles. If the excited center has a large intrinsic moment of momentum, then the emitted mesons have a tendency to be coplanar.[1,2] In addition, because of the deflection of the emitting centers from the direction of the primary particles,[3,4] an asymmetry can arise in the azimuthal angular distribution of the particles of the diffuse and narrow cones observed in the laboratory frame of reference (l system). Koba and Takagi[2] believe that the detection of an azimuthal asymmetry of shower particles exceeding the limits of simple statistical fluctuations would make the two-center model a very plausible one. The problem is all the more important since the distribution over the angle θ (the angle with the direction of the primary particle) characteristic of the two-center model is often of the order of natural statistical fluctuations.[5]

The azimuthal angular distribution of fast particles produced in the collisions of nucleons with complex nuclei was studied using the Pearson criterion.[6] However, the existence of azimuthal anisotropy has not been proved. It should be noted that the use of the Pearson criterion is mathematically sound only for a sufficiently large number of shower particles n_s,[7] not less than 10 m, where m is the number of equal intervals into which we divide the azimuthal angle φ. It is shown below that it is possible to use the χ^2 criterion to detect the azimuthal anisotropy of secondary particles in the case of small n_s if the small number of particles in each shower can be compensated for by a large number of showers.

In the study of the particle angular distribution, the total azimuthal angle 2π is divided into m equal intervals $\Delta\varphi$, and the number of particles n_k is calculated in each interval $(\sum_{k=1}^{m} n_k = n_s)$.[6] As is well known, the quantity

$$\chi_m^2 = \frac{m}{n_s} \sum_{k=1}^{m} \left(n_k - \frac{n_s}{m}\right)^2 = \frac{m}{n_s} \sum_{k=1}^{m} n_k^2 - n_s \qquad (1)$$

has a χ^2 distribution with m − 1 degrees of freedom, if n_s is large, under the assumptions of azimuthal isotropy of shower particles and the statistical independence of their angles of emission φ_i in separate showers with a given n_s. Let us estimate the mathematical expectation and the dispersion of this quantity for an arbitrary n_s. We ascribe to each azimuthal angle of the i-th particle φ_i m random values φ_{ik} (i = 1, 2, ..., n_s; k = 1, 2, ..., m) satisfying the conditions

$$\varphi_{ik} = 1, \qquad (2)$$

if φ_i lies within the k-th among the m equal intervals $\Delta\varphi$, and

$$\varphi_{ik} = 0, \qquad (3)$$

if φ_i does not lie inside this interval. For such a definition of φ_{ik}, we have

$$n_k = \sum_{i=1}^{n_s} \varphi_{ik}. \qquad (4)$$

Taking the statistical independence of the angles φ_i into account, it is easy to find the mathematical expectation of the normalized value $\alpha_m = \chi_m^2/(m-1)$:

$$M(\alpha_m) = 1 + \frac{m}{m-1}(n_s - 1) \sum_{k=1}^{m} \left(p_k - \frac{1}{m}\right)^2, \qquad (5)$$

where p_k is the probability that a particle falls within the k-th interval $\Delta\varphi$, which fully determines the distribution of φ_{ik}. If the azimuthal angular distribution is isotropic, $p_k = 1/m$ and

$$M(\alpha_m) = 1. \tag{6}$$

The calculation of the dispersion α_m is rather tedious. Omitting the calculation, we shall present the final result corresponding to the assumption of azimuthal isotropy of shower particles and statistical independence of their angles φ_i:

$$D(\alpha_m) = \frac{2}{m-1} - \frac{1}{n_s}\frac{2}{m-1}. \tag{7}$$

The fact that the value of the dispersion is finite makes it possible to find the critical limit for the quantity α_m averaged over n showers

$$\bar{\alpha}_m = \frac{1}{n}\sum_{i=1}^{n} \alpha_{mi}, \tag{8}$$

The probability that this limit is exceeded is very small. Denoting the probability of the corresponding event by P, we can write the Chebyshev inequality from Eqs. (6) and (7) as

$$P(|\bar{\alpha}_m - 1| \geqslant t\sqrt{\bar{D}_m}/\sqrt{n}) \leqslant 1/t^2,$$
$$\bar{D}_m = \frac{2}{m-1} - \left(\frac{1}{n_s}\right)_{\text{av}} \frac{2}{m-1}, \tag{9}$$

where t is an arbitrary positive parameter. The more accurate Chebyshev inequality[8] makes it possible to state that*

$$P(\bar{\alpha}_m - 1 \geqslant t\sqrt{\bar{D}_m}/\sqrt{n}) < \exp(-t^2/4), \tag{10}$$

if

$$0 < t \leqslant 3\sqrt{\bar{D}_m}\sqrt{n}/[(n_s)_{max} - 1]. \tag{11}$$

The Chebyshev inequality clearly results in a considerably greater value than the critical limit $\bar{\alpha}_m$. In order to lower the estimate, we can use the Lyapunov theorem, whose limits of applicability are satisfied for a set of showers with a finite number of particles n_s, e.g., for showers with energy smaller than a certain maximum value. Since, for a sufficiently large number of such showers, the distribution of the quantity $\bar{\alpha}_m$ can be regarded as normal, we can, for instance, claim from Eqs. (6) and (7) that

$$P(\bar{\alpha}_m - 1 > t\sqrt{\bar{D}_m}/\sqrt{n}) \approx (2\pi)^{-1/2}\int_t^{\infty} \exp(-x^2/2)\,dx. \tag{12}$$

For t ~ 2.5, the right-hand side of Eq. (12) is already less than 0.01.

By means of the χ^2 criterion, we can study the azimuthal angular distribution of shower particles on the whole, independent of the angle θ with the direction of the primary particle. In order to obtain information about the azimuthal asymmetry of the particles travelling at different angles θ, we can use the quantity introduced in reference 9

$$\alpha = n_s \tan^2\theta_0 (\overline{\cos\theta})^2 / \overline{\sin^2\theta}$$
$$= 1 + \sum_{i \neq j} \sin\theta_i \sin\theta_j \cos(\varphi_i - \varphi_j) \Big/ \sum_{i=1}^{n_s} \sin^2\theta_i;$$
$$\overline{\cos\theta} = \sum_{i=1}^{n_s} \cos\theta_i / n_s, \qquad \overline{\sin^2\theta} = \sum_{i=1}^{n_s} \sin^2\theta_i / n_s, \tag{13}$$

where θ_i is the angle of emission of the i-th particle with respect to the direction of the primary particle in the l system, φ_i is its azimuthal angle, and θ_0 is the angle between the direction of the primary particle and the shower axis going through the center of gravity of the points of intersection of the secondary charged-particle tracks with a sphere of unit radius whose center coincides with the shower vertex.* By means of this quantity, we can solve the problem concerning the deflection of the excited centers from the direction of the primary particles in peripheral interactions of fast nucleons, since such a deflection leads to an increase in θ_0.

Let $f(\theta_1, \varphi_1, \theta_2, \varphi_2, \ldots, \theta_{n_s}, \varphi_{n_s})$ be the probability density of a multi-dimensional distribution. Assuming the azimuthal isotropy of the angular distribution of each particle for an arbitrary θ and for a fixed direction of the remaining $n_s - 1$ particles, the mathematical expectations of the quantity α and its dispersion are, respectively, given by

$$M(\alpha) = \int \alpha f(\theta_1, \varphi_1, \theta_2, \varphi_2, \ldots, \theta_{n_s}, \varphi_{n_s}) \prod_{i=1}^{n_s} d\theta_i\, d\varphi_i$$
$$= \int \alpha f_1(\theta_1, \theta_2, \ldots, \theta_{n_s}) \prod_{i=1}^{n_s} d\theta_i\, d\varphi_i / 2\pi = 1, \tag{14}$$

$$D(\alpha) = \int \Big[\sum_{i \neq j} \sin\theta_i \sin\theta_j \cos(\varphi_i - \varphi_j) \Big/ \sum_{i=1}^{n_s} \sin^2\theta_i\Big]^2$$
$$\times f_1(\theta_1, \ldots, \theta_{n_s}) \prod_{i=1}^{n_s} d\theta_i d\varphi_i/2\pi$$
$$= M[1 - \overline{\sin^4\theta}/n_s(\overline{\sin^2\theta})^2] < 1. \tag{15}$$

Hence, it follows that the substitution

$$\bar{D}_m = 1 \tag{16}$$

leaves the inequality (9) valid for the quantity

$$\bar{\alpha} = \frac{1}{n}\sum_{i=1}^{n} \alpha_i, \tag{17}$$

while the equality (12) becomes an inequality.

---

*Since the quantities α_m, similar to the quantities α and α', considered below, are finite, we have $0 \leqslant \alpha_m \leqslant n_s$.

*The factor $n_s(\overline{\cos\theta})^2/\overline{\sin^2\theta})$ in Eq. (13) is introduced for normalization [see Eq. (14) below].

In a general case, where

$$f(\theta_1, \varphi_1, \theta_2, \varphi_2, \ldots, \theta_{n_s}, \varphi_{n_s}) = f_1(\theta_1, \theta_2, \ldots, \theta_{n_s}) f_2(\varphi_1) f_2(\varphi_2) \ldots f_2(\varphi_{n_s}),$$

$$\int f_2(\varphi)\, d\varphi = 1, \qquad (18)$$

the mathematical expectation α differs from unity by the quantity

$$M(\alpha) - 1 = aM\left[n_s (\overline{\sin\theta})^2 / \overline{\sin^2\theta} - 1\right] \geqslant 0,$$
$$a = [M(\cos\varphi)]^2 + [M(\sin\varphi)]^2. \qquad (19)$$

Since the values of α are finite, we have for a sufficiently large number of showers with a number of particles less than a certain maximum value,

$$\bar{\alpha} \approx M(\bar{\alpha}). \qquad (20)$$

The same properties as α are possessed by the quantity*

$$\alpha' = n_s \tan\theta_0' / \overline{\tan^2\theta} = 1 + \sum_{i \neq j} \tan\theta_i \tan\theta_j \cos(\varphi_i - \varphi_j) \Big/ \sum_{i=1}^{n_s} \tan^2\theta_i, \qquad (21)$$

where θ_0' is the angle between the direction of the primary particle and the straight line going through the vertex of the shower and the center of gravity of the points of intersection of the secondary charged-particle tracks (or their continuations) with the plane tangential to the unit radius sphere at the point of intersection of this sphere with the continuation of the primary-particle track. The experimental values α' can easily be calculated using so-called target diagrams of shower particles.

Before we analyze the experimental data by the above method, let us consider several factors which cause the mathematical expectations α_m, α, and α' to differ from unity.

1. The energy-momentum conservation law subjects the momenta of the particles and their directions to certain constraints which may affect the assumed independence of the φ_i, e.g., in the case of the existence of a particle with a much higher energy and with a very large transverse momentum.† If the transverse momenta of secondary particles are of the same order of magnitude, then, if their number is large and if neutral particles are present, the influence of the energy-momentum conservation law is evidently small. However, if the transverse momenta of nucleons are much greater than those of π mesons,[10] and two nucleons do not have the tendency to be coplanar after their collision, then, for a small (~5) number of charged mesons, the mathematical expectations α_m, α, and α' may increase.

2. As mentioned at the beginning of the article, for small deflection angles of the excited centers from the direction of the primary nucleon, an azimuthal anisotropy of the secondary particle may arise, and the mesons will concentrate in the plane containing the momenta of the primary nucleon and of the isobar. Such an anisotropy will first lead to an increase of $M(\alpha_m)$ for $m > 2$, but will not greatly affect the mean values of α_2, α, and α' since the azimuthal angular distribution remains symmetric. It should be noted that, since the primary particles are described by a plane wave, there will be no azimuthal anisotropy of shower particles in the set of the single showers which is characterized only by the same momenta of primary nucleons but for which the concept of probability has no meaning (see reference 2). The tendency of mesons to be coplanar will make itself felt as a statistical dependence of the angles φ_i of secondary particles, which tends to increase $M(\alpha_m)$. We therefore believe that it is useful to differentiate sharply between the azimuthal anisotropy and the statistical dependence of the secondary-particle angles.

3. The presence of narrowly-correlated groups of particles in their angular distribution, originating from the decay of short-lived particles or isobars, tends to increase the mathematical expectations α_m, α, and α' [see Eqs. (1), (13), and (21)]. The quantities $M(\alpha_m)$, $M(\alpha)$, and $M(\alpha')$ would be much greater than one if the fast moving "fireballs" produced in nucleon-nucleon high-energy collisions were deflected from the direction of the primary particle, and if they had an isotropic distribution of the statistically independent angles φ. If, as a result of a collision in the c.m.s., two nucleons excited in the same way and moving at large angles to the direction of the primary particles are produced, then $M(\alpha_2)$ evidently will not increase, in contrast to the other quantities discussed above which characterize the azimuthal angular distribution of shower particles.

After these remarks, we shall use the proposed method for the analysis of experimental data on the angular distribution of shower particles obtained by J. Pernegr. The values of α, α', and α_m were calculated for 52 showers produced in emulsion by singly-charged cosmic-ray particles having ≤ 5 strongly ionizing particles. The number of secondary shower particles n_s varies from 6 to 42, and the value of the Lorentz factor of the center-of-

---

*We have in mind the equality (14) and inequality (15).

†This assumption does not correspond with experimental data.

Experimental data on the azimuthal angular distribution of shower particles in 52 jets*

Group characteristics	$n_s \leqslant 12$, $\overline{n}_s = 9.3$, $n = 36$				$n_s \geqslant 14$, $\overline{n}_s = 19.5$, $n = 16$			
Azimuthal group characteristics	$\overline{\alpha}$ $(\overline{\alpha}', \overline{\alpha}_m)$	$\sigma(\overline{\alpha})$	$\frac{\lvert\overline{\alpha}-1\rvert}{\sigma(\overline{\alpha})}$	P, %	$\overline{\alpha}$ $(\overline{\alpha}', \overline{\alpha}_m)$	$\sigma(\overline{\alpha})$	$\frac{\lvert\overline{\alpha}-1\rvert}{\sigma(\overline{\alpha})}$	P, %
	1	2	3	4	5	6	7	8
α	0,94	<0.17	—	—	1.07	<0.25	—	—
α'	0,87	<0,17	—	—	1.04	<0.25	—	—
α_2	0.78	0.22	1.0	—	0.63	0.34	1,1	—
α_3	0.91	0.16	—	—	1.80	0.24	3,3	<0.1 $(\leqslant 9)$
α_4	0.80	0.13	1.6	~6	1,41	0.20	2,1	~2
α_5	0.98	0.11	—	—	1.35	0.17	2,0	~2
α_6	1,01	0,10	—	—	1,68	0.15	4.4	$<10^{-3}$ $(\leqslant 5)$
α_7	0.99	0,09	—	—	1.23	0.14	1,7	~5
α_8	0.91	0.08	1.1	—	1.37	0.13	2,9	~0,2
α_9	1.05	0.08	—	—	1.32	0,12	2.7	~0.4
α_{10}	0,98	0.07	—	—	1,45	0,11	3,9	$<10^{-2}$ $(\leqslant 7)$

*Only the values $\lvert\overline{\alpha} - 1\rvert/\sigma(\overline{\alpha}) \geqslant 1$ and of $P < 10\%$ are given.

mass system γ_c from 2.4 to 150. The values of $\overline{\alpha}$, $\overline{\alpha}'$, and $\overline{\alpha}_m$ calculated by us* for two groups of showers with small and large n_s respectively are presented in the table (columns 1 and 5). Columns 2 and 6 show the values of σ, the standard deviation of the quantities $\overline{\alpha}$, $\overline{\alpha}'$, and $\overline{\alpha}_m$ calculated assuming azimuthal isotropy of secondary particles and statistical independence of their angles φ_i. When these conditions are satisfied, the probabilities P that $\overline{\alpha}$ $(\overline{\alpha}', \overline{\alpha}_m)$ are not smaller or not greater than an observed value can also be calculated using the Lyapunov theorem. The corresponding data are shown in columns 4 and 8 of the table; in the parenthesis, the values of P obtained by means of the Chebyshev inequality are shown.

Experimental data for groups of showers with $n_s \leq 12$ agree, within the limits of error, with the assumptions on the azimuthal isotropy of shower particles and the statistical independence of their angles φ_i. However, for large n_s, the values of $\overline{\alpha}_m$ averaged over 16 showers are considerably greater than unity if $m \geq 3$. This increase in $\overline{\alpha}_m$ cannot be due to the influence of the energy-momentum conservation law, since no increase in the quantities $\overline{\alpha}$, $\overline{\alpha}'$, and $\overline{\alpha}_2$ is observed in this shower group and, in addition, such an influence should be even stronger for smaller n_s. The deviation of the excited centers from the direction of primary nucleons, if it exists at all, also does not exhibit any marked influence on the azimuthal angular distribution of secondary particles, since the values of $\overline{\alpha}$ and $\overline{\alpha}'$ are close to unity.

The experimental data of showers with $n_s \geq 14$ points towards a symmetrical but anisotropic azimuthal angular distribution of secondary particles in individual showers, and the symmetry is apparently conserved for any angle θ. The tendency of the emitted mesons to possess an azimuthal anisotropy might possibly also be observed for smaller n_s. In that case, however, the mathematical expectations α_m according to Eq. (5) cannot be great. In addition, for a small number of particles, the influence of the energy-momentum conservation law may be felt, causing a decrease of the mathematical expectations of the quantities under consideration.

The experimental data given above contradict the hydrodynamical theory of jet production in head-on collisions for a cylindrical symmetry of secondary particles, and indicate a considerable role played by peripheral collisions. The data of the table correspond to the emission of mesons mainly around the plane perpendicular to the direction of the intrinsic moment of momentum of the excited center. This fact was predicted theoretically as a consequence of the two-center model of multiple particle production in nucleon-nucleon high-energy collisions.[1,2] For its confirmation, additional statistical material is necessary.

In conclusion, the author wishes to express his gratitude to S. A. Azimov, M. I. Podgoretskiĭ, and D. S. Chernavskiĭ for helpful comments, to J. Pernegr for supplying the experimental data, and to G. M. Chernov for his help.

---

*Azimuthal angles are measured from the plane perpendicular to the emulsion plane.

[1] W. L. Kraushaar and L. J. Marks, Phys. Rev. 93, 326 (1954).

[2] Z. Koba and S. Takagi, Nuovo cimento 10, 755 (1958); Z. Koba and S. Takagi, Fortschr. Physik 7, 1 (1959).

[3] H. W. Meier, Nuovo cimento 11, 307 (1959).

[4] V. Petržilka, Nuovo cimento 13, 1300 (1959).

[5] B. A. Nikol'skiĭ and A. P. Mishakova, JETP **38**, 1507 (1960), Soviet Phys. JETP **11**, 1087 (1960).

[6] Gurevich, Mishakova, Nikol'skiĭ, and Surkova, JETP **34**, 265 (1958), Soviet Phys. JETP **7**, 185 (1958).

[7] N. V. Smirnov and I. V. Dunin-Barkovskiĭ, Краткий курс математической статистики для технических приложений (Short Course on Mathematical Statistics for Technical Applications), Fizmatgiz, 1959.

[8] S. N. Bernshteĭn, Теория вероятностей Theory of Probability, ONTI, 1934.

[9] S. A. Azimov and V. M. Chudakov, Doklady Akad. Nauk Uzbek SSR (in print).

[10] C. F. Powell, Paper presented at the Conference on High-Energy Particle Physics, Kiev, 1959.

Translated by H. Kasha
26

SOVIET PHYSICS JETP VOLUME 13, NUMBER 1 JULY, 1961

INTEGRAL EQUATIONS FOR KN SCATTERING

J. WOLF and W. ZOELLNER

Joint Institute for Nuclear Study

Submitted to JETP editor June 27, 1960

J. Exptl. Theoret. Phys. (U.S.S.R.) **40**, 163-169 (January, 1961)

Integral equations for KN and $\overline{\text{K}}$N scattering in low angular momentum states are derived in the Mandelstam representation on the basis of dispersion relations for forward and backward scattering. An approximation is used in which the equations for KN and $\overline{\text{K}}$N scattering are uncoupled. An estimate of the contribution of the $d_{3/2}$ wave is given in terms of the s- and p-wave amplitudes.

1. Starting from the Mandelstam representation for KN scattering processes, MacDowell[1] has studied the analytic properties of partial wave amplitudes. In this work we derive integral equations for the s-, p- and d-wave amplitudes for these reactions.

In contrast to the program of MacDowell,[1] and the procedure used by Chew and Mandelstam for $\pi\pi$ scattering,[2] we have made use of fixed-angle dispersion relations to derive the integral equations for the partial waves, in particular the dispersion relations for forward and backward scattering. This permits one to avoid a number of serious difficulties encountered by Chew and Mandelstam, and to the study of which a number of papers were devoted.[3,4]

In accordance with the general idea of Mandelstam we consider the following reactions:

$$\text{I. } K+N\to K'+N',$$
$$\text{II. } \overline{K}'+N\to\overline{K}+N',$$
$$\text{III. } \overline{K}'+K\to\overline{N}+N'.$$

The two-particle unitarity condition relates the amplitude for the reaction II to the amplitude for the process

$$\overline{K}+N\to Y+\pi$$

(where Y denotes a Λ or Σ hyperon), and the amplitude for the reaction III to the amplitudes for the processes

$$\overline{K}+K\to\pi+\pi,\quad \pi+\pi\to N+\overline{N}.$$

These three processes have been studied in detail[6,7] and we assume in our work that the amplitudes for these processes are known; in particular one may take into account, for example, the contribution of the pole term or make use of the experimental data as analysed by Dalitz.[8]

The invariants introduced by Mandelstam[9] are given for the reactions I, II, III by

$$\text{I.}\quad \begin{aligned} s &= M^2+m^2+2k^2+2\sqrt{(k^2+M^2)(k^2+m^2)},\\ \overline{s} &= M^2+m^2-2k^2z-2\sqrt{(k^2+M^2)(k^2+m^2)},\\ t &= -2k^2(1-z), \qquad z\equiv\cos\varphi; \end{aligned} \tag{1.1}$$

$$\text{II.}\quad \begin{aligned} s &= M^2+m^2-2\overline{k}^2\overline{z}-2\sqrt{(\overline{k}^2+M^2)(\overline{k}^2+m^2)},\\ \overline{s} &= M^2+m^2+2\overline{k}^2+2\sqrt{(\overline{k}^2+M^2)(\overline{k}^2+m^2)},\\ t &= -2\overline{k}^2(1-\overline{z}), \qquad \overline{z}\equiv\cos\overline{\varphi}; \end{aligned} \tag{1.2}$$

$$\text{III.}\quad \begin{aligned} s &= M^2-m^2-2q^2+2xpq,\\ \overline{s} &= M^2-m^2-2q^2-2xpq,\\ t &= 4(m^2+q^2)=4(M^2+p^2),\\ x &\equiv\cos\vartheta. \end{aligned} \tag{1.3}$$

Here k^2, $\overline{k}^2$, q^2 are the squares of the momentum transfer in the appropriate reaction (in the c.m.s.); M is the nucleon mass, m is the K-meson mass; φ, $\overline{\varphi}$, ϑ are the scattering angles in the corresponding reactions.

The kinematic cut due to the square root in the expressions for $s(k^2)$ and $\overline{s}(k^2)$ can be eliminated by symmetrization with respect to this square root (see Efremov et al.[5]). However, as a result of peculiarities of the kinematics of KN processes, it is possible to take into account the nearest singularities on the negative cut also without symmetrization, by introducing a cut-off at $-m_K^2\approx-13\mu^2$.

2. The matrix elements for the processes I, II, and III are expressed in the form

$$S_{fi}=\delta_{fi}+\frac{i}{(2\pi)^2}\delta(p_1+q_1-p_2-q_2)\frac{M}{\sqrt{4p_1^0p_2^0q_1^0q_2^0}}\overline{u}Tu,$$

where the function T has the structure

$$T=A+\tfrac{1}{2}\gamma(q_1+q_2)B\qquad(\gamma q=\gamma_0q_0-\boldsymbol{\gamma}\mathbf{p}).$$

The function A depends on the isotopic spin of K and N:

$$A = A^{(+)} + \tau_K \tau_N A^{(-)},$$

where $A^{(\pm)}$ are related to the amplitudes with prescribed values of the total isotopic spin of the KN system (A^0 and A^1) by:

$$\text{I.} \quad A^0 = A^{(+)} - 3A^{(-)}, \qquad A^1 = A^{(+)} + A^{(-)};$$
$$\text{II.} \quad A^0 = A^{(+)} + 3A^{(-)}, \qquad A^1 = A^{(+)} - A^{(-)};$$
$$\text{III.} \quad A^0 = A^{(+)}, \qquad A^1 = A^{(+)} + 2A^{(-)}.$$

The function B is related to $B^{(+)}$, $B^{(-)}$ and B^0, B^1 by analogous formulas.

For process I the quantity $\bar{u}Tu$ has the form

$$\bar{u}Tu = (4\pi W / M)\, \chi^+_{N'} \{f_1 + k^{-2} (\sigma q_1)(\sigma q_2) f_2\} \chi_N$$

(the formula for process II is obtained from above by the substitution $k^2 \to \bar{k}^2$, $f \to \bar{f}$), where W is the total energy. The connection between $f_{1,2}$ and A, B is given by

$$\text{I.} \quad f_1 = \alpha A + \beta B, \qquad f_2 = -\gamma A + \delta B, \tag{2.1}$$
$$\text{II.} \quad \bar{f}_1 = \alpha A - \beta B, \qquad \bar{f}_2 = -\gamma A - \delta B,$$

where

$$\alpha = (p_0 + M) / 8\pi W, \qquad \beta = (p_0 + M)(W - M) / 8\pi W,$$
$$\gamma = (p_0 - M) / 8\pi W, \qquad \delta = (p_0 - M)(W + M) / 8\pi W, \tag{2.2}$$

and p_0 is the nucleon energy.

The functions $f_{1,2}$ are connected with the partial wave amplitudes by the relations

$$f_1(k^2, z) = \Sigma \{f_{l+} P'_{l+1}(z) - f_{l-} P'_{l-1}(z)\}, \tag{2.3}$$
$$f_2(k^2, z) = \Sigma \{f_{l-} - f_{l+}\} P'_l(z).$$

Taking into account contributions from partial waves up to f_{2-} we find that ($f_{1,2}(\pm) \equiv f_{1,2}(k^2, z = \pm 1)$):

$$f_0 = \tfrac{1}{2}\{f_1(+) + f_1(-)\} + \tfrac{1}{6}\{f_2(+) - f_2(-)\},$$
$$f_{1-} = \tfrac{1}{6}\{f_1(+) - f_1(-)\} + \tfrac{1}{2}\{f_2(+) + f_2(-)\}, \tag{2.4}$$
$$f_{1+} = \tfrac{1}{6}\{f_1(+) - f_1(-)\}, \qquad f_2 = \tfrac{1}{6}\{f_2(+) - f_2(-)\}.$$

The unitarity condition for process I has the form

$$\operatorname{Im} f_{l\pm} = k\,|f_{l\pm}|^2. \tag{2.5}$$

For the reaction II we obtain

$$\operatorname{Im} \bar{f}_{l\pm} = \bar{k}\,|\bar{f}_{l\pm}|^2 + \bar{k}_Y\,|F_{l\pm}|^2, \tag{2.6}$$

where $F_{l\pm}$ are the partial amplitudes for the process $\bar{K}N \to Y\pi$. The quantity $\bar{k}_Y$ is determined by the formula

$$\bar{k}^2_Y = \tfrac{1}{4}\bar{s}^{-1}\{\bar{s} - (M_Y + \mu)^2\}\{\bar{s} - (M_Y - \mu)^2\},$$

where M_Y, μ denote respectively the hyperon and pion masses.

For the partial amplitudes for the process II we have

$$J_{++} = \frac{1}{pp_0}\sum\left(l + \frac{1}{2}\right)(pq)^l f^l_+ P_l(x),$$
$$J_{+-} = q\sum\frac{l + 1/2}{\sqrt{l(l+1)}}(pq)^{l-1} f^l_- P^{(\prime)}_l(x), \tag{2.7}$$

and exactly the same formulas hold for the reaction $\pi\pi \to N\bar{N}$.

Here J_{++} and J_{+-} are helicity states for these two processes (see Frazer and Fulco[7]), which are in the case of reaction III related to A, B by

$$J_{++} = (1 / 8\pi p^0)\{-pA + qMxB\}, \qquad J_{+-} = (q / 8\pi)\sqrt{1 - x^2}B. \tag{2.8}$$

For partial waves of reaction III the unitarity condition gives

$$\operatorname{Im} f^l_\pm = (q_\pi^{2l+1} / q^0)\, \Pi^{l*} T^l_\pm, \tag{2.9}$$

where Π^l and $T^l_\pm$ are respectively the partial amplitudes for $K\bar{K} \to \pi\pi$ and $\pi\pi \to N\bar{N}$; $q^2_\pi = q^2 + m^2 - \mu^2$.

3. The double Mandelstam representation for the function $B^{(\pm)}(s, \bar{s}, t)$ is of the form

$$B^{(\pm)}(s, \bar{s}, t) = P_\Lambda + \binom{3}{-1} P_\Sigma + \frac{1}{\pi^2}\int\limits_{(M+m)^2} ds'$$
$$\times \int\limits_{(M_\Lambda+\mu)^2} d\bar{s}' \frac{b^{(\pm)}_{12}(s', \bar{s}')}{(s' - s)(\bar{s}' - \bar{s})}$$
$$+ \frac{1}{\pi^2}\int\limits_{(M_\Lambda+\mu)^2} d\bar{s}' \int\limits_{4\mu} dt' \frac{b^{(\pm)}_{23}(\bar{s}', t')}{(\bar{s}' - \bar{s})(t' - t)}$$
$$+ \frac{1}{\pi^2}\int\limits_{4\mu^2} dt' \int\limits_{(M+m)^2} ds' \frac{b^{(\pm)}_{31}(t', s')}{(t' - t)(s' - s)}. \tag{3.1}$$

Here P_Y are the pole terms:

$$4P_Y = g^2_Y / (M^2_Y - \bar{s}).$$

The renormalized coupling constants g^2_Λ and g^2_Σ are determined as residues at the poles of the function $B(s, \bar{s}, t)$ for the second process in isotopic spin states 0 and 1 respectively.

An analogous representation holds for the function $A^{(\pm)}(s, \bar{s}, t)$ with the pole terms multiplied by $(M \pm M_Y)$; the plus sign goes with scalar, the minus sign with pseudoscalar, K mesons.

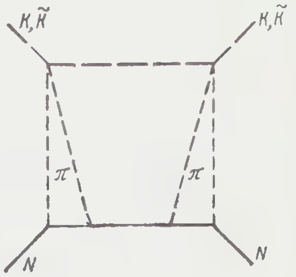

FIG. 1

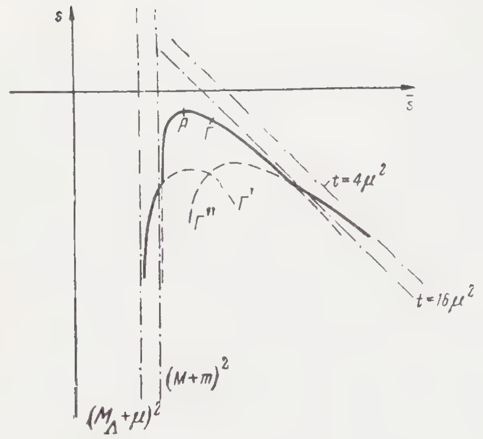

FIG. 2

The boundaries of the region in which the spectral functions fail to vanish will be calculated on the basis of considerations presented by Mandelstam.[10] The nearest singularities are given by diagrams of the type shown in Fig. 1. In the plane of the invariants they correspond to the curves shown in Fig. 2 (the point A has as coordinates $s \approx -20\,\mu^2$, $\bar{s} \approx 113\,\mu^2$, $t \approx 25\,\mu^2$). The curve Γ is symmetric under the exchange of s and $\bar{s}$. The curves Γ′, Γ″ correspond to other diagrams.

The cuts for the functions $A(k^2, z)$ and $B(k^2, z)$ for the case of process I are shown in Fig. 3. The curve P corresponds to two poles at $k^2 = k_Y^2$, at that for $z = +1$ one has $k_\Lambda^2 = -11\,\mu^2$, $k_\Sigma^2 = -12.15\,\mu^2$.

The cuts in the case of process II are shown in Fig. 4. Here P denotes poles at $\bar{k}_\Lambda^2 = -8.9\,\mu^2$ and $\bar{k}_\Sigma^2 = -7.2\,\mu^2$. The cut due to the process $\bar{K}N \to Y\pi$ starts at $-\lambda = -5.4\,\mu^2$; this cut is a consequence of the inequality $(M_Y + \mu)^2 < (M + m)^2$.

In the representation (3.1) the integration over t starts at $4\mu^2$, whereas the kinematic cut due to the root in Eqs. (1.1) and (1.2) does not start until the square of the K-meson mass is reached, so that the interval along the negative k^2 or $\bar{k}^2$ axis from $-m^2$ to $-\mu^2$ remains free of kinematic cuts. Therefore in what follows we restrict integration over negative k^2 or $\bar{k}^2$ to the interval $[-m^2, -\mu^2]$. We note that all kinematic coefficients $\alpha(k^2)$, $\beta(k^2)$, etc. remain real along this interval and do not give rise to any new singularities.

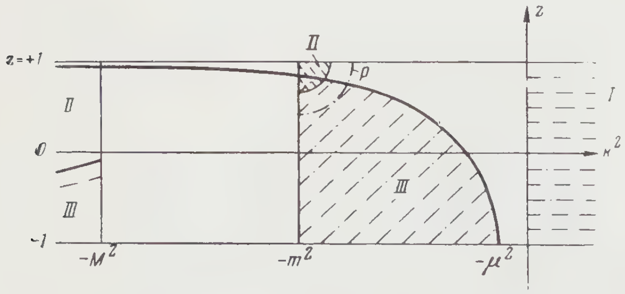

FIG. 3

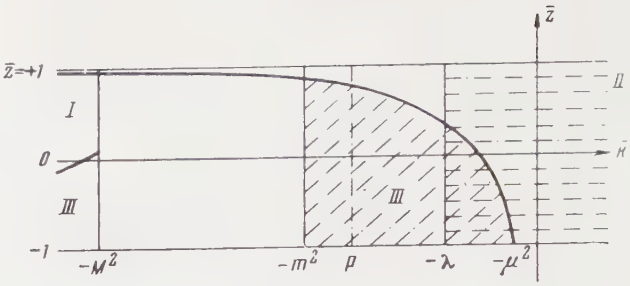

FIG. 4

In view of the analyticity properties (see Fig. 3 and 4) the Cauchy formula can be used for $A^{(\pm)}(k^2, z = \pm 1)$, $B^{(\pm)}(k^2, z = \pm 1)$ and $A^{(\pm)}(\bar{k}^2, \bar{z} = \pm 1)$, $B^{(\pm)}(\bar{k}^2, \bar{z} = \pm 1)$. As an example we write out the dispersion relation for $B^{(\pm)}(k^2, +1)$ $(k^2 \equiv \nu,\ \bar{k}^2 \equiv \bar{\nu})$:

$$B^{(\pm)}(\nu, +1) = \sum_Y B_Y^{(\pm)}(\nu) + \frac{1}{\pi}\int_0^\infty \frac{d\nu'}{\nu' - \nu}\,\mathrm{Im}\,B^{(\pm)}(\nu', +1)$$

$$+ \frac{1}{\pi}\int_{-m^2}^{\mu^2} \frac{d\nu'}{\nu' - \nu}\,\mathrm{Im}\,B^{(\pm)}(\nu', +1), \tag{3.2}$$

where

$$\sum_Y B_Y^{(\pm)}(\nu) = \frac{g_\Lambda^2}{4h(\nu_\Lambda)(\nu_\Lambda - \nu)} + \binom{3}{-1}\frac{g_\Sigma^2}{4h(\nu_\Sigma)(\nu_\Sigma - \nu)},$$

$$h(\nu) = \left|\frac{d}{d\nu}\,\bar{s}(\nu)\right|.$$

Let us note that $B^{(\pm)}(\nu, -1)$ has no pole terms, and that in the case of process II the integration along the right hand cut begins at $-\lambda$.

Introducing the abbreviations $\alpha' = \alpha(\nu')$, $\alpha_Y = \alpha(\nu_Y)$, . . . and

$$\sum A_Y^{(\pm)} = \sum_Y (M \pm M_Y)\, B_Y^{(\pm)}$$

(in what follows we shall omit the summation sign $\sum_Y$), we obtain with the help of Eqs. (3.2), (2.4), and (2.1) the equations for some of the low partial amplitudes for the process I:

$$f_0^{(\pm)}(\nu) = \frac{1}{6}(3\alpha_Y - \gamma_Y)\,A_Y^{(\pm)} + \frac{1}{6}(3\beta_Y + \delta_Y)\,B_Y^{(\pm)}$$

$$+ \frac{1}{\pi}\int_0^\infty \frac{d\nu'}{\nu' - \nu}\,\mathrm{Im}\,f_0^{(\pm)}(\nu')$$

$$+ \frac{1}{\pi}\int_{-m^2}^{-\mu^2} \frac{d\nu'}{\nu' - \nu}\left\{\frac{1}{6}(3\alpha' - \gamma')\,\mathrm{Im}\,A^{(\pm)}(\nu', +1)\right.$$

$$+ \frac{1}{6}(3\beta' + \delta')\,\mathrm{Im}\,B^{(\pm)}(\nu', +1)$$

$$+ \frac{1}{6}(3\alpha' + \gamma')\,\mathrm{Im}\,A^{(\pm)}(\nu', -1)$$

$$\left. + \frac{1}{6}(3\beta' - \delta')\,\mathrm{Im}\,B^{(\pm)}(\nu', -1)\right\}, \tag{3.3}$$

$$f_{1-}^{(\pm)}(\nu) = \frac{1}{6}(\alpha_Y - 3\gamma_Y) A_Y^{(\pm)} + \frac{1}{6}(\beta_Y + 3\delta_Y) B_Y^{(\pm)} + \frac{1}{\pi}\int_0^\infty \frac{d\nu'}{\nu' - \nu} \operatorname{Im} f_{1-}^{(\pm)}(\nu') + \frac{1}{\pi}\int_{-m^2}^{-\mu^2} \frac{d\nu'}{\nu' - \nu} \Big\{ \frac{1}{6}(\alpha' - 3\gamma') \operatorname{Im} A^{(\pm)}(\nu', +1) + \frac{1}{6}(\beta' + 3\delta') \operatorname{Im} B^{(\pm)}(\nu', +1) - \frac{1}{6}(3\gamma' + \alpha') \operatorname{Im} A^{(\pm)}(\nu', -1) + \frac{1}{6}(3\delta' - \beta') \operatorname{Im} B^{(\pm)}(\nu', -1) \Big\}, \tag{3.4}$$

$$f_{1+}^{(\pm)}(\nu) = \frac{1}{6}\alpha_Y A_Y^{(\pm)} + \frac{1}{6}\beta_Y B_Y^{(\pm)} + \frac{1}{\pi}\int_0^\infty \frac{d\nu'}{\nu' - \nu} \operatorname{Im} f_{1+}^{(\pm)}(\nu') + \frac{1}{\pi}\int_{-m^2}^{-\mu^2} \frac{d\nu'}{\nu' - \nu} \Big\{ \frac{1}{6}\alpha' \operatorname{Im} A^{(\pm)}(\nu', +1) + \frac{1}{6}\beta' \operatorname{Im} B^{(\pm)}(\nu', +1) - \frac{1}{6}\alpha' \operatorname{Im} A^{(\pm)}(\nu', -1) - \frac{1}{6}\beta' \operatorname{Im} B^{(\pm)}(\nu', -1) \Big\}, \tag{3.5}$$

$$f_{2-}^{(\pm)}(\nu) = \frac{1}{6}(-\gamma_Y A_Y^{(\pm)} + \delta_Y B_Y^{(\pm)}) + \frac{1}{\pi}\int_0^\infty \frac{d\nu'}{\nu' - \nu} \operatorname{Im} f_{2-}^{(\pm)}(\nu') + \frac{1}{\pi}\int_{-m^2}^{-\mu^2} \frac{d\nu'}{\nu' - \nu} \Big\{ -\frac{1}{6}\gamma' \operatorname{Im} A^{(\pm)}(\nu', +1) + \frac{1}{6}\delta' \operatorname{Im} B^{(\pm)}(\nu', +1) + \frac{1}{6}\gamma' \operatorname{Im} A^{(\pm)}(\nu', -1) - \frac{1}{6}\delta' \operatorname{Im} B^{(\pm)}(\nu', -1) \Big\}. \tag{3.6}$$

Here Im $f_{l\pm}$ is determined by Eq. (2.5).

In order to express the integrals over negative values of k^2 in terms of quantities referring to processes II and III we need to relate the variables of the first process to those of the second and third:

$$\bar{z}(\nu, z) = 1 - \frac{\nu}{\bar{\nu}}(1 - z),$$

$$\bar{\nu}(\nu, z) = \nu \frac{M^2 + m^2 + \nu(1 + z) + 2z\sqrt{(\nu + M^2)(\nu + m^2)}}{M^2 + m^2 - 2\nu z - 2\sqrt{(\nu + M^2)(\nu + m^2)}} \tag{3.7}$$

and

$$x(\nu, z) = -\frac{2\nu(1 + z) + 4\sqrt{(\nu + M^2)(\nu + m^2)}}{\sqrt{4M^2 + 2\nu(1 - z)}\sqrt{4m^2 + 2\nu(1 - z)}},$$

$$q^2(\nu, z) = -m^2 - \frac{\nu}{2}(1 - z). \tag{3.8}$$

Therefore

$$\operatorname{Im} B(\nu, z = +1) = \operatorname{Im} B(\bar{\nu}(\nu, +1), \bar{z} = +1), \tag{3.9a}$$

where $\operatorname{Im} B(\bar{\nu}, +1)$ is expressed in terms of the partial amplitudes $\bar{f}_{l\pm}$ with the help of Eqs. (2.1), (2.4), and (2.6). In just the same way

$$\operatorname{Im} B(\nu, z = -1) = \operatorname{Im} B(q^2(\nu, -1), x = -1) \tag{3.9b}$$

is expressed in terms of the partial amplitudes $f_\pm^l$ of the third process with the help of Eqs. (2.7), (2.8) and (2.9).

The equations for $\bar{f}_{l\pm}$ for process II are analogous. The pole contribution to the equation for $\bar{f}_0^{(\pm)}$ and $\bar{f}_{1-}^{(\pm)}$ is of the form

$$\alpha_Y A_Y^{(\pm)} - \beta_Y B_Y^{(\pm)} \tag{3.10}$$

and

$$-\gamma_Y A_Y^{(\pm)} - \delta_Y B_Y^{(\pm)}, \tag{3.11}$$

respectively; for other partial amplitudes the contribution of the pole terms vanishes. The connection between the processes gives for the negative region

$$\operatorname{Im} B(\bar{\nu}, \bar{z} = +1) = \operatorname{Im} B\{\nu(\bar{\nu}, +1), z = +1\} \tag{3.12a}$$

and

$$\operatorname{Im} B(\bar{\nu}, \bar{z} = -1) = \operatorname{Im} B\{q^2(\bar{\nu}, -1), x = -1\}. \tag{3.12b}$$

With the help of Eqs. (2.1), (2.4), and (2.5) $\operatorname{Im} B(\nu, +1)$ is expressed in terms of the partial amplitudes $f_{l\pm}$, and $\operatorname{Im} B(q^2, -1)$ in terms of $f_\pm^l$.

Since the expansion in partial waves of the imaginary part of the amplitude converges better than the corresponding expansion of the real part, we may neglect in the expressions (3.9) and (3.12) the contributions from the d waves.* In that case Eqs. (3.3) – (3.5) do not depend explicitly on the d waves. The same approximation in Eq. (3.6) gives for f_{2-} an expression which depends only on s and p waves, and so allows an estimate of the size of this amplitude.

We note that the integral equations for KN and $\overline{\text{K}}$N scattering derived by us are not coupled to each other.

The authors express their gratitude to D. V. Shirkov, A. V. Efremov and Chou Hung-Yüan for valuable discussions.

---

[1] S. W. MacDowell, Phys. Rev. **116**, 774 (1959).

[2] G. F. Chew and S. Mandelstam, Phys. Rev. **119**, 467 (1960).

[3] Efremov, Meshcheryakov, Shirkov, and Tzu, On the derivation of Equations from the Mandelstam Representation, preprint E-539 (1960), Joint Inst. Nuc. Res.

[4] Hsien Ting-Ch'ang, Ho Tso-Hsiu, and Zoellner, JETP **39**, 1668 (1960), Soviet Phys. JETP **12**, 1165 (1961).

[5] Efremov, Meshcheryakov, and Shirkov, preprint D-503 (1960), Joint Inst. Nuc. Res.

---

*The same approximation has been used previously[4] for ππ scattering.

[6] P. S. Isayev and M. V. Severinskiĭ, preprint R-550 (1960), Joint Inst. Nuc. Res.

[7] W. R. Frazer and J. R. Fulco, Phys. Rev. **117**, 1603 (1960).

[8] R. H. Dalitz and S. F. Tuan, Ann. of Phys. **8**, 100 (1959). R. H. Dalitz, Report at the Rochester Conference, Geneva (1958).

[9] S. Mandelstam, Phys. Rev. **112**, 1344 (1958).

[10] S. Mandelstam, Phys. Rev. **115**, 1752 (1959).

Translated by A. M. Bincer
27

SOVIET PHYSICS JETP VOLUME 13, NUMBER 1 JULY, 1961

EMERGENCE INTO VACUUM OF THE CERENKOV RADIATION PRODUCED FROM LONGITUDINAL WAVES IN A MEDIUM

B. L. ZHELNOV

Institute of Radio Physics and Electronics, Siberian Section of Academy of Sciences, U.S.S.R.

Submitted to JETP editor June 28, 1960

J. Exptl. Theoret. Phys. (U.S.S.R.) **40**, 170-177 (January, 1961)

The problem treated is that of the radiation from an electron that moves into vacuum from a medium with spatial dispersion. The additional boundary conditions required to take spatial dispersion into account are discussed. It is shown that under certain conditions in addition to the transition radiation there is Cerenkov radiation produced from longitudinal waves in the medium and emerging into the vacuum. For the case of small absorption in the medium the angular distribution of this radiation is determined by the law of refraction together with the condition for Cerenkov radiation in the medium. The main contribution to the transition radiation is the Cerenkov radiation from longitudinal waves, which is produced in the medium near the bounding surface (at a distance of the order of the wavelength). At large distances from the boundary this part of the Cerenkov radiation is a spherical wave and is confined to a narrow range of frequencies lying close to the plasma frequency.

1. INTRODUCTION

WHEN a fast charged particle moves in a region with spatial dispersion there is excitation of longitudinal waves (plasmons).[1,2] The resulting discrete energy loss of the particle is the Cerenkov radiation from the longitudinal waves (cf., e.g., reference 3).

The problem of the emergence of this radiation into vacuum is of undoubted interest, since the radiation has a narrow spectrum that lies near the plasma frequency $\omega_0^2 = 4\pi ne^2/m$ (n, e, and m are the density, charge, and mass of the electrons in the medium), and can be used both for the generation of radio waves (in a plasma) and also for the generation of infrared and ultraviolet rays (in a dielectric). It must be pointed out that Cerenkov radiation from transverse waves actually appears in a medium at relativistic speeds of the particle, whereas Cerenkov radiation from longitudinal waves appears at much smaller speeds. For Cerenkov radiation from longitudinal waves to occur, the speed of the particle must exceed the average thermal speed of the electrons in the medium.[1]

The following are special features of this problem: 1) the passage of a charged particle through the boundary between two media produces a transition radiation, which at large distances from the point of emergence of the particle is indistinguishable from the Cerenkov radiation[4]; 2) when spatial dispersion is taken into account there is a new solution of Maxwell's equations (longitudinal waves), which requires an additional boundary condition.[3]

Subject to a certain assumption regarding the additional boundary condition we find here the radiation fields for the passage of an electron from a medium into vacuum. As Garibyan has shown,[5,6] the transition radiation becomes actually appreciable only at ultrarelativistic speeds. At nonrelativistic particle speeds one can distinguish in the transition radiation a part of the spectrum in which the main contribution comes from the Cerenkov radiation from longitudinal waves.

2. STATEMENT OF PROBLEM AND CHOICE OF BOUNDARY CONDITIONS

Let the motion of the electron be normal to the boundary between the medium and vacuum. We shall regard the radiative energy loss of the electron as negligibly small in comparison with its kinetic energy. We take into account the effects of spatial dispersion for an isotropic medium by writing the connection between D and E in the form

$$\mathbf{D} = (\varepsilon + \delta\Delta)\,\mathbf{E}, \tag{1}$$

where D and E are the electric displacement and field strength at the point $\mathbf{r}$, $\epsilon = \epsilon_0 + i\gamma$ is the complex dielectric constant of the medium, δ is a parameter that characterizes the spatial dispersion of the medium, and Δ is the Laplacian operator. The magnetic permeability of the medium is unity. The expression (1) is equivalent to the inclusion of a term in the dielectric constant proportional to the square of the wave vector.

We shall look for the field of the moving electron in the form of the sum of a longitudinal field (φ) and a transverse field ($\mathbf{A}$) with the gauge div $\mathbf{A} = 0$. We solve the problem by the method proposed by Ginzburg and Frank[7] and developed by Garibyan.[5] For the radiation fields $\varphi'(\mathbf{k})$ and $\mathbf{A}'(\mathbf{k})$ we get as the dispersion relations* for the longitudinal waves (for $\mathbf{k} \neq 0$)

$$k_{\parallel}^2 = \varepsilon/\delta, \tag{2}$$

where $k_{\parallel}^2 = \kappa^2 + \lambda_{\parallel}^2$, κ and $\lambda_{\parallel}$ being the tangential and normal components of the wave vector, and for the transverse waves

$$k_{\perp}^2 = \omega^2 c^{-2} \varepsilon_{\perp}, \tag{3}$$

where

$$\varepsilon_{\perp} = \varepsilon/(1 + \delta\omega^2/c^2), \qquad k_{\perp}^2 = \varkappa^2 + \lambda^2.$$

In vacuum $\varphi'(\mathbf{k}) = 0$.

As has been pointed out earlier, when spatial dispersion is taken into account the usual boundary conditions imposed on the normal and tangential components of the fields are insufficient. We can get a general formulation of the missing boundary condition by setting up a connection, containing some arbitrary constants, which is to hold between the amplitudes of the longitudinal fields and their derivatives at the boundary. Possible forms which are invariant with respect to rotation around the z axis and to reflection in the boundary plane are:

$$\varepsilon\delta\partial\varphi/\partial n + \alpha_1\delta\Delta(\partial\varphi/\partial n) = \alpha_2\varepsilon_{\perp}\delta\dot{A}_n + \alpha_3\delta\dot{A}_n + \alpha_4\delta\Delta\dot{A}_n, \tag{4}$$

$$\varepsilon\delta\partial\varphi/\partial\tau + \beta_1\delta\Delta(\partial\varphi/\partial\tau) = \beta_2\varepsilon_{\perp}\delta\dot{A}_{\tau} + \beta_3\delta\dot{A}_{\tau} + \beta_4\delta\Delta\dot{A}_{\tau}, \tag{5}$$

where δ is the parameter that characterizes the spatial dispersion, $\mathbf{n}$ and τ are the normal and tangent to the boundary plane, and α and β are constants. Dots denote differentiation with respect to time. Ginzburg[3] proposes as the additional boundary condition

$$\mathbf{D}' = \delta\Delta\mathbf{E} = 0. \tag{6}$$

For certain values of the constants α and β the conditions (4) and (5) go over respectively into the normal and tangential components of the condition (6).

If we take Eq. (5) as the additional boundary condition, then the amount of Cerenkov radiation from longitudinal waves emerging into vacuum will be the same for passage of the electron from the medium to vacuum and for its passage from vacuum to the medium. In particular, if we take as the additional boundary condition the tangential component of Eq. (6), then there will be no emergence at all of Cerenkov radiation from the medium into vacuum.

Because of this it seems to us that the condition (5) is physically unjustified. The condition (4), on the other hand, does not have this defect. It can be shown that the amount of Cerenkov radiation emerging into the vacuum has only a weak dependence on the constants α_i that appear in the condition (4). Therefore for a qualitative estimate of the emergence into vacuum of the Cerenkov radiation from longitudinal waves we shall use as the additional boundary condition the normal component of Eq. (6).

3. THE RADIATION FIELDS IN THE VACUUM

The radiation fields in the vacuum are found in exactly the way that has been described by Garibyan.[5] We present the results of the calculation of the radial component of the electric field strength:

$$E'_{\rho}(R, \theta, t) = \frac{e}{v\pi\sqrt{2\pi R \sin\theta}} e^{-3\pi i/4} \int_{-\infty}^{\infty} I(\omega) e^{-i\omega t}\, d\omega, \tag{7}$$

$$I(\omega) = \int_0^{\infty} F(\varkappa) e^{f(\varkappa)R}\, d\varkappa, \tag{8}$$

where the notations used are

$$F(\varkappa) = \varkappa^{3/2}\lambda_0\eta(\varkappa)/\zeta(\varkappa), \qquad f(\varkappa) = i\varkappa\sin\theta + i\lambda_0\cos\theta,$$

$$\eta(\varkappa) = \beta\frac{\omega}{c}\frac{(\varepsilon - 1 - \delta k^2)}{\mu\mu_0}\left(\varepsilon\lambda_{\parallel}\lambda + \frac{\delta\omega^2}{c^2}\varepsilon_{\perp}\varkappa^2\right) + \varepsilon_{\perp}\left(\frac{\varepsilon\lambda_{\parallel} + \delta k^2 k_z}{\mu(\varepsilon - \delta k^2)} - \frac{\varepsilon\lambda_{\parallel}}{\mu_0} - \frac{\delta k^2\omega}{c\mu}\beta\right),$$

$$\zeta(\varkappa) = \delta\omega^2 c^{-2}\varepsilon_{\perp}\varkappa^2 + \varepsilon\lambda_{\parallel}(\lambda + \varepsilon\lambda_0), \quad \mu = k^2 - \omega^2 c^{-2}(\varepsilon - \delta k^2),$$
$$\mu_0 = k^2 - \omega^2/c^2, \qquad \lambda^2 = \omega^2 c^{-2}\varepsilon_{\perp} - \varkappa^2, \qquad \lambda_0^2 = \omega^2/c^2 - \varkappa^2,$$
$$\lambda_{\parallel}^2 = \varepsilon/\delta - \varkappa^2, \qquad \omega = k_z v, \qquad \beta = v/c, \tag{9}$$

R is the distance from the point where the electron leaves the medium to the point of observation, and θ is the angle between R and the z axis. The real and imaginary parts of λ_0, λ, $\lambda_{\parallel}$ are positive. For $\delta \to 0$ Eq. (7) goes over into Eq. (23) of reference 5.

Besides the pole $\mu(\kappa) = 0$ considered by Garibyan,[5] the function $F(\kappa)$ that appears in Eq. (8) has a pole determined by the equation

---

*Here and in what follows the intermediate calculations are not presented (cf. reference 5).

$$\varepsilon - \delta(\varkappa^2 + \omega^2/v^2) = 0. \qquad (10)$$

As Garibyan has shown, the residue at the pole $\mu(\kappa) = 0$ gives the Cerenkov radiation from transverse waves. It will be shown below that the residue at the pole (10) gives the Cerenkov radiation arising in the medium from longitudinal waves.

The integral (8) is calculated by means of a formula of Van der Pol,[8] which takes into account the closeness of the pole to the saddle point. The result is as follows:

$$I(\omega) = -2\left(-\frac{2\pi}{f''(\varkappa_0)R}\right)^{1/2} F(\varkappa_0)\, w e^{f(\varkappa_0)R - w^2} \int_{w}^{i\infty} e^{u^2} du, \qquad (11)$$

where $\kappa_0 = \omega c^{-1} \sin\theta$ is the saddle point of the function $f(\kappa)$; $w = \pm s_0 R^{1/2}$; $s_0^2 = f(\kappa_0) - f(\kappa_1)$; and $\kappa_1^2 = \epsilon/\delta - \omega^2/v^2$ is the pole determined from Eq. (10). The sign of the function w is chosen so that its values lie in the upper half-plane. The closeness of the pole to the saddle point must be taken into account for $|w|^2 \lesssim 1$. For $|w|^2 \gg 1$ we can expand the integral in Eq. (11) in powers of 1/w, and thus get

$$I_1 = e^{f(\varkappa_0)}\left(-\frac{2\pi}{f''(\varkappa_0)R}\right)^{1/2} F(\varkappa_0). \qquad (12)$$

When we deform the original path of integration with respect to $\kappa\ (0 - \infty)$ into the path of steepest descent, for $\gamma = 0$ and $v^2 \geq 4\delta\omega_0^2$ in a certain range of frequencies it is necessary to take into account the residue at the pole κ_1. We shall assume that the speed of the electron satisfies the condition $v^2 \gg 4\delta\omega_0^2$. Then the frequency range in question is determined by the inequalities

$$\omega_1^2 = \omega_0^2(1 + \delta\omega_0^2/v^2) \leqslant \omega^2 \leqslant \omega_0^2(1 + \delta\omega_0^2 a/v^2) = \omega_2^2, \qquad (13)$$

where $a = 1 + \beta^2 \sin^2\theta$. We have taken into account the fact that the influence of spatial dispersion is most important near the plasma frequency ω_0. For the real part of ϵ for $\omega > \omega_0$ we have used the expression $\epsilon_0 = 1 - \omega_0^2/\omega^2$.

If the imaginary part of ϵ, which determines the absorption, satisfies the condition

$$\gamma^2 \lesssim \delta^2\omega^3/Rc^3, \qquad (14)$$

then we have $|w|^2 \lesssim 1$ in a certain range of frequencies around ω' which is determined by the conditions

$$\frac{\partial |w|^2}{\partial\omega} = 0, \quad \Delta\omega \leqslant (1 - |w|^2_{\omega'})^{1/2}\left(\frac{\partial^2 |w|^2}{\partial\omega^2}\right)^{-1/2}_{\omega'}. \qquad (15)$$

The first of these conditions gives the value of ω',

$$(\omega')^2 = \omega_0^2(1 + \delta\omega_0^2 a/v^2) \qquad (16)$$

for $\gamma = 0$. If $\gamma \neq 0$, we get for ω' a value close to the value (16). Using Eq. (16), we get for the second of the conditions (15)

$$\Delta\omega \leqslant \frac{\omega_0}{2}\left[8\left(\frac{\omega_0}{c}\right)^3 \frac{\delta^2}{R}\sin^2\theta\cos^2\theta - \gamma^2\right]^{1/2}. \qquad (17)$$

The values of the integral (8) over the whole range of frequencies are as follows:

ω:	$\omega < \omega_1$	$\omega_1 \leqslant \omega \leqslant \omega' - \Delta\omega$	$\omega' - \Delta\omega \leqslant \omega \leqslant \omega_2$	$\omega_2 \leqslant \omega \leqslant \omega' + \Delta\omega$	$\omega > \omega' + \Delta\omega$
I:	I_1	$I_1 + I_3$	$I_2' + I_3$	I_2	I_1

Here I_1 is the steepest-descent value of the integral for $|w|^2 \gg 1$, I_2 is the value of the integral for $|w|^2 \lesssim 1$; and I_3 is the residue at the point κ_1. In I_2' the function w is taken with the minus sign, and in I_2 with the plus sign.[8] For $\gamma = 0$ the frequency ω' coincides with ω_2. If we take the limiting value $\gamma \sim (\delta^2\omega_0^3/Rc^3)^{1/2}$ for values of R that are small but not in contradiction with the validity of the method of steepest descent $(\omega_0 c^{-1} R \sin^2\theta \gg 1)$, then I_2' becomes negligibly small and can be omitted.

The calculation of the normal component E_n' is made in an analogous way. For the total radiation into the vacuum we have

$$E' = -\frac{e}{v\pi R}\cos\theta\sin\theta \int_{-\infty}^{+\infty}\left(\frac{\omega}{c}\right)^3 \frac{\eta(\varkappa_0)}{\zeta(\varkappa_0)} e^{i\omega(R/c - t)}\, d\omega$$

$$-\frac{\sqrt{2}e}{v\pi\sqrt{R}}\sin\theta e^{-3\pi i/4}$$

$$\times \int_{\omega' - \Delta\omega}^{\omega' + \Delta\omega}\left(\frac{\omega}{c}\right)^{5/2} \frac{\eta(\varkappa_0)}{\zeta(\varkappa_0)}[\pm(\varkappa_1 - \varkappa_0)]\left(e^{-w^2}\int_{w}^{i\infty} e^{u^2} du\right) e^{i\omega(R/c - t)}\, d\omega$$

$$-\frac{e}{v}\sqrt{\frac{2}{\pi R\sin\theta}}\, e^{-\pi i/4}\int_{\omega_1}^{\omega_2} \varepsilon_\perp \frac{\omega^2}{vc}\frac{\varkappa_1^{1/2}}{\zeta(\varkappa_1)} e^{f(\varkappa_1)R - i\omega t}\, d\omega. \qquad (18)$$

It is easy to show that the magnetic field strength is $H' = E'$. The first term in Eq. (8) corresponds to I_1, the second to I_2, and the third to I_3. The choice of the sign of $(\kappa_1 - \kappa_0)$ in the second term corresponds to the choice of the sign of the function w. The regions of integration have been indicated above.

The third term in Eq. (18) represents the amount of Cerenkov radiation produced in the medium from longitudinal waves that emerge into the vacuum.[3] In fact, by expanding the function in the exponent, we find that the field of frequency ω is propagated at the angle $\vartheta(\omega)$,

$$\sin\vartheta(\omega) = c\omega^{-1}\sqrt{\varepsilon_0/\delta - \omega^2/v^2}\,, \tag{19}$$

with the direction of motion of the electron. For the longitudinal waves the index of refraction is $n = c\omega^{-1}(\epsilon_0/\delta)^{1/2}$. By taking the condition for Cerenkov radiation in the medium and using the law of refraction, we get for $\vartheta(\omega)$ in the vacuum the expression (19).

The energy flux dW/ds through unit area during the entire time of flight of the electron can be divided into three parts, corresponding to the three terms in Eq. (18) (cf. also reference 5). The transition radiation, which corresponds to the first term in Eq. (18), is a spherical wave. The energy radiated into the solid angle $d\Omega = \sin\theta\, d\theta\, d\varphi$ with its vertex at the point where the electron passes out of the medium is given by

$$\frac{dW_1}{d\Omega} = \frac{ce^2}{v^2\pi^2}\cos^2\theta\sin^2\theta \int_0^{\infty}{}' \left|\left(\frac{\omega}{c}\right)^3 \frac{\eta(\varkappa_0)}{\zeta(\varkappa_0)}\right|^2 d\omega \tag{20}$$

(the prime on the integral sign means that for values of R that satisfy the condition (14) an interval $\pm\Delta\omega$ around ω' is excluded from the region of integration). For the radiation in the interval $\pm\Delta\omega$ around ω' we get

$$\frac{dW_2}{ds} = \frac{2ce^2}{\pi^2 v^2 R}\sin^2\theta$$
$$\times \int_{\omega'-\Delta\omega}^{\omega'+\Delta\omega} \left|\left(\frac{\omega}{c}\right)^{5/2} \frac{\eta(\varkappa_0)}{\zeta(\varkappa_0)} (\varkappa_1 - \varkappa_0)\, e^{-w^2} \int_w^{i\infty} e^{u^2} du\right|^2 d\omega. \tag{21}$$

As R increases the value of w increases. Then $\Delta\omega$, and consequently also W_2, go to zero, and we must integrate over the entire range of frequencies in Eq. (20).

It must be noted that the condition for distinguishing the second term in Eq. (18) is the same as that for distinguishing the third term, which corresponds to the Cerenkov radiation ($v^2 \geq 4\delta\omega_0^2$). From this we can conclude that the second term in Eq. (18) is a superposition of the transition radiation and the Cerenkov radiation, which is produced near the boundary surface (at a distance of the order of the wavelength). At large distances from the point where the electron comes out, this part of the radiation goes over into a spherical wave. For the Cerenkov radiation, which corresponds to the third term of Eq. (18), the energy emitted between cones of aperature angles θ and $\theta + d\theta$ depends on the distance R and is given by the formula

$$\frac{dW_3}{d\theta} = \frac{4ce^2}{v^2} R \int_{\omega_1}^{\omega_2} \frac{\omega^4}{c^2v^2} \left|\frac{\varepsilon_\perp \varkappa_1^{1/2}}{\zeta(\varkappa_1)} e^{f(\varkappa_1)R}\right|^2 \cos(\theta - \vartheta(\omega))\, d\omega. \tag{22}$$

In the case of passage of an electron from vacuum to a medium the radiation field in vacuum is determined in the same way, the only difference being that the poles do not affect the calculations. Thus there remains only the transition radiation W_1; the amount of such radiation can be found from Eq. (20) by replacing v by − v.

4. QUALITATIVE ESTIMATE OF THE RESULTS

The case of motion of an electron from a medium into vacuum is interesting, since in this case besides the transition radiation there is Cerenkov radiation caused by the excitation of longitudinal waves in the medium.

The parameter δ that characterizes the spatial dispersion is of the order of the square of the Debye radius[3]: $\delta \sim \lambda_D^2 = kT/4\pi ne^2$. Owing to this the condition $v^2 \geq 4\delta\omega_0^2$ for the appearance of Cerenkov radiation can be written in the form $v^2 \geq \langle v^2 \rangle$ ($\langle v^2 \rangle$ is the mean square thermal speed of the electrons in the medium). As is well known (cf., e.g., references 1 and 2), the motion of an electron through a medium with speed satisfying $v^2 \geq \langle v^2 \rangle$ produces longitudinal waves (plasmons). In the following estimates we assume $v^2 \gg 4\delta\omega_0^2$, $v/c = \beta \ll 1$.

In the absence of absorption ($\gamma = 0$), we have $W_3 \to \infty$ for $R \to \infty$, which corresponds to the emergence of the Cerenkov radiation from a semi-infinite trajectory. The angular distribution is then determined by the law of refraction, Eq. (19).

When there is absorption the pole (10) must be taken into account for angles that satisfy the condition $\sin^2\theta > \gamma c^2/\delta\omega_0^2$. It can be seen from this that the Cerenkov radiation with the energy W_3 will be emitted between the bounding surface and a cone of aperture given by $\sin^2\theta \sim \gamma c^2/\delta\omega_0^2$. Moreover, it will be exponentially damped with increase of the distance.

For $\gamma > \delta\omega_0^2$ the pole (10) need not be considered. Both the emerging Cerenkov radiation and the transition radiation will be determined by the single term W_1, in which the integration is taken over the entire range of frequencies. For small values of γ ($\gamma \ll \delta\omega_0^2/c^2$), however, and values of R that are small but do not come within the zone of formation of the radiation ($\delta^2\omega_0^3/\gamma^2 c^3 \gtrsim R \gg c/\omega_0$), the value of W_3 is large. With this statement of the problem one cannot estimate the yield of Cerenkov radiation W_3 (the radiation losses are comparable with the kinetic energy).

Noting that both the spectrum (13) of the Cerenkov radiation and the range $\Delta\omega$ of frequencies around the value ω' of Eq. (16) lie in the neighborhood of the plasma frequency ω_0, let us use the following method to estimate the amount of Cerenkov radiation caused by the excitation of longitudinal waves in the medium when an electron passes through a plate.

Let us take a plate that is "thick" enough for the formation in it of a wave corresponding to the frequency ω_0 (and for the "one-boundary" approximation to the problem to be justified for this frequency), but "thin" enough for the absorption to be negligible. As Garibyan has shown,[6] a plate is thick if $d \gg c/\omega_0$, where d is the thickness of the plate, and it is assumed that $\beta \ll 1$. The absorption can be neglected for the longitudinal waves if $d \ll 1/k''_{\|}$, where $k''_{\|}$, is the imaginary part of the wave vector of Eq. (2). At the frequency ω' this condition means that $d \ll \delta\omega_0/v\gamma$. For the plate thickness d to satisfy both conditions it is necessary for the imaginary part of ϵ to satisfy the condition $\gamma \ll \delta\omega_0^2/c^2$. In this case both conditions on the thickness of the plate can be satisfied.

We can estimate the quantity W_3 by calculating for an electron moving in the medium the energy loss per unit path length owing to the Cerenkov radiation from longitudinal waves, and multiplying it by the thickness of the plate. We shall not find the loss here, however, since it has been calculated by many authors. The most exact calculation of the energy loss per unit time of an electron moving in a medium has been made by Larkin.[2] In our notation the formula is

$$dE/dt = e^2\omega_0^2 v^{-1} \ln (v/\omega_0 \sqrt{\delta}), \tag{23}$$

where it is assumed that $v^2 \gg 4\delta\omega_0^2$ (see also reference 1). Assuming that almost all of the energy radiated in the plate emerges into the vacuum, we get for the estimate of the quantity W_3

$$W_3 \approx e^2\omega_0^2 v^{-2} \ln (v / \omega_0 \sqrt{\delta}). \tag{24}$$

Comparison with the kinetic energy gives the ratio

$$\frac{W_3}{W_\text{K}} = \frac{e^2\omega_0^2 d}{mv^4} \ln \frac{v}{\omega_0 \sqrt{\delta}}. \tag{25}$$

Let us estimate the amount of Cerenkov radiation W_2 that arises at a distance of the order of a wavelength from the boundary of the film through which the electron emerges into the vacuum. For the given plate thickness $(\delta\omega_0/v\gamma \gg d \gg c/\omega_0)$ we can use the expression (21) to estimate the quantity W_2. If γ satisfies the condition (14), we can distinguish W_2 from the transition radiation at distances R_0 in the range

$$\delta^2\omega_0^3 / \gamma^2 c^3 \gtrsim R_0 \gg c / \omega_0. \tag{26}$$

Taking the integrand of Eq. (21) at the point ω' given by Eq. (16) and multiplying by the frequency interval $\Delta\omega$ of Eq. (17), we get for W_2 the value

$$W_2 = \frac{4e^2\omega_0^2}{\pi v^2} R \int_{\theta_1}^{\theta_2} \left[2\delta^2 \left(\frac{\omega_0}{c}\right)^3 \frac{\sin^2\theta \cos^2\theta}{R} - \frac{\gamma^2}{4} \right]^{1/2} \frac{|\xi(\omega')|^2}{\sin\theta} d\theta, \tag{27}$$

where θ_1 and θ_2 are the roots of the radicand and

$$|\xi(\omega')| = |e^{-w^2(\omega')} \int_{w(\omega')}^{i\infty} e^{u^2} du|.$$

For a value of R_0 that satisfies the condition (26), the expression (27) can be estimated in order of magnitude as follows,

$$W_2 \approx \frac{e^2\omega_0}{c} \frac{\langle v^2 \rangle}{v^2} \sqrt{R_0 \frac{\omega_0}{c}}, \tag{27'}$$

where it is assumed that $\delta\omega_0^2 \approx \langle v^2 \rangle$.

Taking the ratio of W_2 to the kinetic energy of the electron, we find

$$\frac{W_2}{W_\text{K}} = \frac{e^2\omega_0}{mv^4} \frac{\langle v^2 \rangle}{c} \sqrt{R_0 \frac{\omega_0}{c}}. \tag{28}$$

The ratio W_3/W_2 is given in order of magnitude by

$$W_3 / W_2 \approx \frac{\omega_0 c}{\langle v^2 \rangle} \frac{d}{\sqrt{R_0\omega_0 / c}} \gg \frac{c^2}{\langle v^2 \rangle} \frac{1}{\sqrt{R_0\omega_0 / c}}. \tag{29}$$

Though at small distances R_0 the energy W_3 of the Cerenkov radiation is much larger than the quantity W_2, still, as was pointed out above, its value falls off exponentially with the distance. On the other hand the part of the Cerenkov radiation that corresponds to W_2 is converted at large distances into an undamped spherical wave.

We can estimate the value of γ for which such a physical picture can be observed, by starting from the condition (14) and noting that the condition $R\omega_0/c \gg 1$ for the applicability of the method of steepest descent must be satisfied. Assuming for dielectrics $\delta \sim 10^{-16}$, $\omega_0 \sim 10^{14}$ and taking $R\omega_0/c \sim 10^4$, we get the value $\gamma \sim 10^{-10}$. For a plasma, assuming $\delta \sim 10^{-6}$, $\omega_0 \sim 10^{10}$, $R\omega_0/c \sim 10^2$, we get $\gamma \sim 10^{-7}$.

Assuming $\beta \sim 10^{-2}$, we get for the thickness of the plate the conditions

$1 \gg d \gg 10^{-4}$ (dielectric) $10^3 \gg d \gg 1$ (plasma)

The quantity W_2 of Eq. (27), like the W_3 of Eq. (24), has a tendency to increase with decreasing speed of the electron. In this case, however, the method that has been presented does not apply, since the radiation losses become comparable with the kinetic energy W_K of the electron [the expressions (25) and (28) approach unity].

The transition radiation, which corresponds to the quantity W_1, has been qualitatively described by Garibyan.[5] Here we shall estimate its value for $\beta \ll 1$ for comparison with the Cerenkov radiation from longitudinal waves.

It is important to take spatial dispersion into account only in a frequency interval close to the plasma frequency ω_0. Since this frequency interval has been taken into account by the term W_2, we can make the estimate of the transition radiation (20) by neglecting spatial dispersion. Then Eq. (20) goes over into the formula of Garibyan [Eq. (28) of reference 5]:

$$W_1 = \frac{2e^2\beta^2}{\pi c}\int_0^{\pi/2} d\theta \frac{\sin^3\theta\cos^2\theta}{(1-\beta^2\cos^2\theta)^2}$$

$$\times \int_0 \left(\frac{(\varepsilon-1)(1-\beta^2 \qquad \sqrt{\varepsilon-\sin^2\theta})}{(\varepsilon\cos\theta+\sqrt{\varepsilon-\sin^2\theta})(1-\beta\sqrt{\varepsilon-\sin^2\theta})}\right)^2 d\omega, \quad (30)$$

Setting $\epsilon_0 = \text{const} \sim 1$, $\epsilon_0 - 1 \sim 1$ for $0 < \omega < \omega_0$ and $\epsilon_0 = 1 - \omega_0^2/\omega^2$ for $\omega_0 < \omega < \infty$, we get the following estimate:

$$W_1 \; W_K \simeq e^2\omega_0/mc^3. \quad (31)$$

It can be seen from a comparison of Eq. (31) with Eqs. (25) and (28) that for $\beta \ll 1$ the transition radiation is much smaller than the emerging Cerenkov radiation that has been produced in the medium from longitudinal waves.

In conclusion I express my gratitude to V. L. Pokrovskiĭ, S. K. Savvinykh, A. P. Kazantsev, A. M. Dykhne, and I. A. Tilinskiĭ for discussions and a number of valuable suggestions.

---

[1] D. Pines and D. Bohm, Phys. Rev. **85**, 338 (1952).

[2] A. I. Larkin, JETP **37**, 264 (1959), Soviet Phys. JETP 10, 186 (1960).

[3] V. L. Ginzburg, JETP **34**, 1593 (1958), Soviet Phys. JETP 7, 1096 (1958).

[4] V. E. Pafomov, JETP **36**, 1853 (1959), Soviet Phys. JETP 9, 1321 (1959).

[5] G. M. Garibyan, JETP **33**, 1403 (1957), Soviet Phys. JETP 6, 1079 (1958).

[6] G. M. Garibyan, JETP **37**, 527 (1959), Soviet Phys. JETP 10, 372 (1960).

[7] V. Ginzburg and I. Frank, JETP **16**, 15 (1946).

[8] L. M. Brekhovskikh, Волны в слоистых средах (Waves in Layered Media), Acad. Sci. Press, 1957, Sec. 20 [Transl: Academic Press].

Translated by W. H. Furry
28

SOVIET PHYSICS JETP VOLUME 13, NUMBER 1 JULY, 1961

ALTITUDE DEPENDENCE OF EXTENSIVE AIR SHOWERS

É. V. GEDALIN

Physics Institute, Academy of Sciences, Georgian S.S.R.

Submitted to JETP editor July 1, 1960

J. Exptl. Theoret. Phys. (U.S.S.R.) 40, 178-179 (January, 1961)

The altitude dependence of extensive air showers is studied assuming that the absolute amount of energy transferred to π mesons in collisions between nucleons with energies $E \gtrsim 10^{12}$ ev and nuclei is constant (in the c.m.s.). As is shown, in order to have the results of the calculation agree with the experimental data, we must assume that, in secondary interactions of particles (other than π mesons) which carry away most of the energy in the nucleon-nucleus collisions, a constant fraction of the incident-particle energy is imparted to the π mesons.

FROM the experiments of the Bristol group[1] we can conclude that, in collisions of nucleons with energy $E_N \gtrsim 10^3$ Bev with nuclei, the absolute amount of energy ~ 50 Bev imparted to π mesons remains constant in the c.m.s. Moreover, the total inelasticity factor varies little because of the increase of the energy transferred to other particles, which we shall henceforth refer to as X particles.

In the present article, the altitude dependence of extensive air showers is discussed, taking this feature of nucleon-nucleus collisions into account. We shall assume that, in collisions of π mesons and nucleons with $E_N < E_p$ ($E_p = 5 \times 10^3$ Bev is the threshold energy) with nuclei, π mesons carry away a constant fraction of the energy of the incident particle.

With respect to the character of the interaction of the X particles with nuclei, we shall make either one of the following two assumptions:

1. In the collision of an X particle with a nucleus, an amount of energy whose absolute value remains constant is transferred to π mesons in the c.m.s. whenever $E_X > E_p$, while a constant fraction of the energy of the incident particle is transferred whenever $E_X < E_p$.

2. In the collision of an X particle with a nucleus, a constant fraction of the energy of the incident particle is transferred to π mesons (for any E_X).

We shall also assume that the spectrum of the secondary particles in nuclear interactions at high energies is given by a power law, $dn/dE \sim E^{-1-\delta}$, where δ is a constant parameter. According to the data of the Bristol group, $\delta = 1/2$ for π mesons. We shall assume the same value $\delta = 1/2$ for the spectra of nucleons and X particles. Neglecting particle decay, we then obtain the following expression for the number of electrons in extensive air showers:

$$\Gamma_e = A \exp\{y_0 s + \lambda (x - x_0)\}$$

for $a^{-2} y_0 \ll x - x_0 < y_0$, and where $y_0 = \ln(E_0/\epsilon)$. E_0 is the primary energy, $\epsilon = 0.07$ is the critical energy for electromagnetic cascade processes, x_0 is the depth of shower initiation, and $a = 2.3$ is the ratio of the nuclear mean free path (for a single interaction) to the radiation length.

Under the assumption 1, we have $s_1 = 0.7$, $\lambda_1 = +0.2$ for $E_0 \gtrsim 10^5$ Bev, i.e., an extensive air shower does not attain the maximum, which contradicts the experimental data[2] ($s_{exp} = 1.2 - 1.4$, $\lambda_{exp} = -0.4$). Under the assumption 2, we have $s_2 = 1.4$, $\lambda_2 = -0.4$. Moreover, the existence of a single interacting X particle produced in one of the first collisions between the nucleon and nuclei is sufficient to obtain these values. This means that, regardless of the fact that the number of produced X particles may be small in each single collision, they may play a considerable role in the development of extensive air showers.

Thus, if in the collision of nucleons with nuclei a constant (in its absolute value) amount of energy is transferred to π mesons in the c.m.s., then, in order to explain the altitude dependence of extensive air showers, it is necessary to assume that the X particles produced in these collisions together with π mesons (the majority of the X particles being most probably K mesons) carry away a large part of the energy imparted to secondary particles, and that, in each of the consecutive collisions, they transfer a constant fraction of it to π mesons.

This conclusion is in good agreement with the results of Hayakawa and Ogita[3] who, assuming that the spectrum of X particles in the showers is similar to that of π mesons at energies $< 10^3$ Bev, and that it remains constant for energies higher than 10^3 Bev (this assumption is equivalent to our assumption 2), found that the theoretical curve of altitude dependence of extensive air showers agrees satisfactorily with the experimental one.

The author wishes to express his gratitude to I. L. Rozental' for supervising the work, and to G. T. Zatsepin for his comments and helpful advice.

---

[1] Duthie, Fisher, Fowler, Kaddoura, Perkins, and Pinkau, Proceedings of the 1959 Moscow International Conference on Cosmic Rays **1**, 1960.

[2] K. Greisen, Progress in Cosmic Ray Physics (North-Holland Publishing Co., Amsterdam, 1956), vol. III.

[3] S. Hayakawa and N. Ogita, Proceedings of the 1959 Moscow International Conference on Cosmic Rays **2**, 1960.

Translated by H. Kasha
29

SOVIET PHYSICS JETP VOLUME 13, NUMBER 1 JULY, 1961

ESTIMATE OF THE ROLE OF THE LAW OF CONSERVATION OF ANGULAR MOMENTUM IN THE STATISTICAL THEORY OF PARTICLE PRODUCTION

Ya. I. GRANOVSKIĬ and G. I. KOPYLOV

Institute of Nuclear Physics, Academy of Sciences, Kazakh S.S.R.

Submitted to JETP editor July 4, 1960

J. Exptl. Theoret. Phys. (U.S.S.R.) 40, 180-182 (January, 1961)

It is shown that the predictions of the statistical theory of multiple meson production remain almost unaltered if the conservation of the z component of the angular momentum is taken into account in the simplest classical way. The resulting anisotropy in the angular distribution of the particles is apparently smaller than that observed in reality.

IT is asserted in several papers on the statistical theory of multiple production of particles that the anisotropy in the angular distribution is due to the restrictions connected with the conservation of the initial angular momentum by the particles in the final state.[1]

However, there is a certain inconsistency in this argument. Indeed, when we replace, in the statistical theory, the quantum mechanical expression for the probability of the process

$$W_n = \int \mathfrak{M}\, \delta(E - \Sigma E_k)\, \delta(\mathbf{P} - \Sigma \mathbf{p}_k)\, d\mathbf{p}_1 \ldots d\mathbf{p}_n \qquad (1)$$

($\mathfrak{M}$ is the square of the modulus of the matrix element) simply by the statistical weight[2]

$$S_n = V^n \int \delta(E - \Sigma E_k)\, \delta(\mathbf{P} - \Sigma \mathbf{p}_k)\, d\mathbf{p}_1 \ldots d\mathbf{p}_n, \qquad (2)$$

we assume that the matrix element is constant, i.e., it conserves angular momentum in a trivial way (invariance under rotations).

The essence of the above-mentioned assertion seems to be that we require an expression for the matrix element which, while being invariant under rotations, depends on the angle in the way prescribed by experiment. Such an expression has not yet been found.

Since a consistent quantum mechanical treatment is impossible, it is of interest to investigate a certain classical model, in which the behavior of the probability W_n is imitated by the statistical weight of a rotating system:[3]

$$S_n = \int \delta(E - \Sigma E_k)\, \delta(\mathbf{P} - \Sigma \mathbf{p}_k)\, \delta(\mathbf{M} - \Sigma [\mathbf{r}_k \times \mathbf{p}_k])\, d\mathbf{p}_1 \ldots d\mathbf{p}_n d\mathbf{r}_1 \ldots d\mathbf{r}_n; \qquad (3)$$

this procedure is consistent with the statistical theory of Fermi and introduces in the simplest classical way angular dependences which are connected with the conservation of angular momentum.

The comparison of (3) and (1) shows that this is equivalent to the replacement

$$\mathfrak{M} \to \mathfrak{M}_{\mathrm{cl}} = \int \delta(\mathbf{M} - \Sigma [\mathbf{r}_k \times \mathbf{p}_k])\, d\mathbf{r}_1 \ldots d\mathbf{r}_n. \qquad (4)$$

This replacement presupposes that the quantity $\mathfrak{M}_{\mathrm{cl}}$ retains some of the characteristic features of the quantum mechanical expression $\mathfrak{M}$.

The calculations with the formula (3) were done by using the Monte Carlo method (method of random stars).[4] Since only one axis — the z axis of the interaction — is fixed experimentally, an average being taken over the other two axes, we must integrate over all values of the transverse components of the angular momentum M_x and M_y in formula (4). Then only a single δ function containing the z component of the angular momentum remains in that formula. Since we have chosen the z axis along the momentum of the incident particle, $M_z = 0$, so that no new parameters appear in our model.

Integrating formula (4) over the volume of the Fermi ellipsoid,[2] we obtain

$$\mathfrak{M}_{\mathrm{cl}} = \int\limits_{(V)} \delta(\Sigma [\mathbf{r}_k \times \mathbf{p}_k])\, d\mathbf{r}_1 \ldots d\mathbf{r}_n$$

$$= \frac{V^n}{2\pi} \int\limits_{-\infty}^{\infty} d\lambda \prod_{k=1}^{n} \frac{1}{V} \int\limits_{(V)} \exp\{i\lambda [\mathbf{r} \times \mathbf{p}_k]_z\}\, d\mathbf{r}$$

$$= \frac{V^n}{\pi} \int\limits_{0}^{\infty} d\lambda \sqrt{9\pi/2} \prod_{k=}^{n} \frac{J_{3/2}(R\lambda p_{\perp k})}{(R\lambda p_{\perp k})^{3/2}}$$

(J is a Bessel function, $p_{\perp k}$ is the transverse momentum of the k-th particle, and R is the radius of the ellipsoid, i.e., the effective radius of the nucleon). Substituting this expression in (1), we can calculate the probability for the production of various systems of particles occurring in the collision.

The method of random stars also allows us to obtain simultaneously the angular and energy distributions and the correlations between the directions of emission of the produced particles. The computations were carried out for collisions of nucleons with energies of 10 Bev; together with the direct creation of the mesons, we also considered the production mechanism going through an isobar. We obtained the following results (for more detail, see reference 5):

1. The statistical weights, after normalization, are not very different from their values in the statistical theory of Fermi, so that the multiplicity is almost unaltered (instead of $\overline{n}_s = 3.68$, one obtains 3.70). The same holds for the momentum distributions. As the energies approach the reaction threshold, the cross sections decrease more slowly than in the Fermi theory.

2. The angular distribution is anisotropic. The anisotropy becomes weaker as the number of particles increases. If we characterize the anisotropy by the ratio of the numbers of particles emitted into the equal solid angles $0° \leq \theta \leq 60°$ and $60° \leq \theta \leq 90°$, respectively, we find for 2, 3, 4, . . . secondary particles the anisotropy 2.5, 1.29, 1.22, . . . (averaged over mesons and nucleons). The experimental values of this quantity are contradictory and display a wide spread; but they are probably higher than our values.[6]

3. The angular correlations between the particles are also almost unchanged. We call attention to the following fact observed by us: the average value of the angle $\overline{\theta}_{ik}$ agrees with the average value of the angle in the plane of the target $\overline{\varphi}_{ik}$; both depend only on the multiplicity. This agreement is also observed in the Fermi model.

Our result that the physical quantities are insensitive to modifications of the statistical weight is evidently due to the fact that our corrected weight $\mathfrak{M}_{cl}$ depends only on the transverse components of the momentum, which vary only little. If, instead of the Fermi ellipsoid, we choose a volume of a different shape (flat disk, the peripheral part of an ellipsoid, etc.), M_{cl} changes very little, retaining all its qualitative features.

These calculations led us to the conclusion that it is futile to try to explain the anisotropy quantitatively using the classical analogy. It appears to us that this effect can only be explained by a quantum mechanical computation of the matrix elements, even if it be of the most approximate nature.

---

[1] E. Fermi, Transl. of Progr. Theoret. Phys. **5**, 570 (1951) and Phys. Rev. **81**, 683 (1951). R. H. Milburn, Revs. Modern Phys. **27**, 1 (1955). J. V. Lepore and M. Neumann, Phys. Rev. **98**, 1484 (1955). J. Koba and Sh. Takagi, Fortschr. Physik 7, 1 (1959). Goldhaber, Goldhaber, Lee, and Pais, preprint UCRL (1960). R. Hagedorn, Nuovo cimento **15**, 434 (1960).

[2] Belen'kiĭ, Maksimenko, Nikishov, and Rozental', Uspekhi Fiz. Nauk **62**, 1 (1957).

[3] L. D. Landau and E. M. Lifshitz, Statistical Physics, Pergamon Press (1958).

[4] Yu. N. Blagoveshchenskiĭ and G. I. Kopylov, preprint R-213, Joint Institute of Nuclear Research, (1958). G. I. Kopylov, JETP **39**, 1091 (1960), Soviet Phys. JETP **12**, 761 (1961).

[5] Ya. I. Granovskiĭ and G. I. Kopylov, preprint, Joint Institute of Nuclear Research.

[6] Bogachev, Bunyatov, Gramenitskiĭ, Lyubimov, Merekov, Podgoretskiĭ, Sidorov, and Tuvdéndorzh, JETP **37**, 1225 (1959), Soviet Phys. JETP **10**, 872 (1960). Botvin, Takibaev, and Chasnikov, Dokl. Akad. Nauk SSSR **135**, 571 (1960), Soviet Phys.-Doklady **5**, in press.

[7] I. M. Dremin and D. S. Chernavskiĭ, JETP **38**, 229 (1960), Soviet Phys. JETP **11**, 167 (1960). Yu. A. Romanov and D. S. Chernavskiĭ, JETP **38**, 1132 (1960), Soviet Phys. JETP **11**, 819 (1960).

Translated by R. Lipperheide
30

SOVIET PHYSICS JETP VOLUME 13, NUMBER 1 JULY, 1961

SUPERFLUIDITY OF NUCLEAR MATTER

L. P. RAPOPORT and S. G. KADMENSKIĬ

Voronezh State University

Submitted to JETP editor July 6, 1960

J. Exptl. Theoret. Phys. (U.S.S.R.) **40**, 183-193 (January, 1961)

Using Bogolyubov's method, we treat the possibility of super-fluidity of nuclear matter and of He^3 for the case of realistic interactions between fermions in S states. We show that in the normal state, near the Fermi surface, repulsion rather than attraction predominates for a pair of nucleons with opposite momenta and spins. However, because of renormalization of the repulsive term in the compensation equation, nuclear matter may become superfluid. The reason for the absence of superfluidity for He^3 is given.

1. INTRODUCTION

In recent years there have appeared a whole series of papers in which Bogolyubov's method[1] is applied to the study of the problem of superfluidity of the nucleus and of nuclear matter.[1-3] The essential feature of this method is the use of ordinary perturbation theory. However, as was shown by Brenig,[4] for an arbitrarily small attractive potential the wave function for a pair of nucleons with energy near the Fermi surface and with opposite momenta has a singularity, so that the use of matrix elements of the potentials computed using plane waves is not possible.

On the other hand, Brueckner's theory,[5,6] which takes account of correlations in the many body system, cannot be simply combined with Bogolyubov's method by replacing the potential V by the K matrix, since the latter has a singularity for a pair of nucleons with opposite momenta near the Fermi surface. At the same time, the correctness of the final result of Bogolyubov's theory, which gives such a good description of superconductivity in metals, permits one to hope that with some modernization this method can also be applied to the problem of superfluidity of nuclei.

Actually, both for Brenig and Bogolyubov the Pauli principle plays the main role in the formation of the energy gap. But it is included entirely differently in the two methods. While in Brenig's method it appears via the singularity of the K matrix and the pairing of real nucleons with energy close to E_F, in Bogolyubov's method it comes from the compensation of the dangerous diagrams when we use second quantization with Fermi quasi-amplitudes.

Continuing this comparison, one may hope to use Bogolyubov's theory for studying superfluidity of nuclear matter by replacing the interaction potential by the K matrix and calculating it so that the correlations near E_F are not included twice. In particular, the K matrix near the Fermi energy E_F can be calculated disregarding the Pauli principle. In the theory of superconductivity of metals such a replacement of the potential by the K matrix disregarding the Pauli principle gives nothing new, since for the relatively weak interactions in the metal the matrix element of the potential is not drastically different from the K matrix omitting the Pauli principle. But in the nuclear case this replacement enables us to treat some interactions which cannot be handled in the usual Bogolyubov scheme, for example the case of an infinite repulsion between nucleons at small distances.

According to the results of Bogolyubov and coworkers,[1] the equation of compensation of dangerous diagrams has a nontrivial solution, which corresponds to a superfluid state, if: a) the interaction is attractive and weak; b) the interaction is attractive and localized on the Fermi sphere; c) the interaction between nucleons is repulsive and highly singular, so that the derivative of the matrix element of the interaction, averaged over angles, is sufficiently large.

Interactions between nucleons of type c) are not known at present. As will be shown in Sec. 2, case b) apparently is also not realized in the nucleus.

In the work of Solov'ev[2] and Dotsenko[3] on the superfluidity of nuclear matter, it is postulated that case a) is satisfied, and by means of a formalism analogous to that developed in reference 1 they obtain an energy gap between the superfluid and normal states. From this they conclude that a superfluid state is favored for nuclear matter; however no specific features of the nucleus appear at all in these papers.

As we shall show, in the general case of the "normal" state a short range repulsion and attraction, for the case of a pair of particles with arbitrary relative orbital angular momenta, affect the wave function of the pair completely differently, so that their influence does not reduce to an effective attractive potential.

For the special case of nuclear matter, the criterion of superfluidity was rewritten by Bogolyubov in the form:

$$|E(k) - E_F|\,\psi(\mathrm{r}) + V(\mathrm{r})\,\psi(\mathrm{r}) = E\psi(\mathrm{r}). \tag{1}$$

If by a suitable choice of ψ we can obtain $E < 0$ from (1), the superfluid state is more favorable than the normal state, which is the criterion for superfluidity.

Equation (1) was used by Cooper, Mills, and Sessler[7] for investigating the possible superfluidity of nuclear matter, by choosing trial functions containing variational parameters. The authors concluded that there was no superfluidity for their class of trial functions. Naturally, however, they could not conclude that superfluidity of nuclear matter is impossible. Besides, as we shall see in Sec. 3, the trial functions used in their work are far from the actual solution of Eq. (1).

2. THE POSSIBILITY OF REPLACING NUCLEAR POTENTIALS BY AN EFFECTIVE ATTRACTION

The fundamental difficulty in the analysis of the interaction of two nucleons is the simultaneous inclusion of the strong repulsion at small distances (which we shall call the "hard core") and the short range attraction.

In most present day work on nuclear theory, it is assumed that the forces between nucleons in the nucleus are almost the same as the forces between isolated nucleons, concerning which we can get information from scattering experiments. This question has been discussed repeatedly in the papers of Weisskopf, Bethe, Brueckner et al., who have succeeded, by starting from this assumption, in explaining a whole host of properties of nuclei.[5,6] There is therefore no reason for supposing that the inetraction of nucleons near the Fermi surface is different from the interaction between isolated nucleons and consequently is no different from that of the other nucleons in the nucleus. An argument in favor of this is the agreement between the parameters of the real part of the optical potential for nucleons having an energy greater than E_F with the parameters of the self-consistent potential for nucleons with energy below E_F. We shall therefore use the Gammel-Thaler[8] potentials for the interaction.

In the theory of superfluidity of nuclear matter, n-n and p-p interactions are of particular interest. In fact, because of the large difference in E_F for neutrons and protons, a neutron and proton with equal and opposite spins and momenta cannot simultaneously lie near the same Fermi surface. But in the interaction of a pair of identical particles, only the central singlet forces are important for the production of superfluidity. In fact, a pair of identical particles ($T = 1$) with even l can occur only in the singlet state, where the tensor forces are equal to zero. In triplet states with $l = 1, 3, 5, \ldots$, where tensor forces are important, the superfluid state is not formed because the interaction of the nucleons in this state will be repulsive.[8]

In many papers on nuclear theory and superfluidity of nuclear matter, it is assumed that the interaction of two nucleons can be approximated by an effective attractive potential. We shall show that in the "normal" state of nuclear matter such a replacement is not possible, i.e. case a) of Sec. 1 does not occur.

In the presence of central forces alone, the wave function for a pair of nucleons with opposite momenta and spins, corresponding to a relative orbital angular momentum l, has the form

$$\psi_l(r) = j_l(kr) + 4\pi \int_0^\infty G_l(r, r')\,V(r')\,\psi_l(r')\,r'^2\,dr', \tag{2}$$

where $G_l(r, r')$ is the Green's function. In defining the Green's function, we must consider the following points, which enable us correctly to select the "normal" state. Far from k_F one could without any contradiction combine the Brueckner procedure with that of Bogolyubov and replace the potential V by the K matrix. Near k_F, a precise inclusion of the Pauli principle leads to a singularity in the K matrix. Therefore in order not to take account of the Pauli principle twice, as pointed out in the introduction, we should in this region replace the potential V by the K matrix and disregard the Pauli principle. Thus for the study of the normal state we must construct Green's function which, in the region far from k_F would coincide with the exact Green's function, which was found in the paper of Brueckner and Gammel,[9] and near k_F would not give a singular K matrix and in particular would not take account of the Pauli principle.

Starting from these considerations, we choose $G_l(r, r')$ in the form

$$G_l(r, r') = (\mu^* k / 4\pi\hbar^2)\, n_l(kr_>)\, j_l(kr_<) \exp\{-\alpha(r_> - a)\}, \tag{3}$$

where μ^* is the effective mass, which takes into account the self-consistent field ($\mu^* = 0.6$ m); n_l and j_l are the spherical Neumann and Bessel functions of half-integral order; a is the radius of the core; $r_>(r_<)$ denotes the larger (smaller) of r, r′; α is a variational parameter which takes account of the effect of the Pauli principle, and is determined from the condition that the total energy be a minimum. This parameter is approximately equal to the reciprocal of the "healing distance".[10]

The Green's function (3) satisfies the following physical conditions: 1) it describes correctly the behavior of the wave function far from k_F; 2) it gives the correct binding energy of the whole system; 3) for $\alpha \to 0$, the function $G_l(r, r')$ goes over into the ordinary Green's function for a pair in a medium, in the "effective mass" approximation in which one disregards the Pauli principle. In this paper, we choose the value $\alpha = 0.8\, k_F$ in agreement with the work of Weisskopf and coworkers.[10] All the following calculations are done for the two cases: $\alpha = 0$ and $\alpha = 0.8\, k_F$.

Let us consider a potential of the type

$$U(r) = \begin{cases} \infty, & r \leqslant a \\ V(r), & r > a \end{cases}. \tag{4}$$

In this case we write (2) in the form

$$\psi_l(r) = j_l(kr) + 4\pi \int_0^a G_l(r, r')\, U(r')\, \psi_l(r')\, r'^2\, dr' + 4\pi \int_a^\infty G_l(r, r')\, V(r')\, \psi_l(r')\, r'^2\, dr'. \tag{5}$$

Following Brueckner and Gammel,[9] to include the effect of the repulsive core we make the following replacement in (5):

$$U(r)\, \psi_l(r) = \lambda \delta(r - a) \quad \text{for} \quad r \leqslant a. \tag{6}$$

Substituting (6) in (5) and using the boundary condition $\psi_l(a) = 0$, we find for λ,

$$\lambda = \frac{j_l(ka)}{4\pi a^2 G_l(a, a)} - \frac{1}{a^2 G_l(a, a)} \int_a^\infty G_l(a, r')\, V(r')\, \psi_l(r')\, r'^2\, dr'. \tag{7}$$

From (5), using (6) and (7) we have

$$\psi_l(r) = S_l(r) + 4\pi \int_a^\infty F_l(r, r')\, V(r')\, \psi_l(r')\, r'^2\, dr', \tag{8}$$

where

$$S_l(r) = j_l(kr)\, [1 - e^{-\alpha(r-a)} \tan h_l(a) / \tan h_l(r)], \tag{9}$$

in which

$$\tan h_l(r) = j_l(kr) / n_l(kr), \tag{10}$$

$$F_l(r, r') = G_l(r, r') - G_l(a, r')\, G_l(r', a) / G_l(a, a). \tag{11}$$

Since $k_F a < 1$ (for the actual density, $k_F = 1.48 \times 10^{13}$ cm^{-1}; a = 0.4 f), expanding $\tan h_l(a)$ in series in $k_F a$ and stopping with the first terms, we obtain

$$\tan h_0(a) = -k_F a, \quad \tan h_1(a) = -(k_F a)^3/3,$$

$$\tan h_2(a) = -(k_F a)^5 / 45. \tag{12}$$

Starting from the relations we have found, we shall give the condition under which one can, in principle, replace the nuclear interaction of the nucleons by an effective attractive potential. It is obvious that the repulsive core is completely compensated by the attractive potential if the wave function $\psi_l(r)$ can be replaced by the free function $j_l(kr)$. Actually this condition is a sufficient criterion for superfluidity, since we then realize case a) of Sec. 1. We can express the mathematical condition for the criterion formulated above by replacing the quantity $\psi_l(r)$ in (8) by the free wave and multiplying the attractive potential by an as yet undetermined function $K_l(r)$, which we shall find later from the condition that the criterion is satisfied. Using (9), we have

$$j_l(kr) = j_l(kr) - n_l(kr) \tan h_l(a)\, e^{-\alpha(r-a)} + 4\pi K_l(r) \int_a^\infty F_l(r, r')\, V(r')\, j_l(kr') r'^2\, dr'. \tag{13}$$

Then using the properties of the Green's function we get for $K_l(r)$,

$$K_l(r) = n_l(kr) \tan h_l(a)\, e^{-\alpha(r-a)} \Big[4\pi \int_a^\infty \Big\{ G_l(r, r') - \frac{\mu^* k}{4\pi\hbar^2} n_l\ r)\, n_l(r'\ \tan h_l(a)\, e^{-\alpha(r-a)} e^{-\alpha(r'-a)} \Big\} \times V(r')\, j_l(kr')\, r'^2\, dr' \Big]^{-1}. \tag{14}$$

We shall evaluate $K_l(r)$, as given by (14), for two limiting cases: when $a \le r \le r_0$ and when $r \to \infty$. The second case is equivalent to the requirement that the phase of the scattered wave be zero. For the case of $\alpha \neq 0$, the function $K_l(r) \equiv 0$ for $r \to \infty$. When we omit the effect of the Pauli principle ($\alpha = 0$), the value $K_l(r) \to K_l^\infty$, where

$$K_l^\infty = \Big[\frac{\mu^* k}{\hbar^2} \int_a^\infty \{ j_l^2(kr') - \tan h_l(a)\, n_l(kr')\, j_l(kr') \} V(r')\, r'^2\, dr' \Big]^{-1} \times \tan h_l(a). \tag{15}$$

It is obvious that in the intermediate range the value of $K_l(r)$ lies between K_l^0 and K_l^∞. Therefore we should take the larger of these values for the condition for replacement of $\psi_l(r)$ by $j_l(kr)$.

Let us consider the case of $l = 0$. As we see from formula (12), the effect of the repulsive core is largest in this state. For comparison with the work of Cooper, Mills and Sessler,[7] we choose the interaction potential for the nucleons in the form

$$U(r) = \begin{cases} \infty, & r \leqslant a \\ -V_0 e^{-\mu(r-a)}, & r > a \end{cases}, \tag{16}$$

where $a = 0.4$, $V_0 = 26$ Mev, $\mu = 0.544 \times 10^{13}\ \text{cm}^{-1}$. Substituting (16) in (14) and averaging over the region $a \leq r \leq 1/\mu$ for $k = k_F$ and arbitrary α, we get

$$K_0^0(\alpha) \approx 11.2\,\frac{(\mu+\alpha)^2 + 4k_F^2}{\mu^2 + 4k_F^2}\,\frac{1+\mu a}{1+\mu a + 2\alpha a}. \tag{17}$$

$K_0^0(\alpha)$ is a monotonically decreasing function, with

$$K_0^0(0) = 11.2, \quad K_0^0(0.8\,k_F) \approx 9.$$

From this it is clear that the operation of the Pauli principle has little effect on the relation between the attractive and repulsive forces near k_F. For $\alpha = 0$, from (15) we have $K_0^\infty = 2.1$.

The estimate of K_0 which we have given for the potential (16) shows that its attractive part is 9 — 11 times too weak to compensate the repulsion. Moreover, as we shall see in Sec. 3, near k_F, for the state of a pair of identical particles with $l = 0$, the repulsive energy is 2.28 times as great as the energy of attraction. Such nucleons can be kept inside the nucleus only through their interaction with other nucleons having $k \neq k_F$ and with nucleons in triplet states. But for pairs with $k \leq k_F$ and in arbitrary relative states ($T = 0,1$; $S = 0,1$; $l \geq 0$) the introduction of an effective attraction is possible only when condition (14) is satisfied. In particular it seems that this replacement can be made for states near k_F, with $l = 2$, since $K_2^0 = 0.4$.

An attempt to introduce an effective attractive interaction potential between nucleons in the shell model was made by Bauer and Moshinsky.[11] Replacing the effect of the repulsive core by the pseudopotential

$$4\pi a\hbar^2\,\delta(\mathbf{r})/\mu^*, \tag{18}$$

and also replacing the attractive potential V by $-g\delta(\mathbf{r})$, where

$$-g\int \delta(\mathbf{r})\,d\mathbf{r} = \int V(\mathbf{r})\,d\mathbf{r},$$

these authors obtained a total attractive potential of the form

$$-4\pi\hbar^2 a^*\,\delta(\mathbf{r})/\mu^*, \tag{19}$$

where $-a^* = a - g\mu^*/4\pi\hbar^2$. All the estimates in their paper are made with this potential. For the two-particle potentials which are known from scattering experiments, the relation $a^* \approx -a$ holds, so that we can apply (19) for the calculation of the interaction energy of nucleons in nuclear matter, using the formalism of Huang and Yang,[12] who calculated the energy of the repulsive core with the pseudopotential (18). Then the interaction energy has the form

$$U = \frac{\hbar^2 k_F^2}{2\mu^*} A \left\{ a^* k_F\,\frac{2}{\pi} + \frac{12}{35}\pi^2(11 - 2\ln 2)\,(a^* k_F)^2 + \ldots \right\}.$$

The total energy of the system is $E = T + U$, where T is the kinetic energy, and has no minimum for any value of k_F, i.e. a system with such an interaction is unstable.

3. SUPERFLUIDITY OF A SYSTEM OF STRONGLY INTERACTING FERMIONS

Let us apply the apparatus of the Bogolyubov theory to derive the criterion for superfluidity of nuclear matter for the case of realistic nucleon-nucleon interactions. We shall consider only n-n and p-p interactions between pairs with opposite spins and momenta, which are the most important for the appearance of superfluidity.[3] We write the compensation equation, which is equivalent to Eq. (1), for the radial non-symmetric case in the linear approximation:

$$C(k, \Omega_k) = -\frac{1}{2}\frac{1}{(2\pi)^3}\int d\Omega_{k'}\int dk'\,k'^2\,J(k, k') \times C(k', \Omega_{k'})/\sqrt{\Delta^2 + \xi^2(k')}, \tag{20}$$

where the matrix element of the interaction, $J(k, k')$ is defined by the formula

$$J(k, k') = (\psi_k(\mathbf{r}),\ V(\mathbf{r})\,\psi_{k'}(\mathbf{r})). \tag{21}$$

Here $\psi_k(\mathbf{r})$ is the wave function of the relative motion of the pair:

$$\psi_k(\mathbf{r}) = (e^{i\mathbf{kr}} \pm e^{-i\mathbf{kr}})/\sqrt{2}, \tag{22}$$

and the sign $+(-)$ holds for even (odd) states; Δ is the width of the energy gap;

$$\xi(k) = k^2\hbar^2/2\mu^* - k_F^2\,\hbar^2/2\mu^*.$$

We know that the superfluid state appears when there is a nontrivial (i.e., one with $C(k, \Omega) \neq 0$) solution of (20). In the general case, the energy of a single-particle excitation in the superfluid state is given by the formula[1]

$$E_e^s(k) = \sqrt{(E_e^n(k))^2 + C^2(k, \Omega)}.$$

The elementary excitations are separated from the ground state by a gap $\Delta = \min C(k_F, \Omega)$. We expand $C(k, \Omega)$ in spherical harmonics:

$$C(k, \Omega_k) = \sum_{l=0}^{\infty} \sum_{m=-l}^{l} C_{lm}(k) Y_{lm}(\theta_k, \varphi_k). \tag{23}$$

From (20) we get

$$C_{lm}(k) Y_{lm}(\theta_k, \varphi_k) = -\frac{1}{2(2\pi)^3} \int d\Omega_{k'} \int \frac{dk' k'^2}{\sqrt{\Delta^2 + \xi^2(k')}} \times J(k, k') C_{lm}(k') Y_{lm}(\theta_{k'}, \varphi_{k'}). \tag{24}$$

From now on the calculations will be done only for even states (including the odd states does not change the final appearance of the formulas).

We represent $e^{i\mathbf{k}\cdot\mathbf{r}}$ in the form

$$e^{i\mathbf{kr}} = 4\pi \sum_{l} \sum_{m=-l}^{l} i^l j_l(kr) Y^*_{lm}(\theta_k, \varphi_k) Y_{lm}(\theta_r, \varphi_r). \tag{25}$$

For the function of a pair in an even state, we then have

$$\psi_k(\mathbf{r}) = \frac{4\pi}{\sqrt{2}} \sum_{l} \sum_{m=-l}^{l} i^l [1 + (-1)^l] j_l(kr) Y^*_{lm}(\theta_k, \varphi_k) Y_{lm}(\theta_r, \varphi_r). \tag{26}$$

In this case the matrix element of the interaction (22) takes the form

$$J(k, k') = \sum_{l, m} \frac{(4\pi)^2}{2} [1 + (-1)^l]^2 \int_0^{\infty} j_l(kr) j_l(k'r) V(r) r^2 dr Y^*_{lm}(\theta_{k'}, \varphi_{k'}) \times Y_{lm}(\theta_k, \varphi_k). \tag{27}$$

Substituting (27) in (24), we get equation (20) in a new form:

$$C_{lm}(k) = -\frac{1}{2} \int \frac{k'^2 dk'}{\sqrt{\Delta^2 + \xi^2(k')}} K_l(k, k') C_{lm}(k'), \tag{28}$$

where

$$K_l(k, k') = \frac{4}{\pi} \int_0^{\infty} j_l(kr) j_l(k'r) V(r) r^2 dr. \tag{29}$$

Formula (29) enables us to determine $K_l(k, k')$ for any potential, when we replace V by the K matrix calculated disregarding the Pauli principle ($\alpha = 0$). Using the K matrix calculated with the Green's function (3) with $\alpha \neq 0$ leads to no fundamental change in the result.

Since Eq. (28) enables us to find C_{lm} only to within a sign factor, it is also impossible to determine $C(k, \Omega_k)$ in (23) uniquely. We shall therefore choose Δ so that we get Eq. (20) in the radially symmetric case which was treated earlier by Bogolyubov, Tolmachev and Shirkov.[1] To do this we assume that $\Delta = \langle C(k_F, \Omega) \rangle$, where the symbol $\langle \ldots \rangle$ means an average over angles. We then get for the energy gap,

$$\Delta = \frac{1}{4\pi} \int \sum_{l, m} C_{lm}(k_F) Y_{lm}(\theta_k, \varphi_k) d\Omega_k = \frac{1}{\sqrt{4\pi}} C_{00}(k_F). \tag{30}$$

The correction to this value coming from including states with higher l values does not exceed a few percent, because of the smallness of the matrix elements of the interaction in these states.

Let us apply (28) to the solution of the problem of superfluidity of nuclear matter. We consider the case of $l = 0$. First we calculate the matrix element (29) for the potential (16). To get the matrix element for the core potential, we first replace it by a finite barrier of height V_0 and width a, and find the wave functions for a pair, for $r \geq a$ and $r \leq a$:

$$\psi_{\mathrm{I}}(r) = A r^{-1} \sinh \beta r, \qquad r \leqslant a;$$

$$\psi_{\mathrm{II}}(r) = B(kr)^{-1} \{\sin kr - D \cos kr\}, \qquad r \geqslant a, \tag{31}$$

where $\beta = [\mu^* \hbar^{-2} (V_0 - \hbar^2 k_F^2/\mu^*)]^{1/2}$. Matching the solutions at $r = a$ and using the normalization condition, we get for $V_0 \to \infty$:

$$\psi_{\mathrm{I}}(r) = (-1)^p \sinh \beta r / \beta \cosh \beta a, \tag{32}$$

$$\psi_{\mathrm{II}}(r) = (-1)^p (kr)^{-1} \sin k(r - a), \tag{33}$$

where

$$p = \begin{cases} 0, & ka \neq \pi(2n+1)/2 \quad ka \neq n'\pi \\ n, & ka = \pi(2n+1)/2. \\ n', & ka = n'\pi \end{cases} \tag{34}$$

The function ψ_{I} has the property (6) which was used by Brueckner and Gammel.[9] In fact,

$$V_0 \psi_{\mathrm{I}}(r) = \frac{(-1)^p \hbar^2 \beta^2}{\mu^*} \frac{\sinh \beta r}{\beta \cosh \beta a} = \begin{cases} 0, & r < a \\ (-1)^p \hbar^2 \beta / \mu^*, & r = a \end{cases}.$$

Applying (32) to the computation of the matrix element of the core potential gives

$$K_1(k, k') = (-1)^p (4\hbar^2/\mu^* \pi k) \sin ka, \tag{35}$$

where p is determined by the value of k′a. The matrix element (35) for $ka \ll 1$ coincides with the matrix element of the core when calculated with the pseudopotential (18). Since $K_1(k, k')$ from (35) is a discontinuous function having jumps, it cannot be substituted immediately in formula (28). However the analysis of the compensation equation in a form more general than (20) shows that including the points of discontinuity of the matrix element (35) gives a zero contribution to the solution of the equation. We shall therefore in the following consider $K_1(k, k')$ without the factor $(-1)^p$.

The matrix element of the potential (16) under the conditions ka, $k'a \ll \pi/2$ has the form

$$K_2(k, k') = -8V_0\mu/\pi [\mu^2 + (k' - k)^2][\mu^2 + (k' + k)^2]. \tag{36}$$

From (35) and (36) we see that with increasing k and k′, the matrix element K_2 falls off much faster than K_1. In particular they are equal for

$k = k' = 0.71\,k_F$, while for $k = k' \sim 2k_F$ the matrix element K_1 is ten times as great as K_2. We may therefore assume that the attraction exists only over a certain range $0 < k \leq \omega$, $0 < k' \leq \omega$. An estimate gives $K_1(k_F, k_F) = 34.4 \times 10^{-39}$ Mev cm^3 and $K_2(k_F, k_F) = 15 \times 10^{-39}$ Mev cm^3. Thus near k_F the energy of repulsion of the core in the "normal" state is 2.28 times as great as the energy of attraction.

Let us represent the coefficient $C_{00}(k)$ in Eq. (28) for $l = 0$ in the form

$$C_{00}(k) = \begin{cases} C_1(k), & 0 \leqslant k \leqslant \omega \\ C_2(k), & \omega \leqslant k < \infty \end{cases}. \tag{37}$$

For $C_2(k)$, we find from (28),

$$C_2(k) = -(2\hbar^2 \sin ak/\pi\mu^* k)\int_0^\infty dk' C_{00}(k')k'^2/\sqrt{\Delta^2 + \xi^2(k')}. \tag{38}$$

Equation (38) has the solution

$$C_2(k) = -(2\hbar^2 \sin ak/\pi\mu^* kN)\int_0^\omega dk'\, C_1(k')\, k'^2/\sqrt{\Delta^2 + \xi^2(k')}, \tag{39}$$

where

$$N = 1 + (2\hbar^2/\pi\mu^*)\int_a^\infty dk' k' \sin ak'/\sqrt{C^2(k_F) + \xi^2(k')}. \tag{40}$$

Substituting (39) in (28), we obtain an equation for $C_1(k)$. Introducing the quantity $C(k) = C_1(k)/4\pi$, we have

$$C(k) = -\frac{1}{2}\int_0^\omega dk' K(k, k')\, C(k')\, k'^2 \,/\sqrt{C^2(k_F) + \xi^2(k')}. \tag{41}$$

Thus, by choosing the gap in the form $\Delta = \langle C(k_F, \Omega)\rangle$, we have in fact arrived at a radially symmetric equation in Bogolyubov's form. Here in Eq. (41),

$$K(k, k') = K_2(k_1 k') - (2\hbar^2/N\pi\mu^*)\, k^{-1} \sin ak. \tag{42}$$

From formula (42) we see that the matrix element of the repulsion appears in renormalized form because of the slower decrease in k-space of the matrix element of the core potential as compared to the attractive potential. Since $K(k, k')$ is small near k_F (this can be seen from the value of the parameter ρ) we can obtain an approximate formula by using Bogolyubov's formalism:[1]

$$C(k) = \frac{K(k, k_F)}{K(k_F, k_F)}\,\tilde{\omega}\mu e^{-1/\rho}, \quad \rho = \rho_2 - \frac{\rho_1}{N}, \tag{43}$$

where

$$\rho_1 = \frac{2\hbar^2 k_F}{\pi\mu^*}\,\frac{\sin ak_F}{E'(k_F)} = 0.75, \quad \rho_2 = -\frac{K_2(k_F, k_F)\, k_F^2}{E'(k_F)} = -0.31,$$

$$\mu = 2\sqrt{E_F(\hbar^2\omega^2/2\mu^* - E_F)},$$

$$\ln\tilde{\omega} = -\frac{1}{2}\int_0^\omega \frac{d}{dk'}\left[\frac{K(k_F, k')^2 k'^2}{K(k_F, k_F)^2 k_F^2}\right] \times \ln\left[\frac{\xi(k') + \sqrt{C^2(k_F) + \xi^2(k')}}{C(k_F)}\right] dk'. \tag{44}$$

A nontrivial solution of equation (43) exists for $\rho > 0$. In this case we find for the gap Δ,

$$\Delta = C(k_F) = \mu\tilde{\omega}e^{-1/\rho}. \tag{45}$$

The quantity N is of great importance in the solution of the problem of superfluidity. N depends strongly on ω, and the choice of ω is difficult. However the estimate of the matrix elements given above enables us to assume that ω is near to k_F. Then for $k_F < \omega < 1.5\,k_F$, we get $\rho > 0$, and the superfluid state should occur. In this case, for values of ω sufficiently close to k_F, we can obtain a wide gap, in particular $\Delta \sim 1$ Mev (see reference 13). Here we should remember that matrix elements for the nucleus may differ markedly from the matrix elements for nuclear matter.

Thus we here meet an extremely peculiar situation, where in the "normal" state near the Fermi surface the repulsion predominates, but because of renormalization of the core matrix element in the compensation equation, the criterion for superfluidity is nevertheless satisfied. Consequently nuclear matter is superfluid not because of the anticipated presence of an effective attractive interaction in the "normal" state, but rather because of the specific character of the nuclear interactions; here the expansion parameter has a value $\rho \ll 1$, i.e., the condition for convergence of the perturbation series is satisfied.

Let us now show that superfluidity is impossible for a system of He^3 atoms which interact in S states. For the interaction potential of the atoms we again choose the expression (16), but with different values of the parameters;[7]

$$V_0 = 10^\circ\,\mathrm{K}, \qquad \mu = 1.85\,\mathrm{A}^{-1}, \qquad a = 2.5\,\mathrm{A}. \tag{46}$$

In this case, because of the very large value of a, the matrix elements of the attraction must be calculated for distorted waves, i.e., by replacing V by the K matrix in which we disregard the Pauli principle. For the distorted wave in $K_2(k, k')$, we use the function (33) with the parameter values in (46). For the parameters $\mu^* = 1.843$ m and $k_F = 0.735\,\mathrm{A}^{-1}$,[14] the matrix element of the attraction for small k and k′ coincides with (36), while it oscillates for large values of k and k′. We may choose π/a as the width of the well. With these values of the parameters we get $\rho_1 = 1.6$, $\rho_2 = 0.7$, and $N < 1$; consequently $\rho < 0$ and the superfluidity criterion is not satisfied. Thus there is no superfluidity of He^3 in this state.

An investigation of the problem of superfluidity of nuclear matter and of He^3 was carried out by Cooper, Mills, and Sessler[7] using the method of trial functions. On the basis of the potential (16), with the parameters (46) which for He^3 give a good approximation to the exact potential of Brueckner and Gammel,[14] they found the required increase in the attractive potential and analyzed the superfluidity criterion in the form (1).

A comparison of the value $K = 9 - 11$ obtained by us in Sec. 2, with the result of Cooper et al.[7] for nuclear matter ($K = 5 - 7$), shows that these estimates do not differ markedly from one another. This is a consequence of the fact that the estimates in reference 7 were made using trial functions close to the functions of the normal state. These estimates somewhat overestimate the role of the repulsive core, whose influence in the superfluid state is drastically suppressed as a result of the renormalization. In the case of He^3, the estimate of reference 7 coincides with ours, even though it was actually made with the same omissions as in the case of nuclear matter.*

The similarity of the results obtained here to the results of Brenig[4] confirms the arguments made in the Introduction concerning the applicability of Bogolyubov's method (with the modifications made above) to the investigation of the problem of superfluidity of nuclear matter, and enables us to understand better the mechanism of appearance of the superfluid state.

[1] Bogolyubov, Tolmachev, and Shirkov, Новый метод в теории сверхпроводимости (New Method in the Theory of Superconductivity) Press of Academy of Sciences, U.S.S.R., 1958; translation, Consultants' Bureau, 1959.

[2] V. G. Solov'ev, Doklady Akad. Nauk SSSR **123**, 437 (1958); JETP **35**, 823 (1958); Soviet Phys. Doklady **3**, 1197 (1958); Soviet Phys. JETP **8**, 572 (1959).

[3] B. B. Dotsenko, Izv. Akad. Nauk SSSR, Ser. Fiz. **23**, 914 (1959), Columbia Tech. Transl. p. 901.

[4] W. Brenig, Z. Physik **156**, 525 (1959).

[5] K. A. Brueckner and C. A. Levinson, Phys. Rev. **97**, 1344 (1955).

[6] H. A. Bethe, Phys. Rev. **103**, 1353 (1956).

[7] Cooper, Mills and Sessler, Phys. Rev. **114**, 1377 (1959).

[8] J. L. Gammel and R. Thaler, Phys. Rev. **107**, 291, 1337 (1958).

[9] K. A. Brueckner and J. L. Gammel, Phys. Rev. **109**, 1023 (1958).

[10] Gomes, Walecka, and Weisskopf, Annals of Physics **3**, 241 (1958).

[11] M. Bauer and M. Moshinsky, Nuclear Phys. **4**, 615 (1957).

[12] K. Huang and C. N. Yang, Phys. Rev. **105**, 767 (1957).

[13] Bohr, Mottelson, and Pines, Phys. Rev. **110**, 936 (1958).

[14] K. A. Brueckner and J. L. Gammel, Phys. Rev. **109**, 1040 (1958).

[15] R. L. Mills et al., Phys. Rev. Letters **3**, 381 (1959).

Translated by M. Hamermesh
31

---

*Our attention was called recently to a paper in which the same authors, through a choice of modified trial functions, concluded that nuclear matter can be superfluid.[15]

SOVIET PHYSICS JETP VOLUME 13, NUMBER 1 JULY, 1961

EXACT SOLUTION OF THE BASIC CASCADE THEORY EQUATIONS

V. S. SYNAKH

Submitted to JETP editor July 8, 1960

J. Exptl. Theoret. Phys. (U.S.S.R.) 40, 194-198 (January, 1961)

Exact numerical solutions of the basic cascade theory equations, obtained by the functional transformation method, are given for small depths (up to two radiation lengths).

IT is well known (see reference 1) that the initial equations of the cascade theory can be written in the form

$$\frac{\partial P(t, E)}{\partial t} = 2\int_E^\infty \Gamma(t, E') W_p(E', E)\, dE' + \int_E^\infty P(t, E') W_e(E', E' - E)\, dE' - \int_0^E P(t, E) W_e(E, E')\, dE', \tag{1a}$$

$$\frac{\partial \Gamma(t, E)}{\partial t} = \int_E^\infty P(t, E') W_e(E', E)\, dE' - \int_0^E \Gamma(t, E) W_p(E, E')\, dE'. \tag{1b}$$

Here t is the depth in radiation lengths, $P(t, E)dE$ is the total number of electrons and positrons in the energy interval $(E, E + dE)$ at a depth t; $\Gamma(t, E)$ is the analogous distribution function for the photons, $W_p(E'\ E)dE$ is the probability per radiation length of creation of a pair with a positron energy in the interval $(E, E + dE)$ from a photon of energy E' and $W_e(E, E')dE'$ is the probability of an electron or positron of energy E emitting a bremsstrahlung quantum in the interval $(E', E' + dE')$, also per radiation length.

The functions W_e and W_p have in the Born approximation, with allowance for the nuclear field only in the ultrarelativistic limit for large collision parameters which are of importance in this case, the following form[2]

$$W_e(E, E')\, dE' = [1 + (1 - E'/E)^2 - \tfrac{2}{3}(1 - E'/E)]\, dE', \tag{2a}$$

$$W_p(E', E)\, dE = [(E/E')^2 + (1 - E/E')^2 + \tfrac{2}{3}(E/E')(1 - E/E')]\, dE/E'. \tag{2b}$$

In writing down the system (1) we have disregarded the Compton effect and the photoeffect for photons, the Rutherford scattering for positrons and electrons, pair annihilation, and other processes which are not significant at high energies. The pair production and bremsstrahlung in the field of the atomic electrons is disregarded in (2). The contribution of the atomic electrons does not exceed 1% of all the effects in the case of heavy elements.

To solve the system of integro-differential equations (1), it is customary to use either the method of functional transformations or the method of moments (see reference 3). The latter is approximate in nature and has limited application. As regard the method of functional transformations, it does permit, in principle, to obtain all the quantities of interest, but the resultant expressions can be calculated analytically only when $t > 1$. In the present paper we obtain exact numerical values for the system (1) in the range of thicknesses up to $t = 2$.

As was shown, for example, in the review by Belen'kiĭ and Ivanenko,[3] the solution of system (1) with the aid of the Laplace-Mellin transformation, subject to the boundary conditions

$$P(t = 0, E) = \delta(E - E_0), \qquad \Gamma(t = 0, E) = 0$$

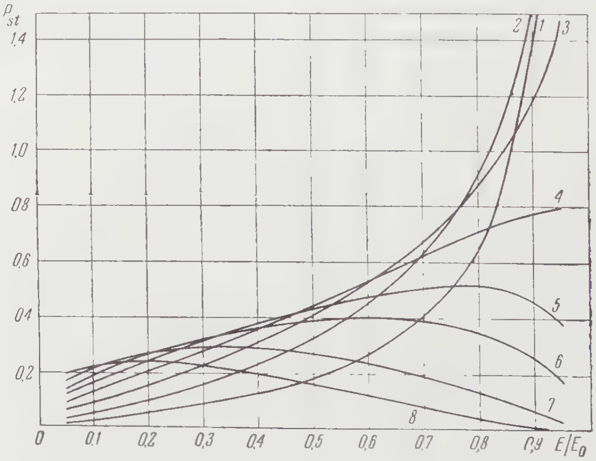

FIG. 1. The P'_{st} curves correspond to the following values of t: 1 – 0.2, 2 – 0.4, 3 – 0.6, 4 – 0.8, 5 – 1.0, 6 – 1.2, 7 – 1.6, 8 – 2.0.

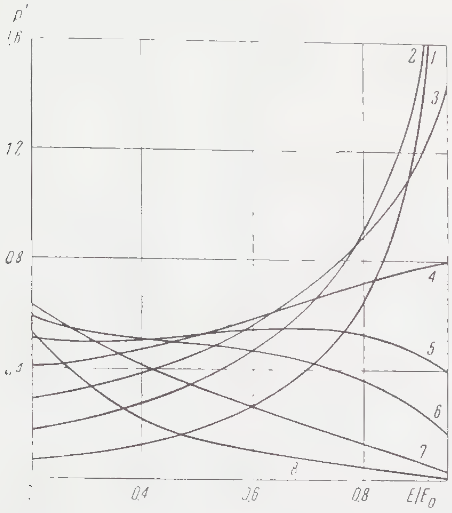

FIG. 2. The P′ curves correspond to the same values of t as in Fig. 1.

has the form

$$P(t,E)=\frac{1}{2\pi iE}\int\limits_{\delta-i\infty}^{\delta+i\infty}\left(\frac{E_0}{E}\right)^s\left[\frac{\sigma+\lambda_1}{\lambda_1-\lambda_2}e^{\lambda_1 t}-\frac{\sigma+\lambda_2}{\lambda_1-\lambda_2}e^{\lambda_2 t}\right]ds,$$

$$\Gamma(t,E)=\frac{1}{2\pi iE}\int\limits_{\delta-i\infty}^{\delta+i\infty}\left(\frac{E_0}{E}\right)^s\frac{C(s)}{\lambda_1-\lambda_2}\left(e^{\lambda_1 t}-e^{\lambda_2 t}\right)ds \qquad (3)$$

and explicit expressions for the functions $\lambda_1(s)$, $\lambda_2(s)$, and $C(s)$ are given, for example, in the book by Belen'kiĭ.[1]

Here σ is the coefficient of γ-quantum absorption. As usual, it is assumed that σ is equal to its ultrarelativistic limit, $\sigma = 0.773$. The integration in (3) is in the complex plane along a straight line parallel to the imaginary axis, subject to the condition $\delta > 0$.

Cascade theory deals also with the quantity $N(t, E)$, i.e., the total number of electrons and positrons at a depth t with energy greater than E:

$$N(t,E)=\int\limits_{E}^{\infty}P(t,E)\,dE=\frac{1}{2\pi i}\int\limits_{\delta-i\infty}^{\delta+i\infty}\left(\frac{E_0}{E}\right)^s\left[\frac{\sigma+\lambda_1}{\lambda_1-\lambda_2}e^{\lambda_1 t}-\frac{\sigma+\lambda_2}{\lambda_1-\lambda_2}e^{\lambda_2 t}\right]\frac{ds}{s}. \qquad (4)$$

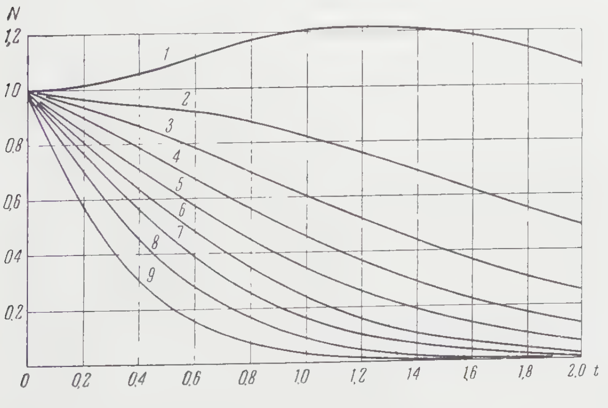

FIG. 3. The N curves correspond to the following values of E/E₀: 1 – 0.1, 2 – 0.2, 3 – 0.3, 4 – 0.4, 5 – 0.5, 6 – 0.6, 7 – 0.7, 8 – 0.8, 9 – 0.9.

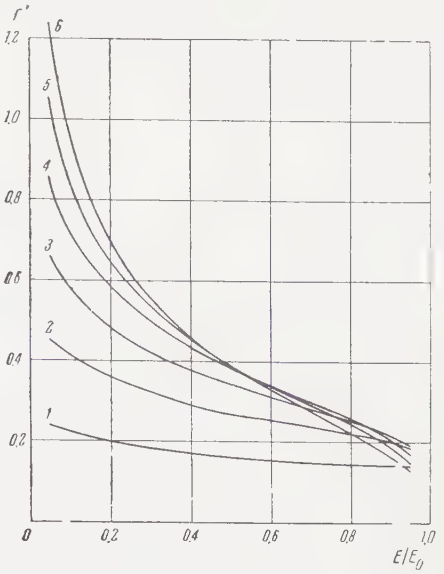

FIG. 4. The Γ′ curves correspond to the following values of t: 1 – 0.2, 2 – 0.4, 3 – 0.6, 4 – 0.8, 5 – 1.0, 6 – 1.2.

The energy distribution of the initial electrons after passing through a layer of thickness t is also of interest. It is found that the well known Bethe-Heitler expression[2] for the probability that an electron with initial energy E_0 will have an energy between E and $E + dE$ after passing through a thickness t

$$P_{st}^{\text{Б}-\Gamma}(t,E)\,dE=\frac{dE}{E_0}\left(\ln\frac{E_0}{E}\right)^{t/\ln 2-1}\Big/\,\Gamma\left(\frac{t}{\ln 2}\right), \qquad (5)$$

is a rather rough approximation.

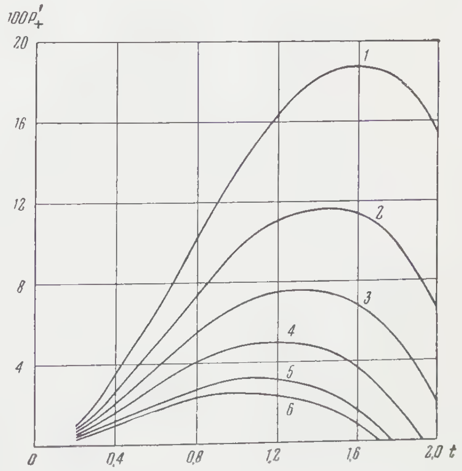

FIG. 5. The P'_+ curves correspond to the following values of E/E₀: 1 – 0.2, 2 – 0.3, 3 – 0.4, 4 – 0.5, 5 – 0.6, 6 – 0.7.

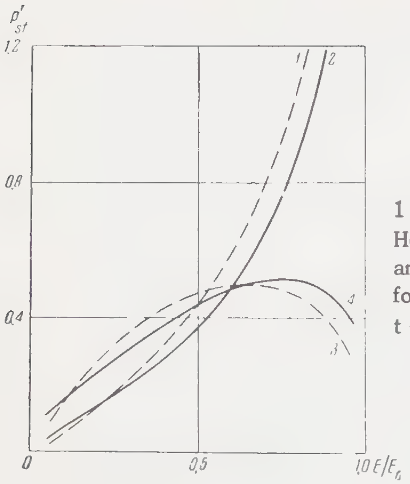

FIG. 6. Curves P'_{st}: 1 and 3 – from the Bethe-Heitler formula (5), 2 and 4 – from (7). t = 0.5 for curves 1 and 2, and t = 1 for curves 3 and 4.

In order to obtain an equation for P_{st} within the framework of the cascade theory, it is evidently sufficient to retain in the right half of (1a) only the terms that describe the radiation retardation

$$\frac{\partial P_{st}(t, E)}{\partial t} = \int_{E}^{\infty} P_{st}(t, E) W_e(E', E' - E)\, dE' - \int_{0}^{E} P_{st}(t, E) W_e(E, E')\, dE', \qquad (6)$$

from which we readily obtain with the aid of the Laplace-Mellin transformation

$$P_{st}(t, E) = \frac{1}{2\pi i E} \int_{\delta - i\infty}^{\delta + i\infty} \left(\frac{E_0}{E}\right)^s e^{-A(s)t}\, ds. \qquad (7)$$

(for an explicit expression for A(s) see reference 1.)

From (3) and (7) we readily obtain the energy distribution function P_+ of the secondary electrons (positrons) at a depth t:

$$P_+(t, E_+) = \tfrac{1}{2}[P(t, E_+) - P_{st}(t, E_+)]. \qquad (8)$$

The expressions given for P, P_{st}, P_+, N, and Γ have been calculated with an electronic computer accurate to ~1%. The results are shown in Figs. 1 – 6. The plots are given for the "primed" quantities, which are more convenient for calculation. The latter are defined, for example, as $P(t, E) = P'(t, E)\,dE/E$, etc. The energy is measured everywhere in units of the initial energy E_0.

In conclusion, the author expresses his gratitude to Z. D. Dobrokhotova and B. I. Shitikov for help in the solution of the problem, to G. I. Budker and V. N. Baĭer for a discussion of the results, and to L. Dobrovinskaya for help in preparing the diagrams.

---

[1] S. Z. Belen'kiĭ, Лавинные процессы в космических лучах (Cascade Processes in Cosmic Rays), Gostekhizdat, 1948.

[2] W. Heitler, The Quantum Theory of Radiation, Oxford, 1954.

[3] S. Z. Belen'kiĭ and I. P. Ivanenko, Usp. Fiz. Nauk **69**, 591 (1959), Soviet Phys. Uspekhi **2**, 912 (1960).

Translated by J. G. Adashko
32

SOVIET PHYSICS JETP VOLUME 13, NUMBER 1 JULY, 1961

ON THE THEORY OF THE ELECTRICAL CONDUCTIVITY OF SEMICONDUCTORS IN A MAGNETIC FIELD. I

V. L. GUREVICH and Yu. A. FIRSOV

Semiconductor Institute, Academy of Sciences, U.S.S.R.

Submitted to JETP editor July 8, 1960

J. Exptl. Theoret. Phys. (U.S.S.R.) 40, 198-213 (January, 1961)

We have developed a quantum theory of the transverse conductivity of semiconductors in a strong magnetic field, taking the inelastic scattering of the electrons into account. If the interaction between the electrons and the scatterers is treated in the Born approximation, we obtain a formula for the conductivity in terms of an integral of the retarded two-particle Green's function of the electron system in a magnetic field. We study this formula for the case where the electrons obey Boltzmann statistics and where one may neglect the influence of their mutual Coulomb interaction on the conductivity. We consider both the classical and the quantum regions of magnetic fields and scattering both by acoustical and by optical phonons. By comparing the results obtained through solving the transport equation with those from quantal calculations in the classical region we show that in practically the whole of that region one can apply the transport equation, with a collision operator which is independent of the magnetic field. We determine the dependence of the transverse low-temperature resistivity, which is caused by the scattering by optical phonons, on the magnetic field. It turns out that it may be a step function with many steps. We obtain in the quantum region equations for the transverse conductivity in different limiting cases. We predict theoretically resonance oscillations in the conductivity which are periodic in 1/H and which are connected with the scattering by optical phonons. Maxima in the oscillations may occur when the limiting frequency of the optical phonons is a multiple of the Larmor frequency. In the classical region the oscillations are a small quantum correction to the conductivity, but they are relatively large in the quantum region.

ADAMS and Holstein[1] developed a theory of the electrical conductivity in a quantized magnetic field by solving directly the equations for the density matrix. They considered a number of different scattering mechanisms, using the Born approximation and assuming the scattering to be elastic. Argyres and Roth[2] used a similar method to study inelastic scattering. They obtained a formula for the transverse conductivity which was a sum over the electron quantum numbers in the magnetic field, but they did not analyze this formula.

It is the aim of the present paper to ascertain the influence of the inelasticity of the scattering on transport phenomena in a strong magnetic field. We restrict ourselves to Boltzmann statistics and consider two characteristic cases: 1) scattering by acoustical phonons where the inelasticity is small and leads to relatively small effects, and 2) scattering by polarized optical vibrations, when account of the inelasticity may change all the characteristic dependences.

We shall call a magnetic field "strong" when the ratio of the diagonal element of the transverse conductivity tensor to its off-diagonal element satisfies the inequality

$$\sigma_{xx}/\sigma_{xy} \ll 1. \tag{1}$$

Only when inequality (1) is satisfied does there exist a small parameter which allows us to write the expressions for σ_{xx} and σ_{xy} as expansions in powers of the scattering potential. Such expansions can, of course, occur only when the Born approximation can be applied. If, however, inequality (1) is not satisfied, it is, generally speaking, impossible to expand the expression for σ_{xx} in a series of ascending powers in the scattering potential, even if the Born approximation is applicable.

We shall differ from references 1 and 2 in starting from Kubo's formula[3] for the transverse conductivity in a magnetic field. It allows us to express σ_{xx} in terms of the electron Green's function in a magnetic field and saves us thereby from unpleasant summations (see, for instance, reference 2). Also, such a method is very general and makes it, for instance, possible to take the Coulomb interaction of the electrons into account.

The range of strong fields includes the classical region where $\alpha = \hbar\Omega/2kT \ll 1$ (Ω is the Larmor frequency, T the temperature) and the quantum region where $\alpha \gtrsim 1$. Although the Boltzmann transport equation can be applied in the first region, we shall use there also quantum calculations. Quantum methods are the only ones which can be applied in the second region.

We have compared in all cases the results from the calculations using Kubo's formula in the classical region with those obtained by solving the transport equation. This has allowed us to ascertain when the collision operator in the transport equation can be assumed to be independent of the magnetic field. It turns out that for the electron-phonon interaction this is possible in practically the whole of the classical region studied.

Since we were not aware of any paper in which the transport equation was solved for the case of electrons scattered in a magnetic field by optical phonons at low temperatures, we solved it in the present paper. We discovered as a result that the plot of the function $\sigma_{xx}(H)$ can consist in this case of two horizontal regions and two steeply drooping regions.

We also evaluated the quantum corrections to σ_{xx} in the classical region. It turns out that when the scattering is by optical phonons these can oscillate and go through a maximum whenever the limiting frequency of the optical vibrations ω_0 is a multiple of the Larmor frequency. These oscillations are periodic in the reciprocal of the field, but in contrast to all other known types of oscillations of the static conductivity, they occur in the case of Boltzmann statistics.

In the quantum region we found the dependence $\sigma_{xx}(H)$ for the case where $\Omega \gg \omega_0$ and where the scattering is by acoustical and optical phonons; this dependence is the same as the one obtained by Adams and Holstein,[1] apart from a logarithmic factor. In the case $\omega_0 \gg \Omega$, where we could not use the methods of Adams and Holstein, we discovered a non-monotonic oscillatory dependence for $\sigma_{xx}(H)$. As in the classical case, σ_{xx} goes through a maximum when the frequency ω_0 is a multiple of Ω, but what is a small correction in the classical limit is part of the main effect in the quantum region.

We studied the oscillations in the classical and the quantum regions for the case of scattering by optical phonons in ionic crystals. It is, however, clear that this effect is caused solely by the presence of a limiting phonon frequency and is independent of the details of the electron-phonon interaction. It can therefore, for instance, also be observed in the case of scattering by optical phonons in atomic semiconductors such as germanium.

1. We shall assume that the electron dispersion law is quadratic and isotropic and that the magnetic field is along the z axis. Kubo's formula, which expresses σ_{xx} in terms of the velocity operators of the motion of the center of the Landau oscillator, is of the form

$$\sigma_{xx} = (e^2\beta / 2V_0) \int_{-\infty}^{\infty} dt \, \mathrm{Sp} \, [e^{\beta F - \beta(\mathcal{H} - \mu N)} \hat{\dot{X}}(t) \hat{\dot{X}}(0)]$$

$$\equiv (e^2\beta / 2V_0) \int_{-\infty}^{\infty} dt \, \langle \hat{\dot{X}}(t) \hat{\dot{X}}(0) \rangle. \tag{2}$$

Here $\beta = 1/kT$, μ is the chemical potential, $\mathcal{H} = \mathcal{H}_e + \mathcal{H}_{sc} + U$, U is the electron-scatterer interaction potential, $\mathcal{H}_{sc}$ is the Hamiltonian of the scatterers, $\mathcal{H}_e$ is the Hamiltonian of the system of electrons including their mutual interaction,

$$\hat{\dot{X}}(t) = e^{i\mathcal{H}t/\hbar} \hat{\dot{X}}(0) e^{-i\mathcal{H}t/\hbar}, \tag{3}$$

V_0 is the normalization volume, N is the particle number operator, and $e^{-\beta F} = \mathrm{Tr}\, e^{-\beta(\mathcal{H} - \mu N)}$. The operator $\hat{X}$ commutes with the Hamiltonian of the free electrons in a magnetic field. One can show by straightforward calculation that $\hat{X}$ commutes also with the electron-electron interaction operator, and this reflects the law of conservation of momentum during two-body collisions. Using the equations of motion we get from this (see reference 3)

$$\hat{\dot{X}} = \sum_{\sigma} \int \psi^*(\mathbf{r}, \sigma) \frac{i}{\hbar} [\mathcal{H}, \hat{X}] \psi(\mathbf{r}, \sigma) \, d^3\mathbf{r}$$

$$= \frac{c}{eH} \sum_{\sigma} \int \psi^*(\mathbf{r}, \sigma) \frac{\partial U}{\partial y} \psi(\mathbf{r}, \sigma) \, d^3\mathbf{r}. \tag{3a}$$

Here σ is the spin variable and

$$\psi(\mathbf{r}, \sigma) = \sum_{\lambda s} a_{\lambda s} \psi_{\lambda s}(\mathbf{r}, \sigma)$$

is the second-quantized electron wave function. The index λ labels the orbital states of the electron and when we choose the gauge $\mathbf{A} = (0, Hx, 0)$ it indicates the totality of the quantum numbers p_z, n, and X; s is the z-component of the electron spin. In the chosen gauge $X = i(c\hbar/eH)\partial/\partial y$.

The electron-phonon interaction operator U is of the form where

$$U(\mathbf{r}) = \sum_{\mathbf{q}} (c_{\mathbf{q}} b_{\mathbf{q}} e^{i\mathbf{qr}} + c_{\mathbf{q}}^* b_{\mathbf{q}}^+ e^{-i\mathbf{qr}}), \tag{4}$$

$b_{\mathbf{q}}$ and $b_{\mathbf{q}}^+$ are the creation and annihilation operators for phonons with wave vector $\mathbf{q}$. For acoustical phonons

$$|c_{\mathbf{q}}|^2 = E_0^2 \hbar q / 2V_0 \rho w. \tag{5}$$

For optical phonons (in polar crystals)

$$|c_{\mathbf{q}}|^2 = A / q^2 V_0, \tag{6}$$

where according to Davydov and Shmushkevich[4]

$$A = 4\pi^2 \hbar (Ze^2 \gamma / a_0)^2 / M a_0 \omega_0, \tag{7a}$$

and according to Krivoglaz and Pekar[5]

$$A = 2\pi\hbar\omega_0 e^2 (1/\varepsilon_\infty - 1/\varepsilon_0). \tag{7b}$$

Here E_0 is the deformation potential constant, ρ the density of the crystal, w the sound velocity, Ze the ion charge, a_0 the distance between neighboring ions, γ the dimensionless constant in the ionic polarizability, M the mass in an elementary cell, ω_0 the limiting frequency of the optical vibrations, and ϵ_0 and ϵ_∞ the dielectric constant of the crystal with and without taking the ionic contribution into account. We shall assume that the frequency of the optical phonons is independent of q and that the frequency of the acoustical phonons is equal to wq.

We restrict ourself to the second approximation in U. After substituting (3) and (4) into (2) we can then replace in the exponents $\mathscr{H}$ by $\mathscr{H}_e + \mathscr{H}_{sc}$ and average over the phonon variables. Writing the remaining term as a sum over the states of the whole of the electron system, we get as the result

$$\sigma_{xx} = \frac{\pi e^2 \beta}{(2\pi)^3} \left(\frac{c}{eH}\right)^2 \int d^3\mathbf{q}\, q_y^2 |c_{\mathbf{q}}|^2 [N_{\mathbf{q}} \Phi_{\mathbf{q}}(\omega_{\mathbf{q}})$$
$$+ (N_{\mathbf{q}} + 1) \Phi_{-\mathbf{q}}(-\omega_{\mathbf{q}})], \tag{8}$$

where $N_q = [\exp(\hbar\omega_q/kT) - 1]^{-1}$, and

$$\Phi_{\mathbf{q}}(\omega) = \hbar \sum_{m,\,n} \exp\{\beta F - \beta(E_n - \mu N_n)\} \delta(\hbar\omega - E_m + E_n)$$
$$\times \Big|\sum_{\lambda\lambda'} \sum_{ss'} \Delta_{\lambda s,\,\lambda' s'}(\mathbf{q}) \langle n | a_{\lambda s}^{+} a_{\lambda' s'} | m\rangle\Big|^2, \tag{9}$$

$$\Delta_{\lambda s,\,\lambda' s'}(\mathbf{q}) = \sum_{\sigma} \int \psi_\lambda^*(\mathbf{r}, \sigma) e^{i\mathbf{q}\mathbf{r}} \psi_{\lambda'}(\mathbf{r}, \sigma)\, d^3\mathbf{r}\, \delta_{ss'}; \tag{10}$$

m and n label the states of the total electron system, and $E_n = (\mathscr{H}_e)_{nn}$.

To evaluate $\Phi_q(\omega)$ we establish the connection between it and the two-particle retarded Green's function with the coordinates pairwise equal, summed over the spin variables:

$$K(\mathbf{r},\mathbf{r}',t) = \begin{cases} i \sum\limits_{\sigma,\,\sigma'} \langle [\psi^+(\mathbf{r}, \sigma, t)\psi(\mathbf{r}, \sigma, t), \psi^+(\mathbf{r}', \sigma', 0)\psi(\mathbf{r}', \sigma', 0)]\rangle, & t > 0 \\ 0, & t < 0 \end{cases} \tag{11}$$

(the symbol [. . . , . . .] indicates a commutator).

Writing as before the trace of (11) as a sum over the states of the electron system, one finds easily the following relation

$$K_{\mathbf{q}}(\omega) = \int_{-\infty}^{\infty} dt\, e^{(i\omega - \nu)t} \int d^3\mathbf{r} \int d^3\mathbf{r}' e^{-i\mathbf{q}(\mathbf{r}-\mathbf{r}')} K(\mathbf{r}, \mathbf{r}', t)$$
$$= \int_{-\infty}^{\infty} d\omega' \Phi_{\mathbf{q}}(\omega')(1 - e^{-\hbar\omega'\beta})(\omega' - \omega - i\nu)^{-1}, \tag{12}$$

where $\nu > 0$, $\nu \to 0$. Since $\Phi_q(\omega)$ is real, we get from this

$$\Phi_{\mathbf{q}}(\omega) = \operatorname{Im} K_{\mathbf{q}}(\omega) / \pi (1 - e^{-\hbar\omega\beta}). \tag{13}$$

Larkin[6] found an expression for $K_q(\omega)$ for a system of interacting electrons for the case $H = 0$. Larkin's method can easily be generalized to the case where $H \neq 0$. We can thus evaluate the screening of phonon potential. This problem will be considered separately. In the present paper we shall not take the interaction between the electrons into account.

In the zeroth approximation in the interaction*

$$K^0(\mathbf{r}, \mathbf{r}', t) = i \sum_{\lambda\lambda'} \sum_{s} \exp\{i(\varepsilon_{\lambda s} - \varepsilon_{\lambda' s}) t/\hbar\} \psi_\lambda^*(\mathbf{r}) \psi_{\lambda'}(\mathbf{r})$$
$$\times \psi_{\lambda'}^*(\mathbf{r}') \psi_\lambda(\mathbf{r}') (n_{\lambda s} - n_{\lambda' s}). \tag{14}$$

Here $\epsilon_{\lambda s}$ is the energy of an electron in the state with quantum numbers λ and s; $n_{\lambda s}$ is the Fermi function of $\epsilon_{\lambda s}$.

For the case of Boltzmann statistics $n_{\lambda s} = \exp\{\beta(\mu - \epsilon_{\lambda s})\}$ and one can sum over λ. This leads to

$$K^0(\mathbf{r}, \mathbf{r}', t) = 2i \cosh(\hbar\Omega_0\beta/2) [G(\mathbf{r}', \mathbf{r}, \beta$$
$$- it/\hbar) G(\mathbf{r}, \mathbf{r}', it/\hbar) - G(\mathbf{r}', \mathbf{r}, -it/\hbar)$$
$$\times G(\mathbf{r}, \mathbf{r}', \beta + it/\hbar)], \tag{15}$$

where according to Sondheimer and Wilson[7]

$$G(\mathbf{r}, \mathbf{r}', \gamma) = \sum_\lambda \psi_\lambda^*(\mathbf{r}') \psi_\lambda(\mathbf{r}) e^{-\gamma\varepsilon_\lambda}$$
$$= e^{i\varphi(\mathbf{r}, \mathbf{r}')} \left(\frac{m}{2\pi\hbar^2\gamma}\right)^{3/2} \frac{\eta}{\sinh\eta} \exp\left\{-\frac{m}{2\hbar^2\gamma}[\eta\coth\eta(\Delta x^2\right.$$
$$\left. + \Delta y^2) + \Delta z^2]\right\}. \tag{16}$$

Here $\Delta x = x - x', \ldots, \eta = \hbar\Omega\gamma/2$, γ is an arbitrary complex number ($\operatorname{Re}\gamma \geq 0$), $\Omega = eH/mc$, $\Omega_0 = eH/m_0c$, m is the effective electron mass, and m_0 is the mass of a free electron. The phase factor φ depends on the choice of gauge but always satisfies the equation

$$\varphi(\mathbf{r}, \mathbf{r}') + \varphi(\mathbf{r}', \mathbf{r}) = 0, \tag{17}$$

because $K^0(\mathbf{r}, \mathbf{r}', t)$ depends only on the difference $\mathbf{r} - \mathbf{r}'$.

Evaluating the Fourier component of $K^0(\mathbf{r} - \mathbf{r}', t)$ with respect to both the coordinates and the time, we find that

---

*Expression (14) is linear in $n_{\lambda s}$. This enables us to write the conductivity for the case of Fermi statistics in an integral in the complex β plane of the conductivity for the case of Boltzmann statistics (see the papers by Rumer[8]).

$$K_{\mathbf{q}}^{0}(\omega)=2nV_0\int_0^\infty dte^{(i\omega-\nu)t}\sin\left(\frac{\hbar q_z^2}{2m}t+\frac{\hbar q_\perp^2}{2m\Omega}\sin\Omega t\right)$$
$$\times\exp\left(-\frac{q_z^2}{2m\beta}t^2-\frac{\hbar^2 q_\perp^2\beta}{2m\alpha}\coth\alpha\sin^2\frac{\Omega t}{2}\right). \qquad (18)$$

Here $q_\perp^2 = q_x^2 + q_y^2$; n is the electron concentration in a magnetic field, and is equal to

$$n=2\cosh\left(\frac{\hbar\Omega_0\beta}{2}\right)\frac{\alpha}{\operatorname{sh}\alpha}\left(\frac{m}{2\pi\hbar^2\beta}\right)^{3/2}e^{\beta\mu}. \qquad (19)$$

Bonch-Bruevich and Mironov[9] obtained the function (18) using a different method.

2. We study the expression for the imaginary part of (18), which determines σ_{xx} by virtue of (8) and (13). As $H \to 0$ we can write the integral over t in closed form and get

$$\operatorname{Im}K_{\mathbf{q}}^{0}(\omega)=\frac{\sqrt{\pi}\,nV_0}{qv_T}\left(1-e^{-\hbar\omega\beta}\right)\exp\left[\frac{\hbar\omega\beta}{2}-\frac{\omega^2}{q^2v_T^2}-\frac{\hbar^2q^2}{8mkT}\right], \qquad (20)$$

where $v_T = \sqrt{2kT/m}$ is the thermal velocity of the electron. This function was obtained by Larkin.[6] We shall use it to evaluate σ_{xx} in the classical region.

For calculations in the quantum region it is convenient to use another form for $\operatorname{Im} K_{\mathbf{q}}^0(\omega)$, which we shall obtain now. Writing the product of two sine terms in the expression for the imaginary part of (18) as the sum of products of four exponentials, we find that

$$\operatorname{Im}K_{\mathbf{q}}^{0}(\omega)=\frac{nV_0}{\Omega}\exp\left\{-\frac{\hbar^2q_\perp^2\beta\coth\alpha}{4m\alpha}\right\}\operatorname{Re}\left[L(\omega)-L(-\omega)\right], \qquad (21)$$

$$L(\omega)=\int_0^\infty dx\exp\left\{-\frac{q_z^2v_T^2}{4\Omega^2}x^2+\frac{\hbar^2q_\perp^2\beta\coth\alpha}{4m\alpha}\cos x\right.$$
$$\left.+i\left(\frac{\hbar q_z^2}{2m\Omega}-\frac{\omega}{\Omega}\right)x+i\frac{\hbar q_\perp^2}{2m\Omega}\sin x\right\}. \qquad (22)$$

We changed here to a new integration variable $x = \Omega t$.

Using the well-known formula

$$\exp\left[\tfrac{1}{2}iz\left(t-1/t\right)\right]=\sum_{N=-\infty}^{\infty}i^N I_N(z)\,t^N, \qquad (23)$$

we get the relation

$$\exp\left(\frac{\hbar^2q_\perp^2\beta\coth\alpha}{4m\alpha}\cos x+i\frac{\hbar q_\perp^2}{2m\Omega}\sin x\right)$$
$$=\sum_{N=-\infty}^{\infty}e^{\alpha N+iNx}I_N\left(\frac{q_\perp^2a^2}{2\sinh\alpha}\right), \qquad (24)$$

and we can use this to write the real part of the integral (22) easily in the form

$$\operatorname{Re}L(\omega)=\sum_{N=-\infty}^{\infty}e^{\alpha N}I_N\left(\frac{q_\perp^2a^2}{2\sinh\alpha}\right)\operatorname{Re}\int_0^\infty dx\exp\left\{-\frac{q_z^2v_T^2}{4\Omega^2}x^2\right.$$
$$\left.+i\left(\frac{\hbar q_z^2}{2m\Omega}+N-\frac{\omega}{\Omega}\right)x\right\}=\frac{\sqrt{\pi}\,\Omega}{|q_z|v_T}\sum_{N=-\infty}^{\infty}e^{\alpha N}I_N\left(\frac{q_\perp^2a^2}{2\sinh\alpha}\right)$$
$$\times\exp\left\{-\left(\frac{\hbar q_z^2}{2m}+N\Omega-\omega\right)^2\Big/q_z^2v_T^2\right\}, \qquad (25)$$

where $a^2 = c\hbar/eH$. Substituting (25) into (21), replacing in the second term N by − N, and using (13) we get finally

$$\Phi_{\mathbf{q}}^{0}(\omega)=\frac{nV_0}{\sqrt{\pi}\,|q_z|v_T}\exp\left(\frac{\hbar\omega\beta}{2}-\frac{q_\perp^2a^2\coth\alpha}{2}\right)\sum_{N=-\infty}^{\infty}I_N\left(\frac{q_\perp^2a^2}{2\sinh\alpha}\right)$$
$$\times\exp\left\{-\frac{(N\Omega-\omega)^2}{q_z^2v_T^2}-\frac{\hbar^2q_z^2}{8mkT}\right\}. \qquad (26)$$

3. It can be seen from the initial equations (2) and (3) that in the second approximation in U, in which all calculations have been made, the different scattering mechanisms do not interfere with one another. The total transverse conductivity is thus a sum of the conductivities related to the various scattering mechanisms, and it is sufficient to evaluate separately each of the terms in this sum.

We start with the solution of the simplest problem: the calculation of the conductivity in the quantum region. First we consider scattering by acoustical phonons. One can see from Eq. (26) that the main contribution to the interaction with the electrons comes from the phonons with wave vectors $q \lesssim 1/a$. We shall assume that for $q \sim 1/a$ the inequality

$$(\hbar\omega/kT)^2\sim(\hbar w/akT)^2\sim\alpha mw^2/kT\ll 1 \qquad (27)$$

which is usually experimentally satisfied, is still satisfied. If (27) is valid we can write

$$N_{\mathbf{q}}\approx N_{\mathbf{q}}+1\approx kT/\hbar\omega_{\mathbf{q}}. \qquad (27a)$$

We substitute (5), (26), and (27a) into (8) and integrate over $q_\perp$ using the formula[10]

$$\int_0^\infty e^{-ax}I_N(bx)\,x^m\,dx=(-1)^m b^{-N}\frac{\partial}{\partial a^m}$$
$$\times\left[\left(a-\sqrt{a^2-b^2}\right)^N\Big/\sqrt{a^2-b^2}\right]\qquad(a>b). \qquad (28)$$

It then turns out that all terms are exponentially small compared with the zeroth term and one needs only take that one into account. If in evaluating the latter we neglect quantities of the order of unity compared to the large logarithm, it turns out in the final result that σ_{xx} depends logarithmically on the magnetic field and we find for ρ_{xx} the following equation

$$\rho_{xx}=\frac{\sigma_{xx}}{\sigma_{xx}^2+\sigma_{xy}^2}\approx\frac{\sigma_{xx}}{\sigma_{xy}^2}=\frac{2}{3\pi}\alpha^2\rho_a\ln\left[\frac{1}{\alpha}\left(\frac{v_T}{w}\right)^2\right], \qquad (29)$$

where $\rho_a = 1/\sigma_a$ is the resistivity, which is determined by the scattering by acoustical phonons in zero magnetic field. It is well known that[4]

$$\sigma_a=\left(4/3\sqrt{\pi}\right)ne^2\tau_a/m, \qquad (30)$$

where the "thermal" relaxation time is

$$\tau_a=\pi\hbar^4\rho w^2/\sqrt{2}\,E_0^2(mkT)^{3/2}. \qquad (31)$$

Expression (29) is essentially the same as the corresponding result of Adams and Holstein,[1] differing from it only by the logarithmic factor. This difference is a natural one, for when we put $\omega = 0$ in (26), i.e., we assume, as in reference 1, that the collisions are elastic and then integrate over q_z, the term with $N = 0$ turns out to diverge for small q_z. Adams and Holstein removed this divergence by taking the finite level width into account. We, however, have studied the case where it is essential to take the inelasticity of the scattering into account. We note that it has been shown by Skobov[11] that when the electrons are scattered by point defects σ_{xx} also depends only logarithmically on H.

To conclude this section we investigate the interesting problem of the expansion parameter used. The Hall conductivity $\sigma_{xy} = nec/H$ is the zeroth term in the expansion in powers of U, while σ_{xx} is a quadratic term. One must therefore expect that the expansion converges sufficiently rapidly if $\sigma_{xx}/\sigma_{xy} \ll 1$ [as a matter of fact this inequality was used when Eq. (29) was derived]. Also, in our case this ratio is of the order of magnitude

$$\frac{\sigma_{xx}}{\sigma_{xy}} \sim \frac{\hbar\Omega}{kT}\,\frac{\hbar}{\tau_a kT}\ln\left[\frac{1}{\alpha}\left(\frac{v_T}{w}\right)^2\right]. \qquad (32)$$

The third factor in Eq. (32) is of the order of magnitude of several units, the second factor is usually very small at low temperatures, and the first factor can be large in strong magnetic fields.

To determine the expansion parameter by a more reliable method, we used the technique proposed by Konstantinov and Perel'[12] to evaluate the correction of order U^4 to σ_{xy}. It turns out that this correction is proportional to H, i.e., its ratio to σ_{xx} increases with the field in the same way as (32). A very strong field, for which the ratio σ_{xx}/σ_{xy} is again $\gtrsim 1$, therefore becomes "weak" in the sense of the criterion (1) and our theory or the theory of Adams and Holstein[1] can not be applied to it.

However, even before such fields are reached it turns out that inequality (27) no longer holds when $q \sim 1/a$. For such q it is already impossible to use the expansion (27a) for the Planck function, and the values $q_\perp \sim kT/\hbar w$ play therefore a role in the integral over $q_\perp$. Klinger[13] has shown that in that case $\sigma_{xx} \sim 1/H^2$. It can thus happen that if inequality (27) is violated before (1), there exists a small expansion parameter in the whole region of strong fields.

4. We turn now to a study of scattering by optical phonons. We shall assume that $\hbar\omega_0\beta \gg 1$, since the quantum limit is practically unattainable if the opposite inequality holds, and we separate two limiting cases. The first one is that of very strong fields, when $\Omega \gg \omega_0$. In the second, more realistic one we have $\Omega < \omega_0$. Substituting (6) into (26) and (8) and going over to dimensionless integration variables in each term of the series

$$v = \hbar q_\perp^2/2m\Omega, \qquad u = \hbar q_z^2/|N_0+\delta+N|\,2m\Omega, \qquad (33)$$

we find that

$$\sigma_{xx} = ne^2(\hbar\omega_0\beta)^{1/2}\left[4\sqrt{\pi}\,m\Omega^2 t_0 \sinh(\hbar\omega_0\beta/2)\right]^{-1}\sum_{N=-\infty}^{\infty} C_N, \qquad (34)$$

$$C_N = \alpha\int_0^\infty du\,u^{-1}\exp\{-\alpha|N_0+\delta+N|(u/2+1/2u)\}$$
$$\times\int_0^\infty v\,dv\,I_N(v/\sinh\alpha)\,(u|N_0+\delta$$
$$+N|+v)^{-1}\exp\{-v\coth\alpha\}, \qquad (35)$$

$$t_0 = 2\pi\hbar^2(\hbar\omega_0/2m)^{1/2}A^{-1}. \qquad (36)$$

Here N_0 is the largest integer contained in the ratio ω_0/Ω; $\delta = \omega_0/\Omega - N_0$.

We split the sum in (34) into three parts

$$S_1 = \sum_{N=0}^{\infty} C_N, \qquad S_2 = \sum_{N=1}^{N_0} C_{-N}, \qquad S_3 = \sum_{N=N_0+1}^{\infty} C_{-N}. \qquad (37)$$

In the quantum limit only the term with $N = 0$ plays a role in the first sum, and all other terms are exponentially small in comparison. In this term the values $v \sim 1$ and $|N_0+\delta|u \sim \omega_0/\Omega$ are important. If $\Omega \gg \omega_0$, then $S_2 = 0$ and S_3 is exponentially small, and in the evaluation of C_0 we can neglect $|N_0+\delta|u$ in comparison with v in the exponent in (35). The integral over v is then equal to unity and we can easily evaluate the integral over u by using the inequality $\hbar\omega_0\beta \gg 1$. As a result we get

$$\rho_{xx} = \sigma_{xx}/\sigma_{xy}^2 = \alpha\rho_0. \qquad (38)$$

Here $\rho_0 = 1/\sigma_0$ is the low-temperature resistivity for $H = 0$, which is connected with the scattering by optical phonons. According to Davydov and Shmushkevich[14] $\sigma_0 = ne^2\tau_1/m$, where

$$\tau_1 = 2\pi\hbar^2(\hbar\omega_0)^{1/2}e^{\hbar\omega_0\beta}(2m)^{-1/2}A^{-1} = t_0 e^{\hbar\omega_0\beta}. \qquad (39)$$

The dependence $\rho_{xx}(H)$ given in Adams and Holstein's paper[1] differs from the one of Eq. (38) only by the logarithmic factor.

If $\omega_0 \gg \Omega$ one can, on the other hand, neglect v in comparison with $|N_0+\delta|u$ when evaluating C_0. Then

$$S_1 \approx C_0 = 2\sqrt{\pi}\,(\hbar\omega_0\beta)^{-1/2}\alpha\Omega\omega_0^{-1}\exp\{-\hbar\omega_0\beta/2\}. \qquad (40)$$

In that case, however, the contribution from S_1 is small compared with the main contribution from S_2. To evaluate the latter we use an approximate method, which enables us to find σ_{xx} apart from a factor of order of magnitude of unity. The important values in the integral (35) are $v \sim N + \coth\alpha$ and $u \sim 1$. The characteristic quantity in S_2 is therefore the sum

$$v + u\,|N_0 + \delta + N| \sim N + N_0 - N = N_0,$$

and we take it outside the integral sign. The integral over v can then easily be evaluated using Eq. (28) and turns out to be equal to $(1 + N)e^{-\alpha N}$. Performing the summation over N and changing the integration variable to $u = e^{-t}$, we find that

$$S_2 \approx (4\alpha^2/\hbar\omega_0\beta)\exp\{-\hbar\omega_0\beta/2\}(S_2' + S_2''), \tag{41}$$

$$S_2' = \int_0^\infty \frac{\exp\{-\alpha\delta(\cosh t - 1)\}}{1 - \exp\{-\alpha\delta(\cosh t - 1)\}}\Big[N_0 + 1 - \frac{1 - \exp\{-\alpha(N_0 + 1)(\cosh t - 1)\}}{1 - \exp\{-\alpha(\cosh t - 1)\}}\Big]dt, \tag{42}$$

$$S_2'' = \int_0^\infty \exp\{-\alpha\delta(\cosh t - 1)\}\frac{1 - \exp\{-\alpha N_0(\cosh t - 1)\}}{1 - \exp\{-\alpha(\cosh t - 1)\}}dt. \tag{43}$$

Using the inequality $N_0 \gg 1$ we get easily the following estimate

$$S_2' = D'(\hbar\omega_0\beta)^{3/2}\alpha^{-2} + (\hbar\omega_0\beta/2\alpha)e^{\alpha\delta}K_0(\alpha\delta), \tag{44}$$

$$S_2'' \sim S_2'/\hbar\omega_0\beta. \tag{45}$$

Here D is a coefficient of the order of unity, and

$$K_0(x) = \int_0^\infty e^{-x\cosh t}dt = \begin{cases}\sqrt{\pi/2x}\exp(-x), & x \gg 1\\ -\ln x, & x \ll 1\end{cases}. \tag{46}$$

The second term in (44) is a small correction to the first one when $\alpha\delta \gg 1$ (there are then also other correction terms of the same order, which we do not write down). If, however, $\alpha\delta \ll 1$, the second term in (44) can be very large and determines the resonance oscillations of the conductivity tensor.

Only the first term plays a role in the sum S_3 (all others are exponentially small). To evaluate it we can neglect $u(1 - \delta)$ compared to v in the integral (35), and we get

$$S_3 \approx C_{-(N_0+1)} = 2\alpha e^{-(1-\delta)\alpha}K_0((1 - \delta)\alpha). \tag{47}$$

As a result we get

$$\sigma_{xx} = \sigma_{xx}^{\mathrm{cl}}[D + F(\alpha, \delta)], \tag{48}$$

where

$$\sigma_{xx}^{\mathrm{cl}} = {}^2/_3(ne^2/m\Omega^2t_0)(\hbar\omega_0/kT)\exp\{-\hbar\omega_0/kT\}. \tag{49}$$

Here D is a constant of order unity and the term $F(\alpha, \delta)$ is negligibly small compared to D if $\alpha\delta(1 - \delta) \gg 1$. If, however, $\alpha\delta(1 - \delta) \ll 1$,

$$F(\alpha, \delta) = -(3/2\sqrt{\hbar\omega_0\beta})\alpha\ln[\alpha\delta(1 - \delta)]. \tag{50}$$

The first term in the quantum formula (48) is the same as the classical expression for the conductivity, which will be obtained in the following. This is natural, for in the case $\omega_0/\Omega \gg 1$ the electron states with large values of the vibrational quantum number $n \sim \omega_0/\Omega \gg 1$ are important. One can evaluate the coefficient D in the classical region. It turns out to be equal to unity.

The second term in (48) describes the specific quantum resonance oscillations of the conductivity, which can be noticed against the background of the classical term when $\hbar\beta\,|\omega_0 - N\Omega| \ll 1$. They are periodic in the reciprocal of the field and occur for the case of Boltzmann statistics, in contrast to all other known types of oscillations of the static conductivity. Their origin can be easily understood. If $\omega_0 = N\Omega$ with good accuracy, then electronic transitions involving the absorption or emission of a phonon are possible, during which the quantum number n changes by N while p_z remains almost unchanged. The transition probability is proportional to the density of the final states, and the total number of transitions for electrons with energies within a given interval is proportional to the density of the initial states. The density of states in a magnetic field near $p_z = 0$ has an integrable singularity of the kind $[\epsilon - \hbar\Omega(n + {}^1\!/_2)]^{-1/2}$ (ϵ is the electron energy). If, however, transitions are possible where only the one quantum number n changes, then both singular factors depend on the same argument, and this leads to a logarithmic divergence of the corresponding integral.*

One can remove this divergence, for instance, by taking the dispersion of the optical phonons into account. More likely to be effective, however, is taking the scattering into account without using the Born approximation, or taking the electron-electron interaction into account. Since the last problem goes beyond the framework of the present paper, we shall not study here the mechanism of removal of the divergence.

5. We turn to the evaluation of σ_{xx} in the classical region. From an analysis of the transport equation in the usual form it is often assumed that in this region the conductivity in a strong field is related to the conductivity for $H = 0$ by a simple order-of-magnitude relation. Indeed, if for $H = 0$

$$\sigma = ne^2\bar{\tau}/m, \tag{51}$$

---

*Because the small q_z are important in the oscillations, one can immediately determine the coefficient of the oscillating term exactly, since one can neglect $u\,|N_0 + \delta + N|$ as com- to v in the corresponding calculations.

where τ is some average relaxation time for the conduction electrons, then

$$\sigma_{xx} \sim ne^2/\Omega^2 \bar{\tau} m. \tag{52}$$

then Eq. (52) is assumed to be an estimate which should yield the correct order of magnitude and the correct field and temperature dependence of σ_{xx}. It is assumed here that in the classical region the collision operator does not appreciably depend on H.

We shall show in the following that even if the collision operator is indeed independent of the field, the situation is sometimes not as simple as that, and (52) may give an incorrect temperature dependence. Also, we shall be able to state the conditions under which the collision operator is independent of the field. To do this we use specific calculations to verify that the assumption that the collision operator in the transport equation is field-independent gives the same formulae for σ_{xx} as are obtained by replacing $\operatorname{Im} K_q^0(\omega)$ in Eq. (8) by its limiting value (20) when $H = 0$. To find out when the collision operator is field-independent, it is then sufficient to ascertain when such a substitution is permissible.

We start again with the case of scattering by acoustical phonons. Substituting (13) and (20) into (8) and assuming that $mw^2 \ll kT$ we get the formula

$$\sigma_{xx} = (8/3\sqrt{\pi})\, ne^2/\Omega^2 m\tau_a. \tag{53}$$

It is the same as the result obtained from the transport equation and verifies the estimate (52).

6. For optical phonons we get by substituting (6), (13), and (20) into (8)

$$\sigma_{xx} = \frac{ne^2}{3\sqrt{\pi} m\Omega^2 t_0} \frac{(\hbar\omega_0\beta)^{3/2}}{\sinh(\hbar\omega_0\beta/2)} K_1\left(\frac{\hbar\omega_0\beta}{2}\right), \tag{54}$$

where K_1 is a Macdonald function. Recognizing that $K_1(z) \approx 1/z$ if $z \ll 1$, and $K_1(z) = \sqrt{\pi/2z}e^{-z}$ for $z \gg 1$, we get at high temperatures $(\hbar\omega_0\beta \ll 1)$

$$\sigma_{xx} = (4/3\sqrt{\pi})\, ne^2/m\Omega^2\tau_0, \tag{55}$$

with the high-temperature relaxation time $\tau_0 = \sqrt{\hbar\omega_0/kT}t_0$.

At low temperatures $(\hbar\omega_0\beta \gg 1)$, Eq. (49) follows from (54). According to Davydov and Shmushkevich,[4] on the other hand, we get for $H = 0$ in the first case $(\hbar\omega_0\beta \ll 1)$

$$\sigma = (8/3\sqrt{\pi})\, ne^2\tau_0/m, \tag{56}$$

and in the second case $(\hbar\omega_0\beta \gg 1)$

$$\sigma_0 = ne^2 t_0 e^{\hbar\omega_0\beta}/m. \tag{57}$$

Equation (55) for high temperatures is the same as the result obtained from the transport equation[4] and verifies the estimate (52).

We know of no papers in which the transport equation in a magnetic field is solved for the scattering by optical phonons at low temperatures. It is, however, at once clear that Eq. (49) gives a different temperature dependence, differing by a factor $2\hbar\omega_0/3kT$ from the estimate (52). To ascertain the cause of such a discrepancy we study the solution of the corresponding transport equation for the case $\hbar\omega_0\beta \gg 1$.

By methods similar to those used by Davydov and Shmushkevich[14] for $H = 0$, we consider two regions of possible values for the electron energy ϵ. In the first region $0 < \epsilon < \hbar\omega_0$, and in the second $\hbar\omega_0 < \epsilon < 2\hbar\omega_0$. Electrons in the first region can only absorb optical phonons, as a result of which they get into the second region. The probability for such a process is proportional to $N_0 \sim \exp(-\hbar\omega_0\beta)$, i.e., exponentially small. For electrons in the second region the most probable process is that of emitting a phonon, as a result of which the electron gets into the first region. The probability for such a process is proportional to $N_0 + 1$, i.e. it is not exponentially small.

We write down the transport equation separately for electrons of each of these two regions. We shall write the correction to the equilibrium distribution function $f_0(\epsilon)$ in the form

$$f' = \hbar \mathbf{p}\chi\, df_0/\partial\varepsilon,$$

where $\hbar\mathbf{p}$ is the quasi-momentum of the electron and the function χ depends only on the energy ϵ. The transport equations for the first and second region are, respectively, of the form

$$e\mathbf{v}\mathbf{E} - \frac{e}{c}[\mathbf{H}\times\chi(\varepsilon_\mathbf{p})]\mathbf{v} = \frac{A}{4\pi^2}\int\frac{d^3\mathbf{q}}{q^2}\{(N_0+1)e^{-\hbar\omega_0\beta}$$
$$(\mathbf{p}+\mathbf{q})\chi(\varepsilon_{\mathbf{p}+\mathbf{q}}) - N_0\mathbf{p}\chi(\varepsilon_\mathbf{p})\}\delta(\varepsilon_{\mathbf{p}+\mathbf{q}} - \varepsilon_\mathbf{p} - \hbar\omega_0), \tag{58}$$

$$e\mathbf{v}\mathbf{E} - \frac{e}{c}[\mathbf{H}\times\chi(\varepsilon_\mathbf{p})]\mathbf{v} = \frac{A}{4\pi^2}\int\frac{d^3\mathbf{q}}{q^2}\{N_0 e^{\hbar\omega_0\beta}(\mathbf{p}-\mathbf{q})\chi(\varepsilon_{\mathbf{p}-\mathbf{q}})$$
$$-(N_0+1)\mathbf{p}\chi(\varepsilon_\mathbf{p})\}\delta(\varepsilon_\mathbf{p} - \varepsilon_{\mathbf{p}-\mathbf{q}} - \hbar\omega_0). \tag{59}$$

Because of the properties of the δ function, one can take $\chi(\epsilon)$ out from under the integral sign and the determination of the right hand sides of (58) and (59) is reduced to the evaluation of integrals of the kind

$$\int(\mathbf{p}-\mathbf{q})\,\delta(\varepsilon_\mathbf{p} - \varepsilon_{\mathbf{p}-\mathbf{q}} - \hbar\omega_0)\frac{d^3\mathbf{q}}{q^2} \approx \frac{8\pi}{3\hbar^2}\left(\frac{m}{2\hbar\omega_0}\right)^{1/2}\left(\frac{\varepsilon - \hbar\omega_0}{\hbar\omega_0}\right)^{3/2}\mathbf{p}. \tag{60}$$

We used here the fact that in the second region $(\epsilon - \hbar\omega_0)/\hbar\omega_0 \sim kT/\hbar\omega_0 \ll 1$.

The other integrals on the right-hand sides of (58) and (59) can be evaluated by similar means. As a result we obtain the following set of equations

$$\tau_1 eE/m + (1 - i\Omega\tau_1)\chi_1 - 2\chi_2/3 = 0,$$
$$\tau_2 eE/m + (1 - i\Omega\tau_2)\chi_2 - {}^2/_3(\varepsilon/\hbar\omega_0)\chi_1 = 0, \tag{61}$$

where $\chi = \chi_x + i\chi_y$, and $E = E_x + iE_y$. The quantity τ_1 is defined by Eq. (39), and $\tau_2 = t_0\sqrt{\hbar\omega_0/\epsilon}$. Moreover, $\chi_1 = \chi(\epsilon)$ in the first region and $\chi_2 = \chi(\epsilon + \hbar\omega_0)$ in the second region, with $\epsilon/\hbar\omega_0 \ll 1$. The correction to the distribution function is

$$f' = \hbar \operatorname{Re}(p_x - ip_y)\,\chi\partial f_0/\partial\varepsilon. \tag{62}$$

Let the field **E** be along the x axis. Then

$$\sigma_{xx} = \frac{2\hbar^2 e}{(2\pi)^3 mE_x}\int d^3\mathbf{p}\,\frac{df_0}{d\varepsilon}\,p_x^2 \operatorname{Re}\chi. \tag{63}$$

It is clear that there are in this case two relaxation times connected with the collision operator, and not one: τ_1, the period an electron stays in the first region, and τ_2, the period an electron stays in the second region. Depending on the ratio of these periods to the Larmor frequency, we obtain different expressions for σ_{xx}.

If we use the inequalities $\epsilon/\hbar\omega_0 \ll 1$ and $kT/\hbar\omega_0 \ll 1$, the solution of the set (51) has the form

$$\operatorname{Re}\chi_1 = -[\tau_1/(1 + \Omega^2\tau_1^2)]\,eE_x/m,$$

$$\operatorname{Re}\chi_2 = -\frac{\tau_2}{1 + \Omega^2\tau_2^2}\,\frac{eE_x}{m} - \frac{(2\varepsilon/3\hbar\omega_0)\,\tau_1(1 - \Omega^2\tau_1\tau_2)}{1 + \Omega^2\tau_1^2(1 + \Omega^2\tau_2^2)}\,\frac{eE_x}{m}. \tag{64}$$

These formulae contain two dimensionless quantities, $\Omega\tau_1$ and $\Omega\tau_2$. The presence of two parameters causes the peculiar behavior of the function $\sigma_{xx}(H)$.

We shall consider this behavior in the whole range of magnetic fields in the classical region. If $\Omega\tau_1 \ll 1$, the current transferred by the electrons in the second region is negligibly small, because their number is exponentially small then. We get for the conductivity the result (57) of Davydov and Shmushkevich, where the time τ_2 is not involved at all.

When the magnetic field is increased so that

$$\Omega\tau_2 \ll 1 \ll \Omega\tau_1, \tag{65}$$

the electrons have time to describe several revolutions while they are in the first region and the conductivity due to them

$$\sigma_{xx} = ne^2/m\Omega^2\tau_1 \tag{66}$$

decreases thus in inverse propertion to H^2.

When the field is further increased the contribution from the electrons in the first region becomes so small that the electrons in the second region begin to play the main part in the transport of current. If this occurs at such fields that inequality (65) is still valid, the corresponding transverse conductivity is equal to

$$\sigma_{xx} = \frac{4}{3}\,\frac{ne^2t_0}{m}\left(\frac{\hbar\omega_0}{kT}\right)^2 \exp\left\{-\frac{\hbar\omega_0}{kT}\right\}. \tag{67}$$

It is independent of H, since the electrons have only time to describe a small part of a revolution during their sojourn in the second region.

If the magnetic field is increased still further so that $1 \ll \Omega\tau_2 \ll \Omega\tau_1$, the electrons will also describe several revolutions while in the second region. As before they will be the main ones involved in the transfer of current. Equation (64) becomes in that case

$$\operatorname{Re}\chi_1 \approx -(\Omega^2\tau_1)^{-1}\,eE_x/m, \qquad \operatorname{Re}\chi_2 \approx -(\Omega^2\tau_2)^{-1}\,eE_x/m, \tag{68}$$

and we obtain for σ_{xx} Eq. (49). It is clear that in this case there is no basis whatever for hoping that the estimate (52) is valid, since the conductivity is determined by the time τ_1 when $H = 0$, and by the time τ_2 in the case $\Omega\tau_1 \gg \Omega\tau_2 \gg 1$. We note that $\sigma_{xy} = ne^2/m\Omega$ in the whole range of fields for which $\Omega\tau_1 \gg 1$.

The presence of several plateaus on the curve of $\sigma_{xx}(H)$ is thus not necessarily connected with the presence of several kinds of carriers. It may be caused by the complex character of the scattering.

7. We shall now ascertain when the collision operator in the transport equation is independent of the magnetic field. We start with the case of acoustical phonons and assume that $\Omega \gg \overline{\omega}$, where $\overline{\omega} \sim w\sqrt{mkT}/\hbar$ is a characteristic frequency for the phonons interacting with the electrons. We can then in all terms of the series (26) (except the zeroth term, which does not contain Ω) neglect ω in comparison to Ω, and we obtain

$$\sigma_{xx} = \frac{ne^2\alpha^2}{2\sqrt{\pi}m\Omega^2\tau_a}\Big[2\sum_{N=1}^{\infty}\int_0^{\infty}\frac{du}{u}\exp\Big\{-\frac{N\alpha}{2}\Big(u + \frac{1}{u}\Big)\Big\}\int_0^{\infty} v\,dv e^{-v\coth\alpha} I_N\Big(\frac{v}{\sinh\alpha}\Big) + \int_0^{\infty}\frac{dy}{y}e^{-y}\int_0^{\infty}\exp\Big\{-v\coth\alpha - \frac{\alpha\xi}{2}\,\frac{v}{y}\Big\}vI_0\Big(\frac{v}{\sinh\alpha}\Big)dv\Big], \tag{69}$$

where $\xi = (w/v_T)^2$ and where the integration variable is $y = \hbar^2 q_z^2/8mkT$.

Using Eq. (28) to evaluate the integral over v, and summing the series obtained in that way in the integral with respect to u, we get

$$\sigma_{xx} = \frac{ne^2\alpha^2}{2\sqrt{\pi}m\Omega^2\tau_a}\Big[2\int_0^{\infty}\frac{du}{u}\,\frac{\exp\{-\alpha[1 + u/2 + 1/2u)\}}{1 + \exp\{-\alpha(1 + u/2 + 1/2u)\}}\Big(\coth\alpha + \frac{1}{1 - \exp\{-\alpha(1 + u/2 + 1/2u)\}}\Big) + \int_0^{\infty}\frac{dy}{y}\,\frac{(\coth\alpha + \xi/2y)\,e^{-y}}{(1 + \xi\alpha y^{-1}\coth\alpha + \alpha^2\xi^2/4y^2)^{3/2}}\Big]. \tag{70}$$

If $\alpha \ll 1$, the first integral in (70) can be evaluated by expanding the denominators in series. It is sufficient here to retain the term of order α. As a result we get

$$\sigma_{xx} = \frac{8ne^2}{3\sqrt{\pi} m\Omega^2\tau_a}\left(1 + \frac{3}{16}\alpha \ln\frac{1}{\xi}\right). \qquad (71)$$

The first term in (71) is the integral of the series, and the second one the integral of the zeroth term. If $^3/_8\,\alpha \ln(v_T/w) \ll 1$, the main term in (71) is the same as Eq. (53), which follows from the solution of the transport equation, and the term with the logarithm is a small quantum correction to (53). In that case one may assume that the collision operator in the transport equation is independent of the magnetic field. Under conditions such that

$$^3/_8\,\alpha \ln(v_T/w) > 1 > \alpha, \qquad (72)$$

we could in principle observe the dependence $\sigma_{xx} \sim 1/H$, but in practice there is usually no region where both inequalities (72) hold.

We shall not analyze the case $\bar{\omega} \gtrsim \Omega$. We note only that here, too, Eq. (53) is valid in practically the whole of the classical region, but the quantum correction to it may be different from the one in (71).

We turn now to scattering by optical phonons. We consider in detail the most interesting case when $\Omega \ll \omega_0$, and show that here, too, we can assume in first approximation the collision operator to be independent of the magnetic field. To do this we come back to the exact Eq. (34). First of all we note that the estimates (42) and (43) for the sum S_2 remain valid also in the classical limit. Indeed, in the integral (35) the main part is played by $v \sim 1/\alpha + N$, but since $N_0 \gg 1/\alpha$, all calculations of Sec. 4 remain valid for most of the terms in the sum. The whole difference from the quantum limit consists only in the fact that the factor α in the argument of the logarithm does not occur in the classical case.

There remains only to estimate the sums S_1 and S_3 and to show that the former is negligibly small and that one can separate from the latter the logarithmic term that leads to oscillations. The main part in S_1 is played by the first $N_1 \sim 1/\alpha$ terms (the sum of all other terms is exponentially small). In these first terms the essential values of $v \sim 1/\alpha + N \sim 2/\alpha$ are much less than the essential values of $|N_0 + N + \delta|u \sim N_0$, so that one may neglect the first term. The series can then easily be summed and as a result we get

$$S_1 = (4/\hbar\omega_0\beta)\, K_0(\hbar\omega_0\beta/2) \ll S_2. \qquad (73)$$

When evaluating the sum S_3 one sees easily that one can, on the other hand, neglect $|N_0 + N + \delta|u$ in comparison with v, and this leads to

$$S_3 = \Delta S_3 + 2\exp\{-\hbar\omega_0\beta/2\}, \qquad (74)$$

where the logarithmic correction is $\Delta S_3 = -2\alpha \exp\{-\hbar\omega_0\beta/2\} \ln(1-\delta)$ if $1-\delta \ll 1$, and is negligibly small in the opposite case.

Substituting the sum of S_2 and ΔS_3 into (34) we get Eq. (49) for σ_{xx}. Its first term gives the classical conductivity and the second term the very interesting oscillating quantum corrections to it. They can in principle be observed if the mechanism which removes the divergence at small q_z (which was discussed in Sec. 4) turns out to be not too effective. We note only that Eq. (50), which is valid in the quantum case when $\alpha\delta(1-\delta) \ll 1$, requires in the classical region the inequality $\delta(1-\delta) \ll 1$, and contains not $\ln[\alpha\delta(1-\delta)]$ but $\ln[\delta(1-\delta)]$.

The ratio Ω/ω_0 is thus essentially the only parameter in the theory of the transverse conductivity caused by the scattering by optical phonons. The quantity α, however, is a parameter only in small ranges of changes in H near resonances. If $\Omega/\omega_0 \ll 1$, the main difference between the quantum and classical regions is that in the former case the oscillations are part of the main effect while in the latter they are small quantum corrections.

We also studied the case $\hbar\omega_0\beta \ll 1$. The result is that the collision operator is again field independent. The quantum corrections can oscillate in this case, too.

In conclusion the authors wish to express their gratitude to A. I. Ansel'm for useful discussions and for his interest in this paper.

---

[1] E. N. Adams and T. D. Holstein, J. Phys. Chem. Solids **10**, 254 (1959).

[2] P. N. Argyres and L. M. Roth, J. Phys. Chem. Solids **12**, 89 (1959).

[3] Kubo, Hasegava, and Hashitsume, J. Phys. Soc. Japan **14**, 56 (1959).

[4] B. I. Davydov and I. M. Shmushkevich, Usp. Fiz. Nauk **24**, 21 (1940).

[5] M. A. Krivoglaz and S. I. Pekar, Izv. Akad. Nauk SSSR, Ser. Fiz. **21**, 3 (1957), Columbia Tech. Transl. p. 1.

[6] A. I. Larkin, JETP **37**, 264 (1959), Soviet Phys. JETP **10**, 186 (1960).

[7] E. H. Sondheimer and A. H. Wilson, Proc. Roy. Soc. (London) **A210**, 173 (1951).

[8] Yu. B. Rumer, JETP **18**, 1081 (1948); **22**, 214 (1952).

[9] V. L. Bonch-Bruevich and A. G. Mironov, Физ. тверд. тел. **2**, 489 (1960), Soviet Phys. Solid State **2**, 454 (1960).

[10] G. N. Watson, Theory of Bessel Functions

(Russ. Transl.) Part I, IIL, 1949, p. 420.

[11] V. G. Skobov, JETP **38**, 1304 (1960), Soviet Phys. JETP **11**, 941 (1960).

[12] O. V. Konstantinov and V. I. Perel', JETP **39**, 197 (1960), Soviet Phys. JETP **12**, 142 (1961).

[13] M. I. Klinger, JETP **31**, 1055 (1956), Soviet Phys. JETP **4**, 831 (1957).

[14] B. Davydov and I. Shmushkevich, JETP **10**, 1043 (1940).

Translated by D. Ter Haar
33

SOVIET PHYSICS JETP VOLUME 13, NUMBER 1 JULY, 1961

CONTRIBUTION TO THE THEORY OF MAGNETOACOUSTIC RESONANCE IN METALS

É. A. KANER, V. G. PESCHANSKIĬ, and I. A. PRIVOROTSKIĬ

Institute of Radiophysics and Electronics, Academy of Sciences, Ukr. S.S.R., and Khar'kov State University

Submitted to JETP editor July 9, 1960

J. Exptl. Theoret. Phys. (U.S.S.R.) 40, 214-226 (January, 1961)

A new effect of resonance absorption of ultrasonic waves in a magnetic field is studied theoretically.* In many respects the resonance mechanism is similar to cyclotron resonance, but is related to the spatial rather than temporal periodicity of the field in the metal. The calculations are performed for closed as well as for open electron trajectories. The positions, widths, and heights of the resonance peaks are determined as a function of the frequency, magnetic field, Fermi surface structure, magnetic field orientation and direction of propagation of the sound relative to the crystallographic axes. A sharp angular dependence of the absorption coefficient has been detected. An investigation of the effects under consideration may yield information on the topology and a number of other important characteristics of Fermi surfaces in metals. The results of the experiments are in good agreement with the predictions of the theory.

1. MECHANISM OF RESONANCE ABSORPTION

SOUND oscillations produce in a metal a spatially-periodic field. In the presence of a magnetic field $\mathbf{H}(0, 0, H)$, this periodicity leads to a non-monotonic dependence of the coefficient of ultrasound absorption α on H. This effect was first explained by Pippard,[1] who determined the period of the oscillations of α from qualitative considerations.

V. Gurevich[2] developed the theory of this phenomenon for closed Fermi surfaces and showed that the periodic variation of α as a function of H^{-1} can be of two kinds, namely harmonic oscillations (which we shall call non-resonant) and smooth increments that occur periodically. These periodic variations of α with H^{-1} have no resonant character in the sense that the relative widths and the forms of the absorption 'lines' remain practically unchanged as the mean free path l tends to infinity.

In the present paper we consider an essentially new effect of resonance absorption of ultrasound in metals. The mechanism of this magnetoacoustic resonance is analogous in many respects to the mechanism of cyclotron resonance in metals,[2] but is connected not with the temporal but with the spatial periodicity of the field in the metal. The magnetoacoustic resonance should take place when the average value (over the period T of the motion in the magnetic field) of the electron velocity along the wave vector $\mathbf{k}$ differs from zero. For closed trajectories this can be realized only when $\mathbf{k}$ is not perpendicular to $\mathbf{H}$. On the open periodic trajectories, resonance should be observed also when $\mathbf{k} \perp \mathbf{H}$, provided the vector $\mathbf{k}$ is not parallel to the direction of the open trajectory.

If the condition $\mathbf{k} \cdot \overline{\mathbf{v}}T \approx 2\pi n$ is satisfied [$n = 1, 2, 3 \ldots$ is an integer, and the bar denotes averaging over the period of the trajectory $p_z = \text{const}$ on the Fermi surface $\epsilon(\mathbf{p}) = \mu_0$], the electron is periodically accelerated by the field in the equal-phase planes, where it remains for a relatively longer time than in the remaining parts of the trajectory. Clearly, the longer the mean free path, the more effective will be the interaction between the electron and the field in these planes.

The dependence of $\mathbf{k} \cdot \overline{\mathbf{v}}T$ on p_z is, however, quite appreciable. If $\mathbf{k} \cdot \overline{\mathbf{v}}T$ is independent of p_z, then the condition $\mathbf{k} \cdot \overline{\mathbf{v}}T = 2\pi n$ will be satisfied simultaneously for all electrons. This is precisely the case realized on open periodic trajectories, when $\mathbf{k} \perp \mathbf{H}$ and the angle θ between $\mathbf{k}$ and the direction of the open trajectory is not small, so that $\mathbf{k} \cdot \overline{\mathbf{v}}T \sim kr \sin\theta \gg 1$. Here the resonance effect will be greater than in the case when $\mathbf{k} \cdot \overline{\mathbf{v}}T$ depends appreciably on p_z. The dependence on p_z leads to a smearing and reduction in the height of the resonance maximum. It is obvious that the electrons for which $\mathbf{k} \cdot \overline{\mathbf{v}}T$ has an extremum with respect to p_z will be relatively more numerous than the other electrons, and therefore the amplitude of resonant absorption will be a maximum precisely for such "extremal" electrons, although its magnitude will be still less than when $\mathbf{k}\cdot\overline{\mathbf{v}}T = \text{const}$.

---

*A preliminary report on this phenomenon was published earlier.[11]

We emphasize that Gurevich[2] did in fact not consider this effect.

Along with magnetoacoustic resonance, the absorption coefficient should be highly anisotropic when the vectors **k** and **H** become slightly nonperpendicular, and also when the vector **k** deviates slightly from the direction of the open periodic trajectory. The reason for this anisotropy is that when $\mathbf{k}\cdot\overline{\mathbf{v}} \equiv 0$ all the electrons fall periodically into the equal-phase plane and participate effectively in the absorption, whereas the absorption when $\mathbf{k}\cdot\overline{\mathbf{v}} \not\equiv 0$ is essentially determined only by the electrons that drift most slowly along **k**. This circumstance brings about a fast reduction in α.

The strong angular dependence of the absorption when $\mathbf{k} \perp \mathbf{H}$, and the presence of magnetoacoustic resonance in this case, are closely linked with the presence of open trajectories, and do not take place in metals with closed Fermi surfaces.

2. GENERAL FORMULA FOR THE ABSORPTION COEFFICIENT

Let us turn to a quantitative examination of the problem. As was shown by Gurevich[2] and Akhiezer, Kaganov, and Lyubarskiĭ,[4] the coefficient of absorption α is connected with the rate of dissipation of energy Q by the relation

$$\alpha = Q/W, \qquad Q = h^{-3}\int d\tau_{\mathbf{p}}\nu\,|\chi^2|\,\delta(\varepsilon-\mu_0), \tag{2.1}$$

where Q is the dissipation function, $\chi\delta(\epsilon-\mu_0)$ is a small non-equilibrium addition to the Fermi distribution function f_0, $\nu(\mathbf{p})$ is the collision frequency [$\nu = t_0^{-1}$ where $t_0(\mathbf{p})$ is the time between collisions], $d\tau_{\mathbf{p}} = dp_x dp_y dp_z = eHc^{-1}d\epsilon\,dt\,dp_z$ is an element of momentum space, $\epsilon(\mathbf{p})$ is the energy, $\mathbf{v} = \partial\epsilon/\partial\mathbf{p}$ is the velocity, t the time of motion along the orbit, $-e$ is the charge, μ_0 is the electron end-point energy, h is Planck's constant, and c is the velocity of light.

The time t is determined by the equation of motion of the electron in a magnetic field[5]

$$d\mathbf{p}/dt = -(e/c)\,[\mathbf{vH}]. \tag{2.2}^*$$

The quantity W is the energy density in the sound wave

$$W = \tfrac{1}{2}\rho\omega^2|\mathbf{u}^2|, \tag{2.3}$$

where ρ is the density of the metal, $\omega = ks$ is the frequency, s is the speed, $\lambda = 2\pi/k$ is the wavelength of sound, and $\mathbf{u}(\mathbf{r}, t) = \mathbf{u}_0 \exp(i\omega t - i\mathbf{k}\cdot\mathbf{r})$ is the displacement vector. The definition (2.1) of the absorption coefficient is certainly valid for $\omega \ll \nu$, which is assumed to be satisfied.

The solution of the linearized kinetic equation for the function χ has the form[2,6]

$$\chi = \int_{-\infty}^{t} dt_1 g(t_1)\exp\Big[\int_{t}^{t_1}(\nu - i\mathbf{kv})\,dt'\Big]; \tag{2.4}$$

$$g = \Lambda_{ik}\dot{u}_{ik} - e\mathbf{E}'\mathbf{v}, \qquad \Lambda_{ik} = \lambda_{ik}(\mathbf{p}) - \langle\lambda_{ik}\rangle,$$

$$\langle\lambda\rangle = \int d\tau_{\mathbf{p}}\lambda\delta(\varepsilon-\mu_0)\Big/\int d\tau_{\mathbf{p}}\delta(\varepsilon-\mu_0),$$

$$u_{ik} = 2^{-1}(\partial u_i/\partial x_k + \partial u_k/\partial x_i),$$

$$e\mathbf{E}' = e\mathbf{E} - (e/c)\,[\dot{\mathbf{u}}\mathbf{H}] - \nabla\langle\lambda_{ik}\rangle u_{ik}. \tag{2.5}$$

Here $\lambda_{ik}(\mathbf{p})$ is the deformation potential, which determines the variation of the dispersion law in the field of the acoustic wave: $\delta\epsilon = \lambda_{ik}u_{ik}$, where u_{ik} is the deformation tensor. In order of magnitude we have $|\lambda_{ik}| \sim |\Lambda_{ik}| \sim \mu_0$. The quantity $\langle\delta\epsilon\rangle = \langle\lambda_{ik}\rangle u_{ik}$ represents the change in the chemical potential of the electrons in the field of the sound wave. The small terms connected with the Stewart-Tolman effect and the change in the temperature can be neglected.[4]

The electric fields induced by the ultrasound should be determined from Maxwell's equations (the field components transverse to the wave vector) and from the conditions for the electroneutrality of the metal, $\mathbf{j}\cdot\mathbf{k} = 0$. For this purpose it is necessary to calculate the current density

$$\mathbf{j} = -2eh^{-3}\int d\tau_{\mathbf{p}}\mathbf{v}\chi\delta(\varepsilon-\mu_0).$$

We shall not deal, however, with the determination of the electric fields, since it can be shown (see reference 2) that in the range of the values of H concerned here the field make the same (or smaller) contribution to the absorption as does the deformation potential, which in turn is known only in order of magnitude. These fields are contained in α only through the slowly varying function g, the form of which does not influence essentially the features of the investigated effects.

Substituting the expression for χ in the dissipative function and integrating by parts, we readily obtain

$$\alpha = h^{-3}W^{-1}\,\mathrm{Re}\int d\tau_{\mathbf{p}} g^*\chi\delta(\varepsilon-\mu_0), \tag{2.6}$$

where g^* is the complex conjugate of g.

---

*$[\mathbf{vH}] = \mathbf{v}\times\mathbf{H}$.

Magnetoacoustic resonance takes place when the trajectories of the electrons in momentum space are periodic in t. The motion on the closed trajectories is always periodic. Periodic open trajectories occur on open Fermi surfaces when the vector **H** lies in the crstallographic plane.[5–7]

Let us calculate the coefficient of absorption for the case when $T\overline{\nu} \ll 1$, and $\max\{kvT\} \gg 1$. This system of inequalities is equivalent to

$$\lambda\!\!\!^{-} \ll 2\pi r \ll l. \qquad (2.7)$$

We can therefore calculate α by the method of stationary phase. It is readily seen that the stationary phase points in the integrals with respect to t form a line of points $\mathbf{k}\cdot\mathbf{v}(t, p_z) = 0$ on the Fermi surface. Simple calculation leads to

$$\alpha \sim eHh^{-3}W^{-1}c^{-1}\,\mathrm{Re}\int dp_z \sum_{0<t_\alpha<T} \sum_{-\infty\leqslant t_\beta\leqslant t_\alpha}{}^{'} g^*_\alpha g_\beta J^*_\alpha J_\beta$$

$$\times \exp\Big[\int_{t_\alpha}^{t_\beta} (\nu - iq)\,dt\Big]; \qquad (2.8)$$

$$J_\alpha = \int_{-\infty}^{\infty} d\tau \exp\left[-\tfrac{1}{2} i q'_\alpha \tau^2 - \tfrac{1}{6} i q''_\alpha \tau^3\right]. \qquad (2.9)$$

Here $q = \mathbf{k}\cdot\mathbf{v}$, the points $t_\alpha(p_z)$ are all the solutions of the equations $q(t_\alpha, p_z) = 0$, $q'_\alpha = dq(t_\alpha)/dt$, $q''_\alpha = d^2q(t_\alpha)/dt^2$, and $g_\alpha = g(t_\alpha)$. The summation with respect to t_α is over all the t_α in the interval $(0, T)$, while the sum with respect to t_β denotes summation over all the roots $t_\beta \leq t_\alpha$, while the first term of the sum, $t_\beta = t_\alpha$, should be multiplied by ½, a fact designated by the prime. Integration with respect to p_z is over those values of p_z for which solutions of the equations $q(t, p_z) = 0$ exist.

We have retained two terms in the exponent of formula (2.9) for J_α, for $q'_\alpha(p_z)$ can vanish in certain important cases (see Sec. 3, item B). The term with q''_α can be neglected if $|q'_\alpha|^3 \gg |q''_\alpha|^2$. In this case

$$J_\alpha = (2\pi/|q'_\alpha|)^{1/2} \exp\left(-\tfrac{1}{4}\pi i s_\alpha\right), \qquad s_\alpha = q'_\alpha/|q'_\alpha|. \qquad (2.10)$$

In the opposite limiting case

$$J_\alpha = (6/|q''_\alpha|)^{1/3}\,\Gamma(1/3)\,3^{-1/2}. \qquad (2.11)$$

Equation (2.8) can be transformed to

$$\alpha = \alpha_0 + \alpha_1, \qquad \alpha_0 = (eH/2h^3Wc)\int dp_z \sum_{0<t_\alpha<T} |g_\alpha J_\alpha|^2, \qquad (2.12)$$

$$\alpha_1 = (eH/h^3Wc)\,\mathrm{Re}\int dp_z\,[1 - \exp(2\pi i\beta - 2\pi\gamma)]^{-1}$$

$$\times \sum_{0<t_\alpha<T} g^*_\alpha J_\alpha \sum_{0<t_\alpha - t_\beta\leqslant T} g_\beta J_\beta \exp\Big[\int_{t_\alpha}^{t_\beta} (\nu - iq)\,dt\Big]. \qquad (2.13)$$

Here $2\pi(\gamma - i\beta) = T(\overline{\nu} - i\overline{q})$. The bar denotes averaging over the period T:

$$\overline{\psi} = \frac{1}{T}\int_0^T \psi\,dt.$$

Contributions to α_0 are obviously made by all values of p_z. It is therefore easy to show, by using the expression (2.10) for J_α, that α_0 coincides with the absorption coefficient for $H = 0$, obtained by Akhiezer et al.[4]:

$$\alpha_0 = \pi h^{-3}W^{-1}\int d\tau_{\mathrm{p}}\,|g|^2\,\delta(\varepsilon - \mu_0)\,\delta(\mathbf{kv}) \sim N\mu_0\omega/\rho s v, \qquad (2.14)$$

where N is the density of the electrons in the metal.

The resonance effects, like the sharp anisotropy of the absorption, are due to the presence of the resonance factor $B(p_z) = [1 - \exp(2\pi i\beta - 2\pi\gamma)]^{-1}$.

3. RESONANT ABSORPTION OF ULTRASOUND ON CLOSED TRAJECTORIES

Let us consider magnetoacoustic resonance on closed trajectories, for which $\overline{v}_x = \overline{v}_y \equiv 0$ and $\overline{v}_z \neq 0$. When $k_z \neq 0$ the function $B(p_z)$ has a series of peaked maxima. For fixed values of the magnetic field and of the frequency, these maxima correspond to values $p_z = p_{zn}$ for which $\beta(p_{zn}) = k_z\overline{v}_z T/2\pi = n$ (n is an arbitrary integer or zero).

The values of p_{zn} do not occur, generally speaking, when $\beta(p_z)$ has extrema. However, if H and ω are such that at some value of n the condition $\beta(p_z) = n$ is satisfied for a value of $\beta(p_z)$ which is extremal with respect to p_z, then the maximum of $B(p_z)$ will be considerably broader than the others, and its contribution to the integral will be greater. Let us show that this maximum leads to resonance oscillations, and not merely to increments in the absorption coefficient, as stated by Gurevich.[2] These increments, as will be made clear in what follows, pertain to the edges of the resonance line and describe its asymmetry.

A. The absorption near the extremum points p_s of the function $\beta(p_z)$ has the form

$$\alpha \sim \frac{eH}{h^3Wc}\left|\sum_{t_\alpha} g_\alpha J_\alpha e^{-iA_\alpha}\right|^2_{p_s} \mathrm{Re}\int_{-\infty}^{\infty} dp_z\,\{1 - \exp$$

$$\times(2\pi i\Delta + \pi i\beta''(p_z - p_s)^2 - 2\pi\gamma)\}, \qquad (3.1)$$

where

$$\Delta = \beta_{ext} - n, \qquad 2\pi|\Delta| \ll 1,$$

$$2\pi|\gamma| \ll 1, \qquad A_\alpha = \int_0^{t_\alpha} q\,dt$$

and the small quantities $\nu(t_\beta - t_\alpha)$ have been neglected.

Expanding the exponential in a series and integrating, we obtain

$$\alpha = (eH/2h^3Wc)\,|\beta''|^{-1/2}\Big|\sum_{t_\alpha} g_\alpha J_\alpha e^{-iA_\alpha}\Big|^2 M,$$

$$M = \gamma(\gamma^2+\Delta^2)^{-1/2}\,[(\gamma^2+\Delta^2)^{1/2}+\sigma\Delta]^{-1/2}. \qquad (3.2)$$

The values of all the functions are taken at $p_z = p_s$, and $\sigma = |\beta''|/\beta''$.

Using (2.10), we obtain the following estimate for the height of the n-th maximum:

$$\alpha_n \sim \alpha_0 (kr\gamma)^{-1/2} \sim \omega^{1/2} H_n \bar{\nu}^{-1}. \qquad (3.3)$$

The relative width of the n-th maximum is $\Delta_n \sim \gamma$ or, expressed in terms of the magnetic field, $\Delta H/H_n \sim (kl)^{-1}$, is independent of n and is determined by the range. The greater l, the narrower the maximum and the higher the peak. Figure 1 shows schematically the dependence of the resonant absorption on H. With increasing n, the amplitude at the maximum decreases as n^{-1}, i.e., varies linearly with the field ($H_n \approx H_1 n^{-1}$).

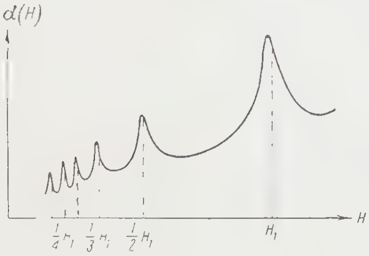

FIG. 1. Approximate course of resonant absorption vs. magnetic field for $\beta'' < 0$.

The form of any individual resonance line is determined by the factor M. Its maximum, of value $3^{3/4}2^{-1}\gamma^{-1/2}$, is reached when $\Delta = -3^{-1/2}\gamma^{-1/2}$, i.e., is shifted somewhat with respect to $\Delta = 0$.

The sharp jumps in the absorption coefficient, referred to by Gurevich,[2] pertain in this case actually to the edges of the resonance lines, and correspond to the limiting case $|\Delta| \gg \gamma$ of the general formula (3.2). These jumps describe the asymmetry of the resonance lines away from resonances when $\sigma\Delta > 0$ we have $M \approx \gamma|\Delta|^{-3/2}$ and when $\sigma\Delta < 0$ the value of M is on the order of $|\Delta|^{-1/2}$ and is $|\Delta|/\gamma \gg 1$ times greater than when $\sigma\Delta > 0$.

In evaluating the integral (3.1) near resonance we have assumed that the numerator, which contains the rapidly oscillating function $\exp\{iA_\alpha(p_z)\}$, varies slowly over the interval $\delta p_z \sim p_s (kl)^{-1/2}$. This assumption is justified if $\alpha_n/\alpha_0 \sim (kr\gamma)^{-1/2} \gg 1$, i.e., in the case of sharply pronounced resonance. In other words, sufficient sharpness of the resonance ensures the correctness of the limiting formula (3.3) If the inequality $\alpha_n \gg \alpha_0$ is not satisfied sufficiently well, then the resonance maxima will be shifted somewhat and "diffuse." In principle it is possible to take this effect into account by determining more accurately the positions of the stationary points in the integral with respect to p_z.

B. We proceed to estimate the contribution due to the limiting value $p_z = p_{z\,\lim}$. The latter is that maximum (minimum) value of p_z on the closed Fermi surface (Fig. 2) for which a unique point $\mathbf{k}\cdot\mathbf{v} = 0$ exists on the curve $p_z = p_{z\,\lim}$, $\epsilon(\mathbf{p}) = \mu_0$. For the sake of simplicity we consider a convex surface $\epsilon(\mathbf{p}) = \mu_0$ with a symmetry center. When $|p_z| < |p_{z\,\lim}|$ the electron trajectory has only two points t_α ($t_1 < t_2$) at which $\mathbf{k}\cdot\mathbf{v}(t) = 0$, and there are no such points at all when $|p_z| > |p_{z\,\lim}|$. The contribution from the limiting value must be estimated with caution, for when $p_z = p_{z\,\lim}$ we have $q'_\alpha = 0$ and expression (2.10) cannot be used for J_α. For small $\Delta p_z = p_{z\,\lim} - p_z$ we have $q'_\alpha \sim |\Delta p_z|^{1/2}$.

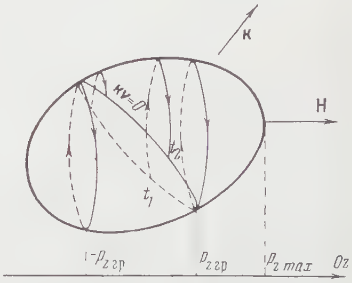

FIG. 2. Schematic form of electron trajectories and line $\mathbf{k}\cdot\mathbf{v}$ = const on closed convex surface $\varepsilon(\mathbf{p}) = \mu_0$.

The resonant part of the absorption coefficient can be written as

$$\alpha = \frac{eH}{h^3Wc}\,\mathrm{Re}\int dp_z \frac{|g_1J_1 + g_2J_2\exp(-iA_{21})|^2}{1-\exp(2\pi i\beta - 2\pi\gamma)}. \qquad (3.4)$$

We have neglected in the numerator the small quantities $\nu(t_\beta - t_\alpha)$, and replaced $\exp(2\pi i\beta)$ by unity.

Let us consider a case when $\beta'_{\lim}\,(d\beta/dp_z)_{\lim} \neq 0$ and $|\Delta| = |\beta_{\lim} - n| \ll (2\pi)^{-1}$. The relative width of the interval $\delta p_z/p_{z\,\lim}$ which makes an appreciable contribution to the integral is on the order of $(|\Delta| + \gamma)(kr)^{-1}$. Here

$$|q_\alpha'^3/q_\alpha''^2| \sim kr\,(\delta p_z/p_{z\,\lim})^{3/2} \ll 1,$$

and expression (2.11) must be used for J_α.

In this case the function $B(p_z)$ is "sharper" than $\exp(-iA_{21})$, since $A_{21}(p_z) = A_2 - A_1$ changes over the interval $\delta p_z \sim (kr)^{-1} p_{z\,\lim}$. Recognizing that $g_1J_1 = g_2J_2$ when $p_z = p_{z\,\lim}$, we obtain for small $|\Delta|$ and γ

$$\alpha_{\lim} = \frac{eH}{3h^3Wc}\frac{|g^2|}{|\beta'|}\left(\frac{6}{|q''|}\right)^{2/3}\Gamma^2(1/3)\left\{1+\frac{2\sigma}{\pi}\,\mathrm{arctg}\,\frac{\Delta}{\gamma}\right\}, \qquad (3.5)^*$$

---

*arctg = $\tan^{-1}$.

where $\sigma = (\beta'|/\beta')_{\lim}$. The factor preceding the curly bracket is of the order of $\alpha_0(kr)^{-2/3}$. Formula (3.5) describe periodic increments in the absorption coefficient, viz. the value of the expression in the curly brackets is 2 when $\sigma\Delta > 0$ and $|\Delta| \gg \gamma$, and is small ($\sim \gamma/|\Delta|$) when $\sigma\Delta < 0$.

The plot of α vs. H, given by Eq. (3.5), has a sawtooth shape with the "tooth" height decreasing with decreasing field. The magnitude of each jump is

$$\Delta\alpha = \frac{2eH\Gamma^2(1/3)\,|g|^2 6^{2/3}}{3h^3Wc\,|\beta'|\,|q''|^{2/3}} \sim \alpha_0(kr)^{-2/3} \sim \omega^{1/3}H_n^{2/3}. \quad (3.6)$$

The absorption increases with increasing H if $\beta' < 0$ and with decreasing H if $\beta' > 0$. On a closed convex Fermi surface, in particular, $\beta' > 0$ and α acquires increments when the magnetic field is decreased.

The dependence of the derivative $d\alpha/dH$ on H should display resonance peaks

$$H\,d\alpha/dH \sim \alpha_0(kr)^{1/3}\sigma\gamma/(\gamma^2 + \Delta^2), \quad (3.7)$$

with an amplitude at the maximum amounting to $(d\alpha/dH)_{\max} \sim \alpha_0(\gamma H)^{-1}(kr)^{1/3}$ and with a position determined by the condition $\beta_{\lim} = n$.

In the case of a quadratic dispersion law, as for any convex closed surface, β' does not vanish anywhere, and the resonance oscillations take place on the $d\alpha'/dH$ curve and are connected only with the limit point.

For a non-convex Fermi surface, the limit point may coincide with the 'extremal' point at some inclination of the vector **k** relative to **H**, i.e., $\beta'_{\lim}$ may vanish. In this case resonant oscillations can occur* when $\gamma(kl)^{1/4} \ll 1$:

$$\alpha_{\lim} = \frac{6^{2/3}\Gamma^2(1/3)\,eH\,|g^2|}{3h^3Wc\,|\beta''|^{1/2}\,|q''|^{2/3}}\,M. \quad (3.8)$$

Their amplitude is treater than in the case (3.3):

$$\alpha_n/\alpha_0 \sim (kr)^{-1/6}\gamma^{-1/2} \sim \omega^{5/6}H_n^{2/3}\nu^{-1/2}.$$

The relative shape and width of the resonance curve is the same as in case A.

C. Let us estimate the contribution to the absorption from the points p_{zn} at which $\beta(p_{zn}) = n$, and $\beta'(p_{zn}) \neq 0$. Near these points, when inequalities (2.7) are satisfied, we have

$$\operatorname{Re} B(p_z) \approx \pi\delta(\beta - n). \quad (3.9)$$

Consequently, the contribution of the points p_{zn} is given by the equation

$$\delta\alpha = \frac{\pi eH}{h^3Wc}\sum_n \int_{\Delta p_{zn}} dp_z\,\delta(\beta - n)\left|\sum_{t_\alpha} g_\alpha|q'_\alpha|^{-1/2}\right.$$
$$\left.\times\exp(-\pi i s_\alpha/4 - iA_\alpha)\right|^2 \quad (3.10)$$

Integration with respect to p_z is carried out in the vicinity of those points ($|p_{zn}| < |p_{z\,\lim}|$) at which $\beta(p_z) = n$, $\beta' \neq 0$, and $q'_\alpha \neq 0$.

It is seen from (3.10) that $\delta\alpha$ has no resonant character. The value of the non-oscillating part of $\delta\alpha$ is on the order of α_0, and the amplitudes of the individual oscillations are of the order of $\alpha_0(kr)^{-1}$ and less than the amplitude of the resonance or of the jumps in the absorption. When the number of terms in (3.10) is large, $\delta\alpha$ is an irregular function of H, owing to the large number of oscillating components with periods and amplitudes of the same order of magnitude.

Along with these singularities, the coefficient of absorption should also acquire smooth increments, connected with the extremal values of p_z (with $p_{z\,\max}$ on a closed convex surface), which were investigated by Gurevich.[2]

D. We investigate finally the sharp anisotropy of absorption when the vectors **k** and **H** deviate little from perpendicularity. We consider for simplicity trajectories on which $\mathbf{k}\cdot\mathbf{v} = 0$ at two points. The absorption can be represented as a sum of a monotonic and an oscillating part:

$$\alpha_{\text{mon}} = h^{-3}W^{-1}\int d\tau_{\mathbf{p}}\,\delta(\varepsilon - \mu_0)\,\delta(\mathbf{kv})\,|g^2|\,\gamma(\gamma^2 + \beta^2)^{-1}, \quad (3.11)$$

$$\alpha_{\text{osc}} = eH(\pi ch^3W)^{-1}\operatorname{Re}\int dp_z\,\gamma(\gamma^2 + \beta^2)^{-1}\,g_1g_2^*J_1J_2^*e^{iA_{21}}, \quad (3.12)$$

where $\beta = k_z\overline{v}_zT/2\pi$, and $k_z = k\sin\varphi$. When $\varphi = 0$, $\beta = 0$ and $\alpha_{\text{mon}} \sim \alpha_0\gamma^{-1}$, $\alpha_{\text{osc}} \sim \alpha_{\text{mon}}(kr)^{-1/2} \sim \alpha_0\gamma^{-1}(kr)^{-1/2}$. This case was investigated by Gurevich.[2] When $\varphi \ll (kl)^{-1}$ the average displacement of the electron in the direction of sound propagation is small ($|\beta| \ll \gamma$), and the absorption has the same form as when $\varphi = 0$.

In the angle interval $(kl)^{-1} \ll \varphi \ll (kr)^{-1}$ the number of electrons with $|\beta| \lesssim \gamma$, and hence the absorption, is $kl\varphi$ times smaller than when $\varphi = 0$. In this case the formula for α_{mon} is obtained from (3.11) by making the substitution $\gamma(\gamma^2 + \beta^2)^{-1} \rightarrow \pi\delta(\beta)$:

$$\alpha_{\text{mon}} = \pi h^{-3}W^{-1}\int d\tau_{\mathbf{p}}\,|g^2|\,\delta(\mathbf{kv})\,\delta(\beta)\,\delta(\varepsilon - \mu_0) \sim \alpha_0(kr\varphi)^{-1}. \quad (3.13)$$

The ratio of the "speeds" of the variations of $(\gamma^2 + \beta^2)^{-1}$ and of $\exp(iA_{21})$ in (3.12) is important for the estimate of α_{osc}. The oscillating factor near the central section, where $A_{21}(p_z)$ has an extremum, changes appreciably in the interval δp_1

---

*When this inequality is satisfied, the "sharpest" is the function $B(p_z)$, and Eq. (2.11) must be used for J_α.

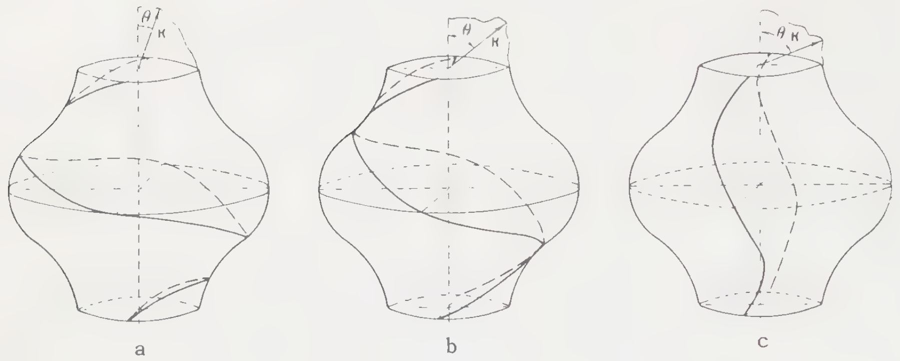

FIG. 3. Line **k·v** = 0 on a "corrugated cylinder" type of surface. a – $\theta < \theta_0$, b – $\theta = \theta_0$, c – $\theta > \theta_0$ (θ_0 is the maximum angle of inclination of the "corrugation" to the cylinder axis).

$\sim p_0(kr)^{-1/2}$, and $(\gamma^2 + \beta^2)^{-1}$ changes over a distance $\delta p_2 \sim p_0(kl\varphi)^{-1}$ (p_0 is the characteristic momentum of the electron). δp_1 is proportional to the number of electrons for which $|A_{21}(p_z) - A_{21}(0)| \lesssim 1$, while δp_2 is proportional to the number of electrons with $|\beta| \leq \gamma$. When $\delta p_2 \ll \delta p_2$ [i.e., $\varphi \ll (\gamma/kl)^{1/2}$] application of the method of stationary phase yields $\alpha_{\mathrm{osc}} \sim \alpha_0\gamma^{-1}(kr)^{-1/2}$. The period of oscillation is the same when $\varphi \ll 1$ as when $\varphi = 0$, and coincides with the extremal diameter of the Fermi surface in the direction of **k** × **H**. In the opposite limiting case, $\delta p_2 \ll \delta p_1$, we can replace $\gamma(\gamma^2 + \beta^2)^{-1}$ by $\pi\delta(\beta)$ and $\alpha_{\mathrm{osc}} \sim \alpha_{\mathrm{mon}} \sim \alpha_0(kr\varphi)^{-1}$.

Thus, the monotonic part of the absorption falls off at small φ much more rapidly than the oscillating part, and when $(\gamma/kl)^{1/2} \ll \varphi \ll (kr)^{-1}$ the amplitude of the oscillations is comparable with the value of α_{mon} (remaining, naturally, smaller than the latter). With further increase in φ, the nonresonant oscillations are replaced by the resonant oscillations investigated above. The latter take place, generally speaking, for all $\varphi \gtrsim (kr)^{-1}$, and particularly also when $\varphi = \pi/2$ (**k** ∥ **H**). However, resonance will occur for $\varphi = \pi/2$ only when the curve $v_z = 0$ is not plane and consequently does not coincide with the curve $\bar{v}_z = p_z = 0$. If the two curves coincide (for example, in the case of quadratic dispersion), then the oscillations will take place only when $|\pi/2 - \varphi| \gg (kr)^{-1}$. Near $\varphi = \pi/2$ ($|\pi/2 - \varphi| < (kr)^{-1}$) the oscillations vanish, and $\alpha = \alpha_0$ il the range of fields under consideration.

All the foregoing statements regarding closed surfaces holds true for closed trajectories on open Fermi surfaces.

4. SINGULARITIES IN THE ABSORPTION OF ULTRASOUND ON OPEN PERIODIC TRAJECTORIES

Most metals have open Fermi surfaces.[5,8,9] When the vector **H** lies in the crystallographic plane, the open trajectories are periodic. Since the electrons absorb sound most effectively when entering the equal-phase plane, an important role is played by the position of the lines **k** · **v** = 0 on the surface $\epsilon(\mathbf{p}) = \mu_0$. Figure 3 shows the lines **k** · **v** = 0 on a surface of the "corrugated" cylinder of revolution type for different angles of inclination θ of the vector k to the cylinder axis x. When $\theta < \theta_0$ (θ_0 is the angle of inclination of the "corrugation" to x at the parabolic point) two closed non-intersecting lines **k** · **v** = 0 (Fig. 3a) exist in each cell of the reciprocal lattice. When $\theta = \theta_0$ they are in contact (Fig. 3b), and when $\theta > \theta_0$ they go into two open periodic curves, which are symmetrical about the plane passing through k and x (Fig. 3c). In the general case these lines are not planar, with the exception of $\theta = 0$ and $\theta = \pi/2$.

For a planar network of "corrugated cylinders,"* when the vector **k** is parallel to the cylinder axis, the lines **k** · **v** = 0 represent an aggregate of closed and open periodic curves (Fig. 4a). As the vector **k** is tilted away from the cylinder axis, the closed and open lines come closer and become tangent at a certain orientation of the vector **k** (Fig. 4b). Further deviation of the vector k causes the lines **k** · **v** = 0 to be closed (Fig. 4a). On the open trajectories we have $\bar{v}_x \equiv 0$ and $|\bar{v}_y T| = cb_x/eH$, where b_x is the period of the open trajectory in momentum space in the direction of x.

On the closed trajectories we have $\bar{v}_x = \bar{v}_y = 0$. The limit between the open and closed trajectories is a self-intersecting curve passing through the saddle point, at which the effective mass and the period T become infinite logarithmically.[8]

If the vector **k** makes, with the direction x of the open periodic trajectory an angle much less than $(kl)^{-1}$, the expression for α has the same form as in the case of closed trajectories when **k** ⊥ **H** (see reference 2). The period of the oscilla-

---

*Such a surface is similar in its topological properties to the Fermi surface in tin.[10]

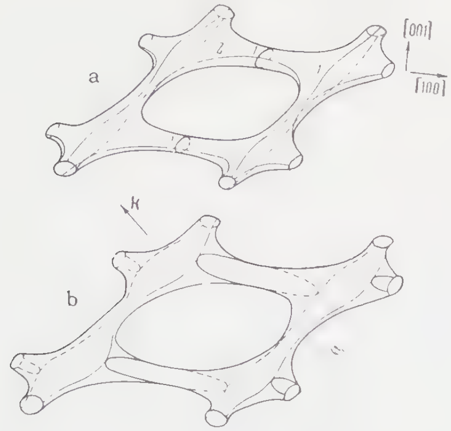

FIG. 4. Lines $\mathbf{k}\cdot\mathbf{v} = 0$ on a surface comprising a planar network of "corrugated cylinders," a) line 1 – $\mathbf{k}$ directed along the 100 axis; 2 – along the 001 axis; b) $\mathbf{k}$ in the (010) plane. The figure shows the instant of tangency between the open and closed lines $\mathbf{k}\cdot\mathbf{v} = 0$.

tions is determined by the extremal dimension of the open trajectory in the $\mathbf{k} \times \mathbf{H}$ direction (for a "corrugated cylinder" — by the height of the "corrugation" on the axial section).

When the vector $\mathbf{k}$ deviates from the xz plane ($\mathbf{H} \parallel z$), the open surface is equivalent to a closed non-convex surface, and the analysis given in Sec. 3 is fully applicable.

When $\mathbf{k} \perp \mathbf{H}$, the contribution to absorption from the open trajectories diminishes rapidly as the vector $\mathbf{k}$ tilts away from the x direction, since the quantity $|\beta| = (kcb_x/2\pi eH)\sin\theta$ (θ is the tilt angle) never vanishes for all the electrons on the unclosed trajectories. Consequently when $(kl)^{-1} \ll \theta \ll (kr)^{-1}$, both the monotonic and the oscillating parts of the absorption from the open trajectories are $(kl\theta)^2$ times smaller than when $\theta = 0$.*

When $\theta \gg (kr)^{-1}$, resonant oscillations are produced. Unlike the closed trajectories, resonant oscillations take place also when $\mathbf{k} \perp \mathbf{H}$. Since β is independent of p_z, it is possible near resonance to take $\operatorname{Re} B(p_z) \approx \gamma_0 [\pi(\gamma_0^2 + \Delta^2)]^{-1}$ outside the integral sign in (2.13), and the absorption will have the form

$$\alpha = \frac{eH\gamma_0}{\pi h^3 Wc\,(\gamma_0^2 + \Delta^2)} \int dp_z \left| \sum_{t_\alpha} g_\alpha J_\alpha e^{-iA_\alpha} \right|^2 \sim \frac{\alpha_0\gamma_0}{\gamma_0^2 + \Delta^2}, \qquad (4.1)$$

where γ_0 is the characteristic value of $\gamma(p_z)$. The integration in (4.1) is over the layer of open trajectories, on which there are points t_α. It is seen from (4.1) that at resonance $\alpha_n \sim \alpha_0\gamma_0^{-1}$ and is comparable with the non-oscillating part of the absorption on the closed trajectories. In this case the resonance is "sharper" than on the closed trajectories with $k_z \neq 0$, since the average displacement $|\bar{v}_y T|$ is the same for all the electrons and there is no additional averaging over p_z.

On these resonance oscillations are superimposed oscillations of relatively small amplitude $[\sim \alpha_0\gamma_0^{-1}(kr)^{-1/2}]$ from the central section (for $\theta < \theta_0$ in the case of a cylinder) with a period $\Delta H^{-1} = |2\pi ec^{-1}(k_x\Delta p_y - k_y\Delta p_x)_0|$, and oscillations from the self-intersecting trajectory (saddle point) with two periods (the periods are different on the sides of the open and closed trajectories), and with an amplitude which is roughly $(kr)^2$ times as small as the amplitude of the resonance oscillations. The phase of these last oscillations has a logarithmically slow dependence on the field.*

The resonant oscillations vanish when $\mathbf{k} \perp \mathbf{H}$ at an angle θ_k of between the vector k and x such that the angle $\mathbf{k}\cdot\mathbf{v} = 0$ shifts on the closed trajectories. In this case the analysis carried out in the preceding section is fully applicable.

The amplitude of the resonance oscillations depends quite sharply on the angle φ between the vector k and the plane $\mathbf{k} \perp \mathbf{H}$. The results given above are valid when $\varphi \ll (kl)^{-1}$. In the region $(kl)^{-1} \ll \varphi \ll (kr)^{-1}$ the amplitude of the resonance has at the maximum an order of $\alpha_0 (kr\varphi)^{-1}$ and is kl times as small as when $\varphi = 0$. In the angle interval $(\gamma_0/kl)^{1/2} \ll \varphi \ll (kr)^{-1}$, when $\theta < \theta$, the amplitude of the resonant oscillations from the central section is comparable with the amplitude of the resonance, similar to what takes place on the closed trajectories (see Sec. 3, item D). In the region of angles $\varphi \gg (kr)^{-1}$, resonant oscillations take place, along with periodic increments in the coefficient of absorption, similar to those that exist on closed trajectories when $k \neq 0$.

5. ANISOTROPY OF THE ABSORPTION ON OPEN PERIODIC OR STRONGLY ELONGATED CLOSED TRAJECTORIES

Trajectories of this type are as a rule insignificant in the absorption of ultrasound. Exceptions are the almost-periodic trajectories with a period on the order of the reciprocal-lattice period. In order to make the following arguments clear, let us consider a specific example of a "corrugated cylinder" surface, when the vector **H** is almost perpendicular to the axis x of the cylinder.

---

*When the vector $\mathbf{k}$ makes with x an arbitrary small angle $\kappa[\kappa \gg (kl)^{-1}]$, then the period of the oscillations is determined by the extremal dimensions of the trajectories in the y direction when $\kappa \ll (\gamma/kl)^{1/2}$, and by the dimensions of the trajectories with $\beta(p_z) \equiv (T/2\pi)(k_y\bar{v}_y + k_z\bar{v}_z) = 0$ when $\kappa \gg (\gamma/kl)^{1/2}$. We note that even at small κ these periods can differ greatly from each other.

*In view of the smallness of the amplitude of the oscillations connected with the saddle point, we do not give the exact formulas and limit ourselves to the remark that we must remember in the calculations that $T \to \infty$ logarithmically near the saddle point. The estimate in the text is valid if $\gamma_0 \ln kr \ll 1$.

In addition to the closed trajectories contained within each reciprocal-lattice cell, there exist strongly elongated closed trajectories,[7] which include $\sim \psi^{-1}$ cells of the reciprocal lattice (ψ is the angle between **H** and the plane perpendicular to x). When **k** is perpendicular to the x axis, then the strongly-elongated trajectories have only two points with $\mathbf{k}\cdot\mathbf{v} = 0$. When $\psi \ll r/l$, the time of motion of the electron between the neighboring points where $\mathbf{k}\cdot\mathbf{v} = 0$ is considerably greater than the time of the free path, t_0. In this case the H-dependent contribution to the absorption from the considered trajectories is exponentially small, and the coefficient of absorption from the strongly elongated trajectories is the same as when H = 0.

When $r/l \ll \psi \ll 1$ and $\mathbf{k} \perp \mathbf{H}$, α_{osc} is on the order of $\alpha_0 (lr)(kr)^{-1/2}\psi^2$, and the order of magnitude of the period of oscillations is ψ^{-1} times as small as in the case of closed Fermi surfaces.

Let **k** be directed parallel to the x axis, and let $q'_\alpha > 0$ when $0 < t_\alpha < T/2$ and $q'_\alpha < 0$ when $T/2 < t_\alpha < T$. The number of points with $\mathbf{k}\cdot\mathbf{v} = 0$ on a strongly elongated closed trajectory is of the order of ψ^{-1}. To estimate the sum under the integral sign in (2.13) let us calculate

$$S = \sum_{0<t_j<t_l<T/2} g_j^* g_l J_j^* J_l \exp\left[\int_{t_l}^{t_j} (\nu - iq)\, dt\right]. \tag{5.1}$$

The remainder of the sum is of the same order as S. Confining ourselves to linear terms in $\psi \ll (kr)^{-1}$, we obtain

$$A_{lj} = \int_{t_j}^{t_l} q\, dt = \begin{cases} A + A\psi(l-j) & (l-j = 2n+1) \\ A\psi(l-j) & (l-j = 2n), \end{cases} \tag{5.2}$$

where $A(p_z) \sim kr$; n is an integer.

Using (5.2) and replacing summation over t_j and t_l in (5.1) by integration with respect to j and l, we obtain

$$S \sim \psi^{-2} |gJ|^2 (1 + e^{iA}) \{(2iA - \pi\gamma)^{-1} + (2iA - \pi\gamma)^{-2}(1 - e^{2iA-\pi\gamma})\}. \tag{5.3}$$

With the aid of (5.3) we can readily estimate the contribution to from strongly elongated trajectories. The results of calculations are listed in the following table:

	$\varphi \ll (kl)^{-1}$	$(kl)^{-1} \ll \psi \ll (kr)^{-1}$; $\psi \ll r/l$	$r/l \ll \psi \ll (kr)^{-1}$
$\alpha_{\text{mon}}/\alpha_0$	l/r	$(kr\psi)^{-2}$	$(kr\psi)^{-2}$
$\alpha_{\text{osc}}/\alpha_0$	$(l/r)(kr)^{-1/2}$	$(kr)^{-3/2}\psi^{-1}$	$(kr\psi)^{-1}$

If the vector **H** is tilted away from a crystallographic plane with small rational indices (nm0) ($\sqrt{n^2 + m^2} \ll l/r$) by an angle less than $(kl)^{-1}$, then the open trajectories make the same contribution to the absorption of the ultrasound as the strictly periodic trajectories.

6. CONCLUSION

Magnetoacoustic resonance can be used to reconstruct the topology and the form of the Fermi surfaces in metals.

a) The presence of resonant oscillations of the non-harmonic type when $\mathbf{k} \perp \mathbf{H}$ is connected with the existence of open periodic trajectories for a given direction of **H**. The observed resonances at $\mathbf{k}\cdot\mathbf{H} \neq 0$ are evidence of the non-convexity of the Fermi surface, i.e., of a sharp deviation of the dispersion from a quadratic law.

b) If open periodic trajectories exist for a given direction of **H**, then the diagram of the rotation of the vector **k** in the plane $\mathbf{k} \perp \mathbf{H}$ should disclose a sharp maximum when the vector **k** is parallel to the direction of the open periodic trajectory. This maximum is the principal (greatest) one and its position is independent of the magnetic field, whereas the position of the lateral maxima shifts with changing H. For closed trajectories, the absorption is almost isotropic when $\mathbf{k} \perp \mathbf{H}$, and there are no resonant oscillations.

c) To determine the form of the Fermi surface we can use non-resonant oscillations of the harmonic type, the period of which is determined by the extremal dimensions of the Fermi surface in the $\mathbf{k} \times \mathbf{H}$ direction. Owing to the sharp anisotropy in the angular dependence of the amplitude of the nonresonant oscillations due to the open periodic trajectories, it is possible to determine the extremal dimensions of the open and closed trajectories separately.

The experimental researches of Galkin and Korolyuk[11] on single crystals of high-purity tin at $\omega/2\pi = 220$ Mc/sec have shown that resonant non-sinusoidal oscillations exist when $\mathbf{k} \perp \mathbf{H}$. All the main characteristics of the experimental curve (periodicity in the reciprocal of the field, vanishing of the oscillation phase, dependence of the width and height of the maximum on the field) confirm fully the theoretical deductions.[11] Galvanomagnetic measurements[9,10] show that the Fermi surface of tin is open in the (001) plane. The period of the reciprocal lattice as calculated from the period of these oscillations is in good agreement with the known crystallographic data (see reference 11).

Recently Morse and co-workers determined the extremal dimensions of the open Fermi surface of gold and silver in the (111) plane from the periods of the nonresonant oscillations. Their data are in good agreement with the results of galvanomagnetic measurements, the de Haas — van Alphen effect, and others.

Thus, an investigation of the absorption of ultrasound in metals in a magnetic field, along with galvanomagnetic and other effects, is a good method of reconstructing the topology of Fermi surfaces in metals. It yields not only the directions of the open trajectories, but also the anisotropy of the diameters and hence the form of the extremal sections on the Fermi surface. The absorption of ultrasound is more convenient than the other high-frequency properties of metals in that it is a volume rather than surface phenomenon, and consequently the need for a perfect surface finish is eliminated.

In conclusion, we are grateful to L. D. Landau, I. M. Lifshitz, M. I. Kaganov, and V. L. Gurevich for a discussion of the results of this investigation.

---

[1] A. B. Pippard, Phil. Mag. **2**, 1147 (1957).

[2] V. L. Gurevich, JETP **37**, 71 (1959), Soviet Phys. JETP **10**, 51 (1960).

[3] M. Ya. Azbel' and É. A. Kaner, JETP **32**, 896 (1957), Soviet Phys. JETP **5**, 730 (1957).

[4] Akhiezer, Kaganov, and Lyubarskiĭ, JETP **32**, 837 (1957), Soviet Phys. JETP **5**, 685 (1957).

[5] Lifshitz, Azbel', and Kaganov, JETP **31**, 63 (1956), Soviet Phys. JETP **4**, 41 (1957).

[6] É. A. Kaner, JETP **38**, 212 (1960), Soviet Phys. JETP **11**, 154 (1960).

[7] I. M. Lifshitz and V. G. Peschanskiĭ, JETP **35**, 1251 (1958) and **38**, 188 (1960), Soviet Phys. JETP **8**, 875 (1959) and **11**, 137 (1960).

[8] I. M. Lifshitz and M. I. Kaganov, Usp. Fiz. Nauk **69**, 419 (1959), Soviet Phys. Uspekhi **2**, 831 (1960).

[9] N. E. Alekseevskiĭ and Yu. P. Gaĭdukov, JETP **35**, 554 (1958), **36**, 447 (1959), and **37**, 672 (1959); Soviet Phys. JETP **8**, 383 (1959), **9**, 311 (1959), and **10**, 481 (1960).

[10] Alekseevskiĭ, Gaĭdukov, Lifshitz, and Peschanskiĭ, JETP **39**, 1201 (1960), Soviet Phys. JETP **12**, 837 (1961).

[11] Galkin, Kaner, and Korolyuk, Dokl. Akad. Nauk SSSR **134**, 74 (1960), Soviet Phys.-Doklady **5**, 1002 (1961).

[12] Morse, Myers, and Walker, Phys. Rev. Lett. **4**, 605 (1960).

Translated by J. G. Adashko
34

SOVIET PHYSICS JETP VOLUME 13, NUMBER 1 JULY, 1961

INTEGRAL EQUATION FOR PION-NUCLEON SCATTERING AT LOW ENERGIES

CHOU HUNG-YÜAN

Joint Institute for Nuclear Research

Submitted to JETP editor July 9, 1960

J. Exptl. Theoret. Phys. (U.S.S.R.) 40, 227-236 (January, 1961)

A set of coupled integral equations for the S and P pion-nucleon scattering wave amplitudes at small energies is deduced on basis of the dispersion relations for forward and backward scattering and the unitarity condition. The contribution of the cut in the nonphysical region is taken into account without applying the analytic continuation by the Legendre expansion. The integral equations include $N\bar{N}$-annihilation amplitudes, which are explicitly connected with the presence of the $\pi\pi$-interaction.

1. INTRODUCTION

SEVERAL authors[1-3] have recently attempted to solve the problem of strong interaction at low energies on the basis of the two-dimensional dispersion relation proposed by Mandelstam.[4-6] They used from the very outset the dispersion relations for the partial amplitudes. The scattering amplitudes in the nonphysical region were obtained by means of an analytic continuation of the Legendre expansion from the physical region, which becomes invalid on the boundary of the region, where the spectral functions do not vanish.

Efremov, Meshcheryakov, Shirkov, and Chou[7] have shown, however, that the higher partial waves in the Legendre expansion cannot be neglected. In particular, if the contribution from the nonphysical region is not cut off at high energies, then the coefficients of the higher partial amplitudes even diverge.

In the present paper we derive a system of coupled integral equations for the amplitudes of the S and P waves of pion-nucleon scattering at low energies, using the dispersion relations for the forward and backward scattering and the unitarity conditions. The dispersion relations for the forward and backward scattering have the advantage that the scattering amplitudes in the nonphysical region can be expressed directly in terms of the amplitudes of the crossing reactions without the use of analytic continuation. The problem of the violation of the Legendre expansion does not arise here. It is very possible that these integral equations will permit a more accurate evaluation of the contribution due to cutoff in the nonphysical region. The dispersion relation for the backward scattering, together with the integral equations, contains the amplitudes of the annihilation reaction $N + \bar{N} \rightarrow \pi + \pi$, so that the influence of the $\pi\pi$ interaction can be taken into account.

The integral equations obtained should be solved simultaneously with the integral equations for the annihilation $N + \bar{N} \rightarrow \pi + \pi$. Quite recently, Efremov, Meshcheryakov and Shirkov[8] obtained a system of integral equations for the scattering, under the assumption that the $N\bar{N}$ annihilation proceeds in the low-energy region predominantly via the S and P states. They have also used the advantage of the dispersion relation for the backward scattering.[9] Their system of integral equations has an interesting feature in that it can be solved without knowledge of the $N\bar{N}$ annihilation amplitudes, provided the $\pi\pi$ scattering phases are known.

The integral equation derived in the present paper is suitable for the case when the real part of the annihilation amplitude in the states with higher moments cannot be neglected compared with the annihilation amplitudes in the S and P states.

In the second section of the present paper we investigate the locations of the singularities of the forward and backward scattering amplitudes.

In Sec. 3 we write out the dispersion relations for the forward and backward scattering, and give the connection between the amplitudes of the S and P waves, on the one hand, and the forward and backward scattering amplitudes on the other. In Sec. 4 we derive integral equations for the amplitudes of the S and P waves. The results obtained are compared with those of Chew, Goldberger, Low, and Nambu.[10]

2. REGION OF VALIDITY OF THE LEGENDRE EXPANSION

The notation used in the present paper is standard. For convenience, however, we shall define it in this section.

As is well known, processes of the form

$$\begin{array}{ll} \text{I.} & \pi(p_1, \alpha) + N(p_3) \rightarrow \pi(-p_2, \beta) + N(-p_4), \\ \text{II.} & \pi(p_2, \beta) + N(p_3) \rightarrow \pi(-p_1, \alpha) + N(-p_4), \\ \text{III.} & N(p_3) + \overline{N}(p_4) \rightarrow \pi(-p_1, \alpha) + \pi(-p_2, \beta) \end{array} \tag{1}$$

are described by a single Green's function. Here π, N, and $\overline{\text{N}}$ are respectively the pion, nucleon, and antinucleon. The p's inside the parentheses denote the corresponding four-momentum vectors, directed inward; α and β are the isotopic spin indices.

In the momentum representation, the Green's function has the form

$$T = \delta_{\beta\alpha}\{-A^{+}(s, \bar{s}, t) + \tfrac{1}{2} i(\hat{p}_1 - \hat{p}_2) B^{+}(s, \bar{s}, t)\}$$
$$+ \tfrac{1}{2}[\tau_3, \tau_\alpha]\{-A^{-}(s, \bar{s}, t) + \tfrac{1}{2} i(\hat{p}_1 - \hat{p}_2) B^{-}(s, \bar{s}, t)\}, \tag{2}$$

where

$$s = -(p_1 + p_3)^2 = -(p_2 + p_4)^2,$$
$$\bar{s} = -(p_1 + p_4)^2 = -(p_2 + p_3)^2,$$
$$t = -(p_1 + p_2)^2 = -(p_3 + p_4)^2, \qquad s + s + t = 2m^2 + 2 \tag{3}$$

(m is the nucleon mass, and the pion mass is set equal to unity). Only two of the three variables s, $\bar{\text{s}}$, and t are independent here.

The invariant functions $A^{\pm}$ and $B^{\pm}$ satisfy the following relations:

$$A^{\pm}(s, \bar{s}, t) = \pm A^{\pm}(\bar{s}, s, t), \qquad B^{\pm}(s, \bar{s}, t) = \mp B^{\pm}(\bar{s}, s, t). \tag{4}$$

According to Mandelstam,[4] they also satisfy the following two-dimensional dispersion relations

$$A^{\pm}(s, \bar{s}, t) = \frac{1}{\pi^2}\int\limits_{(m+1)^2}^{\infty} ds' \int\limits_{(m+1)^2}^{\infty} d\bar{s}' \frac{a_{12}^{+}(s', \bar{s}')}{(s' - s)(\bar{s}' - \bar{s})}$$
$$+ \frac{1}{\pi^2}\int\limits_{(m+1)^2}^{\infty} ds' \int\limits_{4}^{\infty} dt' \frac{a_{13}^{\pm}}{(s' - s)} \frac{(s', t')}{(t' - t)}$$
$$+ \frac{1}{\pi^2}\int\limits_{(m+1)^2}^{\infty} d\bar{s}' \int\limits_{4}^{\infty} dt' \frac{a_{23}(\bar{s}', t')}{(\bar{s}' - \bar{s})(t' - t)},$$
$$B^{\pm}(s, \bar{s}, t) = \frac{g^2}{m^2 - s} \mp \frac{g^2}{m^2 - \bar{s}}$$
$$+ \frac{1}{\pi^2}\int\limits_{(m+1)^2}^{\infty} ds' \int\limits_{(m+1)^2}^{\infty} d\bar{s}' \frac{b_{12}^{\pm}(s', \bar{s}')}{(s' - s)(\bar{s}' - \bar{s})}$$
$$+ \frac{1}{\pi^2}\int\limits_{(m+1)^2}^{\infty} ds' \int\limits_{4}^{\infty} dt' \frac{b_{13}^{\pm}(s', t')}{(s' - s)(t' - t)}$$
$$+ \frac{1}{\pi^2}\int\limits_{(m+1)^2}^{\infty} d\bar{s}' \int\limits_{4}^{\infty} dt' \frac{b_{23}^{\pm}(\bar{s}', t')}{(\bar{s}' - \bar{s})(t' - t)}, \tag{5}$$

where $a^{\pm}$ and $b^{\pm}$ are spectral functions, and g is the renormalized rationalized πN-coupling constant.

To facilitate the analysis we introduce the following variables in the center-of-mass system: k and Φ — momentum and scattering angle for reaction I; $\bar{\text{k}}$ and $\overline{\Phi}$ — momentum and scattering angle for reaction II; p, q, and θ — respectively the nucleon and antinucleon momentum, the pion momentum, and the scattering angle for reaction III. We then have the following relations for reaction I:

$$s = m^2 + 1 + 2k^2 + 2\sqrt{(m^2 + k^2)(1 + k^2)},$$
$$\bar{s} = m^2 + 1 - 2k^2 x - 2\sqrt{(m^2 + k^2)(1 + k^2)}, \tag{6}$$
$$t = -2k^2(1 - x), \qquad x \equiv \cos\Phi.$$

The corresponding relations for reaction II are

$$s = m^2 + 1 - 2\bar{k}^2\bar{x} - 2\sqrt{(m^2 + \bar{k}^2)(1 + \bar{k}^2)},$$
$$\bar{s} = m^2 + 1 + 2\bar{k}^2 + 2\sqrt{(m^2 + \bar{k}^2)(1 + \bar{k}^2)}, \tag{7}$$
$$t = -2\bar{k}^2(1 - \bar{x}), \qquad \bar{x} \equiv \cos\overline{\Phi}.$$

For reaction III we have

$$s = -p^2 - q^2 + 2pqz, \qquad \bar{s} = -p^2 - q^2 - 2pqz,$$
$$t = 4(m^2 + p^2) = 4(1 + q^2), \qquad z = \cos\theta, \tag{8}$$

It is known from experiment that only small values of the momentum are significant for πN scattering at low energies, and the other states can be neglected. As indicated in reference 7, to determine a small number of partial amplitudes it is sufficient to have dispersion relations for only several fixed values of the angle. Thus, in the energy region where all the states except S and P can be neglected, we need dispersion relations for two angles only. The most suitable angles are $\Phi = 0$ and $\Phi = \pi$.

The forward scattering for reaction I is determined by the condition

$$t = 0, \tag{9}$$

which determines also the forward scattering for reaction II. The backward scattering in reaction I is determined by the condition

$$\bar{s}s = (m^2 - 1)^2. \tag{10}$$

Simple calculations show that (10) determines also the backward scattering in reaction II and the forward and backward scattering in reaction III. In Fig. 1, condition (9) is represented by a straight line while condition (2) corresponds to the hyperbola and to the ellipse.

The branch of the hyperbola in region $t \leq 4$ is connected with the backward scattering in reactions I and II. The second branch, in the region $t \geq 4m^2$ is connected with the backward and forward scattering in reaction III. The ellipse, on which s and $\bar{\text{s}}$ are complex, corresponds to the nonphysical region of reaction III, where $4 \leq t \leq 4m^2$.

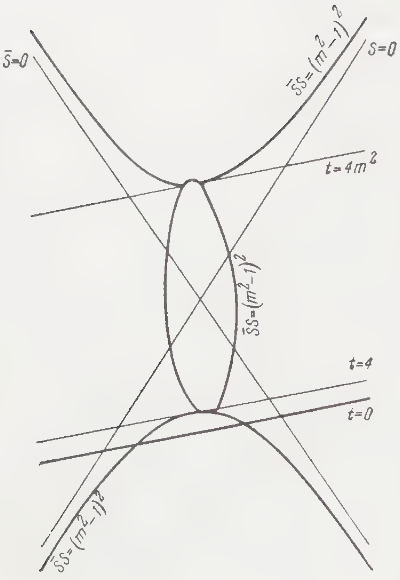

FIG. 1

The dispersion integral for the forward scattering is taken along the line t = 0. The scattering amplitudes for reaction I in the nonphysical region are directly connected with the amplitudes for reaction II in the physical region when cos Φ = 1. Thus, no analytic continuation is necessary.

For the backward scattering the dispersion integral is taken along the curve given by Eq. (10). The scattering amplitudes of reaction I in the nonphysical region are connected not only with the backward scattering in reaction II, but also with the scattering amplitude of reaction III when cos Φ = ± 1. Inasmuch as the unitarity condition for reaction III, as was shown by Mandelstam,[11] is analytically continued in the region $4 \leq t \leq 4m^2$, no further analytic continuation is necessary in this case, too.

The singularities in the cuts of the forward and backward scattering amplitudes for reaction I in the complex s plane can be obtained by projecting the curves of Fig. 1 on this plane. The singularities of the forward scattering amplitudes are well known; the cuts of the backward scattering amplitudes are shown in Fig. 2. The position of the poles is also well known and is therefore not shown in Fig. 2.

3. DISPERSION RELATIONS FOR FORWARD AND BACKWARD SCATTERING

The dispersion relations for the forward scattering have the form

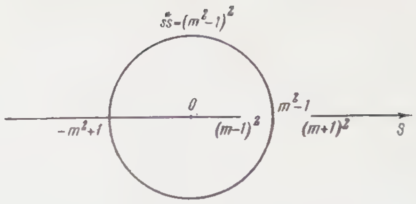

FIG. 2

$$A^{\pm}(s, \cos\Phi = 1) = \frac{1}{\pi}\int\limits_{(m+1)^2}^{\infty} ds' \left(\frac{1}{s'-s} \pm \frac{1}{s'-\bar{s}_+}\right) A_1^{\pm}(s', 1),$$

$$B^{\pm}(s, 1) = \frac{g^2}{m^2-s} \mp \frac{g^2}{m^2-\bar{s}_+} + \frac{1}{\pi}\int\limits_{(m+1)^2}^{\infty} ds' \left(\frac{1}{s'-s} \mp \frac{1}{s'-\bar{s}_+}\right) B_1^{\pm}(s', 1). \tag{11}$$

$A_1^{\pm}$ and $B_1^{\pm}$ have been determined by Mandelstam[4] and coincide with the imaginary parts of $A^{\pm}$ and $B^{\pm}$ in the physical region of reaction I; $\bar{s}_+$ is defined as

$$\bar{s}_+ \equiv 2m^2 + 2 - s. \tag{12}$$

We can also calculate directly the dispersion relations for the backward scattering. The positions of the singularities and of the cuts for this case are shown in Fig. 2. From this follow directly the dispersion relations (the pole terms are separated, the integration contour is chosen as shown in Fig. 3):

$$A^{\pm}(s, \cos\Phi = -1) = \frac{1}{\pi}\int\limits_{(m+1)^2}^{\infty} ds' \frac{A_1^{\pm}(s', -1)}{s'-s} - \frac{1}{\pi}\int\limits_{0}^{(m-1)^2} ds' \frac{A_2^{\pm}(s', -1)}{s'-s} - \frac{1}{\pi}\left\{\int\limits_{g_+} + \int\limits_{g_-} - \int\limits_{-m^2+1}^{0} + \int\limits_{-\infty}^{-m^2+1}\right\} ds' \frac{A_3^{\pm}(s', -1)}{s'-s},$$

$$B^{\pm}(s, -1) = \frac{g^2}{m^2-s} \mp \frac{g^2}{m^2-\bar{s}_-} + \frac{1}{\pi}\int\limits_{(m+1)^2}^{\infty} ds' \frac{B_1^{\pm}(s', -1)}{s'-s} - \frac{1}{\pi}\int\limits_{0}^{(m-1)^2} ds' \frac{B_2^{\pm}(s', -1)}{s'-s} - \frac{1}{\pi}\left\{\int\limits_{g_+} + \int\limits_{g_-} - \int\limits_{-m^2+1}^{0} + \int\limits_{-\infty}^{-m^2+1}\right\} ds' \frac{B_3^{\mp}(s', -1)}{s'-s}. \tag{13}$$

$A_2^{\pm}$, $B_2^{\pm}$ and $A_3^{\pm}$, $B_3^{\pm}$ are also given in Mandelstam's paper. They coincide with the imaginary parts of

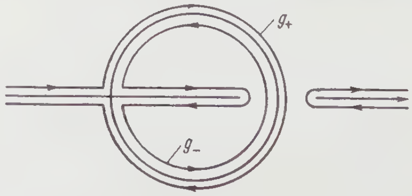

FIG. 3

$A^\pm$ and $B^\pm$ in the physical region of reaction II and III respectively. The contour g_+ is a semicircle in the upper half plane and is followed clockwise, while the contour g_- is a semicircle in the lower half plane and is followed counterclockwise (Fig. 3). s_- is defined as

$$\bar{s}_- \equiv (m^2 - 1)^2 / s. \tag{14}$$

The signs preceding $A_2^\pm$, $B_2^\pm$ and $A_3^\pm$, $B_3^\pm$, which appear in the integrals, must be determined with allowance for the signs of the small imaginary parts of $\bar{s}$ and t in the dispersion relations (5). Let us illustrate the determination of the sign proceeding $A_3^\pm$ in the integral over the contour g_+. For backward scattering $t = -4k^2$. On the semicircle in the upper half plane, s has the form

$$s = \rho e^{i\varphi}, \quad 0 \leqslant \varphi \leqslant \pi. \tag{15}$$

It is readily shown that

$$\operatorname{Im} t = \frac{1}{\rho}\{(m^2-1)^2 - \rho^2\}\sin\varphi. \tag{16}$$

Thus, t has a negative imaginary part outside the semicircle in the upper half plane and a positive imaginary part inside the semicircle of the upper half plane. The sign in front of $A_3^\pm$ in the integral over g_+ should be negative, in contradiction to the result obtained by MacDowell.[12]

The dispersion relations (13) can be recast in a form similar to (11). The integrals in (13) are actually taken along the curve $\bar{s}s = (m^2-1)^2$. In some of these it is convenient to make a change of variables

$$\bar{s} = (m^2 - 1)^2 / s. \tag{17}$$

In particular

$$\begin{gathered}
-\frac{1}{\pi}\int\limits_0^{(m-1)^2} ds'\,\frac{A_2^\pm(s',-1)}{s'-s} = \frac{1}{\pi}\int\limits_{(m+1)^2}^{\infty} d\bar{s}'\,\frac{\bar{s}_-}{\bar{s}'}\,\frac{A_2^\pm(s',-1)}{\bar{s}'-\bar{s}_-}, \\
\frac{1}{\pi}\int\limits_{-m^2+1}^{0} ds'\,\frac{A_3^\pm(s',-1)}{s'-s} = -\frac{1}{\pi}\int\limits_{-\infty}^{-m^2+1} d\bar{s}'\,\frac{\bar{s}_-}{\bar{s}'}\,\frac{A_3^\pm(s',-1)}{\bar{s}'-\bar{s}_-}.
\end{gathered} \tag{18}$$

Applying relations (4) to (18), we obtain

$$\begin{gathered}
-\frac{1}{\pi}\int\limits_0^{(m-1)^2} ds'\,\frac{A_2^\pm(s',-1)}{s'-s} = \pm\frac{1}{\pi}\int\limits_{(m+1)^2}^{\infty} ds'\,\frac{\bar{s}_-}{s'}\,\frac{A_1^\pm(s',-1)}{s'-\bar{s}_-}, \\
\frac{1}{\pi}\int\limits_{-m^2+1}^{0} ds'\,\frac{A_3^\pm(s',-1)}{s'-s} = \mp\frac{1}{\pi}\int\limits_{-\infty}^{-m^2+1} ds'\,\frac{\bar{s}_-}{s'}\,\frac{A_3^\pm(s',-1)}{s'-\bar{s}_-}.
\end{gathered} \tag{19}$$

In a similar manner we obtain

$$\begin{gathered}
-\frac{1}{\pi}\int\limits_0^{(m-1)^2} ds'\,\frac{B_2^\pm(s',-1)}{s'-s} = \mp\frac{1}{\pi}\int\limits_{(m+1)^2}^{\infty} ds'\,\frac{\bar{s}_-}{s'}\,\frac{B_1^\pm(s',-1)}{s'-\bar{s}_-}, \\
\frac{1}{\pi}\int\limits_{-m^2+1}^{0} ds'\,\frac{B_3^\pm(s',-1)}{s'-s} = \pm\frac{1}{\pi}\int\limits_{-\infty}^{-m^2+1} ds'\,\frac{\bar{s}_-}{s'}\,\frac{B_3^\pm(s',-1)}{s'-\bar{s}_-}.
\end{gathered} \tag{20}$$

We recognize further that the integral over g_+ is the complex conjugate of the integral over g_- for physical values of s. Therefore (13) can be reduced to the following form:

$$\begin{aligned}
A^\pm(s,-1) = {} & \frac{1}{\pi}\int\limits_{(m+1)^2}^{\infty} ds'\left(\frac{1}{s'-s} \pm \frac{\bar{s}_-}{s'}\,\frac{1}{s'-\bar{s}_-}\right) A_1^\pm(s',-1) \\
& -\frac{2}{\pi}\operatorname{Re}\int\limits_{g_-} ds'\,\frac{A_3^\pm(s',-1)}{s'-s} - \frac{1}{\pi}\int\limits_{-\infty}^{-m^2+1} ds'\left(\frac{1}{s'-s}\right. \\
& \left.\pm\frac{\bar{s}_-}{s'}\,\frac{1}{s'-\bar{s}}\right) A_3^\pm(s',-1), \\
B^\pm(s,-1) = {} & \frac{g^2}{m^2-s} \mp \frac{g^2}{m^2-\bar{s}_-} + \frac{1}{\pi}\int\limits_{(m+1)^2}^{\infty} ds'\left(\frac{1}{s'-s}\right. \\
& \left.\mp\frac{\bar{s}_-}{s'}\,\frac{1}{s'-\bar{s}_-}\right) B_1^\pm(s',-1) - \frac{2}{\pi}\operatorname{Re}\int\limits_{g_-} ds'\,\frac{B_3^\pm(s',-1)}{s'-s} \\
& -\frac{1}{\pi}\int\limits_{-\infty}^{-m^2+1} ds'\left(\frac{1}{s'-s} \mp \frac{s}{s'}\,\frac{1}{s'-\bar{s}_-}\right) B_3^\pm(s',-1).
\end{aligned} \tag{21}$$

If we can neglect the D wave and the higher waves, then the amplitudes of the S and P waves, $f_{S_{1/2}}^\pm(s)$, $f_{P_{1/2}}^\pm(s)$, $f_{P_{3/2}}^\pm(s)$ can be readily expressed in terms of the forward and backward scattering amplitudes

$$\begin{gathered}
f_{S_{1/2}}^\pm(s) \approx \tfrac{1}{2}\{f_1^\pm(s,1) + f_1^\pm(s,-1)\}, \\
f_{P_{1/2}}^\pm(s) - f_{P_{3/2}}^\pm(s) \approx \tfrac{1}{2}\{f_2^\pm(s,1) + f_2^\pm(s,-1)\}, \\
f_{P_{3/2}}^\pm(s) \approx \tfrac{1}{6}\{f_1^\pm(s,1) - f_1^\pm(s,-1)\}.
\end{gathered} \tag{22}$$

The expressions for $f_1^\pm$ and $f_2^\pm$ have been obtained by Chew, Goldberger, Low, and Nambu (CGLN)[10] and have the following form

$$\begin{aligned}
f_1^\pm(s,x) &= \frac{E+m}{8\pi\sqrt{s}}\{A^\pm(s,x) + (\sqrt{s}-m)B^\pm(s,x)\}, \\
f_2^\pm(s,x) &= \frac{E-m}{8\pi\sqrt{s}}\{-A^\pm(s,x) + (\sqrt{s}+m)B^\pm(s,x)\}.
\end{aligned} \tag{23}$$

Here E is the nucleon energy in the c.m.s.

4. INTEGRAL EQUATIONS

The problem now consists of expressing $A_1^\pm$ and $B_1^\pm$ in terms of the imaginary parts of the partial amplitudes of the πN scattering, and expressing $A_3^\pm$ and $B_3^\pm$ in terms of the imaginary parts of the $N\bar{N}$-annihilation amplitudes. The expressions for $A_1^\pm$ and $B_1^\pm$ can be obtained directly from (22) and (23):

$$\frac{1}{4\pi} A_1^{\pm}(s,\ 1) \approx \frac{\sqrt{s}+m}{E+m} \operatorname{Im}\left\{f^{\pm}_{s_{1/2}}(s) + 3f^{\pm}_{p_{3/2}}(s)\right\}$$

$$-\frac{\sqrt{s}-m}{E-m} \operatorname{Im}\left\{f^{\pm}_{p_{1/2}}(s) - f^{\pm}_{p_{3/2}}(s)\right\},$$

$$\frac{1}{4\pi} A_1^{\pm}(s,\ -1) \approx \frac{\sqrt{s}+m}{E+m} \operatorname{Im}\left\{f^{\pm}_{s_{1/2}}(s) - 3f^{\pm}_{p_{3/2}}(s)\right\}$$

$$-\frac{\sqrt{s}-m}{E-m} \operatorname{Im}\left\{f^{\pm}_{p_{1/2}}(s) - f^{\pm}_{p_{3/2}}(s)\right\},$$

$$\frac{1}{4\pi} B_1^{\pm}(s,\ 1) \approx \frac{1}{E+m} \operatorname{Im}\left\{f^{\pm}_{s_{1/2}}(s) + 3f^{\pm}_{p_{3/2}}(s)\right\}$$

$$+\frac{1}{E-m} \operatorname{Im}\left\{f^{\pm}_{p_{1/2}}(s) - f^{\pm}_{p_{3/2}}(s)\right\},$$

$$\frac{1}{4\pi} B_1^{\pm}(s,\ -1) \approx \frac{1}{E+m} \operatorname{Im}\{f^{\pm}_{s_{1/2}}(s) - 3f^{\pm}_{p_{3/2}}(s)\}$$

$$+\frac{1}{E-m} \operatorname{Im}\{f^{\pm}_{p_{1/2}}(s) - f^{\pm}_{p_{3/2}}(s)\}. \tag{24}$$

In order to express $A_3^{\pm}$ and $B_3^{\pm}$ in terms of the scattering amplitudes of reaction III, it is first necessary to obtain a relation between the values of s and $x \equiv \cos\Phi$ for reaction I, and between t and $z \equiv \cos\theta$ for reaction III. It follows from (6) that for backward scattering

$$t = 2(m^2+1) - s - (m^2-1)^2 s^{-1}. \tag{25}$$

It can be shown that on the integration contours in (21)

$$z = (s - \bar{s})/4pq = -1. \tag{26}$$

The $N\bar{N}$ annihilation reaction was investigated by Fraser and Fulco.[2] It is easy to express $A_3^{\pm}$ and $B_3^{\pm}$ in terms of the partial wave amplitudes $f^{I,J}_{\pm}$ of $N\bar{N}$ annihilation with a definite helicity, where I and J denote respectively the isotopic spin and the total angular momentum of the NN system. The signs + and – pertain to two helicity states. Taking into account the unitarity condition for reaction III, we obtain after simple calculations

$$A_3^{+}(s,\ -1) = \frac{8\pi}{\sqrt{6}} \sum_{J\text{—even}} \left(J+\frac{1}{2}\right) \frac{(pq)^J}{p^2} \left\{\frac{m}{2}\sqrt{J(J+1)}\right.$$

$$\left.\times \operatorname{Im} f^{0,J}_{-}(t) - \operatorname{Im} f^{0,J}_{+}(t)\right\},$$

$$A_3^{-}(s,\ -1) = 4\pi \sum_{J\text{—odd}} \left(J+\frac{1}{2}\right) \frac{(pq)^J}{p^2}$$

$$\left\{-\frac{m}{2}\sqrt{J(J+1)}\operatorname{Im} f^{1,J}_{-}(t) + \operatorname{Im} f^{1,J}_{+}(t)\right\},$$

$$B_3^{+}(s,\ -1) = -\frac{4\pi}{\sqrt{6}} \sum_{J\text{—even}} \left(J+\frac{1}{2}\right)\sqrt{J(J+1)}$$

$$\times (pq)^{J-1} \operatorname{Im} f^{0,J}(t),$$

$$B_3^{-}(s,\ -1) = 2\pi \sum_{J\text{—odd}} \left(J+\frac{1}{2}\right)\sqrt{J(J+1)}\,(pq)^{J-1}\operatorname{Im} f^{1,J}(t). \tag{27}$$

We have here on the contour g_{-} $(0 \leq \varphi \leq \pi)$

$$s = (m^2-1)e^{-i\varphi}, \quad t = 2(m^2+1) - 2(m^2-1)\cos\varphi,$$
$$pq = \tfrac{1}{2} i(m^2-1)\sin\varphi, \tag{28}$$

and for $-\infty < s \leq -m^2+1$

$$t = 2(m^2+1) - s - (m^2-1)^2 s^{-1},$$
$$pq = \tfrac{1}{4}\{(m^2-1)^2 s^{-1} - s\}. \tag{29}$$

It is interesting to note that on the contour g_{-} the quantities A_3^{+} and B_3^{-} are real, and A_3^{-} and B_3^{+} are pure imaginary.

The first few terms of the expansion (27) may be sufficient to represent $A_3^{\pm}$ and $B_3^{\pm}$ adequately for values of t not much greater than 4. This region makes an appreciable contribution to the dispersion relations. It pertains, however, to the nonphysical region of reaction III, which is not amenable to experiment. The actual number of terms that should be retained should be established during the process of solving the integral equation.

Introducing the notation

$$\omega \equiv \sqrt{s} - m, \quad K_{\pm}(s',\ s) = \frac{1}{s'-s} \pm \frac{\bar{s}_{-}}{s'}\,\frac{1}{s'-\bar{s}_{-}}, \tag{30}$$

we obtain from (11) and (21) – (24) equations which, in conjunction with the unitarity condition, yield integral equations for πN scattering. For the amplitude $f^{\pm}_{s_{1/2}}(s)$ we have

$$f^{\pm}_{s_{1/2}}(s) = P^{\pm}_{s_{1/2}}(s) + \mathrm{I}^{\pm}_{s_{1/2}}(s) + \mathrm{II}^{\pm}_{s_{1/2}}(s) + \mathrm{III}^{\pm}_{s_{1/2}}(s);$$

$$P^{\pm}_{s_{1/2}}(s) = \frac{\omega(E+m)g^2}{16\pi\sqrt{s}} \left\{\frac{2}{m^2-s} \mp \left(\frac{1}{m^2-\bar{s}_{+}} + \frac{1}{m^2-\bar{s}_{-}}\right)\right\},$$

$$\mathrm{I}^{\pm}_{s_{1/2}}(s) = \frac{1}{\pi} \int\limits_{(m+1)^2}^{\infty} \frac{ds'}{s'-s} \left\{\frac{E+m}{E'+m}\,\frac{\sqrt{s'}+\sqrt{s}}{2\sqrt{s}} \operatorname{Im} f^{\pm}_{s_{1/2}}(s')\right.$$

$$\left.+\frac{E+m}{2\sqrt{s}}\,\frac{\sqrt{s}-\sqrt{s'}}{E'-m}[\operatorname{Im} f^{\pm}_{p_{1/2}}(s') - \operatorname{Im} f^{\pm}_{p_{3/2}}(s')]\right\},$$

$$\mathrm{II}^{\pm}_{s_{1/2}}(s) = \pm\frac{E+m}{4\pi\sqrt{s}} \int\limits_{(m+1)^2}^{\infty} ds' \left\{3K_{-}(s',\ s)\frac{2m+\omega'-\omega}{E'+m}\operatorname{Im} f^{\pm}_{p_{3/2}}(s')\right.$$

$$+K_{+}(s',\ s)\left[\frac{2m+\omega'-\omega}{E'+m}\operatorname{Im} f^{\pm}_{s_{1/2}}(s') - \frac{\omega'+\omega}{E'-m}\operatorname{Im}(f^{\pm}_{p_{1/2}}(s')\right.$$

$$\left.\left.- f^{\pm}_{p_{3/2}}(s'))\right]\right\},$$

$$\mathrm{III}^{\pm}_{s_{1/2}}(s) = -\frac{E+m}{16\pi\sqrt{s}}\,\frac{1}{\pi}\left\{\int\limits_{-\infty}^{-m^2+1} ds'\,[K_{\pm}(s',\ s)A_3^{\pm}(s',\ -1) +\right.$$

$$+\omega K_{\mp}(s',\ s)B_3^{\pm}(s,\ -1)] + 2\operatorname{Re}\int\limits_{g_{-}} \frac{ds'}{s'-s}[A_3^{\pm}(s',\ -1)$$

$$\left.\left.+\omega B_3^{\pm}(s',\ -1)\right]\right\}. \tag{31}$$

The quantities $A_3^{\pm}$ and $B_3^{\pm}$ in the equation for $\mathrm{III}^{\pm}_{s_{1/2}}(s)$ should be replaced by the expressions in (27). The corresponding equations for $f^{\pm}_{p_{1/2}}(s) - f^{\pm}_{p_{3/2}}(s)$ have the form

$$f^{\pm}_{p_{1/2}}(s) - f^{\pm}_{p_{3/2}}(s) = P^{\pm}_{p_{1/2},\,-3/2}(s) + \mathrm{I}^{\pm}_{p_{1/2},\,-3/2}(s) + \mathrm{II}^{\pm}_{p_{1/2},\,-3/2}(s)$$
$$+ \mathrm{III}^{\pm}_{p_{1/2},\,-3/2}(s);$$

$$P^{\pm}_{p_{1/2},\,-3/2}(s) = \frac{(\sqrt{s}+m)(E-m)\,g^2}{16\pi\sqrt{s}}\left\{\frac{2}{m^2-s}\right.$$
$$\left.\mp\left(\frac{1}{m^2-\bar{s}_+}+\frac{1}{m^2-\bar{s}_-}\right)\right\},$$

$$\mathrm{I}^{\pm}_{p_{1/2},\,-3/2}(s) = \frac{1}{\pi}\int\limits_{(m+1)^2}^{\infty}\frac{ds'}{s'-s}\left\{\frac{E-m}{E'-m}\,\frac{\sqrt{s'}+\sqrt{s}}{2\sqrt{s}}\,\mathrm{Im}\,[f^{\pm}_{p_{1/2}}(s')\right.$$
$$\left.- f^{\pm}_{p_{3/2}}(s')] + \frac{E-m}{E'+m}\,\frac{\sqrt{s}-\sqrt{s'}}{2\sqrt{s}}\,\mathrm{Im}\,f^{\pm}_{s_{1/2}}(s')\right\},$$

$$\mathrm{II}^{\pm}_{p_{1/2},\,-3/2}(s) = \mp\frac{E-m}{4\pi\sqrt{s}}\int\limits_{(m+1)^2}^{\infty}ds'\left\{3K_-(s',\,s)\,\frac{2m+\sqrt{s'}+\sqrt{s}}{E'+m}\right.$$
$$\times\,\mathrm{Im}\,f^{\pm}_{p_{3/2}}(s') + K_+(s',\,s)\left[\frac{2m+\sqrt{s'}+\sqrt{s}}{E'+m}\,\mathrm{Im}\,f^{\pm}_{s_{1/2}}(s')\right.$$
$$\left.\left.+\frac{2m+\omega-\omega'}{E'-m}\,\mathrm{Im}\,(f^{\pm}_{p_{1/2}}(s') - f^{\pm}_{p_{3/2}}(s')\right]\right\},$$

$$\mathrm{III}^{\pm}_{p_{1/2},\,-3/2}(s) = -\frac{E-m}{16\pi\sqrt{s}}\,\frac{1}{\pi}\left\{\int\limits_{-\infty}^{-m^2+1}ds'\,[-K_{\pm}(s',\,s)\,A^{\pm}_3(s',\,-1)\right.$$
$$+ (\sqrt{s}+m)\,K_{\mp}(s',\,s)\,B^{\pm}_3(s',\,-1)]$$
$$\left.+ 2\mathrm{Re}\int\limits_{g_-}\frac{ds'}{s'-s}\,[-A^{\pm}_3(s',\,-1) + (\sqrt{s}+m)\,B^{\pm}_3(s',\,-1)]\right\}. \qquad (32)$$

The equations for the amplitude $f^{\pm}_{p_{3/2}}(s)$ have the form

$$f^{\pm}_{p_{3/2}}(s) = P^{\pm}_{p_{3/2}}(s) + \mathrm{I}^{\pm}_{p_{3/2}}(s) + \mathrm{II}^{\pm}_{p_{3/2}}(s) + \mathrm{III}^{\pm}_{p_{3/2}}(s),$$

$$P^{\pm}_{p_{3/2}}(s) = \mp\frac{\omega\,(E+m)}{48\pi\sqrt{s}}\,g^2\left(\frac{1}{m^2-\bar{s}_+}-\frac{1}{m^2-\bar{s}_-}\right),$$

$$\mathrm{I}^{\pm}_{p_{3/2}}(s) = \frac{1}{\pi}\int\limits_{(m+1)^2}^{\infty}\frac{ds'}{s'-s}\,\frac{E+m}{E'+m}\,\frac{\sqrt{s'}+\sqrt{s}}{2\sqrt{s}}\,\mathrm{Im}\,f^{\pm}_{p_{3/2}}(s'),$$

$$\mathrm{II}^{\pm}_{p_{3/2}}(s) = \pm\frac{E+m}{12\pi\sqrt{s}}\int\limits_{(m+1)^2}^{\infty}ds'\left\{3K_+(s',\,s)\,\frac{2m+\omega'-\omega}{E'+m}\,\mathrm{Im}\,f^{\pm}_{p_{3/2}}(s')\right.$$
$$+ K_-(s',\,s)\left[\frac{2m+\omega'-\omega}{E'+m}\,\mathrm{Im}\,f^{\pm}_{s_{1/2}}(s')\right.$$
$$\left.\left.-\frac{\omega'+\omega}{E'-m}\,\mathrm{Im}\,(f^{\pm}_{p_{1/2}}(s') - f^{\pm}_{p_{3/2}}(s'))\right]\right\},$$

$$\mathrm{III}^{\pm}_{p_{3/2}}(s) = -\tfrac{1}{3}\,\mathrm{III}^{\pm}_{s_{1/2}}(s). \qquad (33)$$

Equations (31) — (33), in spite of their unwieldiness, are rather simple. Each of the amplitudes is the superposition of four terms: $P^{\pm}$, $\mathrm{I}^{\pm}$, $\mathrm{II}^{\pm}$, and $\mathrm{III}^{\pm}$. The term $P^{\pm}$ is the contribution from the poles, while $\mathrm{I}^{\pm}$, $\mathrm{II}^{\pm}$, and $\mathrm{III}^{\pm}$ are the contributions from reactions I, II, and III, respectively.

Since these equations contain the amplitudes of reaction III, they should be solved simultaneously with the integral equations for the $N\bar{N}$ annihilation. It is interesting to compare Eqs. (31) — (33) with the corresponding CGLN result.[10] The main difference lies undoubtedly in the fact that our equations contain the terms $\mathrm{III}^{\pm}_{s_{1/2}}$, $\mathrm{III}^{\pm}_{p_{1/2},-3/2}$, and $\mathrm{III}^{\pm}_{p_{3/2}}$, which are completely missing from their equations. These terms clearly represent the effects of the $\pi\pi$ interaction, since the $\mathrm{Im}\, f^{I,J}_{\pm}$ vanish within the limits of the two-meson approximation for the unitarity condition if the $\pi\pi$ interaction vanishes.

To compare the pole contribution and the contributions from the regions of reaction I and II, we can neglect $\mathrm{Im}\, f^{\pm}_{s_{1/2}}$ and $\mathrm{Im}\, f^{\pm}_{p_{1/2}}$ compared with $\mathrm{Im}\, f^{\pm}_{p_{3/2}}$ and discard terms of order $(\omega/m)^2$ compared with the principal term, as was done in the CGLN paper. We then have the following approximate expressions for $P^{\pm}_{s_{1/2}}$, $\mathrm{I}^{\pm}_{s_{1/2}}$, and $\mathrm{II}^{\pm}_{s_{1/2}}$:

$$P^{\pm}_{s_{1/2}}(s) \approx -\frac{g^2}{4\pi}\,\frac{1}{2\sqrt{s}}\left\{\left(1-\frac{\omega}{2m}\right)\pm\left(1+\frac{\omega}{2m}\right)\right\},$$

$$\mathrm{I}^{\pm}_{s_{1/2}}(s) \approx \frac{2m^2}{\pi\sqrt{s}}\int\limits_{1}^{\infty}\frac{d\omega'}{k'^2}\left(1+\frac{\omega'}{2m}-\frac{\omega}{2m}\right)\mathrm{Im}\,f^{\pm}_{p_{3/2}}(s'), \qquad (34)$$

$$\mathrm{II}^{\pm}_{s_{1/2}}(s) \approx \pm\frac{2m^2}{\pi\sqrt{s}}\int\limits_{1}^{\infty}\frac{d\omega'}{k'^2}\left(1+\frac{\omega'}{2m}-\frac{\omega}{2m}\right)\mathrm{Im}\,f^{\pm}_{p_{3/2}}(s').$$

The approximate equations for $P^{\pm}_{p_{1/2},-3/2}$, $\mathrm{I}^{\pm}_{p_{1/2},-3/2}$, and $\mathrm{II}^{\pm}_{p_{1/2},-3/2}$ are

$$P^{\pm}_{p_{1/2},\,-3/2}(s) \approx -\frac{f^2k^2}{\omega}\left\{\left(1-\frac{\omega}{2m}\right)\pm\left(1+\frac{\omega}{2m}\right)\right\}\left(1-\frac{\omega}{2m}\right),$$

$$\mathrm{I}^{\pm}_{p_{1/2},\,-3/2}(s) \approx -\frac{1}{\pi}\int\limits_{1}^{\infty}d\omega'\,\frac{k^2}{k'^2}\left(\frac{1}{\omega'-\omega}+\frac{1}{m}\right)\mathrm{Im}\,f^{\pm}_{p_{3/2}}(s'), \qquad (35)$$

$$\mathrm{II}^{\pm}_{p_{1/2},\,-3/2}(s) \approx \pm\frac{1}{\pi}\int\limits_{1}^{\infty}d\omega'\,\frac{k^2}{k'^2}\left(\frac{1}{\omega'+\omega}-\frac{1}{m}\right)\mathrm{Im}\,f^{\pm}_{p_{3/2}}(s'),$$

where f is the renormalized pseudo-vector coupling constant, defined as

$$f^2 \equiv g^2/16\pi m^2. \qquad (36)$$

The approximate expressions for $P^{\pm}_{p_{3/2}}$, $\mathrm{I}^{\pm}_{p_{3/2}}$, and $\mathrm{II}^{\pm}_{p_{3/2}}$ have the form

$$P^{\pm}_{p_{3/2}}(s) \approx \pm 2f^2k^2/3\omega,$$

$$\mathrm{I}^{\pm}_{p_{3/2}}(s) \approx \frac{1}{\pi}\int\limits_{1}^{\infty}d\omega'\left(\frac{1}{\omega'-\omega}+\frac{1}{m}\right)\mathrm{Im}\,f^{\pm}_{p_{3/2}}(s'),$$

$$\mathrm{II}^{\pm}_{p_{3/2}}(s) \approx \pm\frac{1}{\pi}\int\limits_{1}^{\infty}\frac{d\omega'}{\omega+\omega'}\left\{1+\frac{2(\omega+\omega')^2}{3k'^2}\left[1-\frac{k^2}{(\omega+\omega')^2}\right]\right.$$
$$\left.-\frac{2\omega}{m}-\frac{2(\omega+\omega')^3}{3mk'^2}\right\}\mathrm{Im}\,f^{\pm}_{p_{3/2}}(s'). \qquad (37)$$

Thus, the pole contribution and $\mathrm{I}^{\pm}_{p_{1/2},-3/2}$ are exactly the same as given by CGLN, within the limits of the approximation made.

$\mathrm{I}^{\pm}_{s_{1/2}}$, $\mathrm{II}^{\pm}_{s_{1/2}}$, and $\mathrm{II}^{\pm}_{p_{1/2},-3/2}$ differ from the corresponding CGLN expression in terms of order ω/m. But $\mathrm{I}^{\pm}_{p_{3/2}}$ and $\mathrm{II}^{\pm}_{p_{3/2}}$ are different from each other. In fact, no subtraction was made in our Eq. (33). If the subtraction is made at $\omega = 1$, then the term $\mathrm{I}^{\pm}_{p_{3/2}}$ becomes analogous to their results, but $\mathrm{II}^{\pm}_{p_{3/2}}$ remains different. This probably will lead to some changes in the behavior of the (3, 3) resonance.

I take pleasure in expressing my gratitude to D. V. Shirkov, V. A. Meshcheryakov, and A. V. Efremov for numerous useful discussions, and also to the participants in Professor Bogolyubov's seminar for interesting comments.

[1] G. F. Chew and S. Mandelstam, Phys. Rev. **119**, 467 (1960).

[2] W. R. Fraser and W. Fulco, Phys. Rev. **117**, 1603 (1960).

[3] Chew, Mandelstam, and Noyes, Phys. Rev. **119**, 478 (1960).

[4] S. Mandelstam, Phys. Rev. **112**, 1344 (1958).

[5] S. Mandelstam, Phys. Rev. **115**, 1741 (1959).

[6] S. Mandelstam, Phys. Rev. **115**, 1752 (1959).

[7] Efremov, Meshcheryakov, Shirkov, and Chou, Preprint, Joint. Inst. Nuc. Res.; Nucl. Phys. (in press).

[8] Efremov, Meshcheryakov, and Shirkov, JETP **39**, 438 (1960), Soviet Phys. JETP **12**, 308 (1961).

[9] Efremov, Meshcheryakov, and Shirkov, JETP **39**, 1099 (1960), Soviet Phys. JETP **12**, 766 (1961).

[10] Chew, Goldberger, Low, and Nambu, Phys. Rev. **106**, 1337 (1957).

[11] S. Mandelstam, Phys. Rev. Lett. **4**, 84 (1960).

[12] S. W. MacDowell, Phys. Rev. **116**, 774 (1959).

Translated by J. G. Adashko
35

SOVIET PHYSICS JETP VOLUME 13, NUMBER 1 JULY, 1961

HIGH ENERGY ELECTRON SCATTERING PROCESSES

S. S. SANNIKOV

Physico-Technical Institute, Academy of Sciences, Ukrainian SSR

Submitted to JETP editor July 14, 1960

J. Exptl. Theoret. Phys. (U.S.S.R.) 40, 237-245 (January, 1960)

A method is developed for calculating cross sections of various processes involving fast polarized electrons, which can be described by two-component spinors. Some helicity properties of the electrons are elucidated. The pair-production cross section in electron-positron collisions is found.

IN the limit of very high velocities polarized electrons can be described by two- rather than four-component spinors, as is done with the neutrino, except that the electron can be polarized either parallel or antiparallel to the direction of motion, while the neutrino is always polarized antiparallel.

The use of two-component spinors to describe the electrons greatly simplifies cross-section calculations for many processes involving high-energy polarized electrons. It is to such a description, together with an elucidation of some helicity properties of the electrons, that the present work is devoted.

1. Let φ and χ be two-component spinors describing fast electrons polarized parallel and antiparallel to the direction of motion. They satisfy the Weyl equation

$$\overset{+}{\sigma}_\mu \frac{\partial}{\partial x_\mu}\varphi = 0, \quad \overset{-}{\sigma}_\mu \frac{\partial}{\partial x_\mu}\chi = 0, \tag{1}$$

where the σ_μ are four independent two-by-two matrices, namely the three Pauli matrices and the unit matrix multiplied by i:

$$\overset{+}{\sigma}_\mu = (\boldsymbol{\sigma}, i), \quad \overset{-}{\sigma}_\mu = (\boldsymbol{\sigma}, -i).$$

These matrices satisfy the commutation relations

$$\overset{+}{\sigma}_\mu\overset{-}{\sigma}_\nu + \overset{+}{\sigma}_\nu\overset{-}{\sigma}_\mu = 2\delta_{\mu\nu}, \qquad \overset{-}{\sigma}_\mu\overset{+}{\sigma}_\nu + \overset{-}{\sigma}_\nu\overset{+}{\sigma}_\mu = 2\delta_{\mu\nu}. \tag{2}$$

The σ_μ matrices form a complete set of two-by-two matrices. The completeness condition can be written

$$\sum_\mu \left(\overset{+}{\sigma}_\mu\right)^{\alpha\dot\beta}\left(\sigma_\mu\right)_{\dot\rho\sigma} = 2\delta^\alpha_\sigma\delta^{\dot\beta}_{\dot\rho} \tag{3}$$

(tensor notation is used here for the spinor indices).

The $\overset{+}{\sigma}_\mu$ and $\overset{-}{\sigma}_\mu$ matrices are related by equations of the form

$$\varepsilon\overset{+}{\sigma}_\mu\varepsilon = \overset{-}{\sigma}{}^T_\mu, \quad \varepsilon\sigma_\mu\varepsilon = \overset{+}{\sigma}{}^T_\mu, \tag{4}$$

where σ^T is the transposed matrix, and ϵ is a metric tensor related to the antisymmetric of the Pauli matrices, $\epsilon = i\sigma_2$.

We shall call particles satisfying the first equation in (1) R-particles (for right-handed helicity), and those satisfying the second equation, L-particles (for left-handed helicity).

It is only in the high-energy limit that the equations for helical particles can be of first order, and then the helicity and polarization become identical. In the more general case which includes also relatively low velocities, the equations for helical particles can be only of second order[1] and there is no simple relation between the helicity and polarization.

2. We perform a plane-wave expansion[2] on φ and χ, writing

$$\varphi(x) = \frac{1}{\sqrt{V}}\sum_{\mathbf{p}}[a_R(\mathbf{p})\,u_R(\mathbf{p})\,e^{ipx} + b_R^+(\mathbf{p})\,v_R(-\mathbf{p})\,e^{-ipx}],$$

$$\chi(x) = \frac{1}{\sqrt{V}}\sum_{\mathbf{p}}[a_L(\mathbf{p})\,u_L(\mathbf{p})\,e^{ipx} + b_L^+(\mathbf{p})\,v_L(-\mathbf{p})\,e^{-ipx}],$$

where $p = (\mathbf{p}, i\epsilon)$, $\epsilon = |\mathbf{p}|$, and $a_R(\mathbf{p})$ and $\overset{+}{b}_R(\mathbf{p})$ are the destruction operators for an R-electron and the creation operator for a R-positron with momentum $\mathbf{p}$ (and $a_L(\mathbf{p})$ and $\overset{+}{b}_L(\mathbf{p})$ are the corresponding L-particle operators). We assume the amplitudes u and v to be normalized according to

$$\begin{aligned} u_R(\mathbf{p})\,\bar u_R(\mathbf{p}) &= v_R(-\mathbf{p})\,\bar v_R(-\mathbf{p}) = -\bar p/2\varepsilon, \\ u_L(\mathbf{p})\,\bar u_L(\mathbf{p}) &= v_L(-\mathbf{p})\,\bar v_L(-\mathbf{p}) = \overset{+}{p}/2\varepsilon, \\ u_R(\mathbf{p})\,\bar u_L(\mathbf{p}) &= v_R(-\mathbf{p})\,\bar v_L(-\mathbf{p}) = 0, \end{aligned} \tag{5}$$

where $\bar u$ is the Hermitian conjugate spinor, and $\bar p = \overset{-}{\sigma}_\mu p_\mu$, $\overset{+}{p} = \overset{+}{\sigma}_\mu p_\mu$. One then easily obtains the following commutation relations for the φ and χ fields:

$$\{\varphi(x), \bar\varphi(x')\} = -i\sigma_-(x - x'),$$

$$\{\chi(x), \bar\chi(x')\} = -i\sigma_+(x - x'), \quad \{\varphi(x), \bar\chi(x')\} = 0. \tag{6}$$

Here we have written

$$\sigma_-(x) = -i\bar{\sigma}_\mu \frac{\partial}{\partial x_\mu}\Delta_0(x), \qquad \sigma_+(x) = i\overset{+}{\sigma}_\mu \frac{\partial}{\partial x_\mu}\Delta_0(x),$$

$$\Delta_0(x) = \frac{i}{(2\pi)^3}\int e^{ipx}\operatorname{sgn}(p_0)\,\delta(p^2)\,d^4p.$$

The remaining commutators vanish. The last of equations (6) indicates the kinematic independence of the φ and χ fields.

The Green's functions for the fields are given by the relations

$$\langle 0|T\varphi(x)\bar{\varphi}(x')|0\rangle = \sigma_-^c(x-x'),$$

$$\langle 0|T\chi(x)\bar{\chi}(x')|0\rangle = \sigma_+^c(x-x');$$

$$\sigma_-^c(x) = -i\bar{\sigma}_\mu \frac{\partial}{\partial x_\mu}\Delta_0^c(x), \qquad \sigma_+^c(x) = i\overset{+}{\sigma}_\mu \frac{\partial}{\partial x_\mu}\Delta_0^c(x),$$

$$\Delta_0^c(x) = -\frac{i}{(2\pi)^4}\int \frac{e^{ipx}}{p^2 - i\delta}\,d^4p.$$

In momentum space these Green's functions may be written

$$\sigma_-^c(p) = -i\bar{p}/(p^2 - i\delta), \quad \sigma_+^c(p) = i\overset{+}{p}/(p^2 - i\delta).$$

We write the Heisenberg-representation equations for the interacting electron-positron and electromagnetic fields in the form

$$i\overset{+}{\sigma}_\mu \frac{\partial}{\partial x_\mu}\varphi + \overset{+}{\sigma}_\mu A_\mu \varphi = 0, \qquad i\bar{\sigma}_\mu \frac{\partial}{\partial x_\mu}\chi + \bar{\sigma}_\mu A_\mu \chi = 0,$$

$$\Box A_\mu = -(j_\mu^R + j_\mu^L), \tag{7}$$

where the current densities of the R and L particles are defined as

$$j_\mu^R(x) = -\tfrac{1}{2}e\,[\bar{\varphi}(x),\ \overset{+}{\sigma}_\mu\varphi(x)],\quad j_\mu^L(x) = \tfrac{1}{2}e\,[\bar{\chi}(x),\ \bar{\sigma}_\mu\chi(x)]. \tag{8}$$

Conservation of j_μ^R and j_μ^L follows from Eqs. (7). Under a space reflection j_μ^R goes over into J_μ^L, and vice versa [which is related to the sign difference between the two equations of (8)]. The scattering matrix is of the usual form

$$S = T\exp\left(i\int(\mathscr{L}_i^R(x) + \mathscr{L}_i^L(x))\,d^4x\right), \tag{9}$$

where $\mathscr{L}_i^R(x)$ and $\mathscr{L}_i^L(x)$ are the interaction Lagrangian densities for the R and L particles in the interaction representation, namely

$$\mathscr{L}_i^R(x) = A_\mu(x)\,j_\mu^R(x), \qquad \mathscr{L}_i^L(x) = A_\mu(x)\,j_\mu^L(x).$$

3. Proceeding by perturbation theory, we may expand the S-matrix as a power series in the coupling constant e, and represent the individual terms of the series by Feynman diagrams. Then in the momentum representation we have the following rules for constructing the mathematical expressions corresponding to these diagrams.

To every incoming free electron line belonging to an R particle of momentum **p** there corresponds a two-component spinor amplitude $u_R(\mathbf{p})$ or $v_R(-\mathbf{p})$ for an electron in the initial state or a positron in the final state, respectively. The amplitudes $\bar{u}_R(\mathbf{p})$ and $\bar{v}_R(-\mathbf{p})$ correspond to outgoing lines belonging to an electron in the final state and a positron in the initial state. For L particles the same free electron lines correspond to the amplitudes $u_L(\mathbf{p})$, $v_L(-\mathbf{p})$, $\bar{u}_L(\mathbf{p})$, and $\bar{v}_L(-\mathbf{p})$. Free photon lines with momentum k, on the other hand, correspond as usual to the amplitudes $e_\mu/\sqrt{2\omega}$ (where e_μ is a polarization unit vector satisfying $e_\mu^2 = 1$).

2) To internal electron lines for R particles with 4-momentum p correspond propagators $\sigma_-^c(p)$, while to internal L particles correspond propagators $\sigma_+^c(p)$. Internal photon lines correspond to the functions $D_{\mu\nu}^c(k) = -i\delta_{\mu\nu}/(k^2 - i\delta)$.

3) Vertex parts at which R-particle electron lines converge correspond to the matrix $e\overset{+}{\sigma}_\mu\delta(p - p' + k)$, while those for L particles correspond to $e\bar{\sigma}_\mu\delta(p - p' + k)$.

The rules for constructing the expressions for the matrix elements are the usual ones, the expressions for the individual elements of the diagrams being ordered in the direction opposite to that of the electron line. The expression obtained for a Feynman diagram according to these rules is then multiplied by $(-1)^{n+l}\delta_p(2\pi)^{4(n-k)}$, where n, k, and l are the number of vertices, internal lines, and closed electrons loops, respectively, and δ_p is 1 or −1 and arises because of the antisymmetry of the electron states (cf. Akhiezer and Berestetskiĭ.[2])

4. As an example of a cross section calculation involving high-energy helical particles, consider electron-electron scattering in the center-of-mass (c.m.) system of the colliding particles.

We note first that the vector nature of the electromagnetic interaction preserves helicity along the electron lines. Let us use the rules given above to write the expression for the matrix element of the direct scattering process of electrons with different helicity:

$$M_{RL} = -i\frac{(2\pi)^4}{(p_1 - q_1)^2}\bar{u}_R(q_1)\overset{+}{\sigma}_\mu u_R(p_1)\,\bar{u}_L(q_2)\,\bar{\sigma}_\mu u_L(p_2)$$

which, using Eq. (3), can be written

$$M_{RL} = -2i\frac{(2\pi)^4}{(p_1 - q_1)^2}\bar{u}_R(q_1)\,u_L(p_2)\,\bar{u}_L(q_2)\,u_R(p_1).$$

Now making use of (5) and calculating some simple traces, we obtain the following expression for the square of the absolute value of the matrix element:

$$|M_{RL}|^2 = \frac{(2\pi)^8}{(p_1 - q_1)^4}\frac{1}{\varepsilon^4}(p_1q_2)(q_1p_2). \tag{10}$$

The expression for the corresponding exchange diagram is obtained from (10) by interchanging q_1 and q_2. In view of (5), the cross-product term between the direct and exchange diagrams vanishes in this case.

From (5) we may arrive at the following general conclusion: the product of two matrix elements will vanish if they correspond to diagrams which differ in the helicity of at least one electron line. This follows from conservation of helicity along electron lines.

Direct calculation will show that if the particles have the same helicity, the square of the matrix element is

$$|M_{LL}|^2 = \frac{(2\pi)^8}{(p_1 - q_1)^4} \frac{1}{\varepsilon^4} (q_1 q_2)(p_1 p_2). \tag{10'}$$

Having obtained the product of matrix elements for the direct and exchange diagrams, we can arrive at the cross section in the usual way.

The final result for the cross section is

$$d\sigma_{RL} = \frac{\alpha^2}{4\varepsilon^2} do \left(\tan^4 \frac{\theta}{2} + \cot^4 \frac{\theta}{2}\right), \quad d\sigma_{LL} = \frac{4\alpha^2}{\varepsilon^2} do \sin^{-4}\theta.$$

Similarly, one easily obtains the cross section for electron-positron scattering in the c.m. system:

$$d\sigma_{RL} = \frac{\alpha^2}{4\varepsilon^2} do \left(\sin^4 \frac{\theta}{2} + \sin^{-4} \frac{\theta}{2}\right),$$

$$d\sigma_{LL} = \frac{\alpha^2}{4\varepsilon^2} do \cos^4 \frac{\theta}{2} \cot^4 \frac{\theta}{2}.$$

We remark that electrons and positrons of different helicity do not undergo scattering by means of virtual annihilation.

Equation (10′) can be obtained from (10) by interchanging p_1 and $-q_1$, and in general we have the following rules.

1) Consider an electron line no parts of which are described by a propagation function, and assume we have an expression for a quadratic combination of matrix elements of any process involving such an electron line with given helicity and with initial and final momenta p and q. If we interchange p and −q, we obtain the corresponding expression for a similar process, but involving an electron line of opposite helicity.

2) Consider an electron line containing sections described by a propagation function, and assume we have an expression for a quadratic combination of matrix elements of any process involving such an electron line with given helicity and with initial and final momenta p and q. If we interchange p and −q and change the sign of the momentum in the electron propagator, we obtain the corresponding expression for the time-reversed process, but involving an electron line of opposite helicity. Here by time-reversed process we mean the process in which the order of events along the electron line is reversed.

Both of these rules follow from CP invariance of the theory.

The second rule simplifies the calculation of the Compton cross section. In the c.m. system, we obtain the following expression for the scattering cross section of polarized photons by helical electrons:

$$d\sigma_R = \frac{\alpha^2}{16\varepsilon^2} do \left[\left(\cos^2 \frac{\theta}{2} + \cos^{-2} \frac{\theta}{2}\right) e_1^2 e_2^2 + 2e_1^2 e_2^2 - 4(e_1 e_2)^2 + \frac{(k_1 e_2)^2 (k_2 e_1)^2}{\varepsilon^4 \cos^4(\theta/2)} + 2 \frac{e_1^2 (k_1 e_2)^2 + 2(e_1 e_2)(k_1 e_2)(k_2 e_1)}{\varepsilon^2 \cos^2(\theta/2)}\right],$$

where θ is the scattering angle, and k_1, e_1, k_2, and e_2 are the photon momenta and polarization before and after collision.

We note that reversal of all particle helicities leaves quadratic combinations of matrix elements invariant. This is because the $\overset{+}{\sigma}$ and $\bar{\sigma}$ matrices satisfy the same commutation relations, namely those of (2).

5. Let us now consider inelastic electron-positron scattering with the emission of a photon, in the c.m. system. The matrix elements corresponding to the Feynman diagrams for an R electron and an L positron are

$$M_1^{RL} = \frac{-i}{\sqrt{2\omega}} \frac{(2\pi)^4}{r_1^2 \alpha_1^2} \bar{u}_R(q_1) \overset{+}{\sigma}_\mu u_R(p_1) \bar{v}_L(-p_2) \bar{\sigma}_\mu \overset{+}{\alpha}_1 \bar{e} v_L(-q_2),$$

$$M_2^{RL} = \frac{-i}{\sqrt{2\omega}} \frac{(2\pi)^4}{r_1^2 \alpha_2^2} \bar{u}_R(q_1) \overset{+}{\sigma}_\mu u_R(p_1) \bar{v}_L(-p_2) \bar{e} \overset{+}{\alpha}_2 \bar{\sigma}_\mu v_L(-q_2),$$

$$M_3^{RL} = \frac{-i}{\sqrt{2\omega}} \frac{(2\pi)^4}{r_2^2 \alpha_3^2} \bar{u}_R(q_1) \overset{+}{e} \bar{\alpha}_3 \overset{+}{\sigma}_\mu u_R(p_1) \bar{v}_L(-p_2) \bar{\sigma}_\mu v_L(-q_2),$$

$$M_4^{RL} = \frac{-i}{\sqrt{2\omega}} \frac{(2\pi)^4}{r_2^2 \alpha_4^2} \bar{u}_R(q_1) \overset{+}{\sigma}_\mu \bar{\alpha}_4 \overset{+}{e} u_R(p_1) \bar{v}_L(-p_2) \bar{\sigma}_\mu v_L(-q_2),$$

where $r_1 = p_1 - q_1$, $r_2 = p_2 - q_2$, $\alpha_1 = -q_2 - k$, $\alpha_2 = -p_2 + k$, $\alpha_3 = q_1 + k$, $\alpha_4 = p_1 - k$, and p_1, p_2, q_1, and q_2 are the electron and positron momenta before and after collision, while k and e are the momentum and polarization of the emitted photon. We are not considering annihilation diagrams, since their contribution at high energies and small scattering and emission angles is negligible because of the large denominators corresponding to virtual photon lines.

Using relations (3) and (5) and calculating the traces, we obtain expressions for quadratic combinations of the matrix elements in the form

$$|M_1^{RL}|^2 = \frac{(2\pi)^8}{2\omega} \frac{S_1^{RL}}{r_1^4 \alpha_1^4} = \frac{(2\pi)^8}{2\omega r_1^4 \alpha_1^4} \frac{1}{\varepsilon^2 \varepsilon_1 \varepsilon_2} [2p_1 p_2 q_2 e (2q_1 \alpha_1 \alpha_1 e - \alpha_1^2 q_1 e) - e^2 p_1 p_2 (2q_1 \alpha_1 q_2 \alpha_1 - \alpha_1^2 q_1 q_2)],$$

$$|M_2^{RL}|^2 = \frac{(2\pi)^8}{2\omega} \frac{S_2^{RL}}{r_1^4 \alpha_2^4} = \frac{(2\pi)^8}{2\omega r_1^4 \alpha_2^4} \frac{1}{\varepsilon^2 \varepsilon_1 \varepsilon_2} [2q_1 q_2 p_2 e (2p_1 \alpha_2 \alpha_2 e - \alpha_2^2 p_1 e) - e^2 q_1 q_2 (2p_1 \alpha_2 p_2 \alpha_2 - \alpha_2^2 p_1 p_2)],$$

$$2\mathrm{Re}\,(M_1^{RL}M_2^{RL^*}) - \frac{(2\pi)^8}{2\omega}\frac{S_{12}^{RL}}{r_1^4\alpha_1^2\alpha_2^2} = 2\,\frac{(2\pi)^8}{2\omega r_1^4\alpha_1^2\alpha_2^2}\frac{1}{\varepsilon^2\varepsilon_1\varepsilon_2}$$
$$\times (p_1\alpha_2p_2e + p_1p_2\alpha_2e - p_1ep_2\alpha_2)(q_1q_2\alpha_1e$$
$$+ q_1\alpha_1q_2e - q_2\alpha_1q_1e).$$

The corresponding expressions for matrix elements 3 and 4 are obtained from (11) by interchanging q_2 and $-p_1$ and p_2 and $-q_1$. The cross terms between the matric elements are calculated just as simply, and we obtain

$$2\mathrm{Re}\,(M_1^{RL}M_3^{RL^*}) = \frac{(2\pi)^8}{2\omega}\frac{S_{13}^{RL}}{r_1^2r_2^2\alpha_1^2\alpha_3^2}$$
$$= 2\,\frac{(2\pi)^8}{2\omega r_1^2r_2^2\alpha_1^2\alpha_2^2}\frac{1}{\varepsilon^2\varepsilon_1\varepsilon_2}\Big[p_1p_2\alpha_1e\,(q_1q_2\alpha_3e - q_1\alpha_3q_2e)$$
$$- p_1p_2q_1e\,(q_2\alpha_1\alpha_3e - \alpha_1\alpha_3q_2e) + \frac{1}{2}\,e^2p_1p_2\,(q_1\alpha_1q_2\alpha_3$$
$$+ q_1\alpha_3q_2\alpha_1 - q_1q_2\alpha_1\alpha_3)\Big],$$
$$2\mathrm{Re}\,(M_1^{RL}M_4^{RL^*}) = \frac{(2\pi)^8}{2\omega}\frac{S_{14}^{RL}}{r_1^2r_2^2\alpha_1^2\alpha_4^2} = 2\,\frac{(2\pi)^8}{2\omega r_1^2r_2^2\alpha_1^2\alpha_4^2}\frac{1}{\varepsilon^2\varepsilon_1\varepsilon_2}(p_2\alpha_4p_1e$$
$$+ p_1p_2\alpha_4e - p_1\alpha_4p_2e)(q_1q_2\alpha_1e + q_1\alpha_1q_2e - q_2\alpha_1q_1e).$$

The expressions for S_{24}^{RL} and S_{23}^{RL} are obtained from S_{13}^{RL} and S_{14}^{RL} by interchanging p_1 and $-q_1$ and p_2 and $-q_2$ (and changing the signs of all the α's).

Rules 1 and 2 can be used to obtain expressions for the quadratic combinations of matrix elements when the colliding particles have the same helicities. We need remark only that the expressions for the $S_{1,2,12}^{LL}$ are obtained from the $S_{1,2,12}^{RL}$ by interchanging p_1 and $-q_1$, while those for $S_{3,4,34}^{LL}$ are obtained from the $S_{3,4,34}^{RL}$ by interchanging p_2 and $-q_2$. The expressions for the $S_{13,24,14,23}^{LL}$ are obtained from the $S_{14,23,13,24}^{RL}$ by interchanging p_1 and $-q_1$ and changing the signs of all the α's.

Summing over the polarizations of the emitted photon, we obtain an expression for the differential cross section for radiation in the RL and LL cases. In the RL case, which is the only one for which we will exhibit the expression, one obtains

$$d\sigma_{RL} = \frac{\alpha^3}{2\pi^2}\,do_2do\,\frac{d\omega}{\omega}\,(\varepsilon-\omega)^2\Big\{[2\varepsilon\,(\varepsilon-\omega)\,z$$
$$+ \omega\,(2\varepsilon-\omega y')\,y - 2\omega\,(\varepsilon-\omega)y']^{-2}\Big(A\,\frac{\sin^2\theta'}{(1-\cos\theta')^2}$$
$$+ B\,\frac{\sin^2\theta}{(1-\cos\theta)^2} - C\,\frac{\sin\theta'\sin\theta\cos\varphi}{(1-\cos\theta')(1-\cos\theta)}\Big)$$
$$+ \frac{1}{4\varepsilon^2(\varepsilon-\omega)^2z^2}\Big(B\,\frac{\sin^2\theta'}{(1+\cos\theta')^2} + B\,\frac{\sin^2\theta}{(1+\cos\theta)^2}$$
$$- D\,\frac{\sin\theta'\sin\theta\cos\varphi}{(1+\cos\theta')(1+\cos\theta)}\Big) + [2\varepsilon\,(\varepsilon-\omega)\,z\,(2\varepsilon\,(\varepsilon-\omega)\,z$$
$$+ \omega\,(2\varepsilon-\omega y')\,y - 2\omega\,(\varepsilon-\omega)\,y')]^{-1}$$
$$\times\Big(\sqrt{ABD} - 2C\cos\varphi\,\frac{1-\cos\theta'\cos\theta}{\sin\theta'\sin\theta}\Big)\Big\}; \qquad (12)$$

$$A = (2\varepsilon^2 - 2\varepsilon\omega + \omega^2)/\varepsilon\,(\varepsilon-\omega), \quad B = (2\varepsilon^2 - 2\varepsilon\omega + \omega^2)/\varepsilon^2,$$
$$C = (2\varepsilon-\omega)^2/\varepsilon\,(\varepsilon-\omega), \qquad D = (2\varepsilon-\omega)^2/\varepsilon^2,$$
$$y' = 1-\cos\theta', \quad y = 1-\cos\theta, \quad z = 1-\cos\theta_2,$$

θ', θ, θ_2 are the angles between $\mathbf{k}$ and $\mathbf{q}_2$, $\mathbf{k}$ and $-\mathbf{p}$, and $\mathbf{q}_2$ and $-\mathbf{p}$, while φ is the angle between the $(-\mathbf{p}, \mathbf{k})$ and $(\mathbf{q}_2, \mathbf{k})$ planes.

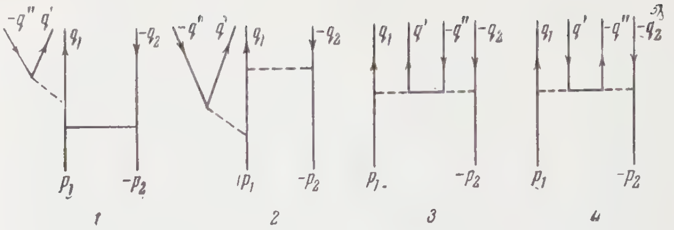

The maxima of $d\sigma_{RL}$ occur when θ_2 and θ are about equal to zero, and when θ_2 is about equal to 0 and θ about equal to π. At these angles $d\sigma_{RL} = d\sigma_{LL}$. Integrating (12) over small θ_2 and θ, with a lower limit in θ_2 equal to $[2m^2/\epsilon\,(\epsilon-\omega)]^{1/2}$ and that for θ of order of magnitude $(m\omega/\epsilon\,(\epsilon-\omega))^{1/2}$ (where m is the electron mass), we obtain, with logarithmic accuracy, the formula first obtained by Garibyan.[3]

Integrating (12) in the region $\theta_2 \sim 0$ and $\theta \sim \pi$ with lower limits $(2m^2/\epsilon^2)^{1/2}$ and about $[m\omega/\epsilon\,(\epsilon-\omega)]^{1/2}$, respectively, we arrive at

$$d\sigma_{RL} \approx 2r_0^2\alpha\,\frac{d\omega}{\omega}\Big(1-\frac{\omega}{\varepsilon}\Big)\ln\frac{\varepsilon\,(\varepsilon-\omega)}{m\omega}, \quad r_0 = \frac{\alpha}{m}. \qquad (13)$$

The radiation described by (13) is due to the recoil electron.

6. Finally, let us consider pair production in fast electron-positron collisions in the c.m.s. system.

Let p_1, p_2, q_1, q_2 be the electron and positron momenta before and after collision, and let q' and q'' be the momenta of the created pair. The region of angles which makes the largest contribution to the cross sections is determined by the minima in the denominators of the matrix elements, and corresponds to small angles of emission for both the created and scattered particles. The figure shows those diagrams which contribute most strongly to the cross section in the region of small angles about the direction of p_1.

Because the phase volumes for q_1 and q' are equal in our region of angles, the diagrams differing by exchange of q_1 and q' give the same contribution as do the direct diagrams pictured here, and thus we can take them into account merely by multiplying the cross section we get by 2.

The contribution from the cross terms between these diagrams and the exchange diagrams, as well as between diagrams 1, 2 and 3, 4 may be neglected as the maxima of their matrix elements do not overlap. One may also neglect pair production by virtual annihilation of the colliding particles, because of the large denominators of the virtual photon lines. Finally, the diagrams in which the pair is created by the positron give no contribution to our region of angles.

The matrix elements corresponding to diagrams 1 and 2 for the collision of an R and an L particle and the creation of a pair of L particles are

$$M_1 = -i\frac{(2\pi)^4}{r^2r_1^2\alpha_1^2}\bar{u}_R(q_1)\overset{+}{\sigma}_\mu\bar{\alpha}_1\overset{+}{\sigma}_\nu u_R(p_1)\bar{v}_L(-p_2)\bar{\sigma}_\nu v_L$$

$$\times(-q_2)\bar{u}_L(q')\bar{\sigma}_\mu v_L(-q''),$$

$$M_2 = -i\frac{(2\pi)^4}{r^2r_2^2\alpha_2^2}\bar{u}_R(q_1)\overset{+}{\sigma}_\mu\bar{\alpha}_2\overset{+}{\sigma}_\nu u_R(p_1)\bar{v}_L(-p_2)\bar{\sigma}_\mu v_L$$

$$\times(-q_2)\bar{u}_L(q')\bar{\sigma}_\nu v_L(-q''),$$

where $r = q' + q''$, $r_2 = p_2 - q_2$, $\alpha_1 = q_1 + q' + q''$, and $\alpha_2 = p_1 - q' - q''$.

Using (3) and (5) we obtain the following expressions for the quadratic combinations of these matrix elements:

$$|M_1|^2 = i\frac{(2\pi)^8}{r^4r_2^4\alpha_1^4}\frac{2}{\varepsilon^2\varepsilon_1\varepsilon_2\varepsilon'\varepsilon''}p_1q_2q_1q''(2p_2\alpha_1q'\alpha_1 - \alpha_1^2p_2q'),$$

$$|M_2|^2 = \frac{(2\pi)^8}{r^4r_2^4\alpha_2^4}\frac{2}{\varepsilon^2\varepsilon_1\varepsilon_2\varepsilon'\varepsilon''}q_1p_2p_1q''(2q_2\alpha_2q'\alpha_2 - \alpha_2^2q_2q'), \quad (14)$$

$$2\mathrm{Re}(M_1M_2^*) = \frac{(2\pi)^8}{r^4r_2^4\alpha_1^2\alpha_2^2}\frac{1}{\varepsilon^2\varepsilon_1\varepsilon_2\varepsilon'\varepsilon''}$$

$$\times\{(p_2q_1q''\alpha_2 + p_2\alpha_2q_1q'' - p_2q''q_1\alpha_2)(p_1q'q_2\alpha_1$$
$$+ p_1q_2q'\alpha_2 - q_2q'p_1\alpha_1) + (q_1q_2q''\alpha_2 + q_1q''q_2\alpha_2$$
$$- q_2q''q_1\alpha_2)(p_1q'p_2\alpha_1 + p_1p_2q'\alpha_1 - p_2q'p_1\alpha_1)$$
$$- p_2q_2[q''\alpha_2(p_1q'q_1\alpha_1 + p_1q_1q'\alpha_1 - q_1q'p_1\alpha_1)$$
$$+ q_1q''(p_1q'\alpha_1\alpha_2 + p_1\alpha_2q'\alpha_1 - p_1\alpha_1q'\alpha_2)$$
$$- q_1\alpha_2(p_1q'q''\alpha_1 + p_1q''q'\alpha_1 - q'q''p_1\alpha_1)]\}.$$

The corresponding expressions for production of a pair of R-particles are obtained from (14), according to rule 1, by interchanging q' and q''. The quadratic combinations for equal helicities of the incoming particles are obtained from the above by interchanging p_2 and $-q_2$.

Writing the expression for the differential cross section in the usual way, integrating over the variables of the scattered positron (corresponding to eliminating the δ function of the momentum variables) and the angle variables of the created positron, with a lower limit equal to $(2m^2/\epsilon^2)^{1/2}$, we obtain the cross section for small angles of scattering and production in the form

$$d\sigma_{RL} = 4r_0^2\frac{\alpha^2}{\pi^2}d\psi\theta_1d\theta_1\theta'd\theta'\frac{\varepsilon^2}{\varepsilon_1^2}\frac{d\varepsilon'd\varepsilon''}{(\varepsilon'+\varepsilon'')^2}$$

$$\times\frac{\sin^2\psi}{\theta_1^2+\theta'^2-2\theta_1\theta'\cos\psi}\frac{\theta_1^2}{(\theta_1^2+\eta^2\theta'^2+2\eta\theta_1\theta'\cos\psi)^2},$$

where $\eta = (\epsilon' + \epsilon'')/\epsilon_1$, and $\epsilon_1 = \epsilon - \epsilon' - \epsilon''$. Integrating over ψ, θ_1, and θ' with lower limits of order m/ϵ, we find, for $\epsilon - \epsilon' - \epsilon'' > \epsilon' + \epsilon''$ (remembering the exchange diagrams), that

$$d\sigma_{RL} \approx 4r_0^2\frac{\alpha^2}{\pi}\frac{d\varepsilon'd\varepsilon''}{(\varepsilon'+\varepsilon'')^2}\ln\frac{\varepsilon}{m}\ln\frac{\varepsilon(\varepsilon'+\varepsilon'')}{m(\varepsilon-\varepsilon'-\varepsilon'')}. \quad (15)$$

In our case of small angles, $d\sigma_{RL} = d\sigma_{LL}$. To find the total cross section let us integrate (15) over ϵ' and ϵ''. with the condition $\epsilon - \epsilon' - \epsilon'' > \epsilon' + \epsilon''$ and lower limits of order m. We obtain

$$\sigma_{RL} \approx 2r_0^2\frac{\alpha^2}{\pi}\ln^3\frac{\varepsilon}{m}.$$

Let us now evaluate the contribution from diagrams 3 and 4. The matrix elements in the RR case of the colliding particles and creation of an L pair are

$$M_3 = -i\frac{(2\pi)^4}{r_1^2r_2^2\alpha_3^2}\bar{u}_R(q_1)\overset{+}{\sigma}_\mu u_R(p_1)\bar{v}_R(-p_2)\overset{+}{\sigma}_\nu v_R$$

$$\times(-q_2)\bar{u}_L(q')\bar{\sigma}_\mu\overset{+}{\alpha}_3\bar{\sigma}_\nu v_L(-q''),$$

$$M_4 = -i\frac{(2\pi)^4}{r_1^2r_2^2\alpha_4^2}\bar{u}_R(q_1)\overset{+}{\sigma}_\mu u_R(p_1)\bar{v}_R(-p_2)\overset{+}{\sigma}_\nu v_R$$

$$\times(-q_2)\bar{u}_L(q')\bar{\sigma}_\nu\overset{+}{\alpha}_4\sigma_\mu v_L(-\bar{q}''),$$

where $r_1 = p_1 - q_1$, $r_2 = p_2 - q_2$, $\alpha_3 = -(p_1 - q_1 - q')$, and $\alpha_4 = p_1 - q_1 - q''$. Using (3) and (5) we arrive at

$$|M_3|^2 = \frac{(2\pi)^8}{r_1^4r_2^4\alpha_3^4}\frac{2}{\varepsilon^2\varepsilon_1\varepsilon_2\varepsilon'\varepsilon''}q_2q''p_1q'(2q_1\alpha_3p_2\alpha_3 - \alpha_3^2q_1p_2),$$

$$|M_4|^2 = \frac{(2\pi)^8}{r_1^4r_2^4\alpha_4^4}\frac{2}{\varepsilon^2\varepsilon_1\varepsilon_2\varepsilon'\varepsilon''}q_1q''p_2q'(2q_2\alpha_4p_1\alpha_4 - \alpha_4^2p_1q_2),$$

$$2\mathrm{Re}(M_3M_4^*) = \frac{(2\pi)^8}{r_1^4r_2^4\alpha_3^2\alpha_4^2}\frac{1}{\varepsilon^2\varepsilon_1\varepsilon_2\varepsilon'\varepsilon''}\{(p_2q'p_1\alpha_4 + p_1q'p_2\alpha_4$$
$$- p_1p_2q'\alpha_4)(q_1q''q_2\alpha_3 + q_2q''q_1\alpha_3 - q_1q_2q''\alpha_3) + (q_2q'p_1\alpha_4$$
$$+ p_1q'q_2\alpha_4 - p_1q_2q'\alpha_4)(q_1q''p_2\alpha_3 + p_2q''q_1\alpha_3 - q_1p_2q''\alpha_3)$$
$$+ p_2q_2[p_1\alpha_4(q_1q''q'\alpha_3 + q'q''q_1\alpha_3 - q_1q'q''\alpha_3)$$
$$- p_1q'(q_1q''\alpha_3\alpha_4 + q_1\alpha_3q''\alpha_4 - q_1\alpha_4q''\alpha_3)$$
$$+ q'\alpha_4(q_1q''p_1\alpha_3 + p_1q''q_1\alpha_3 - p_1q_1q''\alpha_3)]\}.$$

If we now use rule 2 we can find the corresponding expressions for creation of an R pair. The expressions for the RL case of colliding particles are obtained from the above by interchanging p_2 and $-q_2$.

Writing out the expression for the differential cross section and integrating over the variables of the scattered particles [one integration eliminates the δ function of the momentum variables, and the second is taken over angles with lower limit equal to $2m^2/\epsilon\,\epsilon_1)^{1/2}$], the expression we obtain for small angles of the created pair is

$$d\sigma_{RR} = 8r_0^2\frac{\alpha^2}{\pi^2}d\varphi\theta'd\theta'\theta''d\theta''\frac{\varepsilon_1}{\varepsilon}\frac{\varepsilon'^2\varepsilon''^2d\varepsilon'd\varepsilon''}{(\varepsilon'+\varepsilon'')^2}$$

$$\times\frac{\sin^2\varphi}{(\varepsilon'^2\theta'^2+\varepsilon''^2\theta''^2+2\varepsilon'\varepsilon''\theta'\theta''\cos\varphi)^2}.$$

In our region of angles $d\sigma_{RR} = d\sigma_{RL}$. Integrating over and θ' and θ'' with lower limits of order of magnitude m/ϵ, we find for $\epsilon' > \epsilon''$ (recalling the exchange diagrams), that

$$d\sigma_{RR} \approx 8r_0^2 \frac{\alpha^2}{\pi} \frac{\varepsilon_1}{\varepsilon} \frac{d\varepsilon' d\varepsilon''}{(\varepsilon'+\varepsilon'')^2} \ln \frac{\varepsilon}{m} \ln \frac{\varepsilon'^2}{\varepsilon'^2 - \varepsilon''^2}.$$

To find the total cross section we integrate (16) over ϵ' and ϵ'' from m to ϵ. We finally arrive at

$$\sigma_{RR} \approx 2r_0^2 \frac{\alpha^2}{\pi} \ln^2 \frac{\varepsilon}{m}.$$

For θ' and θ'' close to π, the total cross section is of order of magnitude $r_0^2\alpha^2\pi^{-1} \ln(\epsilon/m)$, whereas when $\theta' = 0$, and θ'' is near π, it is of order of magnitude $r_0^2\alpha^2/\pi$.

In conclusion I express my deep gratitude to Professor A. I. Akhiezer for his great help in the work, to Professor V. B. Berestetskiĭ and Professor I. Ya. Pomeranchuk, as well as to P. I. Fomin for interest in the work.

---

[1] R. Feynman and M. Gell-Mann, Phys. Rev. **109**, 193 (1958).

[2] A. I. Akhiezer and V. B. Berestetskiĭ, Квантовая электродинамика (Quantum Electrodynamics,) 2nd Ed., Fizmatgiz, 1959.

[3] G. M. Garibyan, JETP **24**, 617 (1953).

Translated by E. J. Saletan
36

SOVIET PHYSICS JETP VOLUME 13, NUMBER 1 JULY, 1961

REMARK ON THE VARIATIONAL CALCULATIONS OF THE POLARIZABILITY

M. N. ADAMOV and V. A. ZUBKOV

Leningrad State University

Submitted to JETP editor July 14, 1960

J. Exptl. Theoret. Phys. (U.S.S.R.) **40**, 246-248 (January, 1961)

It is shown that in constructing the trial function for the variational calculation of the polarizability of an electron in an excited state it is necessary to take into account the orthogonality of the perturbed wave functions. The polarizabilities of the excited states of an electron in a hydrogen atom or a one-dimensional infinitely deep potential well calculated with account of the above-mentioned orthogonality condition are in satisfactory agreement with the exact values (approaching them from below).

THE formulas of Kirkwood[1] and similar variational formulas for the polarizability have been derived without taking into account the orthogonality of the perturbed wave functions. These formulas, therefore, give values for the polarizability of excited states of the electron which are far too high. It can be shown that the variational values approach the exact values from below if the trial function is properly chosen.

The variational problem of finding the polarizability $\alpha_i = -2E_i^{(2)}$ for the i-th state of the electron must be formulated in the following way:

$$E_i^{(2)} = J[\psi_i^{(1)}]_{min} = \int \psi_i^{(1)}(H_0 - E_i^{(0)})\psi_i^{(1)}\,d\tau + 2\int \psi_i^{(1)} z \psi_i^{(0)} d\tau \qquad (1)$$

with the condition

$$\int \psi_i^{(1)}\psi_i^{(0)} d\tau = 0, \qquad (2)$$

which follows from the normalization of the perturbed function ψ_i, and

$$\int \psi_i^{(1)}\psi_k^{(0)} d\tau = -\int \psi_k^{(1)}\psi_i^{(0)} d\tau = z_{ik}/(E_i^{(0)} - E_k^{(0)}), \qquad (3)$$

which follow from the orthogonality of the function ψ_i to the functions ψ_k corresponding to states with energies lying below that of the i-th state. [We assume that the polarizing field is oriented along the z axis. Formulas (1) to (3) are written in terms of real functions, for convenience.]

The Euler equation for the functional (1) with account of the subsidiary conditions (2) and (3) has the form

$$(H_0 - E_i^{(0)})\psi_i^{(1)} = (\lambda_i - z)\psi_i^{(0)} + \sum_k \lambda_k \psi_k^{(0)}. \qquad (4)$$

It is easy to show that $\lambda_i = E_i^{(1)} = z_{ii}$, $\lambda_k = 0$, so that (4) coincides with the known perturbation theoretical equation for $\psi_i^{(1)}$.

If, instead of looking for an exact solution of Eq. (4), one solves the variational problem approximately by substituting a trial function φ_i with variational parameters in (1), one must require that φ_i satisfy conditions (2) and (3) for arbitrary values of these parameters. For φ_i one often uses an expression of the form

$$\varphi_i = [f_i - (f_i)_{ii}]\psi_i^{(0)}, \qquad (5)$$

where f_i is a function of the variational parameters, and

$$(f_i)_{ik} = \int \psi_i^{(0)} f_i \psi_k^{(0)} d\tau.$$

However, expression (5) does not in general satisfy the conditions (3). Instead of (5), it is reasonable to use the expression

$$\varphi_i = [f_i - (f_i)_{ii}]\psi_i^{(0)} + \sum_k c_{ik}\psi_k^{(0)}, \qquad (6)$$

where

$$c_{ik} = z_{ik}/(E_i^{(0)} - E_k^{(0)}) - (f_i)_{ik}.$$

Expression (6) defines a set of admissible trial functions. Substituting (6) in (1), we find

$$E_i^{(2)} \leqslant J[\varphi_i]_{min} = 2[(z - z_{ii}) + \tfrac{1}{4}(\operatorname{grad} f_i)^2]_{ii} + 2\sum_k c_{ik}[(E_k^{(0)} - E_i^{(0)})f_i + z]_{ik} + \sum_k c_{ik}^2 (E_k^{(0)} - E_i^{(0)}). \qquad (7)$$

Choosing $f_i = a_i z$, where a_i is the variational parameter, we obtain, instead of the Kirkwood formula

$$\alpha_i = 4[z_{ii}^2 - (z_{ii})^2]^2 \qquad (8)$$

the new variational formula*

---

*Formula (9) can also be obtained by averaging, according to Vinti,[2] the denominators of only those terms in $\alpha_i = 2\sum_k' (z_{ik})^2/(E_k^{(0)} - E_i^{(0)})$ which correspond to transitions to a state which lies above the i-th state energetically.

$$\alpha_i = 4\Big[z_{ii}^2 - (z_{ii})^2 - \sum_k (z_{ik})^2\Big]^2 \Big/ \Big[1 + 2\sum_k (E_i^{(0)} - E_k^{(0)})(z_{ik})^2\Big] - 2\sum_k (z_{ik})^2 / (E_i^{(0)} - E_k^{(0)}). \quad (9)$$

In Table I we compare the values of the polarizabilities $\alpha_{n_1 n_2 m}$ of several states of the hydrogen atom calculated with the help of formulas (8) and (9) with the corresponding exact values (see, for example, reference 3). Here $\alpha_{n_1 n_2 m}$ is the polarizability of the state characterized by the parabolic quantum numbers n_1 and n_2 and the magnetic quantum number m.

Table I

	α_{000}	α_{100}	α_{001}	α_{200}	α_{110}	α_{101}	α_{002}
By formula (8)	4	196	144	2916	2916	2450	1296
By formula (9)	4	148	144	1402	1590	1477	1296
Exact value	4.5	168	156	1620	1741	1620	1377

In Table II we make an analogous comparison for several states of an electron moving in an infinitely deep potential well of width $l = 10$ atomic units (α_n is the polarizability of the state characterized by the quantum number n). The exact values of α_n were found by the methods of reference 4. In both tables the polarizabilities are given in atomic units.

Table II

	α_1	α_2	α_3	α_4
By formula (8)	42.7	199,7	241.5	257.0
By formula (9)	42,7	—14.0	—8,5	—5.3
Exact value	43.9	—13,1	—7,8	—4,8

It is clearly evident from Tables I and II that, in contrast to the Kirkwood formula, the new variational formula gives in all cases results which do not exceed the exact values of the polarizability and are, moreover, in satisfactory agreement with the latter.

This formula can be used for the calculation of the polarizability of a many-electron system, regarding the polarizability of the system as the sum of the polarizabilities of the individual electrons. The resulting values of the polarizabilities of atoms and ions are much closer to the values computed by the method of Sternheimer[5] than the usual variational values.

In conclusion we note that the account of the orthogonality of the perturbed wave functions should be important not only in the derivation of the variational formulas for the polarizability, but also in variational calculations of other physical quantities in second order perturbation theory, as, for example, the Van-der-Waals forces.

---

[1] J. G. Kirkwood, Phys. Z. **33**, 57 (1932).

[2] J. P. Vinti, Phys. Rev. **41**, 432 (1932).

[3] L. D. Landau and E. M. Lifshitz, Квантовая механика Quantum Mechanics, Pergamon, 1958.

[4] M. N. Adamov and I. S. Milevskaya, Doklady Akad. Nauk SSSR **109**, 57 (1956), Soviet Phys.-Doklady **1**, 399 (1957).

[5] R. Sternheimer, Phys. Rev. **96**, 951 (1954).

Translated by R. Lipperheide
37

SOVIET PHYSICS JETP VOLUME 13, NUMBER 1 JULY, 1961

MACROSCOPIC EQUATIONS FOR THE MAGNETIC MOMENT IN SOME MAGNETIC RESONANCE PROBLEMS

N. N. KORST

Institute of Chemical Physics, Academy of Sciences, U.S.S.R.

Submitted to JETP editor July 22, 1960

J. Exptl. Theoret. Phys. (U.S.S.R.) 40, 249-255 (January, 1961)

A method is proposed for passing from Bloch's kinetic equations for the density matrix to the equations for the macroscopic magnetic moment of a nuclear system consisting of interacting spins. The method is applied to the problem of three equivalent particles of spin ½ coupled to each other by dipole-dipole interaction. The solution of the equations obtained is given.

THE Boltzmann equation for the density matrix of a spin system[1-3] is used for the description of nuclear magnetic absorption in the general case. Wangsness and Bloch have shown[4] that in certain cases Bloch's phenomenological equation can be applied to the case of noninteracting spins. In this paper we shall give a method for passing from the equations for the density matrix to the system of equations for the expectation values of the spin functions in the general case. By eliminating from this system all the spin functions other than the components of the macroscopic magnetic moment we can obtain an equation analogous to Bloch's phenomenological equation containing higher derivatives with respect to time. Although, apparently, it is not possible to make the transition to the macroscopic equations in the general case, nevertheless in one special case it turns out to be possible to establish certain properties of the relaxation matrix for a system consisting of an arbitrary number of interacting spins. Moreover, investigation of specific problems by means of these equations will perhaps facilitate the understanding of the physical meaning of the relaxation coefficients in the equation for the density matrix.

For the description of the transition to the macroscopic equations we shall need the differential equation for the expectation value of the spin function similar to the one obtained by Wangsness and Bloch in the discussion of a noninteracting system of spins. We shall start with the general equation for the density matrix for a spin system[2] (here and subsequently we shall use the notation introduced by Bloch):

$$\frac{d}{dt}(gv|\sigma|g'v') + i(gv|[E,\sigma]|g'v') = (gv|\Gamma(\sigma)|g'v'),$$

$$(gv|\Gamma(\sigma)|g'v') = \sum_p \sum_{v''v'''} \{2e^{\hbar p/kT}\Gamma^p_{gg'}(vv'v''v''')(g + p, v''|\sigma|g' + p, v''') - \Gamma^p_{gg}(vv'''v''v'')(gv'''|\sigma|gv') - \Gamma^p_{g'g'}(v'''v'v''v'')(gv|\sigma|g'v''')\},$$

$$\Gamma^p_{gg'}(vv'v''v''') = \pi \sum_{u,u'} \int \eta_u(f)\,\eta_{u'}(f-p)\,P(f)\,(gv, fu|G|g + p, v''; f - p, u')(g' + p, v'''; f - p, u'|G|g'v', fu)\,df. \quad (1)$$

Here $(gv|\sigma|g'v')$ is the density matrix of the spin system; g, v are the quantum numbers of the states of the spin system; f, u are the quantum numbers of the states of the heat reservoir; $\eta_u(f)$ is the density of states of the heat reservoir with quantum numbers u; $P(f) = \exp(-\hbar f/kT)$; G is the operator describing the interaction of the spin system with the heat reservoir; E is the interaction energy of the spin system with the external magnetic field **H**.

In order to simplify the subsequent presentation we shall consider a spin system consisting of equivalent particles of spin I coupled by dipole-dipole interaction. Then G has the form

$$G = \sum_{\tau, s<t} I^{\tau}_{st} F^{-\tau}_{st}, \qquad \tau = 0, \pm 1, \pm 2, \quad (2)$$

where s and t are numbers specifying the particles,

$$I^0_{st} = \sqrt{8/3}\,[I_{sz}I_{tz} - \tfrac{1}{4}(I^+_s I^-_t + I^-_s I^+_t)], \quad I^{\pm 1}_{st} = I^{\pm}_s I_{tz} + I_{sz} I^{\pm}_t,$$

$$I^{\pm 2}_{st} = I^{\pm}_s I^{\pm}_t; \qquad F^0_{st} = -\sqrt{3/8}\,C_{st}(1 - 3\cos^2\theta_{st}),$$

$$F^{\pm 1}_{st} = -\tfrac{3}{2} C_{st} \sin\theta_{st} \cos\theta_{st} e^{\pm i\varphi_{st}},$$

$$F^{\pm 2}_{st} = -\tfrac{3}{4} C_{st} \sin^2\theta_{st} e^{\pm 2i\varphi_{st}},$$

where $C_{st} = \hbar\gamma^2/r_{st}^3$, and θ_{st} and φ_{st} are the angles specifying the orientation of the vector $\mathbf{r}_{st}$, between the positions of the particles s and t.

We note that each term in the sum (2) induces transitions only between levels which are separated from each other by $\tau\omega$ ($\omega = \gamma H_0$).

On substituting G in the form (2) into the expression for $\Gamma^p_{gg'}$ we obtain

$$\Gamma^p_{gg'} = \sum_{\tau,\, st,\, s't'} \Phi^{\tau}_{st,\, s't'} (gv \,|\, I_{st}^{-\tau} \,|\, g + \tau\omega, v'') (g' + \tau\omega, v''' \,|\, I^{\tau}_{s't'} \,|\, g'v'), \tag{3}$$

$$\Phi^{\tau}_{st,\, s't'} = \pi \sum_{u,\, u'} \int \eta_u(f)\, \eta_{u'}(f - \tau\omega)\, P(f)\, (fu \,|\, F^{\tau}_{st} \,|\, f - \tau\omega, u') \times (f - \tau\omega, u' \,|\, F^{-\tau}_{s't'} \,|\, fu)\, df. \tag{3'}$$

On taking into account the remark made with respect to the operators I^{τ}_{st}, we obtain

$$\sum_{v''} (gv \,|\, I_{st}^{-\tau} \,|\, g + \tau\omega, v'') (g + \tau\omega, v'' \,|\, Q \,|\, g'v') = (gv \,|\, I_{st}^{-\tau} Q \,|\, g'v') \tag{4}$$

(here Q is an arbitrary spin operator). This relation enables us to write Eq. (1) in operator form

$$\frac{d\sigma}{dt} + i\,[E, \sigma] = \sum_{\tau,\, st,\, s't'} \Phi^{\tau}_{st,\, s't'} \{2e^{\beta\tau} I_{st}^{-\tau}\, \sigma I^{\tau}_{s't'} - I_{st}^{-\tau} I^{\tau}_{s't'} \sigma - \sigma I_{st}^{-\tau} I^{\tau}_{s't'}\}, \tag{5}$$

where $\beta = \hbar\omega/kT$. Then on multiplying both sides of (5) by the spin function and on obtaining the expectation values of the spin functions we can obtain the following equation

$$d\langle Q\rangle / dt = -i\,\langle [Q, E]\rangle + \sum_{\tau,\, st,\, s't'} \Phi^{\tau}_{st,\, s't'} \langle I_{st}^{-\tau}\, [Q, I^{\tau}_{s't'}] + [I_{st}^{-\tau}, Q]\, I^{\tau}_{s't'}\rangle, \tag{6}$$

where

$$\langle Q\rangle = \mathrm{Tr}\,(Q\sigma).$$

If into this equation we substitute in place of Q the operator for the magnetic moment **M**, then on the right hand side we obtain the expectation value of a certain polynomial in the spin operators of the system under discussion. On substituting now into (6) these polynomials in place of Q we shall obtain a system of coupled equations which will contain expectation values of certain spin polynomials. It can be easily seen that for a finite number of spins under consideration the degree of the polynomial will be finite, and consequently the system of equations will be finite. Since for any spin system it is possible to obtain an equation analogous to (6),* then by the same method it is possible to obtain a system of macroscopic equations in the most general case. The number of linearly independent equations in the macroscopic system of equations will in the general case be of the same order as in the equation for the density matrix. However, in certain cases the number of spin functions related by the equations to the components of the magnetic moment may be greatly restricted by the conditions of the problem, while the system of equations for the density matrix contains the complete amount of information with regard to the spin system and, consequently, will be more complicated.

By eliminating from the system of the macroscopic differential equations of the first order all the spin functions with the exception of the magnetic moment we shall obtain an equation of high order with respect to the time derivatives, and nonlinear in the field. In the absence of an alternating field the equation for M_z, for example, must have the form

$$\frac{d^{(N)} M_z}{dt^{(N)}} + \frac{1}{T_1} \frac{d^{(N-1)} M_z}{dt^{(N-1)}} + \ldots + \frac{M_z - M^0}{T_N} = 0, \tag{7}$$

where $T_1, T_2 \ldots T_N$ are expressed in terms of the relaxation coefficients Φ, while N is determined by the number of equations in the macroscopic system of equations. The form of Eq. (7) clearly demonstrates the well known fact that the relaxation process for the components of the magnetic moment of a complex spin system is, generally speaking, described by a large number of exponentials.

The macroscopic equations assume their simplest form in the case of a system of equivalent nuclei, when the relaxation coefficients do not depend on the index τ. This occurs, for example, in a liquid with a sufficiently short correlation time τ_c. Moreover, we shall assume that the temperature is sufficiently high to satisfy the condition $\beta \ll 1$ (this is almost always satisfied). In this case Eq. (5) for the density matrix assumes the form (cf. for example references 2 and 5)

$$\frac{d\sigma}{dt} = -i\,[E, \sigma] + \sum_{\tau,\, st,\, s't'} \Phi^{\tau}_{st,\, s't'} [I^{\tau}_{st}, [I^{-\tau}_{s't'}, \sigma - \sigma_0]]. \tag{8}$$

Here σ_0 is the equilibrium density matrix.

The coefficients $\Phi^{\tau}_{st,s't'}$ [cf. formula (3)] no longer depend on ω, since we assume that $\omega\tau \ll 1$. For the expectation value of the spin function we obtain starting with Eq. (8)

$$d\langle Q\rangle / dt = -i\,\langle [Q, E]\rangle + S(Q),$$

$$S(Q) = \sum_{\tau,\, st,\, s't'} \Phi^{\tau}_{st,\, s't'} \{\langle [I^{\tau}_{st}, [Q, I^{-\tau}_{s't'}]]\rangle - \langle [I^{\tau}_{st}, [Q, I^{-\tau}_{s't'}]]\rangle_0\}; \tag{9}$$

$\langle\ \rangle_0$ denotes averaging with respect to the equilibrium density matrix.

---

*Bloch[3] has obtained such an equation in the most general form in the case of an arbitrary external magnetic field.

As is well known (cf., for example, Ayant's paper[6]), the coefficients $\Phi^{\tau}_{st,s't'}$ are the quantum analogue of the spectral density of the correlation function of the quantities F^{τ}_{st}. Assuming the motion of the medium to be classical we can evaluate these functions when the molecule (the spin system under discussion) undergoes Brownian rotation. Such calculations have been carried out by Aleksandrov[7] and by Hubbard.[5] By utilizing their calculations we can obtain in our case

$$\Phi^{\tau}_{st,\,s't'} = (3\hbar^2\gamma^4\tau_c / 10 r^3_{st} r^3_{s't'})\left(1 - \tfrac{3}{2}\sin^2\vartheta\right) \equiv \Phi_{st,\,s't'}, \quad (10)$$

where ϑ is the angle between the vectors $\mathbf{r}_{st}$ and $\mathbf{r}_{s't'}$. It may be seen from this expression that the coefficients $\Phi^{\tau}_{st,s't'}$ do not depend on τ and $S(Q)$ may now be written in the form

$$S(Q) = \sum_{st,\,s't'} \Phi_{st\;s't'}\,[\langle X_{st,\,s't'}(Q)\rangle - \langle X_{st,\,s't'}(Q)\rangle_0],$$

$$X_{st,\,s't'}(Q) = \sum_{\tau=-2}^{2} [I^{\tau}_{st}, [Q, I^{-\tau}_{s't'}]]. \quad (11)$$

We now show that $X_{st,s't'}(Q)$ transform under rotations of the coordinate system in the same way as Q. In order to do this we consider the rotation of the coordinate system about any two axes (a rotation about a third axis may be expressed in terms of the rotations about the other two axes). We introduce $S_{\varphi} = \exp(-i\varphi I_z)$ the operator for the rotation about the z axis through an angle φ and $S_{\theta} = \exp(-i\theta I_y)$ the operator for the rotation about the y axis (here $\mathbf{I} = \Sigma_s \mathbf{I}_s$). Then, on taking into account the rules for the transformation of the spin operators I_x, I_y, I_z, it may be easily shown that

$$S_{\varphi} I^{\tau}_{st} S^{-1}_{\varphi} = e^{-i\tau\varphi} I^{\tau}_{st}, \quad S_{\theta} I^{\tau}_{st} S^{-1}_{\theta} = \sum_{\mu} q^{\tau}_{\mu}(\theta)\, I^{\mu}_{st}, \quad (12)$$

where the following relations are satisfied by the $q^{\tau}_{\mu}(\theta)$:

$$q^{-\tau}_{-\mu}(\theta) = q^{\tau}_{\mu}(\theta) = q^{\mu}_{\tau}(-\theta), \qquad \sum_{\mu} q^{\tau}_{\mu}(-\theta)\, q^{\mu}_{\lambda}(\theta) = \delta_{\tau\lambda}. \quad (13)$$

By utilizing (12) and (13), we obtain

$$S_{\theta} X_{st,\,s't'}(Q)\, S^{-1}_{\theta} = X_{st,\,s't'}(S_{\theta} Q S^{-1}_{\theta}),$$
$$S_{\varphi} X_{st,\,s't'}(Q)\, S^{-1}_{\varphi} = X_{st,\,s't'}(S_{\varphi} Q S^{-1}_{\varphi}).$$

Thus, under the rotations S_{φ} and S_{θ} the spin functions $X_{st,s't'}(I_{x,y,z})$ transform in the same way as $I_{x,y,z}$. Since $X_{st,s't'}(\mathbf{I})$ is the operator for a vector quantity, the commutation rules of $\mathbf{I}$ with this quantity are known.[8] By using them we obtain

$$-i\langle[\mathbf{X}_{st,\,s't'}, E]\rangle = \gamma[\langle \mathbf{X}_{st,\,s't'}\rangle \mathbf{H}] \quad (14)$$

(γ is the gyromagnetic ratio for the nuclei under consideration). On substituting into (9) the vector spin functions in place of Q we obtain on the right hand side the expectation value also of vector spin functions. As a result, the following system of macroscopic equations is obtained:

$$d\mathbf{x}_i / dt = \gamma[\mathbf{x}_i \mathbf{H}] - \sum_{j=1}^{N} (\mathbf{x}_j - \mathbf{x}^0_j)/T_{ij},$$
$$i = 1, 2, \dots, N, \quad (15)^*$$

where $\mathbf{x}_i = \mathbf{M}$; $\mathbf{x}_j$ for $j \neq 1$ is the expectation value of a vector spin function ($\mathbf{x}^0_j$ is the equilibrium value of $\mathbf{x}_j$), such a function can only be a linear combination of quantities of the type

$$(\mathbf{I}_{s_1}\mathbf{I}_{t_1})(\mathbf{I}_{s_2}\mathbf{I}_{t_2})\dots(\mathbf{I}_{s_n}\mathbf{I}_{t_n})\,\mathbf{I}_s;$$

N is the number of linearly independent equations in the system (15), which is determined not only by the number of particles, but also by the nature of their position with respect to each other; the quantities $1/T_{ij}$ consist of linear combinations of the relaxation coefficients $\Phi_{st,s't'}$.

In the case when the system (15) contains only one equation for $\mathbf{M}$ we obtain the usual Bloch equation with $T_1 = T_2$.

In solving the system (15) it is very convenient to utilize the matrix form of notation. Such a form of notation has been utilized, for example, in the papers by Jaynes[9] and Bloom[10] in investigating Bloch's phenomenological equation. If we introduce the matrices

$$X = \begin{pmatrix} \mathbf{x}_1 \\ \mathbf{x}_2 \\ \cdot \\ \cdot \\ \cdot \\ \mathbf{x}_N \end{pmatrix}, \quad \mathrm{B} = \begin{pmatrix} \beta & 0 & \dots & 0 \\ 0 & \beta & \dots & 0 \\ \cdot & \cdot & \cdot & \cdot \\ 0 & 0 & \dots & \beta \end{pmatrix}, \quad \frac{1}{T} = \begin{pmatrix} \frac{1}{T_{11}} & \dots & \frac{1}{T_{1N}} \\ \cdot & \cdot & \cdot \\ \frac{1}{T_{N1}} & \dots & \frac{1}{T_{NN}} \end{pmatrix},$$

$$\mathbf{x}_j = \begin{pmatrix} x^{+}_j \\ x^{-}_j \\ x_{jz} \end{pmatrix}, \qquad \beta = i\gamma \begin{pmatrix} H_z & 0 & -H^{+} \\ 0 & -H_z & H^{-} \\ -{}^1\!/_2 H^{-} & {}^1\!/_2 H^{+} & 0 \end{pmatrix},$$

$$\frac{1}{T_{ij}} = \frac{1}{T_{ij}} \begin{pmatrix} 1 & 0 & 0 \\ 0 & 1 & 0 \\ 0 & 0 & 1 \end{pmatrix}, \quad (16)$$

where, as usual, $x^{\pm}_j = x_{jx} \pm i x_{jy}$, $H^{\pm} = H_x \pm iH_y$, then the system (15) can be written in the form

$$\left(\frac{d}{dt} + \frac{1}{T} + \mathrm{B}\right) X = \frac{1}{T} X^0. \quad (17)$$

It may be easily seen that the matrices $1/T$ and B commute. This fact greatly simplifies the solution of (17). Indeed, in this case one can immediately obtain the general solution of (17) (similar to Jaynes' paper[9]) in the form

$$X(t) = u(t, 0)\, X(0) + \int_0^t u(t, t')\, dt' \; \frac{1}{T} X^0,$$
$$u(t, t') = R(t, t') \exp\left\{-\frac{t - t'}{T}\right\},$$
$$R(t, t') = \exp\left\{-\int_{t'}^{t} \mathrm{B}(t'')\, dt''\right\}. \quad (18)$$

From this last expression it may be seen that the

$^*[\mathbf{x}_i\mathbf{H}] = \mathbf{x}_i \times \mathbf{H}$

determination of the operator R(t,t′), associated with the external magnetic field, reduces to the similar problem for the Bloch equation. The evaluation of the operator exp [−(t − t′)/T] reduces to the purely algebraic problem of the diagonalization of the matrix 1/T.

As an illustration of the preceding discussion we consider the derivation of the macroscopic system of equations and its solution in the case of a molecule containing three protons which have the same gyromagnetic ratio and which are separated from each other by the same distance r (CH_3 − group). The correlation time in the medium is assumed to be small,* $\tau_c\omega \ll 1$. We shall start with Eq. (9) and expression (11) for S(Q). Since in our system the distance between any pair of particles is equal to r, while the angles between any pair of vectors joining any one particle to the other two are equal to $\vartheta = 60°$, then it follows from formula (10) that

$$\Phi_{st,\,st'} = \Phi\begin{cases} 1, & t = t' \\ -{}^1/_8, & t \neq t' \end{cases}, \qquad \Phi = \frac{3\hbar^2\gamma^4\tau_c}{10r^6}. \tag{19}$$

If in (19) we also take into account the fact that

$$\sum_{\tau}\sum_{st,\,s't'}[I_{st}^{\tau},[Q,I_{s't'}^{-\tau}]] = \tfrac{1}{4}\sum_{\tau}[I^{\tau}[Q,I^{-\tau}]] = \tfrac{1}{4}X(Q),$$

where

$$I^0 = \sqrt{{}^8/_3}\left[I_z^2 - \tfrac{1}{4}(I^+I^- + I^-I^+)\right], \quad I^{\pm 1} = I^{\pm}I_z + I_zI^{\pm},$$

$$I^{\pm 2} = I^{\pm}I^{\pm}, \quad \mathbf{I} = \sum_s \mathbf{I}_s,$$

then we can obtain for S(Q) the following expression

$$S(Q) = \Phi\Big\{\tfrac{9}{8}\sum_{st}\left[\langle X_{st,\,st}(Q)\rangle - \langle X_{st,\,st}(Q)\rangle_0\right]$$
$$- \tfrac{1}{32}\left[\langle X(Q)\rangle - \langle X(Q)\rangle_0\right]\Big\}.$$

Then by utilizing the commutation relations

$$[I_z, I_{st}^{\tau}] = \tau I_{st}^{\tau}, \quad [I_z, I^{\tau}] = \tau I^{\tau},$$

$$[I_{st}^{\tau}, I_{st}^{-\tau}] = \frac{\tau}{2}(I_{sz} + I_{tz}), \qquad \sum_{\tau=1}^{2}\tau[I^{\tau}, I^{-\tau}] = 8I^2I_z - 6I_z,$$

we evaluate $X_{st,st}(\gamma\mathbf{I})$ and $X(\gamma\mathbf{I})$. As a result of this we obtain for $S(\gamma\mathbf{I})$

$$S(\gamma\mathbf{I}) = -(\mathbf{M} - \mathbf{M}^0)/T_{11} + \mathbf{x}/T_{12}.$$

Here

$$\mathbf{M} = \gamma\langle\mathbf{I}\rangle, \quad \mathbf{x} = \gamma\langle\mathbf{s}\rangle, \ \mathbf{s} = \left(\tfrac{1}{2}I^2 - \tfrac{13}{8}\right)\mathbf{I},$$

$$1/T_{11} = 10\Phi, \ 1/T_{12} = \Phi.$$

We have chosen the spin functions $\mathbf{s}$ in such a way that its expectation value with respect to the equilibrium density matrix is equal to zero. Then, on substituting into equation (9) $\mathbf{Q} = \gamma\mathbf{s}$ and on evaluating the commutators, we finally obtain the following system of equations

$$\frac{d\mathbf{M}}{dt} = \gamma[\mathbf{M}\ \mathbf{H}] - \frac{\mathbf{M} - \mathbf{M}^0}{T_{11}} + \frac{\mathbf{x}}{T_{12}},$$

$$\frac{d\mathbf{x}}{dt} = \gamma[\mathbf{x}\ \mathbf{H}] + \frac{\mathbf{M} - \mathbf{M}^0}{T_{21}} - \frac{\mathbf{x}}{T_{22}}, \tag{20}$$

where $1/T_{21} = 5\Phi/16$, $1/T_{22} = 17\Phi/4$.

If from these equations we eliminate $\mathbf{x}$ then the equation for the magnetic moment will have the form

$$\frac{d^2\mathbf{M}}{dt^2} - \gamma\frac{d}{dt}[\mathbf{M}\ \mathbf{H}] + \gamma\left[\frac{d\mathbf{M}}{dt}\mathbf{H}\right] - \gamma^2[[\mathbf{M}\ \mathbf{H}]\mathbf{H}]$$
$$- \left(\frac{1}{T'} + \frac{1}{T''}\right)\frac{d\mathbf{M}}{dt} - \frac{\mathbf{M} - \mathbf{M}^0}{T'T''}$$
$$+ \gamma\left(\frac{1}{T'} + \frac{1}{T''}\right)[\mathbf{M}\ \mathbf{H}] - \frac{\gamma}{T_{11}}[\mathbf{M}^0\ \mathbf{H}],$$

where 1/T′ and 1/T″ are the eigenvalues of the matrix

$$\begin{pmatrix} 1/T_{11} & -1/T_{12} \\ -1/T_{21} & 1/T_{22} \end{pmatrix}.$$

By utilizing the matrix form of notation we can easily obtain the solution of the system (20) in the case of "slow passage" (the stationary solution when the external field is of the form $H_x = H_1 \cos \omega t$, $H_y = -H_1 \sin \omega t$, $H_z = H_0$) and of the spin-echo signal (external transverse field consists of a series of consecutive pulses at the resonance frequency). In both cases the solution may be written in the form

$$\mathbf{M} = \frac{T'T''}{(T' - T'')T_{11}}\left[\frac{T_{11} - T''}{T''}\mathbf{M}_{T'} - \frac{T_{11} - T'}{T'}\mathbf{M}_{T''}\right], \tag{21}$$

where $\mathbf{M}_T$ is the solution of the phenomenological Bloch equation for the corresponding problem (cf., for example, references 9 and 10).

It may be seen from formula (21) that by determining experimentally the relative contribution to the relaxation of the times T′ and T″ we should obtain the same ratio given by $l = (T_{11} - T')\times T''/(T_{11} - T'')T'$, both in the slow passage experiments, and also in methods associated with the spin echo technique. In the example considered by us $l \sim 1/200$, and, therefore, it will hardly be possible to observe two relaxation times in experiments based on utilizing the solution (21).

The author wishes to thank Professor N. S. Sokolov, and also I. V. Aleksandrov for discussions.

---

*The problem of the relaxation of the magnetic moment of such a system was considered in references 5 and 7.

[1] F. Bloch, Phys. Rev. **102**, 104 (1956).

[2] A. G. Redfield, J. Res. Dev. **1**, 19 (1957).

[3] F. Bloch, Phys. Rev. **105**, 1206 (1957).

[4] R. Wangsness and F. Bloch, Phys. Rev. **89**, 788 (1953).

[5] P. Hubbard, Phys. Rev. **109**, 1153 (1958).

[6] Y. Ayant, J. Phys. Radium **16**, 411 (1955).

[7] I. V. Aleksandrov, Thesis, Inst. Chem. Phys., 1958.

[8] L. D. Landau and E. M. Lifshitz, Квантовая механика (Quantum Mechanics), Gostekhizdat, 1948, p. 112 Transl: Addison Wesley, 1958].

[9] E. T. Jaynes, Phys. Rev. **98**, 1099 (1955).

[10] A. L. Bloom, Phys. Rev. **98**, 1105 (1955).

Translated by G. Volkoff.
38

SOVIET PHYSICS JETP VOLUME 13, NUMBER 1 JULY, 1961

ISOTOPIC INVARIANCE IN PROCESSES INVOLVING ANTIHYPERONS

V. A. LYUL'KA

Submitted to JETP editor July 23, 1960

J. Exptl. Theoret. Phys. **40**, 256-261 (January, 1961)

A number of relations between cross section for reactions involving antihyperons is derived on basis of the isotopic invariance hypothesis. Some additional relations between the cross sections arise if interaction of π and K mesons with baryons predominates in states with definite isotopic spin values.

THE experimental investigation of processes in which antihyperons participate is of great interest, since it can be useful in the gathering of various information concerning interactions between elementary particles. As indicated by Amati and Vitale,[1] to obtain antihyperons it is advantageous to use the reaction

$$K + N \rightarrow N + \overline{Y} + N, \tag{1}$$

which can occur in a K-meson beam extracted from an accelerator. Its threshold energy is on the order of 4 Bev, and K mesons of such energy can be obtained in nucleon-nucleon collisions. It can be assumed that various processes in an antiproton beam, for example of the type

$$\overline{p} + N \rightarrow Y_1 + \overline{Y}_2. \tag{2}$$

can be used to obtain antihyperons (particularly low-energy ones).

Assuming that experiments with antihyperons will become feasible in the future, we obtain here, on the basis of the charge-invariance hypothesis, several relations between the cross sections of various processes in which antihyperons participate. An experimental verification of such relations would enable us not only to judge whether the charge-invariants hypothesis can be extended to include phenomena involving interactions of strange particles (in particular, antihyperons) but also, should this hypothesis prove correct, to obtain some information on the interaction between elementary particles in states with definite isotopic spins. We consider here several reactions that are expected in the collision between antihyperons and nuclei having isotopic spins 0 and $1/2$.

1. Let us consider the reactions

$$\begin{aligned} \overline{\Sigma}^{+} + d &\rightarrow n + \pi^{-} + K^{+}, & \overline{\Sigma}^{0} + d &\rightarrow p + \pi^{-} + K^{+}, \\ &\rightarrow n + \pi^{0} + K^{0}, & &\rightarrow p + \pi^{0} + K^{0}. \\ &\rightarrow p + \pi^{-} + R^{0}, & & \end{aligned}$$

The corresponding charge-symmetrical reactions have equal cross sections. Reactions with $\overline{\Sigma}^{+}$ antihyperons were considered in detail by Amati and Vitale[1] and by Matinyan and Khutsishvili.[2] We derive here a few additional relations, including the cross sections of the reactions induced by neutral $\overline{\Sigma}^{0}$ antihyperons.

Assuming charge invariance, we can show that the following equations hold true:

$$\begin{aligned} &d\sigma(\overline{\Sigma}^{+} \rightarrow n\pi^{0}K^{0}) = d\sigma(\overline{\Sigma}^{0} \rightarrow p\pi^{-}K^{+}), \\ &d\sigma(\overline{\Sigma}^{+} \rightarrow n\pi^{-}K^{+}) + d\sigma(\overline{\Sigma}^{+} \rightarrow p\pi^{-}K^{0}) \\ &\quad = d\sigma(\overline{\Sigma}^{+} \rightarrow n\pi^{0}K^{0}) + 2\,d\sigma(\overline{\Sigma}^{0} \rightarrow p\pi^{0}K^{0}). \end{aligned} \tag{3}$$

When experimental data on the cross sections of the reactions induced by negatively charged $\overline{\Sigma}^{+}$ antihyperons become available, these relations will yield information on reactions induced by neutral $\overline{\Sigma}^{0}$ antihyperons, which are very difficult to investigate experimentally, because of the short lifetime of the $\overline{\Sigma}^{0}$.

In addition to the inequalities established in reference 2, we can derive also the following:

$$\begin{aligned} &d\sigma(\overline{\Sigma}^{+} \rightarrow n\pi^{0}K^{0}) + d\sigma(\overline{\Sigma}^{0} \rightarrow p\pi^{0}K^{0}) \geqslant \tfrac{2}{3}\,d\sigma(\overline{\Sigma}^{+} \rightarrow n\pi^{-}K^{+}), \\ &d\sigma(\overline{\Sigma}^{+} \rightarrow p\pi^{-}K^{0}) + \tfrac{1}{3}\,d\sigma(\overline{\Sigma}^{+} \rightarrow n\pi^{0}K^{0}) \geqslant d\sigma(\overline{\Sigma}^{0} \rightarrow p\pi^{0}K^{0}), \\ &d\sigma(\overline{\Sigma}^{0} \rightarrow p\pi^{-}K^{+}) + d\sigma(\overline{\Sigma}^{+} \rightarrow p\pi^{-}K^{0}) \geqslant \tfrac{1}{3}\,d\sigma(\overline{\Sigma}^{+} \rightarrow n\pi^{-}K^{+}). \end{aligned} \tag{4}$$

We note that one of the relations in (4) is the consequence of the other two. In addition,

$$\begin{aligned} &|\{2\,d\sigma(\overline{\Sigma}^{+} \rightarrow p(n)\,\pi^{\pm}K^{0})\}^{1/2} - \{2\,d\sigma(\overline{\Sigma}^{0} \rightarrow p\pi^{0}K^{0})\}^{1/2}| \\ &\quad \leqslant \{d\sigma(\overline{\Sigma}^{0} \rightarrow p\pi K^{+})\}^{1/2} \leqslant \{2\,d\sigma(\Sigma^{\mp} \rightarrow p(n)\,\pi^{\pm}K^{0})\}^{1/2} \\ &\quad + \{2\,d\sigma(\overline{\Sigma}^{0} \rightarrow p\pi^{0}K^{0})\}^{1/2}, \end{aligned}$$

$$\begin{aligned} &|\{2\,d\sigma(\overline{\Sigma}^{+} \rightarrow p(n)\,\pi^{\pm}K^{0})\}^{1/2} - \{d\sigma(\overline{\Sigma}^{0} \rightarrow p\pi^{-}K^{+})\}^{1/2}| \\ &\quad \leqslant \{2d\sigma(\overline{\Sigma}^{0} \rightarrow p\pi^{0}K^{0})\}^{1/2} \leqslant \{2\,d\sigma(\overline{\Sigma}^{+} \rightarrow p(n)\,\pi^{\pm}K^{0})\}^{1/2} \\ &\quad + \{d\sigma(\overline{\Sigma}^{0} \rightarrow p\pi^{-}K^{+})\}^{1/2}, \end{aligned}$$

$$|\{2\,d\sigma(\overline{\Sigma}^0 \to p\pi^0K^0)\}^{1/2} - \{d\sigma(\overline{\Sigma}^0 \to p\pi^-K^+)\}^{1/2}|$$
$$\leqslant \{2\,d\sigma(\overline{\Sigma}^+ \to p\,(n)\,\pi^\pm K^0)\}^{1/2} \leqslant \{2\,d\sigma(\overline{\Sigma}^0 \to p\pi^0K^0)\}^{1/2} + \{d\sigma(\overline{\Sigma}^0 \to p\pi^-K^+)\}^{1/2}. \qquad (5)$$

If the interaction of the π-N system in the state with T = 3/2 predominates, a new relation arises

$$d\sigma(\overline{\Sigma}^+ \to n\pi^+K^0) = \tfrac{1}{2}\,d\sigma(\overline{\Sigma}^0 \to p\pi^0K^0). \qquad (6)$$

We can consider analogously reactions of the type

$$\overline{\Xi} + d \to N + K + K.$$

The charge invariance leads to the relation

$$d\sigma(\overline{\Xi}^- \to pK^+K^0) \geqslant \tfrac{1}{2}\,d\sigma(\overline{\Xi}^- \to nK^+K^+). \qquad (7)$$

At the present time the experimental data apparently point to a strong interaction of the K-N system in the state with T = 1. In this limiting case we obtain

$$d\sigma(\overline{\Xi}^- \to pK^+K^0) = 5\,d\sigma(\overline{\Xi}^- \to nK^+K^+). \qquad (8)$$

2. We now consider the reactions accompanied by the creation of two pions, for example

$$\overline{\Xi} + d \to N + \pi + \pi + K.$$

We construct the wave function of the final state with T = 1 from the wave functions of the system of two pions with t_1 = 0, 1, and 2, and the wave functions of the K-N system with t_2 = 0 and 1. If $A_{t_2}^{t_1}$ is the amplitude of the transition into states with isotopic spins t_1 and t_2, then the amplitudes of the reactions have the following form

$$M(\overline{\Sigma}^+ \to K^+p\pi^-\pi^-) = \left(\tfrac{3}{5}\right)^{1/2} A_1^2,$$
$$M(\overline{\Sigma}^+ \to K^0n\pi^0\pi^0) = -\left(\tfrac{1}{3}\right)^{1/2} A_1^0 \quad \left(\tfrac{1}{15}\right)^{1/2} A_1^2,$$
$$M(\overline{\Sigma}^+ \to K^0p\pi^-\pi^0) = -\tfrac{1}{2} A_0^1 + \left(\tfrac{1}{8}\right)^{1/2} A_1^1 - \left(\tfrac{3}{40}\right)^{1/2} A_1^2,$$
$$M(\overline{\Sigma}^+ \to K^0p\pi^0\pi^-) = \tfrac{1}{2} A_0^1 - \left(\tfrac{1}{8}\right)^{1/2} A_1^1 - \left(\tfrac{3}{40}\right)^{1/2} A_1^2,$$
$$M(\overline{\Sigma}^+ \to K^0n\pi^-\pi^+) = \left(\tfrac{1}{3}\right)^{1/2} A_1^0 - \frac{1}{2} A_1^1 + \left(\tfrac{1}{60}\right)^{1/2} A_1^2,$$
$$M(\overline{\Sigma}^+ \to K^0n\pi^+\pi^-) = \left(\tfrac{1}{3}\right)^{1/2} A_1^0 + \frac{1}{2} A_1^1 + \left(\tfrac{1}{60}\right)^{1/2} A_1^2,$$
$$M(\overline{\Sigma}^+ \to K^+n\pi^0\pi^-) = -\tfrac{1}{2} A_0^1 - \left(\tfrac{1}{8}\right)^{1/2} A_1^1 - \left(\tfrac{3}{40}\right)^{1/2} A_1^2,$$
$$M(\overline{\Sigma}^+ \to K^+n\pi^-\pi^0) = \tfrac{1}{2} A_0^1 + \left(\tfrac{1}{8}\right)^{1/2} A_1^1 - \left(\tfrac{3}{40}\right)^{1/2} A_1^2. \qquad (9)$$

If, as is customarily done, the summation is carried out over the states of the π mesons, we obtain from (9) the inequalities

$$d\sigma(\overline{\Sigma}^+ \to K^0p\pi^-\pi^0) + d\sigma(\overline{\Sigma}^+ \to K^+n\pi^-\pi^0) \geqslant \tfrac{1}{2}\,d\sigma(\overline{\Sigma}^+ \to K^+p\pi^-\pi^-),$$
$$d\sigma(\overline{\Sigma}^+ \to K^0n\pi^+\pi^-) + d\sigma(\overline{\Sigma}^+ \to K^0n\pi^0\pi^0) \geqslant \tfrac{1}{6}\,d\sigma(\overline{\Sigma}^+ \to K^+p\pi^-\pi^-), \qquad (10)$$

which could be verified experimentally.

If the K meson and the nucleon interact only in the state with t = 1, an additional relation appears

$$d\sigma(\overline{\Sigma}^+ \to K^0p\pi^-\pi^0) = d\sigma(\overline{\Sigma}^+ \to K^+n\pi^-\pi^0). \qquad (11)$$

If the pions are produced in states with even orbital momentum (we refer to their relative motion), then the following equality holds

$$d\sigma(\overline{\Sigma}^+ \to K^+n\pi^-\pi^0) = \tfrac{1}{4}\,d\sigma(\overline{\Sigma}^+ \to K^+p\pi^-\pi^-). \qquad (12)$$

The wave function of the final state with T = 1 can also be constructed by considering the functions of the subsystems (πK) and (πM) with isotopic spins t = 1/2 and 3/2. In the limiting case when the interactionof the π-N system in the state with t = 3/2 predominates, we obtain

$$\tfrac{2}{5}\,d\sigma(\overline{\Sigma}^+ \to K^+n\pi^-\pi^0) + \tfrac{29}{10}\,d\sigma(\overline{\Sigma}^+ \to K^+p\pi^-\pi^-)$$
$$+ d\sigma(\overline{\Sigma}^+ \to K^0n\pi^0\pi^0) = \tfrac{2}{3}\,d\sigma(\overline{\Sigma}^+ \to K^0n\pi^-\pi^+)$$
$$+ d\sigma(\overline{\Sigma}^+ \to K^0p\pi^0\pi^-),$$
$$\tfrac{63}{25}\,d\sigma(\overline{\Sigma}^+ \to K^+p\pi^-\pi^-) + \tfrac{3}{2}\,d\sigma(\overline{\Sigma}^+ \to K^0n\pi^0\pi^0)$$
$$= \tfrac{1}{3}\,d\sigma(\overline{\Sigma}^+ \to K^0n\pi^-\pi^+) + \tfrac{2}{25}\,d\sigma(\overline{\Sigma}^+ \to K^+n\pi^-\pi^0)$$
$$+ d\sigma(\overline{\Sigma}^+ \to K^0p\pi^-\pi^0). \qquad (13)$$

If suitable experimental data become available, relations (10) — (13) will enable us to obtain information on the cross sections of reactions with one and two π^0 mesons in the final state, which are very difficult to identify experimentally.

The foregoing analysis can be readily generalized to include heavier nuclei with zero isotopic spin (provided the isotopic spin is a good quantum number for such nuclei).

3. As in the case of nucleon-antinucleon collisions, we can expect in the interaction between antihyperons and nucleons the annihilation to be accompanied by the creation of at least two π^- and K mesons. Such processes will naturally take place also in interactions between antihyperons and nucleons bound in the nucleus.

We have already considered some of these reactions. However, in collision between antihyperons and nuclei, in addition to these usual annihilation processes, so-called "unusual" annihilation can take place, due to the absorption of part of the mesons produced by the remaining nucleons as a result of the elementary act, in analogy with the nucleon-antinucleon annihilation considered by Pontecorvo.[4] Thus, the following processes are possible

$$\overline{\Lambda} + d \to p + K^0, \quad \overline{\Sigma}^0 + d \to n + K^+, \quad \overline{\Sigma}^+ + d \to n + K^0.$$

along with the corresponding charge-symmetrical reactions with equal cross sections.

The isotopic invariance leads in this case to the equation $d\sigma(\overline{\Sigma}^0 \to nK^+) = \frac{1}{2} d\sigma(\overline{\Sigma}^+ \to nK^0)$. Interest attaches also to an experimental investigation of the inverse reactions, for this will afford a check on the spins of the $\overline{\Lambda}$ and $\overline{\Sigma}$ antihyperons, inasmuch as the ratio of the cross sections of the direct and inverse reactions contains the factor $(2S_N + 1)/(2S_{\overline{Y}} - 1)$, where S_N and $S_{\overline{Y}}$ are respectively the spins of the nucleon and the antihyperon.

Let us consider now several reactions of the "unusual" type, caused by the interaction between antihyperons and nuclei that are isotopic doublets (for example He^3 and H^3), i.e., reactions of the type $\overline{\Sigma} + X^3 \to N + N + K$. Denoting by A_{13} and A_{11} the amplitudes of the transitions in the states with T = 1 for the K-N system, and by A_{01} the amplitude with T = 0, we obtain

$$M(\overline{\Sigma}^- \to ppK^+) = A_{13},$$
$$M(\overline{\Sigma}^+ \to nnK^+) = \tfrac{1}{3} A_{13} - \tfrac{1}{3} A_{11} + \left(\tfrac{1}{3}\right)^{1/2} A_{01},$$
$$M(\overline{\Sigma}^+ \to npK^0) = \tfrac{1}{3} A_{13} + \tfrac{2}{3} A_{11},$$
$$M(\overline{\Sigma}^+ \to pnK^0) = \tfrac{1}{3} A_{13} - \tfrac{1}{3} A_{11} - \left(\tfrac{1}{3}\right)^{1/2} A_{01},$$
$$M(\overline{\Sigma}^0 \to ppK^0) = \left(\tfrac{2}{9}\right)^{1/2} A_{13} + \left(\tfrac{1}{18}\right)^{1/2} A_{11} - \left(\tfrac{1}{6}\right)^{1/2} A_{01},$$
$$M(\overline{\Sigma}^0 \to pnK^0) = \left(\tfrac{2}{9}\right)^{1/2} A_{13} - \left(\tfrac{2}{9}\right)^{1/2} A_{11},$$
$$M(\overline{\Sigma} \to npK^+) = \left(\tfrac{2}{9}\right)^{1/2} A_{13} + \left(\tfrac{1}{18}\right)^{1/2} A_{11} + \left(\tfrac{1}{6}\right)^{1/2} A_{01}. \quad (14)$$

Assuming the cross sections over the states of the nucleons, we obtain on the basis of (14) the well known equation[5]

$$d\sigma(\overline{\Sigma}^- \to ppK^+) + d\sigma(\overline{\Sigma}^+ \to pnK^0) + d\sigma(\overline{\Sigma}^+ \to nnK^+)$$
$$= 2[d\sigma(\overline{\Sigma}^0 \to ppK^0) + d\sigma(\overline{\Sigma} \to pnK^+)]. \quad (15)$$

Using the expressions for the amplitudes $M(\overline{\Sigma}^- \to ppK^+)$, $M(\overline{\Sigma}^+ \to nnK^+)$, $M(\overline{\Sigma}^0 \to ppK^0)$, we obtain

$$|\{d\sigma(\overline{\Sigma}^+ \to nnK^+)\}^{1/2} - \{d\sigma(\overline{\Sigma}^- \to ppK^+)\}^{1/2}|$$
$$\leqslant \{2d\sigma(\overline{\Sigma}^0 \to ppK^0)\}^{1/2} \leqslant \{d\sigma(\overline{\Sigma}^+ \to nnK^+)\}^{1/2}$$
$$+ \{d\sigma(\overline{\Sigma}^- \to ppK^+)\}^{1/2},$$
$$|\{2d\sigma(\overline{\Sigma}^0 \to ppK^0)\}^{1/2} - \{d\sigma(\overline{\Sigma}^+ \to nnK^+)\}^{1/2}|$$
$$\leqslant \{d\sigma(\overline{\Sigma}^- \to ppK^+)\}^{1/2} \leqslant \{2d\sigma(\overline{\Sigma}^0 \to ppK^0)\}^{1/2}$$
$$+ \{d\sigma(\overline{\Sigma}^+ \to nnK^+)\}^{1/2},$$
$$|\{2d\sigma(\overline{\Sigma}^0 \to ppK^0)\}^{1/2} - \{d\sigma(\overline{\Sigma}^- \to ppK^+)\}^{1/2}|$$
$$\leqslant \{d\sigma(\overline{\Sigma}^+ \to nnK^+)\}^{1/2} \leqslant \{2d\sigma(\overline{\Sigma}^0 \to ppK^0)\}^{1/2}$$
$$+ \{d\sigma(\overline{\Sigma}^- \to ppK^+)\}^{1/2}.$$

Analogously we can establish the following inequalities

$$d\sigma(\overline{\Sigma}^0 \to ppK^0) + d\sigma(\overline{\Sigma}^+ \to nnK^+) \geqslant \tfrac{1}{3} d\sigma(\overline{\Sigma}^- \to ppK^+),$$
$$d\sigma(\overline{\Sigma}^0 \to ppK^0) + d\sigma(\overline{\Sigma}^0 \to pnK^+) \geqslant \tfrac{2}{3} d\sigma(\overline{\Sigma}^- \to ppK^+),$$
$$d\sigma(\overline{\Sigma}^+ \to nnK^+) + d\sigma(\overline{\Sigma}^+ \to pnK^0) \geqslant \tfrac{1}{3} d\sigma(\overline{\Sigma}^- \to ppK^+). \quad (16)$$

With the aid of experimental data on the interaction between charged antihyperons, we could obtain from relations (16) and (17) information on the cross section of the reactions induced by neutral $\overline{\Sigma}^0$ antihyperons.

A similar analysis can be readily extended to the case of heavier nuclei (Li^7, Be^7), for which the isotopic spin is a good quantum number.

An interesting example of "unusual" reactions of processes of the type

$$\overline{\Sigma} + d \to \Sigma(\Lambda) + K + K.$$

The isotopic invariance gives rise to the relation

$$d\sigma(\overline{\Sigma}^+ \to \Sigma^- K^+ K^0) = d\sigma(\overline{\Sigma}^+ \to \overline{\Sigma}^0 K^0 K^0) + d\sigma(\overline{\Sigma}^0 \to \Sigma^0 K^+ K^0). \quad (17)$$

If the K meson and Σ hyperon interact only in the state with T = ½, then

$$d\sigma(\overline{\Sigma}^+ \to \Sigma^0 K^0 K^0) : d\sigma(\overline{\Sigma}^+ \to \Sigma^- K^+ K^0) : d\sigma(\overline{\Sigma}^0 \to \Sigma^0 K^+ K^0)$$
$$= 1:2:1. \quad (18)$$

In the opposite case of interaction in the state with T = 3/2,

$$d\sigma(\overline{\Sigma}^+ \to \Sigma^0 K^0 K^0) : d\sigma(\overline{\Sigma}^+ \to \Sigma^- K^+ K^0) : d\sigma(\overline{\Sigma}^0 \to \Sigma^0 K^+ K^0)$$
$$= 1:5:4. \quad (19)$$

If, according to Gell-Mann and Pais, all the baryons are isotopic doublets

$$N_1 = \begin{vmatrix} \Sigma^+ \\ Y^0 \end{vmatrix}, \quad Y^0 = \frac{1}{\sqrt{2}}(\Lambda^0 - \Sigma^0),$$
$$N_2 = \begin{vmatrix} Z^0 \\ \Sigma^- \end{vmatrix}, \quad Z^0 = \frac{1}{\sqrt{2}}(\Lambda^0 + \Sigma^0),$$

we have the approximate relation

$$d\sigma(\overline{\Sigma}^+ \to \Sigma^0 K^0 K^0) \approx d\sigma(\overline{\Sigma}^+ \to \Lambda^0 K^0 K^0),$$

the accuracy of which is

$$\delta = (M_\Sigma - M_\Lambda)/M_\Sigma \approx 7\%.$$

I'm grateful to P. É. Nemirovskiĭ, L. B. Okun', L. M. Barkov, A. P. Mishakova and B. A. Nikol'skiĭ for interest in the work and for useful discussions.

---

[1] D. Amati and B. Vitale, JETP **33**, 556 (1957), Soviet Phys. JETP **6**, 435 (1958).

[2] S. G. Matinyan and G. R. Khutsishvili, JETP **35**, 546 (1958), Soviet Phys. JETP **8**, 377 (1959).

[3] E. Fermi, Lectures on Pions and Nucleons (Transl.) IIL, 1956.

[4] B. Pontecorvo, JETP **30**, 947 (1956), Soviet Phys. JETP **3**, 966 (1956).

[5] L. I. Lapidus, JETP **31**, 865 (1956), Soviet Phys. JETP **4**, 740 (1957).

Translated by J. G. Adashko
39

SOVIET PHYSICS JETP VOLUME 13, NUMBER 1 JULY, 1961

RAMAN SCATTERING OF LIGHT IN SUPERCONDUCTORS

A. A. ABRIKOSOV and L. A. FAL'KOVSKIĬ

Institute for Physics Problems, Academy of Sciences, U.S.S.R.

Submitted to JETP editor July 25, 1960

J. Exptl. Theoret. Phys. (U.S.S.R.) **40**, 262-270 (January, 1961)

A computation is carried out of Raman scattering upon reflection of light from the surface of a superconductor. The distribution with angle and frequency of the scattered light and the absolute magnitude of the effect are found.

THE most interesting and important properties of superconductors consist of the special aspects of their behavior in an electromagnetic field. In particular, high-frequency impedance measurements provide the possibility of explaining directly the characteristic features of the electronic energy spectrum of superconductors. The presence of an energy gap Δ in this spectrum leads to the absence of absorption (at $T = 0$) of radiation having a frequency less than the threshold frequency, equal to 2Δ.

In addition to these experiments, which involve measurements at various frequencies, Khaĭkin and Bykov[1] made an attempt to investigate the electron spectrum using the Raman scattering of light in superconductors. The distribution of frequencies of the satellites, given sufficient intensity, might be measured by spectroscopic methods. The fundamental difficulty with this experiment lies in the extremely small amount of scattering. To a significant degree, this is associated with the fact that the skin effect, enables the light to penetrate only into a very thin surface layer of the metal, of the order of 10^{-5} cm. In Khaĭkin and Bykov's experiments, no satellites were found.

The question naturally arises: what increase in sensitivity is required for the successful performance of such an experiment, and what overall pattern is to be expected for the phenomenon? The present calculation was undertaken with this as its object.

Our goal is to derive the distribution with frequency and angle of the light reflected from the plane surface of a superconductor filling the semi-infinite volume $z > 0$. For simplicity, we shall assume $T = 0$, and limit ourselves to the case in which the incident and reflected waves do not make too large angles with the normal to the surface ($\sin^2\theta$, $\sin^2\theta' \ll |\epsilon|$, where ϵ is the complex dielectric constant); the latter limitation is of small significance in practice, since $|\epsilon| \sim 10$ for the majority of metals in the frequency range of interest to us. We shall assume that the frequency of the radiation falls in the optical region.

1. Let the incident wave be characterized by a vector potential

$$\mathbf{A}(z, y) = \mathbf{A}_0 \exp(ik_{0z}z + ik_{0y}y - i\omega t) + \text{compl. conj.}$$

The field which this wave generates in the metal we shall designate by $\mathbf{A}_2$. Under the influence of this field, the system of electrons can undergo a transition with the emission of a quantum $\mathbf{A}_2'$ (outside the metal there arises as a result a field $\mathbf{A}_0'$, corresponding to a quantum having frequency ω', direction in the interval $d\Omega'$ and a given polarization).

Let us introduce a reflection coefficient $d\sigma$, which we shall define as the fraction of the energy falling onto the surface of the superconductor (the latter, it is clear, is equal to $(2\pi)^{-1}\mathfrak{S}t\,|\mathbf{A}_0|^2\omega^2 \times \cos\theta$, where $\mathfrak{S}$ is the area of the surface and t is time), which is reflected into the range of angles of $d\Omega'$ and frequencies $d\omega'$.*

Rather than solve this problem, it is simpler to find the probability of a transition of our system with absorption of a quantum ω'. In accordance with the principle of detailed balancing,[2] if the quantity

$$dW = B^+(\omega', \Omega')V\omega'^2 d\omega' d\Omega' / (2\pi)^3$$

represents the desired probability for the transition of the system (with V the normalization volume), then the probability for absorption of the quantum is $B^-(\omega', \Omega') = B^+(\omega', \Omega')$. The energy of the emitted quantum must not exceed the excitation energy of the system; i.e., in the present case, $\omega - \omega' > 0$.

Normalizing the amplitude of the secondary field outside the metal with the aid of the relation $(2\pi)^{-1}|\mathbf{A}_0'|^2\omega'^2 V = \omega'$, we obtain

---

*Here and in what follows $\hbar = c = 1$.

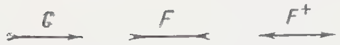

FIG. 1

$$d\sigma = \frac{\omega' dW}{(1/2\pi)\mathfrak{S}t\mathbf{A}_0^2\omega^2\cos\theta} = \frac{(2\pi)^2\,[B^-(\omega',\Omega')/\mathfrak{S}t]}{|\mathbf{A}_0|^2\,|\mathbf{A}_0'|^2\cos\theta\,\omega^2}\;\frac{\omega'^2 d\Omega' d\omega'}{(2\pi)^3}. \tag{1}$$

In the quantum field theory technique the quantity $B^-(\omega', \Omega')$ can be determined from the relation

$$B^-(\omega'\Omega') = \sum_j |S_{j0}|^2,$$

where S_{j0} is the scattering matrix element corresponding to a transition from the ground state to the state j, and the summation proceeds over all possible states attainable by absorption of a quantum. The problem is thus reduced to the calculation of the elements of the S-matrix for electrons in an external field $\mathbf{A}_2 + \mathbf{A}_2'$, bilinear relative to $\mathbf{A}_2$ and $\mathbf{A}_2'$.

In order to find the relation between $\mathbf{A}_2$ and $\mathbf{A}_2'$ and the corresponding fields outside the metal, one can make use of expressions obtained from the theory of the normal skin effect in a normal metal, since in accordance with our assumption the frequency of the light lies in the optical region. (Since $\omega \gg \Delta$, the distinction between normal and superconducting metals is not significant here, while in the optical frequency range the skin-effect in a normal metal is normal.)

2. We shall find the elements of the S-matrix in which we are interested by using a quantum field-theoretical technique developed for application to superconductors by Gor'kov.[3] The quantity Δ entering into the equations for the functions G and F clearly depends on the external field. To take proper account of the corresponding effects it will be more convenient for us not to write down the equations for the functions G and F, but rather to investigate the various Feynman diagrams for normal electrons having the interaction Hamiltonian:

$$\begin{aligned} H_i = {} & ie/m)\,[\mathbf{A}_2(x) + \mathbf{A}_2'(x)]\,(\nabla_x - \nabla_{x'})\,\psi^+(x')\,\psi(x)\,|_{x'\to x} \\ & + (e^2/m)\,\mathbf{A}_2(x)\,\mathbf{A}_2'(x)\,\psi^+(x)\,\psi(x) \\ & + \tfrac{1}{2}g\psi^+(x)\,(\psi^+(x)\,\psi(x))\,\psi(x), \end{aligned}$$

i.e., incorporating the four-fermion interaction that leads to superconductivity.

We shall introduce, as was also done in the paper by Abrikosov and Gor'kov,[4] graphical representations for the functions G, F^+ and F (Fig. 1). As stated above, we are interested in S matrices bilinear in $\mathbf{A}_2$ and $\mathbf{A}_2'$. The simplest Feynman diagrams are represented in Fig. 2. The effect of the magnetic field upon Δ is manifested in the fact that along with the simple diagrams of Fig. 2 there appear the more complex diagrams represented in Fig. 3.

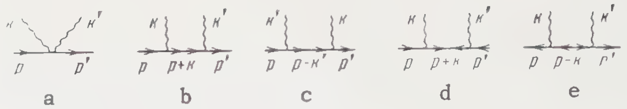

FIG. 2

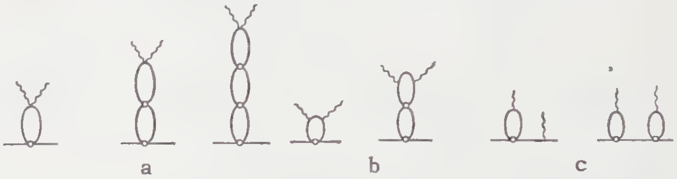

FIG. 3

Let us evaluate all diagrams of the types set forth. We shall demonstrate first that of all the diagrams in Fig. 2, only the diagram 2a is effective. The small contribution of diagrams of the types 2d and 2e follows directly from the form of the function F(p):[3]

$$F(p) = i\Delta/(\varepsilon^2 - \xi^2 - \Delta^2 + i\delta).$$

Since the frequency of the light $\omega \gg \Delta$, we have $F(p+k) \sim \Delta/\omega^2$. Taking into account the fact that each peak with a single potential is proportional to

$$(e/m)\,\mathbf{pA} \sim (e/m)\,p_0 A,$$

it is not difficult to see that the ratio of these diagrams to the diagram 2a is of the order of $\Delta p_0^2/\omega^2 m \ll 1$.

It is possible in similar fashion to demonstrate that the summed contribution of the diagrams in Figs. 2b and 2c is also small. Actually, when summed these diagrams are proportional to

$$G(p+k) + G(p-k) \approx 1/\omega - 1/\omega'.$$

In what follows we shall be interested principally in frequency changes of order Δ, and, in any case, small by comparison with the fundamental frequency. In view of this, the summed contribution of b and c has the relative order of magnitude $(\omega - \omega')/\omega \ll 1$.

For the same reason, diagrams of the type 3b are small by comparison with diagrams 3a. Diagrams 3c can be eliminated if a transverse gauge is chosen for both fields; i.e., $\mathbf{k}\cdot\mathbf{A}_2 = \mathbf{k}'\cdot\mathbf{A}_2' = 0$. This develops quite analogously to what occurs in the derivation of the equations for the electrodynamics of superconductors, since the transverse gauge of the vector potential makes it possible to omit consideration of the variation of Δ with the field. Let us, indeed, consider a loop with a single electromagnetic vertex. This is proportional to

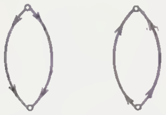

FIG. 4

$\int G(p)\,G(p+k)\,(p\cdot\mathbf{A})\,d^4p$, or to a similar expression containing F functions instead of G's. From symmetry considerations it is clear that this integral will be proportional to $\mathbf{k}\cdot\mathbf{A} = 0$.

Let us now investigate in more detail diagrams of the type 3a. Each of these diagrams will be large only for the case in which the order of the small constant g will be compensated for by a large value for the integrals arising from the loop. It is not difficult to see that the largest integral will be that having two parallel G lines (Fig. 4), which will be of order $\ln(\omega_D/\eta)$, where $\eta = \max(\omega - \omega', \Delta, v|\mathbf{k} - \mathbf{k}'|)$, and ω_D is the Debye frequency. In view of the fact that $g \ln(\omega_D/\Delta) \sim 1$, it is clear that all of the diagrams in Fig. 3a will be equally effective.

At this point, however, it is necessary to make a reservation. In each of the diagrams 3a there must be at least one loop which does not yield a logarithmic integral. This is the loop with the electromagnetic vertex. In view of the fact that at this vertex the electron arrows must be directed to one side (the combination $\psi^+\psi$ enters into the Hamiltonian), the corresponding loop cannot have the same form as in Fig. 4. More precise analysis shows that diagrams of the type 3a are significant only in the most immediate vicinity of the "threshold" value $\omega - \omega' = 2\Delta$ (cf. below); over the whole range $\omega - \omega' - 2\Delta \gtrsim \Delta$, they may be neglected. Below, we shall consider this particular case. Changes which arise in the neighborhood of the threshold point will be indicated in the discussion of the final result.

3. We are thus left with only one diagram illustrated in Fig. 3a. The corresponding element of the S matrix has the form

$$S_{j0} = -i\int \langle j|(e^2/m)(\mathbf{A}_2(x)\,\mathbf{A}_2'(x))\,\overset{+}{\psi}_\alpha(x)\,\psi_\alpha(x)|0\rangle\, d^4x.$$

Inasmuch as we are not interested in the final state of the electronic system, we shall find the summed probability for all probable processes (for the given fields), which is proportional to

$$\sum_j |S_{j0}|^2 = \frac{e^4}{m^2}\int (\mathbf{A}_2^*(x')\,\mathbf{A}_2'(x'))(\mathbf{A}_2(x)\,\mathbf{A}_2'(x)) \times \langle \overset{+}{\psi}_\alpha(x')\,\psi_\alpha(x')\,\overset{+}{\psi}_\beta(x)\,\psi_\beta(x)\rangle\, d^4x\,d^4x'. \qquad (2)$$

The mean over the ground state of the four ψ operators, which enters into Eq. (2), may be reduced to the sum of the products of pairs of ψ operators:

$$\langle \overset{+}{\psi}_\alpha(x')\,\psi_\alpha(x')\,\overset{+}{\psi}_\beta(x)\,\psi_\beta(x)\rangle = \langle \overset{+}{\psi}_\alpha(x')\,\psi_\beta(x)\rangle\langle \psi_\alpha(x')\,\overset{+}{\psi}_\beta(x)\rangle - \langle \overset{+}{\psi}_\alpha(x')\,\overset{+}{\psi}_\beta(x)\rangle\langle \psi_\alpha(x')\,\psi_\beta(x)\rangle$$

(means of the type $\langle \overset{+}{\psi}_\alpha(x')\,\psi_\alpha(x')\rangle = N$ can be neglected, since they do not depend upon the coordinate, and yield zeros when substituted into (2).

The expressions entering here may be found by the same method as the functions G and F in Gor'kov's theory.[3] For an infinite superconductor we find

$$\begin{aligned}
\langle \overset{+}{\psi}_\alpha(x')\,\psi_\beta(x)\rangle &= \delta_{\alpha\beta}\int v_p^2\,\delta(\varepsilon + \varepsilon_p)\,e^{ip(x-x')}\,\frac{d^4p}{(2\pi)^3},\\
\langle \psi_\alpha(x')\,\overset{+}{\psi}_\beta(x)\rangle &= \delta_{\alpha\beta}\int u_p^2\,\delta(\varepsilon - \varepsilon_p)\,e^{ip(x'-x)}\,\frac{d^4p}{(2\pi)^3},\\
\langle \psi_\alpha(x')\,\psi_\beta(x)\rangle &= -I_{\alpha\beta}\int u_p v_p\,\delta(\varepsilon - \varepsilon_p)\,e^{ip(x'-x)}\,\frac{d^4p}{(2\pi)^3},\\
\langle \overset{+}{\psi}_\alpha(x')\,\overset{+}{\psi}_\beta(x)\rangle &= I_{\alpha\beta}\int u_p v_p\,\delta(\varepsilon + \varepsilon_p)\,e^{ip(x-x')}\,\frac{d^4p}{(2\pi)^3}.
\end{aligned} \qquad (3)$$

Here

$$p = (\varepsilon, \mathbf{p}), \qquad \varepsilon_p = \sqrt{\xi_p^2 + \Delta^2}, \qquad \xi_p = v(|\mathbf{p}| - p_0),$$

$$u_p^2 = \tfrac{1}{2}(1 + \xi_p/\varepsilon_p), \quad v_p^2 = \tfrac{1}{2}(1 - \xi_p/\varepsilon_p);$$

$I_{\alpha\beta}$ is a unitary antisymmetric two-row matrix.

In the present case we are dealing with a superconducting half-space. For this the expressions for the means of the operator pairs differ from the corresponding functions for an infinite space.* At the surface, the correlation functions must satisfy the appropriate boundary conditions. We shall limit ourselves here to the case of specular reflection of the electrons from the boundary. In this case the correlation functions fall to zero for $z = 0$ or $z' = 0$.

In place of the functions (3), it is sufficient in this case to take the differences $\Phi(z - z') - \Phi(z + z')$, which satisfy the same equations as the functions (3), as well as the necessary boundary conditions. Upon substitution into (2) we find that, with an accuracy up to insignificant corrections of order a/λ, where a is the inter-atomic distance and λ is the wavelength of the light, the problem reduces to that for an infinite superconductor. For this, the potentials $\mathbf{A}_2$, $\mathbf{A}_2'$ must be extended symmetrically into the region $z < 0$, while the factor $\frac{1}{2}$ appears before the integral in (2).

Substituting the expressions (3) into the integral in (2) we obtain

---

*Strictly speaking, this applies also to the evaluations of the various diagrams carried out above; it can, however, be shown that all results remain correct in the presence of a surface.

$$\sum_i |S_{j0}|^2 = \frac{e^4}{2m^2}\int (\mathbf{A}_2^*(x')\,\mathbf{A}^{*'}_2(x'))\,(\mathbf{A}_2(x)\,\mathbf{A}_2'(x))\,e^{i(p-p')(x-x')}$$

$$\times \frac{1}{2}\left(1 - \frac{\xi_p\xi_{p'}}{\varepsilon_p\varepsilon_{p'}} + \frac{\Delta^2}{\varepsilon_p\varepsilon_{p'}}\right)\delta(\varepsilon+\varepsilon_p)\,\delta(\varepsilon'-\varepsilon_{p'})\frac{d^4p}{(2\pi)^3}$$

$$\times \frac{d^4p'}{(2\pi)^3}\,d^4x\,d^4x' = \frac{e^4}{2m^2}\,t\mathfrak{S}\int R(q_z)\,f(\mathbf{q})\,dq_z, \tag{4}$$

where t represents time; the functions $f(\mathbf{q})$ and $R(q_z)$ have the form

$$f(\mathbf{q}) = \frac{1}{2}\int\frac{d^3\mathbf{p}}{(2\pi)^3}\,\delta(q_0-\varepsilon_p-\varepsilon_{p+q})\left(1-\frac{\xi_p\xi_{p+q}}{\varepsilon_p\varepsilon_{p+q}}+\frac{\Delta^2}{\varepsilon_p\varepsilon_{p+q}}\right), \tag{5}$$

$$R(q_z) = |[\mathbf{A}_2\mathbf{A}_2'(q_z)]|^2 \tag{6}$$

The symbol $[\mathbf{A}_2\mathbf{A}_2'(q_z)]$ represents the Fourier component of the product $\mathbf{A}_2(x)\cdot\mathbf{A}_2'(x$,; i.e.,

$$\mathrm{A}_2(x)\,\mathrm{A}_2'(x) = \int [\mathbf{A}_2\mathbf{A}_2'(q_z)]\,e^{iqx}\,dq_z/2\pi.$$

The projections of the vector $\mathbf{q}$, with the exception of q_z, are equal to the corresponding differences in momentum and frequency between the incident and reflected quanta: $q_x = k_{0x} - k_{0x}'$, $q_y = k_{0y} - k_{0y}'$, $q_0 = \omega - \omega'$.

4. Let us compute first the function $f(\mathbf{q})$. In view of the fact that $\epsilon_p > 2\Delta$, the integral in (5) is different from zero only for $q_0 > 2\Delta$. This was to be expected, for $q_0 = \omega - \omega'$ is the energy transferred to the electronic system, which cannot be less than 2Δ. The integral (5) is fundamentally dependent upon the relation between $v|\mathbf{q}|$ and q_0. For the case $v|\mathbf{q}| \gg q_0$ the integral over $d^3p = (2\pi p_0^2/v)\,d\xi\,d\cos\theta$ may be replaced by

$$\frac{2\pi p_0^2}{v^2|\mathbf{q}|}\int_{-\infty}^{\infty}d\xi\int_{-\infty}^{\infty}d\xi' \qquad (\xi = \xi(q),\ \xi' = \xi(p+q)).$$

Terms in $\xi\xi'$ in the expression under the integral sign vanish. After this we proceed to integration over $d\epsilon$ and $d\epsilon'$.

As a result of all these simple operations we obtain

$$f(\mathbf{q}) = \frac{p_0^2}{\pi^2v^2|\mathbf{q}|}\left[\left(\frac{q_0}{2}+\Delta\right)\mathrm{E}\left(\frac{q_0-2\Delta}{q_0+2\Delta}\right)\right.$$

$$\left. - \frac{q_0\Delta}{q_0/2+\Delta}\,\mathrm{K}\left(\frac{q_0-2\Delta}{q_0+2\Delta}\right)\right], \tag{7}$$

where E and K are complete elliptic integrals.

In accordance with (4) and (6), the function $f(\mathbf{q})$ is unique and depends on Δ. At the transition to the normal metal, therefore, only this function changes. As $\Delta \to 0$ we find

$$f_n(\mathbf{q}) = p_0^2q_0/2\pi^2v^2|\mathbf{q}|. \tag{8}$$

In what follows we shall see that the presence of the factor $1/|\mathbf{q}|$ in $f(\mathbf{q})$ leads to the appearance of a large logarithmic integral over q_z. If $q_0 - 2\Delta \gtrsim \Delta$, then in the region $v|\mathbf{q}| \ll q_0$ the integral (5) does not depend upon $|\mathbf{q}|$. Therefore, the region $v|\mathbf{q}| \gg q_0$ is the principal region of integration over q_z.

In the close vicinity of $q_0 = 2\Delta$ a special situation arises. Analysis of Eq. (5) shows that the range of values of $v|\mathbf{p}|$ for which the integral in (5) is proportional to $1/|\mathbf{q}|$ is determined by the inequality $v|\mathbf{q}| \geq \sqrt{q_0^2 - 4\Delta^2}$. At the same time, however, as has already been mentioned above, all the diagrams 3a assume significance in the vicinity of $q_0 = 2\Delta$.

Analysis of these diagrams, which, is too cumbersome to carry our here, shows that the lower limit of the logarithmic integration over q_z never falls below Δ, while in the immediate vicinity of $q_0 = 2\Delta$ this limit increases; this leads in the end to the elimination of the logarithmic integral, and then to the reduction of the whole effect to zero. In view of all that has been said, we can right up to the extremely close vicinity of the point $q_0 = 2\Delta$, make use of formula (7), and consider $v|\mathbf{q}| \gg q_0$.

5. Let us now go on to the calculation of the function $R(q_2)$. If we take yz as the plane of incidence, and if the field outside the metal is

$$\mathrm{A}(z, y) = \mathrm{A}_0\exp(ik_{0z}z + ik_{0y}y - i\omega t) + \text{compl. conj.},$$

where $k_{0z} = \omega\cos\theta$, and $k_{0y} = \omega\sin\theta$, with θ the angle of incidence, then within the metal the field will have the form

$$\mathrm{A}_2(z, y) = \mathrm{A}_2\exp(ik_{2z}z + ik_{2y}y - i\omega t) + \text{compl. conj.},$$

where $k_{2y} = k_{0y}$, and $k_{2z} = \omega\sqrt{\epsilon - \sin^2\theta}$ (ϵ is the complex dielectric constant), while that value of the radical is chosen for which $\operatorname{Im} k_{2z} > 0$. From Maxwell's equations and the boundary conditions at the surface it is possible to express $\mathbf{A}_2$ in terms of $\mathbf{A}_0$. It is necessary here to take account of the already-adopted condition $\mathbf{k}_2\cdot\mathbf{A}_2 = 0$.

a) If the incident wave is so polarized that the electric field is directed along the x axis, then the field will have the same orientation within the metal as well. In this case, the potentials are directed along the x axis, and the relation

$$A_{2x} = \frac{2\cos\theta}{\sqrt{\varepsilon-\sin^2\theta}+\cos\theta}\,A_{0(x)} \tag{9a}$$

holds.

b) If in the incident wave the magnetic field is directed along the x axis, then the vector potentials $\mathbf{A}_0$ and $\mathbf{A}_2$ lie in the yz plane, and

$$A_{2z} = \frac{2\sin\theta\cos\theta}{\varepsilon\cos\theta+\sqrt{\varepsilon-\sin^2\theta}}\,A_{0(yz)},$$

$$A_{2y} = -\frac{2\cos\theta\sqrt{\varepsilon-\sin^2\theta}}{\varepsilon\cos\theta+\sqrt{\varepsilon-\sin^2\theta}}\,A_{0(yz)}. \tag{9b}$$

The index (yz) indicates that the vector $\mathbf{A}_0$ lies in the yz plane. The same formulas connect $\mathbf{A}'_2$ with $\mathbf{A}'_0$.

In what follows, we shall investigate those angles θ (and θ') for which the condition $|\epsilon| \gg \sin^2\theta$ is fulfilled. In this event the expressions simplify; in particular, in case b) one may neglect A_{2z} by comparison with A_{2y}.

The Fourier component of the product of the vector potentials for the specular case $[\mathbf{A}_2(z) = \mathbf{A}_2(-z)]$ is

$$[\mathrm{A}_2\mathrm{A}'_2(q_z)] = \int\limits_{-\infty}^{\infty} \mathrm{A}_2(z)\,\mathrm{A}'_2(z)\,e^{-q_z z}\,dz$$

$$= (\mathbf{A}_2\mathbf{A}'^{*}_2)\,\frac{2i\,(k_{2z} - k'^{*}_{2z})}{(k_{2z} - k'^{*}_{2z})^2 - q_z^2}\,.$$

We note that in carrying out the integration we shall select only those components of $\mathbf{A}_2(x)$ and $\mathbf{A}'_2(x)$ whose products have a time dependence $\exp\{-i(\omega - \omega')t\}$ (the remaining terms are of no interest, in view of the presence of the δ function in (5) and the condition $\omega - \omega' > 0$). The difference $k_{2z} - k'^{*}_{2z}$ appearing in this expression is equal to $2i\omega\kappa$, $\kappa = \mathrm{Im}\sqrt{\epsilon}$, as a consequence of the inequalities $\sin^2\theta$, $\sin^2\theta' \ll |\epsilon|$.

Substituting all of the terms of the function $R(q_z)$ and carrying out a summation over the polarizations of the scattered, and averaging over those of the incident, light, we obtain

$$R(q_z) = 8\,|\mathbf{A}_0|^2\,|\mathbf{A}'_0|^2\cos^2\theta\cos^2\theta'$$

$$\times\left\{\frac{\cos^2\varphi}{[(n+\cos\theta)^2+\varkappa^2]\,[(n+\cos\theta')^2+\varkappa^2]}\right.$$

$$+\frac{\sin^2\varphi}{[(n\cos\theta+1)^2+\varkappa^2\cos^2\theta]\,[(n+\cos\theta')^2+\varkappa^2]}$$

$$+\frac{\sin^2\varphi}{[(n+\cos\theta)^2+\varkappa^2]\,[(n\cos\theta'+1)^2+\varkappa^2\cos^2\theta']}$$

$$\left.+\frac{\cos^2\varphi}{[(n\cos\theta+1)^2+\varkappa^2\cos^2\theta]\,[(n\cos\theta'+1)^2+\varkappa^2\cos^2\theta']}\right\}$$

$$\times\frac{16\,\varkappa^2\omega^2}{(q_z^2+4\varkappa^2\omega^2)^2}\,. \qquad (10)$$

Here we have used the symbols: $\sqrt{\epsilon} = n + i\kappa$, and φ, the angle between the planes of incidence and reflection. Thus, the function $R(q_z)$ is equal to a constant for $q_z \ll 2\kappa\omega$, and falls off rapidly for $q_z \gg 2\kappa\omega$.

6. Let us now substitute (7) and (10) into (4). Taking $2\kappa\omega \gg q_0/v$, we arrive at the conclusion that the principal contribution to $\sum\limits_j |S_{j0}|^2$ is provided by the logarithmic integral over q_z, in the region delimited by the inequalities $|\mathbf{q}| \gg q_0/v$ and $|q_z| \ll 2\kappa\omega$. In view of the fact that $|q_y| < \omega - \omega' \ll q_0/v$ we may, with logarithmic accuracy, write the result of the integration over q_z in the form

$$\int dq_z/|\mathbf{q}| = 2\ln(2\varkappa\omega v/q_0)$$

(the coefficient 2 results from integration over negative and positive q_z).

Substituting (7), (10), and (4) into (1), with attention to the fact that $\omega - \omega' \ll \omega$, we obtain the final expression for $d\sigma$ for the case $\omega - \omega' > 2\Delta$:

$$d\sigma = \frac{2e^4}{\pi^3}\,\frac{\cos\theta\cos^2\theta'}{\varkappa^2\omega^2}\Big\{[(1+\cos^2\theta)(n^2+\varkappa^2+1)+4n\cos\theta]$$

$$\times[(1+\cos^2\theta')(n^2+\varkappa^2+1)+4n\cos\theta']$$

$$+\sin^2\theta\sin^2\theta'\cos 2\varphi\,(n^2+\varkappa^2-1)^2\Big\}$$

$$\times\{[(n\cos\theta+1)^2+\varkappa^2\cos^2\theta]\,[(n\cos\theta'+1)^2$$

$$+\varkappa^2\cos^2\theta']\,[(n+\cos\theta)^2+\varkappa^2]$$

$$\times[(n+\cos\theta')^2+\varkappa^2]\}^{-1}\left[\left(\frac{\omega-\omega'}{2}+\Delta\right)\mathrm{E}\left(\frac{\omega-\omega'-2\Delta}{\omega-\omega'+2\Delta}\right)\right.$$

$$\left.-\frac{2(\omega-\omega')\,\Delta}{\omega-\omega'+2\Delta}\,\mathrm{K}\left(\frac{\omega-\omega'-2\Delta}{\omega-\omega'+2\Delta}\right)\right]\ln\frac{2\varkappa\omega v}{\omega-\omega'}\,d\omega'd\Omega. \qquad (11)$$

The expression for $d\sigma$ for a normal metal is obtained by substituting $(\omega - \omega')/2$ for the square brackets containing the elliptic integrals E and K.

We note that the ratio of $d\sigma$ to $d\sigma_n$, for the same metal in the normal state, is a universal function of the ratio $(\omega - \omega')/2\Delta$, specifically:

$$(d\sigma - d\sigma_n)/d\sigma_n = \varphi((\omega-\omega')/2\Delta),$$

$$\varphi(x) = \left(1+\frac{1}{x}\right)\mathrm{E}\left(\frac{x-1}{x+1}\right) - \frac{2}{x+1}\,\mathrm{K}\left(\frac{x-1}{x+1}\right) - 1. \qquad (12)$$

A graph of the function $\varphi(x)$ is presented in Fig. 5. It is evident from this fugure that only in the region $\omega - \omega' < 4\Delta$ is there an intrinsic difference between the normal and superconducting metal.

The formula obtained is formally applicable over the whole range of frequencies for which $\ln(\kappa\omega v/|\omega - \omega'|)$ is sufficiently large; i.e., for $\omega - \omega' \ll \kappa\omega v/c$ (in the usual units). In reality, however, it is necessary to consider that treatment of the electrons as free is valid only for energies $\epsilon \ll \omega_D$ (ω_D is the Debye frequency). For $\epsilon \sim \omega_D$ there arises a strong attenuation of the electronic excitations, due to emission of phonons. This imposes the limitation $\omega - \omega' \ll \omega_D$, which more or less coincides with the preceding in the optical region. On the low-frequency side, as has already been stated, Eq. (11) becomes invalid in the region $\omega - \omega' - 2\Delta \ll \Delta$. While this formula yields a finite

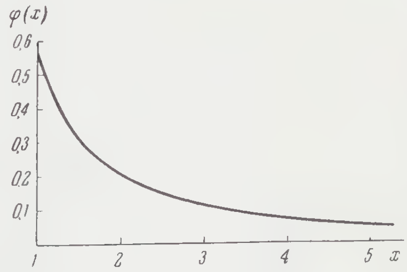

FIG. 5

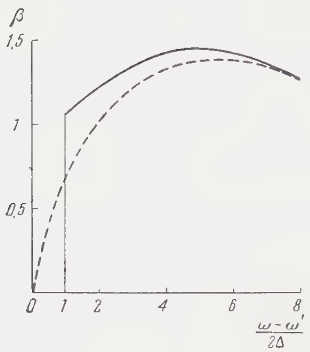

FIG. 6

value at $\omega = 2\Delta$, correct consideration of the graphs 3a gives at this point $d\sigma = 0$. In view of its narrow width, however, this region is not of great interest. For the case of a normal metal the applicability of the derived formula is limited only in the direction of large values of $\omega - \omega'$.

The absolute magnitude of the effect depends to a large degree upon the quantities κ and n. The data available on κ and n for certain metals[5] at $\lambda = 5800$ A and T = 300° K is presented below:

	V	Nb	Ta	Sn	Pb
n	3.03	1.80	2.05	1.48	2.01
$\varkappa$	3.51	2.11	2.31	5.25	3.48

At low temperatures κ changes little, while n decreases slightly. For Nb at $\lambda \approx 5800$ A ($\omega = 3.2 \times 10^{15}$ sec^{-1}), and $\theta = \theta' = 0$:

$$d\sigma = 0{,}6\cdot 10^{-12}\beta\, d\Omega\, d\omega'/2\Delta. \qquad (13)$$

The quantity β in (13) is of order unity; its dependence upon $(\omega - \omega')/2\Delta$ is illustrated in Fig. 6. The dashed line represents this same quantity for the normal state.

It follows from evaluation of (13) that for detection of the effect the sensitivity must be at least 10^5 times as high as in the experiment of Khaĭkin and Bykov.[1]

In conclusion, the authors express their gratitude to Academician L. D. Landau and to M. S. Khaĭkin for their consideration of the results of this work.

---

[1] M. S. Khaĭkin and V. P. Bykov, JETP **30**, 191 (1956), Soviet Phys. JETP **3**, 119 (1956).

[2] L. D. Landau and E. M. Lifshitz, Квантовая механика (Quantum Mechanics), Gostekhizdat, 1948; p. 451.

[3] L. P. Gor'kov, JETP **34**, 735 (1958), Soviet Phys. JETP **34**, 505 (1958).

[4] A. A. Abrikosov and L. P. Gor'kov, JETP **35**, 1558 (1959), Soviet Phys. JETP **35**, 1090 (1959).

[5] Smithsonian Physical Tables, 1954.

Translated by S. D. Elliott
40

SOVIET PHYSICS JETP VOLUME 13, NUMBER 1 JULY, 1961

CONCERNING DISTURBANCES PRODUCED BY A BODY MOVING IN A PLASMA

L. P. PITAYEVSKII and V. Z. KRESIN

Institute of Terrestrial Magnetism, Ionosphere, and Radio Wave Propagation, U.S.S.R.
Academy of Sciences

Submitted to JETP editor July 27, 1960

J. Exptl. Theoret. Phys. (U.S.S.R.) **40**, 271-281 (January, 1961)

An expression is derived for the Fourier components n_q of the disturbance to the electron density, produced by a body moving in a plasma, in the limit as the wave vector $q \rightarrow 0$. It is shown, in particular, that the exact expression for n_q contains terms proportional to $1/q$, which are absent in the first approximation of perturbation theory. The formulas are employed to calculate in various particular cases the effective cross section for scattering of electromagnetic waves of wave lengths considerably in excess of the characteristic dimension of the body.

1. FORMULATION OF THE PROBLEM

In this paper we report on a theoretical investigation of the scattering of electromagnetic waves by a trail left by a moving body in an isotropic electron-ion plasma. This problem has become quite timely of late.[1-3]

We assume that the plasma is sufficiently rarefied, i.e., that the ion mean free path in the plasma is much greater than either the dimensions of the body or the length of the scattered electromagnetic wave:

$$l \gg \lambda, \ R_0. \tag{1}$$

The scattering of an electromagnetic wave by a body moving in a plasma consists of scattering on the body proper, for example a metal sphere, and scattering on the trail produced by the body, i.e., the region of perturbed electron concentration produced by the motion of the body. The scattering by the body itself is described by the usual formulas of diffraction theory and will not be calculated here. We note at once that since the dielectric constant of the trail is low, the scattering from the metallic body itself will be much greater than from a trail region of the same size. It is therefore clear that the trail can make a scattering contribution comensurate with the contribution of the body itself only if trail regions larger than the body participate in the scattering. In the scattering by structures that diminish slowly with distance, such as trails usually are, the regions effectively participating in the scattering have normally dimensions on the order of the wavelength (the contribution from greater distances is strongly reduced by the interference between waves scattered by the different parts of the trail). It is therefore clear beforehand that the trail can make a noticeable contribution to the scattering only at wavelengths much greater than the characteristic dimension of the body R_0:

$$\lambda \gg R_0. \tag{2}$$

We shall confine ourselves to this case throughout.

Since the body produces at large distances away from it only small changes in the dielectric constant (compared with unity), it is natural to employ perturbation theory for the calculation of the scattering. (The validity of the theory will be discussed later on.) Recognizing that the variation of the dielectric constant of the plasma is connected with the perturbation of the electron density δn by the formula

$$\delta\varepsilon(\mathbf{r}) = -\frac{4\pi e^2}{m\omega^2}\delta n(\mathbf{r})$$

(e and m are the electron charge and mass) we obtain by the well-known perturbation theory formula the amplitude of the scattered wave at distances large compared with the wavelength:

$$\mathbf{E}' = \frac{e^2}{m\omega^2\varepsilon}\frac{e^{ikR}}{R} n_{\mathbf{q}} [\mathbf{k}' [\mathbf{k}'\mathbf{E}_0]]. \tag{3}^*$$

Here $\mathbf{E}_0$ is the amplitude of the incident wave, $\mathbf{k}'$ is the wave vector of the scattered wave ($|\mathbf{k}'| = k = \sqrt{\epsilon}\,\omega/c$), ϵ is the dielectric constant of the plasma, and n_q is the Fourier component of the electron-density perturbation:

$$n_{\mathbf{q}} = \int \delta n(\mathbf{r}) e^{-i\mathbf{q}\mathbf{r}} d^3r, \quad \mathbf{q} = \mathbf{k}' - \mathbf{k}, \ |\mathbf{q}| = 2k \sin\frac{\psi}{2} \tag{4}$$

$^*\mathbf{k}'[\mathbf{k}'\mathbf{E}_0] = \mathbf{k}' \times (\mathbf{k}' \times \mathbf{E}_0)$.

($\mathbf{k}$ is the wave vector of the incident wave and ψ is the scattering angle, i.e., the angle between $\mathbf{k}$ and $\mathbf{k}'$). The effective cross section of scattering in a solid-angle element do is given by

$$d\sigma = \frac{1}{16\pi^2\varepsilon^2}\left(\frac{\omega_0}{\omega}\right)^4 \frac{|n_{\mathbf{q}}|^2}{n_0^2} k^4 \sin^2\psi_1 do \tag{5}$$

(ψ_1 is the angle between $\mathbf{k}'$ and $\mathbf{E}_0$, $\omega_0^2 = 4\pi n_0 e^2/m$, and n_0 is the unperturbed electron density). For comparison we give here the formula for the effective cross section of scattering by a metal sphere of radius R_0 for $\lambda \gg R_0$:

$$d\sigma_m = \left(\frac{\omega}{c}\right)^4 \frac{\sigma_0^3}{\pi^3} \sin^2\psi_1 do \qquad (\sigma_0 = \pi R_0^2). \tag{6}$$

As can be seen from (5), the problem of calculating the effective electromagnetic-wave scattering cross section reduces to the calculation of the Fourier components of the variation of the electron density. The perturbations produced in a plasma by a rapidly moving body of dimensions greater than the Debye radius were considered in detail by A. V. Gurevich.[2] To calculate $n_{\mathbf{q}}$ for this case we could therefore, in principle, use Gurevich's results. It turns out, however, that it is simpler to determine $n_{\mathbf{q}}$ directly from the kinetic equation. This yields a more rigorous solution for the problem, for it permits evaluation of certain effects not considered in reference 2, which become significant when $\mathbf{q}$ is small.

2. DERIVATION OF THE GENERAL FORMULA

We consider in the present paper only the case when the velocity V_0 of the body is much less than the thermal velocity of the electrons:

$$V_0 \ll \sqrt{kT/m}. \tag{7}$$

Under these conditions the electron density is directly connected with the electric potential φ by means of the Boltzmann distribution function

$$n = n_0 e^{e\varphi/kT}. \tag{8}$$

On the other hand, the distribution of the ions should be determined simultaneously with the potential. We shall solve this problem with the aid of the kinetic equation for the ion velocity and coordinate distribution function. Inasmuch as the distribution function is independent of the time in a frame fixed in the body, the equation in this frame has the form

$$\frac{\partial f}{\partial \mathbf{r}}\mathbf{v} - \frac{\partial f}{\partial \mathbf{v}}\frac{1}{M}\frac{\partial}{\partial \mathbf{r}}(e\varphi + U) = 0. \tag{9}$$

[By virtue of condition (1) we can neglect collisions between particles.] Here M is the ion mass, $\mathbf{v}$ the ion velocity in the frame in which the body is at rest, and U the energy of interaction between the ions and the surface of the body. Introducing the ion velocity in the system at rest

$$\mathbf{u} = \mathbf{v} + \mathbf{V}_0,$$

we can rewrite (9) as

$$\frac{\partial f}{\partial \mathbf{r}}(\mathbf{u} - \mathbf{V}_0) - \frac{1}{M}\frac{\partial f}{\partial \mathbf{u}}\frac{\partial}{\partial \mathbf{r}}(U + e\varphi) = 0. \tag{10}$$

The electric potential φ satisfies, with allowance for (8), the equation

$$\Delta\varphi = -4\pi e\left(\int f d^3u - n\right) = -4\pi e\left(\int f d^3u - n_0 e^{e\varphi/kT}\right). \tag{11}$$

In Eq. (10) it is convenient to separate from f the coordinate-independent part f_0, which is equal to the distribution function at an infinite distance from the body:

$$f = f' + f_0, \qquad f_0 = n_0 (M/2\pi kT)^{3/2} \exp\{-Mu^2/2kT\}.$$

Substituting this in (10) we get

$$\frac{\partial f'}{\partial \mathbf{r}}(\mathbf{u} - \mathbf{V}_0) - \frac{1}{M}\frac{\partial f_0}{\partial \mathbf{u}}\frac{\partial}{\partial \mathbf{r}}(U + e\varphi) - \frac{1}{M}\frac{\partial f'}{\partial \mathbf{u}}\frac{\partial}{\partial \mathbf{r}}(U + e\varphi) = 0. \tag{12}$$

To solve the system (11) and (12) we change over to Fourier components in the coordinates. Equation (12) in Fourier components becomes

$$i\mathbf{q}(\mathbf{u} - \mathbf{V}_0) f'_{\mathbf{q}} - \frac{e}{M}\frac{\partial f_0}{\partial \mathbf{u}} i\mathbf{q}\varphi_{\mathbf{q}} - \frac{1}{(2\pi)^3 M}\int i\mathbf{q}_1 (U_{\mathbf{q}_1} + e\varphi_{\mathbf{q}_1}) \frac{\partial f'_{\mathbf{q}-\mathbf{q}_1}}{\partial u} d^3q_1 - i\frac{\mathbf{q}}{M}\frac{\partial f_0}{\partial \mathbf{u}} U_{\mathbf{q}} = 0. \tag{13}$$

We now recognize that we are interested only in long waves, i.e., in small values of q, and let $\mathbf{q}$ tend to 0. Since $U_{\mathbf{q}}$ certainly tends to a constant limit as q → 0, the last term in (13) can be discarded. (The first two terms must be retained, since, as will be shown later, $f'_{\mathbf{q}}$ and $\varphi_{\mathbf{q}}$ tend to infinity as q → 0.) In the third term we can also put $\mathbf{q} = 0$. For this purpose it is necessary that the integral in this term converge. But, as we shall see later, the quantities $f'_{\mathbf{q}}$ and $\varphi_{\mathbf{q}}$ are proportional to 1/q as q → 0, and consequently this integral converges. Finally we obtain as q → 0

$$i\mathbf{q}(\mathbf{u} - \mathbf{V}_0) f'_{\mathbf{q}} - \frac{e}{M}\frac{\partial f_0}{\partial \mathbf{u}} i\mathbf{q}\varphi_{\mathbf{q}} = I(\mathbf{u}), \tag{14}$$

$$I(\mathbf{u}) = \frac{1}{M}\int i\mathbf{q}(U_{\mathbf{q}} + e\varphi_{\mathbf{q}}) \frac{\partial f'_{-\mathbf{q}}}{\partial \mathbf{u}} \frac{d^3q}{(2\pi)^3} = \frac{1}{M}\int \frac{\partial f'}{\partial \mathbf{u}}\frac{\partial}{\partial \mathbf{r}}(U + e\varphi) d^3r. \tag{15}$$

Our problem is thus subdivided into two stages — calculation of the function I(u) for the given body and the solution of (14). We note that I(u) is proportional to the product of the potential by the correction to the distribution function, and consequently differs from zero only in the second perturbation-theory approximation in the potential. It is evident therefore that the results of Kraus and Watson,[3] who carried out the calculations in first approximation, are certainly incorrect at large distances.

We change now to Fourier components in (11). We note here that in the expansion of $n_k = n_0 (e^{e\varphi/kT} - 1)_{\mathbf{q}}$ in powers of $e\varphi/kT$,

$$n_{\mathbf{q}} = n_0 \left(\frac{e}{kT} \varphi_{\mathbf{q}} + \frac{e^2}{2k^2T^2} \int \varphi_{\mathbf{q}_1} \varphi_{\mathbf{q}-\mathbf{q}_1} \frac{d^3 q_1}{(2\pi)^3} + \ldots \right), \tag{16}$$

the first term varies as $1/q$, while the others tend to constants and can be neglected. Therefore

$$n_{\mathbf{q}} = n_0 e \varphi_{\mathbf{q}} / kT \tag{17}$$

and instead of (11) we have as $q \rightarrow 0$

$$\varkappa^2 \varphi_{\mathbf{q}} = 4\pi e \int f'_{\mathbf{q}} d^3 u, \tag{18}$$

where $\kappa = \sqrt{4\pi n_0 e^2/kT} = 1/\sqrt{2} R_D$, with R_D the Debye radius.

We note that for small $\mathbf{q}$ the system of inhomogeneous nonlinear equations (11) and (12) is reduced to a system of linear inhomogeneous equations (14) and (18). This result has a simple physical meaning: when $\mathbf{q}$ is small, the large distances from the body, at which the deviations of the distribution function from equilibrium are small, become significant. It follows from (14) and (18) that $f'_{\mathbf{q}}$ and $\varphi_{\mathbf{q}}$ are actually proportional to $1/q$, as pointed out earlier.

Let us divide both halves of (14) by $i\mathbf{q} \cdot (\mathbf{u} - \mathbf{V}_0)$ and integrate over d^3u. The integrals with singular denominators $i\mathbf{q} \cdot (\mathbf{u} - \mathbf{V}_0)$ should, according to Landau,[4] be taken with suitable circuits about the singularities. To take this into account, it is enough to replace $\mathbf{q} \cdot \mathbf{V}_0$ by $\mathbf{q} \cdot \mathbf{V}_0 + i\delta$, where $\delta \rightarrow +0$. As a result we obtain

$$\int f'_{\mathbf{q}} d^3 u - \frac{e}{M} \varphi_{\mathbf{q}} \int \frac{\partial f_0}{\partial \mathbf{u}} \frac{\mathbf{q}}{\mathbf{q}(\mathbf{u} - \mathbf{V}_0) - i\delta} d^3 u$$

$$= \frac{1}{i} \int \frac{I(\mathbf{u})}{\mathbf{q}(\mathbf{u} - \mathbf{V}_0) - i\delta} d^3 u. \tag{19}$$

Solving equations (18) and (19) simultaneously and using the fact that $\partial f_0 / \partial \mathbf{u} = -(\mathbf{u} M/kT) f_0$, we get

$$n_{\mathbf{q}} = \frac{\dfrac{1}{iq} \displaystyle\int \frac{I(\mathbf{u})}{\mathbf{n}(\mathbf{u} - \mathbf{V}_0) - i\delta} d^3 u}{\left[1 + \left(\dfrac{M}{2\pi kT} \right)^{3/2} \displaystyle\int \frac{\mathbf{n}\mathbf{u}}{\mathbf{n}(\mathbf{u} - \mathbf{V}_0) - i\delta} e^{-Mu^2/kT} d^3 u \right]}, \tag{20}$$

where $\mathbf{n} = \mathbf{q}/|\mathbf{q}|$. Writing the integral in the denominator of (20) in Cartesian coordinates with the x axis along $\mathbf{n}$, and using the well known identity

$$\int_{-\infty}^{\infty} \frac{e^{-y^2}}{y - a - i\delta} dy \; - 2\sqrt{\pi} \left[\frac{i\sqrt{\pi}}{2} - \int_0^a e^{x^2} dx \right] e^{-a^2}, \tag{21}$$

we obtain finally

$$n_{\mathbf{q}} = \frac{1}{iq} \int \frac{I(\mathbf{u})}{\mathbf{n}(\mathbf{u} - \mathbf{V}_0) - i\delta} d^3 u \Bigg/ \left[2 - 2a \left(\int_0^a e^{x^2} dx - i \frac{\sqrt{\pi}}{2} \right) e^{-a^2} \right],$$

$$a = \mathbf{n}\mathbf{V}_0 \sqrt{\frac{M}{2kT}}. \tag{22}$$

It follows directly from (22) that the electron density decreases as $1/r^2$ with increasing distance from the body, in agreement with the results of Gurevich.* We note that when $V_0 \gg kT/M$ the denominator of (22) has a rather pronounced angular dependence, namely, $a \gg 1$ when $\mathbf{n} \cdot \mathbf{V}_0 \sim V_0$, and the denominator is equal to zero in this case. At angles for which $\mathbf{n} \cdot \mathbf{V}_0 \sqrt{M/2kT} = a \ll 1$, the denominator is equal to 2. This result can be readily explained. The frequency of the field component with wave vector $\mathbf{q}$ is obviously equal to $\mathbf{q} \cdot \mathbf{V}_0$ in the coordinate system at rest. If $\mathbf{q} \cdot \mathbf{V}_0 \gg q v_T$, where $v_T \sim \sqrt{kT/M}$ is the thermal velocity of the ions, the ions do not have a chance to screen the potential. On the other hand, when $\mathbf{q} \cdot \mathbf{V}_0 \ll q v_T$, the ions screen the potential so that the Debye radius and the potential $\varphi_{\mathbf{q}}$ are each reduced to one half. We note also that the denominator of (22) coincides exactly with the expression for the dispersion of ionic plasma waves. Since, however, these waves are strongly damped, no special significance should be attached to this fact.

Let us proceed now to clarify the physical meaning of the quantity $I(\mathbf{u})$. For this purpose we turn in (14) to the coordinate space and assume that all the quantities depend (in the frame which is at rest) on the time only via the combination $\mathbf{r} - \mathbf{V}_0 t$, so that $\mathbf{V}_0 \partial f' / \partial \mathbf{r} = -\partial f' / \partial t$. We obtain

$$\frac{\partial f'}{\partial t} + \frac{\partial f'}{\partial \mathbf{r}} \mathbf{u} - \frac{e}{M} \frac{\partial f_0}{\partial \mathbf{u}} \frac{\partial \varphi}{\partial \mathbf{r}} = I(\mathbf{u}) \, \delta(\mathbf{r} - \mathbf{V}_0 t). \tag{23}$$

The left half of (23) is the total derivative of the distribution function with respect to time. From the physical meaning of the distribution function it is clear that $I(\mathbf{u}) d^3 u$ is the number of particles per unit time which acquire, by collision with the body, velocities that lie in the interval d^3u about $\mathbf{u}$. Thus $I(\mathbf{u})$ serves so to speak as a sort of a "collision interval" for the ions with the body.

This physical meaning of $I(\mathbf{u})$ enables us, by following the reasoning used to determine the form of the usual collision integral, to recast $I(\mathbf{u})$ in a different form, very useful for approximate calculations. Let us change again to the coordinate system of the body. Let a particle passing near the body with an impact parameter ρ and an azimuth angle φ acquire a velocity $\mathbf{v}$ after scattering (by interaction with the surface of the body and the electric field surrounding it). Then the initial velocity of the ion is $\mathbf{v}_1 = \mathbf{v}_1(\mathbf{v}, \rho, \varphi)$, where the function $\mathbf{v}_1(\mathbf{v}, \rho, \varphi)$ is determined by the scattering law, and the number of particles that acquire a velocity $\mathbf{v}$ in a unit of time is merely the number of incident particles with velocity $\mathbf{v}_1$, i.e.,

---

*The formulas obtained can also be used, naturally, to calculate the perturbed electron density, etc., at large distances from the moving body. In the present paper, however, we shall not consider the transition to coordinate space.

$$\rho d\rho\, d\varphi\, v n_0 (M / 2\pi kT)^{3/2} \exp\{- M [\mathbf{v}_1(\mathbf{v}, \rho, \varphi) + \mathbf{V}_0]^2 / 2kT\}. \tag{24}$$

We have assumed that the scattering is elastic ($|\mathbf{v}_1| = |\mathbf{v}|$) and that the incident particles have at infinity a Maxwellian distribution in the frame which is at rest. To find I is also necessary to subtract from (24) the number of particles with velocity $\mathbf{v}$, knocked out by collision with the body

$$\rho\, d\rho\, d\varphi\, v n_0 (M / 2\pi kT)^{3/2} \exp\{- M (\mathbf{v} + \mathbf{V}_0)^2 / 2kT\}.$$

Finally

$$I(\mathbf{v} + \mathbf{V}_0) = n_0 \left(\frac{M}{2\pi kT}\right)^{3/2} v \int \rho d\rho d\varphi \left[\exp\left\{-\frac{M[\mathbf{v}_1(\mathbf{v},\rho,\varphi)+\mathbf{V}_0]^2}{2kT}\right\} - \exp\left\{-\frac{M(\mathbf{v}+\mathbf{V}_0)^2}{2kT}\right\}\right]. \tag{25}$$

Thus, $\mathrm{I}(\mathbf{u})$ can be readily calculated if the law of scattering of the ions on the body, with allowance for the electric field, is known. Naturally, formula (25) does not permit $\mathrm{I}(\mathbf{u})$ to be calculated in the general case, since the electric field around the body is unknown, if for no other reason. We shall show in the next section, however, that in some important limiting cases this difficulty can be circumvented.

Let us note that $\mathrm{I}(\mathbf{u})$ enables us to express in simple fashion the force acting on the moving body if collisions between the body and neutral molecules can be neglected. Namely, multiplying (23) by $M\mathbf{u}$ and integrating over d^3u and d^3r we obtain the time derivative of the total particle momentum, which is equal to the negative of the sought force. As a result

$$\mathbf{F} = - M \int \mathbf{u} I(\mathbf{u})\, d^3u. \tag{26}$$

In the derivation of the formulas obtained in this section we have assumed that the particles do not lose their identity as they collide with the body and, in particular, that the ions do not become neutralized. It is obvious, however, that the final formula (22) is of great significance. In particular, it can also be used when the ions are partially or completely neutralized. All the effects connected with neutralization modify in this case only the form of the function $\mathrm{I}(\mathbf{u})$, which will no longer satisfy the law of conservation of the number of particles

$$\int I(\mathbf{u})\, d^3u = 0.$$

The results can be readily generalized to include the case of noticeable photoeffect or secondary emission of electrons from the surface of the body.

3. CALCULATION OF THE "COLLISION INTEGRAL" I FOR DIFFERENT PARTICULAR CASES

The function $\mathrm{I}(\mathbf{u})$ can of course not be calculated in general form for arbitrary bodies. In this section we shall determine this function for different limiting cases which are of principal interest. For simplicity we confine ourselves to the motion of a spherically symmetrical body, although in some cases (low and high velocities) the formulas obtained can be applied also to more general cases.

a) Slowly moving body. To illustrate the method we shall consider first the case of the body moving in a plasma at a velocity much lower than the average thermal velocity of the ions (this case is probably only of methodological interest). In this case, in the zeroth approximation in $\mathbf{V}_0$, the potential around the body is spherically symmetrical and independent of $\mathbf{V}_0$. Expanding the exponentials in (25) in powers of $\mathbf{V}_0$ we get

$$I(\mathbf{u}) = n_0 \left(\frac{M}{2\pi kT}\right)^{3/2} \frac{Mu}{kT} e^{-Mu^2/2kT} \int \rho\, d\rho\, d\varphi\, (\mathbf{u} - \mathbf{u}_1)\, \mathbf{V}_0$$
$$= n_0 \left(\frac{M}{2\pi kT}\right)^{3/2} e^{-Mu^2/2kT} \frac{Mu}{kT} \mathbf{u} \mathbf{V}_0 \sigma^*(u),$$

$$\sigma^* = 2\pi \int (1 - \cos\vartheta)\, \rho\, d\rho, \tag{27}$$

where $\vartheta(\rho)$ is the angle between $\mathbf{u}$ and $\mathbf{u}_1$, $\mathbf{u}_1 = \mathbf{v}_1 + \mathbf{V}_0$, and σ^* is the so-called transport cross section of the body (see, for example, reference 5). For an uncharged sphere from which the ions are specularly reflected, we have

$$\sigma^* = \pi R_0^2 = \sigma_0.$$

Substituting (27) into (26) we obtain for the force acting in the body

$$\mathbf{F} = - (M^2 / 3kT)\, \overline{\sigma^* u^3}\, n_0 \mathbf{V}_0, \tag{28}$$

where $\overline{\sigma^* u^3}$ is the average value of $\sigma^*(u) u^3$, taken over the Maxwellian distribution. Formula (28) coincides, as it should, with the formula for the force acting on a heavy particle in a light gas.[5]

b) Rapidly moving body with dimensions which are not small compared with the Debye radius. If the velocity of the body is high

$$V_0 \gg \sqrt{kT/M}, \tag{29}$$

the problem can be greatly simplified, for in this case the electric field exerts a small influence on the scattering of the ions by the body. Actually, as was shown by Gurevich,[2] the electric potential of the body is in this case of order kT/e, or more accurately $(kT/e)\ln(R_0/R_D)$, and when $MV_0^2/2 \gg kT$ it is less than the kinetic energy of the ions relative to the body. Consequently it is natural to neglect in the calculation of I(u) the influence of the field and to consider only scattering of the ions by the surface of the sphere.* Further calculations depend on the law governing this scattering. To be specific, we confine ourselves to specular reflection. All other cases can be analyzed analogously.

It is now natural to represent expression (25) for I(u) in the form $I = I_1 - I_2$ in accordance with the two terms in the integrand. For a sphere, I_2 is simply

$$I_2 \approx n_0 V_0 \sigma_0 (M/2\pi kT)^{3/2}\, e^{-Mu^2/2kT}\,. \tag{30}$$

To calculate I_1 we recognize that

$$(\mathbf{v}_1 + \mathbf{V}_0)^2 = v^2 + V_0^2 + 2vV_0(\cos\vartheta_0\cos\vartheta + \sin\vartheta_0\sin\vartheta\cos\varphi), \tag{31}$$

where ϑ_0 is the angle between $\mathbf{v}$ and $\mathbf{V}_0$ and ϑ is the angle between $\mathbf{v}_1$ and $\mathbf{v}$. In addition, in the case of specular reflection $\rho\, d\rho = \frac{1}{4}R_0^2 \sin\vartheta\, d\vartheta$. Substituting this in (25) we have

$$I_1 = n_0\left(\frac{M}{2\pi kT}\right)^{3/2} v\,\frac{R_0^2}{4}\int d\varphi \sin\vartheta\, d\vartheta \times \exp\left\{-\frac{M}{2kT}\left[v^2 + V_0^2 + 2vV_0(\cos\vartheta_0\cos\vartheta + \sin\vartheta_0\sin\vartheta\cos\varphi)\right]\right\}. \tag{32}$$

Since the exponential function has a large modulus by virtue of (29), we can calculate I_1 by the method of steepest descents. It is easy to verify that the exponent in (32) has a maximum at $\varphi = \pi$, $\vartheta + \vartheta_0 = \pi$. Putting $\varphi = \pi + \varphi'$, $\vartheta + \vartheta_0 = \pi + \vartheta'$, and expanding in φ' and ϑ', we get

$$I_1 = n_0\left(\frac{M}{2\pi kT}\right)^{3/2} v \sin\vartheta_0 \frac{R_0^2}{4}\exp\left\{-\frac{M}{2kT}(v^2 + V_0^2 - 2vV_0)\right\} \times \int \exp\left\{-\frac{MvV_0}{2kT}\varphi'^2\sin\vartheta_0\right\} d\varphi' \int \exp\left\{-\frac{MvV_0}{2kT}\vartheta'^2\sin\vartheta_0\right\} \times d\vartheta' = \frac{n_0}{V_0}\frac{R_0^2}{4}\left(\frac{M}{2\pi kT}\right)^{3/2}\exp\left\{-\frac{M}{2kT}(v - V_0)^2\right\} \tag{33}$$

(We recall that $\mathbf{v} = \mathbf{u} - \mathbf{V}_0$). Thus, the total value of I(u) is

$$I = n_0\sigma_0\left[\left(\frac{M}{2\pi kT}\right)^{1/2}\frac{1}{2V_0}\exp\left\{-\frac{M}{2kT}(v - V_0)^2\right\} - V_0\left(\frac{M}{2\pi kT}\right)^{3/2}\exp\left\{-\frac{Mu^2}{2kT}\right\}\right]. \tag{34}$$

We note that by including terms of higher order in φ' and ϑ' we can readily determine the subsequent terms in the expansion (32) in $\sqrt{kT/MV_0^2}$. We shall not stop, however, to calculate these corrections.

c) Charged body of small size. Let us consider now a body with dimensions much smaller than the Debye radius, carrying a charge that satisfies the condition

$$\epsilon Q \ll R_D M v_i^2,$$

where v_i is the greater of the two quantities $(V_0^2 kT/M)^{1/4}$ and $\sqrt{kT/M}$. (This is precisely the case considered by Kraus and Watson.[3] We have already pointed out that their approximation does not include the effects which we are investigating). In this case the main contribution to I is made by the impact distances ρ which satisfy the condition $R_D \gg \rho \gg r_0$, where r_0 is the greater of the two quantities R_0 and Q/Mv_i^2. For such values of ρ the field can be considered to be a Coulomb field exclusively, and the scattering angle ϑ is small and given by[6]

$$\vartheta = 2Qe\,/\,Mv^2\rho. \tag{35}$$

Expanding the right half of (25) in powers of ϑ, retaining terms up to ϑ^2, and integrating with respect to ρ with cutoff at large when $\rho \sim R_D$ and at small ρ when $\rho \sim r_0$, we obtain

$$I = 2\pi n_0\left(\frac{M}{2\pi kT}\right)^{3/2} e^{-Mu^2/2kT}\, v\left(\frac{M\mathbf{v}\mathbf{V}_0}{2kT} + \frac{M^2}{4(kT)^2}[V_0^2 v^2 - (\mathbf{V}_0\mathbf{v})^2]\right)\int \vartheta^2\rho\, d\rho = \frac{4\pi Q^2 e^2}{MkT}\, n_0\left(\frac{M}{2\pi kT}\right)^{3/2} e^{-Mu^2/2kT}\left(\mathbf{V}_0\mathbf{u} - V_0^2 + \frac{M}{2kT}[u^2V_0^2 - (\mathbf{V}_0\mathbf{u})^2]\right)\frac{1}{v^3}\ln\frac{R_D}{r_0}\,. \tag{36}$$

We note that when $eQ \ll kTR_D$ this formula is suitable for all body velocities $\mathbf{V}_0$. The formula (36) for I can, of course, be obtained without the use of (25), directly from definition (15) for I. For this purpose it is enough to calculate φ_q and f'_q by perturbation theory and substitute in (15). We note also that if $R_0 \ll R_D$, but at the same time $R_0^2 \sim (Q^2e^2/MkTV_0^2)\ln(R_D/r_0)$, we must add to (36) a term due to the scattering by the body itself, as given by (34) (when $V_0 \gg kT/M$). (The two effects are additive in the approximation considered here.)

4. CALCULATION OF THE EFFECTIVE SCATTERING CROSS SECTION

a) Slowly moving body. Substituting (27) in (22) and neglecting everywhere $\mathbf{V}_0$ compared with $\mathbf{u}$, we obtain

$$n_{\mathbf{q}} = \frac{1}{i2q} n_0 (\mathbf{n}\mathbf{V}_0)\frac{M}{kT}\overline{\sigma^* u}, \tag{37}$$

---

*We emphasize that this does not mean that the electric field is in general unimportant; the effect of the field manifests itself in the angular dependence of the denominator of (22).

where $\overline{\sigma^* u}$ is the average value of $\sigma^*(u)u$, taken over a Maxwellian distribution. Substituting in (5), we obtain the effective cross section for a smooth sphere

$$d\sigma = \frac{1}{8\pi^3}\left(\frac{\omega_0}{c}\right)^4 \frac{(\mathbf{n}\mathbf{V}_0)^2 M}{kTq^2}\, \sigma_0^2 \sin^2\psi_1\, do. \tag{38}$$

b) Rapidly moving large body. For this case $I(u)$ is given by formula (34). Let us calculate $n_\mathbf{q}$. We introduce the notation

$$A_1 = \frac{1}{i}\int \frac{I_1(\mathbf{u})\, d^3u}{\mathbf{n}\mathbf{u} - \mathbf{n}\mathbf{V}_0 - i\delta}$$

with A_2 defined analogously. To calculate A_1 we change over from integration over d^3u to integration over d^3v. The integration is best carried out in spherical coordinates with the polar axis along $\mathbf{n}$. In first approximation we can put $\mathbf{v} = \mathbf{V}_0$ in all the factors preceding the exponents and replace the lower limit 0 in the integration with respect to dv by $-\infty$. We then obtain readily

$$A_1 = n_0\sigma_0\pi/2. \tag{39}$$

The quantity A_2 should be calculated in Cartesian coordinates u_x, u_y, and u_z with the x axis along $\mathbf{n}$. With the aid of (21) we obtain

$$A_2 = -n_0\sigma_0\left(\frac{MV_0^2}{2kT}\right)^{1/2}\left(\sqrt{\pi} + 2i\int_0^a e^{x^2}dx\right)e^{-a^2}. \tag{40}$$

Ultimately

$$n_\mathbf{q} = \frac{n_0\sigma_0}{q}\left\{\left[\frac{\pi}{2} - \sqrt{\pi}\left(\frac{MV_0^2}{2kT}\right)^{1/2} e^{-a^2}\right] + i2\left(\frac{MV_0^2}{2kT}\right)^{1/2} e^{-a^2}\int_0^a e^{x^2}dx\right\}$$
$$\times\left[2\left(1 - ae^{-a^2}\int_0^a e^{x^2}dx\right) - ia\sqrt{\pi}e^{-a^2}\right]^{-1} \tag{41}$$

and

$$d\sigma = \frac{\sin^2\psi_1}{16\pi^2}\left(\frac{\omega_0}{c}\right)^4 \frac{\sigma_0^2}{q^2}\left\{\left[\frac{\pi}{2} - \sqrt{\pi}\left(\frac{MV_0^2}{2kT}\right)^{1/2} e^{-a^2}\right]^2\right.$$
$$\left. + 4\left(\frac{MV_0^2}{2kT}\right)\left(e^{-a^2}\int_0^a e^{x^2}dx\right)^2\right\}\left[4\left(1 - ae^{-a^2}\int_0^a e^{x^2}dx\right)^2\right.$$
$$\left. + a^2\pi e^{-2a^2}\right]^{-1} \tag{42}$$

(We recall that $a = \mathbf{n}\cdot\mathbf{V}_0\sqrt{M/2kT}$).

The expression (42) (for a given ψ) has a sharp minimum when $\mathbf{n}\cdot\mathbf{V}_0 \lesssim \sqrt{2kT/M}$ or, introducing the angle α between $\mathbf{n}$ and $\mathbf{V}_0$, when $|\alpha - \pi/2| \lesssim \sqrt{2kT/MV_0^2}$. This is as expected, since the trail of the body has a form which is prolate along $\mathbf{V}_0$, and scattering by a prolate body is always a maximum at the angle of specular reflection from its axis, in this case when $\mathbf{q}\cdot\mathbf{V}_0$ is close to zero. (If $\mathbf{q}\cdot\mathbf{V}_0 = 0$, then $\mathbf{k}\cdot\mathbf{V}_0 = \mathbf{k}'\cdot\mathbf{V}_0$, i.e., the angle of incidence is equal to the angle of reflection.) Let us note also that $n_\mathbf{q}$ increases sharply as $\mathbf{q} \to 0$. (Formally $n_\mathbf{q} \to \infty$ as $\mathbf{q} \to 0$. Actually, however, the formula becomes invalid when $q \sim 1/l$, where l is the mean free path.) This means, in particular, that the trail is capable of "focusing" all possible noises radiated in the plasma above the body.

Formula (41) is valid for sufficiently large wavelengths. It is easy to show that in this particular case this implies the requirement

$$qR_0 = 2\frac{\varepsilon\omega}{c}R_0\sin\frac{\psi}{2} \ll 1. \tag{43}$$

It is seen from (42) that when ψ is not close to zero, and the angle α is not close to $\pi/2$, the order of magnitude of $d\sigma$ is

$$d\sigma \sim \left(\frac{\omega_0}{c}\right)^4 \frac{\sigma_0^2 c^2}{\varepsilon\omega^2}\, do.$$

Comparing this with Eq. (6) for the cross section of the scattering by the body itself, we find that the ratio of the intensity of scattering from the trail to the intensity of scattering from the body itself has an order of magnitude

$$d\sigma/d\sigma_m \sim (\omega_0/\omega)^4 c^2/\varepsilon\omega^2\sigma_0. \tag{44}$$

The scattering cross section in the directions for which $|\alpha - \pi/2| \ll \sqrt{kT/MV_0^2}$ is much greater:

$$d\sigma \sim \frac{MV_0^2}{kT}\left(\frac{\omega_0}{c}\right)^4 \frac{\sigma_0^2 c^2}{\varepsilon\omega^2}\, do.$$

It is seen from (44) that actually, for ordinary body dimensions and not too long waves, the main contribution to the scattering in practically all directions is made by the body itself and not by the trail. We emphasize, however, that this conclusion has been obtained by neglecting the magnetic field, which can change the entire scattering picture appreciably. The influence of the magnetic field is the subject of another investigation. We indicate only that the results obtained in the present article are valid if

$$eH/Mc \ll q_z\sqrt{kT/M},$$

where q_z is the projection of $\mathbf{q}$ on the direction of $\mathbf{H}$.

Let us see now whether the perturbation-theory formula (5) is valid in our case. In order for (5) to be valid it is necessary to have $E' \ll E_0$ over significant distances. It can be verified that in our case the significant distances are $R \sim 1/q$, over which $E' \sim (\omega_0/c)^2\sigma_0 E_0$. This leads to the condition

$$(\omega_0/c)^2\sigma_0 \ll 1$$

(for analogous arguments to justify of the applicability of the Born approximation in quantum mechanics see reference 7). Since the only frequencies that can be used to investigate the scattering are $\omega > \omega_0$, the condition for the validity of formula (5) coincides in our case with the main condition (2).

c) Rapidly moving small body. Since the integral of I, as defined by (36) and contained in the expression for $n_\mathbf{q}$, cannot be calculated for an arbitrary body velocity, we confine ourselves here only to the case when $V_0 \gg \sqrt{kT/M}$. Neglecting u compared with V_0, we obtain

$$I = -\frac{2\pi Q^2e^2}{MkT}\frac{1}{V_0{}^3}\ln\frac{R_D}{R_0}n_0\left(\frac{M}{2\pi kT}\right)^{3/2}e^{-Mu^2/2kT}$$
$$\times\left\{V_0^2 - \frac{M}{2kT}\left[V_0^2u^2 - (\mathbf{V}_0\mathbf{u})^2\right]\right\}.$$

Calculating the integral of I with the aid of (21), we obtain

$$n_\mathbf{q} = \frac{2\pi Q^2e^2n_0}{q\,(2k^3T^3MV_0^2)^{1/2}}\ln\frac{R_D}{r_0}\left[V_0^2 - (\mathbf{V}_0\mathbf{n})^2\right]\left[(1-2a^2)\left(\sqrt{\pi}\right.\right.$$
$$\left.\left.+\,2i\int_0^a e^{x^2}dx\right)e^{-a^2} + 2ia\right]\left[2 - 2a\left(\int_0^a e^{x^2}dx - i\frac{\sqrt{\pi}}{2}\right)e^{-a^2}\right]^{-1}. \qquad (45)$$

It is easy to verify that this formula is suitable when

$$q \ll 1/r_1, \qquad r_1 = (MkT)^{1/2}kTV_0/Qe^3n_0\ln(R_D/r_0).$$

In the case when $eQ/R_D \ll kT$, the formula for $n_\mathbf{q}$ for $q \gg 1/r_1$ can be obtained in the usual manner from the linearized kinetic equation, i.e., in the same approximation as used by Kraus and Watson[3] (a practically analogous calculation for the Fourier components of the potential was also made by Sitenko and Stepanov[8]). For the sake of completeness, we cite the corresponding formula:

$$n_\mathbf{q} = \frac{Q}{e}\left\{2\,(R_Dq)^2 + \left[2 - 2a\left(\int_0^a e^{x^2}dx - \frac{i\sqrt{\pi}}{2}\right)e^{-a^2}\right]\right\}^{-1}. \qquad (46)$$

Substituting (45) and (46) in (5) we obtain $d\sigma$. We shall not write out these formulas.

In conclusion, the authors express their gratitude to Ya. L. Al'pert for interest in the work and for discussions, and to A. V. Gurevich for discussions and for an opportunity to see reference 2 prior to publication.

---

[1] Ya. L. Al'pert, Usp. Fiz. Nauk **71**, 369 (196), Soviet Phys. Uspekhi **3**, 479 (1961). Collection Искусственные спутники земли (Artificial Earth Satellites), Acad. Sci. Press, No 7, 1960.

[2] A. V. Gurevich, Тр. Ин-та земного магнетизма, ионосферы и распространения радиоволн АН СССР (Trans. of Inst. of Terrestrial Magnetism, Ionosphere, and Radio Wave Propagation, U.S.S.R. Acad. Sci., **17** (**23**), 174 (1960). Coll. "Artificial Earth Satellites," No 7, 1960.

[3] L. Kraus and K. Watson, Physics of Fluids **1**, 480 (1958).

[4] L. D. Landau, JETP **16**, 574 (1946).

[5] L. D. Landau and E. M. Lifshitz, Механика сплошных сред (Mechanics of Continuous Media), 1st ed., Gostekhizdat, 1944, p. 437.

[6] L. D. Landau and E. M. Lifshitz, Механика (Mechanics), Gostekhizdat, 1958, p. 75.

[7] N. F. Mott and H. S. W. Massey, Theory of Atomic Collisions (Transl.) Gostekhizdat, 1957, p. 158.

[8] A. G. Sitenko and S. N. Stepanov, Тр. физического отделения физико-математического факультета Харьковского университета (Trans. Phys.-Math. Faculty of the Khar'kov University) No 7, 1 (1958).

Translated by J. G. Adashko
41

SOVIET PHYSICS JETP VOLUME 13, NUMBER 1 JULY, 1961

ON THE APPLICATION OF THE METHODS OF SUPERCONDUCTIVITY THEORY TO THE PROBLEM OF THE MASSES OF ELEMENTARY PARTICLES

V. G. VAKS and A. I. LARKIN

Submitted to JETP editor July 23, 1960

J. Exptl. Theoret. Phys. (U.S.S.R.) 40, 282-285 (January, 1961)

The methods of superconductivity theory are applied to a Heisenberg type four-fermion two-component Lagrangian with cut-off. Owing to the rearrangement of the vacuum state, the two-component nature of the initial field does not hinder the appearance of a fermion mass. Boson excitations are found which are analogous to acoustic excitations in a superconductor. Interaction between the excitations is discussed.

We shall consider the simplest Lagrangian,[1] containing only a two-component spinor field u (x):

$$L = -u^+\sigma p u - \tfrac{1}{4}\lambda\,(ugu)\,(u^+gu^+)$$
$$= -u^+\sigma p u - \tfrac{1}{8}\lambda\,(u^+\sigma_r u)\,(u^+\sigma_r u). \qquad (1)$$

Here $\sigma_r = (\sigma, 1)$, $\sigma p = \sigma_r p_r = \sigma\cdot p - \sigma_0 p_0$, σ is the Pauli spin matrix and $g = i\sigma_y$. The Heisenberg operators u (x) and u^+ (y) obey the usual anti-commutation relations $\{u(x, t), u^+(y, t)\} = \delta(x - y)$. We assume a cut-off at a large momentum Λ, the physical reason for which is not considered. The Lagrangian L is not invariant with respect to the operations $P: x \rightarrow -x$ and $C: u \rightarrow gu^+$, but is invariant under CP and T.

From (1) we have

$$\sigma p u + \tfrac{1}{2}\lambda\,(ugu)\,gu^+ = 0. \qquad (2)$$

We use the methods of the theory of superconductivity in order to solve (2). Following the work of Gor'kov[2] we introduce the quantities

$$G_1 = \langle Tu(x)\,u^+(y)\rangle,$$
$$F = \langle u(x)\,u(y)\rangle, \qquad \Delta = \tfrac{1}{2}\lambda\,\langle u(x)\,gu(x)\rangle; \qquad (3)$$

where the symbol <...> denotes an expectation value for the physical vacuum. Taking into account, as in the theory of superconductivity, only qualitative effects connected with rearrangement of the vacuum, we obtain from (2) and (3)

$$\sigma p G_1(p) - \Delta g F^+(p) = -i, \qquad \tilde{\sigma} p F^+(p) + \Delta^* g G_1(p) = 0; \qquad (4)$$

$$\Delta^* = -\frac{\lambda}{2}\int d^4p\,\mathrm{Sp}\,(F^+(p)\,g) = -i\lambda\Delta^*\int\frac{d^4p}{p^2 + |\Delta|^2 - i\delta}, \qquad (5)$$

where $d^4p = (2\pi)^{-4}dp\,dp_0$, $p^2 < \Lambda^2$, $\delta \rightarrow +0$.

Besides the trivial solution $\Delta^* = 0$, Eq. (5) can have a non-zero solution for the condition $(4\pi)^{-2}\lambda\Lambda^2 > 1$. $|\Delta|^2$ then satisfies the relation

$$1 = -i\lambda\int\frac{d^4p}{p^2 + |\Delta|^2 - i\delta} = \frac{\lambda}{(4\pi)^2}\left(\Lambda^2 - |\Delta|^2\ln\frac{\Lambda^2}{|\Delta|^2}\right). \qquad (6)$$

Assuming that the mass $m = |\Delta| \ll \Lambda$, we find that for (6) to be fulfilled it is essential that $(4\pi)^{-2}\lambda\Lambda^2$ should be very close to 1, i.e. $\lambda m^2 \ll 1$. The hypothesis of such a connection between the interaction constant and the cut-off was put forward in Zel'dovich's work.[3] A more rigorous discussion leads to an integral equation instead of (5), with the constant λ replaced by an irreducible four-pole. We shall find that this only changes the relation between the mass and the parameters λ and Λ.

It is convenient to go over to a four-component description. We introduce

$$\psi = \begin{pmatrix} u \\ (\Delta/m)\,gu^+ \end{pmatrix}, \quad G = \langle\psi(x)\,\psi(y)\rangle. \qquad (7)$$

Equation (4) then takes the form

$$(\hat{p} + m)\,G(p) = -i, \qquad (8)$$

where $\hat{p} = \gamma_r p_r = \boldsymbol{\gamma}\cdot p - \gamma_0 p_0$, γ_r being the usual γ matrix in the Weyl representation. Equations (7) and (8) describe a Majorana particle of mass m: if we introduce the charge-conjugation matrix

$$C = \frac{\Delta}{m}\begin{pmatrix} g & 0 \\ 0 & -g \end{pmatrix},$$

then

$$\psi_c(x) \equiv \bar{\psi}(x)\,C = \psi(x).$$

With the notation of (7), the Lagrangian (1) takes the form

$$L = -\tfrac{1}{2}\bar{\psi}\hat{p}\psi + \tfrac{1}{16}\lambda\,[(i\bar{\psi}\gamma_5\psi)^2 + (\bar{\psi}\psi)^2]$$
$$= -\tfrac{1}{2}\bar{\psi}\hat{p}\psi + \tfrac{1}{32}\lambda\,(i\bar{\psi}\gamma_r\gamma_5\psi)^2, \qquad \gamma_5 = i\gamma_0\gamma_1\gamma_2\gamma_3. \qquad (9)$$

We shall find collective excitations analogous to excitations in a superconductor.[4] For this purpose let us consider the two-particle Green's functions. There are six types of such functions corresponding to the number of possible antisymmetrical ψ combinations:

$$K_{+} = \tfrac{1}{8}\langle i\bar{\psi}(x)\gamma_5\psi(x),\ i\bar{\psi}(y)\gamma_5\psi(y)\rangle,$$

$$K_{-} = \tfrac{1}{8}\langle \bar{\psi}(x)\psi(x),\ \bar{\psi}(y)\psi(y)\rangle,$$

$$K_{r+} = -K_{+r} = \tfrac{1}{8}\langle i\bar{\psi}(x)\gamma_5\gamma_r\psi(x),\ i\bar{\psi}(y)\gamma_5\psi(y)\rangle.$$

As above, if we replace the irreducible four-pole bv the constant λ, we obtain the following equations:

$$K_{-}(q) = \Pi_{-}(q) + i\lambda\Pi_{-}(q)K_{-}(q),$$
$$K_{+}(q) = \Pi_{+}(q) + i\lambda\Pi_{+}(q)K_{+}(q) + i\lambda\Pi_{+r}(q)K_{r+}(q),$$
$$K_{r+}(q) = \Pi_{r+}(q) + i\lambda\Pi_{r+}(q)K_{+}(q) + i\lambda\Pi_{rn}(q)K_{n+}(q);$$
$$\Pi_{\pm} = -\int\frac{d^4p}{s_1s_2}(p_1p_2 \pm m^2), \qquad \Pi_{r+} = -mq_r\int\frac{d^4p}{s_1s_2} = -\Pi_{+r}, \tag{10}$$

$$\Pi_{rn} = \int\frac{d^4p}{s_1s_2}[\delta_{rn}(p_1p_2 - m^2) - 2p_{1r}p_{2n}],$$
$$p_1 = p + q/2, \qquad p_2 = p - q/2, \qquad s_{1,2} = p_{1,2}^2 + m^2. \tag{11}$$

The excitation spectrum is determined by the poles of the functions K. From (11) and (10) taking account of (6), we find that in the region $q^2 \ll \Lambda^2$ the function K_{r_+} does not have a pole, K_+ has a pole $q^2 = 0$ and K has a pole at the point $-q^2 \approx 4m^2 - m^2/\ln(\Lambda^2/m^2)$. Thus there exist odd-CP excitations of zero mass and even CP related to a two-particle state.

Let us examine the interaction between the particles obtained. As an example we shall find the interaction between two fermions through exchange of the massless "K_+ particle". The scattering amplitude of particles with momenta p_1 and p_2 into the state with momenta p_3 and p_4 is given by the expression

$$\langle p_3,\ p_4\left|T\exp\left\{\frac{i\lambda}{16}\int d^4x\,[(\bar{\psi}i\gamma_5\psi)^2 + (\bar{\psi}\psi)^2]\right\}\right|p_1p_2\rangle.$$

Let us look, for example, at the non-exchange term. The term of interest to us is of the form

$$(i\gamma_5)_{3,1}(i\gamma_5)_{4,2}\left[\frac{i\lambda}{2} - \frac{\lambda^2}{16}\int\left\langle i\bar{\psi}\left(\frac{x}{2}\right)\gamma_5\psi\left(\frac{x}{2}\right),\right.\right.$$
$$\left.\left. i\bar{\psi}\left(-\frac{x}{2}\right)\gamma_5\psi\left(-\frac{x}{2}\right)\right\rangle e^{-iqx}d^4x\right]. \tag{12}$$

Using equation (10) for the expression in square brackets in (12) to the accuracy of terms $\sim \lambda m^2$, we obtain

$$\frac{i\lambda'(q)}{2} = \frac{i\lambda}{2}\left(1 + \frac{i\lambda\Pi_+}{1 - i\lambda\Pi_+}\right) = \frac{i\lambda}{2}\,\frac{1}{1 - i\lambda\Pi_+(q)}. \tag{13}$$

According to (6) and (11) we have

$$\frac{i\lambda'(q)}{2} = \frac{i\lambda}{2i\lambda[\Pi_+(0) - \Pi_+(q)]} = \frac{i(4\pi)^2}{q^2[\ln(\Lambda^2/m^2) - {}^3/_4 + 2(1 - \theta\cot\theta)]}, \tag{14}$$

where $\sin^2\theta = -q^2/4m^2$. In spite of the smallness of the primary constant λ, the effective interaction $\lambda'(q)$ is therefore not very small. As was pointed out by Zel'dovich,[3] a similar situation occurs in the problem of resonance scattering, which has some features in common with the model considered.

We shall explain the relation between the results obtained and the usual description of the interaction in the form

$$L_{int} = ei\bar{\psi}(x)\gamma_5\psi(x)\varphi(x). \tag{15}$$

The magnitude of e is determined by comparing (14) with the scattering amplitude for small values of q^2, obtained by perturbation theory from (15). We obtain

$$e^2/4\pi^2 = \left[\ln\frac{\Lambda^2}{m^2} - \frac{3}{4}\right]^{-1}. \tag{16}$$

Let us consider the question of renormalizations for the interaction (5). If we do not taken into account, as in deriving (14), the correction to the function G and the vertex part, we obtain for the effective interaction, analogously to (14)

$$-4e_0^2D(q) = 4ie_0^2/[q^2 + ie_0^2 8\Pi_+(q)]. \tag{17}$$

Here the boson Green's function $D(x - y) = \langle\varphi(x), \varphi(y)\rangle$ and Π_+ is given by Eq. (11). According to the rules of renormalization, we must subtract $ie_0^2 8\Pi_+(0)$ from the demoninator of expressions (7), after which (7) takes the form

$$-4e_0^2D = \frac{4ie_0^2}{q^2}\left[\left(1 + \frac{e_0^2}{(2\pi)^2}\left(\ln\frac{\Lambda_0^2}{m^2} - \frac{3}{4}\right)\right)\right.$$
$$\left. + \frac{e_0^2}{(2\pi)^2}2(1 - \theta\cot\theta)\right]^{-1}. \tag{18}$$

By comparing (18) with (14) we can verify that expression (16) does in fact determine the renormalized physical charge of the usual theory:

$$e^2 = e_0^2\left[1 + \frac{e_0^2}{4\pi^2}\left(\ln\frac{\Lambda_0^2}{m^2} - \frac{3}{4}\right)\right]^{-1}. \tag{19}$$

It can be seen from (19) and (16) that (18) agrees with (14). In this way we can understand in the model discussed the calculated quadratically divergent "self mass" of a boson in the usual renormalization.

The authors thank S. T. Belyaev for valued advice.

Note added in proof (15 December, 1960): After our work was sent to be printed we became aware of a work by Nambu in which analogous results were obtained (Y. Nambu, Report to Midwest Conference on Theoretical Physics, March 1960, preprint).

---

[1] Dürr, Heisenberg, Mitter, Schlieder, and Yamazaki, Z. Naturforsch. **14a**, 441 (1959).

[2] L. P. Gor'kov, JETP **34**, 735 (1958), Soviet Phys. JETP **7**, 505 (1958).

[3] Ya. B. Zel'dovich, JETP **38**, 819 (1960), Soviet Phys. JETP **11**, 594 (1960).

[4] V. M. Galitskiĭ, JETP **34**, 1011 (1958), Soviet Phys. JETP **7**, 698 (1958). Bogolyubov, Tolmachev, and Shirkov, Новый метод в теории сверхпроводимости (A New Method in the Theory of Superconductivity), M., Acad. Sci. Press, 1958.

Translated by R. Berman
42

SOVIET PHYSICS JETP VOLUME 13, NUMBER 1 JULY, 1961

PAIR CORRELATION EFFECTS NEAR CLOSED SHELLS

S. I. DROZDOV and D. F. ZARETSKIĬ

Submitted to JETP editor July 29, 1960

J. Exptl. Theoret. Phys. (U.S.S.R.) 40, 286-295 (January, 1961)

Pair correlation effects are studied for nuclei that are close to closed shell. Equations for the Green's functions are obtained. It is shown that these equations are valid to within corrections of the order $A^{-1/3}$. A possibility is indicated for testing the results by means of stripping or pick-up reactions.

1. INTRODUCTION

THERE are two main methods commonly used in the theory of superconductivity: the canonical-transformation method, developed in the "Bogolyubov papers",[1] and the Green's-function method proposed by Gor'kov.[2] The canonical-transformation method has been used by Belyaev[3] to study the effects of pair correlation in spherical nuclei. In papers by Migdal and his co-workers[4,5] the Gor'kov method has been applied to the study of the influence of superfluidity on the values of the moments of inertia of nonspherical nuclei.

In all these calculations, however, an essential assumption is that there is a large number of correlated pairs. For spherical nuclei this means a large number of particles in unfilled shells, and for nonspherical nuclei it means that the condition $\rho\Delta \gg 1$ must hold, where ρ is the density of one-particle levels near the Fermi surface and Δ is a parameter that characterizes the energy of the pair correlation. It is interesting to examine the properties of nuclei that are near closed shells, in which the stated assumptions are not satisfied because of the smallness of the number of nucleons above the closed shells. This situation calls for more accurate methods, which make it possible to treat pair-correlation effects in this case also.

The purpose of the present paper is to generalize the Gor'kov method so as to find the Green's functions, the density matrices, and the pair-correlation energies in the case of nuclei that are near closed shells.

We shall assume that we can describe the motion of the nucleons in the nucleus by using the Hamiltonian

$$H = \sum_{\lambda} \varepsilon_{\lambda} a_{\lambda}^{+} a_{\lambda} + \tfrac{1}{2} \sum_{\lambda\lambda_1} g_{\lambda\lambda_1} a_{\lambda}^{+} a_{-\lambda}^{+} a_{-\lambda_1} a_{\lambda_1}, \tag{1}$$

where λ is a complete set of quantum numbers necessary for the description of the state of a nucleon (the sets λ and $-\lambda$ differ from each other only in the sign of the projection m of the total angular momentum of the nucleon along some arbitrary axis), ϵ_λ are the eigenvalues of the energy of the nucleon in the self-consistent field $U(\mathbf{r})$:

$$H_0 \varphi_\lambda(\mathbf{r}) = \varepsilon_\lambda \varphi_\lambda(\mathbf{r}), \qquad H_0 = -(\hbar^2/2m_{\text{eff}})\nabla^2 + U(\mathbf{r});$$

m_{eff} is the effective mass of the nucleon, and $g_{\lambda\lambda_1}$ is the interaction matrix element that leads to pairing. The stated Hamiltonian assumes that the interaction between nucleons that leads to pairing occurs in states with opposite signs of the angular-momentum projection m. The part of the interacaction that does not lead to pairing is taken into account by the introduction of the self-consistent field and the effective mass of the nucleon.

For the further exposition we need Green's functions of the system of N nucleons, defined in the following way:

$$\begin{gathered} G_{\lambda}^{N+}(\tau) = -ie^{iE_N\tau} \langle \Phi_N a_\lambda e^{-iH\tau} a_\lambda^{+} \Phi_N \rangle, \quad \tau > 0, \\ G_{\lambda}^{N-}(\tau) = ie^{-iE_N\tau} \langle \Phi_N a_\lambda^{+} e^{iH\tau} a_\lambda \Phi_N \rangle, \quad \tau < 0; \\ G_{\lambda}^{+}(\tau = 0) - G_{\lambda}^{-}(\tau = 0) = -i. \end{gathered} \tag{2}$$

Let us also define the functions

$$\begin{gathered} F_{\lambda}^{N+}(\tau) = (-1)^{\lambda} e^{iE_N\tau} \langle \Phi_{N+2}\, a_{-\lambda}^{+} e^{-iH\tau} a_\lambda^{+} \Phi_N \rangle, \quad \tau > 0, \\ F_{\lambda}^{N-}(\tau) = (-1)^{-\lambda} e^{-iE_N\tau} \langle \Phi_N a_\lambda^{+} e^{iH\tau} a_{-\lambda}^{+} \Phi_{N-2} \rangle, \quad \tau < 0; \\ F_{\lambda}^{N+2-}(0) = F_{\lambda}^{N+}(0), \end{gathered} \tag{3}$$

where Φ_N is the wave function of the ground state of the system of N fermions, E_N is the energy of this state, and $(-1)^\lambda = \text{sign}\,\lambda$.

By the use of the definitions (2), (3) it is easy to obtain the spectral expansions of the Green's functions. In particular, we have for the functions $F_\lambda(\tau)$:

$$\begin{aligned} F_{\lambda}^{N+}(\tau) &= (-1)^{\lambda} \sum_{s} \langle \Phi_{N+2} a_{-\lambda}^{+} \Phi_{N+1,\,s} \rangle \\ &\quad \times \langle \Phi_{N+1,\,s} a_\lambda^{+} \Phi_N \rangle \exp\{-i(E_{N+1,\,s} - E_N)\tau\}, \\ F_{\lambda}^{N-}(\tau) &= (-1)^{-\lambda} \sum \langle \Phi_N a_\lambda^{+} \Phi_{N-1,\,s} \rangle \\ &\quad \times \langle \Phi_{N-1,\,s} a_{-\lambda}^{+} \Phi_{N-1} \rangle \exp\{-i(E_N - E_{N-1,\,s})\tau\}. \end{aligned} \tag{4}$$

Using the Hamiltonian (1), we get the equations for the functions (2) and (3):

$$\left(i\frac{\partial}{\partial\tau}-\varepsilon_{\lambda}\right)G_{\lambda}^{N+}(\tau)+i\sum_{\lambda_1}g_{\lambda\lambda_1}e^{iE_N\tau}\langle\Phi_N a^{+}_{-\lambda}b_{\lambda_1}e^{-iH\tau}a^{+}_{\lambda}\Phi_N\rangle=0,$$

$$\left(i\frac{\partial}{\partial\tau}-\varepsilon_{\lambda}\right)G_{\lambda}^{N-}(\tau)-i\sum_{\lambda_1}g_{\lambda\lambda_1}e^{-iE_N\tau}\langle\Phi_N a^{+}_{\lambda}e^{iH\tau}a^{+}_{-\lambda}b_{\lambda_1}\Phi_N\rangle=0,$$

$$\left(i\frac{\partial}{\partial\tau}-2\mu^{+}_{N}+\varepsilon_{\lambda}\right)F_{\lambda}^{N+}(\tau)$$
$$+\sum_{\lambda_1}(-1)^{-\lambda}g_{\lambda_1\lambda}e^{iE_N\tau}\langle\Phi_{N+2}b^{+}_{\lambda_1}a_{\lambda}e^{-iH\tau}a^{+}_{\lambda}\Phi_N\rangle=0,$$

$$\left(i\frac{\partial}{\partial\tau}-2\mu^{-}_{N}+\varepsilon_{\lambda}\right)F_{\lambda}^{N-}(\tau)$$
$$+\sum_{\lambda_1}(-1)^{\lambda}g_{\lambda_1\lambda}e^{-iE_N\tau}\langle\Phi_N a^{+}_{\lambda}e^{iH\tau}b^{+}_{\lambda_1}a_{\lambda}\Phi_{N-2}\rangle=0, \qquad (5)$$

$$b_{\lambda}=a_{-\lambda}a_{\lambda},\ 2\mu^{+}_{N}=E_{N+2}-E_{N},\qquad 2\mu^{-}_{N}=E_{N}-E_{N-2}.$$

By definition

$$N=-i\sum_{\lambda}G_{\lambda}^{N-}(0).$$

In order to get equations analogous to the Gor'kov equations for the Green's functions, it is necessary to find a connection between the functions $G^{\pm}_{\lambda}$ and $F^{\pm}_{\lambda}$. Such a connection can be obtained if we can calculate the mean values of products of four Fermi amplitudes that appear in Eq. (5). The main content of the present paper is the calculation of these averages in the approximation $A^{-1/3}$ for nuclei that are near closed shells. It must be emphasized that in the existing theories the parameter on which all the approximations are based is the large number of places in the subshell that is in the course of being filled ($\Omega = 2j+1 \gg 1$). This limitation does not exist in the method that is developed in the present paper. The possibility of writing the equations for the Green's functions $G^{\pm}_{\lambda}$ and of the following recurrence scheme for their solution was pointed out by Migdal.[6]

2. THE GREEN'S FUNCTION FOR TWO NUCLEONS ABOVE A CLOSED SHELL

We begin the accomplishment of the program we have indicated with the treatment of nuclei with two nucleons above a closed shell. We shall assume that there is no pairing in the nucleus that corresponds to the doubly closed shell. Let Φ_0 be the wave function of the doubly closed shell. If we neglect the perturbation of the self-consistent field by the addition of one nucleon (an A^{-1} effect), then the wave function of such a nucleus can be written in the form $\Phi_1 = \overset{+}{a}_{\lambda_0}\Phi_0$, where Φ_0 is the state in which the odd particle is placed.

The wave function of the nucleus with two nucleons above the closed shell already cannot be represented in as simple a form as the wave function of the nucleus just mentioned. For two nucleons above the closed shell there are already important pairing effects, which lead to the "smearing out" of the pair of particles over an entire subshell of the given shell. Owing to this we must write the wave function of the ground state of a nucleus with two nucleons above a closed shell in the form

$$\Phi_2=\sum_{j,\,m}c_j C^{00}_{jm\,j-m}b^{+}_{jm}\Phi_0'=\sum_{\lambda}c_{\lambda}b^{+}_{\lambda}\Phi_0', \qquad (6)$$

where $b^{\pm}_{\lambda} = a^{+}_{\lambda}a^{\pm}_{-\lambda}$ is the operator for production of a pair, $|c_j|^2$ is the probability of finding the pair in the subshell j, and Φ_0' is the wave function of the closed shell as perturbed by the presence of pairing; the summation is taken over all states λ.

After these comments, let us go on to the derivation of the equations for the Green's function G^{2-}_{λ}. On the basis of the form of Φ_2 and the commutation rules, we have in the main term of the second equation in (5):

$$\langle\Phi_2 a^{+}_{\lambda}e^{iH\tau}a^{+}_{-\lambda}b_{\lambda_1}\Phi_2\rangle=2c^{*}_{\lambda}\langle\Phi_0' a_{-\lambda}e^{iH\tau}a^{+}_{-\lambda}b_{\lambda_1}\Phi_2\rangle$$
$$+\sum_{\lambda_2}c^{*}_{\lambda_2}\langle\Phi_0' a^{+}_{\lambda}e^{iH\tau}a^{+}_{-\lambda}b_{\lambda_1}\Phi_2\rangle. \qquad (7)$$

Let us consider the first term in the right member of Eq. (7). The effect of the pairing on the closed shell can be treated by perturbation theory. Therefore for $\tau = 0$

$$2c^{*}_{\lambda}\sum_{\lambda_1}g_{\lambda\lambda_1}\langle\Phi_0' a_{-\lambda}a^{+}_{-\lambda}b_{\lambda_1}\Phi_2\rangle=2c^{*}_{\lambda}\sum_{\lambda_1}g_{\lambda\lambda_1}\langle\Phi_0' b_{\lambda_1}\Phi_2\rangle.$$

Here the difference between Φ_0' and Φ_0 is important because of the summation over λ_1.

The dependence of this four-pole on τ is associated with the fixed index λ. Therefore the time dependence of the first term is, in first approximation:

$$2c^{*}_{\lambda}\sum_{\lambda_1}g_{\lambda\lambda_1}\langle\Phi_0' a_{-\lambda}e^{iH\tau}a^{+}_{-\lambda}b_{\lambda_1}\Phi_2\rangle=2c^{*}_{\lambda}e^{i(E_0+\varepsilon_{\lambda})\tau}\sum_{\lambda_1}g_{\lambda\lambda_1}\langle\Phi_0' b_{\lambda_1}\Phi_2\rangle.$$

The difference between Φ_0' and Φ_0 is due to the transition of nucleons from the filled shell into the unfilled shell. For this reason there occurs in the second term of Eq. (7) an additional oscillating factor of the form $e^{i2\omega_0\tau}$, where ω_0 is the distance between the shells.

By means of the commutation rules we find that for $\tau = 0$ the second term is of the order of magnitude of

$$c_{\lambda}\langle\Phi_0' b_{\lambda_1}\Phi_2\rangle.$$

Thus for $\tau = 0$ the first and second terms in Eq. (7) are of the same order of magnitude. Solving Eq. (5) for $G^{2-}_{\lambda}(\tau)$ by using both the first and the second terms, we can convince ourselves that the ratio of the contribution of the second term to that of the first amounts to a quantity

$$\sim (\varepsilon_\lambda - \mu_2)/(\varepsilon_\lambda - \mu_2 + \omega_0),$$

where $2\mu_2 = E_2 - E_0$.

This ratio is small if the states λ are close to the Fermi surface ($\epsilon_\lambda - \mu_2 \ll \omega_0$). Therefore to accuracy $\sim A^{-1/3}$ the equation for $G_\lambda^{2-}(\tau)$ is of the form

$$\left(i\frac{\partial}{\partial\tau} - \varepsilon_\lambda\right) G_\lambda^{2-}(\tau) - i2c_\lambda^* e^{-i(2\mu_2 - \varepsilon_\lambda)\tau} \sum_{\lambda_1} g_{\lambda\lambda_1} \langle \Phi_0' \, b_{\lambda_1} \Phi_2 \rangle = 0. \tag{8}$$

It is convenient to put this equation in the form

$$(i\partial/\partial\tau - \varepsilon_\lambda)\, G_\lambda^{2-}(\tau) - i\Delta_2^* F_\lambda^{2-}(\tau) = 0, \tag{9}$$

$$\Delta_2 = \sum_{\lambda_1} g_{\lambda\lambda_1} (-1)^{\lambda - \lambda_1} F_{\lambda 1}^{2-}(0), \tag{10}$$

where the summation is taken over all λ_1 without exception.

In Eq. (9) we have introduced the notation

$$F_\lambda^{2-}(\tau) = 2c_\lambda^* (-1)^{-\lambda} \exp\{-i(2\mu_2 - \varepsilon_\lambda)\tau\}.$$

It is not hard to see that $F_\lambda^{2-}(\tau)$ can also be represented in the following form:

$$F_\lambda^{2-}(\tau) = (-1)^{-\lambda} e^{-iE_2\tau} \langle \Phi_2 a_\lambda^+ e^{iH\tau} a_{-\lambda}^+ \Phi_0' \rangle. \tag{11}$$

In order to find the Green's function from Eq. (9), we must determine $F_\lambda^{2-}(\tau)$. For this purpose it is convenient to introduce the function

$$F_\lambda^{0+}(\tau) = (-1)^\lambda e^{iE_0\tau} \langle \Phi_2 a_{-\lambda}^+ e^{-iH\tau} a_\lambda^+ \Phi_0' \rangle, \tag{12}$$

with

$$F_\lambda^{2-}(0) = F_\lambda^{0+}(0), \quad \tau = 0.$$

Equations for the determination of $F_\lambda^{2-}(\tau)$ and $F_\lambda^{0+}(\tau)$ follow from the equations (5) by a procedure like that used to get Eq. (9). These equations are

$$\begin{gathered}(i\partial/\partial\tau - 2\mu_2 + \varepsilon_\lambda)\, F_\lambda^{2-}(\tau) = 0,\\ (i\partial/\partial\tau - 2\mu_2 + \varepsilon_\lambda)\, F_\lambda^{0+}(\tau) + i\Delta_2 G_\lambda^{0+}(\tau) = 0,\end{gathered} \tag{13}$$

where $G_\lambda^{0+}(\tau)$ is the Green's function of the magic nucleus:

$$G_\lambda^{0+}(\tau) = -ie^{-i\varepsilon_\lambda\tau}.$$

By means of the spectral representations (4) we get the following solutions of the system (13):

$$\begin{gathered}F_\lambda^{0+}(\tau) = -\tfrac{1}{2}\Delta_2(\varepsilon_\lambda - \mu_2)^{-1} \exp\{-i\varepsilon_\lambda\tau\},\\ F_\lambda^{2-}(\tau) = -\tfrac{1}{2}\Delta_2(\varepsilon_\lambda - \mu_2)^{-1} \exp\{-i(2\mu_2 - \varepsilon_\lambda)\tau\}.\end{gathered} \tag{14}$$

Using Eq. (14), we get the solution of Eq. (9) in the form

$$G_\lambda^{2-}(\tau) = i\,|\Delta_2/2(\varepsilon_\lambda - \mu_2)|^2 \exp\{-i(2\mu_2 - \varepsilon_\lambda)\tau\}. \tag{15}$$

A comparison of the functions $G_\lambda^{2-}(\tau)$ and $F_\lambda^{2-}(\tau)$ with their general expansions (4) shows that, as had been assumed, the excitation energy of the nucleus with one particle above the magic core is determined by the one-particle model, $\Delta E_{12} = \epsilon_\lambda - \epsilon_{\lambda_0}$. Besides this, by means of the Green's functions G_λ^{2-} and F_λ^{2-} we can obtain the following matrix elements:

$$\begin{gathered}\sum_s |\langle \Phi_2 a_\lambda^+ \Phi_{1s} \rangle|^2 = |\Delta_2/2(\varepsilon_\lambda - \mu_2)|^2,\\ \left|\sum_s \langle \Phi_2 a_\lambda^+ \Phi_{1s} \rangle \langle \Phi_{1s} a_{-\lambda}^+ \Phi_0 \rangle\right| = |\Delta_2/2(\varepsilon_\lambda - \mu_2)|,\end{gathered} \tag{16}$$

where the summation is taken over all states Φ_{1s} that correspond to a fixed excitation energy $\Delta E_{1s} = \epsilon_\lambda - \epsilon_{\lambda_0}$.

Since

$$\Phi_2 = \sum_\lambda c_\lambda b_\lambda^+ \Phi_0',$$

the formulas (16) can be simplified for states $\Phi_{1s} = a_{\lambda s}^+ \Phi_0$, and the two formulas reduce to one:

$$|\langle \Phi_2 b_\lambda^+ \Phi_0 \rangle| = |\Delta_2/2(\varepsilon_\lambda - \mu_2)|. \tag{17}$$

Thus the functions G_λ^{2-} and F_λ^{2-} found above do not contradict each other.

The quantities μ_2 and Δ_2 that appear in the expression (15) for the Green's function are determined from Eq. (10) and the normalization condition for the Green's function. In Eq. (10) the sum over filled states can be included as a renormalization of the matrix element $g_{\lambda\lambda_1}$. If besides this we assume the renormalized matrix element to be constant and equal to $\bar{g}$, we then get the following equation for the determination of μ_2 and Δ_2:

$$1 = \tfrac{1}{2}|\bar{g}| \sum_\lambda (\varepsilon_\lambda - \mu_2)^{-1}, \qquad 2 = \sum_\lambda |\Delta_2/2(\varepsilon_\lambda - \mu_2)|^2, \tag{18}$$

where the summation is taken over the states in the unfilled shell.

We can obtain an estimate of the quantities μ_2 and Δ_2 by considering the limiting case of a single level (Sec. 4). In this case

$$2(\varepsilon_\lambda - \mu_2) = |g|\,\Omega, \qquad \Delta_2 = |g|\sqrt{2\Omega},$$

where Ω is the degree of degeneracy of the level ($\Omega \sim A^{1/3}$). Thus near a closed shell the density matrix

$$\rho_\lambda^{(2)} = |\Delta_2/2(\varepsilon_\lambda - \mu_2)|^2$$

is of the order $A^{-1/3}$.

3. THE GREEN'S FUNCTIONS OF ODD NEARLY MAGIC NUCLEI

By using the results of the preceding section, it is not hard to find the equation for the Green's functions of odd nearly magic nuclei. Let us begin the discussion with the case of one nucleon above the closed shell. The wave function of the ground state is $\Phi_1 = a^+_{\lambda_0}\Phi_0$. It follows from Eq. (5) that in this case $G^{1-}_\lambda(\tau)$ satisfies the free equation

$$(i\partial/\partial\tau - \varepsilon_\lambda)\, G^{1-}_\lambda(\tau) = 0, \tag{19}$$

and the equation for $G^{1+}_\lambda(\tau)$ is of the form

$$(i\partial/\partial\tau - \varepsilon_\lambda)\, G^{1+}_\lambda(\tau) = -i\delta_{\lambda-\lambda_1} \sum_{\lambda_1} g_{\lambda_0\lambda_1} e^{iE_1\tau} \langle \Phi_0 b_{\lambda_1} e^{-iH\tau} b^+_{\lambda_0}\Phi_0\rangle. \tag{20}$$

As was to be expected, pairing effects appear in the function $G^{1+}_\lambda(\tau)$ only for $\lambda = -\lambda_0$, since the odd particle is in the state λ_0.

It is not hard to see that the right member of Eq. (20) cannot be calculated by the method of summation over the intermediate states Φ_{2s} by leaving only the term in the sum that corresponds to the ground state Φ_2. In fact, we have for example $\langle\Phi_0 b_\lambda b^+_\lambda \Phi_0\rangle = 1$, whereas $\langle\Phi_0 b_\lambda \Phi_2\rangle\langle\Phi_2 b^+_\lambda\Phi_0\rangle \sim A^{-1/3}$ (cf. Sec. 2).

Let us try to find the function $G^{1+}_\lambda(\tau)$ by using the known solution for $G^{2-}_\lambda(\tau)$. Obviously, for $\lambda \neq \pm\lambda_0$,

$$G^{1+}_\lambda(\tau) = -ie^{-i\varepsilon_\lambda\tau}.$$

Furthermore,

$$G^{1+}_{\lambda_0}(\tau) \equiv 0, \qquad G^{1+}_{-\lambda_0}(0) = -i.$$

Therefore, in accordance with the spectral representation, the function $G^{1+}_\lambda(\tau)$ must have the following form:

$$G^{1+}_\lambda(\tau) = i(\delta_{\lambda\lambda_0} - 1 + \delta_{\lambda-\lambda_0}B)\exp\{-i\varepsilon_\lambda\tau\}$$
$$- i\delta_{\lambda-\lambda_0}B\exp\{-i(2\mu_2 - \varepsilon_\lambda)\tau\}. \tag{21}$$

The first exponential corresponds to the free motion of particles in the excited nucleus with two particles above the core and the second to the ground, paired, state of this nucleus.

The coefficient B is determined by a comparison of the spectral representations for G^{2-}_λ and G^{1+}_λ with the expressions (15) and (21); we get:

$$B = |\langle\Phi_1 a_{-\lambda},\Phi_2\rangle|^2 = |\Delta_2/2(\varepsilon_\lambda - \mu_2)|^2. \tag{22}$$

Thus

$$G^{1+}_\lambda(\tau) = i(\delta_{\lambda\lambda_0} - 1 + \delta_{\lambda-\lambda_0}|\Delta_2/2(\varepsilon_\lambda - \mu_2)|^2)\exp\{-i\varepsilon_\lambda\tau\}$$
$$- i\delta_{\lambda-\lambda_0}|\Delta_2/2(\varepsilon_\lambda - \mu_2)|^2\exp\{-i(2\mu_2 - \varepsilon_\lambda)\tau\}. \tag{23}$$

A comparison of this expression with the general expansion of G^{1+}_λ leads to the following relation ($\lambda \neq \lambda_0$):

$$\sum_s |\langle\Phi_1 a_\lambda \Phi_{2s}\rangle|^2 = 1 - |\Delta_2/2(\varepsilon_\lambda - \mu_2)|^2\,\delta_{\lambda-\lambda_0}, \tag{24}$$

where the summation is taken over all excited states Φ_{2s} that correspond to a prescribed excitation energy $\Delta E_{2s} = \epsilon_\lambda - \epsilon_{\lambda_0} + 2(\epsilon_{\lambda_0} - \mu_2)$. Also it is not hard to see that the function $G^{1+}_\lambda(\tau)$ defined by Eq. (23) satisfies the equation

$$(i\partial/\partial\tau - \varepsilon_\lambda)\, G^{1+}_\lambda(\tau) + i\delta_{\lambda-\lambda_0}\,\Delta_2 F^{2-}_\lambda(\tau) = 0. \tag{25}$$

Let us consider a nucleus with three nucleons above the closed shell. In this case the wave function of the ground state is of the form

$$\Phi_3 = a^+_{\lambda_0}\Phi'_2, \tag{26}$$

where

$$\Phi'_2 = \sum_\lambda c'_\lambda b^+_\lambda \Phi'_0$$

is a state with angular momentum zero, which in general does not coincide with the wave function Φ_2 of the ground state, owing to the perturbing effect of the third particle on the pairing. Obviously in the ground state Φ_3 the one-particle state with angular-momentum component $-\lambda_0$ is a free state.[5] Therefore the Green's function for this state is

$$G^{3-}_{-\lambda_0}(\tau) \equiv 0. \tag{27}$$

It is also not hard to see that to accuracy $\sim A^{-1/3}$ by taking off the odd particle in the state λ_0 [this process is described by the function $G^{3-}_{\lambda_0}(\tau)$] we get a nucleus with two particles above the closed core in the ground state. It is not hard to make the calculation for this case, if in the equations of motion we estimate the terms that arise owing to pairing by breaking the expression up into a sum over intermediate states and keeping only the ground states. By using the spectral representation we thus get:

$$G^{3-}_{\lambda_0}(\tau) = i\exp\{-i(E_3 - E_2)\tau\}. \tag{28}$$

For $\lambda \neq \pm\lambda_0$ the Green's function $G^{3-}_\lambda(\tau)$ is obviously determined like the function $G^{2-}_\lambda(\tau)$ for the two particles above the closed core. In fact, by using the wave function Φ_3 of the ground state and the hypothesis that there is only one paired state for this nucleus, we find from Eq. (5);

$$(i\partial/\partial\tau - \varepsilon_\lambda)\, G^{3-}_\lambda(\tau) - i\Delta_3 F^{3-}_\lambda(\tau) = 0,$$
$$(i\partial/\partial\tau - 2\mu_3 + \varepsilon_\lambda)\, F^{3-}_\lambda(\tau) = 0,$$
$$(i\partial/\partial\tau - 2\mu_3 + \varepsilon_\lambda)\, F^{1+}_\lambda(\lambda) + i\Delta_3 G^{1+}_\lambda(\tau) = 0, \tag{29}$$

where

$$\Delta_3 = \sum_{\lambda_1} g_{\lambda\lambda_1}(-1)^{\lambda-\lambda_1} F^{3-}_{\lambda_1}(0). \tag{30}$$

In these equations the functions $F_\lambda(\tau)$ are defined by the general formulas (3), and the respective spectral representations (4) hold for them. It follows from these definitions that

$$F^{1+}_\lambda(0) = F^{3-}_\lambda(0) = 0 \text{ for } \lambda = \pm\lambda_0. \tag{31}$$

Therefore two terms ($\lambda_1 = \pm\lambda_0$) are absent from the sum (30).

The solution of the equations (29) obtained by using the spectral representation is ($\lambda \neq \pm\lambda_0$)

$$F_{\lambda}^{1+}(\tau) = -\tfrac{1}{2}\Delta_3(\varepsilon_\lambda - \mu_3)^{-1}\exp\{-i\varepsilon_\lambda\tau\},$$
$$F_{\lambda}^{3-}(\tau) = -\tfrac{1}{2}\Delta_3(\varepsilon_\lambda - \mu_3)^{-1}\exp\{-i(2\mu_3 - \varepsilon_\lambda)\tau\},$$
$$G_{\lambda}^{3-}(\tau) = i\,|\Delta_3/2(\varepsilon_\lambda - \mu_3)|^2\exp\{-i(2\mu_3 - \varepsilon_\lambda)\tau\}. \quad (32)$$

The quantities μ_3 and Δ_3 which characterize the pairing in this nucleus are determined from the normalization conditions and Eq. (30). Recalling the relations (28) and (31), we have:

$$1 = |\bar{g}|\sum_{\lambda}{}'(1 - \delta_{\lambda\lambda_0} - \delta_{\lambda-\lambda_0})/2(\varepsilon_\lambda - \mu_3),$$
$$2 = \sum_{\lambda}{}'|\Delta_3/2(\varepsilon_\lambda - \mu_3)|^2(1 - \delta_{\lambda\lambda_0} - \delta_{\lambda-\lambda_0}), \quad (33)$$

where $\bar{g}$ is the renormalized matrix element (Sec. 2).

By means of Eqs. (33) and (18) we can calculate the differences $\mu_3 - \mu_2$ and $\Delta_3 - \Delta_2$. In first approximation we find:

$$\mu_3 - \mu_2 = \Delta_2^2/4(\varepsilon_{\lambda_0} - \mu_2),$$
$$\Delta_3 - \Delta_2 = -\tfrac{1}{4}\Omega_0[\Delta_2/2(\varepsilon_{\lambda_0} - \mu_2)]^4\Delta_2.$$

It follows from this that the pairing energy in an odd nucleus with three particles above a closed core is smaller than the pairing energy in the preceding even nucleus.

4. THE LIMITING CASE OF A SINGLE DEGENERATE LEVEL

In the limiting case of a single degenerate level the derivation of the equations for the Green's function is decidedly simplified. This simplification arises from the fact that the wave functions of the ground and excited states are known in this case.[7] The resulting system of equations for the Green's functions is, for an arbitrary number N of particles in the given degenerate level:

$$(i\partial/\partial\tau - \varepsilon_\lambda - 2g)G_{\lambda}^{N+}(\tau) - i\overset{+*}{\Delta}_N F_{\lambda}^{N+}(\tau) = 0,$$
$$(i\partial/\partial\tau - 2\overset{+}{\mu}_N + \varepsilon_\lambda)F_{\lambda}^{N+}(\tau) + i\overset{+}{\Delta}_N G_{\lambda}^{N+}(\tau) = 0,$$
$$(i\partial/\partial\tau - \varepsilon_\lambda)G_{\lambda}^{N-}(\tau) - i\overset{-*}{\Delta}_N F_{\lambda}^{N-}(\tau) = 0,$$
$$(i\partial/\partial\tau - 2\overset{-}{\mu}_N + \varepsilon_\lambda + 2g)F_{\lambda}^{N-}(\tau) + i\overset{-}{\Delta}_N G_{\lambda}^{N-}(\tau) = 0. \quad (34)$$

The initial conditions are

$$G_{\lambda}^{N+}(0) = G_{\lambda}^{N-}(0) - i, \qquad \overset{-}{\mu}_{N+2} = \overset{+}{\mu}_N, \quad F_{\lambda}^{N+2-}(0) = F_{\lambda}^{N+}(0),$$
$$N = -i\sum_{\lambda} G_{\lambda}^{N-}(0), \qquad \overset{\pm}{\Delta}_N = \sum_{\lambda_1} g_{\lambda\lambda_1}(-1)^{\lambda-\lambda_1} F_{\lambda_1}^{N\pm}(0),$$
$$g = g_{\lambda\lambda}.$$

The equations (34) are obtained by breaking up the four-poles in Eq. (5) into sums over intermediate states. Because of the properties of the wave functions of the ground states, these sums contain only one term, which corresponds to the ground state.

By means of Eq. (15) one can proceed by recurrence to find the Green's functions for all the nuclei that correspond to the filling up of the given level. The recurrence scheme is treated independently for the even and odd nuclei. For the beginning of the recurrence scheme one needs to know the explicit form of the functions $F_{\lambda}^{2-}(0)$ and $F_{\lambda}^{3-}(0)$, which are calculated by means of Eq. (3). Using the initial conditions and the spectral representation we get

$$G_{\lambda}^{2+}(\tau) = i(2 - \Omega)\Omega^{-1}\exp\{-i(\varepsilon_\lambda - 2g)\tau\},$$
$$G_{\lambda}^{2-}(\tau) = i2\Omega^{-1}\exp\{-i(\varepsilon_\lambda + g\Omega)\tau\}. \quad (35)$$

In this case the energy of the ground state of the nucleus with two nucleons in the unfilled level ϵ_λ turns out to be

$$E_2 = 2\varepsilon_\lambda + g\Omega. \quad (36)$$

For the first odd nucleus the pairing will manifest itself only in the state $-\lambda_0$ which is coupled with the state λ_0 in which the odd particle is placed. Therefore $G_{\lambda}^{1-}(\tau)$ corresponds to the free motion of the particle

$$G_{\lambda}^{1-}(\tau) = i\delta_{\lambda\lambda_0}\exp\{-i\varepsilon_\lambda\tau\}.$$

At the same time $G_{\lambda}^{1+}(\tau)$ becomes unfree for $\lambda = -\lambda_0$:

$$G_{\lambda}^{1+}(\tau) = i(\delta_{\lambda\lambda_0} - 1 + \delta_{\lambda-\lambda_0}2\Omega^{-1})\exp\{-i\varepsilon_\lambda\tau\}$$
$$- i\delta_{\lambda-\lambda_0}2\Omega^{-1}\exp\{-i(\varepsilon_\lambda + g\Omega)\tau\}. \quad (37)$$

In the case of a nucleus with three nucleons in the given level the wave function of the ground state can be written in the form

$$\Phi_3 = \overset{+}{a}_{\lambda_0}\Phi_2', \quad (38)$$

where λ_0 is the state in which there is an odd particle, and Φ_2' differs from the wave function Φ_2 of the second nucleus by a factor which is obtained from the normalization requirement for Φ_3:

$$\Phi_2' = \sqrt{\Omega/(\Omega - 2)}\,\Phi_2.$$

Using the wave function Φ_3, one can easily obtain expressions for the Green's functions of the third nucleus:

$$G_{\lambda_0}^{3-}(\tau) = i\left[\frac{2}{\Omega}\exp\{-i[\varepsilon_\lambda + g(\Omega - 2)]\tau\}\right.$$
$$\left.+ \frac{\Omega - 2}{\Omega}\exp\{-i(\varepsilon_\lambda - 2g)\tau\}\right], \qquad G_{-\lambda_0}^{3-}(\tau) \equiv 0,$$
$$G_{\lambda}^{3-}(\tau) = i\frac{2}{\Omega - 2}\exp\{-i[\varepsilon_\lambda + g(\Omega - 2)]\tau\}, \quad \lambda \neq \pm\lambda_0;$$
$$G_{-\lambda_0}^{3+}(\tau) = -i\left[\frac{\Omega - 4}{\Omega}\exp\{-i(\varepsilon_\lambda - 2g)\tau\}\right.$$
$$\left.+ \frac{4}{\Omega}\exp\{-i[\varepsilon_\lambda + g(\Omega - 2)]\tau\}\right], \qquad G_{\lambda_0}^{3+}(\tau) \equiv 0,$$
$$G_{\lambda}^{3+}(\tau) = i\frac{4 - \Omega}{\Omega - 2}\exp\{-i(\varepsilon_\lambda - 2g)\tau\}, \quad \lambda \neq \pm\lambda_0. \quad (39)$$

By using the results for the second and third nuclei and the recurrence scheme which has been indicated, one can obtain the parameters of a system with an arbitrary number N of particles. In particular, the energy of the ground state of a system with an even number of particles is

$$E_N = N\varepsilon_\lambda + \tfrac{1}{2} Ng(\Omega - N + 2). \qquad (40)$$

This expression agrees completely with the quantity obtained by Mottelson.[7] At the same time, the method of quasi-particles gives for this case an expression that agrees with Eq. (40) only in the limit $\Omega \gg 1$.

CONCLUSION

A direct experimental test of the results obtained here can be made by means of stripping or pickup reactions. In fact, a knowledge of the density matrix gives direct information about the nuclear matrix element that determines the cross section of the stripping reaction. For example, for the case of a nucleus with two nucleons above a closed shell

$$\rho_\lambda^{(2)} = \sum_s |\langle \Phi_2 a_\lambda^+ \Phi_{1s}\rangle|^2 = |\Delta_2 / 2(\varepsilon_\lambda - \mu_2)|^2,$$

where all the states s refer to a given level ϵ_λ. If the independent-particle model were valid, then, for example, a pickup reaction could occur only from states corresponding to the single level ϵ_{λ_0}.

In the presence of pairing the pickup reaction can also occur from other levels ϵ_λ. For constant Δ_2 the ratio of the squares of the corresponding matrix elements is given by

$$|(\varepsilon_{\lambda_0} - \mu_2)/(\varepsilon_{\lambda_1} - \mu_2)|^2.$$

Since $\epsilon_{\lambda_1} - \epsilon_{\lambda_0}$ is a quantity of the order of $\epsilon_{\lambda_0} - \mu_2$, this ratio is of the order of unity. Therefore in principle the pickup reaction can occur for all states inside the shell that is being filled up. Incidentally, such reactions can be used to test the hypothesis of the constancy of Δ. The considerations that have been given are of course valid for all spherical even and odd nuclei. If, however, the number of nucleons above the closed shell is large, other effects become important, which can mask the pair-correlation effects.

In conclusion the writers express their deep gratitude to A. B. Migdal for proposing this problem and for many suggestions.

Translated by W. H. Furry
43

---

[1] N. N. Bogolyubov, V. V. Tolmachev, and D. V. Shirkov, Новый метод в теории сверхпроводимости (A New Method in the Theory of Superconductivity), Moscow, Acad. Sci. Press, 1958.

[2] L. P. Gor'kov, JETP **34**, 735 (1958), Soviet Phys. JETP **7**, 504 (1958).

[3] S. T. Belyaev, Kgl. Danske Videnskab. Selskab. Mat.-fys. Medd. **31**, No. 11 (1959).

[4] A. B. Migdal, JETP **37**, 249 (1959), Soviet Phys. JETP **10**, 176 (1960).

[5] Grin', Drozdov, and Zaretskiĭ, JETP **38**, 222 and 1297 (1960), Soviet Phys. JETP **11**, 162 and 936 (1960).

[6] A. B. Migdal, JETP **40**, 684 (1960), Soviet Phys. JETP, in press.

[7] B. R. Mottelson, The Many Body Problem, Dunod, 1958, page 283.

SOVIET PHYSICS JETP VOLUME 13, NUMBER 1 JULY, 1961

POLARIZATION EFFECTS IN THE SCATTERING OF MUONS ON PROTONS

G. V. FROLOV

Radium Institute, Academy of Sciences, U.S.S.R.

Submitted to JETP editor July 29, 1960

J. Exptl. Theoret. Phys. (U.S.S.R.) **40**, 296-297 (January, 1961)

The polarization of recoil protons and scattered μ mesons during the scattering of polarized μ mesons on unpolarized protons is computed by taking into account the proton electromagnetic form factors.

WE report here the calculated polarization of the recoil protons and scattered μ mesons in the scattering of polarized μ mesons by unpolarized protons at rest. The form factors of the protons are taken into account. The calculations were similar to those carried out for electrons,[1,2] the only exception being the account of the μ-meson rest mass m.

We shall define the polarization of the recoil proton in terms of a vector $\mathbf{Z}_2^0$, the average value of the spin operator in the rest system. The polarization vectors for the incident and scattered μ mesons are denoted ζ_1^0 and ζ_2^0, respectively. It is convenient to resolve the polarization vectors into longitudinal and transverse components, defined for the incident meson in the following fashion:

$$\zeta_{1l}^0 = \zeta_1^0 \mathbf{p}_1 / |\mathbf{p}_1|, \qquad \zeta_{1t}^{0\perp} = \zeta_1^0 \mathbf{n}, \quad \zeta_{1t}^{0\parallel} = \zeta_1^0 [\mathbf{p}_1 \mathbf{n}] / |\mathbf{p}_1|. \quad (1)^*$$

Here $\mathbf{n} = (\mathbf{p}_1 \times \mathbf{p}_2)/|(\mathbf{p}_1 \times \mathbf{p}_2)|$, where $\mathbf{p}_1$ and $\mathbf{p}_2$ are the momenta of the incident and scattered mesons. For the recoil proton and the scattered meson the definitions are analogous to (1).

We obtain for the polarization of the recoil protons

$$Z_{2l}^0 = \alpha_{ll} \zeta_{1l}^0 + \alpha_{lt} \zeta_{1t}^{0\parallel},$$
$$Z_{2t}^{0\parallel} = \alpha_{tl} \zeta_{1l}^0 + \alpha_{tt} \zeta_{1t}^{0\parallel}, \qquad Z_{2t}^{0\perp} = \alpha_{22} \zeta_{2t}^{0\perp}, \qquad (2)^*$$

where

$$\alpha_{ll} = 2M\eta\varkappa(1+\mu)[\xi^2 - \eta\xi - m^2(1+\eta)/M^2],$$
$$\alpha_{lt} = m\eta\varkappa(1+\mu)\operatorname{tg}\vartheta[2\eta + 2\eta\xi - \xi^2 + m^2/M^2],$$
$$\alpha_{tl} = M\xi\varkappa(1-\mu\eta)\operatorname{tg}\vartheta[\xi^2 - 2\eta\xi - 2\eta - m^2/M^2],$$
$$\alpha_{tt} = -2m\eta\varkappa(1-\mu\eta)(1+\xi),$$
$$\alpha_{22} = -2m\eta(1+\mu)(1-\mu\eta)/MN,$$
$$\varkappa = (\eta/(\eta+1))^{1/2}(1+\mu)/|p_1|N,$$
$$N = \eta(1+\mu)^2(2\eta - m^2/M^2) + (1+\mu^2\eta)(\xi^2 - 2\eta\xi - \eta).$$

We use the following notation: ϑ — scattering angle, $\xi = E_1/M$, $\mu = b/a$, $\eta = (p_1 - p_2)^2/4M^2$, E_1 — energy of incident meson, a and b — electric and magnetic form factors of the proton, respectively.[1]

For the polarization of the scattered μ mesons we have

$$\zeta_{2l}^0 = \beta_{ll} \zeta_{1l}^0 + \beta_{lt} \zeta_{1t}^{0\parallel},$$
$$\zeta_{2t}^{0\parallel} = \beta_{tl} \zeta_{1l}^0 + \beta_{tt} \zeta_{1t}^{0\parallel}, \qquad \zeta_{2t}^{0\perp} = \beta_{22} \zeta_{1t}^{0\perp}, \qquad (3)$$

where

$$\beta_{ll} = \{(1+\mu^2\eta)[\xi(\xi-2\eta)(1+\cos^2\vartheta) - 2\eta - m^2M^{-2}\sin^2\vartheta] + 2\eta(1+\mu)^2[\xi(\xi-2\eta)\sin^2\vartheta - 2\eta - m^2/M^2]\}/2N\cos\vartheta,$$
$$\beta_{lt} = m\sin\vartheta[(1+\mu^2\eta)(\eta-\xi) + \eta(1+\mu)^2(\xi+2\eta)]/MN,$$
$$\beta_{tl} = m\sin\vartheta[(1+\mu^2\eta)(\xi-\eta) - \eta(1+\mu)^2\xi]/MN,$$
$$\beta_{tt} = \{(1+\mu^2\eta)[\xi(\xi-2\eta)(1+\cos^2\vartheta) - 2\eta - m^2M^{-2}\sin^2\vartheta] - 2\eta(1+\mu)^2 m^2M^{-2}\cos^2\vartheta\}/2N\cos\vartheta,$$
$$\beta_{22} = \{(1+\mu^2\eta)(\xi^2 - 2\eta\xi - \eta) - m^2\eta(1+\mu)^2/M^2\}/N.$$

The proton form factors contained in these formulae are determined from electron-scattering experiments. The only assumptions made in the derivation of the formulae were that the first Born approximation in the electromagnetic field is valid and that the μ meson is point-like. Consequently if the deviations from these formulae exceed the corrections of the second Born approximations, this will serve as evidence of the presence of μ-meson structure.

---

*$[\mathbf{p}_1 \mathbf{n}] = \mathbf{p}_1 \times \mathbf{n}$; tg = tan

[1] Akhiezer, Rozentsveĭg, and Shmushkevich, JETP **33**, 765 (1957), Soviet Phys. JETP **6**, 588 (1957).

[2] G. B. Frolov, JETP **34**, 764 (1958), Soviet Phys. JETP **7**, 525 (1958).

Translated by J. G. Adashko
44

SOVIET PHYSICS JETP VOLUME 13, NUMBER 1 JULY, 1961

SINGULARITIES OF THE SCATTERING AMPLITUDE IN PERTURBATION THEORY

A. Z. PATASHINSKIĬ, A. P. RUDIK, and V. V. SUDAKOV

Submitted to JETP editor July 29, 1960

J. Exptl. Theoret. Phys. (U.S.S.R.) **40**, 298-311 (January, 1961)

The asymptotic behavior of the position of the singularities of the "open envelope" (Fig. 3) perturbation-theory diagram is studied for one of the invariants that tend to infinity. It is shown that in the general case the "open envelope" has two singular curves. A method is developed for reducing the problem of determining the singularities of any perturbation theory diagram with four external lines to the problem of the "open envelope" diagram (Fig. 1) with certain effective masses of virtual particles. Minorants are established for the effective masses. The results are applied to a perturbation-theoretical analysis of $\pi\pi$, KK and NN scattering in the case when one of the invariants that characterize the scattering amplitude tends to infinity. It is found that under these conditions the $\pi\pi$ scattering amplitude has no anomalous singularities in any perturbation-theory approximation. Conditions are indicated under which the absence of anomalous singularities in the perturbation-theory diagram can be established in a number of cases for KK and NN scattering amplitudes.

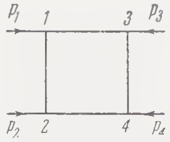

FIG. 1

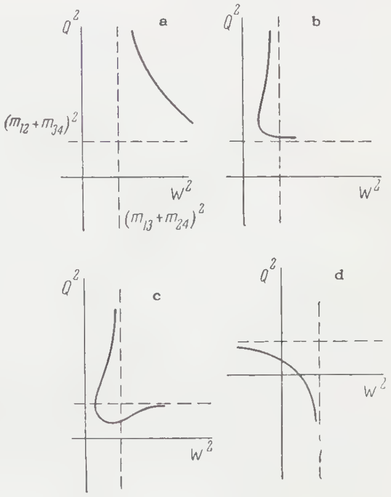

FIG. 2

1. INTRODUCTION

THE present work is devoted to an investigation of the status of the singularities of the scattering amplitude in perturbation theory. For greater clarity in formulation, we recall the properties possessed by the singular curves of the simplest diagram of perturbation theory (Fig. 1), which has been analyzed in detail by Karplus, Sommerfeld, and Wichman,[1] Landau,[2] Mandelstam,[3] Kolkunov,[4] Tarski,[5] and Vladimirov.[6]

In view of the conservation of the 4-momenta of the scattered particles, the 4-momenta of the scattered and virtual particles for any perturbation-theory diagram will lie in a 3-dimensional space.[2,7] It is convenient to use as the basis vectors of this space the following three linearly-independent 4-vectors:

$$W = p_1 + p_2, \quad Q = p_1 + p_3, \quad P = p_1 + p_4. \qquad (1.1)$$

If we put $p_i^2 = M_i^2$ ($i = 1, \ldots, 4$), then

$$2QW = M_1^2 - M_2^2 - M_3^2 + M_4^2,$$

$$2WP = M_1^2 - M_2^2 + M_3^2 - M_4^2, \quad 2QP = M_1^2 + M_2^2 - M_3^2 - M_4^2,$$

$$Q^2 + W^2 + P^2 = M_1^2 + M_2^2 + M_3^2 + M_4^2. \qquad (1.2)$$

As follows from (1.2), the vectors W, Q, and P are orthogonal if $M_1 = M_2 = M_3 = M_4$.

The scattering amplitude is characterized in general by six parameters. It is convenient to use as these parameters the four quantities M_i^2 and two invariants, say W^2 and Q^2. We shall consider the singularities only with real invariants. At the singularity, a certain connection exists between W^2, Q^2, and the masses of the virtual particles. Figure 2 shows cases of singular curves for the diagram of Fig. 1 (the mass m_{ik} corresponds to a virtual particle going from the vertex i to the vertex k). In accordance with the standard terminology, we shall call singular curves of type a

(Fig. 2) normal, while singular curves of type b, c, and d will be called anomalous. We note that a characteristic of normal singular curves is that they are completely contained in the domain $|Q^2| > (m_{12} + m_{34})^2$; $|W^2| > (m_{13} + m_{24})^2$, while anomalous curves are partially located outside this domain.

The question arises of the conditions under which anomalous singularities occur for perturbation-theory diagrams that are more complicated than Fig. 1. An attempt to answer this question is made in the present paper. The analysis is carried out in the asymptotic case, when one of the invariants tends to infinity. As a criterion of an anomalous singular curve we use the condition $|W^2(Q^2)| < |W^2(\infty)|$.

We investigate first the singularities of a diagram of the "open envelope" type (Fig. 3) and establish the asymptotic conditions for the existence of anomalous singularities. It is shown that, unlike the diagram of Fig. 1, the singular curve of the "open envelope" has several branches.

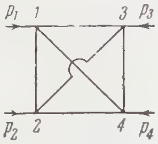

FIG. 3

We then consider an arbitrary complicated perturbation-theory diagram. It is shown that its singularities coincide in the general case (and not only asymptotically) with the singularities of an "open envelope" diagram, in which the masses of the virtual particles are replaced by certain effective masses that depend on W^2 and Q^2. In the general case one succeeds in finding a minorant, independent of the values W^2 and Q^2, for these effective masses. This makes it possible to verify in the asymptotic case the conditions of existence of anomalous singularities for several classes of perturbation-theory diagrams. The method developed is applied to the analysis of pion-pion, kaon-kaon, and nucleon-nucleon scattering amplitudes.

2. METHOD OF DETERMINING THE SINGULARITIES

The singular curves of perturbation-theory diagrams are determined by a method proposed by Landau.[2] It will be found more convenient, however, to modify somewhat the original Landau equations of references 2 and 7. Instead of the 4-momentum q_{ik} of the virtual particle travelling from the vertex i to the vertex k, we introduce the 4-vector $a_{ik} = \alpha_{ik} q_{ik}$ ($a_{ik} = - a_{ki}$), where α_{ik} is the Feynman parameter of the virtual line "ik." In addition we introduce instead of α_{ik} the quantity $\beta_{ik} = 1/\alpha_{ik}$ ($1 \leq \beta_{ik} \leq \infty$). Then the initial equations for finding the singularities of any perturbation-theory diagram have the following form

$$\sum_{(k)}{}' \beta_{ik} a_{ik} = p_i, \tag{2.1}$$

$$\sum_{(c)} a_{ik} = 0, \tag{2.2}$$

$$m_{ik}^2 = \beta_{ik}^2 a_{ik}^2. \tag{2.3}$$

Equations (2.1) express the law of conservation of 4-momenta at each of the vertices of the diagram (for internal vertices $p_i = 0$). The summation in (2.2) is over each independent contour of the diagram. Equations (2.3) signify that the virtual particles lie on the energy surface at the singularity. Simultaneous solution of the system (2.1) — (2.3) yields the dependence of Q^2 on W^2 at the singular point of the diagram. The prime at the summation sign in (2.1) indicates the absence of the term with i = k.

3. THE "OPEN ENVELOPE" DIAGRAM

Let us consider the system (2.1) — (2.3) for the "open envelope." In this case there are four vertices and six 4-vectors a_{ik}, viz. a_{12}, a_{14}, a_{34}, a_{24}, a_{13}, and a_{23}. Using (2.2) for three independent contours, we can express the vectors a_{24}, a_{13}, and a_{23} in terms of a_{12}, a_{14}, and a_{34}. Next, introducing in lieu of p_i the vectors W, Q, and P [according to (1.1)], we transform (2.1) into

$$a_{12}(\beta_{12} + \beta_{23}) + a_{14}(\beta_{14} - \beta_{23}) - a_{34}(\beta_{34} + \beta_{23}) = Q,$$

$$-a_{12}(\beta_{23} + \beta_{24}) + a_{14}(\beta_{13} + \beta_{14} + \beta_{23} + \beta_{24})$$

$$+ a_{34}(\beta_{13} + \beta_{23}) = W,$$

$$a_{12}(\beta_{12} + \beta_{24}) + a_{14}(\beta_{13} - \beta_{24}) + a_{34}(\beta_{13} + \beta_{34}) = P. \tag{3.1}$$

Using (3.1) in conjunction with (2.2) we can express all the a_{ik} in terms of β, P, and the vectors Q, and W. The appropriate formulas are given in Appendix I. Using these values of a_{ik} we obtain, after substituting in (2.3) and eliminating β, the singular curve $Q^2 = Q^2(W^2)$. However, the process of eliminating is in general exceedingly cumbersome.* We therefore confine ourselves merely to a consideration of the asymptotic case $Q^2 \to \infty$. This of necessity implies $\beta_{12} \to \infty$ and $\beta_{34} \to \infty$.[9]

---

*The system (2.3) can be solved easily only if the "open envelope" has a high degree of symmetry.[8]

Introducing

$$\gamma_{ik} = \beta_{ik} / (\beta_{13} + \beta_{14} + \beta_{23} + \beta_{24}) \quad (\gamma_{13} + \gamma_{14} + \gamma_{23} + \gamma_{24} = 1)$$

we obtain from equations (A 1.2), (A 1.3) and (2.3), accurate to terms that tend to zero,

$$m_{12}^2 + W^2 (\gamma_{13} + \gamma_{14})(\gamma_{23} + \gamma_{24}) - [M_1^2 (\gamma_{23} + \gamma_{24}) + M_2^2 (\gamma_{13} + \gamma_{14})] = Q^2 (\gamma_{13}\gamma_{24} - \gamma_{14}\gamma_{23}) / \gamma_{34}, \tag{3.2}$$

$$m_{34}^2 + W^2 (\gamma_{13} + \gamma_{23})(\gamma_{14} + \gamma_{24}) - [M_3^2 (\gamma_{14} + \gamma_{24}) + M_4^2 (\gamma_{13} + \gamma_{23})] = Q^2 (\gamma_{13}\gamma_{24} - \gamma_{14}\gamma_{23}) / \gamma_{12}. \tag{3.3}$$

Before we use the remaining equations of (2.3), let us note the following important fact. Generally speaking, the system (2.1) — (2.3) for the "open envelope" is on the whole a complicated algebraic system of thirty-sixth order. There is therefore no a priori guarantee that the solution of this system is unique. In fact, even for the simplest perturbation-theory diagram, that of Fig. 1, there are two solution branches. To be sure, one of these branches is fictitious in view of the condition $\beta \geq 1$. But in the case of an "open envelope," for which the system (2.1) — (2.3) is more complicated than that for Fig. 1, it turns out that the condition $\beta \geq 1$ is not sufficient to single out one branch of the solution. We shall determine all the possible solutions for the "open envelope" under the condition $Q^2 \to \infty$. The various solutions differ in the manner by which $Q^2 = Q^2(\beta_{12}, \beta_{34}) \to \infty$ as $\beta_{12} \to \infty$ and $\beta_{34} \to \infty$. It is obvious from (2.3) and from (A 1.4) — (A 1.6) that $Q^2/(\beta_{12}, \beta_{34})$ cannot tend to a constant value as $\beta_{12} \to \infty$ and $\beta_{34} \to \infty$ and when $\kappa > 1$. Consequently, only the following two principally different cases are possible: $\kappa < 1$ and $\kappa = 1$.

We consider first the case $\kappa < 1$. Then, as shown in Appendix I

$$\frac{|W|}{m_{13} + m_{14} + m_{23} + m_{24}} = 1 + \frac{Q^2}{2\gamma_{12}\gamma_{34}} \frac{\gamma_{13}\gamma_{24} - \gamma_{14}\gamma_{23}}{(m_{13} + m_{14} + m_{23} + m_{24})^2} + \frac{Q^4 m_{13} m_{24}}{8 (\gamma_{12}\gamma_{34})^2 (m_{13} + m_{14} + m_{23} + m_{24})^6}, \tag{3.4}$$

$$\gamma_{13}\gamma_{24} - \gamma_{14}\gamma_{23} = \frac{m_{13}m_{24} - m_{14}m_{23}}{(m_{13} + m_{14} + m_{23} + m_{24})^2} + \frac{Q^2}{2\gamma_{12}\gamma_{34}} \frac{m_{13}m_{24}}{(m_{13} + m_{14} + m_{23} + m_{24})^4}. \tag{3.5}$$

The value of κ depends on the value of $\epsilon = m_{13}m_{24} - m_{14}m_{23}$. There are two possibilities: a) $\epsilon \neq 0$ and b) $\epsilon = 0$.

a) If $\epsilon \neq 0$, we can neglect the second term in (3.5) and the third term in (3.4). It follows then from (3.2) and (3.3) that $\kappa = 1/2$ and Q^2/γ_{12} (or Q^2/γ_{34}) remains constant as $\beta_{12} \to \infty$ and $\beta_{34} \to \infty$.* Since the right halves of (3.2) and (3.3) are proportional here to the deviation of the quantity $|W|/(m_{13} + m_{14} + m_{23} + m_{24})$ from unity, the following conditions should be satisfied for the case of the anomalous singular curve, when $|W| < (m_{13} + m_{14} + m_{22} + m_{23})$ [the quantities γ_{13}, γ_{14}, γ_{23}, and γ_{24} in (3.2) and (3.3) are now replaced by their values given in (A 1.14)]:

$$m_{12}^2 + (m_{13} + m_{14})(m_{23} + m_{24}) < \frac{M_1^2 (m_{23} + m_{24}) + M_2^2 (m_{13} + m_{14})}{m_{13} + m_{14} + m_{23} + m_{24}}, \tag{3.6}$$

$$m_{34}^2 + (m_{13} + m_{23})(m_{14} + m_{24}) < \frac{M_3^2 (m_{14} + m_{24}) + M_4^2 (m_{13} + m_{23})}{m_{13} + m_{14} + m_{23} + m_{24}}. \tag{3.7}$$

Let us analyze the inequalities (3.6) and (3.7). When both inequalities are satisfied, the "open envelope" has asymptotically anomalous singularities. It is obvious that as the masses of the virtual particles are increased these inequalities are less and less satisfied. When both inequalities (3.6) and (3.7) are violated, the singular curves are of the normal type. Finally, when one of the inequalities, either (3.6) or (3.7), is satisfied while the other is violated, the "open envelope" has no singularities as $Q^2 \to \infty$.

b) If $\epsilon = 0$, it follows from (3.5), (3.2), and (3.3) that $\kappa = 3/4$ and $Q^4/\gamma_{12}\gamma_{13}^2$ (or $Q^4/\gamma_{12}^2\gamma_{34}$) remain finite as $\beta_{12} \to \infty$ and $\beta_{34} \to \infty$. Further, it follows from (3.4) and (3.5) that when $\epsilon = 0$ the value of $|W|/(m_{13} + m_{14} + m_{23} + m_{24})$ is always greater than unity:

$$\frac{|W|}{m_{13} + m_{14} + m_{23} + m_{24}} = 1 + \frac{3Q^4 m_{13} m_{24}}{8 (m_{13} + m_{14} + m_{23} + m_{24})^6 (\gamma_{12}\gamma_{34})^2}, \tag{3.8}$$

that is, in case b) the singular curves are of the normal type.

Let us note another fact. As follows from the derivation of all the formulas in the present section, the results obtained for the "open envelope" can be directly generalized to the case of the simpler diagrams shown in Figs. 1 and 4. For this purpose it is necessary to put $\beta_{14} = \beta_{23} = 0$ for the diagram of Fig. 1, and $\beta_{14} = 0$ for the diagram of Fig. 4. Now the case b) becomes impossible for the diagrams of Figs. 1 and 4, by virtue of the condition $\beta_{13}\beta_{24} \neq 0$, and the solution obtained is unique: Q^2/β_{12} (or Q^2/β_{34}) tends to a constant value as $\beta_{12} \to \infty$ and $\beta_{34} \to \infty$. The conditions for the

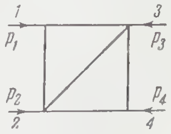

FIG. 4

---

*The connection between β_{12} and β_{34} can be readily obtained from (3.2) and (3.3).

existence of anomalous singularities are obtained for the diagram of Fig. 1 from (3.6) and (3.7) with $m_{14} = m_{23} = 0$, and for the diagram of Fig. 4 with $m_{14} = 0$.

4. SPECIFIC CASE OF "OPEN ENVELOPE" SINGULARITY

Let us consider now the case when $\kappa = 1$. As follows from (3.2) and (3.3), this is possible only when $\gamma_{13}\gamma_{24} - \gamma_{14}\gamma_{23} \rightarrow 0$, as $1/\gamma_{34}$ or $1/\gamma_{12}$.*

Generally speaking, we readily obtain from (2.3) and (A 1.3) — (A 1.7) an equation to relate Q^2, W^2 and β^2 when $\kappa = 1$. In the general case, however, these equations are much more complicated then (A 1.8) — (A 1.11). We therefore confine ourselves only to the case in which

$$Q^2/\gamma_{12}\gamma_{34} \sim (m_{13}m_{24} - m_{14}m_{23})$$
$$\ll (m_{13} + m_{14} + m_{23} + m_{24})^2.$$

Under these conditions, the expansions used to derive (A 1.8) — (A 1.11) are valid, and expressions (3.4) and (3.5) hold accordingly. Recognizing that $\gamma_{13}\gamma_{24} - \gamma_{14}\gamma_{23} \rightarrow 0$, we obtain from (3.4) and (3.5)

$$\frac{|W|}{m_{13} + m_{14} + m_{23} + m_{24}} = 1 + \frac{1}{2}\,\frac{(m_{13}m_{24} - m_{14}m_{23})^2}{m_{13}m_{24}(m_{13} + m_{14} + m_{23} + m_{24})^2}. \tag{4.1}$$

We find therefore that in the case of the "open envelope" there can exist, in addition to the asymptote $W^2 = (m_{13} + m_{14} + m_{23} + m_{24})^2$, also an asymptote at a larger value of W^2, as determined by (4.1). This is the first example known to us in which, as $Q^2 \rightarrow \infty$, the asymptotic value of $W^2(Q^2)$ does not coincide for some perturbation-theory diagram with the square of the sum of the masses over any section of the diagram perpendicular to the vector W.

The asymptotic form of the dependence $W^2 = W^2(Q^2)$ is obtained in Appendix I for $\kappa = 1$, $\beta_{12} \rightarrow \infty$, and $\beta_{34} \rightarrow \infty$. It follows from Fig. 5, that here, too, the singular curves are of the anomalous type if the inequalities (3.6) and (3.7) are satisfied.

We note that although the solution $\kappa = 1$ has been obtained subject to the condition $|m_{13}m_{24} - m_{14}m_{23}| \ll W^2$, there are no grounds for assuming that it will vanish when this condition is violated.

The foregoing analysis of the asymptotic form of singular curves for the "open envelope" indicates that the system (2.1) — (2.3) has in this case three solutions. The first corresponds to the condition $\epsilon \neq 0$ and leads to $\kappa = 1/2$. The second solution corresponds to the particular case $\epsilon = 0$ and leads to $\kappa = 3/4$. (The singular curves are in this case asymptotically of normal form).* The third solution is obtained under the assumption $\epsilon/W^2 \ll 1$ and leads to $\kappa = 1$. Here the value of $W^2(\infty)$ is determined by Eq. (4.1) and does not coincide with $W^2(\infty) = (m_{13} + m_{14} + m_{23} + m_{24})^2$. The singularities of the first and third solutions are of the anomalous types if conditions (3.6) and (3.7) are satisfied.

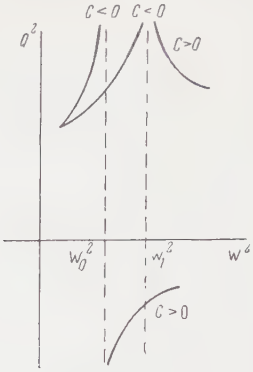

FIG. 5

5. REDUCTION OF SINGULARITIES OF ANY PERTURBATION-THEORY DIAGRAM TO THE SINGULARITIES OF THE "OPEN ENVELOPE" DIAGRAM

Let us analyze the original Landau equations for the determination of the singular curves of an arbitrary perturbation-theory diagram, written in the form (2.1) — (2.3).

Equations (2.1) and (2.2) determine completely the 4-vectors a_{ik} in terms of β and p_i.[7] By virtue of its linearity, the system (2.1) and (2.2) has a unique solution. We seek a_{ik} in the form

$$a_{ik} = a_i - a_k \tag{5.1}$$

Let us consider an arbitrary perturbation-theory diagram with ν vertices. For this diagram, the sum over k in (2.1) contains only terms with indices ik corresponding to vertices ik joined on the diagram. It is more convenient, however, to assume that all the vertices are pairwise interconnected on the diagram but the values of β_{ik} and m_{ik} vanish for all pairs of indices ik corresponding to vertices which are not interconnected on the diagram.

Equation (2.1) for an internal vertex $i = \nu$ can be written, with account of (5.1), in the following form:

---

*It is obvious that the case $\kappa = 0$ cannot be realized for Figs. 1 and 4.

*It follows therefore that the solution obtained in reference 8 for the particular example of "open envelope" is unique when all the masses are equal.

$$\sum_{k=1}^{k=\nu-1} \beta_{k\nu} a_{k\nu} = \sum_{k=1}^{k=\nu-1} \beta_{k\nu} a_k - a_\nu \sum_{k=1}^{k=\nu-1} \beta_{k\nu} = 0. \tag{5.2}$$

Introducing the notation*

$$\gamma_{k\nu} = \beta_{k\nu} \Big/ \sum_{l=1}^{l=\nu-1} \beta_{l\nu}, \qquad \sum_{k=1}^{k=\nu-1} \gamma_{k\nu} = 1, \tag{5.3}$$

we obtain from (5.2) and (5.1)

$$a_\nu = \sum_{k=1}^{k=\nu-1} \gamma_{k\nu} a_k, \quad \alpha_{i\nu} = a_i - a_\nu = \sum_{l=1}^{l=\nu-1} \gamma_{l\nu} a_{il}. \tag{5.4}$$

We now substitute (5.4) into any equation from (2.1), taken for a vertex $n \neq \nu$. We then obtain

$$\sum_{k=1}^{k=\nu-1} (\beta_{kn} + \beta_{n\nu}\gamma_{k\nu}) a'_{kn} = p_n. \tag{5.5}$$

If we now introduce the notation

$$\beta'_{kn} = \beta_{kn} + \beta_{n\nu}\gamma_{k\nu}, \tag{5.6}$$

then Eqs. (5.5) assume the same form as (2.1) for a diagram with $(\nu - 1)$ vertices. Introducing, further, the effective masses m'_{ik} $(i, k \neq \nu)$

$$m'_{ik} = m_{ik} \beta'_{ik} / \beta_{ik}, \tag{5.7}$$

we reduce the problem of finding the singularities of a diagram with ν vertices to the problem of finding of singularities of a diagram with $(\nu - 1)$ vertices† and to the supplementary conditions by which β'_{ik} are expressed in terms of β'_{ik}:

$$m^2_{i\nu} = \beta^2_{i\nu} a^2_{i\nu} = \beta^2_{i\nu} \Big[\sum_{l=1}^{l=\nu-1} \gamma_{l\nu} a_{il} \Big]^2, \quad (i = 1, \ldots, \nu - 1). \tag{5.8}$$

Applying successively the transformations (5.6) and (5.7) to each internal vertex of the diagram, we ultimately reduce the problem of finding the singularities of an arbitrary diagram of perturbation theory to the problem of finding singularities of the "open envelope" diagram (Fig. 3), in which the virtual-particle masses are replaced by certain effective masses, which depend on the variants W^2 and Q^2.

Let us note also a fact, to which our attention was called by I. Ya. Pomeranchuk, that since transformations (5.6) do not make use of (2.3), they are always valid (and not only on the singular curve), and can therefore be used to reduce the denominator of the Feynman integral to the principal axis relative to the 4-vectors over which the integration is carried out.

The results of this section can be formulated as follows:

Theorem 1. The singular curves of any perturbation-theory diagram for the scattering amplitude coincide with the singular curves of the "open envelope" diagram with virtual-particle effective masses that depend on the invariants.

It is obvious that the results obtained can be generalized in an elementary manner to the case of diagrams that describe processes with an arbitrary number of external particles. The role of the "open envelope" will be played here by a diagram with only exterior vertices that are pairwise interconnected by virtual particles with effective masses that depend on the invariants of the process.

6. MINORANTS FOR EFFECTIVE MASSES

The effective masses depend on the invariants W^2 and Q^2. The problem of determining this dependence coincides with the problem of the exact determination of the singular curves of an arbitrary complicated perturbation-theory diagram. The last problem, in turn, cannot be solved in the general case. One can obtain, however, certain minorants for the effective masses, which are independent of the invariants Q^2 and W^2.

First Minorant. From the condition $\beta > 0$ and Eq. (5.6) it follows that the effective mass m'_{ik} for a diagram with $(\nu - 1)$ vertices, obtained by eliminating the ν-th vertex from a diagram with ν vertices containing the ik line,* satisfies the following inequality:

$$m'_{ik} \geqslant m_{ik}. \tag{6.1}$$

In particular, denoting by μ_{ik} $(i, k = 1, \ldots, 4)$ the resultant effective masses of the "open-envelope," we get

$$\mu_{ik} \geqslant m_{ik} \tag{6.1'}$$

for all original (complex) diagrams in which the exterior vertices are directly connected to each other.

The first minorant is valid on the entire singular curve of the complex diagram.

Second minorant. The second minorant for the effective masses pertains to the asymptotic part

---

*$1 \geqslant \gamma_{ik} \geqslant 0$ inasmuch as $1 \leqslant \beta_{ik} \leqslant \infty$ for vertices ik joined on a diagram with each other, and $\beta_{ik} = 0$ for vertices ik which are not joined.

†If the initial diagram does not contain the line ik, the effective mass is determined, in accordance with (5.6) with $\beta_{ik} = 0$, by the equation

$$m'_{ik} = m_{ik} \frac{\beta'_{ik}}{\beta_{ik}} = |a_{ik}| \beta_{i\nu}\beta_{k\nu} \Big/ \sum_{l=1}^{l=\nu-1} \beta_{l\nu}.$$

*Naturally, the first minorant remains valid also when the indices ik correspond to vertices which are not connected to each other on the original diagram. However, the condition $m'_{ik} \geqslant 0$ obtained in this case is useless.

of the singular curve, when any one of the invariants characterizing the diagram tends to infinity. Assume, to be specific, that $Q^2 = (p_1 + p_3)^2$ tends to infinity and the invariant $W^2 = (p_1 + p_2)^2$ remains finite.

Then all the 4-momenta of the virtual particles fall into two classes: 4-momenta with components only along the 4-vector W, and 4-momenta with components both along the 4-vector W and along the 4-vectors Q and P. The 4-momenta of the first class correspond to finite β_{ik} and finite a_{ik}^2; 4-momenta of the second class correspond to β_{ik} which tend to infinity and to a_{ik}^2 which tend to zero (see Appendix I).

Let us examine the sum $\sum_{k=1}^{k=\nu-1} m'_{ik}$ of the effective masses in the diagram with $(\nu - 1)$ vertices, obtained from a diagram with ν vertices.

Using (5.7) we get

$$\sum_{k=1}^{k=\nu-1} m'_{ik} = \sum_{k=1}^{k=\nu-1} m_{ik} + \beta_{i\nu} \sum_{k=1}^{k=\nu-1} \frac{m_{ik}}{\beta_{ik}} \gamma_{k\nu}$$

$$= \sum_{k=1}^{k=\nu-1} m_{ik} + \beta_{i\nu} \sum_{k=1}^{k=\nu-1} |a_{ik}| \gamma_{k\nu}. \qquad (6.2)$$

Retaining in (6.2) only the 4-vectors a_{ik} that belong to the first class, and taking (5.8) into account in a fashion similar to the case when the 4-vector $a_{i\nu}$ pertains to the first class, we arrive at the inequality*

$$\sum_{k=1}^{k=\nu-1} m'_{ik} \geqslant \sum_{k=1}^{k=\nu} m_{ik}, \qquad (6.3)$$

which holds for the indices ik that characterize virtual particles with 4-momenta which belong in the asymptotic case to the first class.

Eliminating successively the interior vertices we obtain in the asymptotic case the following minorants for the resultant "open envelope"

$$\mu_{13} + \mu_{14} \geqslant \sum_{i=1}^{i=\nu} m_{1i}, \quad \mu_{23} + \mu_{24} \geqslant \sum_{i=1}^{i=\nu} m_{2i},$$

$$\mu_{13} + \mu_{23} \geqslant \sum_{i=1}^{i=\nu} m_{3i}, \quad \mu_{14} + \mu_{24} \geqslant \sum_{i=1}^{i=\nu} m_{4i}, \qquad (6.3')$$

where the index i runs through the values corresponding to the 4-vectors a_{si} ($s = 1, \ldots, 4$), belonging to the first class.

7. USE OF NORMALIZED EFFECTIVE MASSES TO DETERMINE THE TYPE OF THE SINGULAR CURVES

We have already obtained the conditions for the existence of anomalous singularities in an "open envelope" (3.6) — (3.7) for $Q^2 = (p_1 + p_3)^2 \to \infty$ and for finite values of $W^2(Q^2) = W^2(\infty)$.

Using the first minorant of the preceding section, we obtain from (3.6) and (3.7) the following theorem:

Theorem 2. An arbitrary scattering diagram is asymptotic and has no anomalous singularities if it includes a simple r diagram (similar to Figs. 1, 4, or 3) based on the exterior vertices, and if this simpler diagram contains asymptotically no singularities of the anomalous type.

Let us consider the scattering of identical particles $M_i^2 = M_2$. Then the right halves of (3.6) and (3.7) contain M^2. Let us recognize now that according to (3.4) we have in the asymptotic case for the "open envelope"*

$$W^2(\infty) = (\mu_{13} + \mu_{14} + \mu_{23} + \mu_{24})^2. \qquad (7.1)$$

Then, neglecting μ_{12}^2 and μ_{34}^2, we obtain from (3.6), (3.7), and (7.1)

$$(\Sigma\mu)\,[\,|W| - \Sigma\mu] \leqslant M^2, \qquad (7.2)$$

where $\Sigma\mu$ is any of the sums of the effective masses, contained in the left halves of (3.6) and (3.7). We choose the smallest among these sums, $(\Sigma\mu)_{\min}$. We can then state the following:

Lemma. Any scattering diagram of identical particles of mass M has asymptotically no anomalous singularities if the inequality

$$W^2 \geqslant [M^2 + (\Sigma\mu)^2_{min}]^2 / (\Sigma\mu)^2_{min}, \qquad (7.3)$$

is satisfied, where $(\Sigma\mu)_{\min}$ is the smallest of the sums contained in the left halves of (3.6) and (3.7).

8. $\pi\pi$, KK, AND NN SCATTERING AMPLITUDES

Let us apply the foregoing method to determine, within the framework of perturbation theory, the types of the singular curves of the $\pi\pi$, KK, and NN scattering amplitudes. We are interested in the possibility of appearance of singular curves of the anomalous type. Let us confine ourselves only to the asymptotic case and use the criterion (3.6) and

---

*It is shown by induction in Appendices II and III that all the 4-vectors a_{ik} of the first class, contained in (5.8), have an identical direction, and that (6.3) and (6.3′) are exact equalities.

*We have confined ourselves to the normal asymptote of the "open envelope" only, for when an anomalous singular curve approaches a normal asymptote, an anomalous singular curve approaches also an anomalous asymptote. On the other hand, if a normal singular curve approaches a normal asymptote, a normal singular curve approaches also an anomalous asymptote (see Fig. 5).

(3.7). We take account of the fact that in the asymptotic case at least one of the following combinations of effective masses of the "open envelope," $\mu_{13}\mu_{24}$ and (or) $\mu_{14}\mu_{23}$, differs from zero, and a nonvanishing combination $\mu_{ik}\mu_{lm}$ corresponds to the 4-vectors a_{ik} and a_{lm}, which belong asymptotically to the first class.

$\pi\pi$ scattering. Since the pion is the lightest strongly-interacting particles, the lowest value of the quantity $(\Sigma\mu)_{\min}$, which enters in (7.3), is $(\Sigma\mu)_{\min} = m_\pi$, where m_π is the pion mass. We then conclude from the lemma that the $\pi\pi$-scattering amplitude has asymptotically no singularity of the anomalous type in any of the perturbation-theory approximations.

KK scattering. Using the conservation of strangeness in strong interactions and recognizing that the K meson is the lightest particle with nonzero strangeness, we conclude on the basis of the lemma that in no approximation of perturbation theory will the KK-scattering amplitude have singularities of the anomalous type as the transferred momentum tends to infinity.

NN scattering. Using the conservation of the baryon charge and recognizing that the nucleon is the lightest of the baryons, we conclude from the lemma that in no approximation of perturbation theory will the NN-scattering amplitude have singularities of the anomalous type as the transferred momentum tends to infinity.

The results obtained in this section can be generalized in the following fashion:

Theorem 3. When the lightest of the elementary like particles with a given quantum characteristic (capability of strong interaction, strangeness, baryon charge, etc.) are scattered, no anomalous singularities arise as the transferred momentum tends to infinity in any perturbation-theory approximation.

By symmetry, it follows from Theorem 3 that in the case of $\pi\pi$ scattering there are no anomalous singular curves at all. For scattering of other elementary particles, along with the conditions listed above for the existence of singular curves of the anomalous type, inequality (7.3) always points to a limiting value of one of the invariants (while the other tends to infinity), above which there exist no anomalous singular curves.

The authors are deeply grateful to V. N. Gribov, B. L. Ioffe, L. D. Landau, L. B. Okun', and I. Ya. Pomeranchuk for interest in this work for useful discussions.

APPENDIX 1

SINGULARITIES OF THE "OPEN ENVELOPE"

We denote by Δ the determinant of the system (3.1)

$$\begin{aligned}\Delta = 2\{&\beta_{12}\beta_{34}(\beta_{13}+\beta_{14}+\beta_{23}+\beta_{24})\\ &+\beta_{12}(\beta_{13}+\beta_{23})(\beta_{14}+\beta_{24})+\beta_{34}(\beta_{23}+\beta_{24})(\beta_{13}+\beta_{14})\\ &+\beta_{13}\beta_{24}(\beta_{14}+\beta_{23})+\beta_{14}\beta_{23}(\beta_{13}+\beta_{24})\}.\end{aligned} \tag{A I.1}$$

We then obtain from (3.1) the following expressions for the 4-vectors a_{ik} $(i, k = 1, \ldots, 4;\ i \neq k)$;

$$\begin{aligned}a_{12}\Delta = {}&Q[\beta_{34}(\beta_{13}+\beta_{14}+\beta_{23}+\beta_{24})+\beta_{13}\beta_{14}+2\beta_{13}\beta_{24}\\ &+\beta_{23}\beta_{24}]-W[\beta_{34}(\beta_{13}+\beta_{14}-\beta_{23}-\beta_{24})+\beta_{13}\beta_{14}\\ &-\beta_{23}\beta_{24}]+P[\beta_{34}(\beta_{13}+\beta_{14}+\beta_{23}+\beta_{24})+\beta_{13}\beta_{14}\\ &+2\beta_{14}\beta_{23}+\beta_{23}\beta_{24}],\end{aligned} \tag{A I.2}$$

$$\begin{aligned}a_{43}\Delta = {}&-Q[\beta_{12}(\beta_{13}+\beta_{14}+\beta_{23}+\beta_{24})+\beta_{13}\beta_{23}+2\beta_{13}\beta_{24}\\ &+\beta_{14}\beta_{24}]-W[\beta_{12}(\beta_{13}-\beta_{14}+\beta_{23}-\beta_{24})+\beta_{13}\beta_{23}\\ &-\beta_{14}\beta_{24}]+P[\beta_{12}(\beta_{13}+\beta_{14}+\beta_{23}+\beta_{24})+\beta_{13}\beta_{23}\\ &+2\beta_{14}\beta_{23}+\beta_{14}\beta_{24}],\end{aligned} \tag{A I.3}$$

$$\begin{aligned}a_{14}\Delta = {}&Q[\beta_{34}(\beta_{23}+\beta_{24})+\beta_{12}(\beta_{13}+\beta_{23})+\beta_{13}\beta_{23}+2\beta_{13}\beta_{24}\\ &+\beta_{23}\beta_{24}]+W[2\beta_{12}\beta_{34}+\beta_{34}(\beta_{23}+\beta_{24})+\beta_{12}(\beta_{13}+\beta_{23})\\ &+\beta_{23}(\beta_{13}+\beta_{24})]-P[-\beta_{34}(\beta_{23}+\beta_{24})+\beta_{12}(\beta_{13}+\beta_{23})\\ &+\beta_{23}(\beta_{13}-\beta_{24})],\end{aligned} \tag{A I.4}$$

$$\begin{aligned}a_{13}\Delta = {}&Q[\beta_{34}(\beta_{23}+\beta_{23})-[\beta_{12}(\beta_{14}+\beta_{24})+\beta_{24}(\beta_{23}-\beta_{14})]\\ &+W[2\beta_{12}\beta_{34}+\beta_{34}(\beta_{23}+\beta_{24})+\beta_{12}(\beta_{14}+\beta_{24})\\ &+\beta_{24}(\beta_{23}+\beta_{14})]+P[\beta_{34}(\beta_{23}+\beta_{24})+\beta_{12}(\beta_{14}+\beta_{24})\\ &+\beta_{14}\beta_{24}+2\beta_{14}\beta_{23}+\beta_{23}\beta_{24}],\end{aligned} \tag{A I.5}$$

$$\begin{aligned}a_{24}\Delta = {}&Q[-\beta_{34}(\beta_{13}+\beta_{14})+\beta_{12}(\beta_{13}+\beta_{23})+\beta_{13}(\beta_{23}-\beta_{14})]\\ &+W[2\beta_{12}\beta_{34}+\beta_{34}(\beta_{13}+\beta_{14})+\beta_{12}(\beta_{13}+\beta_{23})\\ &+\beta_{13}(\beta_{23}+\beta_{14})]-P[\beta_{34}(\beta_{13}+\beta_{14})+\beta_{12}(\beta_{13}+\beta_{23})\\ &+\beta_{13}\beta_{14}+2\beta_{14}\beta_{23}+\beta_{13}\beta_{23}],\end{aligned} \tag{A I.6}$$

$$\begin{aligned}a_{23}\Delta = {}&-Q[\beta_{34}(\beta_{13}+\beta_{14})+\beta_{12}(\beta_{14}+\beta_{24})+\beta_{14}\beta_{24}+2\beta_{13}\beta_{24}\\ &+\beta_{13}\beta_{14}]+W[2\beta_{12}\beta_{34}+\beta_{34}(\beta_{13}+\beta_{14})+\beta_{12}(\beta_{14}+\beta_{24})\\ &+\beta_{14}(\beta_{24}+\beta_{15})]-P[\beta_{34}(\beta_{13}+\beta_{14})\\ &-\beta_{12}(\beta_{14}+\beta_{24})+\beta_{14}(\beta_{13}-\beta_{24})].\end{aligned} \tag{A I.7}$$

When $Q^2 \to \infty$ less rapidly than $\beta_{12}\beta_{34}$, we obtain from (A I.4), (A I.7) and (2.3)

$$\begin{aligned}\frac{m_{14}}{\gamma_{14}|W|} = 1 &+ \frac{(\gamma_{23}+\gamma_{24})(\gamma_{23}+\gamma_{24}-\gamma_{13}-\gamma_{14})}{2\gamma_{12}}\\ &+\frac{(\gamma_{13}+\gamma_{23})(\gamma_{13}+\gamma_{23}-\gamma_{14}-\gamma_{24})}{2\gamma_{34}}+\frac{1}{2}\frac{Q^2}{\gamma_{12}\gamma_{34}W^2}\\ &\times(\gamma_{23}+\gamma_{24})(\gamma_{13}+\gamma_{23})+\frac{1}{2}\frac{(M_1^2-M_2^2)}{W^2}\frac{(\gamma_{23}+\gamma_{24})}{\gamma_{12}}\\ &-\frac{1}{2}\frac{(M_3^2-M_4^2)}{W^2}\frac{(\gamma_{13}+\gamma_{23})}{\gamma_{34}}-\frac{1}{8}\frac{Q^4}{W^4}\frac{(\gamma_{23}+\gamma_{24})^2(\gamma_{13}+\gamma_{23})^2}{(\gamma_{12}\gamma_{34})^2},\end{aligned} \tag{A I.8}$$

$$\frac{m_{13}}{\gamma_{13}|W|} = 1 + \frac{(\gamma_{23}+\gamma_{24})(\gamma_{23}+\gamma_{24}-\gamma_{13}-\gamma_{14})}{2\gamma_{12}}$$
$$+\frac{(\gamma_{14}+\gamma_{24})(\gamma_{14}+\gamma_{24}-\gamma_{13}-\gamma_{23})}{2\gamma_{34}}$$
$$-\frac{1}{2}\frac{Q^2}{\gamma_{12}\gamma_{34}W^2}(\gamma_{14}+\gamma_{24})(\gamma_{23}+\gamma_{24})$$
$$+\frac{1}{2}\frac{(M_1^2-M_2^2)}{W^2}\frac{(\gamma_{23}+\gamma_{24})}{\gamma_{12}}+\frac{1}{2}\frac{(M_3^2-M_4^2)}{W^2}\frac{(\gamma_{14}+\gamma_{24})}{\gamma_{34}}$$
$$-\frac{1}{8}\frac{Q^4}{W^4}\frac{(\gamma_{14}+\gamma_{24})^2(\gamma_{23}+\gamma_{24})^2}{(\gamma_{12}\gamma_{34})^2}, \qquad \text{(A I.9)}$$

$$\frac{m_{24}}{\gamma_{24}|W|} = 1 + \frac{(\gamma_{13}+\gamma_{14})(\gamma_{13}+\gamma_{14}-\gamma_{23}-\gamma_{24})}{2\gamma_{12}}$$
$$+\frac{(\gamma_{13}+\gamma_{23})(\gamma_{13}+\gamma_{23}-\gamma_{14}-\gamma_{24})}{2\gamma_{34}}$$
$$-\frac{1}{2}\frac{Q^2}{\gamma_{12}\gamma_{34}W^2}(\gamma_{13}+\gamma_{14})(\gamma_{13}+\gamma_{23})$$
$$-\frac{1}{2}\frac{(M_1^2-M_2^2)}{W^2}\frac{(\gamma_{13}+\gamma_{14})}{\gamma_{12}}-\frac{1}{2}\frac{(M_3^2-M_4^2}{W^2}\frac{(\gamma_{13}+\gamma_{23})}{\gamma_{34}}$$
$$-\frac{1}{8}\frac{Q^4}{W^4}\frac{(\gamma_{13}+\gamma_{14})^2(\gamma_{13}+\gamma_{23})^2}{(\gamma_{12}\gamma_{34})^2}, \qquad \text{(A I.10)}$$

$$\frac{m_{23}}{\gamma_{23}|W|} = 1 + \frac{(\gamma_{13}+\gamma_{14})(\gamma_{13}+\gamma_{14}-\gamma_{23}-\gamma_{24})}{2\gamma_{12}}$$
$$+\frac{(\gamma_{14}+\gamma_{24})(\gamma_{14}+\gamma_{24}-\gamma_{13}-\gamma_{23})}{2\gamma_{34}}$$
$$+\frac{1}{2}\frac{Q^2}{\gamma_{12}\gamma_{34}W^2}(\gamma_{13}+\gamma_{14})(\gamma_{14}+\gamma_{24})$$
$$-\frac{1}{2}\frac{(M_1^2-M_2^2)}{W^2}\frac{(\gamma_{13}+\gamma_{14})}{\gamma_{12}}+\frac{1}{2}\frac{(M_3^2-M_4^2)}{W^2}\frac{(\gamma_{14}+\gamma_{24})}{\gamma_{34}}$$
$$-\frac{1}{8}\frac{Q^4}{W^4}\frac{(\gamma_{13}+\gamma_{14})^2(\gamma_{14}+\gamma_{24})^2}{(\gamma_{12}\gamma_{34})^2}. \qquad \text{(A I.11)}$$

We introduce the symbol $\lambda = (m_{13}m_{24} - m_{14}m_{23})/(m_{13}+m_{14}+m_{23}+m_{24})^2$, and obtain readily from (A I.8) — (A I.11)

$$\frac{|W|}{m_{13}+m_{14}+m_{23}+m_{24}} = 1 + \frac{Q^2}{2\gamma_{13}\gamma_{34}}\frac{\gamma_{13}\gamma_{24}-\gamma_{14}\gamma_{23}}{(m_{13}+m_{14}+m_{23}+m_{24})^2}$$
$$+\frac{Q^4 m_{13}m_{24}}{8(\gamma_{12}\gamma_{34})^2(m_{13}+m_{14}+m_{23}+m_{24})^6}, \qquad \text{(A I.12)}$$

$$\gamma_{13}\gamma_{24}-\gamma_{14}\gamma_{23} = \lambda + \frac{Q^2}{2\gamma_{12}\gamma_{34}}\frac{m_{13}m_{24}}{(m_{13}+m_{14}+m_{23}+m_{24})^4}, \qquad \text{(A I.13)}$$

$$\gamma_{14} = \frac{m_{14}}{m_{13}+m_{14}+m_{23}+m_{24}}, \qquad \gamma_{13} = \frac{m_{13}}{m_{13}+m_{14}+m_{23}+m_{24}},$$
$$\gamma_{24} = \frac{m_{24}}{m_{13}+m_{14}+m_{23}+m_{24}}, \qquad \gamma_{23} = \frac{m_{23}}{m_{13}+m_{14}+m_{23}+m_{24}}. \qquad \text{(A I.14)}$$

Let us determine the asymptotic form of the dependence of Q^2 and W^2 as Q^2 tends to infinity as $\gamma_{12}\gamma_{34}$, assuming that $Q^2/\gamma_{12}\gamma_{34} \sim \lambda W^2$ and $\lambda \ll 1$.

We denote the right halves of (3.2) and (3.3) by A_{12} and A_{34} respectively. It follows from (3.2), (3.3), (A I.13) and (A I.14) that the signs of A_{12} and A_{34} are the same. We introduce, further the notation

$$\omega = |W|/(m_{13}+m_{14}+m_{23}+m_{24}),$$
$$q^2 = Q^2/(m_{13}+m_{14}+m_{23}+m_{24})^2,$$
$$a = m_{13}m_{14}/2(m_{13}+m_{14}+m_{23}+m_{24})^2, \ \gamma = (\gamma_{12}\gamma_{34})^{1/2}.$$

Then, using (3.2), (3.3), (A I.12), (A I. 13), and (A I.14) we obtain the following single-parameter system of equations, relating W^2 with Q^2

$$\frac{q^2}{\gamma^2} = \frac{2\lambda}{3a}z, \qquad \text{(A I.15)}$$

$$\frac{C}{\gamma} = \frac{(A_{12}A_{34})^{1/2}}{\gamma} = \frac{2\lambda^2}{3a}z\left(1+\frac{2}{3}z\right), \qquad \text{(A I.16)}$$

$$\omega^2 = 1 + \frac{2\lambda^2}{3a}z(1+z). \qquad \text{(A I.17)}$$

In the derivation of (A I.17) we use the fact that $\lambda \ll 1$. Since C is of fixed sign ($C < 0$ and $C > 0$ correspond to the appearance of anomalous and normal singularities respectively), not all the values of the parameters z are allowed. When $C < 0$ we have $-3/2 \le z \le 0$, while when $C \ge 0$ there are two regions, $z > 0$ and $z < -3/2$. Further, when $-1 < z \le 0$ we have $\omega^2 < 1$. For other values of z we have $\omega^2 > 1$. The minimum of the function $\omega^2 - 1$ occurs when $z = -1/2$. The same value, $z = -1/2$, corresponds to the maximum of the function $q^2 = q^2(z)$. When $\lambda > 0$ $q^2(z) < 0$ when $z < 0$ and $q^2(z) > 0$ when $z > 0$. When $z = 0$ and $z = -3/2$, $|q^2(z)| \to \infty$. At these points $\omega^2(0) = 1$ and $\omega^2(-3/2) = \omega'^2$, where ω' is determined from (4.1). When $|z| \to \infty$, $|q^2(z)| \to 0$. The general form of the dependence of Q^2 on W^2, obtained by solving the system (A I.15) — (A I.17), is shown in Fig. 5. When $C < 0$, as seen from Fig. 5, there are two analogous curves $Q^2 = Q^2(W^2)$ starting at a certain point $A(Q^2, W^2)$ and diverging to different asymptotes over W^2. When $C > 0$ the curves have a normal form. We emphasize that the case $\kappa = 1$ corresponds to curves that approach the asymptote ω'.

APPENDIX II

SCATTERING DIAGRAM WITH SIX VERTICES

By way of an example of reduction of the diagrams of perturbation theory to an "open envelope", let us consider a diagram with six vertices (the two interior ones being designated 5 and 6). We assume that all the vertices in this diagram are pairwise inter-connected. We reduce this diagram to the "open envelope" and confine ourselves immediately to a consideration of the asymptotic case $Q^2 = (p_1 + p_3)^2 \to \infty$ only. To simplify the derivations, we assume that none of the β_{ik} with the exception of β_{12} and β_{34}, tend to infinity, that is, all the 4-vectors a_{ik}, except a_{12} and a_{34}, belong to the first class.

It then follows from (A I.2) – (A I.7) that

$$a_{12} = a_{34} = 0,\ a_{13} = a_{14} = a_{23} = a_{24} = W/\delta, \quad \text{(A II.1)}$$

where $\delta = \beta''_{13} + \beta''_{14} + \beta''_{23} + \beta''_{24}$, while β''_{ik} is the particular β_{ik} obtained by eliminating the interior vertices 5 and 6 from the diagram.

Eliminating from the diagram the interior vertex 6 and taking (A II.1) into account, we obtain

$$\begin{aligned} a_{56} &= \gamma_{16}a_{51} + \gamma_{26}a_{52} + \gamma_{36}a_{53} + \gamma_{46}a_{54}, \\ a_{16} &= (\gamma_{36} + \gamma_{46})W/\delta + \gamma_{56}a_{15}, \\ a_{36} &= -(\gamma_{16} + \gamma_{26})W/\delta + \gamma_{56}a_{35}, \\ a_{26} &= (\gamma_{36} + \gamma_{46})W/\delta + \gamma_{56}a_{25}, \\ a_{46} &= -(\gamma_{16} + \gamma_{26})W/\delta + \gamma_{56}a_{45}. \end{aligned} \quad \text{(A II.2)}$$

After eliminating the vertex 6, the remaining diagram has one interior vertex 5, characterized by β'_{ik} which are determined in terms of β_{ik} in accordance with (5.6).

We next eliminate the vertex 5. Then

$$\begin{aligned} a_{15} = a_{25} &= (\gamma'_{35} + \gamma'_{45})W/\delta, \\ a_{35} = a_{45} &= (\gamma'_{15} + \gamma'_{25})W/\delta. \end{aligned} \quad \text{(A II.3)}$$

The primed γ'_{ik}, naturally, are formed from the primed β'_{il} in accordance with (5.3). Substituting (A II.3) in (A II.2) and taking (2.3) into account, we get

$$\frac{m_{16}}{\beta_{16}} = \frac{m_{26}}{\beta_{26}} = \frac{|W|}{\delta}[\gamma_{36} + \gamma_{46} + \gamma_{56}(\gamma'_{35} + \gamma'_{45})],$$

$$\frac{m_{36}}{\beta_{36}} = \frac{m_{46}}{\beta_{46}} = \frac{|W|}{\delta}[\gamma_{16} + \gamma_{26} + \gamma_{56}(\gamma'_{15} + \gamma'_{25})],$$

$$m_{56} = \frac{|W|}{\delta}\beta_{56}|(\gamma_{16} + \gamma_{26})(\gamma'_{35} + \gamma'_{45}) - (\gamma_{36} + \gamma_{46})(\gamma'_{15} + \gamma'_{25})|. \quad \text{(A II.4)}$$

It follows from (A II.4) that

$$|m_{16} + m_{26} - m_{36} - m_{46}| = m_{56}. \quad \text{(A II.5)}$$

The result (A II.5) is quite natural, for as Q^2 tends to infinity we transform the diagram with four exterior vertices to a diagram with two interior vertices, and such a diagram has non-vanishing Feynman parameters at the singular point only when a certain connection exists between the masses of the virtual particles in the interior vertices.[7]

We note that were we to eliminate vertex 5 first, and vertex 6 last, we would obtain instead of (A II.5)

$$|m_{15} + m_{25} - m_{35} - m_{45}| = m_{56}. \quad \text{(A II.5′)}$$

Since the result is independent of the sequence with which we eliminate the internal vertices, a connection is established also between the masses m_{15} and m_{16} ($i = 1, \ldots, 4$).

Let us determine now the effective masses of the virtual particles in accordance with (5.7)

$$m'' = m\beta''/\beta, \quad m' = m\beta'/\beta \quad \text{(A II.6)}$$

and use the following relations, derivable from (A II.3):

$$\frac{m_{15}}{\beta_{15}} = \frac{m_{25}}{\beta_{25}} = (\gamma'_{35} + \gamma'_{45})\frac{|W|}{\delta}, \quad \frac{m_{35}}{\beta_{35}} = \frac{m_{45}}{\beta_{45}} = (\gamma'_{15} + \gamma'_{25})\frac{|W|}{\delta}, \quad \text{(A II.7)}$$

$$m_{13}/\beta_{13} = m_{14}/\beta_{14} = m_{23}/\beta_{23} = m_{24}/\beta_{24} = |W|/\delta \quad \text{(A II.8)}$$

From (A II.7) we obtain still another connection between the effective masses of the virtual particles scattered at the vertex 5

$$m'_{15} + m'_{25} = m'_{35} + m'_{45}. \quad \text{(A II.9)}$$

Using formulas (5.6) to express β''_{ik} in terms of β'_{ik}, we obtain from (A II.6) and (A II.7)

$$\begin{aligned} &m'_{13} + m''_{14} = m'_{13} + m'_{14} + m'_{15}, \quad m''_{13} + m''_{23} = m'_{13} + m'_{23} + m'_{35}, \\ &m''_{14} + m''_{24} = m'_{14} + m'_{24} + m'_{45}, \quad m''_{23} + m''_{24} = m'_{23} + m'_{24} + m'_{25}. \end{aligned} \quad \text{(A II.10)}$$

Taking now (A II.4) into account, we obtain the final expression for the combination of the reduced masses, contained in the inequalities (3.6) and (3.7)

$$\begin{aligned} m''_{13} + m''_{14} &= m_{13} + m_{14} + m_{15} + m_{16}, \\ m''_{13} + m''_{23} &= m_{13} + m_{23} + m_{35} + m_{36}, \\ m''_{14} + m''_{24} &= m_{14} + m_{24} + m_{45} + m_{46}, \\ m''_{23} + m''_{24} &= m_{23} + m_{24} + m_{25} + m_{26}. \end{aligned} \quad \text{(A II.11)}$$

APPENDIX III

SECOND MINORANT

Let us show that the equality sign applies in (6.3) and (6.3′).

Assume that in some diagram having ν vertices all the 4-vectors a_{si} (the subscript s characterizes some interior vertex, while i characterizes any interior vertex subject to the condition that the vector a_{si} is of the first class) have in the asymptotic case the same direction (either +W or −W). Let us consider the diagram with $(\nu + 1)$ vertices, which is reduced upon elimination of the $(\nu + 1)$ – th vertex to the foregoing diagram with ν vertices. Then, on the basis of (5.8),

$$a_{s,\nu+1} = \sum_{l=1}^{l=\nu} \gamma'_{l,\nu+1} a_{sl}.$$

Since $\gamma_{l,\nu+1} \geq 0$, the vector $a_{s,\nu+1}$ has the same direction as the vectors a_{si} $(i = 1, \ldots, \nu)$. Since the initial premise holds for diagrams with five and six vertices (this follows from formulas

(A II.2) and (A II.3)), all the vectors of the first class, arriving at any of the exterior vertices, have the same direction. It then follows from (5.8) and (6.2) that the equality signs apply in expressions (6.3) and (6.3′).

---

[1] Karplus, Sommerfield, and Wichmann, Phys. Rev. **114**, 376 (1959).

[2] L. D. Landau, JETP **37**, 62 (1959), Soviet Phys. JETP **10**, 45 (1960).

[3] S. Mandelstam, Phys. Rev. **115**, 1741 (1959).

[4] V. A. Kolkunov, JETP, in press.

[5] J. Tarski, Preprint, 1959.

[6] V. S. Vladimirov, Preprint R-449 (1959).

[7] L. B. Okun' and A. P. Rudik, Nucl. Phys. **14**, 261 (1960).

[8] Kolkunov, Okun', and Rudik, JETP **38**, 877 (1960), Soviet Phys. JETP **11**, 634 (1960).

[9] A. Z. Patashinskiĭ, JETP **39**, 1744 (1960), Soviet Phys. JETP **12**, 1217 (1961).

Translated by J. G. Adashko
45

SOVIET PHYSICS JETP VOLUME 13, NUMBER 1 JULY, 1961

DETERMINATION OF THE FREQUENCY SPECTRUM OF PHONONS IN CRYSTALS

Yu. KAGAN

Submitted to JETP editor July 30, 1960

J. Exptl. Theoret. Phys. (U.S.S.R.) **40**, 312-318 (January, 1961)

For crystals of arbitrary symmetry, we consider the problem of determining the phonon frequency spectrum, in connection with the investigation of one-phonon transitions in the Mössbauer effect and incoherent scattering of "cold" neutrons.

INTRODUCTION

A knowledge of the distribution function $\psi(\omega)$ for the phonon frequency spectrum is of great importance for the study of the properties of solids. Since the work of Placzek and Van Hove,[1] it is known that incoherent one-phonon scattering of neutrons enables us to establish the frequency spectrum in the case of cubic crystals with a single atom in the unit cell. Recently Visscher[2] pointed out that analogous information concerning the phonon spectrum of an isotropic body can be gotten by studying the resonance absorption of γ rays in a crystal (Mössbauer effect) with emission of one phonon (where the energy change is compensated by the Doppler effect from an appropriate motion of the source). Using the results of a paper of Lamb,[3] Visscher gave a detailed analysis, within the framework of the isotropic approximation, of the conditions under which one can determine $\psi(\omega)$ experimentally.

For both methods, a very important question is the possibility of determining the frequency distribution function for crystals of arbitrary symmetry with any number of atoms in the unit cell. The present paper gives a treatment of this problem. As applied to "cold" neutrons, this question was first treated by Oskot-skiĭ.[4]

The two processes, which at first glance appear to be different in character, permit of analogous descriptions for one- and multiphonon transitions. This is related to the fact that in the resonance absorption we will be interested only in those transitions for which $\hbar\omega \gg \Gamma$ (where $\hbar\omega$ is the energy of the phonon and Γ is the width of the resonance level).

1. THE MÖSSBAUER EFFECT

Suppose a nucleus located at a lattice site makes a transition from an excited state A* to the state A, with emission of a γ quantum. If we take into account a possible change in the phonon distribution, we can write the matrix element for such a transition in the form

$$M_\beta = \langle \mathbf{k},\ A,\ \{n'\} \,|\, H_1 \,|\, A^*,\ \{n\}\rangle = M_{\mathrm{nuc}} \langle \{n'\} \,|\exp\{i\mathbf{k}\mathbf{R}_{\mathrm{m}\beta}\}|\, \{n\}\rangle. \tag{1}$$

Here $\{n\}$, $\{n'\}$ are the sets of phonon occupation numbers before and after decay of the nucleus, M_{nuc} is the matrix element corresponding to the decay of a free nucleus, $\mathbf{k}$ is the wave vector of the γ quantum, $\mathbf{R}_{\mathrm{m}\beta}$ is the coordinate of the nucleus labelled β in the m-th unit cell, at the moment of decay.

The expression for $\mathbf{R}_{\mathrm{m}\beta}$ has the form

$$\mathbf{R}_{\mathrm{m}\beta} = \mathbf{R}^0_{\mathrm{m}\beta} + \mathbf{u}_{\mathrm{m}\beta}, \qquad \mathbf{R}^0_{\mathrm{m}\beta} = \mathbf{r}_{\mathrm{m}} + \boldsymbol{\rho}_\beta, \tag{2}$$

where $\mathbf{r}_{\mathrm{m}}$ and ρ_β denote, respectively, the equilibrium position of a selected site which characterizes the elementary cell, and the position of the β-th atom relative to this site.

The displacement of an arbitrary atom is conveniently represented in the form

$$\mathbf{u}_{m\beta} = \sum_{\mathbf{f},\,\alpha} (\hbar / 2\mu_\beta\,\omega_\alpha(\mathbf{f})\,N)^{1/2} [\mathbf{V}_{\beta\alpha}(\mathbf{f}) \exp\{i\mathbf{f}\mathbf{r}_{\mathrm{m}}\}\, a_\alpha(\mathbf{f}) + \mathbf{V}^*_{\beta\alpha}(\mathbf{f}) \exp\{-i\mathbf{f}\mathbf{r}_{\mathrm{m}}\}\, a^+_\alpha(\mathbf{f})], \tag{3}$$

where $\mathbf{f}$ and ω_α are the wave vector and frequency of the phonon, α is the number of the branch, a and a^+ are the operators for annihilation and creation of the phonon, N is the number of elementary cells in the crystal, and μ_β is the mass of the β-th atom. The complex $\mathbf{V}_{\beta\alpha}$ are orthonormal:

$$\sum_\beta \mathbf{V}_{\beta\alpha}(\mathbf{f})\,\mathbf{V}^*_{\beta\alpha'}(\mathbf{f}) = \delta_{\alpha\alpha'}. \tag{4}$$

Without loss of generality, we set $\mathbf{r}_{\mathrm{m}} = 0$. In accordance with the usual procedure, considering (3), we represent the exponential in (1) as a product of exponentials corresponding to the individual normal vibrations. We expand these exponentials in series, keeping the first three terms (the remaining terms give a contribution which tends to zero when $N \to \infty$). From (3) it follows that only the second term gives a transition which is not diagonal in the occupation numbers.

We average the square modulus of the matrix element (1) over the initial equilibrium distribution, taking account of the independence of the individual oscillators. After transformation, we find for a process in which s phonons participate,

$$|M_\beta^s|^2 = |M_{\mathbf{nuc}}|^2\left(\frac{R_\beta}{N}\right)^s \exp\left\{-\frac{R_\beta}{N}\sum_{\alpha,\mathfrak{f}}{}' \frac{|\mathbf{qV}_{\beta\alpha}(\mathfrak{f})|^2}{\hbar\omega_\alpha(\mathfrak{f})}[2\bar{n}_\alpha(\mathfrak{f})+1]\right\}$$

$$\times\prod_{i=1}^{s}|\mathbf{qV}_{\beta\alpha_i}(\mathfrak{f}_i)|^2[\hbar\omega_{\alpha_i}(\mathfrak{f}_i)]^{-1}\left[\bar{n}_{\alpha_i}(\mathfrak{f}_i)+\tfrac{1}{2}\pm\tfrac{1}{2}\right]. \quad (5)$$

Here R_β denotes the recoil energy for an isolated nucleus,

$$R_\beta = \hbar^2 k^2/2\mu_\beta, \quad (6)$$

and $\mathbf{q}$ is a unit vector in the direction of $\mathbf{k}$; $\bar{n}$ is the equilibrium value corresponding to the crystal temperature. The upper sign inside the brackets in the product in (5) corresponds to phonon emission and the lower to phonon absorption. The prime on the sum in the exponential in (5) means that the s terms with $(\alpha, \mathfrak{f}) = (\alpha_i, \mathfrak{f}_i)$ have been omitted. For finite s, the contribution of these terms to the sum is negligible, and from now on we shall omit the prime.

Now let us determine the probability of emission of a γ quantum in the direction $\mathbf{q}$ with energy E_γ for an s-phonon process, where we take the probability per unit energy range and per unit solid angle.

Using the standard formulas of perturbation theory and changing from summation to an integration over phase space, we find (cf. (5)):

$$W_\beta^s(E_\gamma, \mathbf{q}) = W_0 e^{-Z_\beta}(R_\beta)^s\frac{(v_0)^s}{(2\pi)^{3s}}\frac{1}{s!}S\sum_{\alpha_1\ldots\alpha_s}\int d^3 f_1\ldots d^3 f_s$$

$$\times\prod_{i=1}^{s}|\mathbf{qV}_{\beta\alpha_i}(\mathfrak{f}_i)|^2[\hbar\omega_{\alpha_i}(\mathfrak{f}_i)]^{-1}(\bar{n}_{\alpha_i}+\tfrac{1}{2}\pm\tfrac{1}{2})\,\delta$$

$$\times(E_\gamma - E_0 \pm \hbar\omega_{\alpha_1}\pm\ldots\pm\hbar\omega_{\alpha_s}) \equiv W_0 F_\beta^s(E_\gamma, \mathbf{q}). \quad (7)$$

Here E_0 is the energy of the excited state, W_0 is the probability of γ decay for the free nucleus, v_0 is the volume of the elementary cell, S is a sum over the s + 1 different combinations of absorbed and emitted phonons, and

$$Z_\beta = R_\beta\frac{v_0}{(2\pi)^3}\sum_\alpha\int d^3 f\,\frac{|\mathbf{qV}_{\beta\alpha}(\mathfrak{f})|^2}{\hbar\omega_\alpha(\mathfrak{f})}(2\bar{n}_\alpha(\mathfrak{f})+1) \quad (8)$$

(The energy transfer to the lattice is small compared with the energy of the γ quantum.)

It is not difficult to show that the relation

$$\sum_{s=0}\int F_\beta^s(E_\gamma, \mathbf{q})\,dE_\gamma = 1 \quad (9)$$

holds for the F_β^s.

For resonance absorption of a γ quantum $(E_\gamma, \mathbf{q})$, the probability of an s′-phonon process is given by the same expression (7), except that E_0 and E_γ interchange places in the argument of the δ function. If the source moves with velocity $\mathbf{u}$ and the target is sufficiently thin, the cross section for resonance absorption accompanied by an s-phonon process in the source and by an s′-phonon process in the target is (compare the analogous expression in reference 2):

$$\sigma^{ss'}(\Delta E, \mathbf{q}) = Q\frac{1}{gg'}\sum_{\beta,\lambda}\int F_\beta^s(E_\gamma, \mathbf{q})\,F_\lambda'^{s'}(E_\gamma+\Delta E, \mathbf{q})\,dE_\gamma. \quad (10)$$

In this expression Q is the cross section for resonance absorption by a free nucleus, integrated over energy; g and g′ are the numbers of identical nuclei, having the resonance level, in the elementary cells of source and target [the summation in (10) extends only over these nuclei]. From now on, primed quantities refer to the target.

For the Doppler shift ΔE we have the relation $\Delta E = E_\gamma \mathbf{u}\cdot\mathbf{q}/c$.

The expressions we have found enable us to analyze completely the general case. Suppose that one-phonon processes play the prime role in the range $\Gamma \ll \Delta E < \hbar\omega_{\max}$ (however, see later). Then in this interval the resonance absorption cross section reduces to $(\Delta E > 0)$

$$\sigma^1(\Delta E, \mathbf{q}) \equiv \sigma^{01}(\Delta E, \mathbf{q}) + \sigma^{10}(\Delta E, \mathbf{q}) = Q\frac{v_0}{(2\pi)^3}R\frac{1}{gg'}q^i q^k$$

$$\times\sum_{\beta,\lambda}\exp\{-Z_\beta - Z_\lambda'\}\left\{\sum_\alpha\int d^3 f\,\frac{V_{\beta\alpha}^i(\mathfrak{f})\,V_{\beta\alpha}^{k*}(\mathfrak{f})}{\hbar\omega_\alpha(\mathfrak{f})}(\bar{n}_\alpha(\mathfrak{f})+1)\,\delta\right.$$

$$\times(\Delta E - \hbar\omega_\alpha) + \sum_\xi\int d^3 f\,\frac{V_{\lambda\xi}'^{i}(\mathfrak{f})\,V_{\lambda\xi}'^{k*}(\mathfrak{f})}{\hbar\omega_\xi'(\mathfrak{f})}(\bar{n}_\xi'(\mathfrak{f})+1)\,\delta$$

$$\left.\times(\Delta E - \hbar\omega_\xi')\right\} \quad (11)$$

(where we sum over repeated Latin superscripts).

For the further analysis it is useful to determine the cross section for the true Mössbauer effect, $\sigma^{00}(0, \mathbf{q})$. Expressions (10) and (7) cannot be used for this directly, since (10) contains a product of two δ functions. This result is a consequence of neglecting the width Γ of the excited state. Even when this is valid for transitions involving phonons $(\hbar\omega \gg \Gamma)$, in computing σ^{00} we must consider the fact that Γ is finite. We introduce in place of $\delta(E_\gamma = E_0)$ an expression of the form

$$\frac{1}{\pi}\frac{\Gamma/2}{(E_\gamma - E_0)^2 + \Gamma^2/4}\cdot$$

We then find for σ^{00},

$$\sigma^{00}(0,\mathbf{q}) \equiv \sigma^0(\mathbf{q}) = Q\,\frac{1}{\pi\Gamma}\,\frac{1}{gg'}\sum_{\beta,\lambda}\exp\{-Z_\beta - Z'_\lambda\}. \quad (12)$$

We note that σ^0, like σ', can in general have a sizeable anisotropy. This will especially manifest itself in strongly anisotropic structures, for example in layer lattices. In such cases there are, a priori, directions of the wave vector of the γ quantum for which Z will be especially small.

Let us consider a single crystal of an arbitrary crystal system, having one atom per unit cell. Each of the terms in the curly brackets in (11) is a symmetric tensor of second rank, having the symmetry of the crystal. When it is brought to principal axes, such a tensor has in general three independent components. We determine the ratio

$$\sigma^1(\Delta E, \mathbf{q})/\sigma^0(\mathbf{q})$$

for three mutually perpendicular directions of the vector $\mathbf{q}$ relative to a fixed orientation of source and target, and sum them. If we make use of the condition $\mathbf{V}_\alpha \cdot \mathbf{V}^*_\alpha = 1$, it is easy to see that the result will not contain the polarization vectors. In the integrands in (11) we are then left with only a dependence on the phonon energy. Separating explicitly the integration over ω_α, and introducing the frequency distribution $\psi(\omega)$ for the phonon spectrum normalized in accordance with the relation

$$\tfrac{1}{3}v_0(2\pi)^{-3}\sum_\alpha \int_{\Delta\omega_\alpha = d\omega} d^3f = \psi(\omega)\,d\omega, \quad (13)$$

we get

$$\tfrac{1}{3}\sum_{l}^{3}\sigma^1(\Delta E, \mathbf{q}_l)/\sigma^0(\mathbf{q}_l) = \frac{\pi\Gamma}{\hbar}\,\frac{R}{\Delta E}\,\psi\left(\frac{\Delta E}{\hbar}\right)\,e^{\Delta E/\varkappa T}\,[e^{\Delta E/\varkappa T} - 1]^{-1}$$
$$+ \psi'\left(\frac{\Delta E}{\hbar}\right)e^{\Delta E/\varkappa T'}\,[e^{\Delta E/\varkappa T'} - 1]^{-1}. \quad (14)$$

If the lattices of source and target are the same and $T = T'$, then (14) uniquely determines $\psi(\Delta E/\hbar)$. Thus measurement of the cross sections $\sigma^1(\Delta E, \mathbf{q})$ and $\sigma^0(\mathbf{q})$ for three directions enables us to find the frequency distribution for a crystal of abritrary symmetry.

In the case of uniaxial crystals, the symmetric tensor of second rank has two independent components and it is consequently sufficient to make two measurements, first directing the vector $\mathbf{q}$ along the symmetry axis of the crystal and then along any direction in the plane perpendicular to this axis.

In a cubic crystal, the second rank tensor degenerates into the unit tensor, so that one measurement in an arbitrary direction suffices. The isotropic case, treated by Visscher,[2] is actually equivalent to the case of a cubic crystal.

The presence of the temperature dependence in both terms in (14) opens the attractive possibility (for $T \neq T'$) of separately determining ψ and ψ'. [We note that here it may be useful to reverse the direction of motion of the source ($\Delta E < 0$), which results in the replacement of $\bar{n}$ by $\bar{n} + 1$ in (14).] The realization of this possibility would enable us, on the one hand, to determine the spectrum for the undistorted lattice of the target and, on the other hand, to obtain valuable information concerning changes in the frequency spectrum resulting from defects in the source lattice, in particular concerning the nature of the vibrations of an atom in an interstitial position.

We note that this separation will involve some experimental difficulties, since the necessary increase in temperature of one of the crystals results in a reduction of σ^0 and σ^1. This imposes an obvious limitation on the value of $(Z + Z')_{T=0}$. [See (11) and (12).]

Now we consider crystals having an arbitrary number of atoms in the unit cell. In this case we make the assumption that the factors $\exp\{-Z_\beta - Z'_\lambda\}$, which depend on the integral properties of the spectrum, differ only slightly for any pair β, λ. This will be valid in any case for Z_β, $Z'_\lambda \ll 1$.

Again we determine the sum of the ratios σ^1/σ^0 for three mutually perpendicular directions:

$$\tfrac{1}{3}\sum_{l}^{3}\sigma^1(\Delta E, \mathbf{q}_l)/\sigma^0(\mathbf{q}_l) = \tfrac{1}{3}\pi\Gamma R v_0(2\pi)^{-3}$$
$$\times\left\{\frac{1}{g}\sum_{\alpha,\beta}\int d^3f V_{\beta\alpha}(\mathfrak{f})\,V^*_{\beta\alpha}(\mathfrak{f})\,[\hbar\omega_\alpha(f)]^{-1}(\bar{n}_\alpha + 1)\,\delta(\Delta E - \hbar\omega_\alpha)\right.$$
$$\left. + \frac{1}{g'}\sum_{\xi,\lambda}\int d^3f V_{\lambda\xi}(\mathfrak{f})\,V'^*_{\lambda\xi}(\mathfrak{f})\,[\hbar\omega'_\xi(f)]^{-1}(\bar{n}'_\xi + 1)\,\delta(\Delta E - \hbar\omega'_\xi)\right\}. \quad (15)$$

If we use condition (4) and relation (13) (where the left side of (13) should now contain an additional factor $1/g$), we again arrive at (14). Thus in this case also, when the assumptions made above are valid, it becomes possible to determine the frequency distribution function for a crystal of arbitrary symmetry.

In the general case, when there are atoms of different sorts in the unit cell, $\psi(\omega)$ cannot be determined from the differential cross section of the one-phonon process. This is easily seen by analyzing the general expression (11).

A few words about multiphonon processes. We know that as a rule the frequency distribution function will have at least two maxima. If these maxima are sufficiently sharp, and if twice the smaller critical frequency is greater than the maximum value ω_c, then in the range of values of ΔE from 0 to $\hbar\omega_{max}$ the role of two-phonon and, a fortiori, of multiphonon processes will be markedly reduced.

However, even when the multiphonon processes make a significant contribution to the total cross section $\sigma(\Delta E, \mathbf{q})$, if we use the isotropic approximation for $s + s' \geq 2$ we can consistently include all transitions involving more than one phonon. In fact, for sufficiently low values of $\Delta E (\ll \hbar\omega_{max})$ the contribution of the multiphonon processes is negligible $(\psi(\omega \rightarrow 0) \rightarrow 0)$ and consequently they do not disturb the determination of the frequency distribution in this region. Moreover, for sufficiently low frequencies, $\psi(\omega)$ can be computed directly if we know the elastic constants of the crystal. For an arbitrary ΔE, in multiphonon processes there are created practically no phonons with energies in a sufficiently narrow interval around $\hbar\omega = \Delta E$ (again because $\psi(\omega \rightarrow 0) \rightarrow 0$). Because of this, the quantities σ^{ss} (for $s + s' \geq 2$) can be expressed in terms of the function $\psi(\omega)$ as determined for the region $\omega < \Delta E/\hbar$. From this it is clear that the knowledge of $\psi(\omega)$ for the initial part of the frequency range enables us, once we know the dependence of $\sigma(\Delta E, \mathbf{q})$, to find $\sigma^1(\Delta E, \mathbf{q})$ and with it $\psi(\omega)$ for the whole range of frequencies of the phonon spectrum.

2. "COLD" NEUTRONS

The results presented in the preceding section can be carried over without difficulty to the case of incoherent scattering of "cold" neutrons. The square of the matrix element describing the inelastic scattering of a neutron will have the form (5) with the appropriate value of M_{nuc}, and with $\mathbf{k} = \mathbf{k}_1 - \mathbf{k}_0$, where $\mathbf{k}_0$ and $\mathbf{k}_1$ are the wave vectors of the neutron before and after scattering.

Let us consider the case where the crystal consists of identical atoms. The differential scattering cross section is expressed (for fixed $\mathbf{k}_0$) as

$$d\sigma(\mathbf{k}_1)/d\mathbf{k}_1 = \sum_s d\sigma^s(\mathbf{k}_1)/d\mathbf{k}_1,$$

$$d\sigma^s(\mathbf{k}_1)/d\mathbf{k}_1 = \sigma_\infty(\hbar^2/4\pi k_0 mg)\sum_\beta F_\beta^s(E_1, \mathbf{q}), \tag{16}$$

where $F_\beta^S(E_1, \mathbf{q})$ is defined in accordance with (7), with E_γ and E_0 replaced by the final (E_1) and the initial (E_0) energy of the neutron. (We mention that Eq. (9) will no longer be satisfied, since the quantity R_β cannot be treated as constant for varying E_1.) In (16) we use the following notation: σ_∞ is the total incoherent scattering cross section for a rigidly bound nucleus, and m is the mass of the neutron.

Let us consider a single crystal with arbitrary symmetry. Considering the case of a neutron with energy E_0 less than the Debye energy, and assuming that $T_{cryst} \lesssim \Theta_D$ and $\mu \gg m$, we find for Z_β a value much less than unity. Because of this we will disregard any possible weak dependence of the Debye-Waller factor on β. We then have for the one-phonon process,

$$d\sigma^1(\mathbf{k}_1)/d\mathbf{k}_1 = \sigma^0(\mathbf{k})(\hbar^2 R/mk_0 g)\, q^i q^k v_0 (2\pi)^{-3}$$
$$\times \sum_{\alpha,\beta}\int d^3f\, v_{\beta\alpha}^i(\mathbf{f})\, v_{\beta\alpha}^{k*}(\mathbf{f})\,[\hbar\omega_\alpha(\mathbf{f})]^{-1}[(\bar{n}_\alpha + 1)\,\delta(E_0 - E_1 - \hbar\omega_\alpha)$$
$$+ \bar{n}_\alpha\delta(E_0 - E_1 + \hbar\omega_\alpha)], \tag{17}$$

where $\sigma^0(\mathbf{k})$ is the differential cross section for elastic scattering per unit solid angle.

In the case of the Mössbauer effect there was a simplifying circumstance that was equivalent to the absence of any difference between the directions of the vectors $\mathbf{q}$ and $\mathbf{k}_1$. After fixing the scattering direction in the neutron case (as is done in the experiment), to find the function $\psi(\omega)$ for an arbitrary crystal we must proceed somewhat differently than in the preceding section. Namely, we must determine $d\sigma^1(\mathbf{k}_1)/d\mathbf{k}_1$ and $\sigma^0(\mathbf{k})$ for three positions of the single crystal which differ from one another by a cyclic permutation of the coordinates.

Let us represent (17) in the form

$$(1/\sigma^0(\mathbf{k}))\, d\sigma^1(\mathbf{k}_1)/d\mathbf{k}_1 = q^i q^k T^{ik}. \tag{18}$$

We denote the direction of the principal axes in the first position of the crystal by x, y, z. Then the right side of (18) gives

$$T^{xx}(q^x)^2 + T^{yy}(q^y)^2 + T^{zz}(q^z)^2.$$

For the other two positions of the crystal we have, respectively,

$$T^{zz}(q^x)^2 + T^{xx}(q^y)^2 + T^{yy}(q^z)^2,$$

$$T^{yy}(q^x)^2 + T^{zz}(q^y)^2 + T^{xx}(q^z)^2.$$

Summing the three equations, we find $q^2 T^{ii} = T^{ii}$.

Comparing (18) with (17) and using (4) and (13), we arrive at the relation

$$\frac{1}{3}\sum_l^3 \frac{1}{\sigma^0(\mathbf{k})}\frac{d\sigma^1(\mathbf{k}_1)}{d\mathbf{k}_1}\bigg|_l = \frac{\hbar^3}{2mk_0\mu}\frac{k^2}{\Delta E}\psi\left(\frac{\Delta E}{\hbar}\right)[e^{\Delta E/\varkappa T} - 1]^{-1}, \tag{19}$$

where

$$\Delta E = E_1 - E_0 > 0.$$

Thus, by using three positions of the crystal and determining the cross section for one-phonon incoherent scattering $d\sigma^1(\mathbf{k}_1)/d\mathbf{k}_1$ as a function of E_1, and the elastic scattering cross section $\sigma^0(\mathbf{k})$ for the corresponding values of $\mathbf{k}$, we can find the phonon spectrum of a crystal of arbitrary symmetry having any number of identical atoms in the unit cell.

In the case of uniaxial crystals, two positions of the crystal are sufficient, but it is necessary to know exactly the direction of the symmetry axis. In a cubic crystal a single crystal position is sufficient, and we arrive at the result of Placzek and Van Hove.[1]

If $Z_\beta \ll 1$, which is often the case when working with "cold" neutrons, it is obviously sufficient to measure only $d\sigma^1(\mathbf{k}_1)/d\mathbf{k}_1$.

The arguments concerning the inclusion of multiphonon processes which were presented at the end of the previous section remain valid also for the present case.

The author is indebted to Ya. A. Smorodinskiĭ for valuable discussions.

---

[1] G. Placzek and L. Van Hove, Phys. Rev. **93**, 1207 (1954).

[2] W. Visscher, Annals of Physics **9**, 194 (1960).

[3] W. Lamb, Phys. Rev. **55**, 190 (1939).

[4] V. S. Oskot-skiĭ, Физика твердого тела **2**, 701 (1960), Soviet Phys. Solid State **2**, 647 (1960).

Translated by M. Hamermesh
46

SOVIET PHYSICS JETP VOLUME 13, NUMBER 1 JULY, 1961

SYMMETRIC COMPOSITE MODEL OF STRONGLY INTERACTING ELEMENTARY PARTICLES

Ya. B. ZEL'DOVICH

Submitted to JETP editor July 3, 1960

J. Exptl. Theoret. Phys. (U.S.S.R.) 40, 319-323 (January, 1961)

A scheme is considered in which all baryons (p, n, Λ, Σ, Ξ) are composed of two particles and one antiparticle from a set of three elementary fermions A, B, C. It is shown that the best choice is that in which, as far as charge and strangeness are concerned, A and B are identical to Ξ^0 and Ξ^- and C is identical with Λ. The masses of A, B, and C are assumed to be large so that these particles are unstable with respect to strong interactions and are therefore unobservable. In this scheme the parity of all observable baryons is the same and opposite to the parity of the elementary fermions A, B, and C. Pions and K mesons are pseudoscalar with respect to the baryons.

FERMI and Yang[1] were the first to represent the π meson as being composed of a nucleon and an antinucleon.* The discovery of the strange particles led to a model in which there are three elementary fermions; Markov,[3] Sakata,[4] and Okun'[5,6] (collectively abbreviated SOM) developed such a model and outlined its consequences.

The elementary particles in the SOM scheme are p, n, Λ and their antiparticles $\bar{p}$, $\bar{n}$, $\bar{\Lambda}$; the mesons and the remaining hyperons are represented as composites, e.g., $\pi^+ = p\bar{n}$, $K^+ = p\bar{\Lambda}$, $\Sigma^+ = p\bar{n}\Lambda$, $\Xi^- = \bar{p}\Lambda\Lambda$, etc. Thus there exists a sharp distinction between the three "elementary" baryons and the five "composite" ones (3Σ and 2Ξ); on the other hand, the properties of the baryons, and in particular, their masses, give no justification for such a demarkation.

A number of authors[7-9] emphasize that all eight known baryons are similar to one another in first approximation. There is thus a natural need for a scheme in which this similarity and the internal symmetry are recognized from the beginning. One such scheme, in particular, was proposed by Gell-Mann during a discussion at the Conference on the Physics of High Energy Particles at Kiev, 1959.

Let us consider the problem in its most general form. For this purpose we introduce three elementary fermions A, B, and C, which do not coincide with any of the known particles. We shall represent all known baryons as different composites of two particles and one antiparticle; the mesons will be composites of a particle and an antiparticle. Thus all three particles will be assigned the baryon number (nucleon charge) + 1. We assume further that the strangeness of one particle (C) differs by one unit from the strangeness of the two other particles (A and B); A and B form an isotopic doublet, so that the charge of B differs from that of A by one unit. The masses of the particles A and B forming an isotopic multiplet are equal and their interaction with the third particle (C) is also the same. In such a scheme we have 3 × 3 different mesons and 18 different baryons.

The conclusions with respect to the mesons are identical to those made by Matumoto[10] and Okun'.[5,6] Orthogonalizing the states with account of isotopic invariance, we divide the number of mesons into one triplet with $S = 0$, two doublets with $S = \pm 1$, and two singlets with $S = 0$ (S is the strangeness).

Evidently, the triplet $A\bar{B}$, $(A\bar{A} - B\bar{B})/\sqrt{2}$, $B\bar{A}$ represents the π mesons and the two doublets $A\bar{C}$, $B\bar{C}$ and $C\bar{A}$, $C\bar{B}$ represent the K and $\bar{K}$ mesons.

The two singlets form linear combinations with unknown coefficients $\alpha\xi + \beta\zeta$ and $-\beta\xi + \alpha\zeta$, where $\xi = (A\bar{A} + B\bar{B})/\sqrt{2}$ and $\zeta = C\bar{C}$, $|\alpha|^2 + |\beta|^2 = 1$. These singlets describe hypothetical mesons of the type π_0^0 (or ρ_0), which are the subject of much criticism in the literature.[5,10-12] According to our scheme there should be two of these mesons. However, if their masses are larger than $3m_\pi$ these mesons cannot be experimentally observed as particles.

As was shown by Fermi and Yang,[1] it must be assumed that particle and antiparticle are joined in an ^1S state, i.e., with antiparallel spins; then pions and K mesons are pseudoscalar particles, because the product of the intrinsic parities of a fermion and an antifermion is identically equal to -1

---

*Consequences of the Fermi-Yang model concerning the mass difference between π^+ and π^0 and the β decay $\pi^+ \to \pi^0$ were considered by the author in reference 2.

Let us now turn to the baryons. We have, in a classification according to change of strangeness,

1) one doublet $CC\overline{A}$ and $CC\overline{B}$;

2) one triplet $CA\overline{B}$, $C(A\overline{A} - B\overline{B})/\sqrt{2}$, $CB\overline{A}$ and two singlets consisting of linear combinations of $CC\overline{C}$ and $(A\overline{A} + B\overline{B})/\sqrt{2}$;

3) a quadruplet $AA\overline{B}$, $A(A\overline{A} - B\overline{B})/\sqrt{2}$, $B(A\overline{A} - B\overline{B})/\sqrt{2}$, $BB\overline{A}$ and two doublets consisting of linear combinations of $AC\overline{C}$, $BC\overline{C}$ and $A(A\overline{A} + B\overline{B})/\sqrt{2}$, $B(A\overline{A} + B\overline{B})/\sqrt{2}$;

4) one triplet $AA\overline{C}$, $AB\overline{C}$, $BB\overline{C}$.

It is natural to identify the doublet 1) with the nucleons, the triplet 2) with Σ, one of the singlets 2) with Λ and one of the doublets 3) with Ξ. For this identification we must assume that according to the existing classification A and B have the strangeness $S = -2$, while A is neutral and B has the charge $Q = -e$; C has the strangeness $S = -1$ and is neutral. Thus the conserved quantum numbers (charge, strangeness, baryon number) are the same for the pairs A and Ξ^0, B and Ξ^-, and C and Λ, respectively.

Besides the known baryons, the scheme gives also a number of unobserved particles: a particle U of the Λ type ($Q = 0$, $S = -1$), a doublet V of the Ξ type ($Q = 0, -1$ and $S = -2$), a quadruplet W with $Q = 1, 0, -1, -2$ and $S = -2$, and a triplet R with $Q = 0, -1, -2$ and $S = -3$. The absence of these particles with $S = -1$ and $S = -2$ in experiment can be explained by assuming that they have large masses: $m_U > m_\Sigma + m_\pi$ (for $S = -1$); $m_V, m_W > m_\Xi + m_\pi$ for $S = -2$; then they are unstable against strong decay.

The fact that the particles R with $S = -3$ are not observed can be explained in an analogous way if their mass $m_R > m_\Xi + m_K$. It is possible, however, that these particles exist and will be discovered; the threshold for the production of R with the simultaneous production of 3K is extremely high and the probability for observing R is small.

The condition of Gell-Mann and Rosenfeld[13] according to which the charge of the elementary particles must not be larger than unity is artificial and does not follow from the general ideas of the theory of isotopic invariance and strangeness. Therefore, the appearance of the doubly charged W and R particles is not a deficiency of the scheme.*

In principle, another variant of the scheme (Gell-Mann, Kiev) is possible, in which the quantum numbers of the pairs A and p, B and n, and C and Λ, respectively, coincide. In this variant the physical nucleons are identified with one of the doublets 3) and the cascade hyperons Ξ^- and Ξ^0 are described by the doublet 1). The triplet 4) has strangeness + 1.

We know from experiment that the mass increases as we decrease the strangeness, i.e., as we go from the nucleons ($S = 0$) to the cascade hyperons ($S = -2$). Thus one could easily imagine that the particles with $S = -3$ either do not exist or have not yet been observed. But it is difficult to understand why the particles with $S = +1$ have not been observed if they appear in the scheme. For this reason the first scheme ($A \equiv \Xi^0$, $B \equiv \Xi^-$, $C \equiv \Lambda$) appear to be closer to reality than the second ($A \equiv p$, $B \equiv n$, $C \equiv \Lambda$). There is no basis whatsoever for the pseudo-philosophical assertion, which one sometimes encounters, of the indistinguishability of the results of the different schemes.

Let us turn now to the problem of the relative position of the particles in the composite scheme. We must, evidently, assume mutual attraction between particle and antiparticle (and repulsion between two particles). Hence all particles are in S states with respect to the antiparticles. The spatial parity of all composite particles, i.e., of all physical baryons, is odd in the reference system in which the parity of the unobserved elementary particles A, B, and C is even (we assume that the parity of the antiparticles is odd). Since the parity of all physical baryons is the same, the pion and the K meson are pseudoscalars in the reference system in which the parity of, e.g., p, n, and Λ is assumed to be even; in this reference system the parity of Σ and Ξ is also even, while the parity of A, B, and C is odd.

We note that in the SOM scheme, in which Σ and Ξ consist of p, n, and Λ, we would be led to an odd parity for Σ and Ξ, where the parity of p, n, and Λ is even. Although this conclusion is not conclusively refuted by experiment, it nevertheless seems to be highly improbable.

It would be especially desirable to carry out a direct measurement of the relative parity of Σ^0 and Λ by observing the polarization of the quanta in the decay $\Sigma^0 = \Lambda + \gamma$, as proposed by Feldman and Fulton.[14]

Since the particles repel each other, it is natural to assume that two particles are in an odd state relative to one another. This does not prevent them from being both in an S state with respect to an antiparticle. For example, for the system $AB\overline{C}$ we write

---

*We note that the known "$^3/_2$, $^3/_2$" resonance in the scattering of pions from nucleons corresponds to an unstable state of the nucleons which includes the doubly charged state ($\pi^+ + p$).

$$\psi = \varphi(r_{A\bar{C}})\,\chi(r_{B\bar{C}}) - \chi(r_{AC})\,\varphi(r_{B\bar{C}}),$$

where φ and χ are two different (but both spherically symmetric) functions. This wave function is odd under the interchange of A and B, i.e., if we change the sign of r_{AB}. We can rewrite ψ in the form

$$\psi = \sum_i u_i(r_{AB})\,v_i\left(\tfrac{1}{2}(r_A + r_B) - r_{\bar{C}}\right),$$

both functions u_i and v_i are odd, the overall parity of ψ does not depend on the way in which it is written and is odd if the intrinsic parity of the antiparticles is taken into account, as was already noted earlier.

The relative orientation of the spins is determined by the condition that the spins of particle and antiparticle are antiparallel; that this orientation is favored energetically follows from the fact that it is realized in the case of the mesons. For a baryon, which consists of one antiparticle and two particles, we then obtain the total spin ½, as we should, while the spin wave function is even under the interchange of the two particles. In all, taking both the spin and space parts into account, the wave function changes sign under the interchange of the two particles. This is a characteristic feature of the whole scheme: owing to this antisymmetry, the Pauli principle does not forbid systems with two identical particles, as, for example, $CC\bar{A}$ or $AA\bar{B}$.

If we assumed that the spatial function is symmetric under the interchange of the two particles, while the spin function retains its old properties, all systems with two identical particles would be excluded, and we would obtain 9 systems, which fall into three groups according to strangeness: 4 + 4 + 1. It is not possible to fit the 8 known baryons, which fall into the three strangeness groups 2 + 4 + 2, into such a scheme.

Finally, the variant with symmetric space and antisymmetric spin functions with respect to the interchange of the two particles is equivalent to our proposed variant as far as spin, parity, and the Pauli principle are concerned; but it is less favored energetically for two reasons: the repulsion of the particles and the spin dependence of the attraction between particle and antiparticle.

In the composite model it is assumed that approximate expressions for the masses of the composite particles can be given in the form of sums of the masses of the component elementary particles and terms depending on the pairwise interaction of the elementary particles. In conformity with our assumptions about the wave function, we shall consider only the negative contribution to the mass from the attraction between particle and antiparticle; thus in contrast to Matumoto,[10] we shall not make use of the positive contribution from the repulsion of the two particles. Also, we shall not use the same interaction constant for the particle-antiparticle pair in baryons and mesons, since the wave functions are clearly different in the two cases. Thus seven constants enter into the formula for the mass of the baryons: $m_A = m_B = m$, $m_C = \mu$, the contribution from the interaction $A\bar{C}$ or $B\bar{C}$ equal to $-h$, and four quantities which characterize the interaction and the charge exchange of the three pairs $A\bar{A}$, $B\bar{B}$, and $C\bar{C}$, expressed in matrix form (in this form we taken into account that A and B form a doublet):

$$\begin{array}{cccc} & A\bar{A} & B\bar{B} & C\bar{C} \\ A\bar{A} & k & l & m \\ B\bar{B} & l & k & m \\ C\bar{C} & m & m & n \end{array}$$

In view of the isotopic invariance the interaction of the pairs $A\bar{B}$ and $B\bar{A}$ must be the same as the interaction of the neutral term of the isotopic triplet $(A\bar{A} - B\bar{B})/\sqrt{2}$, i.e., it is characterized by the quantity $k - l$.

Since the number of known different masses is four (the electromagnetic mass differences within the multiplets are neglected), there is sufficient freedom in the set of seven numbers to allow us to satisfy the inequalities necessary to explain non-observability of the elementary particles A, B, and C of the scheme themselves as well as of the supernumerary particles U, V, and W; the mass of R can be either larger or smaller than the sum $m_\Xi + m_K$, so that the formula for the mass does not permit us to draw a definite conclusion about the existence of R.

The main problem to be investigated is that of the role of the unobserved particles as possible excited states and wide resonances, i.e., the problem of how these particles show up in the dispersion relations for processes involving particles which are stable against strong decay. We note that the known "³⁄₂, ³⁄₂" resonance should not be regarded as an unstable particle of our scheme, since in this scheme the spin of all particles — stable and unstable alike — is equal to ½.

---

[1] E. Fermi and C. N. Yang, Phys. Rev. **76**, 1739 (1949).

[2] Ya. B. Zel'dovich, Dokl. Akad. Nauk **97**, 225 and 421 (1954).

[3] M. A. Markov, Report at the 6th Rochester Conference on the Physics of High Energy Particles (1956); Гиперонв и К-мезоны (Hyperons and K mesons) Fizmatgiz (1958).

[4] S. Sakata, Progr. Theor. Phys. **16**, 686 (1956).

[5] L. B. Okun', JETP **34**, 469 (1958), Soviet Phys. JETP **7**, 322 (1958).

[6] L. B. Okun', Usp. Fiz. Nauk **68**, 449 (1949), Ann. Rev. Nuc. Sci. **9**, 61 (1959).

[7] J. Schwinger, Ann. of Phys. **2**, 407 (1957).

[8] A. Salam and J. C. Ward, Nuovo cimento **11**, 568 (1958).

[9] M. Gell-Mann, Phys. Rev. **106**, 1296 (1957).

[10] K. Matumoto, Progr. Theor. Phys. **16**, 583 (1956).

[11] A. M. Baldin, Nuovo cimento **8**, 569 (1958).

[12] Ya. B. Zel'dovich, JETP **34**, 1644 (1958), Soviet Phys. JETP **7**, 1130 (1958).

[13] M. Gell-Mann and A. H. Rosenfeld, Ann. Rev. Nucl. Sci. **7**, 407 (1957).

[14] G. Feldman and T. Fulton, Nucl. Phys. **8**, 106 (1958).

Translated by R. Lipperheide
47

SOVIET PHYSICS JETP VOLUME 13, NUMBER 1 JULY, 1961

HIGHER MOMENTS OF THE CHARGE AND MAGNETIC MOMENT DISTRIBUTIONS OF NUCLEONS

V. B. BERESTETSKIĬ and M. V. TERENT'EV

Submitted to JETP editor August 3, 1960

J. Exptl. Theoret. Phys. (U.S.S.R.) 40, 324-327 (January, 1961)

The unitarity condition with only two-pion intermediate states included is used to calculate the moments of the charge and magnetic moment distributions of nucleons. Asymptotic expressions for these moments are obtained. We calculate how the phase shifts in electron scattering from such nucleons differ from the phase shifts that would be obtained for point nucleons.

1. Chew et al.[1] and Federbush, Goldberger, and Treiman[2] have investigated the spectral distributions g_1^V and g_2^V of the isovector electromagnetic nucleon form factors G_1^V and G_2^V which result from two-pion states. The calculation requires an expression for the pion-nucleon scattering amplitude in the nonphysical region of momentum and energy transfer. If one uses the contribution to this amplitude from the pole term and the experimental data on pion-nucleon scattering, one can obtain an expression for the scattering amplitude only for momentum transfer t close to $t = 4\mu^2$. This is no help whatsoever if one wants to perform a reliable calculation of the anomalous magnetic moment and mean square radius r^2 of the nucleon without additional assumptions on the nature of pion-pion scattering[3] or the contribution from states with large numbers of pions and nucleons.

The problem we have set for ourselves is to calculate the quantities that depend specifically on the spectral distributions for t in the neighborhood of $4\mu^2$. Such quantities are the higher moments of the charge and magnetic moment distribution

$$(\overline{r^{2n}})^V_{1,} = \frac{(-1)^n(2n+1)!}{n!} G^{V(n)}_{1,2}(0) = \frac{(2n+1)!}{\pi}\int^{\infty} \frac{g^V_{1,2}(t)\,dt}{t^{n+1}}$$

or the higher multipole potentials of nucleon transitions, which are related to the nucleon structure and determine, in particular, how the phase shifts in electron-nucleon scattering differ from the values obtained with point nucleons, e.g., expressions of the form

$$a_l = \int \frac{G^V(t) - G(0)}{t} P_l(z)\,dz$$

$$= -\frac{1}{\pi p^2}\int_{4\mu^2}^{\infty} \frac{g^V(t)}{t} Q_l\left(1 + \frac{t}{2p^2}\right) dt, \qquad (2)$$

where P_l and Q_l are Legendre polynomials of the first and second kind, $t = -2p^2(1 - z)$, and p is the momentum in the electron-nucleon center-of-mass system.

For sufficiently large n or l, the integrals in (1) and (2) depend only on a region close to the lower limit, where the g^V functions can be found up to a factor which represents the value of the pion form factor $\Pi(t)$ for $t \sim 4\mu^2$. This quantity can then be measured by comparing the results of calculations according to (1) and (2) with experiment. Unfortunately the asymptotic nature of Eqs. (1) and (2) makes such a comparison difficult.

2. The spectral distributions obtained from the unitarity condition including only the two-pion states are of the form[1]

$$g_1^V\gamma_\mu + \frac{g_2^V}{4M}(\gamma_\mu\hat{q} - \hat{q}\gamma_\mu)$$

$$= \frac{\Pi(t)}{32\pi}\frac{1}{\sqrt{t(t-4M^2)}}\int_{-\sqrt{(t-4M^2)(t-4\mu^2)}}^{\sqrt{(t-4M^2)(t-4\mu^2)}} k_\mu A(t, \nu)\,d\nu, \qquad (3)$$

where $k = k_1 + k_2$, $q = k_1 - k_2 = p_1 - p_2$, p_i and k_i are the nucleon and meson momenta, $\nu = |\mathbf{k}|\,|\mathbf{p}|$, M is the nucleon mass, μ is the meson mass, and A is the isovector amplitude for two-pion nucleon annihilation.

This amplitude A can be divided into a pole term and a regular part, $A = A^p + A'$. Those terms in the g^V obtained by putting A^p in (3) were found by Chew et al.[1] For small $\xi = \sqrt{t/4\mu^2 - 1}$, they may be written (here $\epsilon = \mu/M$)

$$g^V_{1,p} = \tfrac{8}{3} f^2\xi^3/\varepsilon^2, \qquad g^V_{2,p} = 4f^2\xi^5/\varepsilon^4, \qquad \xi \ll \varepsilon/2, \qquad (4)$$

$$g^V_{1,p} = f^2[2\xi - \pi\varepsilon/2 + \varepsilon^2/2\xi],$$

$$g^V_{2,p} = -2f^2[2\xi - \pi\xi^2/2\varepsilon], \quad \varepsilon/2 < \xi \ll 1. \qquad (5)$$

The terms obtained from the regular part of A can be found by inserting the first terms of the expansion of A′ about $t = 4\mu^2$ into (3). These were obtained by Galanin et al.[4] by analytic continuation of the experimental pion-nucleon scattering amplitudes:

$$A' = (g^2/\mu^2)(a_1\nu/M - a_2\hat{k}), \qquad a_1 = 0.0065, \qquad a_2 = 0.0125. \tag{6}$$

Inserting (6) into (3), we obtain the corresponding terms in the g^V, namely

$$g_1^{V'} = \tfrac{4}{3} f^2\xi^3(a_1 - a_2)/\varepsilon^2, \quad g_2^{V'} = -\tfrac{2}{3} f^2\xi^3 a_1/\varepsilon^2$$
$$(f^2 = (\varepsilon/2)^2(g^2/4\pi) = 0.08). \tag{7}$$

3. Comparison of (7) with (4) and (5) shows that the regular part $g^{V'}$ of the spectral distribution is significant only for very small values of ξ. Bosco and Alfaro[5] have used expressions such as (7) to calculate the asymptotic behavior of the isovector part of the charge and magnetic moment distributions, obtaining

$$\rho^V(r) = \frac{1}{(2\pi)^2}\int_{4\mu^2}^{\infty} g^V(t)\frac{1}{r}\exp(-\sqrt{t}r)\,dr. \tag{8}$$

This expression, however, is good only asymptotically for $r \gg 1/\mu\epsilon$, and can therefore not be used to construct the entire $\rho^V(r)$ curve by interpolation, as was attempted by Alfaro and Predazi.[6] This is because in the region $1/2\mu \ll r < 1/\mu\epsilon$ the fundamental role is played by values of ξ in which the g^V are given by the pole term (5).

Inserting (5) into (1), we obtain

$$(\overline{r_1^{2n}})^V = \frac{4f^2(2n+1)!}{(4\mu^2)^n n!}\left[-\frac{(n-1)!\varepsilon}{8} + \frac{(2n-3)!!}{2^{n+1}} + \frac{\varepsilon^2}{4}\frac{(2n-1)!!}{2^{n+1}}\right],$$
$$(\overline{r_2^{2n}})^V = -\frac{f^2(2n+1)!}{\varepsilon(4\mu^2)^n n!}\left[\frac{(n-2)!}{4} - 2\varepsilon\frac{(2n-3)!!}{2^{n+1}}\right]. \tag{9}$$

Inserting (5) into (8), we obtain

$$\rho_1^V(r) = \frac{f^2}{(2\pi)^2}e^{-2\mu r}\left[-\frac{\pi\varepsilon}{r^3} + 3\sqrt{\frac{\pi}{\mu}}\frac{1}{r^{7/2}}\right],$$
$$\rho_2^V(r) = \frac{f^2}{(2\pi)^2}e^{-2\mu r}\left[-6\sqrt{\frac{\pi}{\mu}}\frac{1}{r^{7/2}} + \frac{4\pi}{\mu\varepsilon}\frac{1}{r^4}\right]. \tag{10}$$

4. Expressions can be given for the difference between the electron-nucleon phase shift and their values for a point nucleon. It is more convenient, however, to give the a_i^k and b_i^k, which are related to these differences in the phase shifts by the expressions

$$[\sqrt{l(l-1)}/(2l-1)](a_l^{l-1} - b_l^{l-1}) = 2i\gamma^{l-1},$$
$$[\sqrt{(l+1)(l+2)}/(2l+3)](a_l^{l+1} - b_l^{l+1}) = 2i\gamma^{l+1},$$
$$[(l+2)/(2l+3)]a_l^{l+1} + [(l+1)/(2l+3)]b_l^{l+1} = -2i\,{}^3\delta_l^{l+1},$$
$$[(l-1)/(2l-1)]a_l^{l-1} + [l/(2l-1)]b_l^{l-1} = -2i\,{}^3\delta_l^{l-1},$$
$$a_l^l = -2i\,{}^3\delta_l^l, \quad a_{0,l}^l = -2i\,{}^1\delta_l^l, \quad b_{0,l}^l = 2i\gamma_{0,1}^l. \tag{11}$$

Here ${}^{3,1}\delta_l^J$ are the triplet and singlet phase shifts for total angular momentum J, and $\gamma_{0,1}^J$ and γ^J are parameters which describe the amount of mixing between states with total spin 0 and 1 and states with orbital angular momenta J − 1 and J + 1. Then the a_i^k and b_i^k are given by the following expressions, where we use Eqs. (5) for the spectral distributions:

$$a_l^l = NQ_l(1+2\eta^2)\left\{-\left[\frac{A}{p} + \frac{\omega B}{lM}\right]J_1 + \left[\frac{\omega(1+2\eta^2)}{lM} - 4\frac{l+1}{l}\frac{\eta^4(1-\eta^4)}{M}\right]J_2\right\},$$
$$a_l^{l-1} = NQ_l(1+2\eta^2)\left\{-\left[\frac{A}{p} + \frac{l+1}{l}\frac{\omega B}{M}\right]J_1 + \left[\frac{l+1}{l}\frac{\omega(1+2\eta^2)}{M} + \frac{4(l+1)^2\eta^4(1-\eta^4)}{l(l-1)M}\right]J_2\right\},$$
$$a_l^{l+1} = NQ_l(1+2\eta^2)\left\{-\left[\frac{A}{p} - \frac{\omega B}{M}\right]J_1 + \left[-\frac{\omega(1+2\eta^2)}{M} + \frac{4(l+1)\eta^4(1-\eta^4)}{(l+2)M}\right]J_2\right\},$$
$$b_l^{l-1} = NQ_l(1+2\eta^2)\left\{-\left[\frac{A}{2p} + \frac{l+1}{l}\frac{\omega B}{M}\right]J_1 + \left[\frac{l+1}{l}\frac{\omega(1-2\eta^2)}{M} - \frac{2\eta^2}{M}\right]J_2\right\},$$
$$b_l^{l+1} = NQ_l(1+2\eta^2)\left\{-\left[\frac{A}{2p} - \frac{\omega B}{M}\right]J_1 + \left[-\frac{\omega}{M}(1+2\eta^2) - \frac{2\eta^2}{M}\right]J_2\right\},$$
$$a_{0,l}^l = NQ_l(1+2\eta^2)\left\{-\frac{A}{2p}J_1 - \frac{2\eta^2}{M}J_2\right\},$$
$$b_{0,l}^l = NQ_l(1+2\eta^2)\sqrt{\frac{l+1}{l}}\frac{\eta^2}{\omega}\left[-\frac{\omega^2 B}{\eta M}J_1 - \frac{\omega^2 J_2}{\eta M}\right];$$
$$A = \frac{Mm_e + Mp + p^2}{Mp} + (1+2\eta^2)\frac{p(M+p)}{M(m_e+p)}, \quad B = 1 + \frac{M}{m_e+p};$$
$$J_1 = \frac{f^2\sqrt{\pi}}{2}\frac{1}{L^{3/2}}\left[1 - \frac{\sqrt{\pi}}{8\zeta}\left(1 - \frac{1}{L}\right)\right],$$
$$J_2 = -2f^2\sqrt{\pi}\frac{1}{L^{3/2}}\left[1 - \frac{\sqrt{\pi}}{8\zeta}\left(1 - \frac{1}{L}\right)\right];$$
$$\zeta = \varepsilon\sqrt{L}/2, \quad \eta = \mu/p, \qquad \omega = \eta\sqrt{1+\eta^2},$$
$$N = ie^2p/2\pi, \qquad L = \eta(l+1)/\sqrt{1+\eta^2}. \tag{12}$$

Calculation for the case $l = 4$ and $p = \mu$ leads to very small values (of the order of 10^{-4}) for the differences in the phase shifts and the mixing parameters. This is a reflection of the following situation, which makes it difficult to apply to the present case the methods of calculation suggested by Galinin et al.[4] Equations (12) are the leading terms in a power series expansion in 1/L, where

$$L = l + 1, \qquad \eta \gg 1; \tag{13a}$$
$$L = \eta(l+1), \qquad \eta \ll 1. \tag{13b}$$

On the other hand, angular momenta $l \lesssim l_{\text{eff}}$

$\sim r_0 p$ play a role in the scattering, where r_0 may be called the radius of interaction (for our case it is of the order of the nucleon radius). In case (13a) a satisfactory expansion is one in powers of $1/L$ for $l \gtrsim 4-5$; but then $l_{\text{eff}} \ll 1$, and the phases obtained for $l = 4$, of course, turn out to be very small. For $p \gg \mu$, the value of l_{eff} increases, but the values of l for which the phases can be calculated also increase linearly with p. It is most convenient to investigate the region where $p \sim \mu$, but our calculations have shown that in this case also the differences in the phases and mixing parameters are extremely small.

In conclusion we express our gratitude to I. Ya. Pomeranchuk for his interest in the work and for helpful discussions.

APPENDIX

We give here the formulas relating the phases and mixing parameters with the matrix elements $S^J_{S', l'; S, l}$ of the scattering matrix in the representation in which the total angular momentum J is diagonal (S, l, S′, and l' are the spin and orbital angular momenta before and after scattering):

$$S^J_{1,\,J+1;\,1,\,J+1} = \cos 2\gamma^J \exp\left(2i^3\delta^J_{J+1}\right),$$
$$S^J_{1,\,J-1;\,1,\,J-1} = \cos 2\gamma^J \exp\left(2i^3\delta^J_{J-1}\right),$$
$$S^J_{1,\,J+1;\,1,\,J-1} = i\sin 2\gamma^J \exp\left(i^3\delta^J_{J-1} + i^3\delta^J_{J+1}\right),$$
$$S^J_{0,\,J;\,0,\,J} = \cos 2\gamma^J_{0,1} \exp\left(2i^1\delta^J_J\right),$$
$$S^J_{1,\,J;\,1,\,J} = \cos 2\gamma^J_{0,1} \exp\left(2i^3\delta^J_J\right),$$
$$S^J_{1,\,J;\,0,\,J} = i\sin 2\gamma^J_{0,1} \exp\left(i^1\delta^J_J + i^3\delta^J_J\right).$$

---

[1] Chew, Karplus, Gasiorovicz, and Zachariasen, Phys. Rev. **110**, 265 (1958).

[2] Federbush, Goldberger, and Treiman, Phys. Rev. **112**, 642 (1958).

[3] W. Fraser and J. Fulko, Phys. Rev. **117**, 1609 (1960).

[4] Galanin, Grashin, Ioffe, and Pomeranchuk, JETP **37**, 1663 (1959), Soviet Phys. JETP **10**, 1179 (1960).

[5] B. Bosco and V. Alfaro, Nuovo cimento **13**, 154 (1959).

[6] V. Alfaro and F. Predazi, Nuovo cimento **14**, 448 (1959).

Translated by E. J. Saletan
48

SOVIET PHYSICS JETP VOLUME 13, NUMBER 1 JULY, 1961

PLASMA TURBULENCE IN A MAGNETIC-MIRROR SYSTEM

B. B. KADOMTSEV

Submitted to JETP editor August 3, 1960

J. Exptl. Theoret. Phys. (U.S.S.R.) **40**, 328-336 (January, 1961)

The convective turbulence of a rarefied plasma in a magnetic-mirror system is analyzed theoretically. The turbulence arises as a result of plasma instability. The results which are obtained are in satisfactory agreement with the experimental data of Ioffe, Tel'kovskiĭ, Sobolev, and Yushmanov on plasma lifetime in a system of this kind.[7]

1. INTRODUCTION

THE magnetic-mirror system[1] represents a possible means by which high-temperature plasma can be contained. In its simplest version, a magnetic-mirror system consists of a region of uniform magnetic field H_0 with mirrors at each end, i.e., regions of stronger magnetic field H_m. A schematic diagram of such a system is shown in Fig. 1.

If the magnetic field is strong the Larmor radius of the particles ρ is much smaller than any of the characteristic dimensions and the adiabatic invariant $\mu = Mw^2/2H$ (M is the mass of the particles, w is its transverse velocity) may be considered constant with a high degree of accuracy. For this reason a field configuration of this kind represents a good trapping system for particles for which $\sin\alpha = w/v > H/H_m$ where u is the longitudinal velocity while $v = (u^2 + w^2)^{1/2}$ is the total velocity.

However, the problem of containing a quasineutral plasma is quite difficult. In a magnetic-mirror system the magnetic field falls off in the radial direction and, because it is diamagnetic, the plasma is expelled from the central region toward the walls. As far as the motion of individual particles is concerned, this instability manifests itself in separation of the charges and the appearance of an electric field which causes particles of both signs to drift in the radial direction.

If the plasma pressure is much smaller than the pressure of the magnetic field, only the convective or interchange perturbations lead to instability;[2,3] these correspond to the interchange of neighboring lines of force without perturbation of the magnetic field. In these perturbations the electric field is irrotational and the field potential is constant along the lines of force. Hence, if there is good electrical contact with the end electrodes perturbations of this kind are impossible and a low-pressure plasma will be stable.

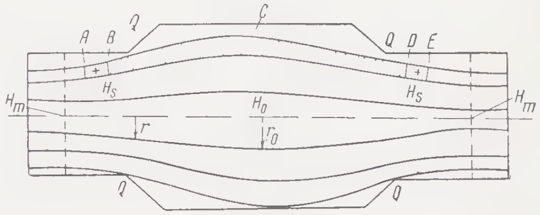

FIG. 1

The concrete details of a given experiment determine whether or not an electrical contact exists. For example, in the pyrotron, described by Post,[4] in which hot plasma is produced by adiabatic compression of a cold plasma which is injected from outside, contact is apparently realized by virtue of the rather dense cold plasma (this question is discussed in a paper by Post et al.[5]). Under other conditions no contact may be formed. Precisely this situation obtains in the system described by Ioffe et al.[6,7] The experimental finding that the plasma is lost from this system primarily in the direction transverse to the magnetic field verifies the fact that no electrical contact is realized.

2. QUALITATIVE ANALYSIS

In the experiment of Ioffe et al.[6] a hot plasma (ion energy, approximately 1 kev and density, approximately 10^9 cm^{-3}) is produced by accelerating ions in a pulsed radial electric field of the order of 1 kv/cm; the field is applied between the chamber and a cold pinch located along the axis of the system. Qualitatively, the way in which the system becomes filled with hot plasma may be described as follows. Following the application of the high voltage, the outer layers of the cold plasma are set into rotational motion. This rotational motion, however, is unstable. The centrifugal force causes the plasma to be "splashed" violently toward the periphery of the system; since this effect is characterized by high electric fields, the "splashing" results in an increase in the energy of the individual ions. As a result the system becomes more or less uniformly filled by plasma with high energy ions; it has been shown experimentally that this process is completed in a time of the order of 10 — 20 μsec.

After the high-voltage pulse ends, plasma rotation ceases and a quieter phase, characteristic of the motion of a diamagnetic plasma in a magnetic field that decays in the radial direction, is observed. The characteristic time for this motion is considerably greater than the ion time-of-flight between the mirrors $t_s \sim 5$ μsec. Hence, an equilibrium distribution of ions and electrons can be set up along the lines of force.

We consider an individual tube containing plasma, ABCDE. Since the electrons remain cold (the electron temperature T_e is of the order of 10 ev) we can write $T_e = 0$; the, from the electron equilibrium condition it follows that φ, the electrical potential along each tube of force containing plasma, is a constant. The potential can not be negative; if it were, the excess electrons would be rapidly repelled from a given tube towards the ends, which are at zero potential. Thus, an individual tube of force can have a potential different from zero only if there is a charge due to positive ions at its ends, the regions AB and DE, where the electron density vanishes.

This charge, however, cannot be arbitrarily large because if the ion charge increases the electric field repels ions toward the ends and then they can be contained only by virtue of the increase in magnetic field from the value H_s at the boundary of the tube to the value H_m at the mirror. It follows that the potential φ satisfies the following condition:

$$0 < \varphi < (T/e)(H_m/H_s - 1), \tag{1}$$

where T is the ion temperature, i.e., ⅔ of the ion mean energy.

This relation allows us to understand why there may be no electrical contact with the ends under the conditions being considered. Because there are large fluctuations in the electric field during the ion acceleration stage, in a plasma produced in this way there are no ions which are reflected very close to the mirrors. In other words, the boundary of the hot plasma is located at some distance from the surface of maximum magnetic field, that is to say, $H_s \neq H_m$. Hence, φ can vary over some finite limit (1) and this means that there is no contact with the end walls.

A consequence is that there is a convective instability in this system: a tube with more dense plasma is expelled towards the walls as a result of the production of the azimuthal electric field, causing a drift $v_e = cH^{-2}(\mathbf{E} \times \mathbf{H})$ and when the tube comes into contact with the wall, ions are emitted and absorbed by the wall; these ions are at a distance of the order of the mean Larmor radius ρ from the wall. Because of the loss of ions, the plasma potential close to the walls drops to zero and the excess electrons escape to the ends along the lines of force. As a result, a layer of thickness ρ next to the walls will be at zero potential and the azimuthal component of the electric field (consequently, the normal component of the velocity) V_e vanishes in the entire wall layer.

It follows that an individual plasma tube cannot be lost to the wall immediately. The tube is slowed down* near the wall and as soon as its density becomes lower than that of the surrounding plasma (because of wall losses) it is forced back into the system. Thus, each individual tube must come in contact with the walls and is forced back into the chamber several times before becoming completely detached from the plasma. The motion as a whole is similar to thermal convection in an ordinary incompressible fluid: the role of the fluid is played by the tubes of force of the magnetic field while the plasma pressure acts as the temperature. For this reason we can make use of the semi-quantitative methods of analysis of ordinary convection.

3. BASIC EQUATIONS

For the conditions considered here, collisions between particles are unimportant so that an exact description of the ion motion is given by the kinetic equation without the collision term:

$$\frac{\partial f}{\partial t} + (\mathbf{v}\nabla)f + \frac{e}{M}\left\{\mathbf{E} + \frac{1}{c}[\mathbf{v}\times\mathbf{H}]\right\}\frac{\partial f}{\partial \mathbf{v}} = 0. \tag{2}$$

For convective flow of a plasma characterized by a plasma frequency which is much lower than the cyclotron frequency $\Omega_H = eH/Mc$ but a characteristic length considerably greater than the Larmor radius ρ, the important terms in Eq. (2) are the last two terms. Hence, in the zeroth approximation

$$\left\{\mathbf{E} + \frac{1}{c}[\mathbf{v}\times\mathbf{H}]\right\}\frac{\partial f}{\partial \mathbf{v}} = 0, \tag{3}$$

whence we have $f = F(\mathbf{v} - \mathbf{v}_0)$, where $\mathbf{v}_0 = H^{-2}c(\mathbf{E} \times \mathbf{H}) = -H^{-2}c(\nabla\varphi_0 \times \mathbf{H})$ while the function F has an axis of symmetry with respect to the direction of the magnetic field.

---

*The fact that a metal wall along the walls of force reduces the normal component of the electric drift to zero, causing retardation of the plasma, was pointed out by L. A. Artsimovich.

If we take account of the remaining terms, then in addition to the electric drift there are supplementary drift velocities which are different for different particles. As an approximation, however, we may assume that all ions move accross the magnetic field with the same velocity $\mathbf{v}_0$; φ_0, however, is no longer the potential of the electric field, but some effective potential which takes account of all forces acting on the ions. This approximation allows us to go from the kinetic description to the hydrodynamic description. If we take $\varphi_0 = \text{const}$ along the lines of force a further simplification is possible and the motion of the individual tubes of force becomes two-dimensional.

In Eq. (2) we can write $f = F(\mathbf{v} - \mathbf{v}_0)$, multiply by $\mathbf{w} = \mathbf{v} - \mathbf{u}\cdot\mathbf{H}/H$, integrate over velocity, and average over the lines of force, thereby obtaining the equation for the transverse motion. We shall assume that the mirror ratio H_m/H_0 is small and that the lines of force of the magnetic field are only slightly distorted. Then we can then neglect the curvature of the lines in the inertia terms, thereby obtaining the following equation for the transverse motion:

$$Mn\left\{\frac{\partial \mathbf{v}_0}{\partial t} + (\mathbf{v}_0\nabla)\,\mathbf{v}_0\right\} + \nabla p + en\nabla\varphi - \frac{ne}{c}[\mathbf{v}_0\times\mathbf{H}] = Mn\mathbf{g}. \quad (4)$$

Here,

$$n = \frac{H_0}{L}\iint f\,d\mathbf{v}\,\frac{dl}{H}$$

is some mean density over the tube of force, L is the mean length of the tubes of force,

$$p = \frac{H_0}{L}\int \frac{p_\perp}{H}\,dl$$

is the mean transverse pressure, the vector **g** is along the radius and is given by

$$g = \frac{1}{MnL}\int (p_\perp + p_H)\,\frac{H_0^2 r_0}{H^2 R r}\,dl \approx \frac{1}{MnL}\int (p_\perp + p_H)\,\frac{H_0^{3/2}}{RH^{3/2}}\,dl,$$

H_0 is the field at the center of the system, $r = r(z)$ is the distance from the line of force to the axis of the system, $r_0 = r(z = 0)$ is the distance from the line of force to the axis in the central plane, dl is an element of length of the line of force, R is its radius of curvature, and

$$p_\parallel = \int Mu^2 f\,dv, \qquad p_\perp = \int \frac{Mw^2}{2}\,f\,d\mathbf{v}$$

are respectively the longitudinal and transverse pressures.

The average field **H** which appears in Eq. (4) may be approximated by a constant so that Eq. (4) coincides exactly with the hydrodynamic equation for the two-dimensional motion of ions in a uniform magnetic field in the presence of a gravitational force Mg. This force, which takes account of the curvature of the lines of force, expresses precisely the average effect of the expulsion of the diamagnetic plasma from the field. We may note that the expression for g given above can be obtained from energy considerations, as has been done by Rosenbluth and Longmire.[2]

The ions can reach an equilibrium state in the longitudinal direction so that the ion distribution function depends explicitly only on v^2 and $\mu = Mw^2/2H$. If the particle density is high enough the plasma is quasi-neutral and the ion density is regions AB and DE (cf. Fig. 1), where the electron density vanishes, is very small. However, this region is entered only by particles characterized by $\sin\alpha = w/v < H/H_S$; consequently, the ion velocity distribution contains no velocities within the cone defined by $\sin\alpha < H/H_S$. We approximate the ion velocity distribution by a Maxwellian function (no velocities in this cone) and assume that the temperature T is a constant. For this distribution

$$n = N\sqrt{1 - H/H_s}, \qquad p_\parallel + 2p_\perp = 3nT,$$

$$p_\parallel = nT\,(1 - H/H_s).$$

In principle, we can calculate g for these relations and find the connection between n and p for a given magnetic field, in which case the problem is reduced to an analysis of the transverse motion alone.

To Eq. (4) we must add the electric field equation

$$\Delta\varphi = -4\pi e\,(n - n_e) \quad (5)$$

and the ion and electron continuity equations:

$$\partial n/\partial t + \operatorname{div}(\mathbf{v}_0 n) = 0, \quad (6)$$

$$\partial n_e/\partial t + \mathbf{v}_e\nabla n_e = 0. \quad (7)$$

Here we have neglected end leakage because it has been shown experimentally[7] that leakage is responsible for less than 20% of the total particle loss from the system; we assume that the electrons experience an electric drift $\mathbf{v}_e = cH^{-2}(\mathbf{H}\times\nabla\varphi)$ only. Eqs. (4) — (7) completely describe the behavior of plasma in the system.

4. STABILITY

We first find the density at which the plasma becomes unstable. We assume that

$$4\pi e^2 n/M\Omega_H^2 = 4\pi nMc^2/H^2 \ll 1.$$

Under these conditions the inertia terms in Eq. (4) can be neglected and we obtain the following expression

$$\mathbf{v}_0 = -\frac{1}{\Omega_H}[\mathbf{h}\times\mathbf{g}] + \frac{1}{M\Omega_H n}[\mathbf{h}\times\nabla p] + \frac{c\,[\mathbf{h}\times\nabla\varphi]}{H}, \qquad (8)$$

where $\mathbf{h}$ is a unit vector along $\mathbf{H}$ (i.e., the z axis).

We take $p = nT$ and assume that T is a constant. Furthermore, for the curvature of the lines of force we can write $g = Tr/MaR_0$ where a is the radius of the chamber and R_0 is some mean radius of curvature for the lines of force close to the walls. Substituting Eq. (8) in Eq. (6) we have

$$\frac{\partial n}{\partial t} - \omega_0 \frac{\partial n}{\partial \vartheta} + \frac{c}{H}\mathbf{h}\,[\nabla\varphi, \nabla n] = 0, \qquad (9)$$

where $\omega_0 = T/MaR_0\Omega_H$ is the angular drift velocity of the ions under the effect of the force Mg.

Suppose that in the equilibrium state $n = n_e = n_0$ and $\varphi_0 = 0$. Assuming that the perturbations of density and potential n', n'_e and φ' vary according to $\exp\{-i\omega t + im\vartheta\}$, from Eqs. (5), (7), and (9) we can obtain a single equation for φ:

$$\omega(\omega + m\omega_0)\,\Delta\varphi' + \frac{4\pi e^2 m^2 \omega_0}{M\Omega_H}\frac{1}{r}\frac{dn_0}{dr}\varphi' = 0. \qquad (10)$$

In the simplest case, where the density n_0 is given by the parabolic relation $n_0 = N(1 - r^2/a^2)$, the solution of Eq. (10) is of the form $\varphi^1 = J_m(\alpha_{mn} r/a)$ where α_{mn} is the n-th root of the Bessel function J_m. Then the oscillation frequency is given by

$$\omega = -\tfrac{1}{2} m\omega_0 \pm m\sqrt{\tfrac{1}{4}\omega_0^2 - 2\Omega_0^2\omega_0/\Omega_H\alpha_{mn}^2},$$

where $\Omega_0^2 = 4\pi e^2 N/M$. From these considerations it is apparent that an instability arises only when the density becomes high enough to make Ω_0^2 greater than $\frac{1}{8}\alpha_{mn}^2\omega_0\Omega_H$. Under these conditions the instability arises first for perturbations with the greatest wavelength, i.e. for $m = 1$ and $\alpha_{mn} = \alpha_{11} = 2.83$. The stability condition can be written approximately in the form

$$r_d^2 > aR_0, \qquad (11)$$

where $r_D^2 = T/M\Omega_0^2$ is the square of the Debye radius.

The stability condition assumes a similar form for other density distributions $n_0(r)$. In particular, if n_0 experiences a steep drop at a distance δ from the walls (which are assumed to be metal), the stability condition becomes $r_D^2 > R_0\delta$. Since δ cannot be smaller than ρ, for a plasma density high enough so that $r_D^2 < R_0\rho$ there will be an instability for any distribution n_0 which vanishes at the walls. This is precisely the situation which obtains in the experiment[6] where $r_D \sim \rho \sim 1$ cm, while R_0 is approximately 10^2 cm.

5. TURBULENT CONVECTION

The condition $r_D^2 < R_0\rho$ together with the plasma neutrality condition, represent the criteria for convective motion on all scales of length to the minimum of approximately ρ. The equations of motion can be simplified for this particular case. For this purpose we subtract Eq. (7) from Eq. (6) and express the difference $n - n_e$ in terms of φ by means of Eq. (5). We thus obtain

$$\frac{\partial}{\partial t}\Delta\varphi + \mathbf{v}_e\nabla(\Delta\varphi) - 4\pi e\,\mathrm{div}\,(n(\mathbf{v}_0 - \mathbf{v}_e)) = 0, \qquad (12)$$

where $\mathbf{v}_e = cH^{-1}(\mathbf{h}\times\nabla\varphi)$. For two-dimensional flow, however, $\nabla\varphi = (H/c)\,\mathrm{curl}\,\mathbf{v}_e$ so that Eq. (12) can be integrated once, yielding

$$\frac{\partial \mathbf{v}_e}{\partial t} + (\mathbf{v}_e\nabla)\,\mathbf{v}_e - \frac{4\pi ec}{H^2} n\,[\mathbf{v}_0 - \mathbf{v}_e,]\times\mathbf{H} + \nabla f = 0, \qquad (13)$$

where f is an arbitrary function of r and ϑ.

As an approximation, in the first term of Eq. (4) we replace $\mathbf{v}_0$ by $\mathbf{v}_e$ and n by some mean density N, multiply Eq. (4) by $4\pi c^2/H^2$, and subtract from Eq. (13). We then obtain the approximate equation

$$\frac{\partial \mathbf{v}_e}{\partial t} + (\mathbf{v}_e\nabla)\,\mathbf{v}_e + \nabla p^* = g^* n, \qquad (14)$$

where $\mathbf{v}_e \approx \mathbf{v}_0$ is the macroscopic plasma velocity, p^* is an arbitrary function of r and ϑ, and $g^* = 4\pi e^2 g/M(\Omega_H{}^2 + \Omega_0^2)$, $\Omega_0^2 = 4\pi e^2 N/M$. If we take account of the neutrality condition $n = n_e$ and the condition

$$\mathrm{div}\,\mathbf{v}_e = 0 \qquad (15)$$

Eqs. (14) and (7) coincide exactly with the equations for an incompressible inhomogeneous fluid in a gravitational field of force. Hence there is a very close analogy with the familiar convection of an incompressible fluid.

Since Eq. (14) does not contain a viscosity term, the convection described by this equation is of a turbulent nature. Thus, the problem of plasma lifetime in the system becomes essentially the determination of the coefficient of turbulent diffusion. We shall assume that the chamber walls are exactly along the lines of force. Let x be the distance from the wall while q is the diffusion flux of plasma to the wall. In the region next to the walls the flux q may be assumed constant. Eqs. (14) and (15) contain only one dimensional parameter g^* which appears in the form of a product with n. It then follows from similitude considerations that the turbulent state of the plasma must be determined only by the parameter g^*q. But, from the quantities g^*q and x the dimensionality of the diffusion coefficient can be constructed in only one way, namely,

$$D = A(g^*q)^{1/3}x^{4/3} = A\,[4\pi e^2 Tq/R_0 M(\Omega_H^2 + \Omega_0^2)]^{1/3}x^{4/3}, \qquad (16)$$

where A is a numerical factor of order unity. Knowing D, from the relation $q = D - dn_0/dr = D\,dn_0/dx$ we find the distribution close to the walls n_0:

$$n_0 = N - 3q / A (g^* q)^{1/3} x^{1/3}, \tag{17}$$

where $N = \text{const}$ is the density inside the chamber, i.e., at $x \to \infty$.

The distribution given by Eq. (17) holds only when $x > \rho = \sqrt{T/M\Omega_H^2}$. At $x = \rho$ we must impose a boundary condition. Let ξ be the fraction of the plasma lost in contact of the tube with the wall and let n_s be the mean density (17) at $x = \rho$. The density fluctuation n' due to the fact that the plasma tubes move back and forth at the wall is a quantity of order $n' \sim \frac{1}{2} \xi n_s$. In order-of-magnitude terms, the flux at the wall q is $n'v'$ where $v' \sim D/x$ is the velocity fluctuation. Hence, as an approximation we can write the following boundary condition:

$$q = \tfrac{1}{2} \xi n_s (D/x)_{x=\rho}.$$

Now, expressing n_s by means Eqs. (17) we can find the relation between q and N and the plasma lifetime τ_0:

$$\tau_0 \approx \frac{\pi a^2 N}{2\pi a q} = Ca \left(\frac{\Omega_H^2 + \Omega_0^2}{\Omega_0^2} \frac{R_0 M}{\rho T} \right)^{1/2}, \qquad C = \frac{1}{2} \left(\frac{2 + 3\xi}{A\xi} \right)^{3/2}. \tag{18}$$

The expression for τ_0 contains one unknown parameter ξ. The quantity τ_0 is rather sensitive to ξ, but it is an extremely complicated problem to calculate ξ because this parameter is directly related to the "roughness" of the wall; experimentally, the walls never coincide completely with the lines of force. For this reason, the tube running along the wall does not lose ions over its entire length, but only at separated points of contact. In the remaining portions the tube potential (consequently, its velocity) is maintained for some period of time. Hence, to find ξ we must solve the complete kinetic equation, taking account of the longitudinal motion. In view of the complexity of this probelm and the lack of adequate experimental data on wall roughness we do not treat this problem and shall assume that ξ is a numerical constant of order unity.

In the derivation of Eq. (18) we have not taken any account of end effects. According to Eq. (1), however, end effects impose certain limitations on the potential φ. As a result, the velocity $v'_\lambda \sim C\varphi'_\lambda/\lambda H$ of a fluctuation of order λ cannot be larger than $(cT/\lambda H)(H_m/H_s - 1)$. Hence, the turbulent diffusion coefficient $D \sim \langle \lambda' v \rangle$ cannot be larger than

$$D_m = B \frac{cT}{H} \left(\frac{H_m}{H_s} - 1 \right), \tag{19}$$

where B is a numerical factor of order unity.

An estimate shows that (16) is actually much smaller than (19); however, if there is a diaphragm this relation may not hold. When plasma retardation at the wall is not important and we modify the first approach by introducing velocity limitations due to end effects, the plasma flow loses its diffusion nature because the tubes do not close inside the chamber. For this reason Eq. (19) does not give the true diffusion coefficient; it can, however, be used for making estimates.

	V, kv	45	30	20	10
H, kg	T, kev	1.2	1.0	0.9	0.4
5	experiment	0.15	0.2	0.4	1.0
	theory	0.35	0.4	0.45	0.7
6	experiment	0.16	0.4		
	theory	0.45	0.5		
8	experiment	0.7	1.5		
	theory	1.0	1.1		

6. COMPARISON WITH THE EXPERIMENTAL DATA

In the table we compare the dependence of τ_0 (in milliseconds) on T and H as computed from Eq. (18) with the experimentally measured relation[6] for a mirror ratio $H_m/H_0 = 1.5$. The calculation is carried out as follows: the radius of curvature $R_0 \approx 3 \times 10^2$ cm is computed from the experimentally measured magnetic field under the assumption of a Maxwellian ion-velocity distribution with the cone excluded (depending on the cone angle α, R_0 can vary by 20%.) The ion temperature is $\frac{2}{3}$ of the mean ion energy, which is estimated experimentally from the rate of removal due to charge exchange. According to reference 6 the density N is 10^9 for fields of 5 and 6 kilogauss and 5×10^8 for a field of 8 kilogauss. The constant C is taken as 20, corresponding approximately to $A = \xi \approx \frac{1}{2}$. The chamber radius $a = 22$ cm and V is the acceleration potential.

The fact that the lifetime which we have computed is of the order of magnitude of the experimental lifetime for a completely reasonable choice of the constants A and ξ is an indication of the usefulness of the considerations developed above. However, the experimental dependence of τ_0 on H and T is much sharper than the theoretical dependence. This result is probably due to the fact that the chamber in the experimental apparatus has a complicated shape with protrusions (Q in Fig. 1) which act as diaphragms or that ξ itself is not a constant but increases with diminishing τ_0, that is to say, with increased intensity of the convective oscillations.

The finding that convection is responsible for plasma loss from this system is also supported by probe measurements.[7] These measurements show

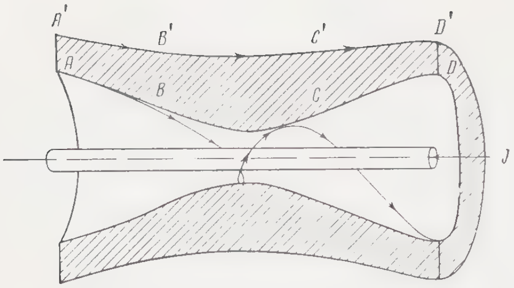

FIG. 2

that the currents to the wall probes are well correlated along the lines of force, that is to say, the plasma actually escapes to the wall in complete tubes. Furthermore, the probe currents exhibit oscillations with a period of approximately 5 — 10 μsec. If we assume that in the vicinity of the walls the ions rotate in azimuth with a velocity $v_0 = a\omega_0 = T/MR_0 \sim 10^5$ (and that the electric drift velocity is of the same order of magnitude) while the minimum correlation length $\rho \sim 1$ cm, the oscillation period is approximately $\rho/v_0 \sim 10$ μsec, in agreement with experimental results.

The dependence of lifetime on density N can be determined from the experimental dependence of τ_0 on time.[6] For example, using the experimental $\tau = \tau(pt)$ curve for $p = 2 \times 10^{-6}$ mm Hg we can estimate the time for τ_0 to increase by a factor of e as 0.3 — 0.4 msec. But the mean lifetime for this interval (taking account of charge exchange) is approximately 0.15 msec. Thus, τ_0 increases in time in accordance with a function of the form $\tau_0 \sim N^{-1/2}$, which follows from Eq. (18) if $\Omega_0^2\Omega_H^2 < 1$, as is the case if $N < 10^9$.

7. CONCLUSION

In spite of the numerous simplifications which have been introduced, our theoretical analysis is in satisfactory agreement with the experimental results and both lead to the conclusion that plasma instability arises in a system of this kind as a consequence of convection. In order to avoid instability it is necessary to have a magnetic field configuration which increases in all directions as seen from the region occupied by plasma. One configuration of this kind, which has only two mirrors, is shown in Fig. 2. This field consists of a meridian field, with lines of force of which lie in the planes of r and z, and an azimuthal field which is produced by a current I along the axis. If the force line A′B′C′D′ of the meridian field has a negative curvature, as shown in Fig. 2, the field increases with increasing radial distance from this line. The field increases in the outward direction from the cross-hatched region at sections AB and CD in exactly the same way.

If we now choose a current I which makes the azimuthal field small at the line A′B′C′D′ but converts the force line ABCD into a rather sharp spiral in BC, than all the force lines at the boundary of the cross-hatched torroidal region exhibit negative curvature, that is to say, the field increases in all directions. Actually, the presence of a current I causes some elongation of the lines of force close to the axis of the system so that the longitudinal pressure of the plasma will tend to push the plasma tube toward the axis. But if the longitudinal pressure is smaller than the transverse pressure, effects due to elongation of the lines of force will be small and the plasma will be stable in the cross-hatched region, since a rotational diamagnetic force acts upon it.

In conclusion, the author wishes to express his gratitude to M. S. Ioffe and V. G. Tel'kovskiĭ, who maintained constant contact with this work.

---

[1] G. I. Budker, Физика плазмы и проблема управляемых термоядерных реакций (Plasma Physics and the Problem of a Controlled Thermonuclear Reaction) Acad. of Sci. U.S.S.R. Press, 1958, Vol. 3, p. 3.

[2] M. Rosenbluth and C. Longmire, Ann. of Phys. **1**, 120 (1957).

[3] B. B. Kadomtsev, op. cit. ref. 1, Vol. 4, p. 16.

[4] R. F. Post, Report P/377, Second International Conference on the Peaceful Uses of Atomic Energy, Geneva, 1958.

[5] Post, Ellis, Ford and Rosenbluth, Phys. Rev. Letters **4**, 166 (1960).

[6] Ioffe, Sobolev, Tel'kovskiĭ, and Yushmanov, JETP **39**, 1602 (1960), Soviet Phys. JETP **12**, 1117 (1961).

[7] Ioffe, Sobolev, Tel'kovskiĭ, and Yushmanov, JETP 40, 40 (1961), this issue p. 27.

Translated by H. Lashinsky
49

SOVIET PHYSICS JETP VOLUME 13, NUMBER 1 JULY, 1961

ON THE MANDELSTAM REPRESENTATION IN PERTURBATION THEORY FOR AN ANOMALOUS MASS RELATION

V. N. GRIBOV, M. V. TERENT'EV, and K. A. TER-MARTIROSYAN

Submitted to JETP editor August 8, 1960

J. Exptl. Theoret. Phys. (U.S.S.R.) **40**, 337-340 (January, 1961)

The analytic properties of the box diagram are investigated in perturbation theory. With this diagram as an example, it is demonstrated how the Mandelstam representation must be modified in the case of an anomalous relation between the particle masses.

As is well known, the Mandelstam integral representation for scattering amplitudes[1] is valid only if the process does not contain "anomalous" diagrams. In this paper we discuss the modification of the Mandelstam representation in the anomalous case by considering the simplest diagram, namely the box diagram shown in Fig. 1. The notation is as follows: p_i, k_i are particle four-momenta; m, μ are the masses of the "internal" particles; $p_1 + p_2 + p_3 + p_4 = 0$. We consider the case when $p_1^2 = p_2^2 = p_3^2 = p_4^2 = M^2$. The diagram is a function of the invariants $s = (p_1 + p_2)^2$ and $t = (p_2 + p_3)^2$:

$$A(s,t) = \frac{1}{i\pi^3} \times \int \frac{\delta(p_1 + k_4 - k_1)\,\delta(p_2 + k_1 - k_2)\,\delta(p_3 + k_2 - k_3)\,d^4k_1\,d^4k_2\,d^4k_3\,d^4k_4}{(k_1^2 - \mu^2 + i\varepsilon_1)(k_2^2 - m^2 + i\varepsilon_2)(k_3^2 - \mu^2 + i\varepsilon_3)(k_4^2 - m^2 + i\varepsilon_4)}.$$

For the "normal" case when $M^2 < m^2 + \mu^2$ we can write

$$A(s, t) = \frac{1}{\pi^2} \int\limits_{\Omega_N} \frac{\rho(s', t')\,ds'\,dt'}{(s' - s - i\delta)(t' - t - i\sigma)};$$

$$\rho(s, t) = \pi / \sqrt{-stf(s, t)},$$

$$f(s, t) = 4(M^2 - m^2 - \mu^2)^2 + (t - 4\mu^2)(4m^2 - s). \qquad (1)$$

The region of integration Ω_N is bounded by the curve L_N in the st-plane (see Fig. 2); and $f(s, t) = 0$ on the curves L_N and L_A.

The quantity $A(s, t)$ may also be represented in the form

$$A(s, t) = \frac{1}{\pi} \int\limits_{4m^2}^{\infty} \frac{A_1(s', t)}{s' - s - i\delta}\,ds',$$

$$A_1(s, t) = \frac{1}{\sqrt{-stf(s, t)}} \ln \frac{\sqrt{f(s, t)} + \sqrt{t(4m^2 - s)}}{\sqrt{f(s, t)} - \sqrt{t(4m^2 - s)}}, \quad t < 0, \qquad (2)$$

where the integral is to be calculated along the contour C_1 in the complex s-plane shown in Fig. 3. The function $A_1(s, t)$, which is for $t < 0$ formally continued into the region $s < 4m^2$, has two branch points:

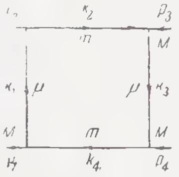

FIG. 1

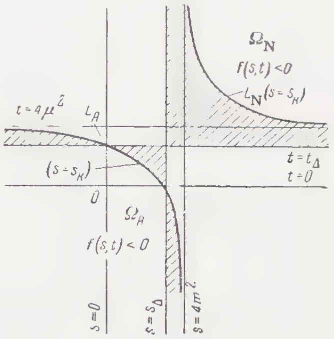

FIG. 2

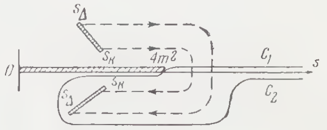

FIG. 3

at $s = s_\Delta = 4m^2 - (M^2 - m^2 - \mu^2)^2/\mu^2$

a logarithmic type branch point, and at

$$s = s_k = 4m^2 + 4(M^2 - m^2 - \mu^2)^2/(t - 4\mu^2)$$

a root type branch point. The function $A_1(s, t)$ may be made single-valued in the complex s-plane by introducing a cut from s_Δ to s and from 0 to $4m^2$ (see Fig. 3).

Let us investigate in more detail the motion of the singular points s_Δ and s_k as the mass M changes, making use of the method proposed by Mandelstam.[2] Let at first $M^2 < m^2 + \mu^2$. We make the substitution $M^2 \rightarrow M^2 + i\epsilon$. Then the points

s_Δ and s_k move off the real axis. As M increases these points move in the manner shown by the dashed lines in Fig. 3; when $M^2 = m^2 + \mu^2$ they cut the contour C_1 to the right of the point $s = 4m^2$, and then, for $M^2 > m^2 + \mu^2$, take up positions to the left of the point $s = 4m^2$, as shown in Fig. 3. In order to avoid cutting the contour of integration when passing to the anomalous case it is necessary to replace in the expression (1) from the very beginning the contour C_1 by the contour C_2. In the anomalous case this leads to the appearance of the integral over the discontinuity of the function $A_1(s, t)$ in the interval $s_\Delta < s < s_k$. Passing to the limit $\epsilon \to 0$ and evaluating the jump in A_1 in this interval, one can obtain for $M^2 > m^2 + \mu^2$

$$A(s, t) = a(s, t) + \frac{1}{\pi}\int_{4m^2}^{\infty} \frac{A_1(s', t)}{s' - s - i\delta}\, ds', \tag{3}$$

$$a(s, t) = \frac{1}{\pi}\int_{s_\Delta}^{s_k} \frac{a_1(s', t)}{s' - s - i\delta}\, ds', \qquad a_1(s, t) = \frac{2\pi}{\sqrt{stf(s, t)}}\,. \tag{4}$$

The integral in Eq. (4) can be evaluated directly. As a result it turns out that for $t < 0$ and $s_\Delta < s < s_k$ the function a is of the form

$$a(s, t) = \frac{2}{\sqrt{stf(s, t)}}\left[\ln\frac{\sqrt{st(s_\Delta - 4m^2)} + \sqrt{-s_\Delta f(s, t)}}{\sqrt{st(s_\Delta - 4m^2)} - \sqrt{-s_\Delta f(s, t)}} + i\pi\right] \tag{5}$$

(it is obvious that a is symmetric under the exchange s → t, μ → m).

Now the function a(s, t) may be analytically continued into the region $s > 4m^2$, and then in the variable t into the region $t > 0$. As a result the following representation is obtained for a(s, t) for t in the various regions as indicated:

$$a(s, t) = \begin{cases} \dfrac{1}{\pi}\displaystyle\int_{s_k}^{s_\Delta} \frac{a_1(s', t)}{s' - s - i\delta}\, ds', & 0 < t < t_\Delta \\ -\dfrac{1}{\pi}\displaystyle\int_{-\infty}^{s_k} \frac{a_1(s', t)}{s' - s - i\delta}\, ds' + \frac{1}{\pi}\int_{\infty}^{s_\Delta} \frac{a_1(s', t)}{s' - s - i\delta}\, ds', & t_\Delta < t < 4m^2; \\ \dfrac{1}{\pi}\displaystyle\int_{s_k}^{s_\Delta} \frac{a_1(s', t)}{s' - s - i\delta}\, ds', & t > 4m^2 \end{cases}$$

$$t_\Delta = 4\mu^2 - (M^2 - m^2 - \mu^2)^2 / m^2. \tag{6}$$

Thus the diagram of Fig. 1 may be represented in the anomalous case in the form

$$A(s, t) = a(s, t) + \frac{1}{\pi^2}\int_{\Omega_N} \frac{\rho(s', t')\, ds'\, dt'}{(s' - s - i\delta)(t' - t - i\sigma)} = a(s, t) + A_0(s, t), \tag{7}$$

where the function a is determined by the relations (6) and (4) and has discontinuities in the variable s for fixed real t in the dashed-in region in Fig. 2 (it is obvious that in the same region a(s, t) has analogous discontinuities in the variable t for fixed s).

It is interesting to note that as t → 0 the function a(s, t) has as $s \to s_k \to s_\Delta$ a pole type singularity, namely

$$a(s, 0) \underset{s \to s_\Delta}{=} \frac{\xi}{s - s_\Delta}, \qquad \xi = \frac{1}{\mu^2}\sqrt{(4m^2 - s_\Delta)/s_\Delta}.$$

We are most grateful to L. D. Landau who called to our attention the fact that in the anomalous case there must necessarily exist the singular region shown shaded in Fig. 2.

One can verify that for the function A(s, t) the curve L_N is not singular in the anomalous case, since along this curve the singularities of the functions a and A_0 compensate each other. Indeed, for $t > 4\mu^2$ the function $A_0(s, t)$ has the following representation:

$$A_0(s, t) = \frac{1}{\pi}\int_{4m^2}^{\infty} \frac{1}{i\sqrt{s'tf(s', t)}} \times \ln\left(\frac{\sqrt{f(s', t)} + i\sqrt{t(s' - 4m^2)}}{\sqrt{f(s', t)} - i\sqrt{t(s' - 4m^2)}}\right)\frac{ds'}{s' - s - i\delta}\,.$$

Let us separate out of A_0 the part that is singular at $s = s_k$ (for $t > 4\mu^2$); then $A(s, t) = A'_0 + a'$, where

$$A'_0 = \frac{1}{\pi}\int_{4m^2}^{\infty} \frac{1}{i\sqrt{s'tf}} \ln\left(\frac{i\sqrt{t(s' - 4m^2)} + \sqrt{f}}{i\sqrt{t(s' - 4m^2)} - \sqrt{f}}\right)\frac{ds'}{s' - s - i\delta},$$

$$a'(s, t) = \int_{s_k}^{s_\Delta} \frac{2\, ds'}{\sqrt{s'tf}(s' - s - i\delta)} + \int_{4m^2}^{\infty} \frac{ds'}{\sqrt{s'tf}(s' - s - i\delta)}.$$

The function A'_0 has no branch points at $s = s_k$. After performing the integration a' may be written in the form (for $0 < s < s_\Delta$)

$$a'(s,t) = \frac{1}{\sqrt{stf}}\left\{2\ \ln\ \frac{\sqrt{s_\Delta(s_k-s)}-\sqrt{s(s_k-s_\Delta)}}{\sqrt{s(s_k-s_\Delta)}+\sqrt{s_\Delta(s_k-s)}}\right.$$
$$+\ln\frac{\sqrt{4m^2(s_k-s)}+\sqrt{s(s_k-4m^2)}}{\sqrt{4m^2(s_k-s)}-\sqrt{s(s_k-4m^2)}}$$
$$\left.+\ln\frac{i\sqrt{s_k-s}-\sqrt{s}}{i\sqrt{s_k-s}+\sqrt{s}}\right\}.$$

It is easy to show after analytic continuation into the region $s \sim s_k$ that the function a' also has no singularities along the line $s = s_k$.

If one considers the case when the anomaly appears only in the simplest diagrams shown in Fig. 1, 4 and 5 (it is possible that this is the case for the real scattering processes of Σ and Λ hyperons[3]) then the exact scattering amplitude F(s, t) may be represented by

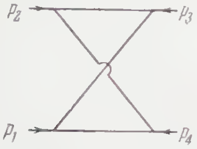

FIG. 4

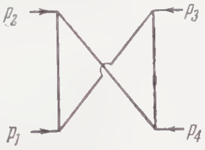

FIG. 5

$$F(s,t) = a(s,t) + a(s_c,t) + a(s,s_c) + F_0(s,t),$$

where $s_c = 4M^2 - s - t$, and the function $F_0(s,t)$ has the usual Mandelstam representation.

In conclusion it is important to note that the diagram under consideration, symmetric in the masses of the particles, constitutes a very special case. For arbitrary masses of the particles with the structure of the integrand preserved the region of integration involved in the determination of the function a(s, t) is substantially modified. In addition, if the particle stability condition is violated the diagrams develop complex singularities, with the result that the contour of integration in a(s, t) is no longer entirely along the real axis.

---

[1] S. Mandelstam, Phys. Rev. **112**, 1344 (1958).

[2] S. Mandelstam, Phys. Rev. Lett. **4**, 84 (1960).

[3] Patashinskiĭ, Rudik, and Sudakov, JETP, in press.

Translated by A. M. Bincer
50

SOVIET PHYSICS JETP VOLUME 13, NUMBER 1 JULY, 1961

PAIRING FORCES AND PAIR CORRELATIONS IN THE Pb^{206} *NUCLEUS*

V. N. GUMAN, L. A. SLIV, and G. A. SOGOMONOVA

Leningrad Physico-Technical Institute, Academy of Sciences, U.S.S.R.

Submitted to JETP editor August 10, 1960

J. Exptl. Theoret. Phys. (U.S.S.R.) **40**, 341-351 (January, 1961)

The residual pairing forces acting between the nucleons in the nucleus are determined. The importance of taking these pairing forces and the pair correlations into account in determining the position and the properties of the levels is demonstrated. The energies, eigenfunctions, and transition probabilities of the levels of the Pb^{206} nucleus are derived and compared with experiment.

THE current models of the nucleus are based on the assumption, confirmed by experiment, that there exists a self-consistent field in the nucleus in which the nucleons move. However, the self-consistent field is not the only force acting on the individual nucleon; there also exist the so-called residual forces. The consideration of the residual forces is essential in the study of the behavior of the nucleons in the neighborhood of the Fermi energy surface. The importance of this circumstance follows from the application of the ideas of the theory of superconductivity to the study of the nucleus.

The present paper is devoted to the determination of the forces, including the residual ones, capable of explaining and describing all properties of the nuclear ground and excited states up to an excitation energy of 3 Mev.

CHOICE OF FORCES

Let us first consider a nucleus with one particle above the filled proton and neutron shells. The interaction of the extra particle with the particles in the core is described by the sum of a central potential $V_C(r, \mathbf{s}\cdot\mathbf{l})$ and a quadrupole potential $V_S(r, \theta, \varphi)$. More precisely, V_C and V_S are the first two terms in the expansion of the self-consistent potential. This is shown most easily by the example of two-particle forces: $V(\mathbf{r}_i) = \sum_k V(\mathbf{r}_i - \mathbf{r}_k)$. Expanding $V(\mathbf{r}_i - \mathbf{r}_k)$ in terms of the Legendre polynomials $P_l(\cos\omega_{ik})$ and averaging over the states of all particles except the i-th, we find that the term with $l = 0$ gives the central potential V_C and the term with $l = 2$ the quadrupole potential V_S. So far there has been no evidence that the higher multipole terms must be included in the potential for the outer nucleons; these terms will therefore be regarded as small. The potentials V_C and V_S represent the long range part of the total self-consistent potential, while the neglected terms give the short range part.

The central potential V_C is best determined from the calculations of the level spectra of nuclei with a single nucleon above closed shells or with a single hole. This was done by one of the authors and Volchok,[1] who found a potential of the form

$$V_C(r, \mathbf{ls}) = V(r) - \lambda\left(\frac{\hbar}{2Mc}\right)^2 \frac{\mathbf{ls}}{r}\frac{\partial V(r)}{\partial r}, \tag{1}$$

where

$$V(r) = -V_0/(1 + e^{\alpha(r-r_0)}). \tag{2}$$

The parameters V_0, r_0, α, and λ turned out to be nearly the same over the range of nuclei from O^{17} to Pb^{209}. The potential V_C can therefore be regarded as known.

The potential V_S is usually written in the form

$$V_S(\mathbf{r}_k) = \pm\varkappa(r_k)\sum_\mu \alpha_{2\mu} Y_{2\mu}(\theta_k, \varphi_k); \tag{3}$$

The $-$ and $+$ signs correspond to particles and holes, respectively. The potential V_S can be regarded formally as an interaction of the outer particle with the remaining ones which leads to a deformation of the potential surface of the core. For small deformations of the potential surface,

$$\varkappa(r) = r\partial V(r)/\partial r, \tag{4}$$

where $V(r)$ is given by (2), we can compute the matrix elements

$$\langle nl|\varkappa(r)|n'l'\rangle = \int_0^\infty R_{nl}(r) R_{n'l'}(r) r^3 \frac{\partial V}{\partial r} dr, \tag{5}$$

where $R_{nl}(r)$ are the radial functions of the particle in the potential (1), as derived in reference 1.

It turns out that, except for small deviations,

$$\langle nl\,|\,\varkappa(r)\,|\,n'l'\rangle \approx (-1)^{n+n'}\cdot 40\ [\text{Mev}]. \qquad (5')$$

for all states of nuclei in the neighborhood of lead. This value will be used in the following.

The other parameter of the interaction with the surface, α_μ, can be represented in the form[2]

$$\alpha_\mu = \sqrt{\hbar\omega/2C}\,(b_\mu + (-1)^\mu b^*_{-\mu}), \qquad (5'')$$

where C is the effective surface tension. Here we assume that the surface of the core undergoes ellipsoidal oscillations with the phonon energy $\hbar\omega$; b_μ and b^*_μ are annihilation and creation operators for a phonon with spin 2 and spin component μ along the z axis.

Let us now turn to a nucleus in which there are two extra particles or holes in addition to closed shells. The potential in which the extra nucleons move is

$$V = V_C + V_S + V_p(1, 2). \qquad (6)$$

The first two potentials, V_C and V_S, are single-particle potentials, whereas V_p is a two-nucleon potential. The potential V_p cannot be included in the first two terms, because its main short range part plays an important role. For in the case of two extra nucleons the potential V_p not only gives a contribution to the energy but also changes the character of the states. The pair interaction V_p is taken of the form

$$V_p = -[v_t\pi_t + v_s\pi_s]\exp\{-|\mathbf{r}_1 - \mathbf{r}_2|^2/\rho^2\}. \qquad (7)$$

Here v_t and v_s are the parameters of the triplet and singlet interactions, and π_t and π_s are the corresponding operators:

$$\pi_t = \tfrac{1}{4}(3 + \sigma_1\sigma_2), \qquad \pi_s = \tfrac{1}{4}(1 - \sigma_1\sigma_2),$$

ρ is the effective range of the pair interaction.

Thus the spin dependent part of the interaction consists of a mixture of triplet and singlet forces. We leave out tensor forces, because there are no clear effects at low energies which would permit us to separate the tensor forces from the ordinary spin forces. The choice of a Gaussian shape for the radial dependence of the forces is somewhat arbitrary; any other strongly decreasing function would be just as good. Since the results depend on the integral effect, details cannot play any role, only the depth and the range of the potential well being of importance. We neglected the repulsive forces between the particles at distances $r_{12} \leq 0.5$ f, i.e., the so-called "hard core." The introduction of a hard core and the corresponding correction of the functions with the help of a cut-off factor of the type $1 - \exp(-r_{12}^2/r_C^2)$ give a negligible contribution to the energy. Hence the nature of the forces at small distances does not come into play in our problem.

METHOD OF CALCULATION

As the first nucleus to be studied we chose Pb^{206}, a nucleus with two neutrons missing from the filled shell. The choice of Pb^{206} was dictated by the fact that this nucleus has been investigated extensively and is therefore convenient for analysis. About 30 levels of the Pb^{206} nucleus are known, the spins are identified, and the transition probabilities or relative intensities have been determined. Several theoretical papers have been devoted to the study of the Pb^{206} nucleus with an analysis of the levels (see reference 3, and the literature quoted there); these can be used for an orientation in our calculations. We regard the Pb^{206} nucleus as a system consisting of two nucleons (holes) and the surface of the core. The Hamiltonian of this system is written as

$$\hat H = \hat H_S + \hat H_p(1) + \hat H_p(2) + \hat V_S(1) + \hat V_S(2) + \hat V_p\ (12), \qquad (8)$$

where

$$\hat H_S = \hbar\omega\left(\tfrac{5}{2} + \sum_\mu b_\mu^* b_\mu\right), \qquad \hat H_p = -(\hbar^2/2M)\,\Delta + V_C;$$

V_C, V_S, and V_p are given by formulas (1), (3), and (7).

The eigenfunctions of the Hamiltonian $\hat H_S$ are functions of the quadrupole oscillation of the surface with the energy $\hbar\omega$ and the number of quanta N; the eigenfunctions of the Hamiltonian $\hat H_p$ are functions of the shell model potential (1). We therefore choose basis functions of the type

$$|\,j_1 j_2 J;\ NR;\ IM\rangle,$$

corresponding to a state where two nucleons with spins j_1 and j_2 are coupled with total angular momentum J; N phonons contribute the angular momentum R and together with J give the total angular momentum of the nucleus I with projection M.

We shall seek the eigenfunctions of the Hamiltonian $\hat H$ given by (8) in the form of an expansion in terms of the basis functions

$$|\,IM\rangle = \sum_{j_1 j_2 J;\,NR} c(j_1 j_2 J; NR)\,|\,j_1 j_2 J;\ NR;\ IM\rangle. \qquad (9)$$

The energies and eigenfunctions of the single-particle states of Pb^{206} were determined in reference 1; the results needed here are shown in Fig. 1.

We must now calculate the various matrix elements. The matrix elements of the interaction with the surface oscillations were computed according to the scheme[3]

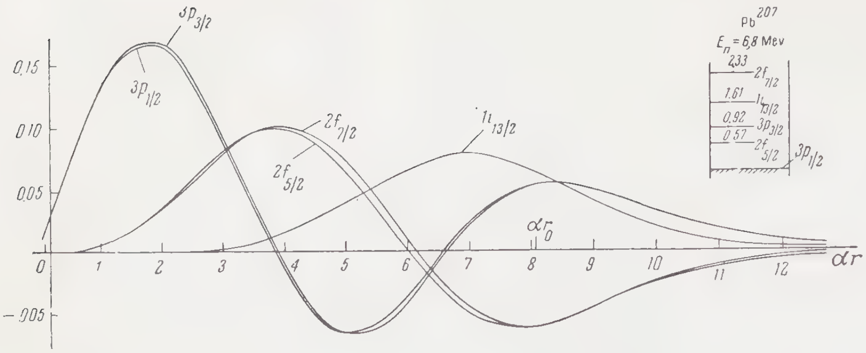

FIG. 1. Single-particle wave functions and energy levels of the Pb^{207} nucleus.

$$
\begin{aligned}
&\langle j_1 j_2 J;\ NR; I \,|\, \sum_{1,2} \varkappa\,(r) \sum_{\mu} \alpha_{2\mu}\, Y_{2\mu}\,(\theta, \varphi) \,|\, j_1'\, j_2'\, J';\, N'R';\, I\rangle \\
&\quad = \varkappa \sqrt{\hbar\omega/2C}\,(NR \,\|\, b^2 \,\|\, N'R')\ W(JRJ'R';\ I\,2) \\
&\quad \times \sqrt{(2J+1)(2J'+1)}\ (-1)^{J+R'-I}\,\{\delta_{j_1 j_1'}\,(-1)^{j_1'-j_2-J'} \\
&\quad \times (j_2 \,\|\, Y^2 \,\|\, j_2')\, W\,(j_2\ J\ j_2'\, J';\, j_1\, 2) + \delta_{j_2 j_2'}\,(-1)^{j_2-j_1'-J} \\
&\quad \times (j_1 \,\|\, Y^2 \,\|\, j_1')\, W\,(j_1\, J j_1'\, J';\ j_2\ 2)\},
\end{aligned} \tag{10}
$$

where $\kappa = (-1)^{n_1+n_2+n_3+n_4} \times 40$ [Mev]. The reduced matrix elements $(NR \parallel b^2 \parallel N'R')$ are given in the paper by Raz,[4] and the W's are Racah coefficients.

For the calculation of the matrix elements of the pair interaction V_p we expanded the coordinate part in a series:

$$
\begin{aligned}
\exp\{-r_{12}^2/\rho^2\} &= \sum_{k=0}^{\infty} f_k(r_1, r_2)\, P_k(\cos\omega_{12}) = \sum_k f_k(r_1, r_2) \\
&\quad \times \sum_{m=-k}^{k} \frac{4\pi}{2k+1}\, Y_{km}^{*}(\theta_1, \varphi_1)\, Y_{km}(\theta_2, \varphi_2) \\
&= \sum_k f_k(r_1, r_2)\,(\mathbf{T}^k(1)\cdot\mathbf{T}^k(2));
\end{aligned} \tag{11}
$$

T^k is the irreducible tensor operator of the k-th rank. The radial parts of the matrix elements of the interactions have the form of Slater integrals:

$$
\begin{aligned}
&F^k(n_1 l_1, n_2 l_2;\ n_1' l_1',\ n_2' l_2') \\
&\quad = \int R_{n_1 l_1}(r_1) R_{n_2 l_2}(r_2)\, f_k(r_1, r_2)\, R_{n_1' l_1'}(r_1)\, R_{n_2' l_2'}(r_2)\, dr_1\, dr_2,
\end{aligned} \tag{12}
$$

they were computed numerically on the electronic computer "Strela." The dependence of the integrals F^k on the parameter ρ for different k is shown in Fig. 2. Finally we have

$$
\begin{aligned}
&\langle j_1 j_2, JM \,|\, v_s \pi_s \sum_k f_k(r_1 r_2)\,(\mathbf{T}^k(1)\cdot\mathbf{T}^k(2) \,|\, j_1' j_2',\ JM\rangle \\
&\quad = -v_s A\begin{pmatrix} l_1 & 1/2 & j_1 \\ l_2 & 1/2 & j_2 \\ J & 0 & J \end{pmatrix} A \begin{pmatrix} l_1' & 1/2 & j_1' \\ l_2' & 1/2 & j_2' \\ J & 0 & J \end{pmatrix} F^k(n_1 l_1, n_2 l_2;\ n_1' l_1',\ n_2' l_2') \\
&\quad \times (-1)^{l_1+l_2'-J} \sqrt{(2l_1'+1)(2l_2'+1)} \\
&\quad \times C^{l_1 0}_{l_1' 0\, k\, 0}\, C^{l_2 0}_{l_2' 0\, k\, 0}\, W\,(l_1 l_2,\ l_1' l_2';\ Jk),
\end{aligned} \tag{13}
$$

where the A's are the coefficients for the transformation from jj to ls coupling,[5] and the

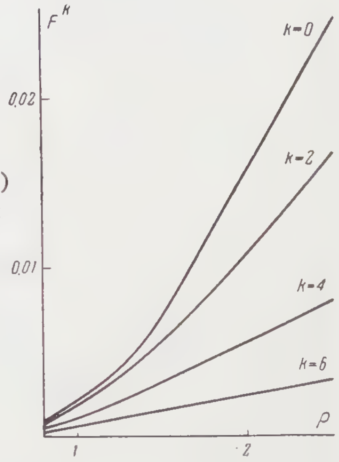

FIG. 2. Dependence of the integrals $F^k(n_1l_1, n_2l_2; n_1'l_1', n_2'l_2')$ on the parameter ρ for different values of k.

$C^{lm}_{l_1 m_1 l_2 m_2}$ are Clebsch-Gordan coefficients. An analogous expression holds for the triplet forces.

The set of matrix elements corresponding to given spin and parity forms the energy matrix. By reducing this matrix to its diagonal form, we obtain the energy levels and the eigenfunctions of the operator $\hat{H}$ defined by (8). Our method of calculation is approximate in that we include only a limited number of levels in the matrix. The lower levels will then be determined more accurately than the higher-lying ones. Thus, if we require that the first four low-lying levels with a given I be obtained with some desired accuracy, we thereby determine at which levels the matrix should be cut off. In our paper the rank of the matrices does not exceed twenty. These matrices were diagonalized on the "Strela" computer.

DETERMINATION OF THE PARAMETERS

The pair interaction contains three parameters: v_t, v_s, and ρ. However, in the case of Pb^{206}, where we have two identical particles, all basic matrix elements contain v_s and v_t approximately in the unique combination $2v_s + v_t$. Under these circumstances we may retain only one constant, for example, v_s, which will be regarded as the effective sum of two constants.

The interaction with the surface contains two parameters, the phonon energy $\hbar\omega$ and the effective surface tension C. Hence we must determine four constants: ρ, v_S, $\hbar\omega$, and C.

Not all of the required physical quantities are equally sensitive to these four constants. Thus the distance between the first 2^+ level and the ground state 0^+ depends mainly on the depth of the well v_S; small variations of the parameter ρ lead to appreciable changes in the binding energy of the two nucleons, but do not affect greatly the distance between the levels 2^+ and 0^+. The probability for the transition $2^+ \rightarrow 0^+$ is mainly determined by the ratio $\hbar\omega/C$. This allows us to make a crude determination of the possible values of the required parameters before the diagonalization.

First let us carry out the diagonalization taking only the pair interaction into account. The corresponding results are shown in Figs. 3 and 4. They lead to the following important conclusions:

1) The matrix elements of the pair interaction are large for levels with spin I = 0, approximately half as large for the levels with I = 2, even smaller for I = 4, and altogether unimportant for the other levels. The inclusion of the nondiagonal matrix elements, or in other words, of the pair correlations, leads to a considerable widening of the distance between the levels with given I. Since this shift is largest for the first level I = 0, there appears an energy gap of 0.8 to 1.0 Mev between the ground state with spin I = 0 and the other levels.

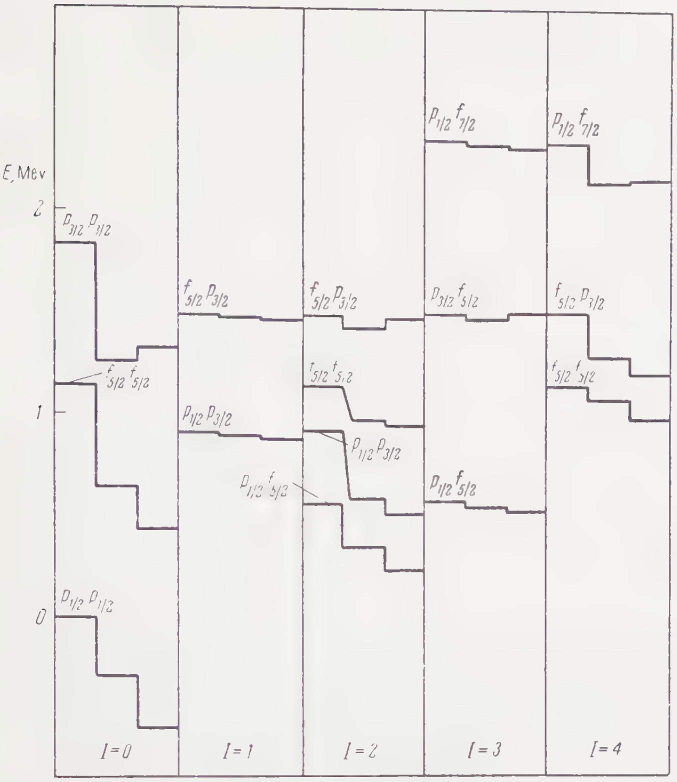

FIG. 3. Shift of the level positions as a result of the pairing forces. On the left of each column we show the single-particle level, in the center, the level after inclusion of the diagonal term of the pairing interaction only, and on the right, the level after the pair correlations have also been included. The ordinate gives the energy in Mev.

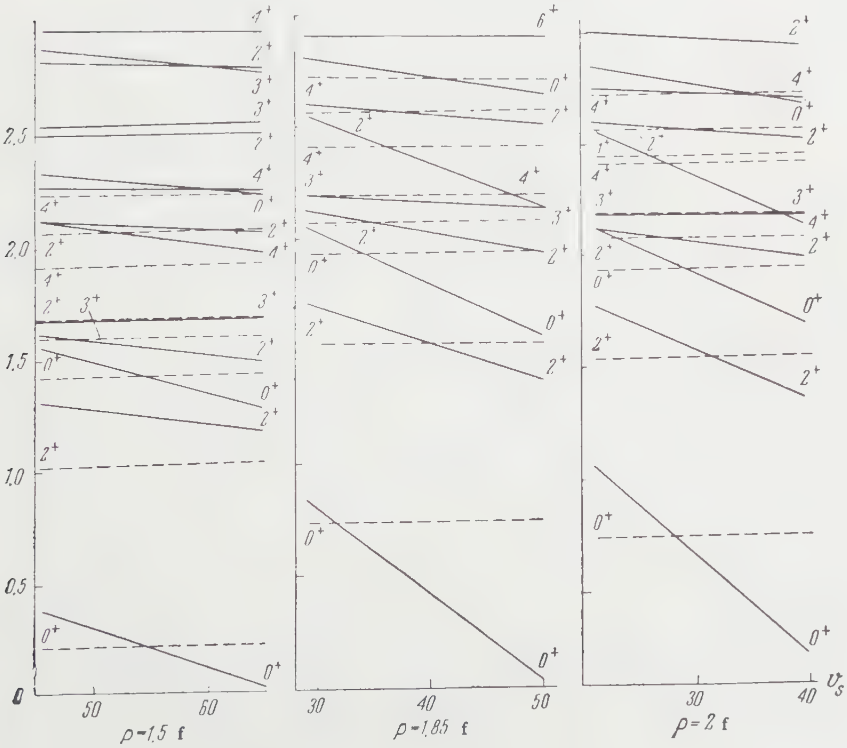

FIG. 4. Relative positions of the energy levels of the Pb^{206} nucleus for different values of the parameters ρ and v_s. The experimental levels are indicated by dotted lines.

Table I. Matrix elements of the pairing interaction using the radial wave functions of an oscillator and a diffuse potential

Configuration	Oscillator potential	Diffuse potential	Ratio
$(p_{1/2})^2 0^+$	—0,427	—0.349	0.817
$(f_{5/2})^2 0^+$	—0,685	—0.581	0,848
$(p_{3/2}\, f_{5/2}) 1^+$	0	0	—
$(p_{1/2}\, f_{5/2}) 2^+$	—0,329	—0.236	0,717
$(p_{1/2}\, p_{3/2}) 2^+$	—0,520	—0.399	0,767
$(p_{3/2})^2 2^+$	—0,260	—0,199	0.765
$(f_{5/2})^2 2^+$	—0,235	—0,195	0,830
$(p_{3/2}\, f_{5/2}) 2^+$	—0,094	—0.069	0.734
$(p_{1/2}\, f_{5/2}) 3^+$	—0.037	—0.026	0.676
$(p_{3/2}\, f_{5/2}) 3^+$	—0.046	—0,036	0.783
$(f_{5/2})^2 4^+$	—0.101	—0.083	0.822
$(p_{1/2}\, f_{5/2}) 4^+$	—0.364	—0.265	0.728

Table II. The coefficients c (j_1, j_2, J; NR) for the basic components of the wave functions of the levels of the Pb^{206} nucleus for I = 0

$j_1\, j_2$, J; NR	*E*, Mev			
	—1,06 7	0,26	1.00	2.4
$p_{1/2}\ p_{1/2}$, 0; 00	0.836	—0.355	—0,267	—0,026
$f_{5/2}\ f_{5/2}$, 0; 00	0.283	0.838	—0.089	—0.113
$p_{3/2}\ p_{3/2}$, 0; 00	0.264	0,014	0,898	0.053
$i_{13/2}\ i_{13/2}$, 0; 00	—0.051	—0.077	—0.047	0,859
$f_{7/2}\ f_{7/2}$, 0; 00	0.073	0.110	0.038	—0.148
$p_{1/2}\ p_{1/2}$, 0; 20	0,045	0.002	—0,003	0.033
$f_{5/2}\ f_{5/2}$, 0; 20	0.023	0.040	—0,013	0,070
$p_{1/2}\ f_{5/2}$, 2; 12	0.271	0.067	—0.139	0.077
$p_{1/1}\ p_{3/2}$, 2; 12	—0.216	0.076	—0.151	—0.089
$f_{5/2}\ f_{5/2}$, 2; 12	0.099	0.368	—0.071	0.441
$f_{5/2}\ f_{3/2}$, 2; 12	—0.049	—0.069	—0.102	—0,010
$p_{3/2}\ p_{3/2}$, 2, 12	0.056	0.004	0.226	0,046
$f_{5/2}\ f_{5/2}$, 4; 24	0.029	0,037	—0.030	0,073
$f_{5/2}\ p_{3/2}$, 4; 24	—0.051	—0,009	—0.024	—0,041

2) The inclusion of the pair interaction alone is not sufficient to obtain the correct energy levels, let alone the correct transition probabilities.

3) For $\rho < 1.5$ f and $\rho < 2.5$ f the level ordering does not agree with experiment. This discrepancy cannot be removed by taking the interaction with the surface into account. It follows, in particular, that, for reasons of simplicity, δ forces can be used to obtain various qualitative results; but they are inadequate for a quantitative investigation.

It is interesting to compare our results with the calculations with oscillator functions. For this purpose we list in Table I the values of some matrix elements of the pair interaction from the paper of True and Ford[3] together with our values, after they have been reduced to the same ρ and v_S. It is seen that the use of oscillator functions gives too large matrix elements.

We must now include the interaction with the surface before diagonalizing the matrix. Regarding the choice of the parameters of the surface interaction $\hbar\omega$ and C we note that the number of possible single-particle levels with spin $I = 2^+$ is equal to the number of the known experimental levels with that spin up to excitation energies of 2 Mev. Hence $\hbar\omega$ cannot be smaller than 2 Mev. We have investigated all values from 2 to 10 Mev

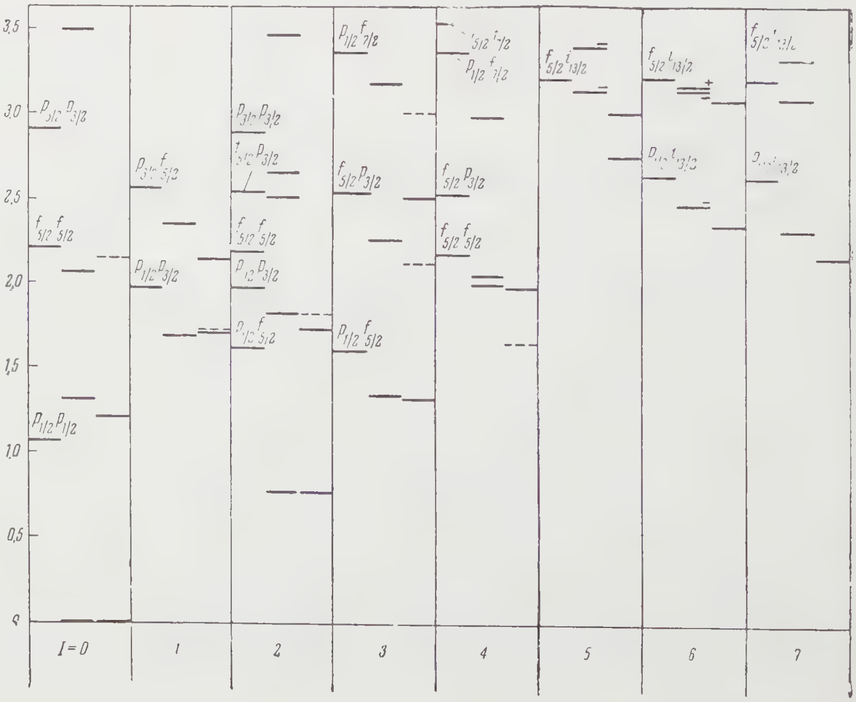

FIG. 5. Comparison of the results obtained for the energy levels of Pb^{206} with the experimental data. On the left of each column we give the position and configuration of the single-particle levels; in the center, the final positions of the levels after the inclusion of the pairing forces and the interaction with the surface of the core; and on the right, the experimental levels. Dotted lines designate levels which have not been determined with sufficient reliability. A minus sign above a level denotes negative parity of the level.

Table III. The coefficients c (j_1, j_2, J; NR) for the basic components of the wave functions of the levels of the Pb^{206} nucleus for I = 2

$j_1\ j_2,\ J;\ NR$	E, Mev					
	—0.30	0.38	0.76	1.48	1.60	2.71
$p_{1/2}\,p_{1/2}$, 0; 12	0,200	—0,043	—0,064	0,071	—0.056	0,921
$f_{5/2}\,f_{5/2}$, 0; 12	0.094	0.044	0.109	—0.041	—0.014	0,147
$p_{3/2}\,p_{3/2}$, 0; 12	0.067	—0.085	—0.007	—0.056	0.081	0.235
$p_{1/2}\,f_{5/2}$, 2; 00	0.766	0.508	—0,240	0.105	0.016	—0.141
$p_{1/2}\,p_{3/2}$, 2; 00	—0.440	0.803	0.055	—0.196	0.255	0.154
$f_{5/2}\,f_{5/2}$, 2; 00	0.209	0,064	0,935	0.033	—0.003	0.012
$f_{5/2}\,p_{3/2}$, 2; 00	—0.143	0.041	0.003	0.933	0.252	—0.017
$p_{3/2}\,p_{3/2}$, 2; 00	0.144	—0.222	—0,005	—0.184	—0.912	0.013
$p_{1/2}\,f_{5/2}$, 2; 12	0.152	0.046	0.154	—0.052	—0.038	—0.099
$p_{1/2}\,p_{3/2}$, 2; 12	—0.102	0.109	0.018	0,106	—0.162	0.080
$f_{5/2}\,f_{5/2}$, 2; 12	0,097	0.072	—0.124	—0.023	—0.005	—0.057
$p_{1/2}\,f_{5/2}$, 2; 20	0.036	0.004	0.003	—0.000	—0.002	0.059
$f_{5/2}\,f_{5/2}$, 4; 12	0.103	0.077	0.097	0.122	0.032	—0.039
$f_{5/2}\,p_{3/2}$, 4; 12	—0.166	0.074	0,020	0.072	0.007	0.085

in the three-phonon approximation and found that the best results are obtained for $\hbar\omega = 3$ Mev and C = 1000 Mev.

In Fig. 5 and Tables II to V we give the main results of the diagonalization of the energy matrix, where the interaction parameters have the following values: $v_S = 25$ Mev, $\rho = 2$ f, $\hbar\omega = 3$ Mev, and C = 1000 Mev.*

The results show that our choice of forces reproduces all experimentally known excited levels up to an excitation energy of 3 Mev. The only exception is the 4^+ level at 1.66 Mev. One should, therefore, first re-examine the experimental evidence for the existence of this level. The theoretical spectrum contains many more levels than the experimental one. This is plausible, since the transition probabilities from certain levels are very small and difficult to observe.

As we have obtained the eigenfunctions for the levels of the nucleus, we can compute the transition probabilities. The transition probability for a γ ray of given multipolarity λ is equal to

$$T(\lambda) = \frac{8\pi(\lambda+1)}{\lambda[(2\lambda+1)!!]^2}\frac{1}{\hbar}\left(\frac{\Delta E}{\hbar c}\right)^{2\lambda+1} B(\lambda), \qquad (14)$$

$$B(\lambda) = (2I+1)^{-1}\,|\langle\alpha I \parallel \hat{M}_\lambda \parallel \beta I'\rangle|^2,$$

where I′ and I are the nuclear spins in the initial and final states, respectively; α and β are additional quantum numbers characterizing the states; $\hat{M}_\lambda$ is the operator of the multipole transition; ΔE is the transition energy. The complete expressions for the operator $\hat{M}_\lambda$ and the quantity $B(\lambda)$ for the electric and magnetic transitions with various values of the initial and final quantum numbers j_1, j_2, N, R, and I have already been given.[2-4] We shall, therefore, not write down the formulas by which the probabilities were computed, but only give the final results (see Table VI).

Table IV. The coefficients c (j_1, j_2, J; NR) for the basic components of the wave functions of the levels of the Pb^{206} nucleus for I = 3

$j_1 j_2,\ J;\ NR$	E, MeV		
	0.320	1.20	2.14
$p_{1/2}\,f_{5/2}$, 3; 00	0.969	0.057	0.022
$p_{3/2}\,f_{5/2}$, 3; 00	—0.037	0.955	0.116
$p_{1/2}\,f_{7/2}$, 3; 00	—0.012	—0.091	0.945
$f_{5/2}\,f_{7/2}$, 3; 00	—0.007	0.024	—0.032
$p_{3/2}\,f_{7/2}$, 3; 00	0,013	0.023	—0.017
$p_{1/2}\,p_{3/2}$, 1;12	0,025	—0.109	0.227
$f_{5/2}\,p_{3/2}$, 1; 12	—0.067	0.099	0.013
$f_{5/2}\,f_{7/2}$, 1; 12	0.001	—0.013	0.073
$p_{1/2}\,f_{5/2}$, 2; 12	—0.061	0.107	0.153
$p_{1/2}\,p_{3/2}$, 2; 12	0.062	0.148	—0.100
$p_{1/2}\,f_{5/2}$, 3; 12	—0.134	0.132	—0.021
$p_{3/2}\,f_{5/2}$, 3; 12	0 081	—0.044	—0.001
$f_{5/2}\,f_{5/2}$, 4; 12	0.149	0.043	0,010

For an understanding of the above results we recall that the functions of the initial and final states are mixtures of various single-particle and collective levels. The transition probability will therefore be of the form of the square of the modulus of a sum of transition matrix elements between different components of the mixture. The terms in this sum will have either sign, and it is therefore not surprising that two levels of the same type can have transition probabilities which differ by two orders of magnitude. The contribution of a given level to the mixture is determined by the force parameters and the position of the level. The E2 transition probabilities are particularly sensitive to the parameters of the interaction with the surface ħω and C; here the E2 transition from the first level 2_1^+ is less sensitive to these parameters than that from the other levels. Thus one can reproduce the experimentally observed value of the probability for the E2 transition with the parameters ħω = 3 Mev, C = 1000 Mev as well as with ħω = 10 Mev, C = 1000 Mev.* However, for the second choice of parameters the probability for an E2 transition from the second level 2_2^+ to 0^+ will be only one fifth of the true value. The pair correlations, on the other hand, lead to a decrease of the probability of E2 transitions, especially for the high-lying levels.

---

*The single-particle level energies for Pb^{207} used by us were obtained without corrections for the interaction with the surface. These corrections can be easily included. They have significant effect on the computations; possibly the parameter v_s is somewhat increased while ρ becomes a little smaller. The levels with large I are lowered somewhat if the single-particle level in Pb^{206} lies lower than in Pb^{207}.

Table V. The coefficients $c(j_1, j_2, J; NR)$ for the basic components of the wave functions of the levels of the Pb^{206} nucleus for I = 4

$j_1 j_2$, J; NR	*E*, Mev			
	0 .965	1,02	1,95	2,69
$f_{5/2} f_{5/2}$, 4; 00	0.977	—0.087	0.071	0,066
$f_{5/2} p_{3/2}$, 4; 00	0.080	0,941	—0.226	0.004
$p_{1/2} f_{7/2}$, 4; 00	—0.038	0,229	0.903	—0.119
$f_{5/2} f_{7/2}$, 4; 00	—0.063	0.049	0.115	0,959
$p_{3/2} f_{7/2}$, 4; 00	0.011	—0.107	—0.052	0.028
$f_{5/2} f_{5/2}$, 4; 12	0.100	0,063	—0.001	0.135
$f_{5/2} p_{3/2}$, 4; 12	0.088	0.186	0,076	—0,107
$p_{1/2} f_{7/2}$, 4; 12	0.011	—0,010	—0.134	—0.110
$p_{1/2} p_{5/2}$, 2; 12	0.002	—0.005	—0.393	0.022
$p_{1/2} p_{3/2}$, 2; 12	0.005	—0.046	—0.291	0.086
$f_{5/2} f_{5/2}$, 2; 12	0,120	0.007	0.007	—0.103
$p_{1/2} p_{1/2}$, 0; 24	—0.001	0,006	0.049	—0.021
$f_{\ /2} f_{5/2}$, 0; 24	0.012	0,001	0.006	—0.018
$p_{1/2} f_{5/2}$, 2; 22	0,005	—0.001	—0.004	0,010

Table VI. Transition probabilities * between the levels of the Pb^{206} nucleus

Initial state	Final state	Type of transition	ΔE, Mev	B	T	Initial state	Final state	Type of transition	ΔE, Mev	B	T
2_1	0_1	E2	0.815	0.254	0.092	2_4	0_1	E2	2,400	0.003	0.252
2_2	0_1	E2	1,460	0,008	0,053	2_5	0_1	E2	2,650	0,002	0,327
2_2	2_1	M1	0,650	2,125	0,570	3_1	2_1	E2	0.560	0.010	0,001
0_2	2_1	E2	0,360	0,033	0.0002	3_2	2_1	E2	1,430	0,001	0.004
0_3	2_1	E2	1.250	0.001	0,002	4_1	2_1	E2	1.200	0,015	0.037
2_3	0_1	E2	1.800	0,001	0.010						

*The transition probability $T_{E2}(2_1 \to 0_1) = 0.103 \times 10^{12}$ sec^{-1} was found experimentally. For the transitions from the level 2_2 the following relation holds: $T_{M1}(2_2 \to 2_1) : T_{E2}(2_2 \to 0_1) = 4:1$. The relative intensities for the other levels are given in the paper of Alburger and Pryce.[6] In the table $B = T(\lambda)/(\Delta E)^{2\lambda+1}$, where ΔE is in Mev.

It is of interest to determine the mean radius of a pair. With the functions obtained above we find $(|\mathbf{r}_1 - \mathbf{r}_2|^2)^{1/2}$ cm, which is approximately equal to the nuclear radius.

CONCLUSIONS

The account of the surface and pair forces leads not only to a change in the energies of the single-particle states. A more important effect is the change of the character of the states as expressed in the structure of the wave functions. In the first place, all states, for all values of the spin I, contain a considerable admixture of collective states which complicate the properties of the levels. In the second place, the pair correlations lead to a mixing of single-particle states, which becomes more pronounced as the level density increases.

The probability for transitions from the second, third, etc. levels with a given I are very sensitive to the interaction parameters. Thus the E2 transition $2_2 \to 2_1$ neglecting the surface interaction is smaller by three orders of magnitude than the value found with our choice of parameters (if the surface interaction is included in a perturbation treatment, we find a value which is smaller by one order of magnitude than the value corresponding to our choice of parameters). The mixing of states sometimes decreases the transition probability by several orders of magnitude. For example, the E2 transitions $2_3 \rightarrow 0_1$ and $0_3 \rightarrow 2_1$ have, despite the admixture of collective states, a vanishingly small transition probability. In particular, the mixing of states has as a consequence that not all high E2 transitions will be enhanced.

---

*For ħω = 10 Mev and C = 1000 Mev the results are close to those obtained by perturbation methods.

All this shows that a correct account of the forces acting on the nucleons in the nucleus leads to a considerably more detailed picture of the properties of the nucleus than is provided by the existing models. On the other hand, the picture is not too complicated to permit a theoretical description.

In future papers we shall give the results for other nuclei with two and more particles outside closed shells.

[1] L. A. Sliv and B. A. Volchok, JETP **36**, 539 (1959), Soviet Phys. JETP **9**, 374 (1959).

[2] A. Bohr and B. Mottelson, Kgl. Danske Vidensk. Selskab, Mat.-fys. Medd. **27**, Nr. 16 (1953).

[3] W. W. True and K. W. Ford, Phys. Rev. **109**, 1675 (1958).

[4] B. J. Raz, Phys. Rev. **114**. 1116 (1959).

[5] Сб. Строение атомного ядра (под. ред. А. С. Давыдова) (Structure of the Atomic Nucleus), Collected Papers, edited by A. S. Davydov, IIL, p. 375 (1959).

[6] D. E. Alburger and M. H. L. Pryce, Phys. Rev. **95**, 1482 (1954).

Translated by R. Lipperheide
51

SOVIET PHYSICS JETP VOLUME 13, NUMBER 1 JULY, 1961

TRANSFORMATIONS OF THE INHOMOGENEOUS LORENTZ GROUP AND THE RELATIVISTIC KINEMATICS OF POLARIZED STATES

V. I. RITUS

P. N. Lebedev Physics Institute, Academy of Sciences, U.S.S.R.

Submitted to JETP editor August 12, 1960

J. Exptl. Theoret. Phys. (U.S.S.R.) 40, 352-364 (January, 1961)

Representations of the inhomogeneous Lorentz group are considered which correspond to physical systems possessing mass, momentum, and intrinsic angular momentum, for which the polarization is described by values of the projection of the intrinsic angular momentum along a prescribed direction or of the total angular momentum along the direction of the momentum (the helicity). Representations are also considered which correspond to physical systems with zero mass, for which the polarization is described only by the projection of the total angular momentum along the direction of the momentum. For these representations all of the transformations of the inhomogeneous Lorentz group which determine the relativistic kinematics of the polarization are found in explicit form. The representations for systems with zero mass are obtained from those for systems with mass $\kappa \neq 0$ by passage to the limit $\kappa \to 0$.

1. GENERAL REMARKS

THE transformations of the inhomogeneous Lorentz group consist of space-time displacements, space rotations, and transformations in which a velocity is imparted to the system (pure Lorentz transformations). In a displacement of a system in space and time its coordinates x_μ go over into

$$x'_\mu = x_\mu + a_\mu, \tag{1}$$

where the four-vector* a_μ characterizes the magnitude and direction of the displacement. Under the displacement a state Φ of the system goes over into a state $\Phi^D = D\Phi$ by the action of a unitary operator $D(a)$, which is of the form

$$D(a) = \exp(-ia_\mu p_\mu), \tag{2}$$

where the four-vector p_μ is the momentum four-vector of the system.

In a space rotation of the system around an axis **n** through the angle φ the coordinates x_μ are transformed into

$$\mathbf{x}' = \mathbf{n}(\mathbf{nx}) + [\mathbf{x} - \mathbf{n}(\mathbf{nx})]\cos\varphi + [\mathbf{nx}]\sin\varphi, \qquad x_0' = x_0, \tag{3†}$$

and a state Φ of the system goes over into a state $\Phi^R = R(\mathbf{n}, \varphi)\Phi$ by the action of a unitary operator $R(\mathbf{n}, \varphi)$, which is of the form

$$R(\mathbf{n}, \varphi) = \exp(-i\varphi\,\mathbf{nM}), \tag{4}$$

where the axial vector **M** is the angular-momentum operator of the system. When a velocity **v** is imparted to the system* (pure Lorentz transformation) the coordinates undergo the transformation

$$\mathbf{x}' = \mathbf{x} + \mathbf{v}\left[\frac{\mathbf{vx}}{v^2}(\gamma - 1) + \gamma x_0\right], \qquad x_0' = \gamma(x_0 + \mathbf{vx}), \tag{5}$$

and a state Φ of the system goes over into $\Phi^L = L(\mathbf{v})\Phi$ by the action of a unitary operator $L(\mathbf{v})$, which is of the form

$$L(\mathbf{v}) = \exp(-i\chi\,\mathbf{c}\,\mathbf{N}), \qquad \operatorname{th}\chi = v, \qquad \mathbf{c} = \mathbf{v}/v, \tag{6†}$$

where the vector **N** is the generator of the pure Lorentz transformation.

The operators **M**, **N** form the antisymmetric angular-momentum tensor $M_{\mu\nu}$:

$$\mathbf{M} = (M_{23}, M_{31}, M_{12}), \qquad i\,\mathbf{N} = (M_{41}, M_{42}, M_{43}). \tag{7}$$

The operators p_μ and $M_{\mu\nu}$ satisfy the following commutation relations[1,2]:

$$[p_\mu, p_\nu] = 0, \tag{8}$$

$$[M_i, p_j] = i\varepsilon_{ijk}p_k, \quad [M_i, p_0] = 0,$$
$$[N_i, p_j] = -i\delta_{ij}p_0, \quad [N_i, p_0] = -ip_i, \tag{9}$$

$$[M_i, M_j] = i\varepsilon_{ijk}M_k, \quad [M_i, N_j] = i\varepsilon_{ijk}N_k,$$
$$[N_i, N_j] = -i\varepsilon_{ijk}M_k. \tag{10}$$

---

*The notation used is $a_\mu = (\mathbf{a}, a_0)$, $a_\mu b_\mu = \mathbf{a}\cdot\mathbf{b} - a_0 b_0$.

†$[\mathbf{nx}] = \mathbf{n} \times \mathbf{x}$; $(\mathbf{nx}) = \mathbf{n}\cdot\mathbf{x}$.

*Hereafter we shall use, besides the ordinary velocity **v**, the corresponding four-velocity $u_\mu = (\mathbf{u}, \gamma)$, where $\mathbf{u} = \gamma\mathbf{v}$ and $\gamma = (1 - v^2)^{-1/2}$.

†$\operatorname{th}\gamma = \tanh\gamma$.

Although the operators p_μ, $M_{\mu\nu}$ that define the inhomogeneous Lorentz group are Hermitian and correspond to physical quantities they do not form a complete set of commuting operators, and therefore cannot be used for a consistent description of physical systems. We can, however, construct from the operators p_μ and $M_{\mu\nu}$ a complete set of Hermitian operators A, whose eigenstates Φ_a form a representation of the inhomogeneous Lorentz group. Those of the operators A that commute not only with each other but also with the operators p_μ and $M_{\mu\nu}$ are called invariants of the group. To each set of eigenvalues of the invariants of the group there corresponds its own representation, i.e., its own system of states Φ_a, which transform only among themselves under all the transformations of the group. A detailed classification of the representations of the inhomogeneous Lorentz group has been derived in papers by Wigner,[3] Bargmann and Wigner,[4] and Shirokov.[5]

We shall here consider representations that are characterized by a complete system of conserved operators A, i.e., operators that commute with the S matrix and with the operator p_0.[1]

2. CONSERVED OPERATORS AND THE INTRINSIC ANGULAR MOMENTUM OF A SYSTEM

Let us consider a physical system which possesses the four-momentum p_μ and the four-dimensional angular momentum $M_{\mu\nu}$. When a velocity $\mathbf{v}$ is imparted to such a system the components of the vector p_μ and the tensor $M_{\mu\nu}$ are transformed in the following way:[6]

$$\mathbf{p}' = \mathbf{p} + \mathbf{v}\,[(\mathbf{vp})\,v^{-2}(\gamma - 1) + \gamma p_0], \qquad p_0' = \gamma(p_0 + \mathbf{vp}), \quad (11)$$

$$\begin{aligned}\mathbf{M}' &= \mathbf{M} + [\mathbf{v}\,[\mathbf{vM}]]\,v^{-2}(1-\gamma) + \gamma\,[\mathbf{vN}],\\ \mathbf{N}' &= \mathbf{N} + [\mathbf{v}\,[\mathbf{vN}]]\,v^{-2}(1-\gamma) - \gamma\,[\mathbf{vM}].\end{aligned} \quad (12)$$

If we choose for the velocity $\mathbf{v}$ the value $\mathbf{v} = -\mathbf{p}/p_0$, then the center of mass of the transformed system will be at rest, so that $\mathbf{p}' = 0$, $p_0' = \kappa$, and $\mathbf{M}' = \mathbf{M} - \kappa^{-1}(p_0 + \kappa)^{-1}\mathbf{p} \times [\mathbf{p} \times \mathbf{M}] - \kappa^{-1}[\mathbf{p} \times \mathbf{N}]$.

The angular momentum $\mathbf{M}'$, which is the angular momentum of the stationary system (or the angular momentum of the system in the center-of-mass coordinate system) is naturally called the intrinsic angular momentum of the system. Let us denote it by $\mathbf{J}$

$$\mathbf{J} = \mathbf{M} - \frac{[\mathbf{p}\,[\mathbf{pM}]]}{\varkappa\,(p_0 + \varkappa)} - \frac{[\mathbf{pN}]}{\varkappa}. \quad (13)$$

If, following Pryce,[7] we introduce the coordinate $\mathbf{r}$ of the center of mass of the system, defined by the relation*

$$\mathbf{r} = \varkappa^{-1}\,[-\mathbf{N} - \overline{(p_0 + \varkappa)^{-1}\,[\overline{\mathbf{pM}}]} + \overline{p_0^{-1}(p_0 + \varkappa)^{-1}\,\mathbf{p}\,(\overline{\mathbf{pN}})}], \quad (14)$$

then the operator $M_{\mu\nu}$ can be written in terms of the momentum $\mathbf{p}$, the intrinsic angular momentum $\mathbf{J}$, and the coordinate $\mathbf{r}$ of the center of mass, in the following way[5,8,9]

$$\mathbf{M} = [\mathbf{rp}] + \mathbf{J}, \qquad \mathbf{N} = -\overline{p_0\,\mathbf{r}} - (p_0 + \varkappa)^{-1}\,[\mathbf{pJ}]. \quad (15)$$

Thus the angular momentum $\mathbf{M}$ of the system is the sum of the intrinsic angular momentum $\mathbf{J}$ and the angular momentum $\mathbf{r} \times \mathbf{p}$, which can be interpreted as the angular momentum of the center of mass.

From the definitions (13) — (14) and the relations (8) — (10) it follows that the operators $\mathbf{r}$, $\mathbf{J}$, $\mathbf{p}$ satisfy the following commutation relations:

$$\begin{gathered}[r_i, r_j] = 0, \qquad [r_i, p_j] = i\delta_{ij}, \qquad [r_i, p_0] = i p_i p_0^{-1},\\ [J_i, J_j] = i\varepsilon_{ijk} J_k, \qquad [J_i, r_j] = 0,\\ [J_i, p_j] = 0, \qquad [J_i, p_0] = 0.\end{gathered} \quad (16)$$

Furthermore

$$[r_i, M_j] = i\varepsilon_{ijk} r_k,$$

$$\begin{aligned}[r_i, N_j] = i\,(&-p_0^{-1}\,\overline{p_i r_j} + p_0^{-1}(p_0 + \varkappa)^{-2}\,p_i\,[\mathbf{pJ}]_j\\ &+ (p_0 + \varkappa)^{-1}\,\varepsilon_{ijk} J_k),\end{aligned}$$

$$\begin{gathered}[J_i, M_j] = i\varepsilon_{ijk} J_k, \qquad [J_i, N_j] = i\,(p_0 + \varkappa)^{-1}\,(\delta_{ij}\,\mathbf{pJ} - p_i J_j),\\ [\mathbf{J}^2, J_i] = 0, \qquad [\mathbf{J}^2, M_i] = 0, \qquad [\mathbf{J}^2, N_i] = 0.\end{gathered} \quad (17)$$

Thus the operators p_μ, $M_{\mu\nu}$ are expressed in terms of the operators p_μ, $\mathbf{J}$, $\mathbf{r}$ (and conversely). It follows from the commutation relations (16) — (17) that the operators p_μ, $\mathbf{J}^2$, and one of the components of $\mathbf{J}$, for example J_z, form a complete system of conserved operators:

$$p_\mu,\ \mathbf{J}^2,\ J_z \quad \text{or} \quad p_\mu^2,\ \mathbf{p},\ \mathbf{J}^2,\ J_z. \quad (18)$$

The operators (18) exhaust the possibilities for forming sets of independent conserved operators from p_μ and $M_{\mu\nu}$.

The operators p_μ^2 and $\mathbf{J}^2$ are invariants of the group. The eigenvalues of the operator p_μ^2 are κ^2, where κ is the energy of the stationary system, or the energy in the center-of-mass system (c.m.s.). For nonelementary systems† (for example, a system of two colliding particles) κ is a continuous variable. The momentum $\mathbf{p}$, $p_0 = (\mathbf{p}^2 + \kappa^2)^{1/2}$

---

*A stroke over the product of two noncommuting Hermitian operators means the product made Hermitian operators means the product made Hermitian by symmetrization; that is, $\overline{ab} = \frac{1}{2}(ab + ba)$.

†For the definition of an elementary system see reference 10.

always has a continuous spectrum of eigenvalues. The eigenvalues of the operators $\mathbf{J}^2$ and J_Z are obviously $J(J+1)$, where $J = 0, \frac{1}{2}, 1, \ldots$, and $m = J, J-1, \ldots, -J$. In the representation of p_μ^2, $\mathbf{p}$, $\mathbf{J}^2$, J_Z the operators (15) take the forms

$$\mathbf{M} = -i\left[\mathbf{p}\frac{\partial}{\partial \mathbf{p}}\right] + \mathbf{J}, \qquad \mathbf{N} = -ip_0\frac{\partial}{\partial \mathbf{p}} - (p_0 + \varkappa)^{-1}[\mathbf{pJ}], \tag{19}$$

and $\mathbf{J}$ is represented by the well known $(2J+1)$-rowed square matrices.

For each κ and J the eigenstates $\Phi_{\mathrm{p}Jm}$ of the operators (18) form an irreducible representation of the inhomogeneous Lorentz group and correspond to a system with mass κ, intrinsic angular momentum J, momentum $\mathbf{p}$, and projection of intrinsic angular momentum m. The mass κ and the intrinsic angular momentum J are invariants of this representation, and therefore as a rule we shall write the eigenstates of the operators (18) in the simple form $\Phi_{\mathrm{p}m}$.

3. THE REPRESENTATION OF MOMENTUM AND INTRINSIC ANGULAR MOMENTUM FOR A SYSTEM WITH MASS NOT EQUAL TO ZERO

Let $U(a, \Lambda)$ be the operator that corresponds to the inhomogeneous Lorentz transformation $x'_\mu = \Lambda_{\mu\nu}x_\nu + a_\mu$, and let $U_{\mathrm{p}'m', \mathrm{p}m}$ be the matrix element of the operator $U(a, \Lambda)$ in the representation (18). It follows from general considerations[3,4] that this matrix element must have the form

$$U_{\mathbf{p}'m', \mathbf{p}m}(a, \Lambda) = e^{-ip'a}Q_{m'm}(\Lambda, p)\,\delta_{\mathbf{p}', \Lambda\mathbf{p}}, \tag{20}$$

where $Q(\Lambda, p)$ is a unitary operator in the space of the projection of the intrinsic angular momentum, which depends on the transformation Λ and the momentum p_μ. Thus the action of the operator $U(a, \Lambda)$ on the eigenstate $\Phi_{\mathrm{p}m}$ leads to the state

$$\Phi'_{\mathbf{p}m} \equiv U(a, \Lambda)\,\Phi_{\mathbf{p}m} = \sum_{\mathbf{p}'m'}\Phi_{\mathbf{p}'m'}U_{\mathbf{p}'m'\,\mathbf{p}m}$$

$$= e^{-i\Lambda pa}\sum_{m'}\Phi_{\Lambda\mathbf{p}m'}Q_{m'm}(\Lambda, p), \tag{21}$$

and the action of the operator $U(a, \Lambda)$ on an arbitrary state Φ leads to a new state $\Phi' = U\Phi$ whose wave function $\Phi'(\mathrm{p}'m')$ is connected with the wave function $\Phi(\mathrm{p}m)$ by the relation $(\mathrm{p}' = \Lambda\mathrm{p})$:

$$\Phi'(\mathbf{p}'m') \equiv U(a, \Lambda)\,\Phi(\mathbf{p}'m') = \sum_{\mathbf{p}m}U_{\mathbf{p}'m', \mathbf{p}m}(a, \Lambda)\,\Phi(\mathbf{p}m)$$

$$= e^{-ip'a}\sum_{m}Q_{m'm}(\Lambda, p)\,\Phi(\mathbf{p}m). \tag{22}$$

The operator $Q(\Lambda, p)$ satisfies the group relation

$$Q(\Lambda_2\Lambda_1, p) = Q(\Lambda_2, \Lambda_1 p)\,Q(\Lambda_1, p). \tag{23}$$

It is obvious that the explicit form of any transformation of the inhomogeneous Lorentz group, $U(a, \Lambda)$, will be known if the operators $Q(R, p)$ and $Q(L, p)$ for rotations and pure Lorentz transformations are known. In order to find these operators, let us represent the operators $R(\mathbf{n}, \varphi)$ and $L(\mathbf{v})$ [cf. Eqs. (4) and (6)] in the form

$$\exp\left[-\lambda\frac{\partial}{\partial x} + \lambda f(x, \mathbf{J})\right], \tag{24}$$

where x is a variable which determines the position and magnitude of the four-momentum p_μ, and a change of which by the amount λ characterizes the transformation. For example, if the value $x = x_0$ corresponds to a momentum p_μ, then the value $x = x_0 + \lambda$ corresponds to the momentum $p'_\mu = \Lambda_{\mu\nu}(\lambda)\,p_\nu$. Let us now represent

$\exp\left[-\lambda\frac{\partial}{\partial x} + \lambda f(x, \mathbf{J})\right]$ in the form

$$\exp\left[-\lambda\frac{\partial}{\partial x} + \lambda f(x, \mathbf{J})\right] = \exp F(x_0, \lambda, \mathbf{J})\exp\left(-\lambda\frac{\partial}{\partial x}\right)$$

$$(x_0 = x - \lambda); \tag{25}$$

then it is not hard to show[11]* that if $f(x, \mathbf{J})$ commutes with its derivatives with respect to x, then

$$F(x, \lambda, \mathbf{J}) = \int_x^{x+\lambda} f(x', \mathbf{J})\,dx', \tag{26}$$

from which we have

$$Q(\Lambda(\lambda), p(x_0)) = \exp F(x_0, \lambda, \mathbf{J}). \tag{27}$$

This same formula also follows from the group relation (23). In fact, let us set in Eq. (23) $\Lambda_1 = \Lambda(\lambda)$ and $\Lambda_2 = \Lambda(d\lambda) = I + \Lambda'(0)\,d\lambda$. Then, since $Q(I + \Lambda'(0)\,d\lambda, \Lambda(\lambda)\,p(x) = Q(I + \Lambda'(0)\,d\lambda, p(x+\lambda)) = I + f(x+\lambda, \mathbf{J})\,d\lambda$, then in virtue of the group relation $\Lambda(d\lambda)\Lambda(\lambda) = \Lambda(\lambda + d\lambda)$ we have from Eq. (23) the equation for $Q(\Lambda(\lambda), p)$:

$$dQ(\Lambda(\lambda), p(x)) = f(x+\lambda, \mathbf{J})\,Q(\Lambda(\lambda), p(x))\,d\lambda, \tag{28}$$

which in the case in which $f(x, \mathbf{J})$ commutes with $f(x', \mathbf{J})$ (or with all of its own derivatives with respect to x) has the solution

$$Q(\Lambda(\lambda), p(x)) = \exp\int_x^{x+\lambda} f(x', \mathbf{J})\,dx'. \tag{29}$$

Let us examine the special cases of the formula (27).

Rotations. In the case of rotations $-i\varphi\mathbf{n}\cdot\mathbf{M} = -\varphi\partial/\partial x - i\varphi\mathbf{n}\cdot\mathbf{J}$, where x is the angle in the plane perpendicular to $\mathbf{n}$ that determines the direction of the momentum $\mathbf{p}$, so that $\lambda = \varphi$ and $f(x, \mathbf{J}) - i\mathbf{n}\cdot\mathbf{J}$. Therefore

---

*The writer is extremely grateful to D. A. Kirzhnits for remarks connected with the formulas (25) and (26).

$$Q(R_{\mathbf{n},\varphi},\ p) = \exp(-i\varphi\,\mathbf{n}\mathbf{J}). \tag{30}$$

This is an obvious result, since in a rotation of a physical system around the axis $\mathbf{n}$ through the angle φ its intrinsic angular momentum as well as its momentum is rotated through the angle φ around $\mathbf{n}$.

Pure Lorentz transformations. In this case $-i\chi\mathbf{cN} = -\chi\partial/\partial x + i\chi(\mathbf{c}[\mathbf{pJ}])(p_0+\varkappa)^{-1}$, where x is the angle in the plane of $\mathbf{v}$ and p_0 that characterizes the magnitude and direction of the four-momentum p_μ, so that*

$$\mathbf{p}_\parallel = \mathbf{v}\sqrt{p_\perp^2+\varkappa^2}\,\mathrm{sh}\,x, \qquad p_0 = \sqrt{p_\perp^2+\varkappa^2}\,\mathrm{ch}\,x, \qquad \lambda = \chi.$$

Therefore

$$f(x, \mathbf{J}) = -i([p \times c]\mathbf{J})[(p_\perp^2+\kappa^2)^{1/2}\cosh x + \kappa]^{-1},^*$$

and

$$Q(L_\mathbf{v},\ p) = \exp(-i\omega\mathbf{n}\mathbf{J}), \qquad \mathbf{n} = [\mathbf{pv}]/|[\mathbf{pv}]|; \tag{31}$$

$$\omega = 2\,\mathrm{arc\,tg}\frac{|[\mathbf{pu}]|}{\mathbf{pu}+(p_0+\varkappa)(\gamma+1)}\,. \tag{32}^*$$

Thus when a velocity $\mathbf{v}$ is imparted to a physical system its momentum $p_\mu = (\mathbf{p}, p_0)$ is transformed into a momentum $p'_\mu = (\mathbf{p}', p'_0)$ [cf. Eq. (11)], and the intrinsic angular momentum is turned through the angle ω around the axis $\mathbf{p} \times \mathbf{v}$. The angle of rotation ω of the intrinsic angular momentum plays an important role in the relativistic theory of reactions with polarized particles, and therefore we shall discuss it in more detail.

4. RELATIVISTIC KINEMATICS OF THE INTRINSIC ANGULAR MOMENTUM OF A SYSTEM

We shall present a different derivation of the angle ω by which the intrinsic angular momentum $\mathbf{J}$ of a system is rotated when a velocity $\mathbf{v}$ is imparted to the system. By definition, the intrinsic angular momentum $\mathbf{J}$ of a physical system A, which has four-momentum p_μ and four-dimensional angular momentum $M_{\mu\nu}$ is the space part of the four-dimensional angular momentum $M^c_{\mu\nu}$ of the stationary system A^c which is obtained from the system A by imparting to it the velocity $\mathbf{v} = -\mathbf{p}/p_0$. Under a pure Lorentz transformation the system A goes over into a system A′ having the four-momentum p'_μ and the four-dimensional angular momentum $M'_{\mu\nu}$.† By definition, the intrinsic angular momentum $\mathbf{J}'$ of the transformed system A′ is the space part of the four-dimensional angular momentum $M'^c_{\mu\nu}$ of the stationary system A'^c that is obtained from A′ by imparting to it the velocity $\mathbf{v}' = -\mathbf{p}'/p'_0$.

In the general case the intrinsic angular momenta $\mathbf{J}$ and $\mathbf{J}'$ defined in this way for the system A and the Lorentz-transformed system A′ do not coincide, but differ by a space rotation. To see this we note that if for the system A we introduce the four-vector

$$\Gamma_\mu = (1/2\,i\varkappa)\,\varepsilon_{\mu\nu\lambda\sigma}M_{\nu\lambda p_\sigma},$$

then the intrinsic angular momentum of the system A coincides with the space part of the four-vector Γ^c_μ of the system A^c. The four-vectors Γ^c_μ and Γ'^c_μ of the systems A^c and A'^c, and consequently also the intrinsic angular momenta $\mathbf{J}$ and $\mathbf{J}'$ of the systems A and A′, are connected with each other by the product of three Lorentz transformations:

$$\Gamma'^c_\mu = L_{\mu\nu}(\mathbf{v}_3)\,L_{\nu\lambda}(\mathbf{v}_2)\,L_{\lambda\sigma}(\mathbf{v}_1)\,\Gamma^c_\sigma \equiv R_{\mu\sigma}\Gamma^c_\sigma, \tag{33}$$

where $\mathbf{v}_1$, $\mathbf{v}_2$, $\mathbf{v}_3$ are the velocities of the systems A, A′, A'^c relative to A^c, A, and A′, respectively. It is obvious that

$$\mathbf{v}_1 = \mathbf{p}/p_0,\ \ \mathbf{v}_2 = (\mathbf{p}'-\mathbf{p})(p'_0+p_0)/(p'^2_0+p^2_0+p'_0p_0-\mathbf{p}'\mathbf{p}-\varkappa^2)$$

$$\mathbf{v}_3 = -\mathbf{p}'/p'_0\,. \tag{34}$$

The resultant transformation $R_{\mu\sigma}$ does not change the velocity of the system A^c, and therefore is a pure space rotation,* so that $R_{00} = 1$, $R_{ik} = R_{ik}(\mathbf{n}, \omega)$. The direction $\mathbf{n}$ of the axis of rotation and the angle of rotation ω can be found from the relations

$$2\,n_i\sin\omega \equiv -\varepsilon_{ijk}R_{jk}(\mathbf{n},\ \omega) = -\varepsilon_{ijk}L_{j\nu}(\mathbf{v}_3)\,L_{\nu\lambda}(\mathbf{v}_2)\,L_{\lambda k}(\mathbf{v}_1),$$

from which it follows that

$$\mathbf{n}\sin\omega = [\mathbf{u}_1\mathbf{u}_2]\frac{1+\gamma_1+\gamma_2+\gamma_3}{(1+\gamma_1)(1+\gamma_2)(1+\gamma_3)}\,. \tag{35}$$

This formula, which was first obtained by Stapp[12] (see also reference 9) corresponds exactly to the formula (32) found above.

This derivation brings out a definite symmetry in the dependence of the angle ω on the velocities $\mathbf{u}_1$, $\mathbf{u}_2$, $\mathbf{u}_3$. The velocities $\mathbf{u}_1$, $\mathbf{u}_2$, $\mathbf{u}_3$ form a closed triangle, which must be understood in the sense that $\mathbf{u}_3$ is the relativistic sum of the velocities $-\mathbf{u}_2$ and $-\mathbf{u}_1$, and so on (see Fig. 1). If we introduce a function $\omega(x, y, \theta)$ that depends on the dimensionless variables x, y and the angle θ and is symmetrical in x and y,

---

*Sh = sinh, ch = cosh, arctg = $\tan^{-1}$.

†It is obvious that p'_μ and $M'_{\mu\nu}$ are connected with p_μ and $M_{\mu\nu}$ by relations (11) and (12), where

$$\mathbf{v} = (\mathbf{p} - \mathbf{p})(p_0 + p_0)/(p_0 \top \nu_0 \top \nu_0 p_0 - \mathbf{p}\,\mathbf{p} - \varkappa^2)$$

is the velocity of the Lorentz transformation, i.e., the velocity of the system A′ relative to the system A.

*It must be kept in mind that pure Lorentz transformations with nonparallel velocities do not form a group (cf. reference 13).

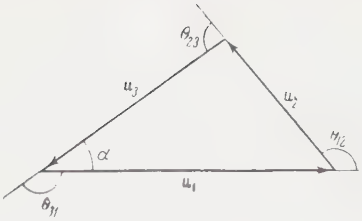

FIG. 1

$$\omega(x,\ y,\ \theta) = 2\ \operatorname{arc\,tg} \frac{xy \sin\theta}{xy\cos\theta + (x_0+1)(y_0+1)},$$

$$x_0 = \sqrt{x^2+1},\quad y_0 = \sqrt{y^2+1}, \tag{36}$$

then the symmetry of the dependence of ω on $\mathbf{u}_1$, $\mathbf{u}_2$, $\mathbf{u}_3$ can be expressed by the relation

$$\omega = \omega(u_1,\ u_2,\ \theta_{12}) = \omega(u_2,\ u_3,\ \theta_{23}) = \omega(u_3,\ u_1,\ \pi - \theta_{31}) \tag{37}$$

or, if in accordance with Eq. (34) we go over to the momenta $\mathbf{p}$, $\mathbf{p}'$ and the velocity $\mathbf{u}$ of the Lorentz transformation, by the relation

$$\omega = \omega(p/\varkappa,\ u,\ \theta) = \omega(u,\ p'/\varkappa,\ \theta') = \omega(p'/\varkappa,\ p/\varkappa,\ \alpha), \tag{38}$$

where θ, θ', α are the respective angles between the vectors $\mathbf{p}$ and $\mathbf{u}$, $\mathbf{p}'$ and $-\mathbf{u}$, $\mathbf{p}'$ and $\mathbf{p}$.

When one of the velocities u_1, u_2, u_3 goes to infinity, another also automatically goes to infinity. It is not hard to see that

$$\omega(x,\ y,\ \theta)\,|_{x\to\infty,\ y\to\infty} = \theta.$$

Therefore it follows from Eq. (38) that $\omega \to \theta$ for p/κ, $u \to \infty$; $\omega \to \alpha$ for p/κ, $p'/\kappa \to \infty$, and $\omega \to \theta'$ for p'/κ, $u \to \infty$. In particular it follows that if we let the mass κ of the system go to zero, then the angle of rotation of the intrinsic angular momentum approaches the angle of rotation α of the momentum (which in the case $\kappa = 0$ is the angle of aberration of light).

It is useful to present the formula for the angle α through which the momentum $\mathbf{p}$ of the system is turned in a pure Lorentz transformation. Starting from Eq. (11), one can show without difficulty that

$$\sin\alpha = \frac{|[\mathbf{pu}]|\,[\mathbf{pu} + p_0(\gamma+1)]}{(\gamma+1)\,p\sqrt{(\gamma p_0 + \mathbf{pu})^2 - \varkappa^2}},$$

$$\cos\alpha = \frac{p^2(\gamma+1) + (\mathbf{pu})^2 + \mathbf{pu}\,p_0(\gamma+1)}{(\gamma+1)\,p\sqrt{(\gamma p_0 + \mathbf{pu})^2 - \varkappa^2}},$$

$$\alpha = 2\operatorname{arc\,tg}\left\{|[\mathbf{pu}]|\left[\mathbf{pu} + (\gamma+1)\frac{p^2 + p\sqrt{(\gamma p_0 + \mathbf{pu})^2 - \varkappa^2}}{\mathbf{pu} + p_0(\gamma+1)}\right]^{-1}\right\} \tag{39}$$

We call attention to the fact that the angles α and ω are angles of rotation around the same axis $\mathbf{p} \times \mathbf{v}$, the angle ω being always less than α, except in the case $\kappa = 0$, when $\omega = \alpha$. Thus in a pure Lorentz transformation the intrinsic angular momentum always rotates through a smaller angle than the momentum does.

In conclusion we present plots of the functions $\omega(x, y, \theta)$ and $\omega(x, \infty, \theta)$ (see Figs. 2 and 3). It is interesting to note that in Lorentz transformations in which the momentum is rotated through

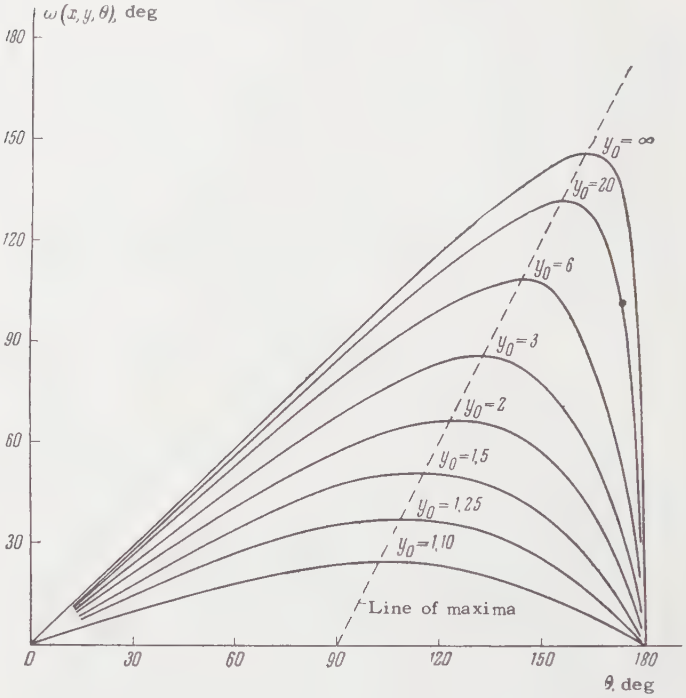

FIG. 2. Graphs of the function $\omega(x, y, \theta)$ plotted against θ for parameter values $1 < y_0 < \infty$, $x_0 = 20$.

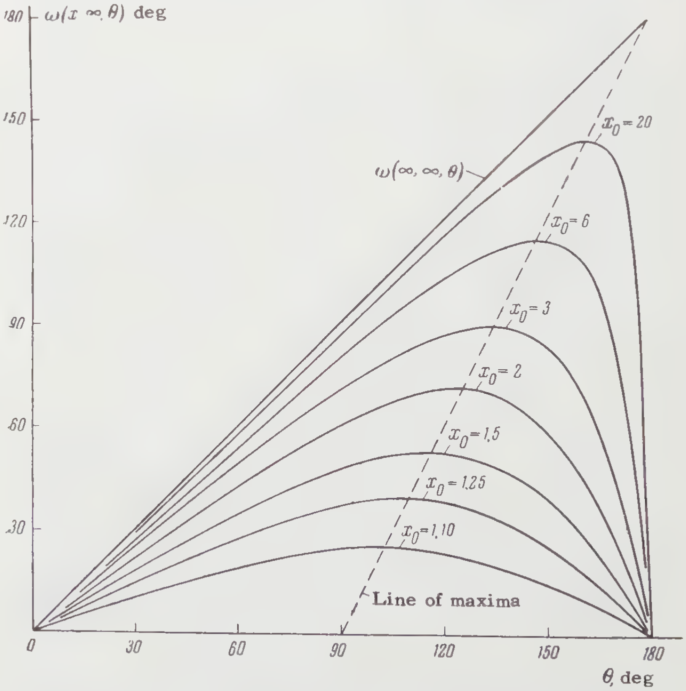

FIG. 3. Graphs of the function $\omega(x, y, \theta)$ plotted against θ for parameter values $1 < x_0 < \infty$, $y = \infty$

exactly 180° the intrinsic angular momentum is not rotated at all, whereas in Lorentz transformations in which the momentum is rotated through almost 180° the intrinsic angular momentum can be rotated through large angles close to 180°.

5. THE REPRESENTATION OF MOMENTUM AND HELICITY FOR SYSTEMS WITH NONZERO MASS

The definition of the intrinsic angular momentum of a system as the angular momentum of the system with its center of mass at rest is possible only for systems with nonzero rest mass. The representation of momentum and intrinsic angular momentum considered above holds only for systems of this kind. There is, however, another representation of the inhomogeneous Lorentz group — the representation of momentum and helicity* — which holds for systems with $\kappa \neq 0$ and also for those with $\kappa = 0$. We shall consider this representation first for $\kappa \neq 0$, and then, by going to the limit $\kappa \to 0$, also for $\kappa = 0$.

Accordingly, assume that the rest mass of the system is not zero. Let us consider an eigenstate Φ_{pkm} with momentum pk along the axis **k** and component m of the intrinsic angular momentum along the axis **k** (**k** is the unit vector along the z axis of quantization). We shall define the eigenstate χ_{pm} of the system with momentum p and helicity m as the state obtained by rotating the state Φ_{pkm} around the axis [**k**p] by an angle θ equal to the angle between the momentum p and the direction **k**:

$$\chi_{\mathbf{p}m} = R([\mathbf{kp}],\ \theta)\,\Phi_{p\mathbf{k},\,m} = \exp\left[-i\theta([\mathbf{kp}]\,\mathbf{M})/p\sin\theta\right]\Phi_{p\mathbf{k},\,m}. \tag{40}$$

The action of the operator U(a, Λ) on the eigenstate χ_{pm} leads to a state χ'_{pm}:

$$\chi'_{\mathbf{p}m} \equiv U(a,\ \Lambda)\,\chi_{\mathbf{p}m} = \sum_{\mathbf{p}'m'} \chi_{\mathbf{p}'m'}\,U_{\mathbf{p}'m',\ \mathbf{p}m}(a,\ \Lambda)$$

$$= e^{-i\Lambda pa} \sum_{m'} \chi_{\Lambda\mathbf{p},m'}\,S_{m'm}(\Lambda,\ p), \tag{41}$$

and the action of the operator U(a, Λ) on an arbitrary state Φ leads to a new state Φ′ = UΦ, whose wave function in the representation of momentum and helicity, $\Phi'(p'm') = (\chi_{p'm'}, \Phi')$, is connected with the wave function $\Phi(pm) = (\chi_{pm}, \Phi)$ in this same representation by the relation

$$\Phi'(\mathbf{p}'m') = U(a,\ \Lambda)\,\Phi(\mathbf{p}'m')$$

$$= e^{-ip'a} \sum_{m} S_{m'm}(\Lambda,\ p)\,\Phi(\mathbf{p}m),\quad p' = \Lambda p. \tag{42}$$

In the relations (41) and (42), unlike (21) and (22), S(Λ, p) is a unitary operator in the helicity space, which depends on the transformation Λ and the momentum p_μ.

By using Eqs. (40) and (41) we can see without difficulty that in the helicity representation the operator S(Λ, p) is equal to the product of three operators Q in the intrinsic-angular-momentum representation (p′ = Λp):

$$S_{m'm}(\Lambda,\ p) = Q_{m'n'}(R^{-1}_{[\mathbf{kp}'],})\,\theta',$$

$$p'\mathbf{k})\,Q_{n'n}(\Lambda,\ \mathbf{p})\,Q_{nm}(R_{[\mathbf{kp}],})\,\theta\ ,\ p\mathbf{k}). \tag{43}$$

This formula essentially solves the problem of going from the intrinsic-angular-momentum representation to the helicity representation for systems with nonzero mass. It is useful, however, to get the generators of rotations and pure Lorentz transformations for the representation of momentum and helicity.

For a rotation through the angle φ around the axis **n** Eq. (43) takes the form

$$S(R_{\mathbf{n},\ \varphi},\ p) = \exp\left[i\theta'([\mathbf{kp}']\,\mathbf{J})/p\sin\theta'\right]\exp\left[-i\varphi\mathbf{nJ}\right]$$

$$\times\exp\left[-i\theta([\mathbf{kp}]\,\mathbf{J})/p\sin\theta\right]. \tag{44}$$

If the angle of rotation φ is small, then

$$\mathbf{p}' = \mathbf{p} + \varphi[\mathbf{np}],\quad \theta' = \theta - \varphi(\mathbf{k}[\mathbf{np}])/p\sin\theta.$$

Therefore the first exponential in Eq. (44) can be put in the form exp (a + b), where the operator a is $a = i\theta([\mathbf{k}\times\mathbf{p}]\mathbf{J})/p\sin\theta$ and the operator b is proportional to φ and consequently is small. Then using the formula[14]

$$e^{a+b} = e^{a}\left(1 + \int_0^1 e^{-a\eta}\,b\,e^{a\eta}\,d\eta + \ldots\right), \tag{45}$$

and also the fact that $\exp(-a\eta)$ is the operator of rotation through the angle $\theta\eta$ around the axis $\mathbf{k}\times\mathbf{p}$, we get

$$\exp\left[i\theta'\,\frac{([\mathbf{kp}']\,\mathbf{J})}{p\sin\theta'}\right] \approx \exp\left[i\theta\,\frac{([\mathbf{kp}]\,\mathbf{J})}{p\sin\theta}\right]$$

$$\times\left(\mathrm{I} + i\varphi\mathbf{nJ} - i\varphi(\mathbf{pJ})\,\frac{p\mathbf{nk}+\mathbf{np}}{p^2+p\mathbf{pk}}\right). \tag{46}$$

Returning to Eq. (44) and expanding $\exp(-i\varphi\mathbf{n}\cdot\mathbf{J}) \approx \mathrm{I} - i\varphi\mathbf{n}\cdot\mathbf{J}$, we get for small φ

$$S(R_{\mathbf{n},\ \varphi},\ p) = \mathrm{I} - i\varphi(\mathbf{kJ})\,\frac{p\mathbf{nk}+\mathbf{np}}{p+\mathbf{pk}}, \tag{47}$$

from which it follows that in the representation of

---

*By this term we mean the component of the total angular momentum **M** along the direction of the momentum, and not merely its sign.

momentum and helicity the generator of rotations is the operator

$$\mathbf{M} = -i\left[\mathbf{p}\,\frac{\partial}{\partial \mathbf{p}}\right] + (\mathbf{kJ})\,\frac{p\mathbf{k}+\mathbf{p}}{p+\mathbf{pk}}\,. \tag{48}$$

For a pure Lorentz transformation with the velocity $\mathbf{v} = c\mathrm{v}$ the formula (43) takes the form

$$S(L_{\mathrm{v}},\ p) = \exp\left[i\theta'\,([\mathbf{kp}']\,\mathbf{J})/p'\sin\theta'\right]\exp\left[-i\omega\mathbf{nJ}\right]$$

$$\times\exp\left[-i\theta\,([\mathbf{kp}]\,\mathbf{J})/p\sin\theta\right], \tag{49}$$

where $\mathbf{n} = [\mathbf{p}\times\mathbf{v}]/|[\mathbf{p}\times\mathbf{v}]|$. If the speed v of the Lorentz transformation is small, the angle α through which the momentum vector $\mathbf{p}$ is turned is also small [cf. Eq. (30)], and

$$\mathbf{p}'/p = \mathbf{p}/p' + \alpha\,[\mathbf{np}]/p, \quad \theta' = \theta - \alpha\,(\mathbf{k}\,[\mathbf{np}])/p\sin\theta.$$

Then by repeating the same arguments as for the case of a rotation, we get for small speeds v (and consequently small angles α and ω)

$$S(L_{\mathrm{v}},\ p) = \mathrm{I} - i(\alpha-\omega)\,\frac{([[\mathbf{kp}]\,\mathbf{k}]\,\mathbf{J})\,p\mathbf{nk} - ([\mathbf{kp}]\,\mathbf{J})\,([\mathbf{kp}]\,\mathbf{n})}{p^2-(\mathbf{pk})^2}$$

$$- i\alpha\mathbf{kJ}\,\frac{\mathbf{nk}p}{p+\mathbf{pk}}$$

$$= \mathrm{I} - i\left\{\varkappa\,\frac{([[\mathbf{kp}]\,\mathbf{k}]\,\mathbf{J})\,(\mathbf{k}\,[\mathbf{pv}])\,p - ([\mathbf{kp}]\,\mathbf{J})\,([\mathbf{kp}]\,[\mathbf{pv}])}{p^2\,(p^2-(\mathbf{pk})^2)}\right.$$

$$\left. + \mathbf{kJ}\,\frac{(\mathbf{k}\,[\mathbf{pv}])\,p_0}{p\,(p+\mathbf{pk})}\right\}. \tag{50}$$

It follows from this that in the representation of momentum and helicity the generator of pure Lorentz transformations is the operator

$$\mathbf{N} = -ip_0\,\frac{\partial}{\partial\mathbf{p}} + \varkappa\,\frac{p\,([[\mathbf{kp}]\,\mathbf{k}]\,\mathbf{J})\,[\mathbf{kp}] - ([\mathbf{kp}]\,\mathbf{J})\,[[\mathbf{kp}]\,\mathbf{p}]}{p^2\,(p^2-(\mathbf{pk})^2)}$$

$$+ \mathbf{kJ}\,\frac{p_0\,[\mathbf{kp}]}{p\,(p+\mathbf{pk})}. \tag{51}$$

Let us examine the appearance of the mass in the components of $\mathbf{J}$ that are orthogonal to $\mathbf{k}$. The operators $\mathbf{M}$, $\mathbf{N}$ and the momentum operator p_μ satisfy the commutation relations (8) – (10). The operators

$$p_\mu^2,\ \mathbf{p},\ \mathbf{J}^2,\ \mathbf{Mp}/p \equiv \mathbf{kJ} \tag{52}$$

form a complete system of conserved operators, and the operators p_μ^2 and $\mathbf{J}^2$ are invariants of the group. For each κ and J the eigenstates $\chi_{\kappa\mathrm{pJm}}$ of the operators (52) form an irreducible representation of the inhomogeneous Lorentz group and correspond to a system with mass κ, intrinsic angular momentum J, momentum p, and helicity m.

We shall now obtain explicit expressions for the operators S(R, p) and S(L, p) that correspond to finite transformations.

Rotations. As in Sec. 3, for the construction of the operator $S(R_{\mathbf{n}}, \varphi, \mathrm{p})$ we shall use Eq. (29), in which in the present case

$$f(x,\ \mathbf{J}) = -i(\mathbf{kJ})\,\frac{p\mathbf{nk}+\mathbf{np}}{p+\mathbf{pk}}$$

$$= -i(\mathbf{kJ})\,\frac{p\mathbf{nk}+\mathbf{np}}{p\,[1+\sin\alpha\sin\beta\cos(x-\gamma)+\cos\alpha\cos\beta]}\,.$$

Here α, β are the angles made by the vectors $\mathbf{p}$, $\mathbf{k}$ with the axis of rotation $\mathbf{n}$, and x, γ are the azimuthal angles of the vectors $\mathbf{p}$, $\mathbf{k}$ in the plane perpendicular to $\mathbf{n}$. By integrating Eq. (29) we get

$$S(R_{\mathbf{n},\,\varphi},\ p) = \exp\left[-i\eta\mathbf{kJ}\right], \tag{53}$$

where the angle η is given by

$$\eta = 2\,\mathrm{arc\,tg}\,\frac{(p\mathbf{nk}+\mathbf{np})\,\mathrm{tg}\,(\varphi/2)}{p+\mathbf{pk}+(\mathbf{k}\,[\mathbf{np}])\,\mathrm{tg}\,(\varphi/2)}\,. \tag{54}$$

Thus when a state with momentum p and helicity m is rotated it goes over into a state with the momentum $\mathrm{p}' = \mathrm{Rp}$ and the same helicity m, and is merely multiplied by a phase factor $\exp(-i\eta\mathrm{m})$. This is naturally a result of the fact that when the system is rotated its intrinsic angular momentum is turned through the same angle as its momentum. We call attention to the fact that in special cases, when the axis of rotation $\mathbf{n}$ is parallel to the momentum $\mathbf{p}$ or to the quantization axis $\mathbf{k}$, the angle η is equal to the angle of rotation φ.

Pure Lorentz transformations. Unfortunately, we cannot use the formula (29) for the construction of the operator $S(L_{\mathrm{v}}, \mathrm{p})$, since in this case $f(x, \mathbf{J})$ does not commute with $f(x', \mathbf{J})$. Since, however, the operator $S(L_{\mathrm{v}}, \mathrm{p})$ is the product of three rotations in the space of the intrinsic angular momentum of the system [cf. Eq. (49)], $S(L_{\mathrm{v}}, \mathrm{p})$ is also a rotation operator in this space and must have the form

$$S(L_{\mathbf{v}},\ p) = \exp\left[-i\lambda\mathbf{mJ}\right]. \tag{55}$$

The direction $\mathbf{m}$ of the rotation axis and the angle of rotation λ can be found if we use Eq. (49) for the simplest representation, which corresponds to the intrinsic angular momentum $1/2$, so that $\mathbf{J} = \sigma/2$. We then get

$$\mathbf{m} = \left[\left(p\mathbf{nk}\,\mathrm{tg}\,\frac{\alpha}{2}\right)^2 + \left(p+\mathbf{pk}+\mathbf{k}\,[\mathbf{np}]\,\mathrm{tg}\,\frac{\alpha}{2}\right)^2\sin\frac{\alpha-\omega}{2}\right]^{-1/2}$$

$$\times\left\{[[\mathbf{kp}]\,\mathbf{k}]\,\frac{p\,(\mathbf{nk})}{p+\mathbf{pk}}\sin\frac{\alpha-\omega}{2} + [\mathbf{kp}]\left(\mathrm{tg}\,\frac{\alpha}{2} + \frac{(\mathbf{k}\,[\mathbf{np}])}{p+\mathbf{pk}}\right)\right.$$

$$\left.\times\sin\frac{\alpha-\omega}{2} + \mathbf{k}p\,(\mathbf{nk})\,\mathrm{tg}\,\frac{\alpha}{2}\cos\frac{\alpha-\omega}{2}\right\}, \tag{56}$$

$$\lambda = 2\,\mathrm{arc\,tg}\left[\left(\frac{p\mathbf{nk}\,\mathrm{tg}\,(\alpha/2)}{p+\mathbf{pk}+(\mathbf{k}\,[\mathbf{np}])\,\mathrm{tg}\,(\alpha/2)}\right)^2\sec^2\frac{\alpha-\omega}{2} + \mathrm{tg}^2\,\frac{\alpha-\omega}{2}\right]^{1/2}. \tag{57}$$

We turn our attention to the fact that the operator $S(L_{\mathbf{v}}, p)$ can be written in the form

$$S(L_{\mathbf{v}}, p) = Q^{-1}_{[\mathbf{kp}'],\,\theta'} Q_{\mathbf{n},\,\alpha} Q_{[\mathbf{kp}],\,\theta} \cdot Q^{-1}_{[\mathbf{kp}],\,\theta} Q^{-1}_{\mathbf{n},\,\alpha} Q_{\mathbf{n},\,\omega} Q_{[\mathbf{kp}],\,\theta}.$$

The first three operators Q obviously give the operator $S(R_{\mathbf{n}}, \alpha, p)$, and the last four give the operator $S(R_{\mathbf{r}}, \alpha-\omega, p)$, where $\mathbf{r}$ is the unit vector obtained by turning the vector $\mathbf{n}$ through the angle θ around the axis $\mathbf{k}\times\mathbf{p}$. It is not hard to see that

$$\mathbf{r} = \frac{p(\mathbf{nk})\,[[\mathbf{kp}]\,\mathbf{k}] - (\mathbf{n}\,[\mathbf{kp}])\,[\mathbf{kp}]}{p^2 - (\mathbf{pk})^2}. \tag{58}$$

Consequently, the operator $S(L_{\mathbf{v}}, p)$ can be represented as the product

$$S(L_{\mathbf{v}}, p) = \exp[-i\lambda\mathbf{kJ}]\exp[-i(\alpha-\omega)\,\mathbf{rJ}] \tag{59}$$

of two rotations in the space of the intrinsic angular momentum: a rotation through the angle $\alpha-\omega$ around the axis $\mathbf{r}\perp\mathbf{k}$, and a rotation around the axis $\mathbf{k}$ through the angle λ, with

$$\lambda = 2\,\mathrm{arc\,tg}\,\frac{p\mathbf{nk}\,\mathrm{tg}(\alpha/2)}{p + \mathbf{pk} + (\mathbf{k}\,[\mathbf{np}])\,\mathrm{tg}(\alpha/2)}. \tag{60}$$

Thus when a state with momentum p and helicity m is given an additional velocity $\mathbf{v}$ it is transformed into a superposition of states with the momentum $p' = L_{\mathbf{v}}p$ and various helicities m'. The fact that a state with definite helicity m is transformed into a set of states with different helicities m' is due to the fact that for a system with nonzero mass the angle of rotation ω of the intrinsic angular momentum is not equal to the angle of rotation α of the momentum.

6. THE REPRESENTATION OF MOMENTUM AND HELICITY FOR SYSTEMS WITH ZERO MASS

We shall treat this representation as the limit for $\kappa \to 0$ of the representation for systems with mass $\kappa \neq 0$. First of all we must define the limiting expression for the intrinsic-angular-momentum operator of a system with momentum $p\mathbf{k}$ along the quantization axis $\mathbf{k}$, since the state $\Phi_{p\mathbf{k},\,m}$ is the starting point for the construction of states with arbitrary momentum p and helicity m (cf. Sec. 5).

It is not hard to see from Eq. (13) that for $\kappa \to 0$ (and finite $\mathbf{M}$ and $\mathbf{N}$) the component of $\mathbf{J}$ along the momentum does not change, and the components orthogonal to the momentum go to infinity. Since we are dealing with a state whose momentum is directed along $\mathbf{k}$, this means that for $\kappa \to 0$ the component $J_3 = \mathbf{k}\cdot\mathbf{J}$ remains unchanged, and $J_1, J_2 \to \infty$. From this it also follows that $J \to \infty$ for $\kappa \to 0$. Depending on the nature of the approach of J to infinity for $\kappa \to 0$ one can get two quite different representations corresponding to $\kappa = 0$.

1) If $\kappa J \to \Xi \neq 0$, then it follows from the explicit expression for the matrix elements of J_1, J_2, J_3 that for $\kappa \to 0$ the operators κJ_1, κJ_2, J_3 go to I_1, I_2, I_3, where

$$(I_1)_{m'm} = \tfrac{1}{2}\,\Xi\,(\delta_{m'm-1} + \delta_{m'm+1}),$$
$$(I_2)_{m'm} = \tfrac{1}{2}\,i\Xi\,(\delta_{m'm-1} - \delta_{m'm+1}),$$
$$(I_3)_{m'm} = m\delta_{m'm}, \qquad -\infty < m,\ m' < \infty. \tag{61}$$

We now find that instead of Eq. (16) we have as the commutation relations for these operators those of the two-dimensional Euclidean group, i.e., the group of displacements and rotations in a plane,

$$[I_1, I_2] = 0, \quad [I_2, I_3] = iI_1, \quad [I_3, I_1] = iI_2. \tag{62}$$

Then I_1, I_2 are the generators of displacements along the axes 1, 2, and I_3 is the generator of rotations in the plane 1, 2.

It is not hard to verify that the conserved operators

$$p_\mu,\ \Xi^2 = I_1^2 + I_2^2,\ I_3 \quad \text{or} \quad p_\mu^2,\ \mathbf{p},\ \Xi^2 = I_1^2 + I_2^2,\ I_3 \tag{63}$$

form a complete set, and the operators p_μ^2 and Ξ^2 are invariants of the group. For $\kappa = 0$ and any $\Xi \neq 0$ the eigenstates $\chi_{\kappa=0,\,\Xi pm}$ of the operators (62) form an irreducible representation of the inhomogeneous Lorentz group and correspond to a system with zero mass, infinitely large intrinsic angular momentum ($J = \kappa^{-1}\,\Xi$), momentum p, and helicity m. We shall not consider this representation, since physical systems with zero mass and infinite intrinsic angular momentum are not observed. One can, however, get the generators of rotations and pure Lorentz transformations for this representation from Eqs. (48) and (51) by the replacement of $\kappa J_{1,2}$ by $I_{1,2}$ and of J_3 by I_3. The operators that correspond to finite transformations can be obtained from Eqs. (53), (55), and (59) by replacing $(\alpha-\omega)J_{1,2}$ by $|\mathbf{p}\times\mathbf{u}|\,I_{1,2}/p(\gamma p + \mathbf{pu})$ and J_3 by I_3, since $\alpha-\omega$ goes to zero for $\kappa \to 0$ like $\kappa\,|\mathbf{p}\times\mathbf{u}|/p(\gamma p + \mathbf{pu})$.

2) If $\kappa J \to 0$, then it follows from the explicit expression for the matrix elements of J_1, J_2, J_3 that for $\kappa \to 0$ the operators κJ_1, κJ_2, J_3 go over into I_1, I_2, I_3, where

$$I_1 = I_2 = 0, \quad (I_3)_{m'm} = m\delta_{m'm}, \quad -\infty < m,\ m' < \infty. \tag{64}$$

The operators

$$p_\mu,\ I_3 \quad \text{or} \quad p_\mu^2,\ \mathbf{p},\ I_3 \tag{65}$$

form a complete set of conserved operators, and the operators p_μ^2 and I_3 are invariants of the group. For $\kappa = 0$ and each value of m the eigenstates $\chi_{\kappa=0pm}$ of the operators (65) form an irreducible representation of the inhomogeneous Lorentz group and correspond to a system with zero mass, helicity m, and momentum **p**.

Using the expressions (48) and (51) and going to the limit $\kappa \to 0$, we find that in the representation (65) the generators of rotations and of pure Lorentz transformations are the operators

$$\mathbf{M} = -i\left[\mathbf{p}\frac{\partial}{\partial \mathbf{p}}\right] + I_3\frac{p\mathbf{k}+\mathbf{p}}{p+\mathbf{pk}}, \qquad \mathbf{N} = -ip\frac{\partial}{\partial \mathbf{p}} + I_3\frac{[\mathbf{kp}]}{p+\mathbf{pk}}. \tag{66}$$

In a similar way one can obtain the operators $S(R_{\mathbf{n},\,\varphi},\, p)$ and $S(L_{\mathbf{v}},\, p)$ corresponding to finite rotations and pure Lorentz transformations [cf. Eqs. (53), (55), (59)].

Rotations:

$$S(R_{\mathbf{n},\,\varphi},\, p) = \exp(-i\eta I_3),$$

$$\eta = 2\,\mathrm{arc\,tg}\frac{(p\mathbf{nk}+\mathbf{np})\,\mathrm{tg}\,(\varphi/2)}{p+\mathbf{pk}+(\mathbf{k}\,[\mathbf{np}])\,\mathrm{tg}\,(\varphi/2)}. \tag{67}$$

Pure Lorentz transformations:

$$S(L_{\mathbf{v}},\, p) = \exp(-i\lambda I_3),$$

$$\lambda = 2\,\mathrm{arc\,tg}\frac{p\mathbf{nk}\,\mathrm{tg}\,(\alpha/2)}{p+\mathbf{pk}+(\mathbf{k}\,[\mathbf{np}])\,\mathrm{tg}\,(\alpha/2)}, \quad \mathbf{n} = \frac{[\mathbf{pv}]}{|[\mathbf{pv}]|}. \tag{68}$$

The angle α through which the momentum is turned in a Lorentz transformation is given by Eq. (39) with $\kappa = 0$ (the angle of aberration of light). Then

$$\lambda = 2\,\mathrm{arc\,tg}\frac{(\mathbf{k}\,[\mathbf{pu}])}{\mathbf{pu}+p\mathbf{ku}+(p+\mathbf{pk})(\gamma+1)}. \tag{69}$$

Thus under a rotation or a pure Lorentz transformation a state with momentum **p** and helicity m goes over into a state with momentum $\mathbf{p}' = R_{\mathbf{n},\,\varphi}\mathbf{p}$ or $\mathbf{p}' = L_{\mathbf{v}}\mathbf{p}$ and the same helicity m, being changed by a mere phase factor $\exp(-i\eta m)$ or $\exp(-i\lambda m)$, where η or λ is given by Eq. (67) or Eq. (69).

---

[1] C. Møller, Kgl. Danske Videnskab. Selskab, Mat.Fys. Medd. **23**, No. 1 (1945).

[2] P. A. M. Dirac, Revs. Mod. Phys. **21**, 392 (1949).

[3] E. P. Wigner, Ann. Math. **40**, 149 (1939).

[4] V. Bargmann and E. P. Wigner, Proc. Natl. Acad. Sci. U.S. **34**, 211 (1948).

[5] Yu. M. Shirokov, JETP **33**, 861, 1196, 1208 (1957), Soviet Phys. JETP **6**, 664, 919, 929 (1958).

[6] C. Møller, The Theory of Relativity, Oxford University Press, 1955.

[7] M. H. L. Pryce, Proc. Roy. Soc. **A150**, 166 (1935); **A195**, 62 (1948).

[8] L. L. Foldy, Phys. Rev. **102**, 568 (1956).

[9] Chou Kuang-Chao and M. I. Shirokov, JETP **34**, 1230 (1958), Soviet Phys. JETP **7**, 851 (1958).

[10] T. D. Newton and E. P. Wigner, Revs. Mod. Phys. **21**, 400 (1949).

[11] D. A. Kirzhnits, Dissertation, Physics Institute, Academy of Sciences, U.S.S.R.

[12] H. Stapp, Phys. Rev. **103**, 425 (1956).

[13] V. Lalan, Compt. rend. **236**, 2297 (1953). A. Metz, Compt. rend. **237**, 29 (1953).

[14] R. P. Feynman, Phys. Rev. **84**, 108 (1951).

Translated by W. H. Furry
52

SOVIET PHYSICS JETP VOLUME 13, NUMBER 1 JULY, 1961

ON THE THEORY OF LOW-TEMPERATURE, HIGH-FREQUENCY MAGNETIC SUSCEPTIBILITY OF A FERRODIELECTRIC

I. A. AKHIEZER, V. G. BAR'YAKHTAR, and S. V. PELETMINSKIĬ

Institute for Technical Physics, Academy of Sciences, Ukrainian S.S.R.

Submitted to JETP editor July 18, 1960

J. Exptl. Theoret. Phys. (U.S.S.R.) 40, 365-374 (January, 1961)

Quantum field theory methods are used to evaluate the transverse components of the magnetic susceptibility tensor of a ferrodielectric, taking both the exchange and the relativistic interaction between spin waves into account. We find the ferromagnetic resonance line width. We show that a knowledge of the magnetic susceptibility enables us to study the relaxation of the magnetic moment of a ferrodielectric, and we evaluate the transverse relaxation time.

1. In ferromagnetic resonance theory the line width is usually introduced phenomenologically by adding to the equation of motion of the magnetic moment a relaxation term either in the Landau-Lifshitz or in the Bloch form. The aim of the present paper is to find the ferromagnetic resonance line shape starting from a microscopic theory of the interaction between spin waves.

It is well known that one can find the average lifetime of a spin wave and the relaxation time of the magnetic moment of a ferrodielectric by using a transport equation which determines the change with time of the spin wave distribution function. The transport equation method does, however, not enable us to determine completely the magnetic susceptibility tensor as a function of frequency and wave vector, since the transverse components of the magnetic moment can not be expressed in terms of the spin-wave occupation number.* To find the magnetic susceptibility we use therefore here field theoretical methods and we connect the magnetic susceptibility with the double-time spin-wave Green's function.

To evaluate the spin-wave Green's function we start from a Hamiltonian which takes both the exchange and the relativistic interaction between spin waves into account; the interactions between the spin-waves and the lattice vibrations will, however, not be taken into account. The method applied is particularly convenient to evaluate the transverse components of the magnetic susceptibility tensor, which are alone of importance for studying the ferromagnetic resonance line shape. Knowledge of the magnetic susceptibility as a function of the frequency and wave vector enables us to determine the behavior of the relaxation of the magnetic moment and, in particular, to track the rotation of the magnetic moment when it approaches its equilibrium value.

2. We first connect the magnetic susceptibility of a ferrodielectric with the spin-wave Green's function.* The average value of the magnetic moment density is well known to be defined by the formula

$$\mathfrak{M}(\mathbf{r},t) = \operatorname{Sp} \mathbf{M}(\mathbf{r}) \rho(t), \tag{1}$$

where $\mathbf{M}(\mathbf{r})$ is the magnetic moment density operator in the Schroedinger representation and $\rho(t)$ the system density matrix, which satisfies the equation

$$i \frac{\partial}{\partial t} \rho = [\mathcal{H} + \mathcal{H}^e, \rho], \tag{2}$$

where $\mathcal{H}$ is the total Hamiltonian of the ferrodielectric when there is no external field and $H^e(t)$ the Hamiltonian of the interaction between the ferrodielectric and the variable external magnetic field $\mathbf{h}(\mathbf{r}, t)$:

$$\mathcal{H}^e(t) = -\int \mathbf{M}(\mathbf{r}) \mathbf{h}(\mathbf{r}, t)\, d\mathbf{r}. \tag{3}$$

To find the magnetic moment in weak magnetic fields we change in Eqs. (1) — (3) to the Heisenberg representation. In the first approximation in the external field, the density matrix in the Heisenberg representation is of the form

---

*Akhiezer[1] and Kaganov and Tsukernik[2] used the transport equation to evaluate the longitudinal component of the magnetic susceptibility tensor. Kaganov and Tsukernik[3] evaluated the imaginary part of the transverse magnetic susceptibility far from resonance, but their result is incorrect (private communication from the authors), owing to an incorrect application of perturbation theory.

*Kubo[4] developed a general theory of irreversible processes using the density matrix.

$$\hat{\rho}(t) = \hat{\rho}_0 - i \int_{-\infty}^{t} [\hat{\mathscr{H}}^e(t'), \hat{\rho}_0]\, dt', \tag{4}$$

where $\hat{\rho}_0 = \exp(\Omega - \hat{\mathscr{H}})/T$ is the equilibrium density matrix when there is no external field, Ω the thermodynamic potential of the system, and T the temperature. Using (4) one obtains easily the following expression for the magnetic moment density

$$m_i(\mathbf{r}, t) \equiv \mathfrak{M}_i(\mathbf{r}, t) - \mathfrak{M}_i^0$$
$$= \int_{-\infty}^{\infty} dt'\, d\mathbf{r}' K_{il}^R(\mathbf{r} - \mathbf{r}', t - t')\, h_l(\mathbf{r}', t'), \tag{5}$$

where $\mathfrak{M}_i^0$ is the equilibrium value of the magnetic moment at the given temperature and $K_{il}^R(\mathbf{r}, t)$ is the retarded double-time Green's function

$$K_{il}^R(\mathbf{r} - \mathbf{r}', t - t') = i\theta(t - t')\langle[\hat{M}_i(\mathbf{r}, t), \hat{M}_l(\mathbf{r}', t')]\rangle,$$
$$\theta(t) = \begin{cases} 0, & t < 0 \\ 1, & t > 0 \end{cases}, \qquad \langle f\rangle = \mathrm{Sp}\, \rho_0 f. \tag{6}$$

Expanding the quantities $m_i(\mathbf{r}, t)$, $h_i(\mathbf{r}, t)$ and $K_{il}^R(\mathbf{r}, t)$ in terms of the Fourier integral,

$$K_{il}^R(\mathbf{r}, t) = \frac{1}{(2\pi)^4} \int_{-\infty}^{\infty} e^{-i\omega t + i\mathbf{k}\mathbf{r}} K_{il}^R(\mathbf{k}, \omega)\, d\mathbf{k}\, d\omega,$$

we can rewrite Eq. (5) as

$$m_i(\mathbf{k}, \omega) = K_{il}^R(\mathbf{k}, \omega)\, h_l(\mathbf{k}, \omega). \tag{7}$$

The magnetic susceptibility tensor $\chi_{il}(\mathbf{k}, \omega)$ is thus the same as the retarded double-time Green function:

$$\chi_{il}(\mathbf{k}, \omega) = K_{il}^R(\mathbf{k}, \omega) \tag{8}$$

3. We shall show that a knowledge of the magnetic susceptibility tensor enables us to study the relaxation of the magnetic moment. Let there be initially at time $t = 0$ some distribution of the magnetic moment $\mathbf{m}^0(\mathbf{r})$ in the system which would be an equilibrium distribution if there were present a constant magnetic field $\mathbf{h}^0(\mathbf{r})$ which is connected with the initial magnetic moment distribution through the relation

$$m_i^0(\mathbf{k}) = \chi_{il}(\mathbf{k}, \omega)\, h_l^0(\mathbf{k})\,|_{\omega=0}.$$

The magnitude of the magnetic moment at $t > 0$ is determined by Eq. (5), where we must take for the variable magnetic field

$$\mathbf{h}(\mathbf{r}, t) = \theta(-t)\, e^{\varepsilon t}\, \mathbf{h}^0(\mathbf{r}), \qquad \varepsilon \to +0. \tag{9}$$

Such a choice for $\mathbf{h}(\mathbf{r}, t)$ corresponds to an adiabatic switching on of the field at $t = -\infty$ and an instantaneous switching off at $t = 0$. Using Eqs. (5), (6), and (9), we get

$$m_i(\mathbf{r}, t) = i \int_{-\infty}^{0} dt'\, d\mathbf{r}'\, e^{\varepsilon t'} \langle[\hat{M}_i(\mathbf{r}, t), \hat{M}_l(\mathbf{r}', t')]\rangle\, h_l^0(\mathbf{r}'). \tag{10}$$

Noting that according to (6)

$$i\langle[\hat{M}_i(\mathbf{r}, t), \hat{M}_l(\mathbf{r}', t')]\rangle$$
$$= K_{il}^R(\mathbf{r} - \mathbf{r}', t - t') - K_{li}^{R*}(\mathbf{r}' - \mathbf{r}, t' - t),$$

and using Eq. (8) for the Fourier component of the function K_{il}^R we get the following equation for the relaxation of the magnetic moment

$$m_i(\mathbf{r}, t) = -\frac{i}{(2\pi)^4} \int d\mathbf{k}\, e^{i\mathbf{k}\mathbf{r}} h_l^0(\mathbf{k}) \int_{-\infty}^{\infty} d\omega \frac{e^{i\omega t}}{\omega} [\chi_{il}(\mathbf{k}, \omega)$$
$$- \chi_{li}^*(\mathbf{k}, \omega)]. \tag{11}$$

We see that the relaxation of the magnetic moment is determined by the anti-Hermitian part of the magnetic susceptibility tensor χ_{il}. It is well known[5] that the anti-Hermitian part of the χ_{il} tensor determines also the absorption of energy from a variable magnetic field. One can check this by differentiating the energy of the system $Q(t)$ with respect to the time

$$\dot{Q}(t) = \frac{d}{dt}\mathrm{Sp}\,\{\hat{\rho}(t)[\mathscr{H} + \hat{\mathscr{H}}^e]\}$$
$$= -\mathrm{Sp}\,\{\hat{\rho}(t) \int \hat{M}_i(\mathbf{r}, t) \frac{\partial}{\partial t} h_i(\mathbf{r}, t)\, d\mathbf{r}\}.$$

Using Eq. (4) for $\hat{\rho}(t)$ we find

$$\dot{Q}(t) = -\mathrm{Sp}\left\{\rho_0 \int \hat{M}_i(\mathbf{r}, t) \frac{\partial}{\partial t} h_i(\mathbf{r}, t)\, d\mathbf{r}\right\}$$
$$- \int_{-\infty}^{\infty} dt'\, d\mathbf{r}'\, d\mathbf{r}\, h_i(\mathbf{r}', t') \frac{\partial h_l(\mathbf{r}, t)}{\partial t} K_{li}^R(\mathbf{r} - \mathbf{r}', t - t'). \tag{12}$$

If in the case of a magnetic field which is periodic in time

$$h_i(\mathbf{r}, t) = \frac{1}{(2\pi)^3} \sum_{\omega_n} \int d\mathbf{k}\, h_i(\mathbf{k}, \omega_n)\, e^{i\mathbf{k}\mathbf{r} - i\omega_n t}$$
$$\left(\omega_n = \frac{2\pi n}{t_0}, \quad n = 0, \pm 1, \ldots\right)$$

we average Eq. (12) over the period t_0, we get the final expression for the average absorption of energy from a variable magnetic field per unit time

$$\bar{\dot{Q}} = -i(2\pi)^{-3} \int d\mathbf{k} \sum_{\omega_n > 0} \omega_n h_l(\mathbf{k}, \omega_n)\, [\chi_{li}(\mathbf{k}, \omega_n)]$$
$$- \chi_{il}^*(\mathbf{k}, \omega_n)]\, h_i^*(\mathbf{k}, \omega_n). \tag{13}$$

4. We shall now connect the retarded double-time Green's function $K_{il}^R(\mathbf{r}, t)$ with the Matsubara Green's function $\mathscr{K}_{il}(\mathbf{r}, \tau)$, for the evaluation of which we shall apply a diagram technique. The function $\mathscr{K}_{il}(\mathbf{r}, \tau)$ is defined by the equation

$$\mathscr{K}_{il}(\mathbf{r} - \mathbf{r}', \tau - \tau') = \langle T_\tau\{\hat{M}_i(\mathbf{r}, \tau)\, \hat{M}_l(\mathbf{r}', \tau')\}\rangle,$$
$$\hat{M}_i(\mathbf{r}, \tau) = e^{\mathscr{H}\tau} M_i(\mathbf{r})\, e^{-\mathscr{H}\tau}, \tag{14}$$

where T_τ is the chronological operator for the variable τ.

We expand the function $\mathcal{K}_{il}(\mathbf{r}, \tau)$ in a Fourier series in τ

$$\mathcal{K}_{il}(\mathbf{r}, \tau) = \frac{T}{(2\pi)^3} \sum_{k_4} \int d\mathbf{k} e^{i\mathbf{kr} - ik_4\tau} \mathcal{K}_{il}(\mathbf{k}, \mathbf{k}_4)$$

$$(\mathbf{k}_4 = 2\pi nT;\ n = 0, \pm 1, \ldots).$$

Using furthermore a method similar to the one applied by Abrikosov, Gor'kov, and Dzyaloshinskiĭ[6] and Fradkin[7] we get, using (8),

$$\chi_{il}(\mathbf{k}, \omega) = K^R_{il}(\mathbf{k}, \omega) = \mathcal{K}_{il}(\mathbf{k}, -i\omega + 0). \tag{15}$$

Writing (14) in the k-representation we find

$$\mathcal{K}_{il}(\mathbf{k}, k_4) = \frac{1}{2} \int_{-1/T}^{1/T} d\tau e^{ik_4\tau} \sum_{\mathbf{k}'} \langle T_\tau \{\hat{M}_i(\mathbf{k}, \tau) \hat{M}_l(\mathbf{k}', 0)\}\rangle, \tag{16}$$

where $M_i(\mathbf{k}, \tau)$ are the Fourier components of the magnetic moment density operator

$$\hat{M}_i(\mathbf{r}, \tau) = \frac{1}{\sqrt{V}} \sum_{\mathbf{k}} \hat{M}_i(\mathbf{k}, \tau) e^{i\mathbf{kr}}$$

(V is the volume of the system).

5. We turn to an evaluation of the magnetic susceptibility of a ferrodielectric. Following Holstein and Primakoff[8] and introducing spin-wave creation and annihilation operators $c^+_{\mathbf{k}}$ and $c_{\mathbf{k}}$ we write the Hamiltonian of the ferrodielectric in the form*

$$\mathcal{H} = \mathcal{H}_0 + \mathcal{H}_3 + \mathcal{H}_4, \tag{17}$$

where $\mathcal{H}_0$ is the basic Hamiltonian

$$\mathcal{H}_0 = \sum_{\mathbf{k}} \varepsilon_{\mathbf{k}} c^+_{\mathbf{k}} c_{\mathbf{k}} \tag{18}$$

($\epsilon_{\mathbf{k}}$ is the spin wave energy) and $\mathcal{H}_3$ and $\mathcal{H}_4$ are the Hamiltonians of the spin wave — spin wave interaction†

$$\mathcal{H}_3 = \frac{1}{\sqrt{V}} \sum_{1, 2, 3} \{\Phi(1, 2; 3) c^+_1 c^+_2 c_3 \Delta(\mathbf{k}_1 + \mathbf{k}_2 - \mathbf{k}_3) + \text{compl. conj.} + \Phi_1(1, 2, 3) c^+_1 c^+_2 c^+_3 \Delta(\mathbf{k}_1 + \mathbf{k}_2 + \mathbf{k}_3) + \text{compl. conj.}\},$$

$$\mathcal{H}_4 = \frac{1}{V} \sum_{1, 2, 3, 4} \{\Psi(1, 2; 3, 4) c^+_1 c^+_2 c_3 c_4 \Delta(\mathbf{k}_1 + \mathbf{k}_2 - \mathbf{k}_3 - \mathbf{k}_4) + \Psi_1(1, 2, 3; 4) c^+_1 c^+_2 c^+_3 c_4 \Delta(\mathbf{k}_1 + \mathbf{k}_2 + \mathbf{k}_3 - \mathbf{k}_4) + \text{compl. conj.} + \Psi_2(1, 2, 3, 4) c^+_1 c^+_2 c^+_3 c^+_4 \Delta(\mathbf{k}_1 + \mathbf{k}_2 + \mathbf{k}_3 + \mathbf{k}_4) + \text{compl. conj.}\}. \tag{19}$$

The spin wave energy is $\epsilon_{\mathbf{k}} = \sqrt{A^2_{\mathbf{k}} - |B_{\mathbf{k}}|^2}$, where

$$A_{\mathbf{k}} = \Theta_c (ak)^2 + \mu(H_0 + \beta M_0) + 2\pi\mu M_0 \sin^2\theta_{\mathbf{k}},$$

$$B_{\mathbf{k}} = 2\pi\mu M_0 \sin^2\Theta_{\mathbf{k}} e^{2i\varphi_{\mathbf{k}}}.$$

Here μ is twice the Bohr magneton, a the lattice constant, Θ_c a quantity of the order of the Curie temperature, M_0 the saturation magnetic moment, β the anisotropy constant, H_0 the constant external magnetic field, and $\theta_{\mathbf{k}}$ and $\varphi_{\mathbf{k}}$ the polar angles of the vector $\mathbf{k}$.

The quantities Φ and Ψ_1 describe the splitting of one spin wave into two or three, respectively, Φ_1 and Ψ_2 describe the creation of three or four spin waves, respectively, and Ψ describes the spin wave — spin wave scattering process. The quantities Φ and Φ_1 are relativistic in origin while the quantities Ψ, Ψ_1, and Ψ_2 are caused by exchange and relativistic interactions.

For actual calculations we restrict ourselves to the range of large wave vectors ($1 \gg ak \gg \sqrt{\mu M_0/\Theta_c}$), when the exchange interaction is the main agency, and to the region of small wave vectors ($ak \ll \sqrt{\mu M_0/\Theta_c}$), where the relativistic interaction plays the main part. In these regions the quantities Φ, Φ_1, Ψ, Ψ_1, and Ψ_2 are determined by the following asymptotic formulae

$$\left.\begin{array}{c} \Psi(1, 2; 3, 4) = -\mu(4M_0)^{-1}\Theta_c a^2 (\mathbf{k}_1\mathbf{k}_2 + \mathbf{k}_3\mathbf{k}_4) \\ |\Psi_2| \ll |\Psi_1| \ll |\Psi| \end{array}\right\} \text{when } 1 \gg ak \gg \sqrt{\frac{\mu M_0}{\Theta_c}} \tag{20}$$

$$\Phi(1, 2; 3) = -\pi\mu\sqrt{2\mu M_0}\{\sin 2\theta_1 (e^{-i\varphi_1} u_1^* + e^{i\varphi_1} v_1^*)(u_2^* u_3 + v_2^* v_3) + \sin 2\theta_2 (e^{-i\varphi_2} u_2^* + e^{i\varphi_2} v_2^*)(u_1^* u_3 + v_1^* v_3) + \sin 2\theta_3 (e^{i\varphi_3} u_3 + e^{-i\varphi_3} v_3)(v_1^* u_2^* + v_2^* u_1^*)\}, \tag{21}$$

$$\left.\begin{array}{c} |\Phi_1| \sim |\Phi|; \quad |\Psi_1| \sim |\Psi_2| \sim |\Psi| \\ \Psi(1, 2; 3, 4) = -{}^1\!/\!_2\, \mu^2\beta\{u_1^* u_2^* u_3 u_4 + 4u_1^* v_2^* v_3 u_4 + v_1^* v_2^* v_3 v_4\} \end{array}\right\}$$

$$\text{when } ak \ll \sqrt{\frac{\mu M_0}{\Theta_c}}, \tag{22}$$

where*

$$u_{\mathbf{k}} = \sqrt{(A_{\mathbf{k}} + \varepsilon_{\mathbf{k}})/2\varepsilon_{\mathbf{k}}},$$

$$v_{\mathbf{k}} = -e^{2i\varphi_{\mathbf{k}}} \sqrt{(A_{\mathbf{k}} - \varepsilon_{\mathbf{k}})/2\varepsilon_{\mathbf{k}}}.$$

In the present paper we shall be interested in the transverse components of the magnetic susceptibility tensor; to evaluate these it is sufficient to know the transverse components of the magnetic moment. Restricting ourselves to the first terms in the expansion of the moment operators in the spin wave creation and annihilation operators, we have

---

*The Holstein-Primakoff model presupposes that the Hamiltonian and the moment operators are expanded in the parameter $\frac{1}{2}$s. We note that Dyson[9] has shown that in fact the expansion in the exchange interaction is in a parameter ~(1/10)s (s is the spin of the atom).

†See, for instance, reference 10.

*To eliminate the indeterminacy in the quantities $u_{\mathbf{k}}$ and $v_{\mathbf{k}}$ as $\mathbf{k} \to 0$, it is necessary to take the shape of the sample into account.[11]

$$\hat M^+(\mathbf k,\tau) = \hat M_x(\mathbf k,\tau) + i\hat M_y(\mathbf k,\tau)$$
$$= \sqrt{2\mu M_0}\,\{u^*_{\mathbf k}\hat c^+_{-\mathbf k}(\tau) + v_{\mathbf k}\hat c_{\mathbf k}(\tau)\},$$
$$\hat M^-(\mathbf k,\tau) = \hat M_x(\mathbf k,\tau) - i\hat M_y(\mathbf k,\tau)$$
$$= \sqrt{2\mu M_0}\,\{u_{\mathbf k}\hat c_{\mathbf k}(\tau) + v^*_{\mathbf k}\hat c^+_{-\mathbf k}(\tau)\}; \qquad (23)$$

where

$$\hat c_{\mathbf k}(\tau) = e^{\mathscr H\tau}c_{\mathbf k}e^{-\mathscr H\tau}, \qquad \hat c^+_{\mathbf k}(\tau) = e^{\mathscr H\tau}c^+_{\mathbf k}c^{-\mathscr H\tau}.$$

We introduce the single-particle spin-wave Green's function:

$$G(\mathbf k,\tau)\,\Delta(\mathbf k-\mathbf k') = \langle T_\tau\{\hat c_{\mathbf k}(\tau)\,\hat c^+_{\mathbf k'}(0)\}\rangle. \qquad (24)$$

Its Fourier component $G(\mathbf k, k_4)$ satisfies the Dyson equation

$$G(\mathbf k, k_4) = G_0(\mathbf k, k_4) + G_0(\mathbf k, k_4)\,\Sigma(\mathbf k, k_4)\,G(\mathbf k, k_4). \qquad (25)$$

Here

$$G_0(\mathbf k, k_4) = (\varepsilon_{\mathbf k} - ik_4)^{-1} \qquad (26)$$

is the zeroth-approximation spin-wave Green's function and $\Sigma(\mathbf k, k_4)$ is the mass operator. Substituting (23) into (16) and taking into account that $\langle T_\tau\{\hat c^+_{\mathbf k}(\tau)\,\hat c^+_{\mathbf k'}(0)\}\rangle$ and $\langle T_\tau\{\hat c_{\mathbf k}(\tau)\,\hat c_{\mathbf k'}(0)\}\rangle$ are equal to zero in the zeroth approximation in the interaction, we express the function $\mathscr K_{il}(\mathbf k, k_4)$ in terms of the single-particle Green's function $G(\mathbf k, k_4)$

$$\mathscr K_{++}(\mathbf k, k_4) = 2\mu M_0 u^*_{\mathbf k}v_{\mathbf k}\{G(\mathbf k, k_4) + G(-\mathbf k, -k_4)\},$$
$$\mathscr K_{+-}(\mathbf k, k_4) = 2\mu M_0\{|v_{\mathbf k}|^2 G(\mathbf k, k_4) + |u_{\mathbf k}|^2 G(-\mathbf k, -k_4)\},$$
$$\mathscr K_{-+}(\mathbf k, k_4) = 2\mu M_0\{|u_{\mathbf k}|^2 G(\mathbf k, k_4) + |v_{\mathbf k}|^2 G(-\mathbf k, -k_4)\},$$
$$\mathscr K_{--}(\mathbf k, k_4) = 2\mu M_0 u_{\mathbf k}v^*_{\mathbf k}\{G(\mathbf k, k_4) + G(-\mathbf k, -k_4)\}. \qquad (27)$$

It follows from (15), (27), and (26) that the transverse components of the magnetic susceptibility tensor tend to infinity in the zeroth approximation of the spin wave — spin wave interaction, if the frequency of the magnetic field and its wave vector are the same as the spin-wave frequency and wave vector:

$$\omega_{\mathbf k} = \pm\varepsilon_{\mathbf k}. \qquad (28)$$

6. We use Eq. (25) to evaluate the complete Green function $G(\mathbf k, k_4)$:

$$G(\mathbf k, k_4) = [\varepsilon_{\mathbf k} - ik_4 - \Sigma(\mathbf k, k_4)]^{-1}. \qquad (29)$$

The magnetic susceptibility near resonance is determined by the quantity $G(\mathbf k, -i\epsilon_{\mathbf k} + 0)$; we shall not be interested in the small correction to the position of the resonance line, which is caused by the real part of the function Σ. Introducing therefore a quantity $\gamma(\mathbf k)$:

$$\gamma(\mathbf k) = \operatorname{Im}\Sigma(\mathbf k, -i\varepsilon_{\mathbf k} + 0), \qquad (30)$$

we get from (15), (27), and (29) for the magnetic susceptibility near resonance

$$\chi_{xx}(\mathbf k,\omega) = \tfrac{1}{2}\mu M_0 U_1(\mathbf k)\{[\varepsilon_{\mathbf k} - \omega - i\gamma(\mathbf k)]^{-1}$$
$$+ [\varepsilon_{\mathbf k} + \omega + i\gamma(\mathbf k)]^{-1}\},$$
$$\chi_{yy}(\mathbf k,\omega) = \tfrac{1}{2}\mu M_0 U_2(\mathbf k)\{[\varepsilon_{\mathbf k} - \omega - i\gamma(\mathbf k)]^{-1}$$
$$+ [\varepsilon_{\mathbf k} + \omega + i\gamma(\mathbf k)]^{-1}\},$$
$$\chi_{xy}(\mathbf k,\omega) = -\tfrac{1}{2}i\mu M_0\{U(\mathbf k)[\varepsilon_{\mathbf k} - \omega - i\gamma(\mathbf k)]^{-1}$$
$$- U^*(\mathbf k)[\varepsilon_{\mathbf k} + \omega + i\gamma(\mathbf k)]^{-1}\},$$
$$\chi_{yx}(\mathbf k,\omega) = \tfrac{1}{2}i\mu M_0\{U^*(\mathbf k)[\varepsilon_{\mathbf k} - \omega - i\gamma(\mathbf k)]^{-1}$$
$$- U(\mathbf k)[\varepsilon_{\mathbf k} + \omega + i\gamma(\mathbf k)]^{-1}\}; \qquad (31)$$

$$U_1(\mathbf k) = |u_{\mathbf k}|^2 + |v_{\mathbf k}|^2 + u^*_{\mathbf k}v_{\mathbf k} + u_{\mathbf k}v^*_{\mathbf k},$$
$$U_2(\mathbf k) = |u_{\mathbf k}|^2 + |v_{\mathbf k}|^2 - u^*_{\mathbf k}v_{\mathbf k} - u_{\mathbf k}v^*_{\mathbf k},$$
$$U(\mathbf k) = 1 + u^*_{\mathbf k}v_{\mathbf k} - u_{\mathbf k}v^*_{\mathbf k}. \qquad (32)$$

We consider now the relaxation of the transverse part of the magnetic moment. Substituting (31) into (11) and integrating over ω, we get

$$m_x(\mathbf r, t) = \frac{\mu M_0}{(2\pi)^3}\int\frac{d\mathbf k}{\varepsilon_{\mathbf k}}e^{i\mathbf{kr}-\gamma(\mathbf k)t}\,\{h^0_x(\mathbf k)\,U_1(\mathbf k)\cos\varepsilon_{\mathbf k}t$$
$$+ h^0_y(\mathbf k)\operatorname{Im}[U(\mathbf k)\,e^{-i\varepsilon_{\mathbf k}t}]\},$$
$$m_y(\mathbf r, t) = \frac{\mu M_0}{(2\pi)^3}\int\frac{d\mathbf k}{\varepsilon_{\mathbf k}}e^{i\mathbf{kr}-\gamma(\mathbf k)t}\,\{h^0_x(\mathbf k)\operatorname{Im}[U(\mathbf k)\,e^{i\varepsilon_{\mathbf k}t}]$$
$$+ h^0_y(\mathbf k)\,U_2(\mathbf k)\cos\varepsilon_{\mathbf k}t\}. \qquad (33)$$

We see that the quantity $\gamma(\mathbf k)$ determines the relaxation time of the transverse components of the magnetic moment. That the quantity $\gamma(\mathbf k)$ is positive follows from the Lehmann representation of the Green's function

$$G(\mathbf k, -i\omega + 0) = \int_{-\infty}^{\infty} d\omega'\,\rho(\mathbf k,\omega')\,/\,(\omega' + \omega + i0), \qquad (34)$$

where

$$\rho(\mathbf k,\omega) = \sum_{n,n'}[\exp\{(\Omega - E_n)/T\}$$
$$- \exp\{(\Omega - E_{n'})/T\}]\langle n|c_{\mathbf k}|n'\rangle\langle n'|c^+_{\mathbf k}|n\rangle\,\delta(\omega + E_n - E_{n'})$$

(E_n are the energy levels of the system). One sees easily that the quantity $\rho(\mathbf k,\omega)$ is real, an odd function of ω, and positive for $\omega > 0$. From (34) it follows that the imaginary part of the Green's function is of the form

$$\operatorname{Im} G(\mathbf k, -i\omega + 0) = -\pi\rho(\mathbf k, -\omega).$$

From Eq. (29) it follows that the sign of the imaginary part of $\Sigma(\mathbf k, -i\omega + 0)$ is the same as the sign of the imaginary part of $G(\mathbf k, -i\omega + 0)$; the quantity $\gamma(\mathbf k)$, which is the same as $\operatorname{Im}\Sigma(\mathbf k, -i\omega + 0)$, is thus positive for $\omega = \epsilon_{\mathbf k} > 0$.

7. We turn now to finding the resonance line width $\gamma(\mathbf k)$, which is connected with the mass operator $\Sigma(\mathbf k, k_4)$ through Eq. (30). We use perturbation theory and diagram methods to evaluate the quantity $\Sigma(\mathbf k, k_4)$. We show in Figs. 1 — 5 the diagrams of the first and second approximation for the quantity Σ. The solid lines in the

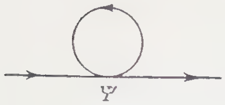

FIG. 1

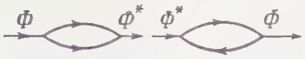

FIG. 2

diagrams correspond to the function G_0, and the vertices to the functions Φ, Φ_1, Ψ, Ψ_1, Ψ_2, and a δ-function expressing the conservation of $\mathbf{k}$ and k_4. One integrates over the momentum $\mathbf{k}$ of internal lines and sums over k_4. The general coefficient in front of the analytical expression corresponding to an arbitrary diagram is equal to $(-1)^{n+1}qT^p(2\pi)^{-3p}$, where q is the number of equivalent diagrams, n the number of vertices, and p the number of independent momenta of virtual spin waves.

In the first perturbation-theory approximation (see Fig. 1) the mass operator is equal to

$$\Sigma_1(\mathbf{k}) = -4(2\pi)^{-3}\int d\mathbf{k}'\,\Psi(\mathbf{k}, \mathbf{k}'; \mathbf{k}, \mathbf{k}')\,n_{\mathbf{k}'}, \qquad (35)$$

where $n_{\mathbf{k}} = [\exp(\epsilon_{\mathbf{k}}/T) - 1]^{-1}$ is the Bose distribution function of the spin waves. The quantity $-\Sigma_1(\mathbf{k})$ is real, independent of k_4, and is a small correction to the spin wave energy.

In Figs. 2 and 3 we give the second-order diagrams for the mass operator which are caused by the term $\mathscr{H}_3$ in the interaction Hamiltonian. The analytical expression for the diagrams of Fig. 2 is of the form

$$\Sigma_\Phi(\mathbf{k}, k_4) = 2T(2\pi)^{-3}\sum_{k'_4}\int d\mathbf{k}'\,|\Phi(\mathbf{k}', \mathbf{k} - \mathbf{k}'; \mathbf{k})|^2 G_0(\mathbf{k}', k'_4)G_0(\mathbf{k}-\mathbf{k}', k_4-k'_4)$$
$$+ 4T(2\pi)^{-3}\sum_{k'_4}\int d\mathbf{k}'\,|\Phi(\mathbf{k}, \mathbf{k}'; \mathbf{k} + \mathbf{k}')|^2 G_0(\mathbf{k}', k'_4)\,G_0(\mathbf{k} + \mathbf{k}', k_4 + k'_4). \qquad (36)$$

Summing over k'_4 and performing the substitution $k_4 = -i\omega + 0$ we get

$$\Sigma_\Phi(\mathbf{k}, -i\omega + 0) = 2(2\pi)^{-3}\int d\mathbf{k}'\,|\Phi(\mathbf{k}', \mathbf{k} - \mathbf{k}'; \mathbf{k})|^2\,(n_{\mathbf{k}'} + n_{\mathbf{k}-\mathbf{k}'} + 1)(\varepsilon_{\mathbf{k}'} + \varepsilon_{\mathbf{k}-\mathbf{k}'} - \omega - i0)^{-1}$$
$$+ 4(2\pi)^{-3}\int d\mathbf{k}'\,|\Phi(\mathbf{k}, \mathbf{k}'; \mathbf{k} + \mathbf{k}')|^2(n_{\mathbf{k}'} - n_{\mathbf{k}+\mathbf{k}'})\times(\varepsilon_{\mathbf{k}+\mathbf{k}'} - \varepsilon_{\mathbf{k}'} - \omega - i0)^{-1}.$$

The imaginary part of this expression which we need to evaluate the ferromagnetic resonance line width is equal to

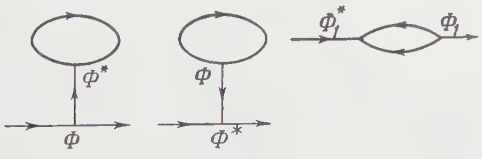

FIG. 3

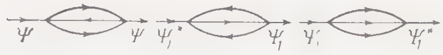

FIG. 4

$$\operatorname{Im}\Sigma_\Phi(\mathbf{k}, -i\omega + 0) = (2\pi)^{-2}\int d\mathbf{k}'\,|\Phi(\mathbf{k}', \mathbf{k} - \mathbf{k}'; \mathbf{k})|^2[(n_{\mathbf{k}'} + 1)(n_{\mathbf{k}-\mathbf{k}'} + 1) - n_{\mathbf{k}'}n_{\mathbf{k}-\mathbf{k}'}]\,\delta(\omega - \varepsilon_{\mathbf{k}'} - \varepsilon_{\mathbf{k}-\mathbf{k}'})$$
$$+ 2(2\pi)^{-2}\int d\mathbf{k}'\,|\Phi(\mathbf{k}, \mathbf{k}'; \mathbf{k}+\mathbf{k}')|^2[n_{\mathbf{k}'}(n_{\mathbf{k}+\mathbf{k}'} + 1) - (n_{\mathbf{k}'} + 1)\,n_{\mathbf{k}+\mathbf{k}'}]\,\delta(\omega + \varepsilon_{\mathbf{k}'} - \varepsilon_{\mathbf{k}+\mathbf{k}'}). \qquad (37)$$

The terms of the mass operator which correspond to the diagrams of Fig. 3 are determined by the expressions

$$\Sigma_a(\mathbf{k}) = \frac{4}{(2\pi)^3}\left(\exp\frac{\varepsilon_0}{T} - 1\right)^{-1}\Phi(\mathbf{k}, 0; \mathbf{k})\int d\mathbf{k}'\,\Phi^*(\mathbf{k}', 0; \mathbf{k}')\,n_{\mathbf{k}'} + \text{compl. conj.},$$
$$\Sigma_b(\mathbf{k}, k_4) = \frac{18T}{(2\pi)^3}\sum_{k'_4}\int d\mathbf{k}'\,|\Phi_1(\mathbf{k}, \mathbf{k}', -\mathbf{k} - \mathbf{k}')|^2\times G_0(\mathbf{k}', k'_4)G_0(-\mathbf{k}-\mathbf{k}', -k_4-k'_4). \qquad (38)$$

By integrating the first of Eqs. (38) over the angles of the vector $\mathbf{k}'$ we verify easily that the quantity $\Sigma_a(\mathbf{k})$ vanishes. Summing the second of Eqs. (38) over k'_4 and separating off the imaginary part of the quantity $\Sigma_b(\mathbf{k}, -i\omega + 0)$ we get

$$\operatorname{Im}\Sigma_b(\mathbf{k}, -i\omega+0) = -\frac{9}{(2\pi)^2}\int d\mathbf{k}'\,|\Phi_1(\mathbf{k}, \mathbf{k}', -\mathbf{k} - \mathbf{k}')|^2[(n_{\mathbf{k}'} + 1)(n_{\mathbf{k}+\mathbf{k}'} + 1) - n_{\mathbf{k}'}n_{\mathbf{k}+\mathbf{k}'}]\,\delta(\omega + \varepsilon_{\mathbf{k}'} + \varepsilon_{\mathbf{k}+\mathbf{k}'}).$$

One sees easily that near resonance ($\omega = \epsilon_{\mathbf{k}}$) this quantity tends to zero and thus does not contribute to the line width $\gamma(\mathbf{k})$.

We show in Figs. 4 and 5 the second-order diagrams for the mass operator which are caused by the term H_4 in the interaction Hamiltonian. We are led to analytical expressions only for those diagrams the imaginary part of which differs from zero for $k_4 = -i\omega + 0$ near the resonance point $\omega = \epsilon_{\mathbf{k}}$ (Fig. 4)

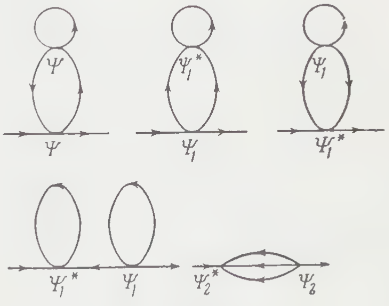

FIG. 5

$$\Sigma_\Psi(\mathbf{k}, k_4) = 8T^2(2\pi)^{-6}\sum_{k_4', k_4''}\int d\mathbf{k}'\,d\mathbf{k}''\,|\Psi(\mathbf{k}, \mathbf{k}'; \mathbf{k}'', \mathbf{k}+\mathbf{k}'-\mathbf{k}'')|^2 G_0(\mathbf{k}', k_4')G_0(\mathbf{k}'', k_4'')G_0(\mathbf{k}+\mathbf{k}'-\mathbf{k}'', k_4+k_4'-k_4'') + 18T^2(2\pi)^{-6}\sum_{k_4', k_4''}\int d\mathbf{k}'\,d\mathbf{k}''\,|\Psi_1(\mathbf{k}, \mathbf{k}', \mathbf{k}''; \mathbf{k}+\mathbf{k}'+\mathbf{k}'')|^2 G_0(\mathbf{k}', k_4')G_0(\mathbf{k}'', k_4'')G_0(\mathbf{k}+\mathbf{k}'+\mathbf{k}'', k_4+k_4'+k_4'') + 6T^2(2\pi)^{-6}\sum_{k_4', k_4''}\int d\mathbf{k}'\,d\mathbf{k}''\,|\Psi_1(\mathbf{k}', \mathbf{k}'', \mathbf{k}-\mathbf{k}'-\mathbf{k}''; \mathbf{k})|^2 G_0(\mathbf{k}', k_4')G_0(\mathbf{k}'', k_4'')G_0(\mathbf{k}-\mathbf{k}'-\mathbf{k}'', k_4-k_4'-k_4''). \quad (39)$$

For the imaginary part of the quantity $\Sigma_\Psi(\mathbf{k}, -i\omega+0)$ we get

$$\operatorname{Im}\Sigma_\Psi(\mathbf{k}, -i\omega+0) = \frac{4}{(2\pi)^5}\int d\mathbf{k}'\,d\mathbf{k}''\,|\Psi(\mathbf{k}, \mathbf{k}'; \mathbf{k}'', \mathbf{k}+\mathbf{k}'-\mathbf{k}'')|^2[n_{\mathbf{k}'}(n_{\mathbf{k}''}+1)(n_{\mathbf{k}+\mathbf{k}'-\mathbf{k}''}+1) - (n_{\mathbf{k}'}+1)n_{\mathbf{k}''}n_{\mathbf{k}+\mathbf{k}'-\mathbf{k}''}]\,\delta(\omega+\varepsilon_{\mathbf{k}'}-\varepsilon_{\mathbf{k}''}-\varepsilon_{\mathbf{k}+\mathbf{k}'-\mathbf{k}''}) + \frac{9}{(2\pi)^5}\int d\mathbf{k}'\,d\mathbf{k}''\,|\Psi_1(\mathbf{k}, \mathbf{k}', \mathbf{k}''; \mathbf{k}+\mathbf{k}'+\mathbf{k}'')^2|\,[n_{\mathbf{k}'}n_{\mathbf{k}''}\times(n_{\mathbf{k}+\mathbf{k}'+\mathbf{k}''}+1) - (n_{\mathbf{k}'}+1)(n_{\mathbf{k}''}+1)n_{\mathbf{k}+\mathbf{k}'+\mathbf{k}''}]\,\delta(\omega+\varepsilon_{\mathbf{k}'}+\varepsilon_{\mathbf{k}''}-\varepsilon_{\mathbf{k}+\mathbf{k}'+\mathbf{k}''}) + \frac{3}{(2\pi)^5}\int d\mathbf{k}'\,d\mathbf{k}''\,|\Psi_1(\mathbf{k}', \mathbf{k}'', \mathbf{k}-\mathbf{k}'-\mathbf{k}''; \mathbf{k})|^2[(n_{\mathbf{k}'}+1)(n_{\mathbf{k}''}+1)(n_{\mathbf{k}-\mathbf{k}'-\mathbf{k}''}+1) - n_{\mathbf{k}'}n_{\mathbf{k}''}n_{\mathbf{k}-\mathbf{k}'-\mathbf{k}''}]\,\delta(\omega-\varepsilon_{\mathbf{k}'}-\varepsilon_{\mathbf{k}''}-\varepsilon_{\mathbf{k}-\mathbf{k}'-\mathbf{k}''}). \quad (40)$$

One verifies easily that the imaginary part of the terms of the mass operator which are given by Fig. 5 tend to zero near resonance.

It is clear from Eqs. (30), (37), and (40) that the quantity $\gamma(\mathbf{k})$ is proportional to the probability that a spin wave makes a transition from an initial state with momentum $\mathbf{k}$ to any of all the possible final states.

8. To determine the shape of the homogeneous resonance line we must know the quantity $\gamma(0) = \operatorname{Im}\Sigma(0, -i\epsilon_0+0)$ where ϵ_0 is the homogeneous resonance frequency which is determined by the shape of the body.[12] If the ferrodielectric has the shape of a disc and if the axis of easiest magnetization lies in the plane of the disc, we have*

$$\varepsilon_0 = \mu(H_0+\beta M_0)^{1/2}(H_0+\beta M_0+4\pi M_0)^{1/2}. \quad (41)$$

The exchange interaction does not contribute to the homogeneous resonance width. The quaternary relativistic interaction is small compared with the ternary relativistic interaction so that the main contribution to the line width $\gamma(0)$ comes from the quantity $\operatorname{Im}\Sigma_\Phi(0, -i\epsilon_0+0)$ which is proportional to the probability that a spin wave with $\mathbf{k} = 0$ splits up into two spin waves

$$\gamma(0) = \operatorname{Im}\Sigma_\Phi(0, -i\varepsilon_0+0) = \frac{1}{(2\pi)^2}\operatorname{cth}\frac{\varepsilon_0}{4T}\int d\mathbf{k}\,|\Phi(\mathbf{k}, -\mathbf{k}; 0)|^2\,\delta(2\varepsilon_{\mathbf{k}}-\varepsilon_0). \quad (42)^*$$

This quantity differs from zero in the region where the anisotropy of the ferrodielectric and the external magnetic field are sufficiently small:

$$H_0/M_0+\beta < 4\pi/3.$$

We give the expression for the quantity $\gamma(0)$ in two limiting cases

$$\gamma(0) = \begin{cases} \dfrac{2}{5\pi}\left(\dfrac{3}{8}\right)^{7/2}\operatorname{cth}\dfrac{\varepsilon_0}{4T}\left(\dfrac{\mu M_0}{\Theta_c}\right)^{3/2}\left(\dfrac{4\pi}{3}-\dfrac{H_0}{M_0}-\beta\right)^{5/2}\mu M_0, \\ \qquad\qquad \dfrac{4\pi}{3}-\dfrac{H_0}{M_0}-\beta \ll 1 \\ A\operatorname{cth}\dfrac{\varepsilon_0}{4T}\left(\dfrac{\mu M_0}{\Theta_c}\right)^{3/2}\left(\dfrac{H_0}{M_0}+\beta\right)^{1/2}\mu M_0, \quad \dfrac{H_0}{M_0}+\beta \ll 1 \end{cases} \quad (43)^*$$

$$A = \frac{\pi}{4}\int_0^{\pi/6}\cos^2\vartheta\sqrt{1-4\sin^2\vartheta}\,d\vartheta.$$

If the anisotropy of the ferrodielectric and the external magnetic field are such that

$$H_0/M_0+\beta \geqslant 4\pi/3,$$

then one spin wave with $\mathbf{k} = 0$ cannot split into two and $\gamma(0)$ is determined by the quantity $\operatorname{Im}\Sigma_\Psi(0, -i\epsilon_0+0)$ and only the first of the three terms in (40) is different from zero and is proportional to the probability that a spin wave is scattered by a background spin wave:

$$\gamma(0) = \operatorname{Im}\Sigma_\Psi(0, -i\varepsilon_0+0) = 4(2\pi)^{-5}(e^{\varepsilon_0/T}-1)\times\int d\mathbf{k}'\,d\mathbf{k}''\,|\Psi(0, \mathbf{k}', \mathbf{k}'', \mathbf{k}'-\mathbf{k}'')|^2(n_{\mathbf{k}'}+1)n_{\mathbf{k}''}n_{\mathbf{k}-\mathbf{k}''}\,\delta\times(\varepsilon_0+\varepsilon_{\mathbf{k}'}-\varepsilon_{\mathbf{k}''}-\varepsilon_{\mathbf{k}'-\mathbf{k}''}). \quad (44)$$

In the temperature range $\epsilon_0 \ll T \ll \Theta_c$ the homogeneous resonance line width is of the form

$$\gamma(0) \approx \frac{\mu M_0}{\Theta_c}\left(\frac{T}{\Theta_c}\right)^2\mu M_0, \qquad \frac{H_0}{M_0}+\beta \gtrsim \frac{4\pi}{3};$$

$$\gamma(0) = \frac{\beta^2}{192\pi}\frac{\mu M_0}{\Theta_c}\left(\frac{T}{\Theta_c}\right)^2\mu M_0, \qquad \beta \gg \frac{4\pi}{3}. \quad (45)$$

We turn now to the evaluation of the quantity $\gamma(\mathbf{k})$ in the region of large values of the wave vector $\mathbf{k}$ ($ak \gg \sqrt{\mu M_0/\Theta_c}$). The main part is then played by the quantity $\Sigma_\Phi(\mathbf{k}, -i\epsilon_{\mathbf{k}}+0)$ which is caused by the exchange interaction between the spin waves. Using (40) and (20) we get

$$\gamma(\mathbf{k}) = \operatorname{Im}\Sigma_\Psi(\mathbf{k}, -i\varepsilon_{\mathbf{k}}+0) = \frac{1}{4(2\pi^5)}\left(\frac{\mu\Theta_c}{M_0}\right)^2\left(\exp\frac{\varepsilon_{\mathbf{k}}}{T}-1\right)\times a^4\int d\mathbf{k}'\,d\mathbf{k}''\,(\mathbf{k}\mathbf{k}'+\mathbf{k}\mathbf{k}''+\mathbf{k}'\mathbf{k}''-\mathbf{k}''^2)^2(n_{\mathbf{k}'}+1)+n_{\mathbf{k}''}n_{\mathbf{k}+\mathbf{k}'-\mathbf{k}''}\,\delta(\varepsilon_{\mathbf{k}}+\varepsilon_{\mathbf{k}'}-\varepsilon_{\mathbf{k}''}-\varepsilon_{\mathbf{k}+\mathbf{k}'-\mathbf{k}''}). \quad (46)$$

When $\epsilon_{\mathbf{k}} \sim T$ the quantity $\gamma(\mathbf{k})$ determines the time it takes to establish thermal equilibrium in the spin system; in that case

---

*The x axis is along the normal to the disc.

*Cth = coth.

$$\gamma(\mathbf{k}) \approx (T / \Theta_c)^4 \Theta_c. \qquad (47)$$

Comparing Eqs. (47) and (45) we see easily that $\gamma(\mathbf{k})$ for $\epsilon_{\mathbf{k}} \sim T$ is much larger than $\gamma(0)$ if the temperature is such that $T/\Theta_c \gg \sqrt{\mu M_0/\Theta_c}$. This means, according to (33) that first, after a time on the order of $\gamma(\mathbf{k})^{-1}$, a uniform distribution of the magnetic moment is established in the ferrodielectric. Then, after a time on the order of $\gamma(0)^{-1}$, the transverse part of the magnetic moment $\mathbf{m}_\perp$ slowly approaches its equilibrium value rotating with the homogeneous resonance frequency ϵ_0. The end point of $\mathbf{m}_\perp$ describes then the ellipse

$$m_x^2(t) / U_1(0) + m_y^2(t) / U_2(0) = \mathrm{const.} \qquad (48)$$

9. In the solutions of the Maxwell equations there occurs usually a tensor $\widetilde{\chi}_{il}$ which connects the magnetic moment density $\mathbf{M}$ with the total magnetic field in the system $\mathbf{h} + \mathbf{h}^i$:

$$M_i = \widetilde{\chi}_{il}(h_l + h_l^i). \qquad (49)$$

We shall connect the tensor χ_{il} occurring in Sec. 2 with the tensor $\widetilde{\chi}_{il}$. Solving the Maxwell equations one finds easily the connection between the field $\mathbf{h}^i$ and the magnetic moment density $\mathbf{M}$; in the magnetostatics approximation we have

$$\mathbf{h}^i = -4\pi\mathbf{k} / k^{-2}(\mathbf{k}\mathbf{M}). \qquad (50)$$

Eliminating the quantity $\mathbf{h}^i$ from Eq. (49) and using (50) we get

$$(\delta_{il} + 4\pi\widetilde{\chi}_{im} k_m k_l / k^{-2}) M_l = \widetilde{\chi}_{il} h_l.$$

Comparing this formula with Eqs. (7) and (8) we get the following equation which connects the quantities χ_{il} and $\widetilde{\chi}_{il}$

$$(\delta_{im} + 4\pi\widetilde{\chi}_{in} k_n k_m / k^{-2}) \chi_{ml} = \widetilde{\chi}_{il}. \qquad (51)$$

In conclusion the authors express their gratitude to A. I. Akhiezer for valuable advice.

---

[1] A. Akhiezer, J. Phys. (U.S.S.R.) **10**, 217 (1946).

[2] M. I. Kaganov and V. M. Tsukernik, JETP **37**, 823 (1959), Soviet Phys. JETP **10**, 587 (1960).

[3] M. I. Kaganov and V. M. Tsukernik, JETP **38**, 1320 (1960), Soviet Phys. JETP **11**, 952 (1960).

[4] R. Kubo, J. Phys. Soc. Japan **12**, 570 (1957).

[5] L. D. Landau and E. M. Lifshitz, Электродинамика сплошных сред (Electrodynamics of Continuous Media), Gostekhizdat, M., 1957.

[6] Abrikosov, Gor'kov, and Dzyaloshinskiĭ, JETP **36**, 900 (1959), Soviet Phys. JETP **9**, 636 (1959).

[7] E. S. Fradkin, JETP **36**, 1286 (1959), Soviet Phys. JETP **9**, 912 (1959).

[8] T. Holstein and H. Primakoff, Phys. Rev. **58**, 1098 (1940).

[9] F. J. Dyson, Phys. Rev. **102**, 1217 (1956).

[10] Akhiezer, Bar'yakhtar, and Kaganov, Usp. Fiz. Nauk **71**, 533 (1960), Soviet Phys. Uspekhi **3**, 567 (1961).

[11] V. G. Bar'yakhtar and G. I. Urushadze, JETP **38**, 1253 (1960), Soviet Phys. JETP **11**, 905 (1960).

[12] C. Kittel, Phys. Rev. **71**, 270 (1947).

Translated by D. ter Haar
53

SOVIET PHYSICS JETP VOLUME 13, NUMBER 1 JULY, 1961

Letters to the Editor

γ TRANSITIONS IN THE Sm^{146} NUCLEUS

E. E. BERLOVICH, V. N. KLEMENT'EV,
L. V. KRASNOV, and M. K. NIKITIN

Leningrad Physico-Technical Institute,
Academy of Sciences, U.S.S.R.

Submitted to JETP editor August 28, 1960

J. Exptl. Theoret. Phys. (U.S.S.R.) 40, 375-377 (January, 1961)

We investigated γ radiation of Sm^{146} resulting from electron capture in Eu^{146}. The source consisted of a gadolinium fraction separated by a chromatographical method from a tantalum target bombarded by 660-Mev protons from the synchrocyclotron of the Joint Institute for Nuclear Research. After the decay of the short-lived Gd^{147} (29 hr) and Gd^{149} (9.3 days), the basic activity was due to Gd^{146} (60 days) and its daughter nucleus Eu^{146} (5 days). According to our estimate, the contribution from the relatively soft radiation of Eu^{146} in the region of the Sm^{146} lines was insignificant. The sources used by us had been stored for 40 and 180 days.

The measurements were made on a double scintillation coincidence spectrometer. The investigated lines were separated by means of a single-channel amplitude analyzer and the entire pulse spectrum picked up by the other branch was fed to a coincidence circuit with a resolving time of $2\tau = 10^{-7}$ sec. The coincidence pulses were used to trigger a 100-channel analyzer of type AI-100. The spectrum was fed to this analyzer with a suitable delay.

The Eu^{146} decay has been studied previously,[1,2] and γ transitions of energies 0.64 and 0.74 Mev have been discovered. Moreover, transitions have been found[3] with energies of 0.66 and 0.89 Mev.

We discovered a number of γ transitions arising during the decay of Eu^{146}. The energies and relative intensities of these transitions are shown in the table. As there are a number of lines in the γ spectrum with close-lying energies, we have indicated the total intensity for such groups of lines, and we list the mean energy of such a group; the energies of the lines forming the group are shown in the parentheses. The intensities were determined by resolution into the standard line shape. The intensity of the 0.74-Mev transition was taken as unity. The 0.64-Mev transition was not single transition; according to our estimate, its intensity is approximately equal to the intensity of the 0.74-Mev transition. The errors in the intensity determination were ~ 30%.

E_γ, Mev	I_γ
0.64	~1
0.74	1.00
0.91	0.10
1.1 (1.07+1.17)	0.14
1.3 (1.26+1.31)	0.10
1.5 (1.45+1.56)	0.13
1.8	0.02
2.1 (1.94+2,06+2.19)	0.04
2.4	0.01

The region of the spectrum above 0.9 Mev was investigated with a lead filter 28 g/cm² thick to eliminate the effect of the summation of the most intensive quanta of 0.64 and 0.74 Mev which were emitted in coincidence.

Our experiments confirmed the presence of coincidences (see reference 1) between the 0.74- and 0.64-Mev quanta. Figure 1 shows the spectrum of coincidences with each of these two quanta (in both cases lead filters 6 g/cm² thick were used).

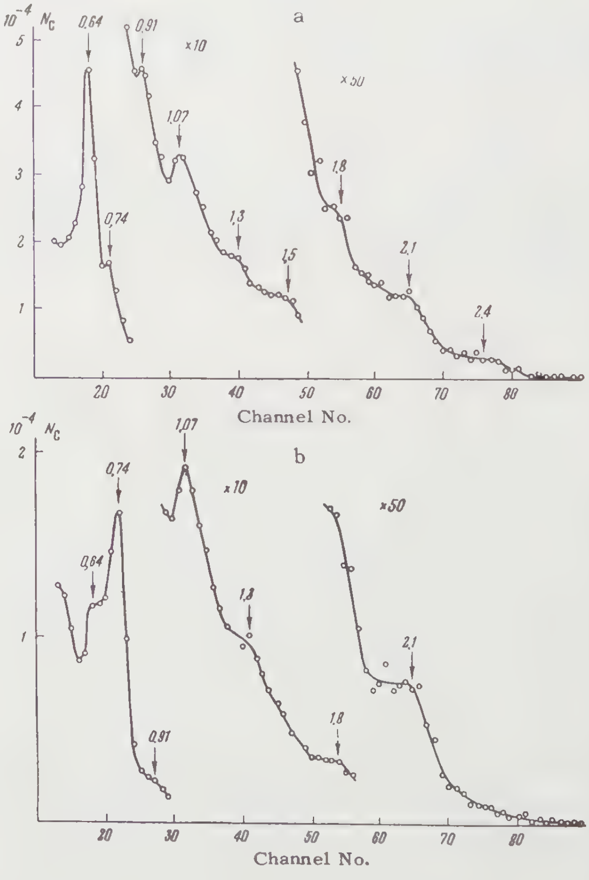

FIG. 1

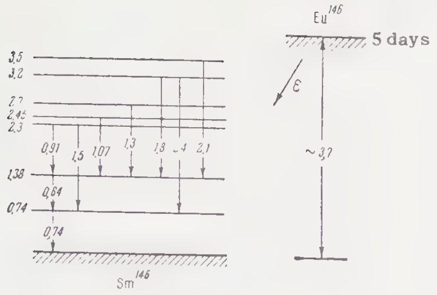

FIG. 2

We found coincidences of 0.74-Mev quanta (Fig. 1a) with quanta of 0.64, 0.91, 1.07, 1.3, 1.5, 1.8, 2.1, and 2.4 Mev. We also observed coincidences of 0.64-Mev quanta (Fig. 1b) with all the quanta enumerated above, except for 1.5 and 2.4 Mev; we also found self coincidences of the 6.4-Mev quanta, which compells us to assume that there is still one more quantum with energy close to 0.64 Mev. Moreover, we investigated coincidences with various parts of the hard region of the spectrum in the range of 2.4, 2.1, 1.8, 1.5, 1.3, 1.1, and 0.9 Mev.

In the spectrum of coincidences with 0.24-Mev quanta the peak at 0.74 Mev is plainly visible, while the 0.64-Mev peak is absent, which is in agreement with the data of the spectrum of 0.64-Mev coincidences. In the case of the coincidences with 2.1-Mev quanta, both peaks are absent. Coincidences with parts of the spectrum in the regions of 0.9, 1.1, and 1.3 Mev give peaks at 0.64 and 0.74 Mev of approximately the same intensity. However, while investigating the coincidences with the part in the region of 1.5 Mev, we observed a sharp increase in the intensity of the 0.74-Mev peak, which is in agreement with the results of experiments on coincidences with 0.64-Mev quanta and gives a basis to assume that the 1.5- and 0.64-Mev transitions are not in cascade. It thus follows that the 0.74-Mev transition is the lower one in the 0.64-0.74 Mev cascade, since the 1.5- and 2.4-Mev transitions proceed directly to the 0.74 level. As regards the remaining transitions, it can be said that they go to the 1.38-Mev level.

In neither the singles spectrum nor in the coincidence spectrum was there observed a direct transition from the 1.38-Mev level of intensity greater than 5% of the 0.74-Mev lines.

In conclusion, we propose a variant of the decay scheme of the Eu^{146} nucleus which is in agreement with the results of the present work (Fig. 2). The energy of the Eu^{148} decay into Sm^{146} is 3350 kev according to Cameron's formula and 3700 kev according to Levi's formula,[4] which allows the existence of the levels introduced by us up to 3.5 Mev.

Some of the transitions occurring in coincidence are probably individual components of the groups shown in the table (for example, the 1.07-Mev line from the group of 1.1-Mev lines.

We noted a γ line of energy 280 kev which was in coincidence with quanta of 115 — 120 kev; they are apparently associated with the decay of Gd^{146} or Eu^{147}.

---

[1] Gorodinskiĭ, Murin, Pokrovskiĭ, and Preobrazhenskiĭ, Izv. Akad. Nauk SSSR, Ser. Fiz. **21**, 1624 (1957), Columbia Tech. Transl. p. 1611.

[2] Anton'eva, Bashilov, Dzhelepov, and Preobrazhenskiĭ, JETP **36**, 28 (1959), Soviet Phys. JETP **9**, 20 (1959).

[3] Gorodinskiĭ, Murin, Pokrovskiĭ, Preobrazhenskiĭ, and Titov, Dokl. Akad. Nauk SSSR **112**, 405 (1957), Soviet Phys.-Doklady

[4] B. S. Dzhelepov and G. F. Dranitsina, Систематика энергий β-распада (Systematics of the β-Decay Energy), Press of the Acad. Sci. U.S.S.R., 1960.

Translated by E. Marquit
54

ON THE THEORY OF PARAMAGNETIC RESONANCE OF Ti *AND* Co *IONS IN CORUNDUM*

S. A. AL'TSHULER and M. M. ZARIPOV

Kazan' State University

Submitted to JETP editor November 2, 1960

J. Exptl. Theoret. Phys. (U.S.S.R.) **40**, 377-379 (January, 1961)

As a result of recent experimental investigations of paramagnetic resonance in Al_2O_3 crystals containing different paramagnetic impurities it has been found that the magnetic properties of Ti ions[1] and of Co ions[2,3] differ appreciably from the properties of these ions in other crystals studied previously. If we make certain natural assumptions then, as our calculations have shown, the whole set of experimental facts relating to the paramagnetic resonance spectra and the spin-lattice relaxation times can be simply explained.

In the case of Ti in corumdum an anisotropy of the g-factor has been experimentally obtained which is unusually large for ions of the iron group with an odd number of electrons: $g_{\parallel} = 1.067$, $g_{\perp} < 0.1$. As the temperature was lowered from 9 to 1.55° K the spin-lattice relaxation time increased from $T_1 = 5 \times 10^{-8}$ to $T_1 = 0.1$ sec. We assume that the trigonal component of the crystalline field is much stronger than the spin-orbit interaction and, therefore, the effects of the cubic and the trigonal components must be taken into account simultaneously. Moreover, we shall assume that the constant of the trigonal field is negative, as the result of which the lowest energy level turns out to be an orbital doublet. The assumptions made by us find confirmation in the structure of the corundum crystalline unit cell. The spin-orbit interaction splits the ground orbital level into two Kramers spin doublets separated by a gap of $\delta = 70\ \text{cm}^{-1}$. The character of the symmetry of the wavefunctions of the lowest doublet is such that even when higher order approximations are taken into account we have $g_{\perp} = 0$. For a definite ratio of the constants of the cubic and the trigonal fields we can easily obtain $g_{\parallel} = 1.07$. It is well known that in corundum the covalent bonds between the metal ion and the oxygen atoms surrounding it play an appreciable role. Taking this bonding into account for the titanium ion will lead to $g_{\perp}$ somewhat different from zero. The relatively small value of the gap δ leads to a very strong spin-lattice interaction. Even at helium temperatures two-phonon processes play the predominant role, as a result of which $T_1 \sim T^{-7}$.

If we assume that the Co^{2+} ions in corundum are situated in a crystalline field of the same character and magnitude as the Ti^{3+} ions, then the lowest orbital level will be a singlet separated from the nearest orbital level by a gap of 1300 cm^{-1}. Taking into account the spin-orbit coupling in second-order perturbation theory, and also the effect of the external magnetic field and of the hyperfine interactions leads to the following spin-Hamiltonian:

$$\mathcal{H} = D\left[S_z^2 - \tfrac{1}{3}S(S+1)\right] + g_{\parallel}\beta H_z S_z + g_{\perp}\beta(H_x S_x + H_y S_y) + A I_z S_z + B(I_x S_x + I_y S_y),$$

where $S = 3/2$. Agreement with experimental values of $g_{\parallel}$, $g_{\perp}$, A and B is obtained if we alter somewhat the constant of the trigonal field, in such a way that the initial splitting of the spin quadruplet is equal to $2D = 24\ \text{cm}^{-1}$. In this case the coefficient describing the contribution to the hyperfine structure of higher electronic configurations containing S states has been taken equal to $K = 0.25$; in order of magnitude the coefficient K agrees with values obtained in the study of paramagnetic resonance spectra in other crystals.[4]

Measurements of the spin-lattice relaxation of Co^{2+} ions have shown that while at 25° K the spin-lattice coupling of the Co^{2+} ions is much stronger than of Cr^{3+} ions, on the other hand at helium temperatures the relaxation time T_1 for the Cr^{3+} ions is much shorter than for the Co^{2+} ions. This fact may be explained as follows.

As a result of the fact that the gap between the lowest orbital energy levels of the Co^{2+} ions is relatively small, the spin-lattice coupling is strong, and at temperatures above helium temperatures is determined by two-phonon processes. In this case the principal role is played by the relaxation transitions between spin levels belonging to different Kramers doublets. The probabilities of these transitions are higher by several orders of magnitude than the probabilities of transitions within Kramers doublets. The exceptionally strong increase of the relaxation time T_1 as the temperature is lowered from 30° to 6° K is related to the fact that this is accompanied by a very rapid diminution in the population of the upper Kramers doublet. Calculations show that for $\Theta < T < 6°$ K (Θ is the Debye temperature)

$$1/T_1 \sim e^{\varepsilon/T}\,(120T^7 + 60\varepsilon T^6 + 12\varepsilon^2 T^5 + \varepsilon^3 T^4),$$

where $\epsilon = 2Dk/\hbar = 35°$. At temperatures below helium temperatures $T_1 \sim 1/T$, since the relaxation is determined by the single phonon processes associated with the transitions between the spin levels of the lowest Kramers doublet. Calculations show that in this case $T_1(Co^{2+})/T_1(Cr^{3+}) = 560$ if the magnetic field is equal to 3000 oe.

---

[1] L. S. Kornienko and A. M. Prokhorov, JETP **38**, 1651 (1960), Soviet Phys. JETP **11**, 1189 (1960).

[2] A. M. Prokhorov and G. M. Zverev, JETP **36**, 647 (1959), Soviet Phys. JETP **9**, 451 (1959).

[3] J. E. Geusic, Bull. Am. Phys. Soc., Ser. II, **4**, 261 (1959).

[4] A. Abragam and M. H. L. Pryce, Proc. Roy. Soc. (London) **A206**, 173 (1951).

Translated by G. Volkoff
55

CRITICAL VELOCITIES IN SUPERFLUID HELIUM

V. P. PESHKOV

Institute for Physics Problems, Academy of Sciences, U.S.S.R.

Submitted to JETP editor November 24, 1960

J. Exptl. Theoret. Phys. (U.S.S.R.) 40, 379-381 (January, 1961)

MORE than 20 years ago Daunt and Mendelssohn,[1] in films, and Allen and Misener,[2] in fine capillaries, noted that the flow velocity of helium II is independent of the pressure head. The clearest picture of the critical velocity was derived by Kapitza,[3] in his papers on the investigation of the thermo-mechanical effect. Critical velocities are manifested in the fact that beyond a certain value the flow velocity of the superfluid component of helium, in films and in fine capillaries and slits, does not increase with further increase in head. In large capillaries (larger than 10^{-3} cm), beginning at a certain critical velocity, there appear forces of interaction between the normal and superfluid components. Landau, in his first paper on superfluid helium,[4] formulated the conditions for destruction of superfluid motion as a consequence of the appearance of excitations in the superfluid helium. The ratio of the energy of an excitation to its momentum must be smaller than the flow velocity of the superfluid component relative to the walls: $\epsilon/p < v_s$. Proceeding from these premises, one may conclude that a velocity greater than the velocity of sound is required for formation of phonons, and one greater than 70 m/sec for formation of rotons.

Using dimensional and certain other concepts, a number of authors have proposed for the critical velocity the relations $v_s = \hbar/md$ and $v_s = \hbar/m\sqrt{ad}$, where m is the mass of the helium atom, d the diameter of the capillary or width of the slit, and a a quantity of the same order as the interatomic distance. Feynman,[5] assuming that superfluidity is destroyed as a result of the formation of vortices at the exit of the superfluid current from the capillary, derived the formula $v_s = (\hbar/md)\cdot\ln(d/a)$. These formulas give the correct order of magnitude for the critical velocity and its dependence upon the dimensions, for a certain range of capillary diameters, but for capillary dimensions of less than 10^{-3} cm they are not borne out, either qualitatively or quantitatively. Suggestions indicating that the reason for the destruction of superfluidity lies in the generation of vortices, however, appear to be correct. As is well-known,[5,6] the energy of a vortex ring of radius R is, approximately

$$\varepsilon \approx (\rho_s R h^2/2m^2) \ln (R/a), \qquad (1)$$

while its momentum $p \approx \rho_s \pi R^2 h/m$, where ρ_s is the superfluid component density, and $h = 2\pi\hbar$. Thus, in addition to phonons and rotons, there exists still another form of excitations — vortex rings. Assuming that a vortex ring of minimal size is a roton of energy $\Delta = k \cdot 8.9° = 1.23 \times 10^{-15}$ erg, and momentum $p_0 = 2.1 \times 10^{-19}$ g cm/sec, we obtain $a \approx 10^{-8}$ cm, and $R = 2.6 \times 10^{-8}$ cm, while the vortex ring spectrum will have the form

$$\varepsilon = \Delta \sqrt{\frac{p}{p_0}} \left(1 + \frac{1}{2} \ln \frac{p}{p_0}\right). \qquad (2)$$

Inasmuch as the condition for generation of the excitations is $v_s > \epsilon/p$, it is evident from the form of the spectrum that the development of vortices with the largest p — i.e., the largest radius — is the most profitable. Moreover, there should exist an analogy between the development of turbulence in an ordinary liquid and the generation of vortices in superfluid helium; i.e., the energy for formation of the vortices may not be acquired instantaneously, but only after a relaxation time τ. One may therefore presume that superfluidity is destroyed through formation of a vortex of maximal radius R with the energy (1). This energy is acquired at the expense of a fraction (α) of the kinetic energy of the superfluid current in the capillary over a segment of its length on the order of $R + v_s\tau$; i.e.,

$$\alpha \frac{\rho_s v_s^2}{2} \pi R^2 (R + v_s \tau) = \rho_s \frac{R h^2}{2m^2} \ln \frac{R}{a}$$

or

$$v_s^2 R (R + v_s \tau) = \frac{h^2}{\alpha \pi m^2} \ln \frac{R}{a}. \qquad (3)$$

For $\alpha = 0.122$, $\tau = 4 \times 10^{-4}$ sec, and $a = 10^{-8}$ cm, (3) yields for $v_s(R)$ a dependence that agrees to within the limits of experimental error with the experimental data available (cf. reference 6), at T = 1.3°K, from $R = 3 \times 10^{-6}$ cm to R = 0.2 cm. For films, R is taken to be the total thickness d, and for slits, the quantity d/2. If one takes $a = 3 \times 10^{-7}$ cm (the value obtained by Hall[7] from experiments on the oscillation of vortices), then for $\alpha = 0.116$ and $\tau = 2 \times 10^{-4}$ sec satisfactory agreement is also obtained. In the figure, the circles represent the experimental data, the solid curve is computed from equation (3) with $a = 10^{-8}$ cm, $\tau = 4 \times 10^{-4}$ sec, and $\alpha = 0.122$, and the

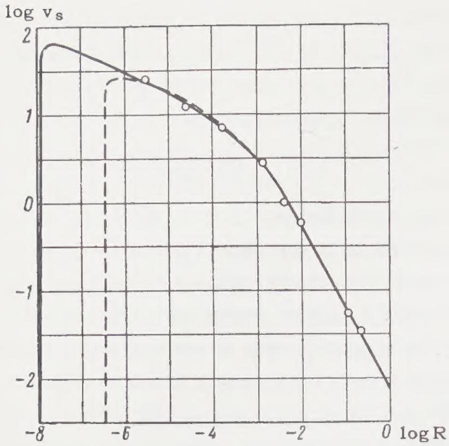

dashed curve, with $a = 3 \times 10^{-7}$ cm, $\tau = 2 \times 10^{-4}$ sec, and $\alpha = 0.116$.

The appearance of a trans-critical regime in the capillary under conditions of slight supercriticality is represented in the following form: At certain points in the capillary, due to nonuniformity of its walls, there will exist more suitable conditions for the formation of a ring vortex. When the vortex has moved along the capillary, another vortex arises at the same point, but with two vortices present near one another one vortex begins to move into the other. After a third vortex has formed, it too begins to take part in the collective vortex motion. Thus, the vortices forming at individual points due to slight supercriticalities begin gradually to fill the capillary, through an extremely complex collective motion. In the presence of a thermal current along the capillary the vortices existing therein increase the thermal resistance; the gradual filling of the capillary with vortices is therefore accompanied by a real, experimentally observable, slow (e.g., 0.2 cm/sec) advance of a front of increased thermal gradient. This pattern has been observed by Mendelssohn and Steele.[8] The vortices formed are more stable when their momenta are in the direction of motion of the normal component than when they are oppositely directed; when trans-critical regimes are present in capillaries, therefore, a velocity distribution is established which is similar to that proposed by Gorter and Mellink,[9] wherein the difference $v_s - v_n$ remains constant over the entire cross-section of the capillary.

---

[1] J. G. Daunt and K. Mendelssohn, Proc. Roy. Soc. **A170**, 423, 439 (1939).

[2] J. F. Allen and A. D. Misener, Proc. Roy. Soc. **A172**, 467 (1939).

[3] P. L. Kapitza, JETP **11**, 581 (1941).

[4] L. D. Landau, JETP **11**, 592 (1941).

[5] R. P. Feynman, Progr. in Low Temp. Phys. **1**, Amsterdam, 1955, p. 17.

[6] K. R. Atkins, Liquid Helium, Cambridge, 1959.

[7] H. E. Hall, Proc. Roy. Soc. **A245**, 546 (1958).

[8] K. Mendelssohn and W. A. Steele, Proc. Phys. Soc. **73**, 144 (1959).

[9] C. J. Gorter and J. H. Mellink, Physica **15**, 285 (1949).

Translated by S. D. Elliott
56

ORIGINS OF THE NERNST EFFECT IN FERROMAGNETIC METALS

E. I. KONDORSKIĬ

Moscow State University

Submitted to JETP editor October 24, 1960

J. Exptl. Theoret. Phys. (U.S.S.R.) **40**, 381-382 (January, 1961)

THIS article treats a relativistic effect connected with the movement of current carriers that possess a nonvanishing mean magnetization. An estimate of the transverse electric field intensity connected with this effect shows that it needs to be taken into account in the theory of the Nernst effect in ferromagnetic metals. It is shown that from the sign of the Nernst field one can determine how the magnetization of the current carriers is directed with respect to the resultant spontaneous magnetization of the metal.

In the existing theories, the fractional values of the magnetic moments of ferromagnetic metals are explained[1] on the basis of the assumption that the current carriers possess a magnetization directed parallel or antiparallel to the magnetization of the metal.

Let us consider the simplest possible model, in which the current carriers are free electrons with mean magnetization $I_e = a_e I_z$, where a_e is a positive or negative coefficient and I_z is the magnetization. Under the influence of an electric field E_x, there is excited an electric current of density $j_x = env_x = -enuE_x$, where u is the mobility. It is known that if a system possessing magnetic moment **I** moves with velocity **v**, a stationary observer records in it an electric polarization **P** and an electric field $\mathbf{E} = -4\pi\mathbf{P} = -(4\pi/c)\mathbf{v} \times \mathbf{I}$. In the case being considered, this field is directed along the y axis and is equal to $E = (a_e v_x/c) 4\pi I_z$. Therefore the Lorentz force is $F_y = e(E - v_x B_z/c)$, and the Hall current density is $j_y = -(\sigma v_x/c)(B_z - a_e \cdot 4\pi I_z)$. This current vanishes after appearance of surface charges that produce an electric field $E_{H1} = j_y/\sigma$. The Hall field intensity is $E_{Hy} = E_{H1} + E = v_x B_z/c$, whence $R_0 = 1/cne$. Thus in the case of free electrons possessing magnetization, the Hall constant remains the same as if the whole magnetization were produced exclusively by bound electrons. In this case the derivation given differs from the usual one only in the treatment of the physical interpretation of the terms that enter E_{Hy}.

The effect considered plays an essential role in the Nernst effect, where because of the electrical polarization connected with current carriers that possess a magnetization, there can arise a field, two orders of magnitude larger than the usual Nernst field, which is produced by the difference of speeds of electrons moving toward the hot and the cold ends of the conductor.

Current carriers of any type moving toward the hot end of the metal have a larger mean magnetization than carriers that are moving in the opposite direction. Therefore when a heat current flows along the conductor, there is a transfer not only of energy but also of magnetic moment. As a result, in this case also there is produced an electric polarization, which leads to the appearance of a transverse electric field. Calculation of the part Q_{se} of the ferromagnetic Nernst constant Q_s that is due to the effect under consideration leads to the expression

$$Q_{se} = \frac{2\tau(\eta)\,\eta a_e}{3cm^* I_s}\frac{\partial I_s}{\partial T}\cdot 300 = \frac{K a_e}{c C_0 I_s}\frac{\partial I_s}{\partial T}\cdot 300 \text{ [v/deg-gauss]}. \tag{1}$$

Here $\tau(\eta)$ is the relaxation time, η is the Fermi energy, K is the thermal conductivity, C_0 is the electronic heat capacity, and I_s is the spontaneous magnetization. It is easily demonstrated that at temperatures near the Curie point and for $|a_e| \geq 0.1$, we have $Q_{se} \gg Q_s'$, where Q_s' is the usual Nernst constant.

In the Nernst field there is also included a field connected with spin-orbit interaction of the current carriers with the ions. If in first approximation, as was done by Karplus and Luttinger,[2-3] we describe the spin-orbit interaction by means of an effective field $H_{eff} = H_{spo} I_e/I_s$, then we can derive a formula for the part of the Nernst constant connected with this interaction; it will differ from (1) only by a positive multiplier. Comparison with experimental data[4-5] on nickel and on iron-nickel alloys shows that (1) describes well the temperature dependence of Q_s from room temperature to the Curie point and gives the right order of magnitude for the value of Q_s.

It follows from (1) that, independently of the type of current carrier, the coefficient Q_s is positive if the magnetization of the carriers is directed opposite to the spontaneous magnetization of the metal, and is negative if both magnetizations are parallel. Thus from the sign of Q_s it is possible to determine the signs of the magnetizations of the current carriers. As Smith's[4] experimental data show, Q_s is negative in iron and positive in nickel and cobalt. Consequently, the magnetization of the current carriers is directed along the spontaneous magnetization in iron and opposite to it in cobalt and in nickel.

---

[1] S. V. Vonsovskiĭ, Современное учение о магнетизме (Modern Theories of Magnetism), Gostekhizdat, 1953, pp. 224-227.

[2] R. Karplus and J. M. Luttinger, Phys. Rev. **95**, 1154 (1954).

[3] J. M. Luttinger, Phys. Rev. **112**, 739 (1958).

[4] A. Smith, Phys. Rev. **33**, 295 (1911); **17**, 23 (1921).

[5] R. P. Ivanova, Физика металлов и металловедение (Phys. of Metals and Metallography) **8**, 851 (1959).

Translated by W. F. Brown, Jr.
57

CORRECTION TO THE ARTICLE BY D. P. GRECHUKHIN 'SOME EXPERIMENTAL POSSIBILITIES FOR VERIFICATION OF THE MODEL OF NONAXIAL NUCLEI WITH A ROTATIONAL SPECTRUM'

JETP **38**, 1891 (1960), Soviet Phys. JETP **12**, 1359 (1960).

THROUGH an oversight on the part of the author, the coefficient of the third term of Eq. (4) is in error. The rigorously correct formula is

$$\langle r^2\rangle_{\mathrm{DF}} = \frac{3}{5} Z R_0^2 \Big\{1 + \frac{5}{4\pi}\beta^2 + \frac{25}{12\pi}\sqrt{\frac{5}{4\pi}}\,(C_{2020}^{20})^2 \beta^3 \cos\gamma\,[1 - 4\sin^2\gamma]\Big\}.$$

Recognizing that $(C_{2020}^{20})^2 = 2/7$ and $(50)/21)\sqrt{5/\pi} \approx 3.004$, we obtain, with sufficient accuracy

$$\langle r^2\rangle_{\mathrm{DF}} = \frac{3}{5} Z R_0^2 \Big\{1 + \frac{5}{4\pi}\beta^2 + \frac{3}{8\pi}\beta^2 \cos\gamma\,[1 - 4\sin^2\gamma]\Big\}.$$

The author is deeply grateful to É. E. Fradkin for calling his attention to the error and for undertaking the recalculation of $<r^2>_{\mathrm{DF}}$.